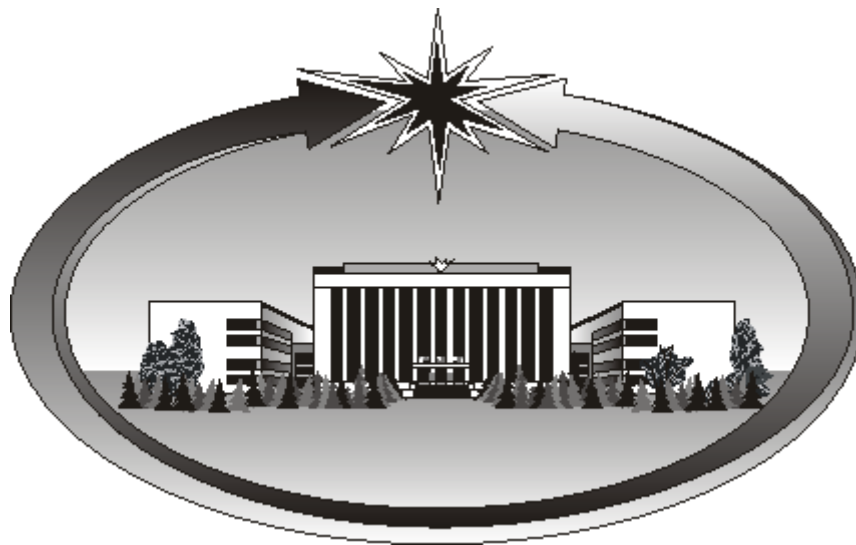


Siberian Branch of Russian Academy of Sciences

BUDKER INSTITUTE OF NUCLEAR PHYSICS



# **ANNUAL REPORT**

## **2010**

NOVOSIBIRSK 2011

# Contents

<b>Introduction</b>	<b>7</b>
<b>1. Physics of Elementary Particles</b>	<b>13</b>
1.1 CMD-3	15
1.2 The SND detector	16
1.2.1 SND upgrade and results of the first experiments at VEPP-2000	16
1.2.2 VEPP-2M data analysis	18
1.2.3 Participation in international projects	19
1.3 Detector KEDR	20
1.4 Results of work of the KEDR detector at the VEPP-4M collider in 2010	21
1.4.1 Measurement of parameters of $J/\psi$ -meson	22
1.4.2 Measurement of the $\psi(2S)$ -mesons parameters	23
1.4.3 Measurement of the $\psi(3770)$ -meson parameters	25
1.4.4 Measurement of the $\tau$ -lepton mass	25
1.4.5 Search for narrow resonances	26
1.5 Detector for HEP	27
1.6 X-ray detectors	27
1.7 Other works	27
1.8 Microstructure gas detectors	28
1.8.1 Cryogenic two-phase avalanche THGEM-based detectors	28
1.8.2 Modernization of the system of scattered electrons in the KEDR experiment	29
1.8.3 Low-pressure gas THGEM-based detector	31
1.8.4 Participation in collaborations	31
1.9 Participation of BINP in the LHCb in 2010	32
1.9.1 Technical support of the LHCb	32
1.9.2 Physical results	33
1.10 Belle Experiment	37
1.10.1 Main results	37
1.10.2 Data analysis of the Belle experiment	37
1.10.3 Detector upgrade	43
1.11 Experiment BABAR	46
1.12 Participation in the ATLAS experiment on the Large Hadron Collider (LHC)	47
1.13 The Photon Collider	50
<b>2. Electro - and photonuclear physics</b>	<b>51</b>
2.1 Experiments with internal targets	53
<b>3. Theoretical physics</b>	<b>55</b>
3.1 Strong interaction	57
3.2 SP nonconservation	61
3.3 Quantum electrodynamics	61
3.4 Gravity	64
3.5 Astrophysics	64
3.6 Nonlinear dynamics and chaos, quantum	65
<b>4. Plasma physics and controlled thermonuclear fusion</b>	<b>69</b>
4.1 Scientific report about research results on GDT device for 2010 year	71

4.1.1	Introduction.....	71
4.1.2	The study of plasma motion at the vortex confinement .....	72
4.1.3	The maximum achievable electron temperature and energy balance.....	75
4.1.4	High-frequency electromagnetic oscillations .....	76
4.2	Plasma theory.....	77
4.2.1	Plasma equilibrium and stability .....	77
4.2.2	Dynamic plasma confinement .....	77
4.2.3	Terahertz radiation .....	77
4.2.4	Nonneutral plasmas.....	77
4.2.5	Theory of plasma dust formation .....	77
4.2.6	Theory of plasma wakefield acceleration .....	77
4.2.7	Simulation of turbulent plasma heating by a powerful electron beam.....	78
4.3	Beam Injectors of Hydrogen Atoms and Ions .....	78
4.3.1	Beam Injectors of Hydrogen Atoms .....	78
4.3.2	Project of powerful continuous injector of beam of fast hydrogen atoms.....	79
4.4	GOL-3 Facility .....	79
4.4.1	Introduction .....	79
4.4.2	Experiments on injection of a beam with smoothly increasing power.....	80
4.4.3	Measurement of electron distribution function .....	81
4.4.4	Studies of sub-Terahertz plasma emission.....	82
4.4.5	Results of plasma magnetic activity measurements.....	84
4.4.6	Experimental investigations of tungsten erosion after powerful plasma stream irradiation.....	85
4.4.7	Development of diagnostic capabilities .....	87
4.4.8	Development of technology of creation of a long-pulse intensive electron beams based on plasma emitters .....	89
4.4.9	Sammary .....	89
<b>5.</b>	<b>Electron-Positron Colliders.....</b>	<b>91</b>
5.1	VEPP-2000 in 2010.....	93
5.1.1	First experimanal work with SND and CMD-3 detectors $2\times(500-950\text{MeV})$ .....	93
5.1.2	Radiative polarization and energy calibration .....	94
5.1.3	Correcting the orbit and magnetic structure of VEPP-2000.....	96
5.1.4	Optimizing the correctors strength.....	98
5.1.5	Correcting the accelerator structure .....	99
5.1.6	Luminosity measurements.....	101
5.1.7	Booster BEP modernization.....	102
5.2	The accelerator complex VEPP-4 .....	106
5.2.1	Distribution of working time .....	106
5.2.2	High Energy Physics .....	107
5.2.3	Modernization of the CBS system .....	107
5.2.4	Upgrade of the "Positron" injector.....	109
5.2.5	VEPP-4M longitudinal feedback system .....	111
5.2.6	The temperature monitoring system .....	113
5.3	VEPP-5 injection complex.....	114
5.4	Linear inductive accelerator LIA - 2 .....	119
5.5	Electron beam welding .....	122
5.6	Design and construction of electron guns.....	125
5.7	Creating electron cooling for a beam energy of up to 2 MeV .....	127
5.8	Work with the accelerator mass spectrometer.....	128
5.9	Developing of hadron cancer therapy .....	129

5.10	Vacuum systems.....	129
5.10.1	High-vacuum infrared optical window .....	129
5.10.2	Cryogenic equipment for testing the accelerating modules XFEL (DESY).....	131
5.10.3	Vacuum system of the NSLS-II booster.....	134
5.11	Electron-beam sources of multicharge ions MIS-1. ....	136
5.12	Works on the electron-positron factories and beam physics .....	138
5.13	Pulse magnet for the positron source of the KEK Super-B Factory .....	138
5.14	Works on the injection-extraction systems .....	140
<b>6.</b>	<b>Synchrotron Radiation Sources and Free Electron Lasers.....</b>	<b>143</b>
6.1	Works on SR beams from VEPP-3 .....	145
6.1.1	Station "Explosion (Extreme states of matter)" .....	145
6.1.2	Station "LIGA technology and X-ray lithography" .....	148
6.1.3	Station "Anomalous Scattering" .....	151
6.1.4	Station "Precision Diffractometry" .....	154
6.1.5	Station "X-ray fluorescent elemental analysis" .....	156
6.1.6	Station "Diffractometry using hard X-rays" .....	159
6.1.7	Station " X-ray Microscopy and Tomography" .....	162
6.1.8	Station "Diffractive Movie" .....	165
6.1.9	Station "EXAFS Spectroscopy" .....	167
6.1.10	Application of a 9-channel SCD to fluorescent XAFS-spectroscopy .....	171
6.2	Work on SR beams from VEPP-4M .....	173
6.2.1	Station "Cosmos".....	173
6.3	Working with beams of terahertz radiation.....	176
6.3.1	Novosibirsk terahertz free electron laser .....	176
6.3.2	Experimental stations on THz radiation beams .....	176
6.3.3	The second stage of Novosibirsk FEL.....	193
6.3.4	Results of the year 2010 and plans for the year 2011 .....	194
6.4	Development and creation of specialized generators of SR .....	194
6.4.1	Superconductive wigglers.....	194
6.4.2	Radiation-resistant dipole magnet for the ion accelerator under construction at GSI (Germany).....	195
6.4.3	Technological storage ring complex (TSRC "Zelenograd") .....	196
6.4.4	Development of the new synchrotron radiation source for the Siberian Centre for Synchrotron and Terahertz Radiation .....	197
6.4.5	MARS at the RRC "Kurchatov Institute" .....	199
6.5	Conferences, meetings, seminars.....	199
6.5.1	XVIII International Conference on Synchrotron Radiation application "SR-2010" .....	199
6.5.2	International Symposium on the generation and application of terahertz radiation .....	200
6.5.3	School for Young Professionals "Synchrotron radiation in the Earth sciences" ..	201
6.5.4	Conference of students and graduates working at the SCSTR .....	202
6.5.5	Participation of SCSTR members in other academic activities.....	202
<b>7.</b>	<b>Radiophysics and electronics.....</b>	<b>205</b>
7.1	Power supply sources for electrophysics facilities .....	207
7.1.1	Stabilized current sources .....	207
7.1.2	High-voltage sources. Electronics for diagnostic and heating injectors of neutral atoms.....	209
7.1.3	High-voltage sources. Power electronics for electron beam welding (EBW) .....	210
7.2	Development of measuring systems and devices for automation of the physical	

---

experiments.....	210
7.3 Research related to the modelin and solving the electrostatic and electrodynamic problems of accelerator physics.....	214
7.4 RF generator for the resonance electron accelerator based on a coaxial resonator .....	214
7.5 Manufacturing and tuning of the elements of the accelerating structure for the modustrial linear electron accelerator for 10 MeV/100 kW .....	218
7.6 Project of 100 MHz continuous wave RF generator with an output power of 540 kW .....	221
7.7 Upgrading the RF Continuous-power generators for the FEL .....	225
7.8 Defining parameters of the RF system of the storage ring Siberia-2 for ensuring the stability of longitudinal motion of electrons for in-phase dipole oscillations .....	227
7.9 Status of the RF system of the 2.2 GeV storage ring in Zelenograd.....	228
7.10 RF sistem of the neutral beam injectors of the COMPASS tokamak .....	229
7.11 New RF system for the electron-positron storage ring BEP .....	229
7.12 Preparation of the VEPP-4M RF system for work at an energy of 4 GeV.....	231
7.13 CCDTL accelerating structures for Linac4, CERN .....	231
<b>8. Powerful Electron Accelerators and Beam Technologies .....</b>	<b>235</b>
8.1 Radiation technologies and ELV series electron accelerators.....	237
8.2 ILU accelerators and their applications .....	243
8.2.1 Accelerator supplies .....	243
8.2.2 Development of modular industrial electron accelerator ILU-14.....	244
8.2.3 New technologis development.....	245
<b>9. Physics for medicine.....</b>	<b>247</b>
9.1 Status of BNCT .....	249
9.2 X-ray detectors for medicine and examination of people.....	250
9.2.1 Medical Radiography .....	250
9.2.2 X-ray Inspection Sistem "Sibscan" for examination of people.....	250
9.2.3 Works for High Energy Physics .....	250
<b>Bibliography .....</b>	<b>251</b>
<b>List of publications.....</b>	<b>251</b>
Preprints.....	299
Authorial papers - 2010 .....	302
Participation in conferences.....	303
<b>List of Collaboration Agreements.....</b>	<b>306</b>
<b>Research Personnel .....</b>	<b>309</b>
Members of Russian Academy of Science .....	309
Director board.....	309
Scientific council .....	309
Specialized sections of scientific council.....	310
Research staff and publications.....	313

## Introduction

The Institute of Nuclear Physics of the USSR Academy of Sciences was established in accordance with the decision of the Council of Ministers in May 1958. The Institute was based on the laboratory of new acceleration methods, directed by G.I. Budker, at the Institute of Atomic Energy, headed by Igor Kurchatov. RAS member A.N. Skrinsky has been the director of the Institute since 1977.

Currently, BINP is the largest academic institute of the country (about 2700 employees). The scientific staff of the Institute of 4141 members includes 10 members and corresponding members of the RAS and 226 PhDs. A distinctive feature of BINP is the large-scale experimental workshop (about 1000 employees) with high-level technical and technological equipment.

The Institute is actively engaged in the training of research and technical personnel of high qualification. BINP is the base institute for seven sub-departments of the Physics Department of Novosibirsk State University (NSU) and the Physical Engineering Department of Novosibirsk State Technical University (NSTU), which educate about 200 students. 50 young people pursue post graduate studies at BINP, NSU and NSTU.

BINP is one of the world's leading centers for a number of fields in high-energy physics, accelerator physics, and plasma and controlled fusion physics. The Institute conducts large-scale experiments in elementary particle physics on electron-positron colliders and a unique complex of open plasma traps and develops up-to-date accelerators, intense sources of synchrotron radiation and free electron lasers. As concerns most of BINP research directions, there are no other institutes in Russia that can be compared with BINP.

The major achievements of BINP in science and technology include the following:

### **In the field of elementary particle physics and nuclear physics:**

- pioneering work on the development of the method of colliding beams, which is now the main method in high energy physics):
  - the first experiments on electron-electron interaction (simultaneously with the Princeton-Stanford works), 1965,
  - the world's first experiments on electron-positron interaction (1967)
  - the world's first observation of double bremsstrahlung (1967);
  - pioneering works on two-photon physics (1970);
- study of the characteristics of vector mesons on colliding electron-positron beam facilities: VEPP-2, VEPP-2M and VEPP-4 (since 1967);
- discovery of the phenomenon of multiple production of hadrons in the electron-positron annihilation (1970);
- precise measurement of the contribution of hadronic vacuum polarization to the value of anomalous magnetic moment of muon for one of the most sensitive tests of the Standard Model, conducted in collaboration with Brookhaven National Laboratory (1984 - 2005);
- development of the method of resonant depolarization for precise measurements of the mass of elementary particles, reaching a record-high precision of measurements of the mass of  $K^-$ ,  $\rho^-$ ,  $\omega^-$ ,  $\phi^-$ ,  $\psi^-$  and  $\nu$ -mesons (1975 - 2004);
- discovery of parity nonconservation in atomic transitions and confirmation of the unified theory of electroweak interaction (1978);
- development of conduction of experiments on internal hyperfine targets in storage rings (since 1967) and study of the electromagnetic structure of deuteron in polarization experiments (1984);
- development of the method for generation of intense fluxes of tagged high-energy gamma quanta through the use of inverse Compton scattering (1980 - 1982) and experimental observation of photon splitting in a Coulomb nuclear field (1997);

- development of new methods for detection of high-energy charged and neutral particles and creation of unique detectors for colliding beams (OLYA, CMD-1, MD-1, CMD-2, CMD-3, ND, SND, and KEDR) (since 1974);
- development of X-ray detectors for medical purposes and creation on their basis of the low-dose digital radiographic device with ultra-low patient exposure and X-ray inspection system for screening people («Sibskan», since 1981).

**In the field of theoretical physics:**

- development of the resonance theory of dynamical chaos and pseudo chaos in classical and quantum mechanics (since 1959);
- the first calculation of charge renormalization in the Yang-Mills theory (1969);
- development of the QCD sum rule technique (1979 - 1984);
- prediction of large enhancement of parity violation in neutron resonances in heavy nuclei (1980 - 1985);
- development of the theory of hard exclusive reactions in QCD (1977 -1984);
- development of an operator approach to quantum electrodynamics in external fields (1974 - 1976);
- development of quantum electrodynamics in periodic structures, including a laser wave (1972 - 1997);
- development of the theory of radiation effects during the passage of charged particles and high-energy photons through single oriented crystals (since 1978);
- derivation of the evolution equation in QCD for parton energy distribution (the BFKL equation) (1975 - 1997)
- prediction of the coherence effect in emission of gluons in QCD and study of its effect on hadron distributions (1981 - 1982).

**In the field of accelerator physics and technology:**

- successful long-term experience in creating storage rings and colliders;
- invention, development and experimental testing of the method of «electron cooling» of beams of heavy particles, which is currently used at laboratories around the world; equipping accelerator complexes for heavy ions in Germany and China and at CERN with effective «coolers» (1965-2005);
- invention and development of new types of high-power RF generators (Gyrocon, relativistic klystron, and Magnicon) (since 1967);
- suggestion of the method of linear electron-positron colliding beams for production of ultrahigh energies (1968) and presentation of a physically self-consistent project (1978);
- development of elements of large-field pulsed magnetic optics (X-lenses and lithium lenses), which are currently used at various laboratories (since 1962);
- invention and experimental verification of the charge-exchange injection method, which is used now on all large proton accelerators (1960-1964);
- theoretical and experimental studies of the production of polarized beams and spin dynamics in accelerators and colliders, the conceptual design and creation of high-spin rotators and "Siberian snakes" for a number of accelerator complexes (1966 - 1995);
- theoretical and experimental investigations into the stochastic instability and collision effects limiting the luminosity of colliding beam facilities (since 1966);
- development of the physical concept of the new generation of electron - positron colliders of very high luminosity, the so-called electron - positron factories (since 1987);
- proposal and development of the method of ionization cooling of muons for creation of muon colliders and neutrino factories (1969 -1981 - 2002);
- development and creation of high-power and low-energy electron accelerators for various technological applications, environmental protection among them, including the 500 kW ELV-12 accelerators with an energy of 1 MeV and the ILU-10 accelerators with power as high as 50 kW and an energy of 5 MeV (since 1963);
- proposal and implementation of the energy recovery linac scheme for high-efficiency free electron lasers (1979 - 2003).

**In the field of plasma and fusion physics:**

- invention (1954) and creation (1959) of the “classical” open magnetic trap (magnetic mirror) for hot plasma confinement;
- invention and development of new schemes of open traps: multimirror, with a rotating plasma, ambipolar, gas-dynamic; pilot multimirror confinement of plasma with sub-thermonuclear parameters in the GOL-3 trap; pilot stabilization of MHD instabilities in the axially symmetric gas dynamic trap on the GDT facility (since 1971);
- discovery of collisionless shock waves in plasma (1961);
- development of the method of plasma heating with relativistic electron beams (since 1971);
- development of high-intensity surface-plasma sources of negative ions, which became widespread throughout the world (1969 - 1981);
- proposal and development of the concept of high-power thermonuclear neutron source based on open trap for materials science (1987);
- theoretical prediction of the Langmuir collapse (1972) and experimental detection of strong Langmuir turbulence and collapse of Langmuir waves in a magnetic field (1989 - 1997);
- creation of a series of unique high-power precision sources of hydrogen atoms for high-temperature plasma study for a number of large facilities (since 1997).

**In the field of synchrotron radiation and free electron lasers:**

- application of the synchrotron radiation of the BINP storage rings to various scientific and technological objectives and creation of the Siberian Centre for Synchrotron Radiation based on VEPP-2M, VEPP-3, and VEPP-4 (since 1973);
- theoretical and experimental studies of emission of particles in periodic structures (undulators, wigglers, and crystals) (since 1972);
- development and creation of specialized sources of synchrotron radiation (since 1983);
- development and creation of one- and two-coordinate detectors for experiments with synchrotron radiation (since 1975);
- invention and development of the optical klystron (1977) and generation of coherent radiation in the infrared to ultraviolet spectrum (since 1980);
- development and creation of the powerful free-electron laser (for photochemical research and technological applications as well as for transferring energy from the Earth to a satellite) on the basis of the most promising scheme using a ERL microtron; generation of high-power (400 W) laser radiation in the terahertz range (since 1987);
- creation of a series of high-field superconducting magnetic devices for SR sources and electron storage rings (wigglers and bending magnets with a field of up to 10 T and solenoids with a field of up to 13 T) (since 1996).

The unique plants and equipment of the Institute make a core infrastructure for a wide range of interdisciplinary scientific and technological research at the four share-use centers established at the Institute: the Siberian Synchrotron Radiation Center, the Center for Photochemical Research, the Center for Geochronology of the Cenozoic, and the Center for Electron Beam Technology. Hundreds of organizations work on the facilities each year.

The application works of BINP are entirely based on the results of its fundamental studies and focused in the following key areas:

- high-power industrial electron accelerators used for modification of polymers; for purification of industrial and domestic waste; production of nanopowders of pure metals, silica, and metal oxides, carbides and nitrides; radiation processing of food; sterilization of medical equipment and disposable instruments and clothing; and other technological applications;
- low-dose digital radiographic installation of scanning type with ultra-low patient exposure, for medical and security systems;
- development of nuclear medicine facilities for proton, ion, and boron-neutron capture therapy of malignant tumors;
- plants for electron beam welding;
- radiographic equipment for the defense research.

Over the past 20 years BINP has actively used the basic and applied research funding received due to execution of contract works. Annually, BINP develops, manufactures and supplies diversified high-tech products in the value of more than half a billion rubles for customers in Europe, Asia, and North and South America (20 countries) as well as in Russia. Funds received in this way made it possible to complete and commission the VEPP-4M accelerator complex with the unique detector KEDR and design and build new large up-to-date unique facilities: the electron-positron collider VEPP-2000, the free electron laser, and the new injection complex ensuring the work of the existing and future installations of BINP. Since the disintegration of the USSR, these funds have supported the continuous work of BINP facilities and infrastructure.

BINP activity is characterized by the wide long-term international cooperation with most major foreign and international centers. A striking example of such cooperation is the BINP participation in the today's largest international project – the creation of the Large Hadron Collider at CERN (Geneva). Within the framework of this work, BINP has developed, manufactured and delivered to CERN unique high-tech equipment in the value of over 100 million Swiss francs. Another example of international cooperation is the participation in the projects of B-factories in the U.S.A. and Japan and major European projects: synchrotron radiation source PETRA-III and X-ray free electron laser (DESY, Hamburg), heavy-ion accelerator complex (GSI, Darmstadt) and many others.

BINP has a key role in several major Russian projects, including the Center for Synchrotron Radiation at the Research Center "Kurchatov Institute", the synchrotron radiation source of the TSC in Zelenograd, the neutron source for the JINR in Dubna, and the radiographic equipment for defense studies for the Federal State Unitary Enterprise "VNIITF", Snezhinsk.

The Institute takes an active part in the shaping of the innovation economy of the country. A striking example of this is the development in conjunction with the ICG SB RAS and the company "Siberian Center for Pharmacology and Biotechnology" of a unique technology of electron-beam immobilization of biomolecules on an inert carrier, which is used for mass production of the world's first oral thrombolytic "Trombovazim".

The Institute is deeply integrated into the work of RAS and SB RAS, exercising implementation of 20 projects under the program of the Presidium and Branches of the RAS, 16 interdisciplinary integration projects, and 8 joint projects of SB RAS with regional RAS institutes, the National Academies of Sciences of Ukraine, Belarus and China, two custom projects of SB RAS (as a co-executor), 4 state contracts under the Federal Program "Research and development on priority directions of scientific-technological complex of Russia in the years 2007 - 2012" (unique stands and installations and share-use centers); 19 government contracts under the Federal Program "Research and educational personnel of the innovation Russia" for the years 2009 - 2013 and over 50 RFBR projects.

Every year the Institute members present about 300 reports at Russian and international conferences, publish about 300 articles in leading Russian and foreign scientific journals, and issue monographs and training aids. According to materials published in the review "Bibliometric indicators of the Russian Science and Russian Academy of Sciences" (*Herald of the Russian Academy of Sciences*, June 2009, Volume 79, № 6), the number of references to works by BINP members in 1997-2007 accounted in the reputable international database ESI is 28 267. According to the survey, this value is the highest result among all the institutions of the Russian Academy of Sciences. 4 members of the Institute have got the special award of Elsevier Publishing as the most cited authors in the natural sciences in the area of the former USSR.

### **The BINP Scientific Council found the following works to be the best in 2010:**

#### **In the field of physics of elementary particles and fundamental interactions:**

1. The fundamental parameters of the family of  $\psi$ -mesons – the masses and leptonic widths – were measured with the world's best accuracy in the experiment with the KEDR detector on VEPP-4M.
2. The meson-photon transition form factors for pseudoscalar mesons  $\pi^0$ ,  $\eta$ ,  $\eta'$  and  $\eta_c$  were measured with the world's best accuracy at large squared transfer momenta – from 4 to 40  $\text{GeV}^2$  – in the BABAR experiment (Stanford, USA).
3. The upper limit on the mass of the right intermediate boson in the mirror-symmetry model was found in the experiment with the ATLAS detector on the Large Hadron Collider with the record energy  $2E = 7 \text{ TeV}$ .
4. A new powerful technique of calculating loop integrals, based on the dimensional recurrence relation and analyticity of integrals as functions of the space-time dimension, was formulated and developed.

**In the field of basic nuclear physics:**

5. The difference in the elastic scattering of electrons and positrons on a proton was measured for the first time with high accuracy in the experiment DEUTERON on VEPP-3.

**In the field of plasma physics:**

6. The theoretical model and a set of programs for calculating the nonlinear relaxation of high-power electron beams in a plasma were developed. They describe well the existing experiments and predict high efficiency of collective plasma heating in an open-trap fusion reactor.

7. The collective relaxation of a relativistic electron beam in the plasma of the multimirror trap GOL-3 was shown to occur with high efficiency even at a strong longitudinal plasma inhomogeneity: the beam passes up to 55% of its energy to the plasma.

**In the field of physics and technology of particle accelerators, synchrotron radiation and FEL sources:**

8. In experiments with colliding beams of heavy ions on the Large Hadron Collider at record energies, the jet suppression phenomenon was observed directly for the first time. A key element that allowed storing ions of required intensity is the electron cooling system that was designed and developed by BINP and installed on the low-energy ion storage ring LEIR.

9. The high-current injector of the linear induction accelerator was completed and successfully tested. The design parameters of the installation, dramatically surpassing those of all the world's counterparts, were attained.

10. Stable generation of epithermal neutrons was realized on the facility BNCT, equipped with an electrostatic tandem accelerator. The first experiments on irradiation of tumor cells with neutrons were carried out.

11. They on the electron-positron collider VEPP-2000 attained luminosity in the mode of round colliding beams throughout the energy range of the storage ring. The first experiment with the SND and CMD-3 detectors was carried out in the energy range of 1000 - 1900 MeV with an integrated luminosity of 15 inverse picobarns.

12. A unique 119-pole superconducting wiggler with a period of 3 cm was created for the Synchrotron Radiation Center ALBA-CELLS (Spain).

13. The X-ray position detector DIMEX with microsecond time resolution was developed for the study of the dynamics of fast processes and nanostructures with the use of synchrotron radiation.

In 2010, in accordance with the presidential decree No. 678 dated 06.06.2010, Nikolai A. Vinokurov was awarded the State Prize of the Russian Federation in Science and Technology, 2009, for the achievements in the development and creation of the free electron lasers. A team of six members of the Institute, including A.N. Skrinsky, G.N. Kulipanov, V.V. Kubarev, O.A. Shevchenko, M.A. Scheglov and V.M. Petrov, was awarded the State Prize of the Novosibirsk region for their cycle of works "Development and creation of the high-power terahertz free electron laser." According to the results of the 2009 contest, a team of young scientists of the Institute, consisting of A.V. Bogomyagkov, I.B. Nikolaev and K.J. Todyshev, was awarded the RAS medal for young scientists in the field of nuclear physics for their work «Precise measurement of the  $\tau$ -lepton mass». A team of young scientists of the Institute, including E.I. Soldatkina and V.V. Prikhodko, was awarded the award of the Government of the Novosibirsk region in 2010 in the category of «physical and mathematical sciences» for their work «Methods for improving plasma confinement in a thermonuclear neutron source model based on a gas dynamic trap.» Postgraduates K.A. Martin and V.I. Aleinik got grants of the Novosibirsk mayor contest for young scientists and specialists in the sphere of innovation activity in 2010.

Four research teams of the Institute under the guidance of RAS members Skrinsky, Kruglyakov, and Kulipanov and Professor Onuchin have the status of leading scientific schools, which is adjudged by the Council on Grants of the President of the Russian Federation. The same Council distinguished three teams of young scientists of the Institute as young PhDs. Three BINP Dissertation Councils with the right to examine PhD theses continued their work in 2010. A total of 15 meetings were held, at which 15 PhD theses were defended.

Over 50 tours to the BINP facilities were organized for about 1700 pupils, students, and teachers of schools and universities, employees of other organizations and guests of the Institute.

Offsite lectures were given at Novosibirsk schools.



1

ELEMENTARY PARTICLES  
PHYSICS



## 1.1 CMD-3 Detector

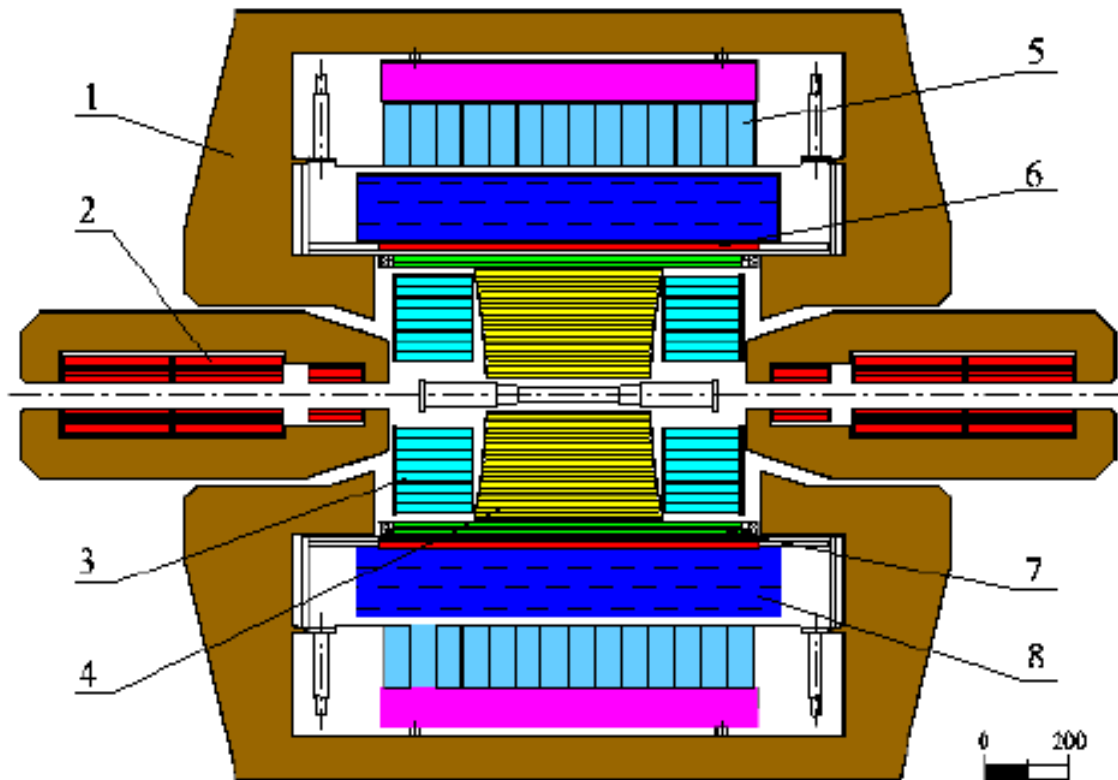


Fig.(1.1)1. CMD-3 detector. 1 – the magnet yoke, 2 – the superconducting solenoids of VEPP-2000, 3 – the crystal-BGO electromagnetic calorimeter; 4 – the drift chamber; 5 – the crystal-CsI electromagnetic calorimeter; 6 – the superconducting solenoid of CMD-3, 7 – the Z-chamber, 8 – the liquid-xenon electromagnetic calorimeter.

A schematic longitudinal section of the CMD-3 detector is shown in Fig.(1.1)1.

Experiments with the CMD-3 detector on the VEPP-2000 collider started in 2010. Events of goes with  $e^+ e^-$  beams were used for measurement of experimental resolutions of the detector systems. The spatial resolution of the drift chamber of the detector in a plane perpendicular to the axis of the beams was about 100 microns; the average particle momentum resolution in events of  $e^+ e^-$  scattering at a beam energy of 850 MeV was found to be  $\sigma_p/p = 5\%$ . The energy resolution of the barrel electromagnetic calorimeter, which includes a crystal-CsI calorimeter and a liquid-xenon calorimeter, was  $\sigma_E/E = 6\%$ .

From March to June 2010, experimental data corresponding to a luminosity integral of  $1.5 \text{ pb}^{-1}$  were recorded in the center-of-mass system at 7 energy points in the range of 1.3-1.9 GeV. Preliminary analysis of data for measurement of cross sections of the processes  $e^+ e^- \rightarrow \pi^+ \pi^-$  and  $e^+ e^- \rightarrow \pi^+ \pi^- \pi^+ \pi^-$  was performed; the results of the analysis for  $e^+ e^- \rightarrow \pi^+ \pi^- \pi^+ \pi^-$  are shown in Fig. (1.1) 2. It can be seen that even the small number of events recorded in the early experiments was sufficient to significantly improve the accuracy of the measurement of cross section of production of four charged pions at energy above 1.4 GeV in the center-of-mass system.

During the summer of 2010 the staff of the laboratory was actively working on finalizing the T2Q and ADIS boards to adapt them to the physical requirements of the charged and neutral triggers of the detector. Reading signals from sectors of the Z-camera was switched from T2A boards of the KLYUKVA standard to T2Q boards. To switch the reading of signals from the strips of the liquid-xenon calorimeter and cathode strips of the Z-camera to the new electronics, the members of the laboratory are developing the AWF-32 board. It is necessary to make 100 such boards, which can be done by the fall of 2011. In December 2010, a physical go into the energy of the  $\phi$  (1020) resonance was carried out with the CMD-3 detector. The experimental data obtained correspond to a luminosity integral of  $0.67 \text{ pb}^{-1}$  in the resonance scanning mode.

In the peak of the  $\phi(1020)$  resonance, the integrated luminosity was  $0.46 \text{ pb}^{-1}$ . The energy dependences of the cross sections of the processes  $\phi \rightarrow K^+ K^-$  and  $\phi \rightarrow K_L^0 K_S^0$  were investigated. The VEPP-2000 collider energy was calibrated by the measurements of the  $\phi(1020)$  mass in this study.

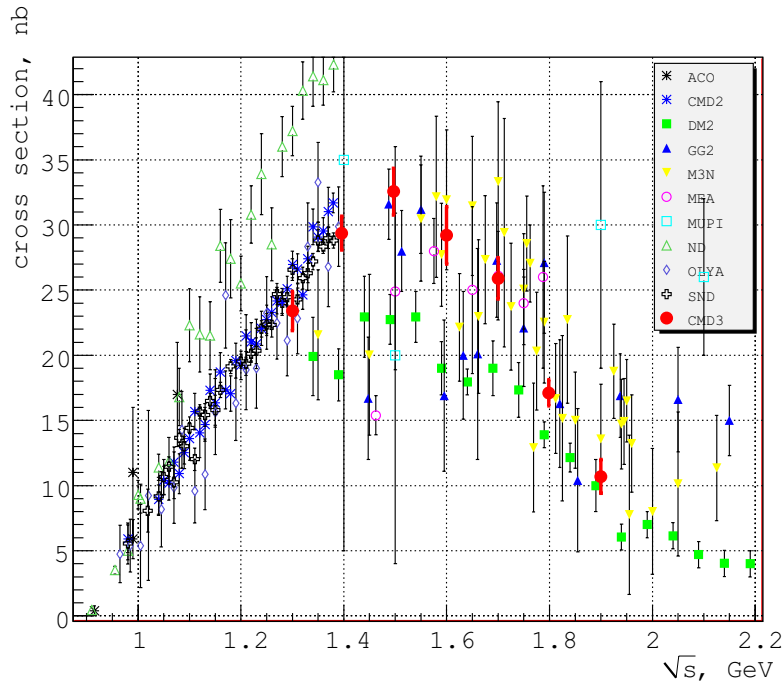


Fig.(1.1)2. Energy dependence of the cross section of production of four charged pions, obtained with the CMD-3 detector on the VEPP-2000 collider, in comparison with results of other experiments.

Besides, processing of the data obtained with the CMD-2 detector on the VEPP-2M collider continued in 2010. Basing on joint analysis of the four main channels of the  $\phi(1020)$  meson decay, the electron width of this resonance was measured. The following value was obtained:  $\Gamma_{ee} = 1.235 \pm 0.006 \pm 0.022 \text{ keV}$ . This measurement is consistent with the results of previous experiments, and its accuracy is comparable with the world's average value.

## 1.2 The SND detector

### 1.2.1 SND upgrade and results of the first experiments at VEPP-2000

During the experiments at the VEPP-2000 collider in February-June and December 2010 the tracking system has shown a stable and satisfactory performance.

In 2010, production has begun of the second exemplar of the SND tracking system with a modified structure of the internal cathode allowing to reduce mutual interferences between the strips. The second exemplar uses a new element base for high-voltage power supply. In March-May the body of the new tracking system was assembled and since October work began to install and tighten the wire structure.

Aerogel Cherenkov counters subsystem, with a aerogel refractive index  $n=1.13$ , was used in experiments since the time of its installation at the SND detector in 2009. In experiments with recorded cosmic rays, data from the Cherenkov counters were used for testing and calibration of various detector subsystems. The collected experimental data has allowed to measure the dependence of the maximum number of photoelectrons and the light collection inhomogeneity of the counters on time. It was found that at the end of the pilot experimental season of 2009-2010 the average amplitude of the counters for electrons was at the level of 4-5 photoelectrons. Such a low level of the signal is caused mainly by the deterioration of the aerogel properties, namely by decrease of the scattering length in it. It was decided to rebuild the sub-

system counters to conduct tests of each element of the counter: aerogel, shifter and photomultiplier tube (PMT with MCP). As a result, properties of the aerogel were almost completely recovered after annealing procedures and the shifter plates have not shown any sign of deterioration of their properties. Two photomultipliers had to be replaced due to degradation of their photocathode quantum efficiency.

At present, the subsystem is fully restored and installed at the SND detector. With renewed subsystem, experiments were conducted and the collected data will allow to get the value of the maximum amplitude of the signal for charged particles in near future. Besides the response of the counter for various types of charged particles will be also investigated experimentally. In particular, the threshold behavior of the amplitude as a function of the momentum for the charged  $\pi$ -mesons and subthreshold probability for the counter to be triggered by charged  $K$ -mesons were measured.

In 2010, the calibration of the SND calorimeter was performed by using the events of the process  $e^+e^- \rightarrow e^+e^-$  collected during the scanning of the center-of-mass energy interval from 1 to 2 GeV. The obtained energy resolution is consistent with the one in experiments performed in 1995-2000. New front-end electronics plates were developed for the calorimeter and their production was launched. Four plates of the new modification have been installed on the calorimeter first layer and regularly worked for the past six months.

In 2010, the development of the SND detector data acquisition system (DAS) software was continued. In particular, the following tasks were performed:

- item support of DAS during the experiments in the course of 2010, support of DAS users, solution of problems in case of failures in electronics and computer network subsystems;
- item development of the operator's interface;
- item the number of active windows was increased;
- item interfaces of the launching and operational managements of the run were refined, as well as interfaces which control the DAS processes, display the current values of scalers and information from the VEPP collider, allow viewing of the raw events;
- item preservation of parameters of VEPP and the detector into the database was organized, work was started on visualization, a prototype code was developed to show the history of the signal changes in the last 12 hours;
- item reading of the new digitizer plates for the signals from the proportional chamber was implemented;
- item processes of the slow control of the electronics and control of the detector state based on the recorded events were integrated in DAS;
- item computer farms, performing tasks of the tertiary trigger, were reformatted by using the virtual machines (XEN technology based approach).

The following tasks were performed in the realm of "offline" software:

- item the software development process organization was modified (transition to subversion, TRAC, wiki);
- item cluster-finding algorithm was refined for strips;
- item simulation of the strips in the proportional chamber was realized;
- item merging of the strip clusters and tracks in the drift chamber in an object "particle" was implemented;
- item an algorithm which takes into account a possible displacement of phase in the drift chamber reconstruction was realized;
- item profiling of the simulation and reconstruction jobs, and their optimization were carried out;
- item a set of control algorithms was enlarged for processes of the detector control by using recorded events;
- item a set of adapted primary generators for simulation was significantly enlarged;
- item a lot of errors were corrected in already implemented software modules.

In 2010, an experiment was conducted with the upgraded SND detector at the new electron-positron collider VEPP-2000 in the energy range  $2E=1.0\div 1.9$  GeV. Integrated luminosity was about 6 inverse picobarns that is comparable to the luminosity recorded at the previous  $e^+e^-$  colliders. Recorded data is currently being processed. Using the new data to calibrate the collider energy, excitation curve of the  $\phi$  meson in channels  $\phi \rightarrow 3\pi$ ,  $K_S K_L$  was measured.

Experimental data at the energy  $2E = 1900$  MeV (above the threshold of the nucleon pairs production) were used to obtain preliminary results for the nucleon-antinucleon pairs production cross section and to estimate the background. The results are shown in Fig.(1.2)1 and Fig.(1.2)2. For the process  $e^+e^- \rightarrow p\bar{p}$  the obtained cross section is fairly reasonable  $\sigma(e^+e^- \rightarrow p\bar{p}) = (0.8 \pm 0.2)$  nb. While for the process  $e^+e^- \rightarrow n\bar{n}$  the background was too high and work continues at present to reach its suppression.

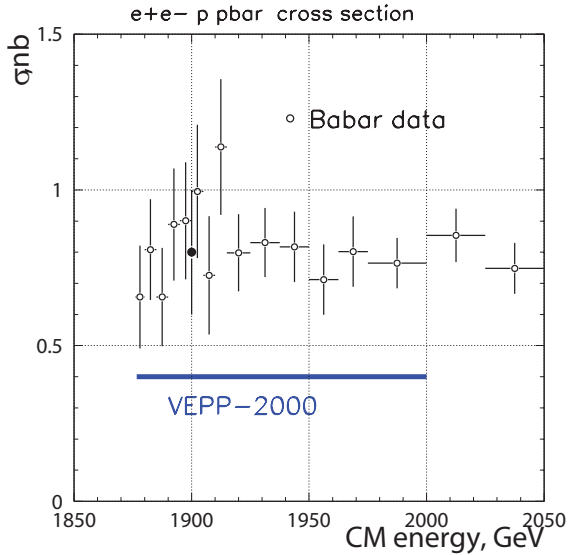


Fig.(1.2)1 Cross section of the  $e^+e^- \rightarrow p\bar{p}$  process. the black dot shows the preliminary result of the SND measurement using a part of the accumulated experimental data. For comparison, results of the previous measurements of BaBar is also shown.

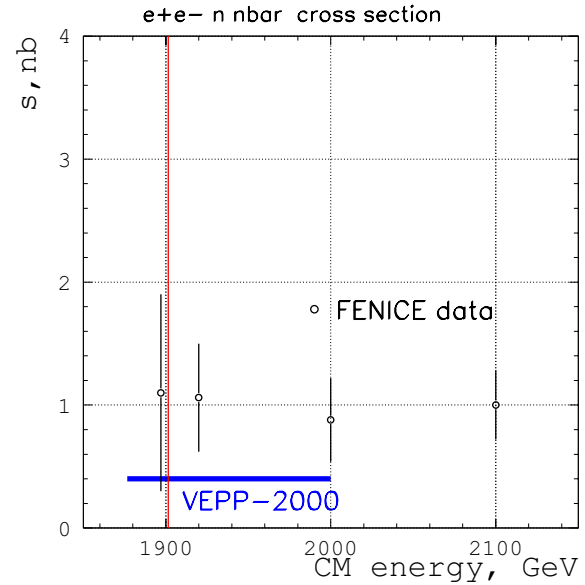


Fig.(1.2)2 Cross section of the  $e^+e^- \rightarrow n\bar{n}$  process. Vertical stripe specifies the region for which the SND experimental data is currently under processing.

In 2010, work was invested in the design and development of a energy calibration system for VEPP-2000 based on the Compton backscattering method. CO-laser was purchased and launched. Vacuum chamber was manufactured, with high-vacuum window made of ZnSe, for insertion of the laser radiation into the collider vacuum chamber.

### 1.2.2 VEPP-2M data analysis

Analysis was continued of the data of experiments conducted with the SND detector at VEPP-2M in the period from 1995 to 2000. In 2010, the SND team obtained the following main results in the elementary particle physics:

The cross section of the process  $e^+e^- \rightarrow \eta\pi^+\pi^-$  was measured in the channel  $\eta \rightarrow 2\gamma$  in the energy range  $2E = 1.0 \pm 1.4$  GeV. The used integrated luminosity was  $9.05 \text{ pb}^{-1}$  accumulated at the collider VEPP-2M. The results obtained (Fig.(1.2)3) does not contradict the previous data from BaBar and CMD-2 and have higher statistical accuracy. Our data confirm the vector dominance model and will be used to refine this and other models.

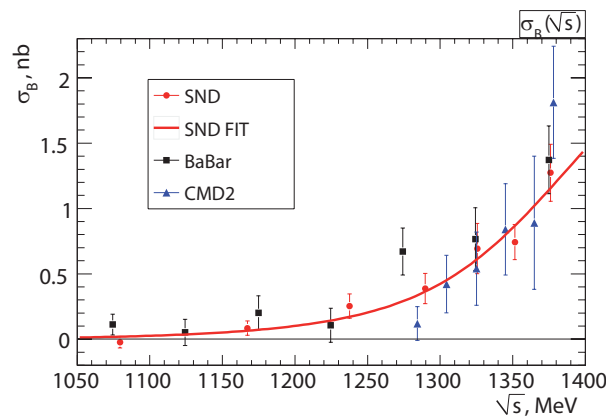


Fig.(1.2)3 Cross section of the process  $e^+e^- \rightarrow \eta\pi^+\pi$  depending on the energy measured by SND and the approximating curve. For comparison, results of previous BaBar and CMD-2 measurements are also shown.

Search of the lepton number violation process  $e^+e^- \rightarrow e\mu$  was undertaken in the experiment with SND detector in the energy range of about 1 GeV. A model independent upper limits, at the 90 % confidence level, were obtained for the  $e^+e^- \rightarrow e\mu$  process cross section:  $\sigma_{e\mu} < 0.6$  nb, as well as for the corresponding decay  $\phi \rightarrow e\mu$ :  $B(\phi \rightarrow e\mu) < 2 \cdot 10^{-6}$ . In this energy region, these limits were obtained for the first time and they can be used, together with the similar limits for the  $J/\psi$ -meson, to constrain a hypothetical  $e \rightarrow \mu$  transition.

An article was published devoted to the search of the process  $e^+e^- \rightarrow K^+K^-\pi^0$  in the energy range from 1.2 to 1.38 GeV. The following upper limits were obtained on the cross sections  $\sigma(e^+e^- \rightarrow \phi\pi \rightarrow K^+K^-\pi^0) < 0.023$  nb and  $\sigma(e^+e^- \rightarrow KK^*(982) \rightarrow K^+K^-\pi^0) < 0.059$  nb at the 95 % confidence level.

Analysis is finished for the following processes:  $e^+e^- \rightarrow e^+e^-\gamma\gamma$ ,  $e^+e^- \rightarrow K^\pm K_{S\pi}^\pm (K_S \rightarrow \pi^+\pi)$ ,  $e^+e^- \rightarrow e^+e^-\gamma\gamma$  and the corresponding articles are being prepared for publication.

Work is continued on the analysis of the following processes:

$e^+e^- \rightarrow \pi^0\gamma$ ,  $e^+e^- \rightarrow \pi^+\pi(2E > 1 \text{ GeV})$ ,  $e^+e^- \rightarrow \pi^+\pi\pi^+\pi$ ,  $e^+e^- \rightarrow \pi^+\pi\gamma$ .

### 1.2.3 Participation in international projects

In 2010, the Beijing  $c$ - $\tau$  factory (BEPC-II) energy measurement system was launched. It is based on the Compton backscattering method. A systematic uncertainty in the beam energy determination turned out to be about 50 keV. This number was obtained by comparing the measured mass of the  $\phi'$  resonance, obtained by using the Compton backscattering system, with the PDG value of the mass.

In the work participated:

G.N. Abramov, E.G. Avdeeva, P.M. Astigeevich, M.N. Achasov, V.M. Aulchenko, A.Yu. Barnyakov, K.I. Beloborodov, A.V. Berdyugin, V.E. Blinov, A.G. Bogdanchikov, A.A. Botov, D.A. Bukin, A.V. Vasiljev, V.M. Vesenev, V.B. Golubev, T.V. Dimova, V.P. Druzhinin, L.V. Kardapoltsev, D.P. Kovrizhin, A.A. Korol, S.V. Koshuba, E.A. Kravchenko, A.Yu. Kulpin, K.A. Martin, A.E. Obrazovskiy, A.P. Onuchin, V.M. Popov, E.V. Pakhtusova, S.I. Serednyakov, Z.K. Silagadze, A.A. Sirotkin, K.Yu. Skovpen, A.N. Skrinsky, I.K. Surin, A.I. Tekutev, Yu.A. Tikhonov, Yu.V. Usov, P.V. Filatov, A.G. Kharlamov, Yu.M. Shatunov, D.A. Shtol, A.N. Shukaev.

## 1.3 Detector KEDR

The KEDR detector is an universal magnetic detector working on the  $e^+e^-$  collider VEPP-4M in the energy region from 2 to 11 GeV in the center of mass system.

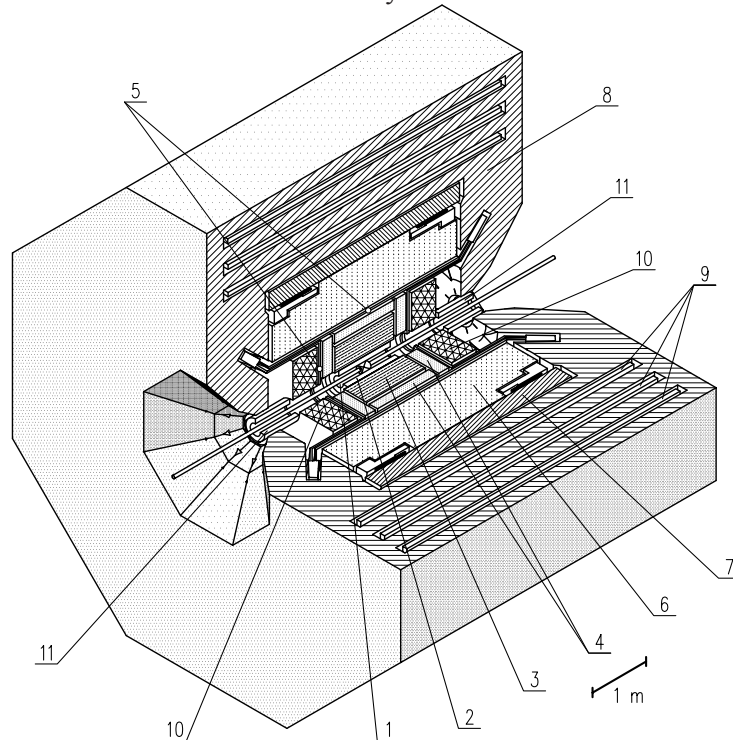


Fig.(1.3)1. The KEDR detector. 1 - vacuum chamber of the collider, 2 - vertex detector, 3 - drift chamber, 4 - aerogel Cherenkov counters, 5 - time of flight counters, 6 - liquid krypton barrel electromagnetic calorimeter, 7 - superconducting solenoid, 8 - magnet yoke, 9 - muon chambers, 10 - end cap electromagnetic calorimeter based on CsI crystals, 11 - compensating solenoid.

The main systems of the KEDR detector are shown in Fig.(1.3)1. Besides this, the detector includes the system of detection of the scattered electrons for study of the  $\gamma\gamma$  physics, and the luminosity monitor. Parameters of the detector are similar to those of the best detectors, operating in the world in this energy region; in detail, the detector is described elsewhere.

An unique feature of experiments with the KEDR detector is a possibility of the precise beam energy determination. Two methods are used for this: the resonant depolarization method and the Compton back-scattering method. Determination of the beams energy with high precision plays important role for receiving meaningful physical results from the detector.

The most important results of works of 2010 on the modernization and improvement of the detector systems operation are described below.

### GEM-detectors are included in the electron tagging system

In 2010 an upgrade of the electron tagging system (TS) was performed: the two-coordinate triple-GEM (Gas Electron Multiplier) detectors were placed in front of each module. Usage of the GEM detectors allows to improve resolution in the radial coordinate and, consequently, in the energy of scattered electrons measured in the TS. This also, due to measurement of the vertical coordinate, helps to suppress the background from the single bremsstrahlung.

The design and dimensions of the two-layer plate with strip structure of the GEM detector is shown in Fig.(1.3)2. The line string in the center of the picture shows change of the slope of strips of the lower layer (from  $30^\circ$  at the center up to  $11^\circ$  at the edge).

The distribution of difference between the measured in the GEM detector coordinate and the calculated one is shown in Fig.(1.3)3. The width of the distribution is  $89 \mu\text{m}$ , corresponding to the resolution of one chamber  $\sigma_{det} \simeq \sigma_{meas} / \sqrt{3/2} \simeq 73 \mu\text{m}$  in direction transverse to strips of the upper layer.

The detector efficiency attains the 98% plateau at the gas amplification  $2.5 \cdot 10^4$ . One should note, that during the 2009-2010 season the GEM-TS detectors worked at the gas amplification in the range  $(3-6) \cdot 10^4$  without breakdowns and other visible problems due to the high voltage. Budker INP is one of three places in the world (with the CERN and the BNL), where these new devices are used.

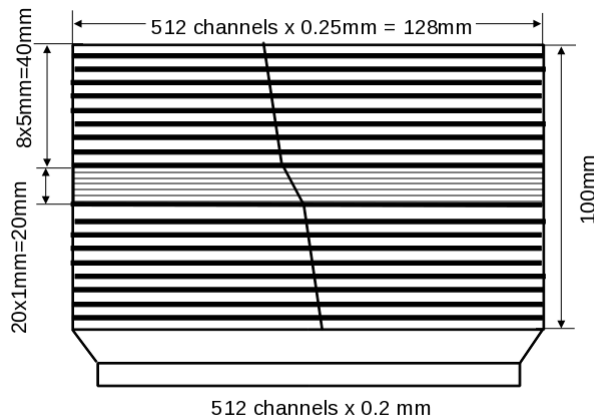


Fig.(1.3)2. Design and dimensions of the read-out plate of the GEM detector with varying inclination of the lower layer strips.

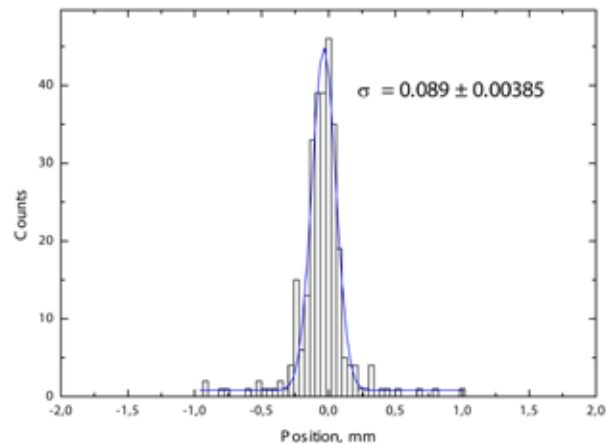


Fig.(1.3)3. Distribution of the difference between the measured and calculated coordinate from the GEM detector. Space resolution  $\sigma_{det} \simeq 73 \mu\text{m}$ .

### Laser calibration system of the TS started operation

The laser calibration of the TS uses two lasers with different wave lengths, which by turns give some light to beam. The spectrum of electrons scattered due to the Compton effect has a sharp edge, unambiguously connected with the initial photon frequency (accuracy  $10^{-6}$ ) and with the accelerator energy (accuracy  $5 \cdot 10^{-5}$ ). Measurement of the coordinate of the spectrum edge allows to perform the TS calibration with accuracy better than  $\Delta E/E < 10^{-4}$  ( $E$  and  $\Delta E$  are the scattered electron energy and its error). Now the optical system is tuned for operation with one laser. The systematic errors due to the orbit instabilities are under study. For inclusion of the second laser additional optical elements are necessary, which are in production.

### The consumption of liquid helium in the cryogenic system of the detector is reduced in two times

In the season of 2010-2011 considerable lower consumption of the liquid helium in the cryogenic system of the superconducting magnets provision of the KEDR detector was reached: from 700-900 to 360-500 liters per twenty-four hours. For the gas-expansion piston of the helium refrigerator a pistol pair with diminished (on  $4 \mu\text{m}$ ) slot clearance was produced. As a result the leakage of cold helium from the working area was diminished considerably and by this the efficiency of work was improved noticeably.

## 1.4 Results of work of the KEDR detector at the VEPP-4M collider in 2010

In the season 2010 the KEDR detector continued the experiment at the VEPP-4M collider, processing of the statistics collected earlier and the new one. The most important results are the following.

- Collection of statistics: in 2010 the luminosity integral  $2.1 \text{ pb}^{-1}$  at the  $\psi(2S)$ -meson and  $0.65 \text{ pb}^{-1}$  in the energy interval  $2E=1850 - 3100 \text{ MeV}$  scanning was written.
- Measurement of parameters of the  $J/\psi$ -meson: the values of the mass and the decay probability  $J/\psi \rightarrow \eta_c \gamma$  were obtained.
- Measurement of parameters of the  $\psi(2S)$ -meson: precision in the value of the mass was improved considerably, preliminary results of the values  $\Gamma_{ee} \times Br(\psi(2S) \rightarrow \text{hadrons})$ ,  $\Gamma_{ee} \times Br(\psi(2S) \rightarrow e^+e^-)$ ,  $\Gamma_{ee} \times Br(\psi(2S) \rightarrow \mu^+\mu^-)$  и  $\Gamma_{ee} \times Br(\psi(2S) \rightarrow \tau^+\tau^-)$  were obtained.

- Measurement of parameters of the  $\psi(3770)$ -meson: the form of resonance excitation curve was done more precise, the mass and the width were obtained.
- Measurement of the  $\tau$ -lepton mass: the work on the mass estimation using full statistics is being carried out.
- Search for narrow resonances: in the energy region  $2E=1850-3100$  MeV the limit on the product of electron width of narrow resonance to probability of its decay to hadrons was lowered.

Description of these works in some detail follows below.

### 1.4.1 Measurement of parameters of $J/\psi$ -meson

In 2010 the processing of the experimental statistics collected for study of the  $J/\psi$ -meson properties was continued. New results are presented here.

#### Measurement of the $J/\psi$ mass

On statistics of 2003 and 2005 a new value of the  $J/\psi$ -meson mass with the best in the world accuracy was obtained:

$$M_{J/\psi} = 3096.913 \pm 0.006 \pm 0.009 \text{ MeV (KEDR)}.$$

The accuracy of the  $M_{J/\psi}$  was improved in comparison with our measurement (published in 2003), which determines average value of the  $J/\psi$ -meson mass in the tables of elementary particles of the Particle Data Group (PDG). Measurement of the  $J/\psi$ -meson mass in different experiments and the average value of the mass from the PDG tables of 2010 (vertical band of 2 standard errors width) are shown in Fig.(1.4)1.

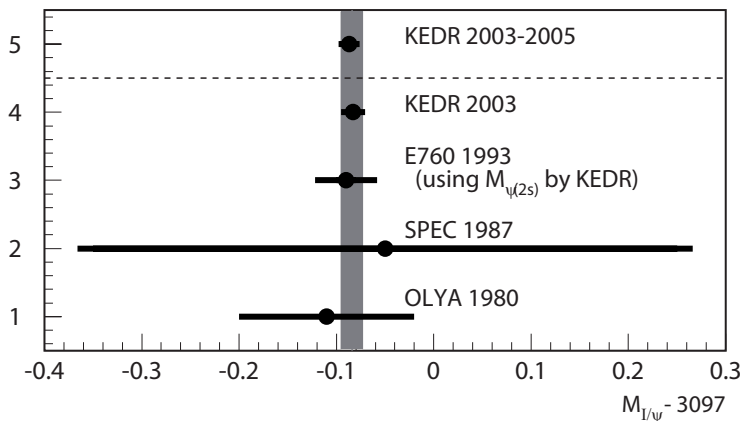


Fig.(1.4)1. Mass of the  $J/\psi$ -meson in different experiments and its average value (shown with the vertical band).

#### Radiative decay $J/\psi \rightarrow \eta_c \gamma$

Interest to measurement of the branching ratio  $J/\psi \rightarrow \eta_c \gamma$  is due to the fact, that during long time there was only one measurement of this probability done by the Crystal Ball group, and the result differed noticeably from the theoretical calculations. Only recently, in 2009, a new measurement of this branching by the CLEO was published. Circles in Fig.(1.4)2 represent experimental results (CLEO 09 and CBAL 86), which PDG uses for determination of the average value ( $Br(J/\psi \rightarrow \eta_c \gamma) = (1.7 \pm 0.4)\%$ ), and the result of measurement of this value by the KEDR detector (in 2010):

$$Br(J/\psi \rightarrow \eta_c \gamma) = (2.59 \pm 0.16 \pm 0.31)\% \text{ (KEDR)}.$$

The theory calculations (squares) are shown also. Average decay probability from the PDG-2010 is shown in Figure (1.4).2 with vertical band. Our result agrees with the CLEO result and is close to the theory predictions.

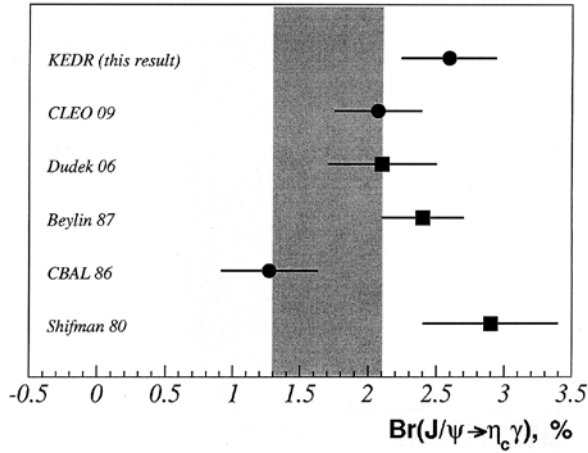


Fig.(1.4) 2. Value of the  $Br(J/\psi \rightarrow \eta_c \gamma)$  in different experiments and its average value (shown with the vertical band), as well as the theory predictions (squares).

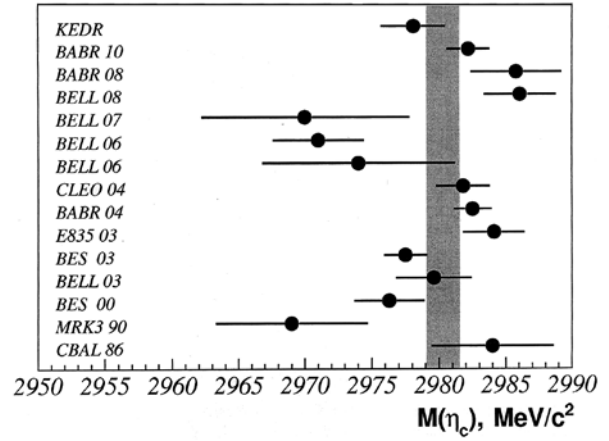


Fig.(1.4) 3. Value of the  $\eta_c$ -meson mass in different experiments and its average value (shown with the vertical band).

In this experiment the mass of the  $\eta_c$ -meson was measured also:

$$M_{\eta_c} = 2978.1 \pm 1.4 \pm 2.0 \text{ MeV (KEDR).}$$

Our measurement is close in accuracy to the best measurements of the  $\eta_c$ -meson mass (Fig.(1.4)3) and agrees within one standard error with the average value of this mass in the tables PDG-2010 ( $M_{\eta_c} = 2980.3 \pm 1.2 \text{ MeV}$ ).

### Measurement of the $J/\psi$ lepton widths

In assumption of the lepton universality, the value

$$\Gamma_{ee} \times Br(J/\psi \rightarrow l^+ l^-) = 0.3320 \pm 0.0041 \pm 0.0050 \text{ keV (KEDR)}$$

was obtained (2010). Using the independent value  $Br(J/\psi \rightarrow e^+ e^-) = (5.94 \pm 0.06)\%$  (PDG-2008), one obtains result for the lepton width:

$$\Gamma_{ll} = 5.59 \pm 0.12 \text{ keV (KEDR),}$$

which has a better accuracy, than the table average (PDG-2008)  $\Gamma_{ee} = 5.55 \pm 0.14 \pm 0.02 \text{ keV}$ .

The full width equals

$$\Gamma = 94.1 \pm 2.7 \text{ keV (KEDR).}$$

This value agrees with the average value  $\Gamma = 93.2 \pm 2.2 \text{ keV (PDG-2008)}$ .

## 1.4.2 Measurement of the $\psi(2S)$ -meson parameters

In 2010 processing of the statistics, collected for research of the  $\psi(2S)$ -meson properties, was continued. New results are submitted here.

### Measurement of the mass

In 2010 an accuracy of the mass measurement of the  $\psi(2S)$ -meson has been greatly improved in comparison with the result, published in 2003 (based on the scan of 2002). The new value is obtained as the average of the scans of 2002, 2004, and 2006, systematic errors have been made more accurate as well. The new value of the mass is equal to

$$M_{\psi(2S)} = 3686.123 \pm 0.008 \pm 0.012 \text{ MeV (KEDR).}$$

This value is within one standard error consistent with the table value  $M_{\psi(2S)} = 3686.093 \pm 0.034$  (PDG-2010) and has two times better accuracy.

Data of different measurements are shown in Fig.(1.4)4.

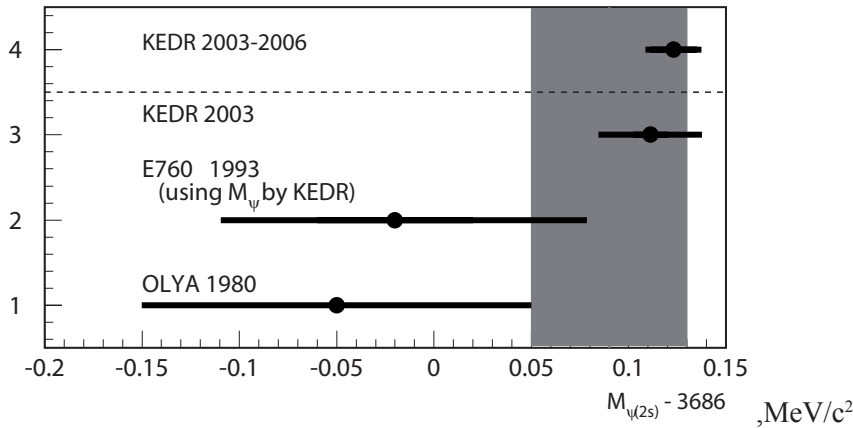


Fig.(1.4)4. The mass of the  $\psi(2S)$  from various experiments. Vertical band is the average value without new result of KEDR.

In 2010, our measurements of the  $J/\psi$  - and  $\psi(2S)$ -meson masses equalized in terms of accuracy, they are on 5th-6th place among the most accurate measured masses of elementary particles: between  $\pi^\pm$  and  $\pi^0$ .

#### Measurement of $\Gamma_{ee} \times Br(\psi(2S) \rightarrow hadrons)$

In 2010, the data analysis was performed to measure the value of  $\Gamma_{ee} \times Br(\psi(2S) \rightarrow hadrons)$ . The following result was obtained

$$\Gamma_{ee} \times Br(\psi(2S) \rightarrow hadrons) = 2.27 \pm 0.02 \pm 0.04 \text{ keV (KEDR).}$$

This result is in a good agreement with the value in the PDG tables of 2010:  $2.30 \pm 0.04$  keV.

#### Measurement of the lepton widths

In 2010 processing of data sample of  $4.9 \text{ pb}^{-1}$ , recorded at the  $\psi(2S)$  resonance and in the continuum, was done with the aim of direct measurement of values  $\Gamma_{ee} \times Br(\psi(2S) \rightarrow l^+l^-)$ . The following preliminary results were obtained:

$$\Gamma_{ee} \times B_{ee} = 21.7 \pm 0.7 \pm 1.6 \text{ eV}, \quad \Gamma_{ee} \times B_{\mu\mu} = 22.2 \pm 0.9 \pm 1.1 \text{ eV (KEDR).}$$

Measurement of these quantities for the  $\psi(2S)$  has been done for the first time in the world, therefore they are absent in the PDG tables. Our measurement agrees with the value  $19 \pm 2$  eV, which can be obtained as the product of values  $\Gamma_{ee}$  and  $Br(\psi(2S) \rightarrow l^+l^-)$  from the PDG tables. (Note that the table values  $B_{\mu\mu}$ ,  $B_{ee}$  and  $\Gamma_{ee}$  were obtained as a result of joint fitting the results of many experiments on the measurement of the  $\psi(2S)$  parameters). We have plans to improve accuracy of our measurements by the inclusion in the processing the statistics, collected on the  $\psi(2S)$  in 2010 (full luminosity integral equals  $6 \text{ pb}^{-1}$ ).

Data of the KEDR detector allow to calculate the value  $\Gamma_{ee}$ . Using the above results for the  $\Gamma_{ee} \times Br(\psi(2S) \rightarrow hadrons)$  and the independent value  $Br(\psi(2S) \rightarrow hadrons) = (97.85 \pm 0.13) \%$  (PDG-2010), we obtain the following value of the electron width  $\Gamma_{ee}$  for the  $\psi(2S)$  meson:

$$\Gamma_{ee} = 2.320 \pm 0.045 \text{ keV (KEDR).}$$

This value differs from the table value ( $\Gamma_{ee} = 2.350 \pm 0.040$  keV) less than by 1 sigma and has comparable accuracy.

During the data processing for the tau-lepton mass measurement (see below) simultaneously the value  $\Gamma_{ee} \times Br(\psi(2S) \rightarrow \tau^+\tau^-)$  was obtained. The preliminary value is equal to

$$\Gamma_{ee} \times Br(\psi(2S) \rightarrow \tau^+\tau^-) = 9.0 \pm 2.6 \text{ eV (KEDR).}$$

It is in agreement with the table value equal to  $7.2 \pm 0.8$  eV (PDG-2010).

### 1.4.3 Measurement of the $\psi(3770)$ -meson parameters

In 2010 new results in processing of the experiment on measurement of the  $\psi(3770)$ -meson parameters were obtained. For processing we used statistics of  $2.7 \text{ pb}^{-1}$ , collected in three scans of the  $\psi(2S)$ - $\psi(3770)$  region in 2004-2006. Data were fitted with the non-relativistic p-wave Breit-Wigner distribution with the energy dependent full width. The non-resonant  $D\bar{D}$  pairs production cross section was taken proportional to the sum of cubes of the D-meson momenta. In our analysis parameters of the  $\psi(3770)$ -meson were determined with account of the  $\psi(3770)$ -meson form factor described with the vector dominance model. Interference of the resonance with the non-resonant  $D\bar{D}$ -pairs production was taken into account also.

Visible cross section in the three scans (data have different detection efficiency) depending on the energy in the center of mass in a wide range of  $W = 3650 \div 4000 \text{ MeV}$  is presented in Fig.(1.4)5. Fig.(1.4)6 shows a joint fitting of data near the  $\psi(3770)$  peak and above after subtracting the substrate of the light quarks.

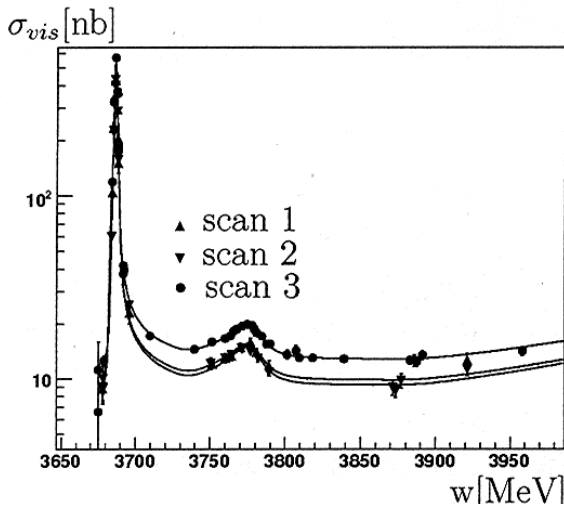


Fig.(1.4)5. Visible cross section in three scans as a function of the center mass energy.

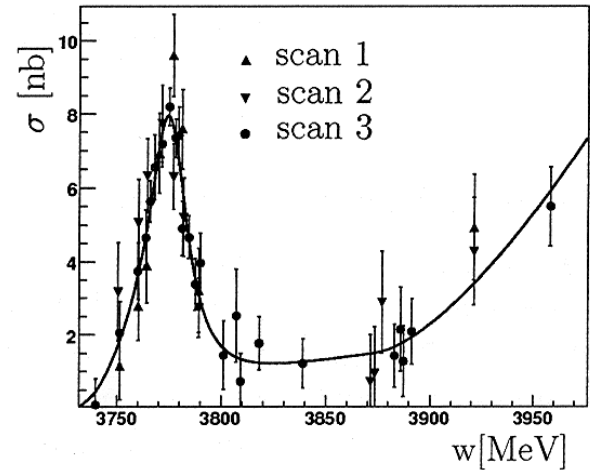


Fig.(1.4)6. Visible cross section in three scans as a function of the center mass energy after subtracting the light quarks substrate.

The following values of the  $\psi(3770)$ -meson mass and full width were obtained:

$$M_{\psi(3770)} = 3778.0_{-1.5}^{+1.6} \text{ MeV (KEDR)},$$

$$\Gamma = 22.4_{-3.4}^{+3.9} \text{ MeV (KEDR)}.$$

They are in agreement with the table data (PDG-2010) for average values of the  $\psi(3770)$ -meson mass and full width:  $M_{\psi(3770)} = 3775.2 \pm 1.7 \text{ MeV}$ ,  $\Gamma = 27.6 \pm 1.0 \text{ MeV}$ .

### 1.4.4 Measurement of the $\tau$ -lepton mass

The lepton universality principle is one of the fundamental principles of the Standard Model. It consists in requirement of equality of weak interaction constants for leptons  $e^\pm$ ,  $\mu^\pm$ ,  $\tau^\pm$ .

In the presence of  $\mu$ - $\tau$  universality we must have

$$\left( \frac{G_\tau}{G_\mu} \right)^2 = \left( \frac{m_\mu}{m_\tau} \right)^5 \left( \frac{t_\mu}{t_\tau} \right) B(\tau \rightarrow e \nu_\tau \bar{\nu}_e) \cdot \frac{F_{cor}(m_\mu, m_e)}{F_{cor}(m_\tau, m_e)} \equiv 1$$

(Since  $Br(\mu \rightarrow e \nu_\mu \bar{\nu}_e) = 1$ ). Using PDG data of 2010, for the experimental value of this ratio one obtains  $1.0029 \pm 0.0045$ , which is different from 1 less than by  $1\sigma$ .

The main contribution to the error yields from uncertainties with which the life time of the  $\tau$ -lepton ( $\pm 0.34\%$ ) and the value  $\text{Br}(\tau \rightarrow e \nu_\tau \bar{\nu}_e)$  ( $\pm 0.28\%$ ) are known. An error in the average value of the  $\tau$ -lepton mass is  $\pm 0.009\%$ , its contribution to the presented above ratio is small now ( $\pm 0.045\%$ ). The value of this error was diminished noticeably, after inclusion in the PDG tables our measurement of the  $m_\tau$  with the best in the world precision (2007). Nevertheless, the measurement of the  $\tau$ -lepton mass with the best possible accuracy remains an interesting task and can be claimed in the future. Such an experiment with participation of physicists from the Budker INP is planned at the  $e^+e^-$ -collider in Beijing. In 2010, we continued analysis of the full recorded statistics ( $15.2 \text{ pb}^{-1}$ ) in order to improve the precision of measuring of the  $\tau$ -lepton mass, to diminish the systematic errors of the measurement. The following value of the mass was obtained

$$m_\tau = (1776.69^{+0.17}_{-0.19} \pm 0.15) \text{ MeV (KEDR)}.$$

We are continuing analysis of the systematic errors, it is possible that this result will be improved.

#### 1.4.5 Search for narrow resonances

In 2010 we continued processing of the experiment on search for narrow resonances in the energy region  $2E=1.85\text{-}3.1 \text{ GeV}$ . Method of measurement and the data analysis are described elsewhere. The upper limit was lowered in comparison with the result of 2009, since in the past year additional statistics was written in the ‘‘problematic’’ points of this energy interval. The integral luminosity, included in the data processing, was  $\int L dt = 300 \text{ nb}^{-1}$ .

Fig.(1.4)7 shows the value of the upper limit on the product of the electron width by the probability of the narrow resonance decay to hadrons in the energy range 1.85 - 3.1 GeV.

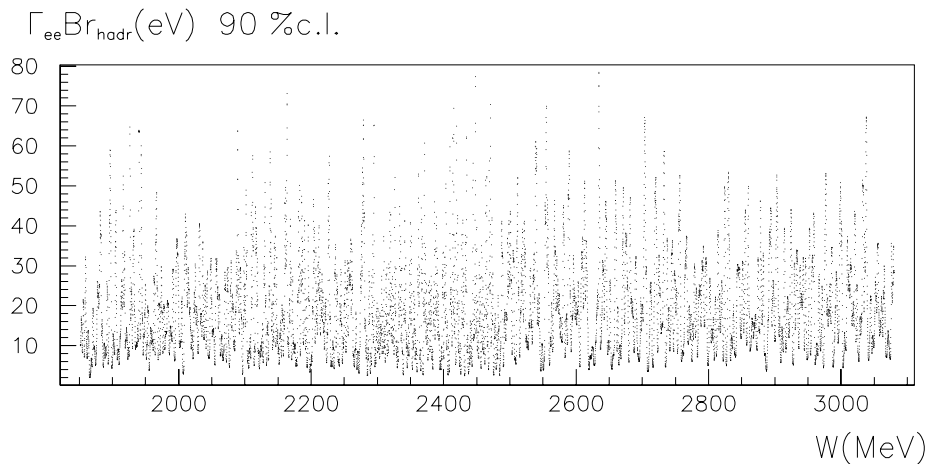


Fig.(1.4)7. Upper limit on the product of the narrow resonance electron width by the probability of its decay to hadrons in the energy range  $2E=1.85 - 3.1 \text{ GeV}$ .

Detection efficiency of the final states has been obtained using the  $J/\psi$ -meson hadronic decays. Accounting of the detection efficiency dependence on the type of final state and the energy in the cms, as well as the uncertainty, with which the beam energy spread in the storage ring is known, increases the limit in 1.5 times. The final value of limit on the value of  $\Gamma_{ee}^R \times \text{Br}(R \rightarrow \text{hadrons})$  in region  $2E = 1.85\text{-}3.1 \text{ GeV}$  is equal to

$$\Gamma_{ee}^R \times \text{Br}(R \rightarrow \text{hadrons}) < 120 \text{ eV, 90\% CL (KEDR)}.$$

In conclusion note that the measurement with the best in the world accuracy of the fundamental parameters of the psi-mesons family: masses and lepton widths was recognized the best work of the Budker INP in 2010 in the field of elementary particles physics and fundamental interactions.

In 2010 results of experiments with the KEDR detector were published in 7 articles, 2 preprints, 3 reports were submitted at the 35-th International conference on high energy physics (July 2010, Paris), 3 reports were submitted at the 4-th International workshop on the charm physics (October 2010, Beijing),

one report was submitted at the XI Workshop on the tau-lepton physics (September 2010, Manchester), one report was submitted at the III-th All-Russian conference on fundamental constants (December 2010, Saint-Peterburg), one PhD dissertation was defended.

This work was supported in part by the RFBR grants 08-02-00142-a, 08-02-00258-B, 08-02-00251-a, 09-02-01035-a, 09-02-01143-B, 10-02-00904-B, 10-02-05033-C, as well as by the Grant of President RF for support of leading scientific schools of the Russian Federation NS-6943.2010.2.

## 1.5 Detectors for HEP

In 2010, the electronics of the detectors KEDR and SND were operating at full scale, providing stable acquisition of statistic data. Breakdowns arising from time to time were eliminated promptly.

A number of issues related to the system of scattered electrons of the KEDR detector were resolved in 2010. The system was completely integrated into the data acquisition system of the detector. Thus, the data acquisition system of the detector acquired significant additional capabilities.

The channel of the fast ADC (Flash ADC) for the electronics of the calorimeter was finalized in 2010. The nomenclature of component elements was determined and their purchase was ordered. Besides, work on the gradual modernization of the inner electronics (preamplifiers and backplanes) of the detector was continued.

Digitizing electronics (about ninety 32-channel boards) for the calorimeters of the CMD-3 detector worked in full scale and demonstrated high reliability.

## 1.6 X-ray detectors

In early 2010, a new one-coordinate detector DIMEX-3 for 512 channels was transferred to users for regular work. It was used in the experimental studies of the dynamics of explosions and measurement of samples on the VEPP-3 SR beam line.

Another two detectors of this modification were made in the second half of 2010. One of them is intended for the VEPP-4 SR beam line, where large-sample experiments on the explosion dynamics will continue.

The case of the OD-4 detector for experiments on SR wide-angle scattering was fabricated in 2010. A multi-stage gas electron multiplier (GEM) is used in OD-4 instead of a wire structure, as, for instance, in ODP-3, which allows, along with a high gas amplification (over 10000), creating a detector in the form of arc with an arbitrary angular aperture. A substantial effort was made on the development of the electronics of the detector.

Two X-ray detectors OD-3M, designed to modernize the OD-3 series in order to increase the reliability and improve performance, were produced in 2010. Earlier, in 2009, two such detectors were made and delivered to the customers (ISSCM SB RAS and Institute of Catalysis SB RAS).

## 1.7 Other works:

In the framework of international projects the sector staff continued active participation in the works connected with the development of new data acquisition system of the BELLE-II detector (KEK, Japan). The prototypes of the new electronics for the barrel part of the calorimeter on CsI(Tl) crystals were fabricated and after correction subjected to tests. In late 2010, enterprises in Korea fabricated and delivered a new shaper in the VME standard to KEK. The shaper was made by the BINP design. At the moment it is being tested.

Among the sector staff there are coauthors of more than 15 publications issued within the framework of the BELLE collaboration (KEK, Japan).

## 1.8 Microstructure gas detectors

The development of detectors based on gas electron multipliers (GEMs) was continued in 2010.

The work was carried out in several directions:

- 1) Cryogenic two-phase avalanche detectors based on thick GEMs (THGEMs).
- 2) Modernization of the system of scattered electrons in the KEDR experiment.
- 3) Low-pressure THGEM-based gas detector.

4) Participation in collaborations: RD51 at CERN (development of the microstructure gas detectors) and TPC for the International Linear Collider.

### 1.8.1 Cryogenic two-phase avalanche THGEM-based detectors

The main objective of the project is to develop methods for detecting neutrinos and dark matter and medical imaging through the development of special detectors based on gas electron multipliers and operating in dense noble gases at cryogenic temperatures in the avalanche amplification mode. Many of the applications mentioned above are based on the unique ability of GEMs to operate with high gain in pure noble gases at cryogenic temperatures, in the gas and two-phase modes. GEM-based cryogenic avalanche detectors can be applied to registration of coherent scattering of neutrinos on nuclei using two-phase Ar and Xe, solar neutrino detection using two-phase or compressed He and Ne, registration of dark matter using two-phase Ar and Xe, and positron emission tomography (PET) using two-phase Xe.

A new upgraded facility with a cryogenic chamber of 9 liters was put into operation in 2010. It was extensively exploited for a year, which resulted in a series of research cycles on it.

a) Characteristics of Geiger multipixel avalanche photodiodes (G-APDs or SiPMs) were investigated at cryogenic temperatures. The amplitude and noise characteristics of G-APDs (Fig. (1.8)1) were improving with decreasing temperature. In particular, at 87 K, the rate of noise was as low as a few Hz on an efficiency plateau, and the maximum gain of G-APDs was 4 times higher than that at room temperature. Fig. (1.8)2 also shows the dependence of the quenching resistance of G-APD pixel on temperature. At 87 K it increases by almost 3 orders of magnitude, which may affect the response speed of the device at cryogenic temperatures.

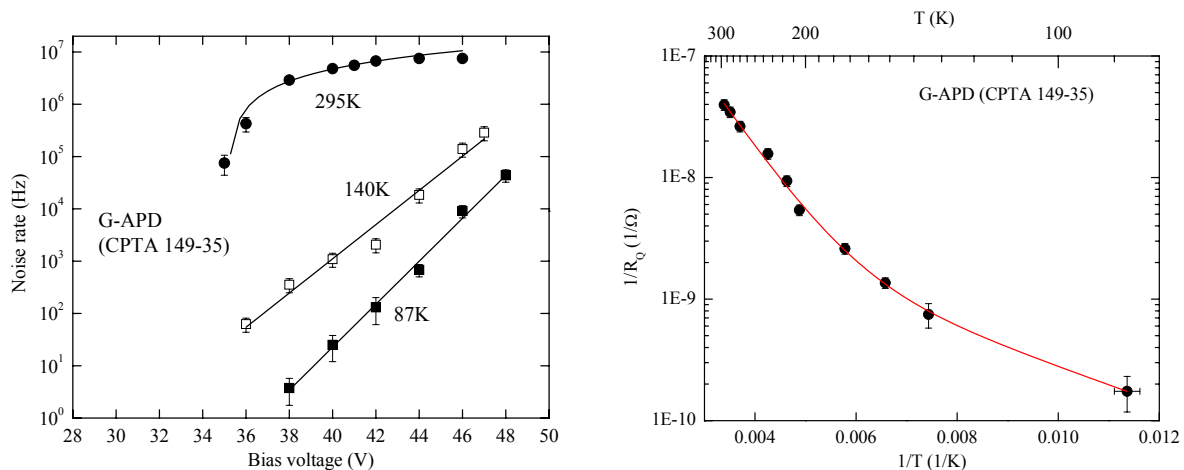


Fig.(1.8)1. Characteristics of the “CPTA 149-35” G-APD at cryogenic temperatures. Left: rate of single-electron noise in dependence on bias voltage. Right: dependence of quenching resistance pixel on temperature.

b) A two-phase THGEM-based avalanche Ar detector with optical readout of signal using G-APD was studied. The new concept of registration of optical readout of signal in two-phase detectors was investigated, with using a G-APD registering photon avalanche scintillations from the THGEM. Effective registration of avalanche scintillations in THGEM orifices in two-phase Ar with G-APD and without re-emitter, i.e. insensitive to VUV radiation of Ar, was demonstrated. This means that scintillations occurred in the near infrared region, where the G-APD is highly sensitive. For instance, Fig.(1.8)2 shows a typical scintillation signal from the G-APD (bipolar and unipolar after filtering), together with the charge signal

from the THGEM. It also shows the correlation between the amplitudes of scintillation and charge signals. The amplitude of scintillation signal was significant: at an avalanche gain of 400, the amplitude was 640 photoelectrons of the G-APD for 60 keV X-ray photons absorbed in liquid Ar. This corresponds to 0.7 photoelectrons per initial electron (before multiplication in THGEM), i.e. the detector is practically capable of working in the mode of primary electron counting. The avalanche scintillation light yield was about 4-5 infrared photons per avalanche electron into complete solid angle, which is comparable with the light yield of argon in the VUV.

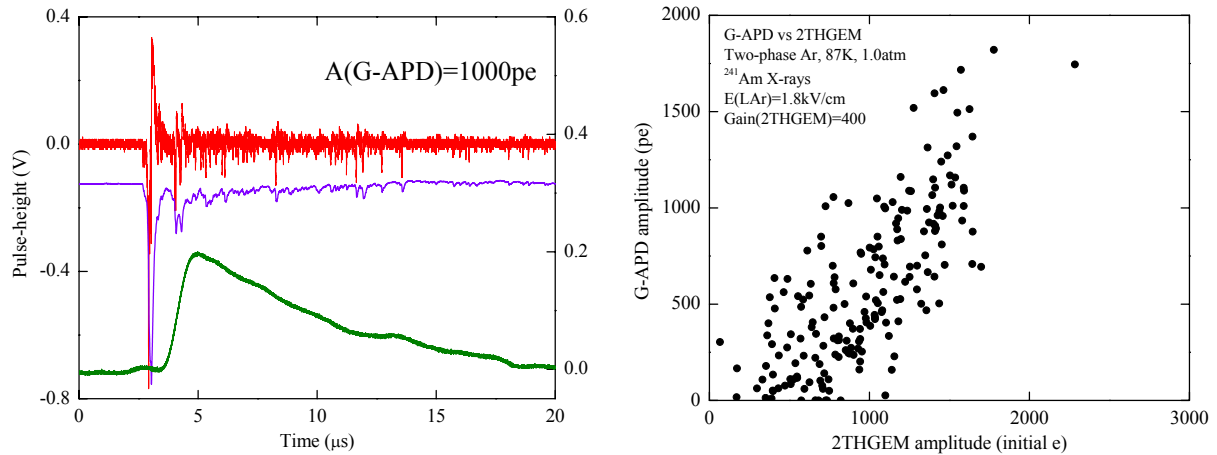


Fig.(1.8)2. Illustration of the Ar operation of the two-phase THGEM-based avalanche detector with optical readout using G-APD at an avalanche gain of 400. Left: a typical scintillation signal (top and middle) and a charge signal (bottom) at a scintillation signal amplitude of 1000 photoelectrons. Right: correlation between the amplitudes of scintillation and charge signals expressed in G-APD photoelectrons and primary (before amplification in the THGEM) electrons.

c) The work of the two-stage THGEM based on the new insulating material (Kapton) in gaseous and two-phase Ar was studied. The samples were prepared in Moscow. The Kapton THGEM operated unstably in two-phase Ar, failing in reaching gains more than a few dozens. Moreover, the Kapton THGEM resistance with a given insulator thickness (240 μm) to breakdowns, even in Ar gas, turned out to be insufficient for operation at cryogenic temperatures with gains up to 10 000: after several minutes of work it burned down completely. It is obvious that we must find a manufacturer of better and thicker Kapton THGEMs.

d) Studies on the measurements of infrared scintillation light yield in gaseous and liquid Ar were begun.

e) Research on the work of two-stage GEM in two-phase and gaseous xenon was begun.

Exploration of cryogenic avalanche detectors will continue in 2011.

## 1.8.2 Modernization of the system of scattered electrons in the KEDR experiment

The system of registration of scattered electrons is an essential part of the KEDR experiment and makes it possible to register electrons scattered from the place of meeting at small angles. These electrons are a characteristic feature of photon-photon interaction, and their registration and precise measurement of momentum is an important physical task.

In order to attain the ultimate resolution in the momentum of scattered electrons, which is determined by parameters of beam in the accelerator, as well as improve the separation of signal and background, we equipped each of the 8 stations of the system with a detector based on a triple GEM with two-coordinate readout. The detectors will allow measuring the coordinate in the orbital plane with a resolution of  $\sim 0.1$  mm. In the direction perpendicular to the plane of the orbit, the spatial resolution will be  $\sim 0.25$  mm within  $\pm 1$  cm from the orbit and  $\sim 1$  mm at a greater distance from the plane of the orbit. To obtain the required parameters we developed a special design of the readout plane with a variable angle of stereo strips. The dimensions of the detector are 125\*100 mm to 250\*100 mm depending on the type of station.

During 2010, the system of GEM-based detectors (GEM SRSE) was completely launched and began continuous operation as part of the KEDR data acquisition system. Since November 2010, the system has been involved in statistics acquisition in the energy range of 3.2 - 3.7 GeV. Fig.(1.8)3 and Fig.(1.8)4 show the coefficient of gas amplification and the efficiency of all the 8 detectors of the system in dependence on the time since the beginning of the season.

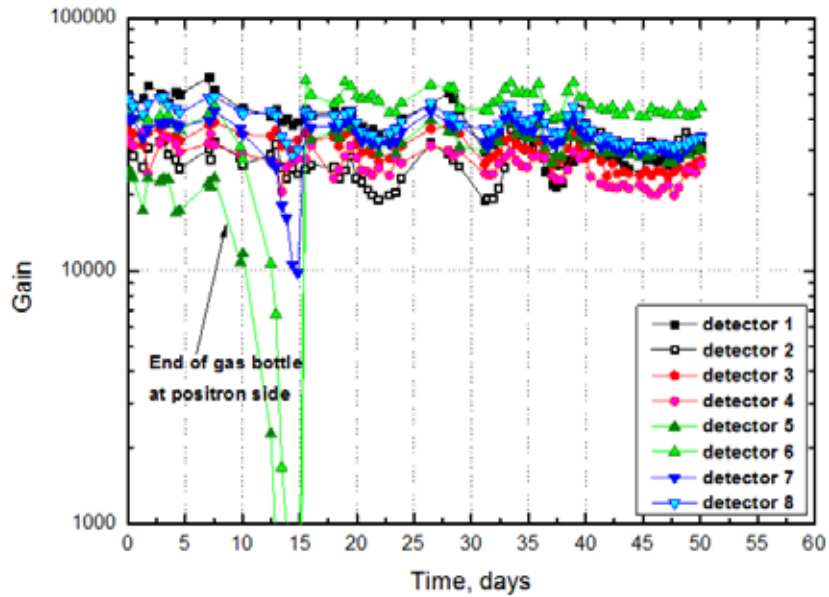


Fig.(1.8)3. Coefficient of gas amplification of the GEM SRSE detectors in dependence on time.

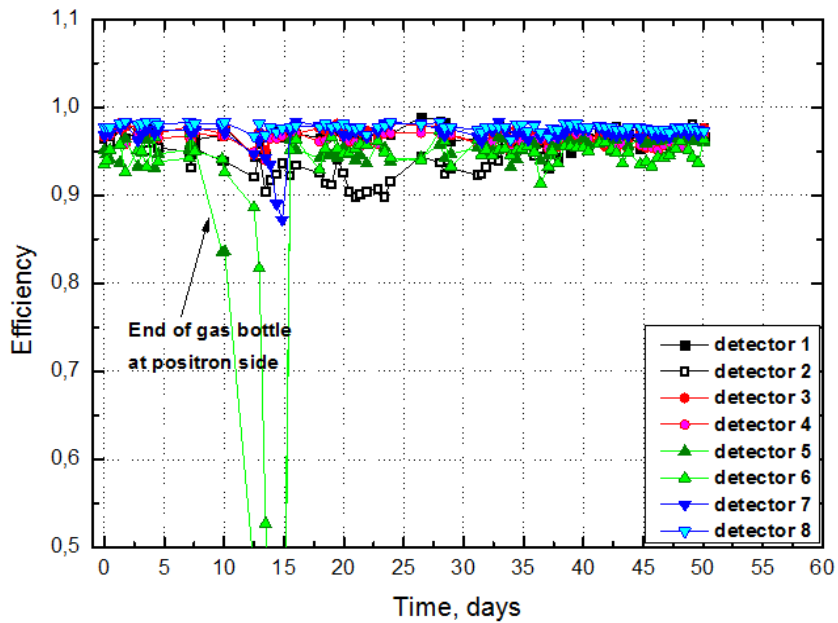


Fig.(1.8)4. Effectiveness of the GEM SRSE detectors in dependence on time.

It can be seen that the detectors operate stably for a long time with a high gain (20000 - 40000) and efficiency of 95-97%. No signs of breakdown and subsequent damage to the structure of the detectors and electronics have been observed.

The first results of the joint operation of GEM SRSE and hodoscopes on drift tubes are shown in Fig. (1.8)5. The figure presents a correlation between the coordinates of the tracks in both systems.

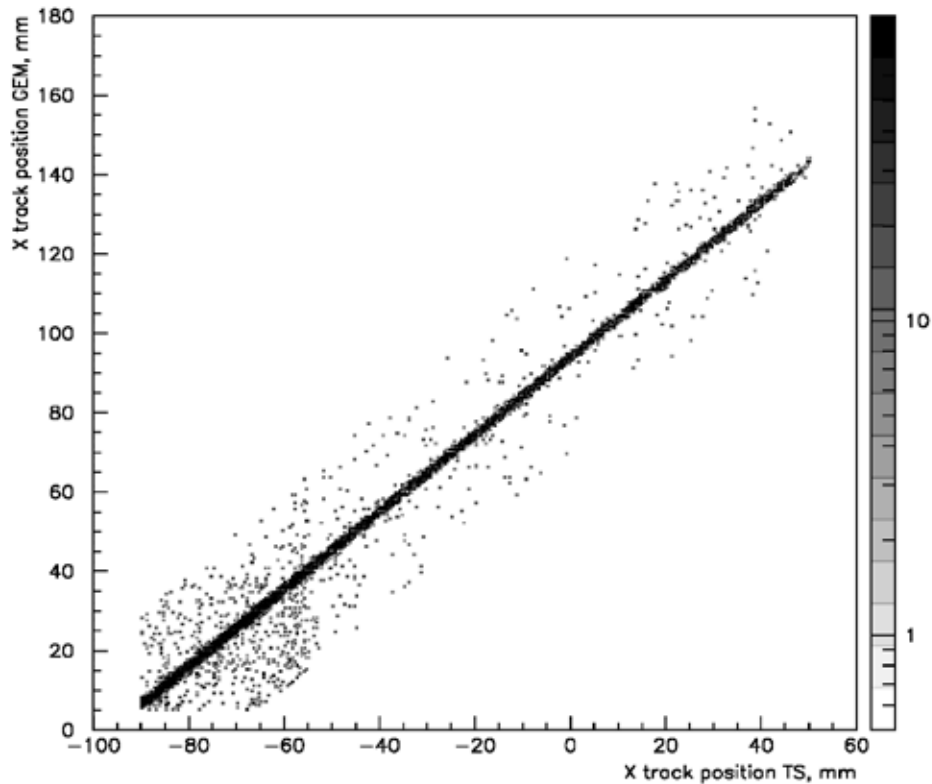


Fig.(1.8)5. Correlation of track coordinates recorded in a hodoscope on drift tubes (horizontal axis) and in a GEM SRSE detector (vertical axis).

### 1.8.3 Low-pressure gas THGEM-based detector

The low-pressure gas THGEM-based detector is intended for identification of ions on the AMS facility. Measurements of low-pressure detectors were continued in 2010. The amplification characteristics of thick and thin GEMs were measured in isobutane at a pressure of several tens of Torr.

### 1.8.4 Participation in collaborations

The BINP group of microstructure gas detectors participates in the international collaboration RD51 (CERN) on the development of microstructure gas detectors. The collaboration was formed in 2008. In 2010, the group continued its participation in this collaboration.

In 2010, members of the group of microstructure gas detectors continued their participation in the development of TPC for the International Linear Collider (ILC). Currently, a cascade GEM is regarded as the most likely candidate as the end registering detector of the TPC.

The work was done with the participation of V.I. Aul'chenko, A.E. Bondar, A.F. Buzulutskov, A.A. Grebenyuk, V.V. Zhulanov, R.G. Snopkov, A.V. Sokolov, Yu.A. Tikhonov, A.V. Chegodaev, E.O. Shemyakina, and L.I. Shekhtman.

## 1.9 Participation of BINP in the LHCb in 2010

### 1.9.1 Technical support of the LHCb

Data stream from the LHCb detector, which is recorded for subsequent storage and processing, consists of events of approximately 30 kB passing through a high-level trigger (HLT2) with a frequency of about 2 kHz. Thus, the data stream to store is about 60 MB/sec or around 600 TB per year of operation. This volume is too large to provide each analysis. Instead, the LHCb experiment is conducted with the application of centralized off-line pre-selection of events (the so-called “stripping”). About 10% of the events are separated from the total amount of data, which are then written to several (5-8) flows. Thus, each stream, which contains similar events (for example, all the channels with muons in the final state or events from the D-meson decay may be grouped in one stream), encloses a much smaller number of events that can be handled in a relatively short time in the GRID system. In addition, data files after “stripping” already contain information about candidate particles and combinations thereof, which additionally significantly reduces the time of processing and obtaining a physical result. A disadvantage of this approach is that the pre-selection procedure should be available already at the stage of data acquisition. To some extent, this problem is solved by inclusive selection (such as muons with large transverse momenta, “topological” selection and so on)

Members of the BINP group are responsible for developing and supporting the software environment that provides pre-selection of events (“stripping”) by selection criteria specified by the developers of physical analysis. Since such pre-selection has much in common with a high-level trigger (which is also a software algorithm on the LHCb), the “stripping” environment is a modification of the software for trigger HLT2. The “stripping” environment allows simultaneous operation of several hundreds of physical event selection processes, sends them for recording to several streams (DST files), and contains modules for perfection of the selection criteria and monitoring the results.

Besides that, the BINP group is responsible for supporting pre-selection of angles  $\gamma$  measured from tree decays of B mesons. These analyses include the channels of B decay to DX, where B is a charged ( $B^\pm$ ) or neutral ( $B_d$  or  $B_s$ ) B meson, D is a charged or neutral D meson which is reconstructed in one of the states  $D \rightarrow hh$ ,  $D \rightarrow hhh$ ,  $D \rightarrow hhhh$ ,  $D \rightarrow Kshh$ ,  $D \rightarrow K\pi\pi^0$  (here h is a charged kaon or pion), and X is a kaon, pion or a combination  $\pi\pi$ ,  $K\pi$  or  $KK$ . These decay channels cover almost all possible methods for measuring the angle  $\gamma$  – both from the ratio of the amplitudes of allowed and forbidden decays  $B \rightarrow DK$  and with the help of time-dependent analyses or analyses of the Dalitz distribution.

Members of the BINP group continued works on the modeling of the radiation background in the LHCb pit and surrounding areas. Earlier this work was done using the FLUKA package and more concise versions of the LHCb geometry. In particular, direct flows of particles, doses, and flows of hadrons with energies above 20 MeV and an equivalent neutron flux of 1 MeV were calculated in 2000-2002 for silicon. These calculations were necessary to evaluate the performance of the electronics located in the corresponding areas and, where appropriate, to develop radiation-hard pieces of equipment. Later on, in 2004-2007, the activation of components, in particular, the distribution of activity in the materials of the LHCb experiment, and the distribution of dose rates from induced radioactivity were calculated. Currently it is necessary to resume simulation of direct radiation fluxes to determine the degree of danger for the electronics located in service areas around the LHCb with the updated geometry of the experiment and modified script of the accelerator operation.

In 2010, the required infrastructure was restored (the latest version of the FLUKA package was installed, the geometry was tested and so on) and test runs of simulations with limited statistics were conducted. Fig.(1.9)1 shows a comparison of the old simulation with the new one. The dependence of the absorbed dose on the coordinate along the z axis of the experiment is presented.

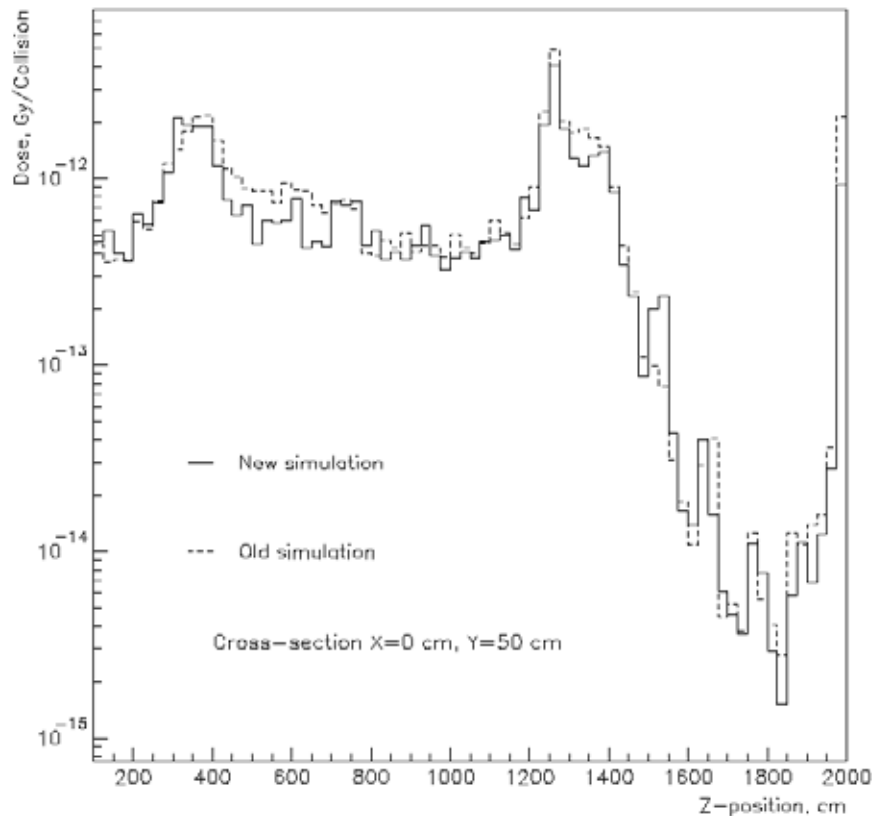


Fig.(1.9)1. Dependence of the absorbed dose on the z coordinate.

## 1.9.2 Physical results

The research program of BINP in the LHCb experiment is aimed at watching the effects beyond the Standard Model of electroweak interactions. A particular problem within this overall project is the precise measurement of quantities that undergo CP violation – of the angle  $\gamma$  in the unitarity triangle and the D meson mixing parameters.

The CP violation is responsible for the asymmetry of matter and antimatter in the universe. Within the Standard Model, the CP violation is described by the Cabibbo-Kobayashi-Maskawa (CKM) matrix, which characterizes transitions between different generations of quarks due to the weak interaction. One of the CKM matrix representations is the so-called unitarity triangle (UT). Various processes are sensitive to the lengths of the sides and the angles of the triangle. Effects beyond the Standard Model become evident in the mismatch of measurements of UT parameters (for example, in the sum of the angles of the triangle differing from 180 degrees). Thus, precision measurements of the UT parameters complement the direct search of the effects of "new physics" at high energies in such installations as ATLAS or CMS.

Many of the CP violating processes, which are the most sensitive to the UT parameters, are observed in B meson decays. To date, only one angle of the UT (often called  $\beta$ ) is measured with an accuracy of about 1 degree in the Belle and BaBar experiments at the electron-positron colliders. The LHCb experiment will significantly clarify many other parameters of CP violation. In particular, the angle  $\gamma$  can be measured with an accuracy of a few degrees.

Another effect with a significant potential for observing "New Physics" manifestations is mixing of D mesons, where a neutral D meson, initially in a state with a definite flavor (e.g.,  $D^0$ ) acquires an admixture of the opposite flavor ( $\bar{D}^0$ ) in the process of evolution over time. This phenomenon is predicted by the Standard Model and has already been observed experimentally. However, the CP violating effects in the mixing of D mesons are expected to be ultimately small, and the "New Physics" effects could lead to significant CP violation. Sensitivity achieved to date does not allow us to put any significant constraints on CP violation in D mixing.

Both measurements have many similar properties: they require considerable experimental statistics, can potentially be accomplished with very high accuracy because of the vanishingly small theoretical

uncertainties, and use the unique (for experiments on hadron accelerators) ability of the detector LHCb to record decay channels with exclusively hadronic final states with high efficiency. Our group proposed a research program that uses the advanced technique of model-independent analysis of the Dalitz distribution for precise measurement of the angle  $\gamma$  and D meson mixing parameters.

The most accurate measurement of the angle  $\gamma$  uses multiparticle decays of neutral D mesons from the transitions  $B \rightarrow DK$  (such as  $K^0 \pi^+ \pi^-$ ). These analyses study the so-called Dalitz distributions, which characterize the dynamics of multiparticle D decay in the phase space volume. In the simplest (and most often used) case of three-particle decay, the phase space volume and the Dalitz distribution are described by two variables. Since D mesons that appeared in decays of B are a mixture of  $D^0$  and  $\bar{D}^0$ , these distributions differ from those observed in the case of decay of the “pure” state of  $D^0$  or  $\bar{D}^0$  and contain information on the angle  $\gamma$ . Similarly, the most precise measurements of CP violation in D mixing use the change in the Dalitz distribution of the multiparticle decay of D over time.

Analyses of this kind, however, suffer from the uncertainty in the description of the decay amplitude of the «pure» state of D: this amplitude is a complicated complex function of variables describing the phase space. Although the modulus of this function can be obtained from decays of “pure”  $D^0$ , which are available in large quantities, its complex phase cannot be determined from this statistics. All analyses that had been carried out so far are based on model assumptions on the behavior of the decay amplitude of D and therefore contain a model uncertainty computed rather unreliably. Such an approach would limit the accuracy of LHCb high-statistics measurements.

Recently, with the participation of BINP members, a method was developed which solves the problem of model uncertainty in the measurement of the angle  $\gamma$ . The missing information on the complex phase in the D decay amplitude is taken from the quantum correlations of pairs of neutral D mesons produced at electron-positron colliders at the kinematic threshold. The fact that two D mesons are observed in a coherent state leads to correlations between the Dalitz distributions for multiparticle decays of two D mesons and makes it possible to determine the complex phase (more precisely, the phase difference for the decays of  $D^0$  and  $\bar{D}^0$  in one element of the phase space volume – exactly that information which is required at measuring  $\gamma$ ). Technically, this approach requires dividing the phase space into regions (“bins”) with a concomitant deterioration of the statistical accuracy. However, the proposed method of optimal dividing allows achieving a statistical sensitivity to  $\gamma$  by only  $\sim 10\%$  worse than with the model-dependent method, without dividing. Using this method, the CLEO collaboration recently received results on the measurement of the complex phase, which can be used at the LHCb.

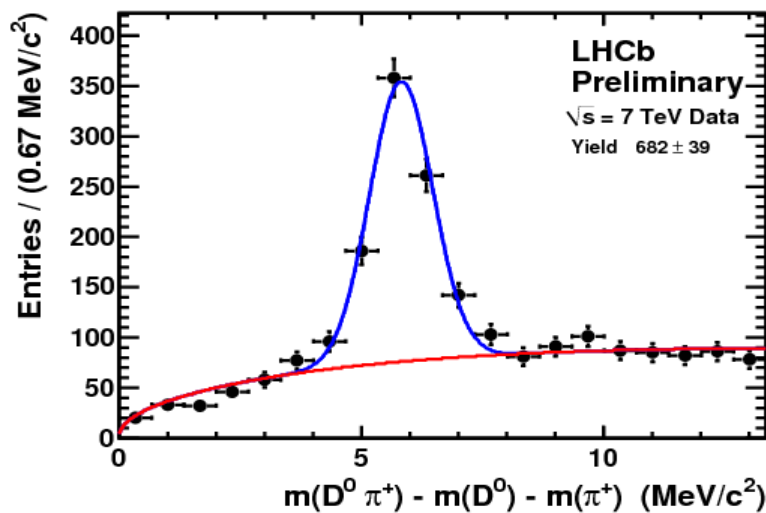


Fig.(1.9)2. Signal  $D^* \rightarrow D\pi$ ,  $D \rightarrow K_s \pi \pi$  observed by the LHCb detector with a statistics of  $124 \text{ nb}^{-1}$ .

The measurement of D meson mixing using multiparticle D decays is much like the measurement of  $\gamma$  and also suffers from the model uncertainty. Recently it was shown that in the measurement of mixing one can apply a similar model-independent approach using phase information obtained from the quantum correlations in the DD system decays, which makes it possible to eliminate the potentially dominant model uncertainty. Since a substantial statistics content of D decays will be acquired at the LHCb already

in 2011, this analysis will provide competitive results in the near future. Preparation for such analysis was performed in 2010 – assessment of the detection efficiency and reconstruction restoration of the decay time and debugging of the event selection procedures and separation of signal from the background using the already accumulated data. Fig.(1.9)2 shows a signal of the process  $D^* \rightarrow D\pi$ ,  $D \rightarrow K_s \pi \pi$ , which was selected from a small portion of the LHCb data accumulated by now.

One more way to measure the angle  $\gamma$  was proposed and published in 2010. It can extend the research program at the LHCb. If a neutral B meson decays into a multiparticle state  $DK\pi$ , with a D meson that then also decays to a multiparticle state, one can perform analysis of the «double» Dalitz distribution – two correlated distributions in the phase space of the decays of B and D. A unique feature of this analysis is that, since the relative admixture of the opposite flavor of D is much greater than in the two-particle decay of charged B to DK, both the angle  $\gamma$  and the complex phases in the amplitudes of B and D can be obtained independently without involving other measurements. In particular, the phase information from the correlated decays of  $D\bar{D}$  also becomes unnecessary, and hence exact model-independent measurement of the angle  $\gamma$  can be made solely from the LHCb data. Moreover, the extracted information about the phase in the decay  $B \rightarrow DK\pi$  can then be used in analysis which uses two-particle decays of D from the process  $B \rightarrow DK\pi$ . Application of this method, however, will require a considerable statistical content of B decays (a few years of the LHCb operation).

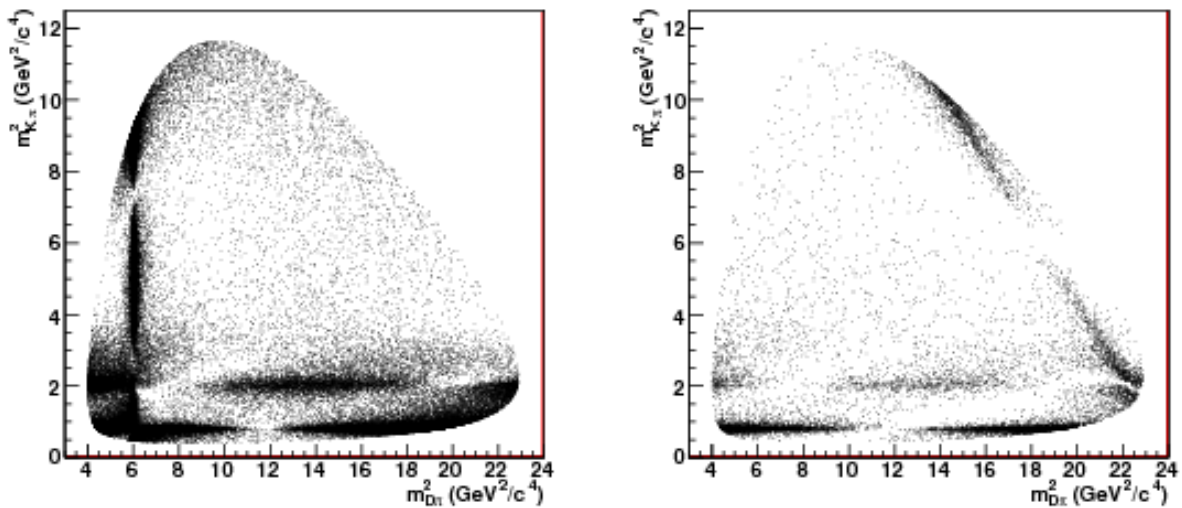


Fig.(1.9)3. Dalitz distribution of the decays  $B \rightarrow D^0 K\pi$  (left) and  $B \rightarrow \bar{D}^0 K\pi$  (right). Result of Monte Carlo simulation.

Monte Carlo simulation was performed for verification of the practical applicability of the proposed technique and determination of the accuracy of extraction of the angle  $\gamma$  (Fig.(1.9)3). Since the proposed method also suggests dividing the Dalitz distribution into regions, a method of optimal dividing was proposed (Fig.(1.9), 4 and 5), which improves the statistical accuracy of  $\gamma$  determination. The obtained accuracy of  $\gamma$  determination is about 1 degree for a luminosity integral at the LHCb of about  $50 \text{ fb}^{-1}$  (such a luminosity value is expected to be acquired after upgrading the LHC collider and detector). This accuracy is comparable with other methods of  $\gamma$  measuring and does not contain theoretical uncertainties or uncertainties associated with parameters determined from other measurements. Thus, the proposed method will provide an additional independent measurement with accuracy competitive with that of other techniques, which not only is important to improve the statistical accuracy but also serves as an additional test of possible systematic effects.

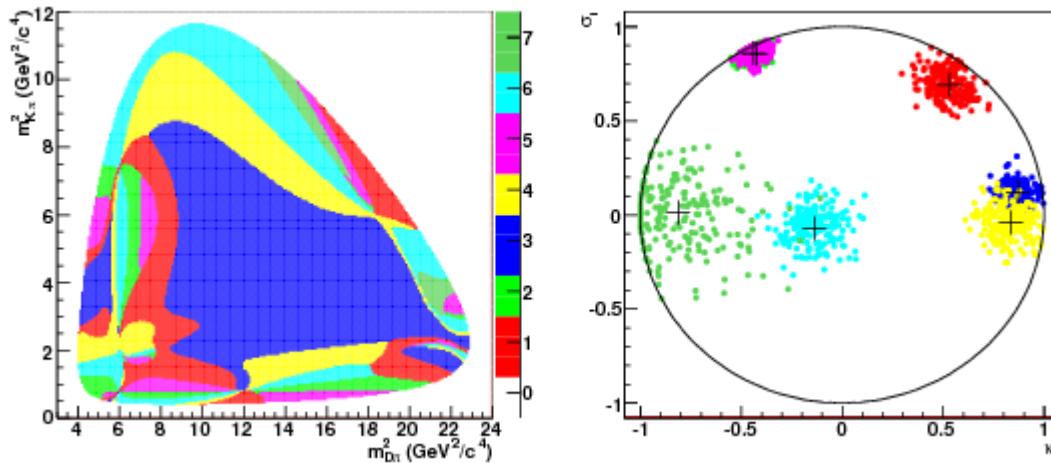


Fig.(1.9)4. Optimal division of the Dalitz distribution of the decay  $B \rightarrow DK\pi$  into regions (left) and phase coefficients obtained for such a division in the simulation (right).

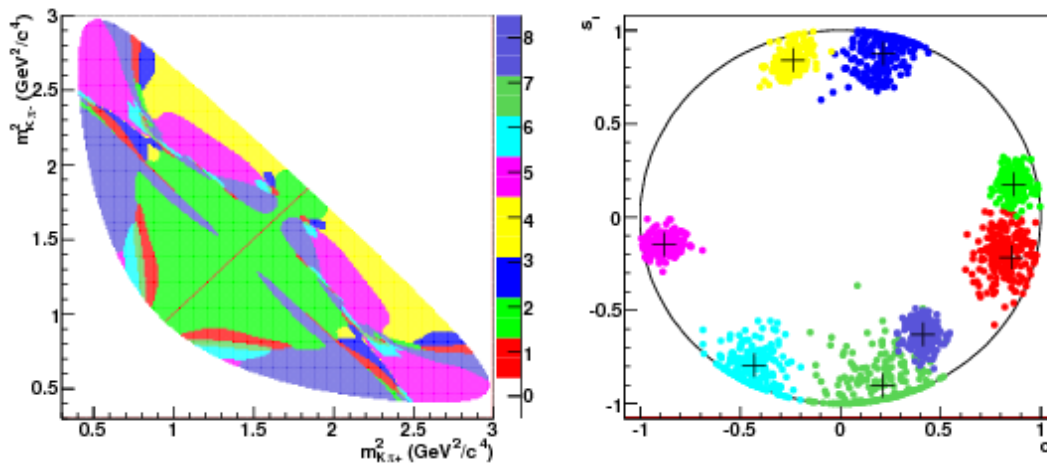


Fig.(1.9)5. Optimal division of the Dalitz distribution of the decay  $D \rightarrow K_s \pi\pi$  into regions (left) and phase coefficients obtained for such a division in the simulation (right).

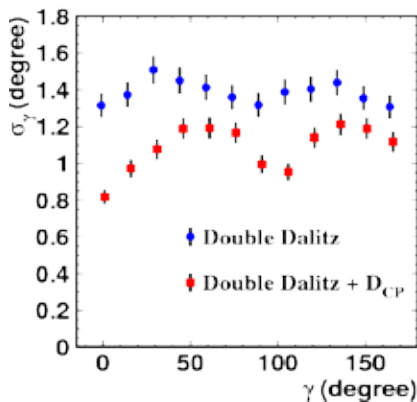


Fig.(1.9)6. The accuracy of measuring the angle  $\gamma$  in dependence on its value for the method of «double Dalitz analysis» for a statistics content of  $50 \text{ fb}^{-1}$  (after upgrading the LHC and LHCb).

In addition, the BINP group takes active participation in the investigation of the possibilities of research of heavy quarkonia in the LHCb experiment, namely, the charmonium and bottomonium – bound states of  $c$  and  $b$  quarks. More than ten new charmonium-like states were discovered at the B-factories at SLAC and KEK in the past five years, with properties that poorly fit into the picture of charmonium by theoretical models. Some of these new states were later observed in experiments at Tevatron. Therefore, there is reason to believe that an appreciable number of such states can be produced in experiments at the LHC, in particular, LHCb, which will enable a detailed exploration of their properties. A study was conducted that showed that the LHCb experiment is also promising in terms of learning the different states of bottomonium.

The works were made with the participation of A.V. Bobrov, E.A. Cooper, S.A. Poluektov, L.I. Shekhtman, and S.I. Eidelman.

## 1.10 Belle experiment

### 1.10.1 Main results

- Integrated luminosity of the Belle experiment has exceeded 1040 inverse femtobarn.
- Partial widths of the decay of  $\tau$ -lepton into 3 charged hadrons have been measured.
- Search for  $\tau$  decays with the violation of lepton flavor or lepton number has been performed.
- High precision Dalitz analysis of the decay  $D^0 \rightarrow \pi^+ \pi^- \pi^0$  from  $D^* \rightarrow D^0 \pi$  has been started.
- Work on the interference study in  $B^\pm \rightarrow K^\pm \eta_c^{(\prime)}$  decays and determination of parameters of  $\eta_c$  и  $\eta_c'$  charmonia has been completed.
  - A study of the combined CP-parity violation in three-body decays using full data has been continued.
  - A method of the model-independent measurement of the neutral D mesons mixing parameters and the parameters of CP-violation in mixing using binned Dalitz analysis has been developed.
  - A study of the resonant structure of the  $K^+ \pi^+ \pi^-$  final state in  $B^+ \rightarrow J/\psi K^+ \pi^+ \pi^-$  and  $B^+ \rightarrow \psi' K^+ \pi^+ \pi^-$  decays has been performed. Parameters of the  $K_1(1270)$  intermediate state have been determined and branching fractions of the above-mentioned decays have been measured.

The main course of the Working group is the collaboration in the field of elementary particle physics with the High Energy Accelerator Research Organization (KEK), Tsukuba, Japan, which is one of the largest and fast developing laboratories in the field of high energy physics. Lately, KEK administration actively extends the international cooperation in order to make KEK an international centre in this field of physics. Today one of the main experiments in elementary particle physics in Japan is a study of CP-violation in B meson decays with the Belle detector at the electron-positron collider KEKB with a very high luminosity (so called B-factory).

A group of scientists from the Budker Institute of Nuclear Physics actively participates in the Belle project from the beginning. Novosibirsk physicists made a large contribution to the construction of the electromagnetic calorimeter of the Belle detector. They participated in the design project, element prouction, assembly, and setup of this world's biggest calorimeter based on cesium iodide monocrystals.

In 2010 the Belle detector operation was stopped for an upgrade. The currently accumulated integrated luminosity exceeds 1040 inverse femtobarn. The analysis of this experimental data is still in process. Furthermore, the detector and accelerator upgrade is under way to increase the device luminosity and prepare experiments, which will allow a one order increase of the measurement precision of the CP-violation parameters and, perhaps, an observation of the physical phenomena beyond the Standard Model.

BINP physicists actively participate both in detector upgrade and analysis of the accumulated experimental data.

### 1.10.2 Data analysis of the Belle experiment

In 2010 one can single out two main directions in the physics of  $\tau$ -lepton: determination of the  $\tau$ -lepton properties in allowed (non-suppressed) decays and search for new physics in rare and suppressed decays.

1. The  $\tau$ -lepton decays into three charged hadrons (different  $\pi^\pm$  и  $K^\pm$  mesons combinations) and a neutrino have been studied with the 666 fb<sup>-1</sup> data samples. As a result, the branching fractions of four decay modes have been measured and mass spectra of 3-particle hadron system have been obtained (see Table(1.10) 1).

Table(1.10)1. Obtained branching fractions of  $\tau \rightarrow (h_1 h_2 h_3) \nu_\tau$ .

Decay mode	Branching fraction
$\pi\pi\pi, 10^{-2}$	$8.42 \pm 0.00^{+0.26}_{-0.25}$
$K\pi\pi, 10^{-3}$	$3.30 \pm 0.01^{+0.16}_{-0.17}$
$KK\pi, 10^{-3}$	$1.55 \pm 0.01^{+0.06}_{-0.05}$
$KKK, 10^{-5}$	$3.29 \pm 0.17^{+0.19}_{-0.20}$

Comparison with other experiments is shown in Fig.(1.10) 1.

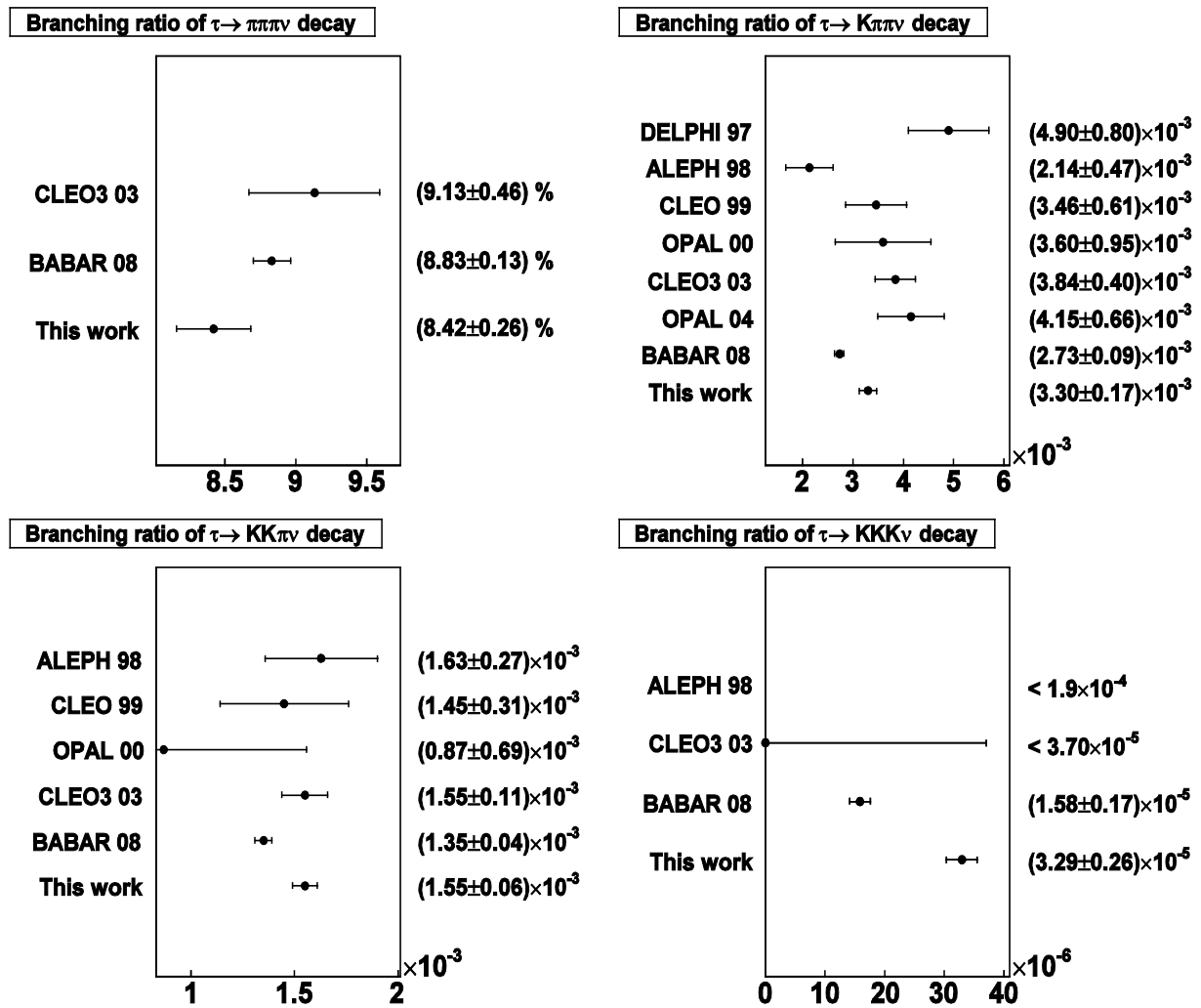


Fig.(1.10)1. Comparison of the  $\tau$  decay branching fractions, obtained in different experiments.

The invariant mass distribution of the hadronic system is given in Fig.(1.10) 2. One can see that consistency with the simulation by the current version of TAUOLA program is unsatisfactory.

Furthermore, the analysis aimed at the  $\tau$ -lepton lifetime determination is being completed. The precision improvement of this important parameter will allow carrying out more sensitive tests of the lepton universality.

2. Decays of  $\tau$ -lepton with the violation of lepton flavor or lepton number are forbidden in the Standard Model. Discovery of the neutrino oscillations removed the full prohibition, but the probability of such decays is extremely small, which makes their observation almost impossible. New physics models (beyond the Standard Model) increase the probability of the mentioned decays by many orders and at some parameter values bring it up to  $10^{-7} - 10^{-8}$ . Such probability values can be reached at the Belle and BaBar experiments, therefore an intensive search of the discussed decays is carried out. Even their non-observation, accompanied by the upper limit improvement, plays an important role, since it allows setting the constraint on the parameter space in the new physics models. In 2010, noticeably increasing the sensitivity due to the new selection criteria and using larger integrated luminosity (hence a larger number of  $\tau$ -lepton pairs), the Belle collaboration continued a search for such decays.

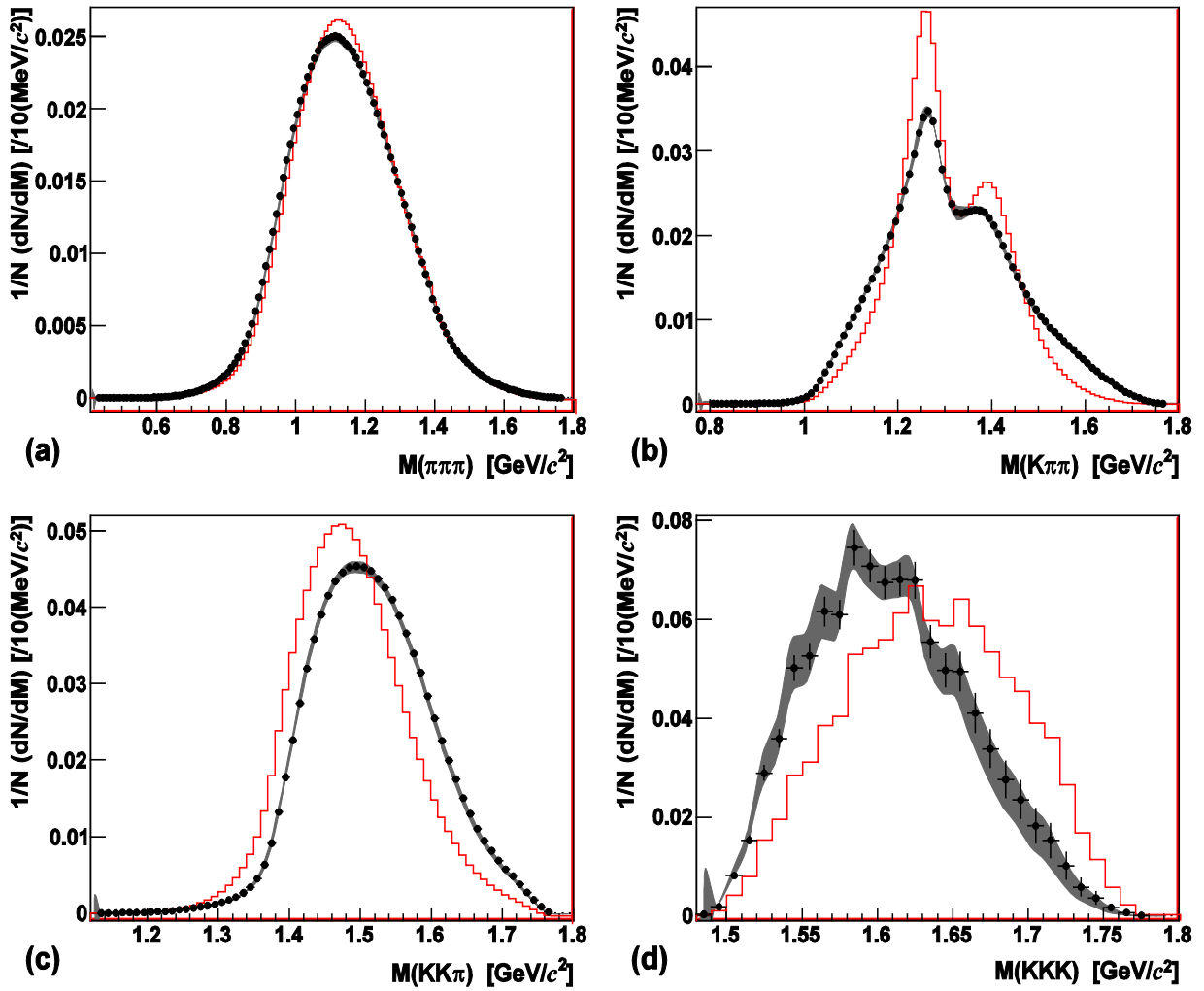


Fig.(1.10)2. Invariant mass distribution of the hadronic system.

Thus, a search for  $\tau$ -lepton decays into lepton  $l$  ( $\mu$ ,  $e$ ) and a pair of charged mesons  $h$  ( $\pi^\pm$ ,  $K^\pm$ ) has been carried out with the  $671 \text{ fb}^{-1}$  luminosity runs. The results are shown in Table(1.10) 2. One can see that the upper limits have been increased by (1.6-8.8) times.

Table(1.10)2. 90% upper limits on the branching fractions of  $\tau \rightarrow (lh, h_2)$  decays.

Decay of $\tau$	Belle		BaBar		CLEO	
	Branching, $10^{-8}$	$N_{\tau\tau}, 10^6$	Branching, $10^{-8}$	$N_{\tau\tau}, 10^6$	Branching, $10^{-8}$	$N_{\tau\tau}, 10^6$
$\mu^+\pi^+\pi^-$	3.3		29		820	
$\mu^+\pi^+\pi^-$	3.7		7		340	
$\mu^+\pi^+K^-$	16		26		750	
$\mu^+\pi^+K^+$	10	616.6	32	203.5	740	4.4
$\mu^+\pi^+K^-$	9.4		22		700	
$\mu^+K^+K^-$	6.8		25		1500	
$\mu^+K^+K^-$	9.6		48		600	
$e^+\pi^+\pi^-$	4.4		12		220	
$e^+\pi^+\pi^-$	8.8		27		190	
$e^+\pi^+K^-$	5.8		32		640	
$e^+\pi^+K^+$	5.2	616.6	17	203.5	380	4.4
$e^+\pi^+K^-$	6.7		18		210	
$e^+K^+K^-$	5.4		14		600	
$e^+K^+K^-$	6.0		15		380	

In another experiment a search for  $\tau$ -lepton decays into 3 other leptons was performed with the  $782 \text{ fb}^{-1}$  data samples. The results are shown in Table(1.10)3. A noticeable improvement of upper limits can be seen.

Table(1.10)3. 90% upper limits on the branching fractions of  $\tau \rightarrow (l_1 l_2 l_3)$  decays.

Decay of $\tau$	Belle		BaBar		CLEO	
	Branching, $10^{-8}$	$N_{\tau\tau}, 10^6$	Branching, $10^{-8}$	$N_{\tau\tau}, 10^6$	Branching, $10^{-8}$	$N_{\tau\tau}, 10^6$
$e^-e^+e^+$	2.7	718.7	4.3	438.4	290	4.4
$e^-\mu^+\mu^+$	2.7		3.7		180	
$e^+\mu^-\mu^-$	1.7		5.6		150	
$\mu^-e^+e^+$	1.8		8.0		170	
$\mu^-\mu^+\mu^+$	2.1		5.3		190	
$\mu^+e^-e^-$	1.5		5.8		150	

Finally, a search for  $\tau$ -lepton decays into lepton  $l$  ( $\mu, e$ ) and one or two  $K_s^0$  has been carried out with the  $671 \text{ fb}^{-1}$  data samples [4]. The results are shown in Table(1.10) 4. One can see a noticeable improvement of upper limits.

Table(1.10)4. 90% upper limits on the branching fractions of  $\tau \rightarrow lK_s^0$  and  $\tau \rightarrow lK_s^0 K_s^0$  decays.

Decay of $\tau$	Belle		BaBar		CLEO	
	Branching, $10^{-8}$	$N_{\tau\tau}, 10^6$	Branching, $10^{-8}$	$N_{\tau\tau}, 10^6$	Branching, $10^{-8}$	$N_{\tau\tau}, 10^6$
$e^-K_s^0$	2.6	616.6	3.3	431	91	12.8
$\mu^-K_s^0$	2.3		4.0		95	
$e^-K_s^0 K_s^0$	7.1		—	—	220	
$\mu^-K_s^0 K_s^0$	8.0		—	—	340	

The group performed a high precision Dalitz analysis of the decay  $D^0 \rightarrow \pi^+ \pi^- \pi^0$  from  $D^{*0} \rightarrow D^0 \pi$  based on  $673 \text{ fb}^{-1}$  of data accumulated by the Belle detector, which corresponds to more than  $200 \cdot 10^3$  signal events. The decay model includes the vector resonances  $\rho(770)$ ,  $\omega$ ,  $\rho(1450)$ , and  $\rho(1700)$ , the scalar states  $\sigma(600)$ ,  $f_0(980)$ ,  $f_0(1370)$ , and  $f_0(1500)$ , and also the tensor resonance  $f_2(1270)$  (see Fig.(1.10) 3). A study of this decay will provide a more precise measurement of the scalar component in the  $\pi^+ \pi^-$  channel of D meson decays and will allow a determination of the CP-violation degree in neutral D mesons with a high sensitivity. Along with other CP-symmetric  $D^0$  final states, a detailed study of  $D^0 \rightarrow \pi^+ \pi^- \pi^0$  can be used to increase statistics of the measurement of the  $\phi_3$  angle of the Cabibbo-Kobayashi-Maskawa matrix. Furthermore, data separation into  $D^0$  and anti- $D^0$  is being carried out to determine CP-asymmetry parameters of the  $D^0 \rightarrow \pi^+ \pi^- \pi^0$  decay model.

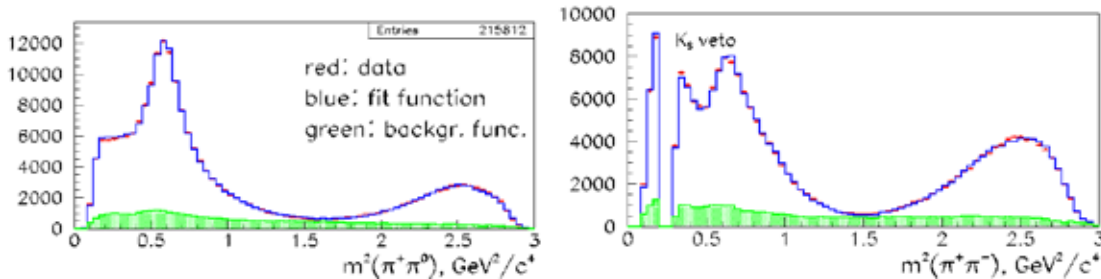


Fig.(1.10)3. Projections of the Dalitz distribution (data is shown red, fitting function after the parameter optimization – blue, background - green).

A group of BINP scientists has studied properties of particle  $\eta_c$  and its excited state  $\eta_c(2S)$ . These particles are bound states of  $c$  and anti- $c$  quarks (so called charmonia). Their source was considered to be B meson decay into K meson and charmonium, followed by the charmonium decay into hadrons  $K_s K \pi$ . In Fig.(1.10) 4 the mass distribution of  $(K_s K \pi)$  invariant mass is shown red (peaks correspond to  $\eta_c, J/\psi, \chi_{c1}$ , and  $\eta_c(2S)$  resonances), the combinatorial background is marked black. One can see that some events are neither signal (peaks), nor combinatorial background – this is a so called non-resonant amplitude. In-

interference with the non-resonant amplitude leads to a considerable model error of the measurement of B meson and charmonium decays branching product. The procedure of taking the interference into account, which was proposed in this work, for the first time contains no assumptions about the interference phase or absolute value, i.e. is model independent. Results of this study are the B meson and charmonium decays branching product and the mass and width values of  $\eta_c$  and  $\eta_c(2S)$  mesons. Due to the large data sample, the results have small statistical errors and allow the improvement of the corresponding world average values. The results are being prepared for publication.

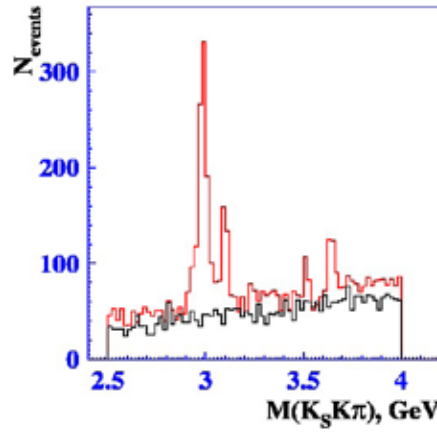


Fig.(1.10)4.  $K_s K \pi$  invariant mass distribution.

Among B meson decays into final states without charmed particles, the decays into three-body final states are of great interest. Examples of such processes are decays  $B \rightarrow K \pi \pi$  and  $B \rightarrow K K K$ , which were discovered for the first time in BINP. Special feature of multi-body (including three-body) decays is that they usually include intermediate quasi-two-body states. Figure (1.10) 5 shows the invariant mass distributions of two-particle combinations  $K^+$  and  $\pi^-$ , and also  $\pi^+$  and  $\pi^-$  mesons from  $B^+ \rightarrow K^+ \pi^+ \pi^-$  decay. One can see that there are intermediate  $K^*(892)$  and  $K^*(1430)$  resonances in the  $M(K^+ \pi^-)$  spectrum, and also  $\rho(770)$  and  $f_0(980)$  resonances in the  $M(\pi^+ \pi^-)$  spectrum. Analysis of decays into multi-body final states allows the measurement of both the probability of the corresponding b quark transitions and the relative phases between constituent quasi-two-body amplitudes. This provides a much better sensitivity of multi-body B meson decays to the direct violation of CP-parity. Work describes the first analysis of CP-violation in  $B^\pm \rightarrow K^\pm \pi^\pm \pi^\mp K^\pm \pi^\pm \pi^\mp$  decays, where the indication of the direct CP-violation in  $B^\pm \rightarrow \rho^0 K^\pm$  decays is detected. At present time, the analysis of the full data sample of B meson decays accumulated at the Belle detector is under way.

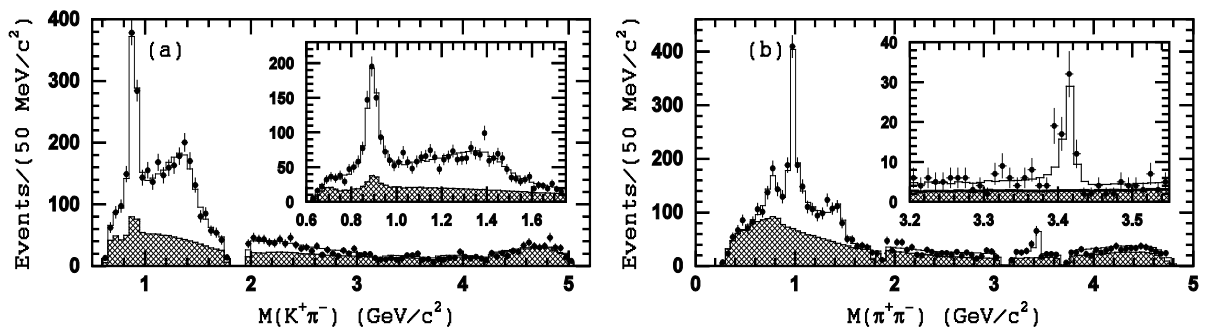


Fig.(1.10)5. Invariant mass distributions of  $K^+ \pi^-$  (left) and  $\pi^+ \pi^-$  (right) pairs in  $B^+ \rightarrow K^+ \pi^+ \pi^-$  decays.

Within the Belle experiment framework, scientists conduct a study of model-independent measurement of neutral D meson mixing parameters and CP-violation parameters in mixing. Mixing parameters are fundamental parameters, which cannot be precisely obtained by theoretical methods. Precise measurement of these parameters will allow the decrease of theoretical uncertainty in other dimensions, particularly, the measurement of the angle  $\gamma$  of the unitarity triangle. Measurement of the CP-violation parameters

will provide a test for the Standard Model, since in this model these parameters are strictly limited. The advantage of this method is the opportunity to avoid uncertainties, associated with the model of the amplitude of the three-body D meson decay, using binned analysis of the Dalitz diagrams (see Fig.(1.10) 6). In 2010 a paper describing this method was published in Physical Review D.

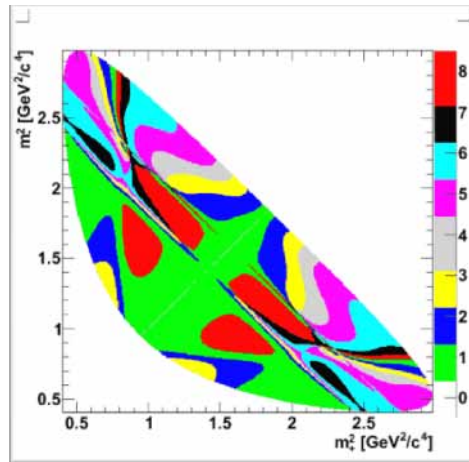


Fig.(1.10)6. Binned Dalitz diagram of the  $D^0 \rightarrow K_s \pi^+ \pi^-$  decay.

BINP scientists participated in the study of the resonant structure of the  $K^+ \pi^+ \pi^-$  final state in  $B^+ \rightarrow J/\psi K^+ \pi^+ \pi^-$  and  $B^+ \rightarrow \psi' K^+ \pi^+ \pi^-$  decays. In this study the amplitude analysis of invariant masses of the decay final particles was carried out, taking into account the interference between different intermediate states. Besides, the analysis of the spin-dependent angular distributions of the final state was performed. It was shown that the intermediate state  $K_1(1270)$  makes a dominant contribution both in  $B^+ \rightarrow J/\psi K^+ \pi^+ \pi^-$  and  $B^+ \rightarrow \psi' K^+ \pi^+ \pi^-$  decays. The branching fractions of  $K_1(1270)$  decay into  $K\rho$ ,  $K\omega$ ,  $K^*(892)\pi$ , and  $K_0^*(1430)\pi$  final states were determined (fit results are shown in Fig.(1.10) 7). Furthermore, mass  $(1248.1 \pm 3.3(\text{stat}) \pm 1.4(\text{syst}))$  MeV/ $c^2$  and width  $(119.5 \pm 5.2(\text{stat}) \pm 6.7(\text{syst}))$  MeV/ $c^2$  of  $K_1(1270)$  state were obtained. This is one of the first measurements of these parameters, where  $K_1(1270)$  is extracted purely enough. Besides, precise measurements of  $B^+ \rightarrow J/\psi K^+ \pi^+ \pi^-$  and  $B^+ \rightarrow \psi' K^+ \pi^+ \pi^-$  decay branchings were performed. Study results are published in Physical Review D.

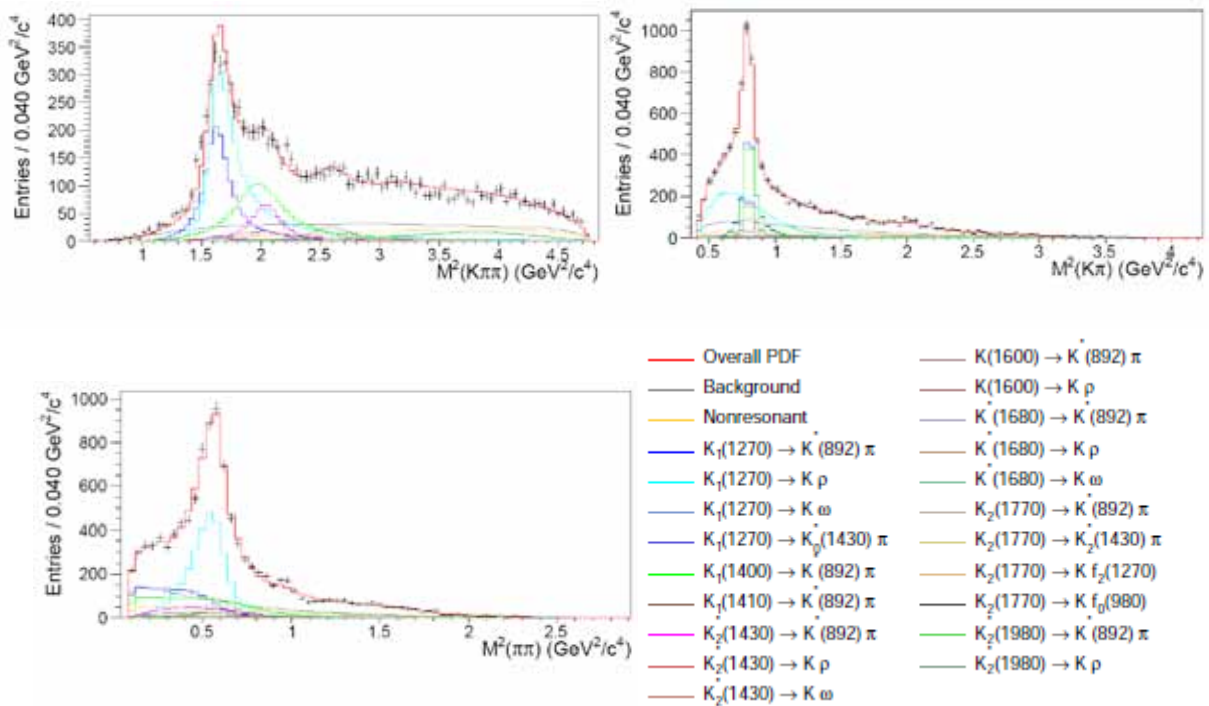


Fig.(1.10)7. Fit results for  $B^+ \rightarrow J/\psi K^+ \pi^+ \pi^-$  decay. Data (points) and fit (histograms) are shown as projections over three axes.

### 1.10.3 Detector upgrade

The next stage of B-factory operation is the upgrade of both the detector (Belle II) and the collider to increase the luminosity up to  $8 \times 10^{35} \text{ cm}^{-2} \text{ s}^{-1}$ . The new experiment will allow the measurement of all angles of the unitarity triangle with a few percent precision and, perhaps, will give the opportunity to go beyond the Standard Model. Besides the study of the CP-violation mechanism, a large data sample accumulated in this experiment will allow new results on B meson, D meson, and  $\tau$ -lepton decay physics to be obtained.

Increase of the luminosity and background load on the collider sets new requirements on the detector systems. To provide effective calorimeter operation, it needs to be upgraded. BINP group participates in R&D work on the upgrade of the detector calorimeter system. It has developed and proposed the calorimeter upgrade scheme.

For the barrel part of the calorimeter, the counter electronics will be replaced by the scheme with pipeline readout followed by the data fit with a known response function. Such procedure allows the determination of both the energy and the signal arrival time. Usage of the time information allows the suppression of the fake cluster rate.

For the end-caps, where the background conditions are most severe, first the electronics upgrade is planned, and then the replacement of the CsI(Tl) scintillation crystals by the crystals of non-activated CsI with a smaller decay time. This will allow a 30 times improvement of the counter time resolution, and taking into account a fit of the signal shape, will provide background suppression by more than 150 times.

In 2010 the BINP scientists carried out measurements of the parameters of shaper-digitizer and concentrator modules in the VME standard, which were developed in BINP (see Fig.(1.10)8).

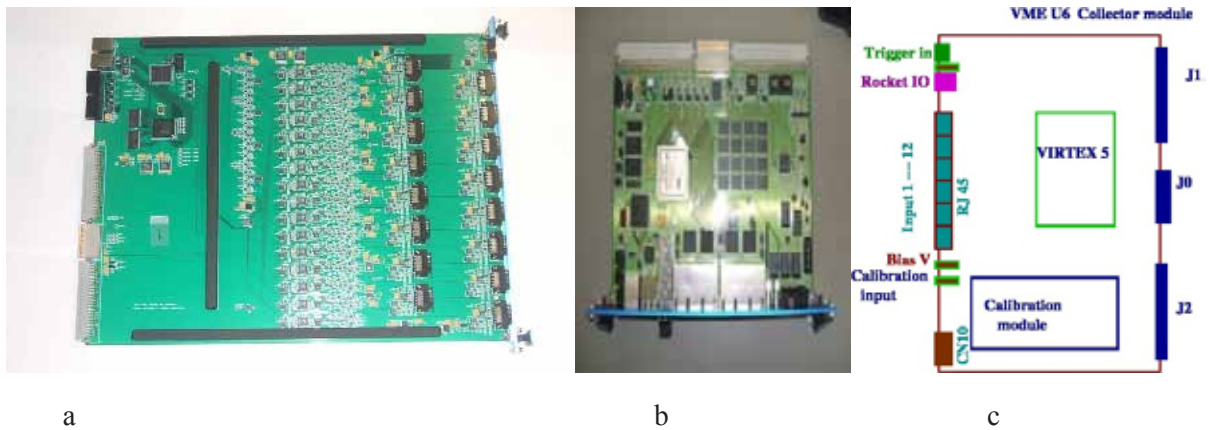


Fig.(1.10)8. (a) 16-channel shaper-digitizer electronic module in the VME standard; (b), (c) Concentrator electronic module in the VME standard.

Noise and linearity measurements were conducted for the shaper-digitizer. The linearity turned out to be better than  $2 \times 10^{-3}$  for the dynamic range, which corresponds to 10 MeV – 10 GeV energy range (see Fig. (1.10) 9).

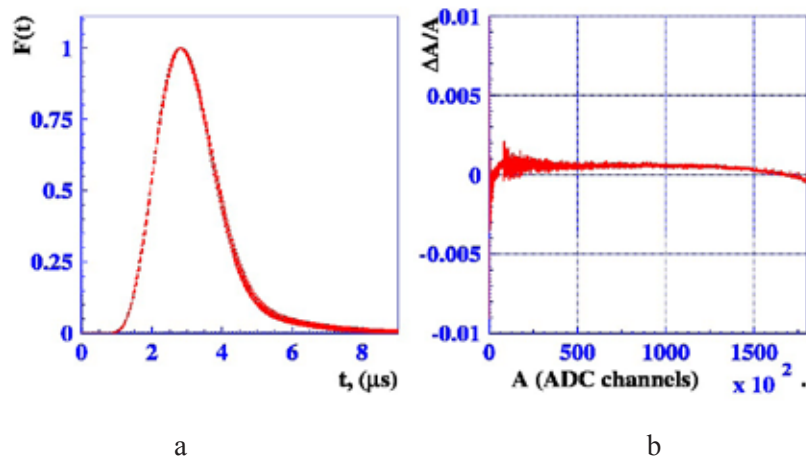


Fig.(1.10)9. (a) Pulse shape after the shaper; (b) Deviation from the linear dependency of the shaper module.

For the concentrator module, the XLINX project was worked out. This project allows working with calorimeter modules in a stand-alone mode using the scheme shown in Fig.(1.10) 10. Special software was developed to load the algorithm and the coefficient array for the reconstruction of time and energy of the signals from crystals. This is done from a personal computer (PC) into the shaper module. After loading projects into the XLINX scheme of the shaper and concentrator, the program activating these projects in modules is launched at PC. After the launch signal (external or internal), the projects pack the data and send it from the shaper module to the concentrator module, and after that to PC, where the data is written to file. Projects and the corresponding software were developed and tested. This software allows reading 64 amplitudes from 16 channels with a 300 Hz frequency. For working with a real data acquisition system, usage of the optic connection line is planned. This will allow a noticeable increase of the concentrator module reading frequency. Project and software development for the optic connection line are planned for the next year.

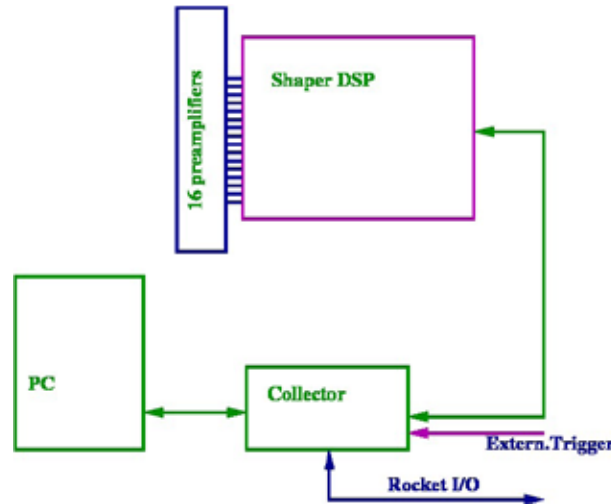


Fig.(1.10)10. Scheme of the calorimeter modules operation in stand-alone mode.

The concentrator module includes a calibration module. This module allows generation of signals with given shape to imitate signals from crystals. Fig.(1.10) 11 shows the signal from the CsI(Tl) counter and the signal from the calibration module. Difference of these signals does not exceed 2%.

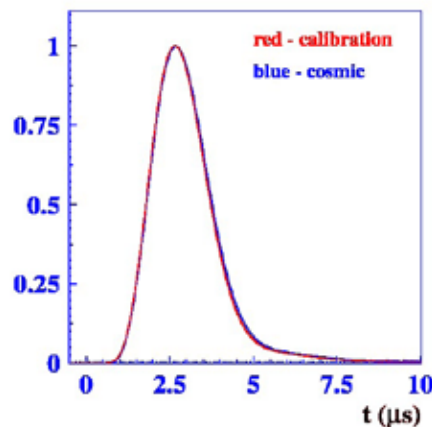


Fig.(1.10)11. Shapes of the signal from the CsI(Tl) counter (blue) and the signal of the calibration module (red).

For the end-cap calorimeter, where the usage of pure CsI crystals is planned, the use of new photodetectors is needed. It is planned to use photopentodes – photomultipliers with three diodes (see Fig.(1.10) 12). These devices can operate in 1.5 T magnetic field.

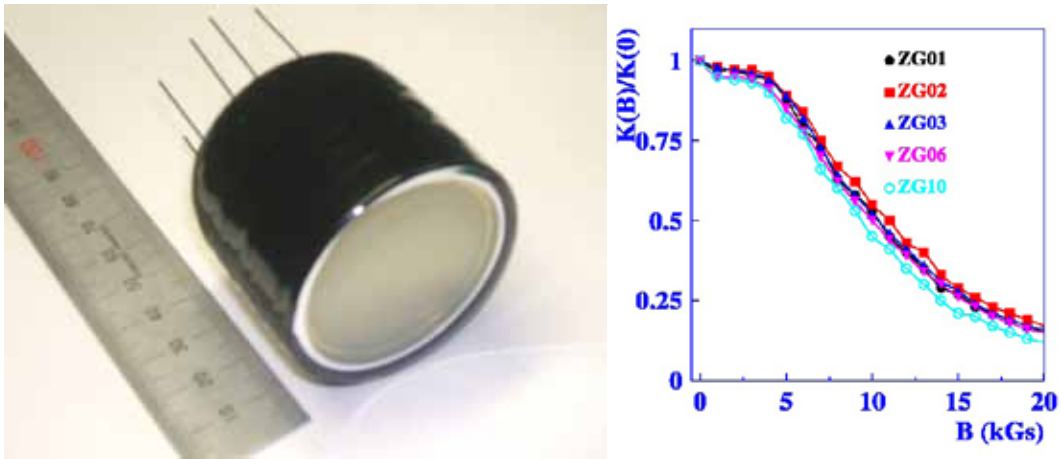


Fig.(1.10)12. Vacuum photopentode by Hamamatsu company.

For operation inside a large machine, long-term working capacity and stability of the device characteristics are very important. The BINP team continued photopentode characteristics tests in the conditions of heavy light load. Sensitivity variation of the photopentodes because of the light loads does not exceed 2% (see Fig.(1.10)13).

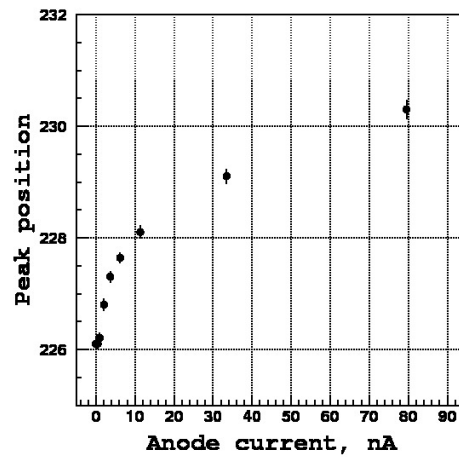


Fig.(1.10)13. Dependency of the  $^{137}\text{Cs}$  peak position on the average anode current of the photopentode.

In studies participated: K. Arinstein, V. Aulchenko, A. Bondar, A. Buzulutskov, S. Eidelman, D. Epifanov, N. Gabyshev, A. Garmash, A. Kuzmin, D. Matvienko, A. Poluektov, V. Shebalin, B. Shwartz, Yu. Usov, A. Vinokurova, V. Vorobiev, V. Zhilich, V. Zhulanov, O. Zyukova.

## 1.11 Experiment BABAR

The BABAR collaboration involves 11 BINP employees. The BABAR detector was gaining statistics on the PEP-II storage ring at SLAC (USA) from 1999 to 2008. The accumulated data are still being processed. Currently, about 100 processes are being analyzed. Some thirty papers were published in 2010.

The main purpose of this experiment is the measurement of the CP violation in the decays of neutral B mesons. Another task of no less importance is precision measurement of the decays of B and D mesons and  $\tau$  leptons as well as search for their rare decays. Although the detector is optimized for the study of CP asymmetry, it is also suitable for study of other processes in this energy region.

BINP members of the collaboration participate in the analysis of the results of measurements of the cross sections of the  $e^+e^-$  annihilation into hadrons using the radiative return and two-photon processes with registration of scattered electrons. Our physicists also work on the analysis of semileptonic decays and measurement of the module of the  $V_{ub}$  element of the CKM matrix.

Series of analysis on the measurement of the meson-photon transition form factors for pseudoscalar mesons  $\pi^0$ ,  $\eta'$ ,  $\eta$  and  $\eta_c$  at high squared transfer momentum ( $Q^2$ ), of 4 to 40  $\text{GeV}^2$ , was completed in 2010.

The data obtained for the meson-photon transition form factors makes it possible to get unique information about the meson wave functions. These functions describe the momentum distributions of quarks inside mesons and are used for theoretical calculations of many processes in quantum chromodynamics (QCD). The most important and unexpected result of these measurements is that the wave function of  $\pi^0$  meson is very different from the wave functions of other light mesons  $\eta$  and  $\eta'$ . The measured normalized form factors for  $\pi^0$ ,  $\eta$ , and  $\eta'$  mesons are shown in Fig.(1.4)1 as functions of  $Q^2$ . The horizontal line shows the value of the asymptotic limit of the form factor calculated within the framework of QCD. The form factor of  $\pi^0$  meson, in contrast to the form factors of  $\eta$  and  $\eta'$ , exceeds the asymptotic limit at  $Q^2 \simeq 10 \text{ GeV}^2$  and will approach it from above. Such behavior can be explained by the assumption that the wave function of  $\pi^0$  meson is much broader than the corresponding functions for  $\eta$  and  $\eta'$ .

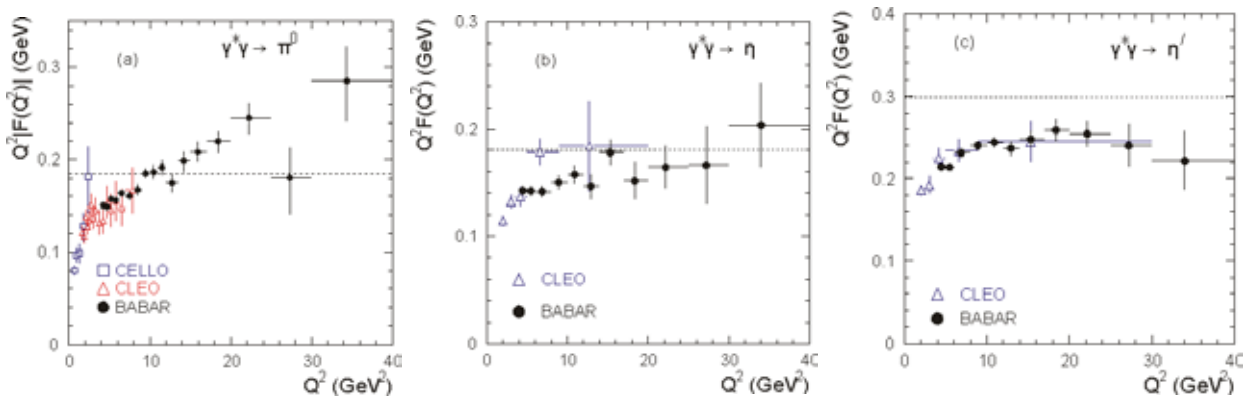


Fig.(1.4)1. Normalized meson-photon transition form factors for  $\pi^0$  (a),  $\eta$  (b) and  $\eta'$  (c) mesons. The horizontal dotted line shows the value of the asymptotic limit for the form factor.

Due to the large mass of c quark, the form factor of  $\eta_c$  meson is expected to weakly depend on the shape of the wave function. Measurements made with the BABAR detector confirm this QCD prediction.

Results obtained on the BABAR and Belle detectors showed the need for further experiments in this energy region but with a much higher luminosity. A decision was made to build such SuperB factory in Italy. BINP physicists actively participate in the development of the accelerator and the detector.

Identification of particles in the detector for SuperB will be performed by the DIRC – system for registration of Cherenkov rings. BINP physicists are involved in the development of the modeling program for light collection in this system. They suggested supplementing the DIRC with the detector of Cherenkov rings based on “focusing” Aerogel (FARICH). This proposal is now being studied by the collaboration. The FARICH detector is to be placed between the drift chamber and end cap calorimeter. The detector uses multilayer focusing aerogel and pixel photon detectors based on microchannel plates. The total number of channels of the electronics is expected to be about 20 thousands. This system increases the solid angle for identification of particles. The modelling shows that the reliability of identification of pions and kaons will exceed 5 standard deviations in the momentum range of up to 5  $\text{GeV}/c$ .

## 1.12 Participation in the ATLAS experiment on the Large Hadron Collider (LHC)

The year 2010 became the first successful year of full-scale experiments on the Large Hadron Collider. On March 30, collisions of proton beams were obtained at a record-high energy of 7 TeV in the center-of-mass system. During the year, parameters of the collider were steadily improving: the number of proton bunches exceeded 400; the peak luminosity reached  $2 \cdot 10^{32} \text{ cm}^{-2} \text{ s}^{-1}$ ; and the energy stored in the beams attained 28 MJ.

The integral of acquired statistics was 45 inverse picobarns. Analysis of these data made it possible to measure the cross sections of the known processes of the Standard Model in the new energy region and start the search for the New Physics. In particular, more than 20,000 events of production of vector bosons (W and Z) and dozens of events with the production of a top quark and antiquark were reconstructed. 25 papers were published, some of them setting the world's best upper limits for new or exotic processes.

During one month at the end of the year, data were acquired at collisions of lead ions. These events are characterized by a multiplicity of charged particle tracks (about 1000 per collision) which is even greater than that at collision of protons. The ATLAS detector for the first time revealed the effect of significant imbalance in the energy of hadron jets at central collisions of heavy ions, which indicates formation of a qualitatively new state of matter at very high energy densities. This effect was predicted by theorists (e.g. by Bjorken) as early as in the 80s.

In 2010, BINP physicists took part in the data acquisition in the experiment control room (ATLAS point 1) within the system of liquid-argon calorimeters. They were also working on the monitoring and analysis of the quality of the data of the calorimeters and their calibration. As before, special attention was paid to the "presampler" (preshower mini-detector) of the end electromagnetic calorimeter – BINP was fully responsible for this system at all phases, from design and beam tests to installation in the detector and putting into operation.

Work on the analysis of the physical processes is also getting more vigorous.

Since the spring of 2009, within the framework of the collaboration with the Universities of Pittsburgh and Uppsala, BINP members have been exploring the possibility to observe heavy Majorana neutrinos in a channel with two leptons and two jets in the final state, within the Left-Right Symmetric Model, see Fig. (1.12)1. This model can explain the presence of a nonzero mass of ordinary light neutrinos (which follows from observation of their oscillations) as well as the emergence of asymmetry between matter and antimatter (the baryon number B and the lepton number L can be violated separately under the condition of B-L conservation). One can notice that this model is complementary to many supersymmetric models since the latter are characterized by large missing transverse energy in an event.

Full simulation and reconstruction of the processes of the effect (for several values of the masses of heavy intermediate boson  $W_R$  and Majorana neutrinos) and background processes were carried out. All the statistics acquired by the ATLAS detector in 2010 and available for analysis (34 inverse picobarns) was processed. The number of selected events in the data is consistent with the expected contribution from the background processes of the Standard Model. Fig.(1.12)2 shows the region of masses of the right vector boson and Majorana neutrino that was excluded at the level of 95%. Even with a small statistics acquired so far, it is a significant improvement as compared with the Tevatron results (the limit on the heavy vector boson mass is at the level of 740 GeV). A report made by the BINP member Kirill Skovpen "ATLAS sensitivity to Left-Right Symmetry at 7 TeV" at the CERN-ISTC workshop (September 1-5, 2010, BINP, Novosibirsk, Russia) took the first place in the competition of young scientists.

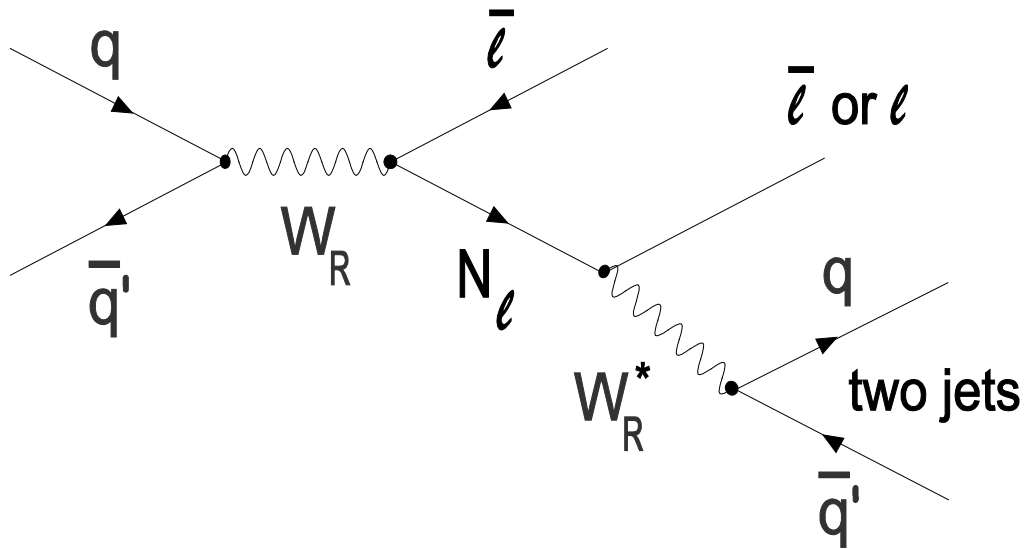


Fig.(1.12)1. Chart of the production of heavy right  $W_R$  boson with subsequent decay to lepton and heavy Majorana neutrino  $N_l$  in the Left-Right Symmetric Model. Two leptons and two hadron jets are detected in the final state.

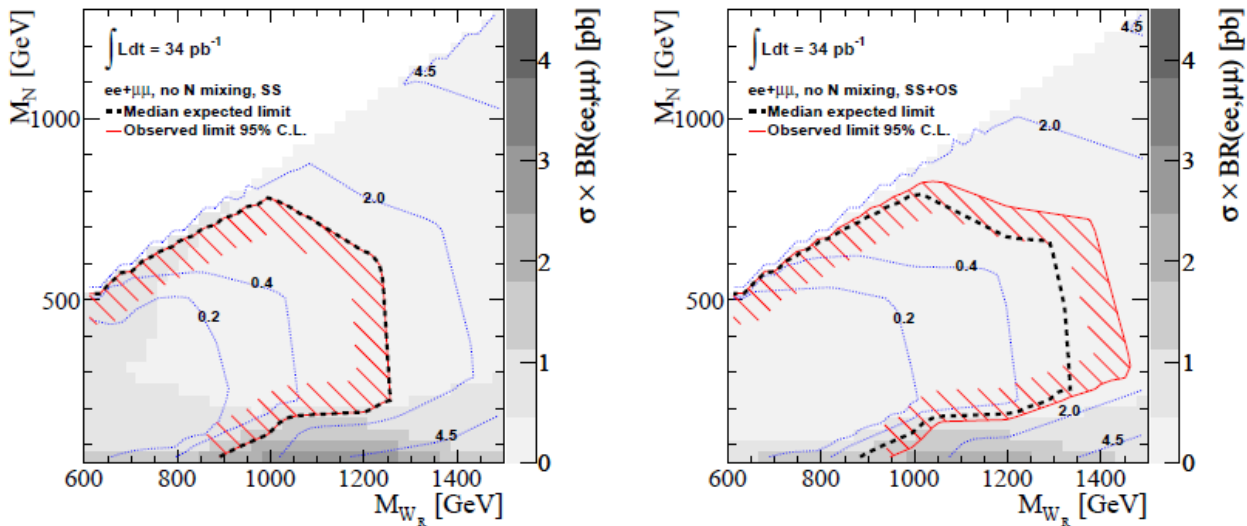


Fig.(1.12)2. Median expected and observed upper limits on the masses of heavy right  $W_R$  boson and heavy Majorana neutrino  $N$ . The left chart is for events with leptons of the same type and sign (SS = Same Sign) in the final state, the right chart also includes events with leptons of the opposite sign (OS = Opposite Sign). The boundary of the singled out (at the level of 95%) area is shown with the red shading. The contours show the corresponding upper limits on the cross sections (pikobarns).

Much effort is also made on the development of the computer infrastructure and related software. Data from an experiment of such scale (several petabytes of data input per year) can be stored and processed only with well-coordinated work of many powerful computing clusters worldwide, using the advanced technology of distributed computing GRID. The peak load of the network was as high as 6 gigabits per second.

BINP programmers had made and continue to make a substantial contribution to the creation and development of critical services and utilities for management of the distributed computing system (ATLAS GRID) - Monitoring of Data Replicating and Information System.

The power of the BINP GRID cluster increases; the capacity of communication channels is improved. Cooperation with the computer centers of NSU and SB RAS is developed.

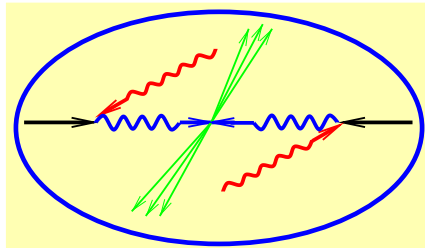
Besides, physicists and computer programmers of BINP are actively working in the group of system administrators for the data acquisition system and the trigger. They provide installation and maintenance of the software of the whole system for data acquisition and monitoring. An important part of the work is putting the computer hardware for the High Level Trigger (HLT) into operation. 10 crates of new equipment were put into operation in the third and fourth quarters of 2010, which added 5 000 cores to the HLT farm.

Currently, a draft for upgrading the LHC collider is being developed with a purpose to increase the luminosity by an order, to  $10^{35} \text{ cm}^{-2}\text{s}^{-1}$ . In this regard, works were started on upgrading the ATLAS detector for operation at such luminosity.

The BINP group takes part in the experiment on the study of the performance of the liquid-argon calorimeters for the ATLAS detector at a luminosity of  $10^{35} \text{ cm}^{-2}\text{sec}^{-1}$ . For these purpose, mini-modules of calorimeters (electromagnetic, hadron and forward) were fabricated and placed in cryostats with liquid argon. The modules are being irradiated with the extracted proton beam of the U-70 accelerator in Protvino with an energy of 50 GeV (the intensity of the beam can be varied in a wide range:  $10^7 \div 10^{12}$  particles per second). The BINP group is fully responsible for the mini-module of the electromagnetic calorimeter and participates in the data acquisition and analysis (the last run was held in April 2010).

The work is carried out with the participation of A.V. Anisenkov, O.L. Beloborodova, S.D. Belov, V.S. Bobrovnikov, A.G. Bogdanchikov, A.R. Buzykaev, A.S. Zaitsev, V.F. Kazanin, V.I. Kaplin, A.A. Korol', D.S. Krivashin, R.E. Kuskov, D.A. Maksimov, A.L. Maslennikov, I.O. Orlov, S.V. Peleganchuk, A.I. Senchenko, K.Yu. Skovpen, A.M. Sukharev, A.A. Talyshev, Yu.A. Tikhonov.

## 1.13 The Photon Collider



In 2004, the project of International Linear Collider (ILC) based on a superconducting technology was launched. In addition to the  $e^+e^-$  physics program, the ILC will provide an opportunity to study  $\gamma\gamma$  and  $\gamma e$  interactions (photon collider or PLC), where high energy photons can be obtained using Compton backscattering of the laser light off the high energy electrons. In 2007 the ILC Reference Design Report (RDR) was published. In 2008 two detector conceptions were approved for further development. Owing to a high ILC cost further plans are quite uncertain. The situation can change after discovery of new physics at the LHC.

Meanwhile the ILC community is searching for possible ways of the cost reduction. One of such suggestions is a construction of the photon collider Higgs factory as a precursor to ILC. In order to produce a single Higgs boson with the mass 120 GeV at the photon collider one needs the electron energy  $2E=160$  GeV, while the Higgs production in  $e^+e^-$  to HZ requires  $2E=230$  GeV and a positron production system. We reported our view on this suggestion at the conference ILC08/LCWS08. A detailed discussion took place at TILC09. Although we are most interested in creation of the photon collider but, in our opinion, it would be more reasonable to construct from the very beginning the linear collider on the energy  $2E=230$  GeV capable to produce the Higgs boson (if it really exists) in  $e^+e^-$  mode. From a financial points of view such photon collider is unlikely to be significantly cheaper because  $e^+e^-$  beams will be constructed in parallel, all this will lead only to incremental cost of the collider. Moreover, the physics community will never agree with additional delay of  $e^+e^-$  experiments by 5-6 years.

Participant of the work: V.I. Telnov.

2

ELECTRO- AND  
PHOTO-NUCLEAR  
PHYSICS



## 2.1 Experiments with internal targets

The results of the experiment on the measurement of the ratio ( $R = \sigma_{e+p}/\sigma_{e-p}$ ) of elastic electron-proton and positron-proton scattering cross sections were processed in 2010. This experiment is interesting because of the possibility of determination of the contribution of two-photon exchange (TPE) to this process. Information on TPE, in turn, will probably give an opportunity to explain the dramatic contradictions in the results of recent polarization-technique experiments at TJNAF, USA, on the measurement of the proton form-factors and the results of earlier, non-polarization measurements, where the form-factors were determined from analysis of differential cross sections of the reaction in the assumption of validity of the one-photon approximation.

An important stage of the processing is the introduction of radiation corrections. Formulas provided by Fadin and Feldman to describe the emission of real photons in this reaction were applied. Comparison of the radiation corrections made by complete formulas with the so called soft-photon approximation shows the difference in their results.

Preliminary results of the experiment are shown in Fig.(2.1)1. Results of this experiment are still being processed.

There are plans to continue the TPE measurements with a higher accuracy under other kinematic conditions.

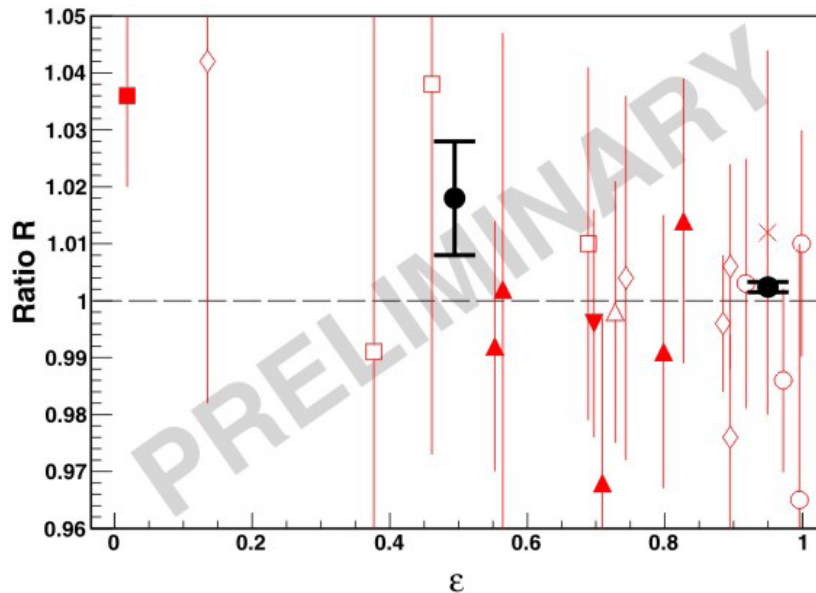


Fig.(2.1)1. Preliminary results of the experiment (black circles) compared with the available data.

Besides, the works on the construction of the photon tagging system (PTS) are underway. Dipole magnets D1 and D3 were made and subjected to tests and magnetic measurements. The measurements, in general, confirmed the correctness of calculations from field integrals and field homogeneity. For example, Fig. 2 shows field integrals of magnets D1 and D3 along the electron beam trajectory in dependence on the current in the coils of the magnets. One can see small differences in the field integrals; they will be eliminated by currents of trim coils. The development effort on magnet D2 is completed. The fabrication of the magnet is underway in the workshop of the institute.

The vacuum chamber of the experimental section is divided into three parts. The fabrication of the first (along the beam trajectory) part of the vacuum chamber as well as the central one with a storage cell is completed. The development effort on the last (along the beam trajectory) section of the vacuum chamber is completed; its fabrication is underway in the workshop of the Institute.

The engineering development of secondary members for diagnostics of electron beam position in the PTS experimental section was almost completed. It only remains to develop the imaging of the output of the third receiver (located after dipole D2) of synchrotron radiation from the vacuum chamber of the section. It is necessary for the on-line control of electron beam in the vertical direction.

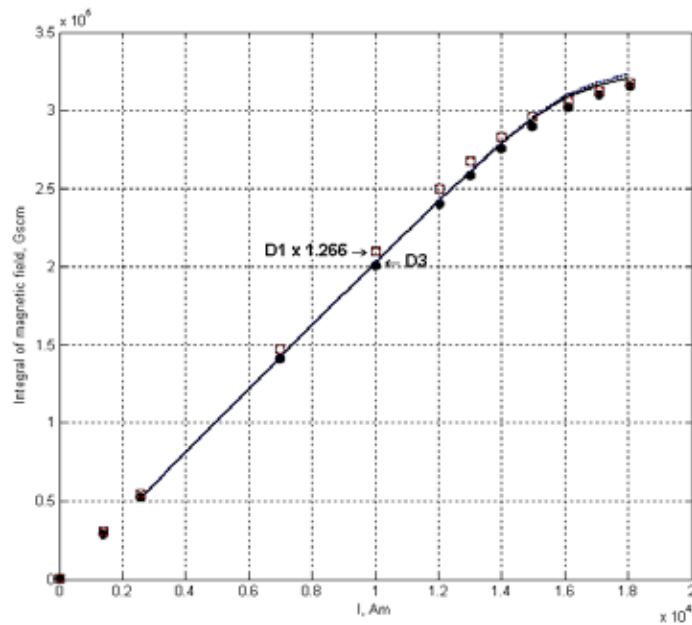


Fig.(2.1)2. Field integrals of magnets D1 and D3 along the electron beam trajectory in dependence on the current of the coils of the magnets. The black dots show the results of measurements of magnet D1 (multiplied by a "correct" coefficient of 1.266); the hollow squares are for the measurements of magnet D3. The solid and dashed lines present the results of the calculation of magnets D1 and D3 by the MERMAID program.

The tagging system will include three coordinate detectors and two scintillation counters ("sandwiches"). The coordinate detectors will be created based on the cascade gas electron multipliers (GEMs). The GEMs were chosen because of a number of advantages. For instance, they can have high spatial resolution and work in intense particle fluxes. Another important argument was the fact that BINP had already developed 3-layer 2-coordinate GEMs for the scattered-electron system of the KEDR detector on the VEPP-4 collider. The parameters of these detectors are well suited for the PTS and can be adapted for our case. In addition, the copper coating on the GEM elements will be made 1 micron thick, which will reduce the thickness of the detectors to 0.15%  $X_0$  ( $X_0$  is the radiation unit of length). It is important for achieving high resolution of the PTS in the energy and angles of electron emission. The manufacturing of these detectors was started.

A new stage of modeling the tagging system was completed. The total resolution of the PTS in the electron energy varies from 4 to 11 MeV for final electron energies of 500 to 1000 MeV (at an initial energy of 2 GeV). The resolution in the horizontal angle is about 2 mrad, which is about 1 mrad in the vertical angle.

To improve the parameters of the tensor polarized deuterium target, we installed an additional pump in the source of polarized deuterium atoms, which improved the vacuum in the second stage of the source pump-out. This additional pump-out gave us an opportunity to study the formation of a free molecular jet from the transient flow regime. This process is underexplored; the knowledge of the position and size of the area after which the flow becomes a free-molecular one is necessary to select the focusing properties of the magnetic system of the source.

This work was supported by RFBR grant № 08-02-01155 and Federal Agency of Education (State contract P522 dated August 5, 2009).

The experiments with internal targets are carried out in collaboration with groups from Tomsk, St. Petersburg, NIKHEF (Netherlands), ANL (USA), and IKF JGU (Mainz, Germany).

BINP members participating in the work: L.M. Barkov, A.V. Gramolin, V.F. Dmitpiev, S.A. Zevakov, I.V. Karnakov, B.A. Lazarenko, E.B. Levichev, S.I. Mishnev, N.Yu. Muchnoi, D.M. Nikolenko, I.A. Rachek, R.Sh. Sadykov, D.K. Toporkov, Yu.V. Shestakov, and L.I. Shekhtman.

3

THEORETICAL PHYSICS



## 3.1 Strong interaction

### Matching of the low-x evolution kernels.

V.S. Fadin, R. Fiore, A.V. Grabovsky  
Nucl. Phys. B 831 (2010) 248-261

It is demonstrated that the ambiguity of the low-x evolution kernels in the next-to-leading order (NLO) permits one to match the Möbius form of the BFKL kernel and the kernel of the colour dipole model and to construct the Möbius invariant NLO BFKL kernel in  $N=4$  supersymmetric Yang-Mills theory.

### Scalar contribution to the BFKL kernel.

R.E. Gerasimov, V.S. Fadin  
Yadernaya Fizika, 73, No. 7 (2010) pp. 1254-1268,  
Physics of Atomic Nuclei, 73, No. 7 (2010) pp. 1214-1228

Supersymmetric non-Abelian gauge theories, in particular the Yang-Mills theory with  $N=4$  supersymmetry which is intensively discussed now in connection with its integrability, contain scalar particles. The contribution of such particles to the kernel of the BFKL equation is calculated. A great cancellation between the virtual and real parts of this contribution, analogous to the cancellation in the quark contribution in QCD, is observed. The reason of this cancellation is discovered. This reason is common for contribution of particles with any spin. Understanding of this reason permits to obtain the total contribution without the complicated calculations, which are necessary for finding separate pieces.

### Möbius representation of the BFKL kernel.

V.S. Fadin  
In: Subtleties in Quantum Field Theory, Ed. D.Diakonov, Gatchina, 2010, p.76-103

Discovered by L.N. Lipatov, conformal (Möbius) invariance of the BFKL equation for scattering of colourless particles in the leading logarithmic approximation (LLA) is extremely significant for integrability of the equation. Therefore, it is very important to know conformal properties of the BFKL kernel in the next-to-leading order (NLO). Evidently, in QCD the conformal invariance is violated by running of  $\alpha_s$ . It turns out, that the ambiguity of the NLO kernel, caused by the possibility to redistribute radiative corrections between the kernels and the impact factors, makes possible to find the quasi-conformal representation of the kernel, where the Möbius invariance is violated only by terms proportional to the  $\beta$ -function. It permits also to get agreement between the BFKL approach and the colour dipole model.

### Check of the gluon reggeization condition in the next-to-leading order: quark part.

M.G. Kozlov, A.V. Reznichenko, V.S. Fadin  
Preprint INP 2010-26, 27 p.; accepted Phys.Atom.Nucl. 74 (2011),  
Yad. Phys.: 74 (2011) 784-796

The bootstrap condition for gluon production in the multi-Regge kinematics in the next to leading order is considered. The bootstrap conditions result from the requirement of the compatibility of the Regge form of QCD amplitudes with the  $s$ -channel unitarity and represent non-linear restraints on the Reggeized gluon trajectory and vertices. Their fulfillment provides the gluon Reggeization, i.e. the Regge form of elastic and inelastic amplitudes. The condition under consideration remained only one to be checked. The demonstration of its fulfillment is the last step in the proof of the gluon Reggeization in the next-to-leading approximation. In this paper this demonstration is presented for the quark part of the bootstrap condition.

**Low- $x$  evolution equations in Möbius representation.**

V.S. Fadin, R. Fiore, A.V. Grabovsky and A. Papa  
Physics of Particles and Nuclei, 41, No.6(2010), pp. 935-938

The Möbius form of the BFKL kernel in the next-to-leading order (NLO) in theories containing fermions and scalars in arbitrary representations of the colour group is presented. The ambiguity of the NLO kernels permits to get agreement between the BFKL approach and the colour dipole model and to find the quasi-conformal representation of the BFKL kernel.

**Quantum Chromodynamics: Perturbative and Nonperturbative aspects.**

B.L. Ioffe, V.S. Fadin, L.N. Lipatov  
Cambridge University Press, 2010

The book is devoted to the strong interaction theory - QCD. It contains a brief introduction in QCD and description of the most important properties of QCD, such as asymptotic freedom, spontaneous violation of chiral symmetry, quantum anomalies and vacuum structure of QCD. Besides this, the book covers various aspects of perturbative and nonperturbative approaches to QCD, which are not so widely discussed in other sources: divergence of perturbation series, QCD sum rules, evolution equations, colour coherence in soft gluon emission, BFKL approach, high energy effective action, integrability of the BFKL dynamics.

**Spin-dependent part of  $p\bar{p}$  interaction cross section and Nijmegen potential.**

V. F. Dmitriev, A. I. Milstein, S. G. Salnikov  
Physics Letters B 690, 427 (2010)

Low energy proton-antiproton interaction is considered taking into account the polarization of both particles. The corresponding cross sections are calculated using the Nijmegen nucleon-antinucleon optical potential. Then they are applied to the analysis of the polarization buildup which is due to the interaction of stored antiprotons with polarized protons of a hydrogen target. It is shown that, at realistic parameters of a storage ring and a target, the filtering mechanism may provide a noticeable polarization in a time comparable with the beam lifetime.

**Matching QCD and HQET heavy-light currents at three loops.**

S. Bekavac, A.G. Grozin, P. Marquard, J.H. Piclum, D. Seidel, M. Steinhauser  
Nucl. Phys.B 833 (2010) 46-63

We consider the currents formed by a heavy and a light quark within Quantum Chromodynamics and compute the matching to Heavy Quark Effective Theory to three-loop accuracy. As an application we obtain the third-order perturbative corrections to ratios of  $B$ -meson decay constants.

**Matching heavy-quark fields in QCD and HQET at three loops.**

A.G. Grozin  
Phys. Lett.B 692 (2010) 161-165

The relation between the heavy-quark field in QCD and the corresponding field in HQET is derived up to three loops, and to all orders in the large- $\beta_0$  limit. The corresponding relation between the QED electron field and the Bloch-Nordsieck one is gauge invariant to all orders. We also prove that the  $\overline{MS}$  anomalous dimension of the QED electron field depends on the gauge parameter only at one loop.

**Matching QCD and HQET at three loops.**

A.G. Grozin

Nucl. Phys.B (Proc. Suppl.)205-206 (2010) 301-307

QCD/HQET matching for the heavy-quark field and heavy-light quark currents with three-loop accuracy is discussed.

**Mass spectrum in supersymmetric QCD and problems with the Seiberg duality.  
Equal quark masses.**

V.L. Chernyak

JETP,110(2010)383-405,(ЖЭТФ, 137 (2010), стр. 437-459)

The mass spectra are found analytically in supersymmetric Quantum Chromodynamics (SQCD) with arbitrary numbers of  $N_c$  colors and  $N_f$  flavors of quarks with equal small masses, within the dynamical scenario where the quarks can condense in colorless flavored pairs ( $\bar{Q}_j$ - $Q^i$ ), while the color remains unbroken. The results appeared to be even qualitatively different from numerous previous publications in the literature based on the hypothesis of duality proposed by N. Seiberg. It is shown that, unlike the ordinary (that is, non-supersymmetric) Quantum Chromodynamics (QCD), the mass spectra and even the phase states of this theory are highly sensitive to the ratio  $N_f/N_c$ . The mass spectra of the original (direct) theory and its dual variant proposed by N. Seiberg are compared and shown to be parametrically different, so that these two theories are not equivalent.

**On mass spectrum in SQCD. Unequal quark masses.**

V.L. Chernyak

JETP,111 (2010) 949-961, (ЖЭТФ, 138 (2010), стр. 1-12)

In supersymmetric Quantum Chromodynamics (SQCD) with arbitrary numbers of  $N_c$  colors and  $N_f$  flavors of quarks with unequal small masses, the mass spectra and phase states are found analytically, within the dynamical scenario where the quarks can condense in colorless flavored pairs ( $\bar{Q}_j$ - $Q^i$ ). It is shown that, depending on the values of  $N_c$ ,  $N_f$  and the values of quark masses the theory can be in the four different phase states. The properties of each of these phases and their mass spectra are described.

**Exclusive  $\gamma\gamma$  – processes.**

V.L. Chernyak

Chinese Physics C,34 (2010) 822-830

A short review of the current state of experimental and theoretical studies of various exclusive reactions with the two-photon initial state is presented. It is discussed in detail what information about the hadron wave functions properties can be extracted from the recent experimental measurements of such processes. A comparison is made with predictions of different theoretical models.

**Nucleon polarization in the process  $e^+e^- \rightarrow N\bar{N}$  near threshold**

A.E. Bondar, V.F. Dmitriev, A.I. Milstein, V.M. Strakhovenko

e-Print: arXiv:1012.4638 [hep-ph] Dec 2010.

The process  $e^+e^- \rightarrow N\bar{N}$  is studied nearby a threshold with account for polarizations of all initial and final particles. The nucleon polarization  $\zeta^N$  reveals a strong energy dependence due to that of the nucleon electromagnetic form factors  $G_E(Q^2)$  and  $G_M(Q^2)$  caused by the final-state interaction of nucleons. It is shown that the modulus of the ratio of these form factors and their relative phase can be determined by measuring  $\zeta^N$  along with the differential cross section. The polarization degree is analyzed using Paris  $N\bar{N}$  optical potential for calculation of the form factors. It turns out that  $|\zeta^N|$  is high enough in a rather wide

energy range above the threshold. Being especially high for longitudinally polarized beams,  $|\zeta^N|$  is noticeable even if both  $e^+e^-$  beams are unpolarized.

### Effect of quark-mass variation on big bang nucleosynthesis

J.C.Berengut, V.F.Dmitriev, V.V.Flambaum  
Phys.Lett.,B683,(2010),114

We calculate the effect of variation in the light-current quark mass,  $m_q$ , on standard big bang nucleosynthesis. A change in  $m_q$  at during the era of nucleosynthesis affects nuclear reaction rates, and hence primordial abundances, via changes the binding energies of light nuclei. It is found that a relative variation of  $\delta m_q/m_q = 0.016 \pm 0.005$  provides better agreement between observed primordial abundances and those predicted by theory. This is largely due to resolution of the existing discrepancies for  ${}^7\text{Li}$ . However this method ignores possible changes in the position of resonances in nuclear reactions. The predicted  ${}^7\text{Li}$  abundance has a strong dependence on the cross-section of the resonant reactions  ${}^3\text{He}(d,p){}^4\text{He}$  and  $t(d, n){}^4\text{He}$ . We show that changes in  $m_q$  at the time of BBN could shift the position of these resonances away from the Gamow window and lead to an increased production of  ${}^7\text{Li}$ , exacerbating the lithium problem.

### Space-time dimensionality $\mathcal{D}$ as complex variable: Calculating loop integrals using dimensional recurrence relation and analytical properties with respect to $\mathcal{D}$ .

R.N. Lee  
Nucl.Phys. B830 (2010) 474-492.

We show that dimensional recurrence relation and analytical properties of the loop integrals as functions of complex variable  $\mathcal{D}$  (space-time dimensionality) provide a regular way to derive analytical representations of loop integrals. The representations derived have a form of exponentially converging sums. Several examples of the developed technique are given.

### Analytic Results for Massless Three-Loop Form Factors.

R.N. Lee, A.V. Smirnov, V.A. Smirnov.  
JHEP 1004(2010) 020

We evaluate, exactly in  $d$ , the master integrals contributing to massless three-loop QCD form factors. The calculation is based on a combination of a method recently suggested by one of the authors (R.L.) with other techniques: sector decomposition implemented in FIESTA, the method of Mellin-Barnes representation, and the PSLQ algorithm. Using our results for the master integrals we obtain analytical expressions for two missing constants in the  $\epsilon$ -expansion of the two most complicated master integrals and present the form factors in a completely analytic form.

### Dimensional recurrence relations: an easy way to evaluate higher orders of expansion in $\epsilon$ .

R.N. Lee, A.V. Smirnov, V.A. Smirnov  
Nucl.Phys.Proc.Suppl. 205-206 (2010) 308-313

Applications of a method recently suggested by one of the authors (R.L.) are presented. This method is based on the use of dimensional recurrence relations and analytic properties of Feynman integrals as functions of the parameter of dimensional regularization,  $d$ . The method was used to obtain analytical expressions for two missing constants in the  $\epsilon$ -expansion of the most complicated master integrals contributing to the three-loop massless quark and gluon form factors and thereby present the form factors in a completely analytic form. To illustrate its power we present, at transcendentality weight seven, the next order of the  $\epsilon$ -expansion of one of the corresponding most complicated master integrals. As a further application, we present three previously unknown terms of the expansion in  $\epsilon$  of the three-loop non-planar massless propagator diagram. Only multiple  $\zeta$ -values at integer points are present in our result.

## Calculating multiloop integrals using dimensional recurrence relation and $\mathcal{D}$ -analyticity.

R.N. Lee.

Nucl.Phys.Proc.Suppl. 205-206 (2010) 135-140

We review the method of the calculation of multiloop integrals recently suggested by the author. A simple method of derivation of the dimensional recurrence relation suitable for automatization is given. Some new analytic results are given.

## 3.2 CP nonconservation

### Upper Limits on Electric and Weak Dipole Moments of $W$ -Boson.

A.E. Blinov, A.S. Rudenko

Phys. Lett. B 699, 287 (2011)

The total cross-sections of the reaction  $e^+e^- \rightarrow W^+W^-$ , as measured at LEP-II at centre-of-mass energies  $2E \simeq 200$  GeV are used to derive the upper limits on the parameters of  $CP$ -violating ( $P$ -odd and  $C$ -even) triple gauge-boson couplings  $WW\gamma$  and  $WWZ$ .

### Can $CP$ -violation be observed in heavy-ion collisions?

A.S. Rudenko, I.B. Khriplovich

Canadian Journal of Physics 89, 63, 2011

We demonstrate that, at least at present, there is no convincing way to detect  $CP$ -violation in heavy-ion collisions.

### $K_{13\gamma}^+$ decay revisited: branching ratio and $T$ -odd momenta correlation.

A.S. Rudenko, I.B. Khriplovich

Soviet Journal of Nuclear Physics 74, 1 2011

We calculate the branching ratios of the  $K_{13\gamma}^+$  decays, and the  $T$ -odd triple momenta correlations, due to the electromagnetic final state interaction, in these processes. The contributions on the order of  $\omega^{-1}$  and  $\omega^0$  to the corresponding amplitudes are treated exactly. For the branching ratios the corrections on the order of  $\omega^0$  are estimated and demonstrated to be small. We compare the results with those of other authors. In some cases our results differ considerably from the previous ones.

## 3.3 Quantum electrodynamics

### Pair creation by a photon in an electric field.

V.N. Baier, V.M. Katkov

Phys. Lett. A, 374, (2010) 2201-2206.

The total probability of pair creation by a photon in a constant and homogeneous electric field is found with using the polarization operator in this field. The approximations of this probability are developed in four overlapping regions of photon energy. At high energy the corrections to the standard quasiclassical approximation have been calculated. In the region of intermediate energies the saddle point method is used for the calculation of the process probability. The probability of pair creation in an electric field in this energy interval exceeds essentially the probability in the corresponding magnetic field. For smaller photon energy the low energy approximation has been developed. At very low photon energy the probability of the absorption of soft photon by the particles creating by internal field is calculated.

**Exact theory of the photoproduction of charged particles in external fields.**

V.M. Katkov

Book of abstracts of the International conference "Channaling 2010", Ferrara - Italy, p.15

The probability of pair creation by a photon in a constant and homogeneous electromagnetic field of an arbitrary configuration is calculated with using the imaginary part of the polarization operator. Separating of the photon energy divisions is the same as in an electric field. It is shown that, in the energy region higher than the threshold of pair creation in a magnetic field, a weak electric field vanishes the root divergence in the probability of pair creation on the Landau energy levels. At low photon energy the electric field action onto the process dominates and an influence of magnetic field is connected with its interaction with the magnetic moment of creating particles. This interaction, in particular, has appeared in the distinction of the pair creation probability by field for scalar and spinor particles.

**Application of the DRA method to the calculation of the four-loop QED-type tadpoles.**

R.N. Lee, I.S. Terekhov.  
arXiv:1010.6117 [hep-ph]

We apply the DRA method to the calculation of the four-loop QED-type tadpoles. For arbitrary space-time dimensionality  $D$  the results have the form of multiple convergent sums. We use these results to obtain the epsilon-expansion of the integrals around  $D=3$  and  $D=4$ .

**Analytic Epsilon Expansions of Master Integrals Corresponding to Massless Three-Loop Form Factors and Three-Loop  $g-2$  up to Four-Loop Transcendentality Weight.**

R.N. Lee, V.A. Smirnov.  
arXiv:1010.1334 [hep-ph]

We evaluate analytically higher terms of the epsilon-expansion of the three-loop master integrals corresponding to three-loop quark and gluon form factors and to the three-loop master integrals contributing to the electron  $g-2$  in QED up to the transcendentality weight typical to four-loop calculations, i.e. eight and seven, respectively. The calculation is based on a combination of a method recently suggested by one of the authors (R.L.) with other techniques: sector decomposition implemented in FIESTA, the method of Mellin-Barnes representation, and the PSLQ algorithm.

**The induced charge generated by the potential well in graphene.**

A. I. Milstein, I. S. Terekhov  
Phys.Rev. B 81, 125419 (2010)

The induced charge density,  $\rho_{ind}(r)$ , generated in graphene by the potential well of the finite radius  $R$  is considered. The result for  $\rho_{ind}(r)$  is derived for large distances  $r \gg R$ . We also obtained the induced charges outside of the radius  $r \gg R$  and inside of this radius for subcritical and supercritical regimes. The consideration is based on the convenient representation of the induced charge density via the Green's function of electron in the field.

**Effect of a strong laser field on  $e^+e^-$  photoproduction by relativistic nuclei.**

A. Di Piazza, E. Lotstedt, A.I. Milstein, C. H. Keitel  
Phys. Rev. A 81, 062122 (2010)

We study the influence of a strong laser field on the Bethe-Heitler photoproduction process by a relativistic nucleus. The laser field propagates in the same direction as the incoming high-energy photon, and

it is taken into account exactly in the calculations. Two cases are considered in detail. In the first case, the energy of the incoming photon in the nucleus rest frame is much larger than the electron's rest energy. The presence of the laser field may significantly suppress the photoproduction rate at soon-available values of laser parameters. In the second case, the energy of the incoming photon in the rest frame of the nucleus is less than and close to the electron-positron pair-production threshold. The presence of the laser field allows for the pair production process, and the obtained electron-positron rate is much larger than in the presence of only the laser and the nuclear field. In both cases, we have observed a strong dependence of the rate on the mutual polarization of the laser field and on the high-energy photon, and the most favorable configuration is with laser field and high-energy photon linearly polarized in the same direction. The effects discussed are, in principle, measurable with presently available proton accelerators and laser technology.

### **Polarization of the electron and positron produced in combined Coulomb and strong laser fields.**

A. Di Piazza, A.I. Milstein and C.Muller  
Phys. Rev. A 82, 062110 (2010)

The process of  $e^+e^-$  production in the superposition of a Coulomb and a strong laser field is considered. The pair production rate integrated over the momentum and summed over the spin projections of one of the particles is derived exactly in the parameters of the laser field and in the Born approximation with respect to the Coulomb field. The case of a monochromatic circularly polarized laser field is considered in detail. A very compact analytical expression of the pair production rate and its dependence on the polarization of one of the created particles is obtained in the quasiclassical approximation for the experimentally relevant case of an undercritical laser field. As a result, the polarization of the created electron (positron) is derived.

### **High-energy $e^+e^-$ photoproduction cross section close to the end of spectrum.**

A. Di Piazza, A.I. Milstein  
Phys. Rev. A 82, 042106 (2010)

We consider the cross section of electron-positron pair production by a high-energy photon in a strong Coulomb field close to the end of the electron or positron spectrum. We show that the cross section essentially differs from the result obtained in the Born approximation as well as from the result which takes into account the Coulomb corrections under the assumption that both electron and positron are ultrarelativistic. The cross section of bremsstrahlung in a strong Coulomb field by a high-energy electron is also obtained in the region where the final electron is not ultrarelativistic.

### **A positron source using channeling in crystals for linear colliders.**

X.Artru, R.Chehab, M.Chevallier, T. Kamitani, T. Omori, L. Rinolfi,  
V.M. Strakhovenko, T. Suwada, A. Variola, A. Vivoli  
Int.J.Mod.Phys.A25(2010)106

An alternative way to the conventional positron source is presented. This source is using two successive targets: the first one is a tungsten crystal, which  $\langle 111 \rangle$  axis is aligned with the beam direction, and the second is an amorphous target put at some distance from the crystal. Between the two targets a sweeping magnet takes off all or part of the charged particles coming out from the crystal. A large amount of photons is emitted from electrons of the primary beam channelled in a crystal. Consecutively, these photons create numerous  $e^+e^-$  pairs in the amorphous target. An optimization procedure is carried out, aiming to obtain the highest accepted yield after the capture system and the minimum Peak Energy Density Distribution in order to avoid thermal gradients, which are destructive for the target.

## 3.4 Gravity

### **Integration over connections in the discretized gravitational functional integrals.**

V. M. Khatsymovsky  
Mod. Phys. Lett. A, Vol. 25, pp. 351-368 (2010)

The result of integration over connections is poorly defined in the discrete field theory with non-compact gauge group with the Haar measure exponentially growing in some directions. This point is studied in the case of the functional integral for the discrete first order Einstein gravity. The result is defined as generalized function of the edge vectors or area tensors. The singular part of this function has support in the non-physical region. The regular part is exponentially suppressed at large areas/lengths and possesses a number of maxima at approximately the equidistant nonzero values of area. In other words, the most probable are a number of the equidistant values of the elementary area (of the order of Plank scale ( $10^{-33}\text{cm}^2$ )).

### **Defining integrals over connections in the discretized gravitational functional integrals.**

V. M. Khatsymovsky  
Mod.Phys.Lett.A, Vol. 25, pp. 1407-1423 (2010)

Integration over connections is studied in the discrete functional integral for the first order formulation of the Einstein gravity. The result is defined as generalized function of the edge vectors or area tensors. The result of the preceding work is obtained immediately in the Minkowsky spacetime, without passing to the Euclidean spacetime. The singular part of this function has support in the non-physical region. The regular part is exponentially suppressed at large areas/lengths. The basis integrals are calculated over which the general functional integral can be expanded.

### **A version of the connection representation of Regge action.**

V. M. Khatsymovsky  
Class. Quantum Grav., Vol. 27, p. 065003 (2010)

We define for any 4-tetrahedron (4-simplex) the simplest finite closed piecewise flat manifold consisting of this 4-tetrahedron and of the one else 4-tetrahedron identical up to reflection to the present one (call it bisimplex). Gravity action for the arbitrary piecewise flat manifold can be expressed in terms of sum of the actions for the bisimplices built on the 4-simplices constituting this manifold. We use representation of each bisimplex action in terms of rotation matrices (connections) and area tensors. Application of this representation to the path integral formalism is considered. One of the consequences is exponential suppression of the result at large areas or lengths (compared to Plank scale). It is important for the consistency of the simplicial description of spacetime.

## 3.5 Astrophysics

### **Capture of dark matter by the Solar System. Simple estimates.**

I.B. Khriplovich  
International Journal of Modern Physics D 20, 1, 2011

We consider the capture of galactic dark matter by the Solar System, due to the gravitational three-body interaction of the Sun, a planet, and a dark matter particle. Simple estimates are presented for the capture cross-section, as well as for density and velocity distribution of captured dark matter particles close to the Earth.

## 3.6 Nonlinear dynamics and quantum, chaos

### **Electron Quantum Transport Trough a Mesoscopic Device: Dephasing and Absorption Induced by Interaction with a Complicated Background.**

Valentin V. Sokolov

“Topics on Chaotic Systems; Selected Papers from CHAOS2009 International Conference”,  
World Scientific, pp. 309-319, (2010)

Decoherence during ballistic quantum transport trough a 2D mesoscopic open structure is an issue of great interest from the both, theoretical as well as experimental, points of view. Effects induced by interaction with a complicated many-body environment with a weak disorder is analyzed. The doorway resonance states excited in the structure via external channels are damped not only because of escape through such channels but also due to the ulterior population of the long-lived environmental states. Transmission of an electron with a given incoming through the structure turns out to be an incoherent sum of the flow formed by the interfering damped doorway resonances and the retarded flow of the particles re-emitted into the structure by the environment. Though the number of the particles is conserved in each individual event of transmission, there exists a probability that some part of the electron’s energy can be absorbed due to environmental many-body effects thus violating the time-reversal symmetry and, as a consequence, suppressing the weak localization phenomenon. Besides the electron can disappear from the resonance energy interval and elude observation at the resonant transmission energy imitating thereby loss of the particles. The both decoherence and absorption phenomena are treated within the framework of a unit microscopic model based on the general theory of the resonance scattering. All the effects discussed are controlled by the only parameter: the spreading width of the doorway resonances, that uniquely determines the decoherence rate.

### **Ballistic electron Quantum transport in a presence of a disordered background.**

Valentin V. Sokolov

J. Phys. A: Math. Theor. 43(2010) 265102

Effect of a complicated many-body environment is analyzed on the electron random scattering by a 2D mesoscopic open ballistic structure. A new mechanism of decoherence is proposed. The temperature of the environment is supposed to be zero whereas the energy of the incoming particle  $E_{in}$  can be close to or somewhat above the Fermi surface in the environment. The single-particle doorway resonance states excited in the structure via external channels are damped not only because of escape through such channels but also due to the ulterior population of the long-lived environmental states. Transmission of an electron with a given incoming  $E_{in}$  through the structure turns out to be an incoherent sum of the flow formed by the interfering damped doorway resonances and the retarded flow of the particles re-emitted into the structure by the environment. Though the number of the particles is conserved in each individual event of transmission, there exists a probability that some part of the electron’s energy can be absorbed due to environmental many-body effects. In such a case the electron can disappear from the resonance energy interval and elude observation at the fixed transmission energy  $E_{in}$  thus resulting in seeming loss of particles, violation of the time reversal symmetry and, as a consequence, suppression of the weak localization. The both decoherence and absorption phenomena are treated within the framework of a unit microscopic model based on the general theory of the resonance scattering. All the effects discussed are controlled by the only parameter: the spreading width of the doorway resonances, that uniquely determines the decoherence rate.

## Classical Versus Quantum Dynamical Chaos: Sensitivity to External Perturbations, Stability and Reversibility.

Valentin V. Sokolov, Oleg V. Zhirov, and Yaroslav A. Kharkov

to appear in: "Topics on Chaotic Systems: Selected Papers from the CHAOS2010 International Conference" (Chania, Crete, Greece, 1-4 June 2010), World Scientific, (2011)

The extraordinary complexity of classical trajectories of typical nonlinear systems that manifest stochastic behavior is intimately connected with exponential sensitivity to small variations of initial conditions and/or weak external perturbations. In rigorous terms, such classical systems are characterized by positive *algorithmic complexity* described by the Lyapunov exponent or, alternatively, by the Kolmogorov-Sinai entropy. The said implies that, in spite of the fact that, formally, any however complex trajectory of a perfectly isolated (closed) system is unique and differentiable for any certain initial conditions and the motion is perfectly reversible, it is impractical to treat that sort of classical systems as closed ones. Inevitably, arbitrary weak influence of an environment crucially impacts the dynamics. This influence, that can be considered as a noise, rapidly effaces the memory of initial conditions and turns the motion into an irreversible random process.

In striking contrast, the quantum mechanics of the classically chaotic systems exhibit much weaker sensitivity and strong memory of the initial state. Qualitatively, this crucial difference could be expected in view of a much simpler structure of quantum states as compared to the extraordinary complexity of random and unpredictable classical trajectories. However the very notion of trajectories is absent in quantum mechanics so that the concept of exponential instability seems to be irrelevant in this case. The problem of a quantitative measure of complexity of a quantum state of motion, that is a very important and nontrivial issue of the theory of quantum dynamical chaos, is the one of our concern. With such a measure in hand, we quantitatively analyze the stability and reversibility of quantum dynamics in the presence of external noise.

To solve this problem we point out that individual classical trajectories are of minor interest if the motion is chaotic. Properties of all of them are alike in this case and rather the behavior of their manifolds carries really valuable information. Therefore the phase-space methods and, correspondingly, the Liouville form of the classical mechanics become the most adequate. It is very important that, opposite to the classical trajectories, the classical phase space distribution and the Liouville equation have direct quantum analogs. Hence, the analogy and difference of classical and quantum dynamics can be traced by comparing the classical ( $W^{(c)}(I, \theta; t)$ ) and quantum (Wigner function  $W^{(q)}(I, \theta; t)$ ) phase space distributions both expressed in identical phase-space variables but ruled by different(!) linear equations.

The paramount property of the classical dynamical chaos is the exponentially fast structuring of the system's phase space on finer and finer scales. On the contrary, degree of structuring of the corresponding Wigner function is restricted by the quantization of the phase space. This makes Wigner function more coarse and relatively "simple" as compared to its classical counterpart. Fourier analysis affords quite suitable ground for analyzing complexity of a phase space distribution, that is equally valid in classical and quantum cases.

We demonstrate that the typical number of Fourier harmonics is indeed a relevant measure of complexity of states of motion in both classical as well as quantum cases. This allowed us to investigate in detail and introduce a quantitative measure of sensitivity to an external noisy environment and formulate the conditions under which the quantum motion remains reversible. It turns out that while the mean number of harmonics of the classical phase-space distribution of a non-integrable system grows with time exponentially during the whole time of the motion, the time of exponential upgrowth of this number in the case of the corresponding quantum Wigner function is restricted only to the Ehrenfest interval  $0 < t < t_E$  - just the interval within which the Wigner function still satisfies the classical Liouville equation. We showed that the number of harmonics increases beyond this interval *algebraically*. This fact gains a crucial importance when the Ehrenfest time is so short that the exponential regime *has no time to show up*. Under this condition the quantum motion turns out to be quite stable and reversible.

**Quantum chaos versus noisy environment.**

Ya.A. Kharkov, V.V. Sokolov and O.V. Zhirov

J. Sib. Fed. Univ. Math. Phys., 2010, Volume 3, Issue 3, Pages 303-310

Quantum dynamics of a classically chaotic 1D system in the presence of external noise is studied. Stability and reversibility properties of the motion (characterized by the Peres fidelity) as functions of the noise level  $\sigma$  are considered. We calculate fidelity analytically in the cases of weak and very strong noise and find critical value,  $\sigma_c(t)$ , below which the effect of perturbation remains small. Decay of critical perturbation with time is found to be power-like after the Ehrenfest time  $t_E$ . An estimate of the decoherence time  $t_d(\sigma)$  is presented after that the averaged density matrix becomes diagonal and its evolution turns into Markovian process.

**Google matrix, dynamical attractors and Ulam networks.**

D.L. Shepelyansky, O.V. Zhirov

e-print: arXiv:0905.4162 (2009); Phys. Rev. E 81, 036213 (2010)

We study the properties of the Google matrix generated by a coarse-grained Perron-Frobenius operator of the Chirikov typical map with dissipation. The finite-size matrix approximant of this operator is constructed by the Ulam method. This method applied to the simple dynamical model generates directed Ulam networks with approximate scale-free scaling and characteristics being in certain features similar to those of the world wide web with approximate scale-free degree distributions as well as two characteristics similar to the web: a power-law decay in PageRank that mirrors the decay of PageRank on the world wide web and a sensitivity to the value in PageRank. The simple dynamical attractors play here the role of popular websites with a strong concentration of PageRank. A variation in the Google parameter  $\alpha$  or other parameters of the dynamical map can drive the PageRank of the Google matrix to a delocalized phase with a strange attractor where the Google search becomes inefficient.

**Towards Google matrix of brain.**

D.L. Shepelyansky, O.V. Zhirov

e-print: arXiv:1002.4583v2.[cond-mat.dis-nn](2010); Phys. Lett. A 374, 3206 (2010)

We apply the approach of the Google matrix, used in computer science and World Wide Web, to description of properties of neuronal networks. The Google matrix  $G$  is constructed on the basis of neuronal network of a brain model discussed in PNAS 105 (2008) 3593. We show that the spectrum of eigenvalues of  $G$  has a gapless structure with long living relaxation modes. The PageRank of the network becomes delocalized for certain values of the Google damping factor  $\alpha$ . The properties of other eigenstates are also analyzed. We discuss further parallels and similarities between the World Wide Web and neuronal networks.

**Quantum compacton vacuum.**

O.V.Zhirov, A.S.Pikovskiy and D.L.Shepelyansky

it e-print: arXiv:1005.0778v1 [cond-mat.stat-mech] (2010)

We study the properties of classical and quantum strongly nonlinear chains by means of extensive numerical simulations. Due to strong nonlinearity, the classical dynamics of such chains remains chaotic at arbitrarily low energies. We show that the collective excitations of classical chains are described by sound waves whose decay rate scales algebraically with the wave number with a generic exponent value. The properties of the quantum chains are studied by the quantum Monte Carlo method and it is found that the low-energy excitations are well described by effective phonon modes with the sound velocity dependent on an effective Planck constant. Our results show that at low energies the quantum effects lead to a suppression of chaos and drive the system to a quasi-integrable regime of effective phonon modes.

**Two-dimensional ranking of Wikipedia articles.**

A.O.Zhirov, O.V.Zhirov, D.L.Shepelyansky

e-print: arXiv:1006.4270v1 [cs.IR] (2010), Eur. Phys. J.B 77, p.523 (2010)

The Library of Babel, described by Jorge Luis Borges, stores an enormous amount of information. The Library exists ab aeterno. Wikipedia, a free online encyclopaedia, becomes a modern analogue of such a Library. Information retrieval and ranking of Wikipedia articles become the challenge of modern society. While PageRank highlights very well known nodes with many ingoing links, CheiRank highlights very communicative nodes with many outgoing links. In this way the ranking becomes two-dimensional. Using CheiRank and PageRank we analyze the properties of two-dimensional ranking of all Wikipedia English articles and show that it gives their reliable classification with rich and nontrivial features. Detailed studies are done for countries, universities, personalities, physicists, chess players, Dow-Jones companies and other categories.

4

PLASMA PHYSICS  
AND CONTROLLED  
THERMONUCLEAR  
FUSION



## 4.1 Scientific report about research results on GDT device for 2010 year

### 4.1.1 Introduction

Most projects of thermonuclear reactors based on open magnetic systems for plasma confinement have the common structure. The main part of the reactor is a mirror trap where thermonuclear power is produced. Special magnetic cells for longitudinal losses of particles and energy fluxes suppression are attached to the ends of the mirror trap. As mentioned in earlier investigations the simplest configuration of thermonuclear reactor based on mirror machine cannot have a power amplification coefficient essentially higher than unity because of longitudinal losses high level. At different times some effective methods of longitudinal losses of particles and energy restriction were suggested: ambipolar cells, multimirror traps, etc.

Independent from the methods of longitudinal losses suppression the aim of competitive thermonuclear systems development makes demands to the main reactor part – central mirror trap. One of the demands comes from the problem of future reactor size minimization. It's necessary to have a maximally achievable from technical point of view magnetic field magnitude. This demand leads to necessity of the simplest axially symmetric magnetic configuration using. Furthermore reactor volume minimization demands confinement of plasma with relative pressure of about  $\beta \approx 1$  ( $\beta$ - relation of plasma pressure to magnetic field pressure,  $\beta = 8\pi p/B^2$ , where  $p$  – plasma pressure,  $B$  – magnetic field value). Third important requirement comes from the circumstance of that thermonuclear plasma conventionally cannot have an isotropic ion distribution function in velocity space. It can be caused by absence of ions inside of "loss cone" and by injection of atomic beams with narrow angle distribution for plasma heating and particle balance sustaining.

Therefore the central mirror cell of thermonuclear reactor should be axially symmetric and provide the confinement of non-equilibrium plasma with thermonuclear parameters and  $\beta \approx 1$ . Requirements specified are particularly hard for reactor projects with relatively low or zero neutron flux level on so-called alternative fuels:  $d\text{-}^3\text{He}$ ,  $p\text{-}^{11}\text{B}$ .

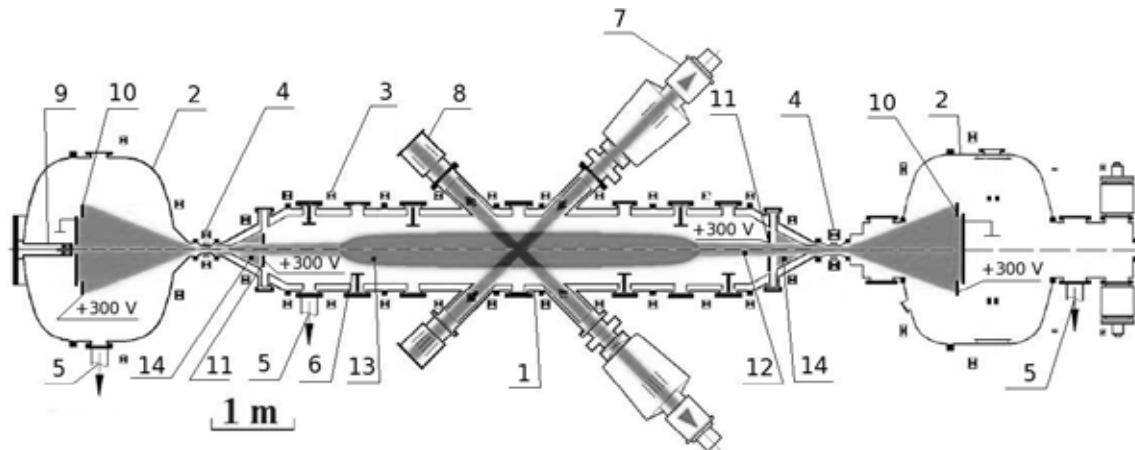


Fig.(4.1)1. Scheme of Gas Dynamic Trap device: 1 – central vacuum chamber; 2 – end tanks; 3 – coils of central solenoid; 4 – mirror coils; 5 – ports of vacuum pumping; 6 – titanium evaporators; 7 – neutral beams injectors; 8 – beams absorbers; 9 – generator of preparatory plasma; 10 – sectioned plasma absorbers (central disks are grounded, outer rings are under potential of about +300 V); 11 – limiters (also under potential of about +300 V); 12 – warm plasma; 13 – hot ions; 14 – systems of gas puffing.

Gas Dynamic Trap (GDT) device in Budker Institute of Nuclear Physics SB RAS is a good model of thermonuclear reactor central cell. GDT has an axially symmetric magnetic system and designed for non-equilibrium high beta plasma confinement.

The main part of GDT device (fig. (4.1)1) is an axially symmetric mirror trap with high mirror ratio designed for confinement of plasma which has two ion components with drastically different energies. One of components is warm with isotropic distribution in velocity space which has temperature of about 200 eV and density  $n_w \approx 2 \cdot 10^{19} m^{-3}$ . This component is confined in gas dynamic regime. Another ion component

is hot one created by oblique injection of neutral hydrogen or deuterium beams. Energy of injected atoms is in range from 23 to 25 keV, fast ions formed by atoms ionization are confined adiabatically and oscillate between turning points near the magnetic mirrors. Energetic confinement time of fast ions is mostly defined by collisions with electrons and appears much less than characteristic time of their angular scattering. Therefore hot ions have anisotropic distribution function, relatively low angular spread and peaked density and pressure near the turning points. Mean energy of fast ions is about  $E_h \approx 10 \text{ keV}$ , density near the turning points  $n_h \approx 5 \cdot 10^{19} \text{ m}^{-3}$ . Moreover electron temperature is up to  $T_e = 200 \text{ eV}$ .

Research program on GDT is mostly oriented on decision of fundamental scientific problem of non equilibrium high beta plasma confinement in axially symmetric mirror trap. This problem includes following tasks:

1. To achieve the low level of transverse losses relate to longitudinal ones in regimes with high beta. Note that axially symmetric mirror trap does not have a favorable configuration for MHD stability of plasma in general.
2. To investigate the microinstabilities influence on plasma confinement. Microinstabilities are the phenomena connected with electromagnetic waves generation in non equilibrium plasma. Electromagnetic waves can sufficiently modify kinetic processes in plasma and consequently influence on its confinement.
3. To provide research on MHD equilibrium of high beta plasma. Condition  $\beta \approx 1$  means significant difference of magnetic field value inside of plasma from vacuum one. This fact can lead to number of processes appearing which define the equilibrium configurations.

At the beginning of 2010 sufficient progress in GDT device experiment development has been made. GDT had been modified: atomic injection power had been increased, magnetic field magnitude had been increased, diagnostic complex had been improved. Furthermore the series of investigations on realization and explanation of vortex confinement method for transverse plasma losses suppression were carried out. Mentioned results allowed us to achieve values of relative pressure up to 0,6 which is a record for axially symmetric open systems for plasma confinement.

This report includes description and results of three cycles of experimental investigations on GDT device. First series of experiments was oriented on completion of vortex confinement method substantiation and dedicated to the direct demonstration of vortex movement of plasma. Simultaneously measurements of maximally achievable electron temperature were carried out in optimized regimes with vortex confinement as well as measurements of energy transversal losses. In the last series of studies the survey experiments on possible microinstabilities observation was provided.

#### 4.1.2 The study of plasma motion at the vortex confinement

Vortex confinement method assumes the refusal from MHD stabilization. Its idea is to modify unstable motion of plasma column transverse the magnetic field in such a way to close the flux lines. It can be realized by differential rotation zone creation near the radial boundary of plasma by means of special electrodes: sectioned plasma absorbers and radial limiters (see fig.(4.1)1).

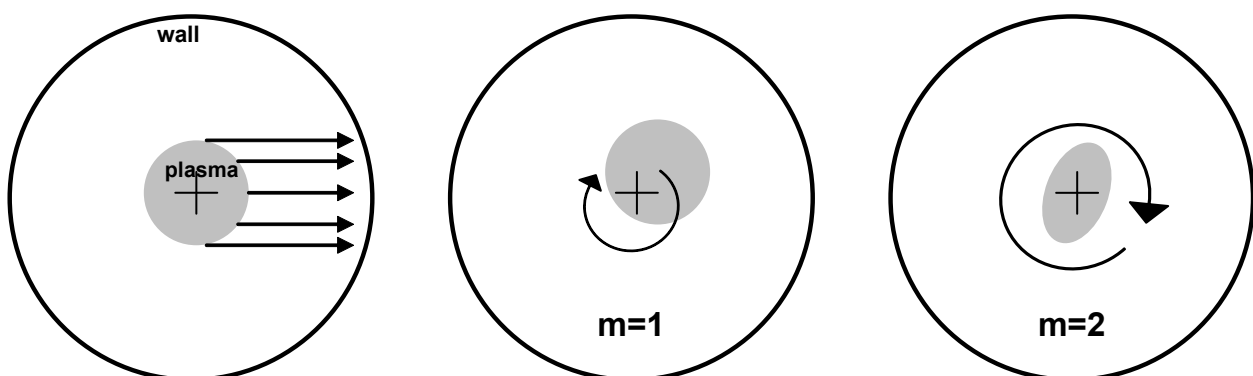


Fig.(4.1)2. Simplified scheme of plasma column motion without vortex confinement (left) and with vortex confinement realization (center and right): according to theoretical model only  $m = 1$  and  $m = 2$  modes are available at differential rotation.

According to numerical simulations plasma column cross section movement in the plane perpendicular to magnetic field can be either a rotation around the GDT device axis with small displacement relate to the axis (azimuthal mode  $m=1$ ) or plasma cross section has an elliptical form and rotates around the ellipse symmetry axis which coincides with GDT device axis (fig.(4.1)2). Such a perturbations should spread along the magnetic field on the entire length of the device (flute character of oscillations). At the beginning of 2010 vortex confinement method was sufficiently justified theoretically and experimentally, but from the experimental side there was a lack of a very important detail – the direct observation of vortex motion of the plasma. Since, according to the findings of the theory, the method of vortex confinement can be used in thermonuclear systems, its final justification is extremely important.

To study the motion of the plasma column two systems of miniature magnetic probes (Mirnov coils) was designed and built. These probes are capable to measure fluctuations of the radial component of the magnetic field at frequencies up to 100 kHz. One system was a ring on which 16 probes were attached equidistantly. Ring enveloped the plasma column near the hot ions turning point. Another system was an assembly of the 12 probes located equidistantly on the line rod length 0.9 m. The linear assembly was located parallel to the axis of the installation near the plasma column. Center of the assembly was located in an area with mirror ratio 2. Each probe was connected to a channel of digital recorder of waveforms having adequate time and amplitude resolution.

During the experiments, which were performed in regimes with electron temperature up to  $T_e = 200$  eV and relative pressure of up to  $\beta = 0,55$ , we studied the spatial and frequency spectra of plasma column oscillations by means of Mirnov coils and other diagnostics.

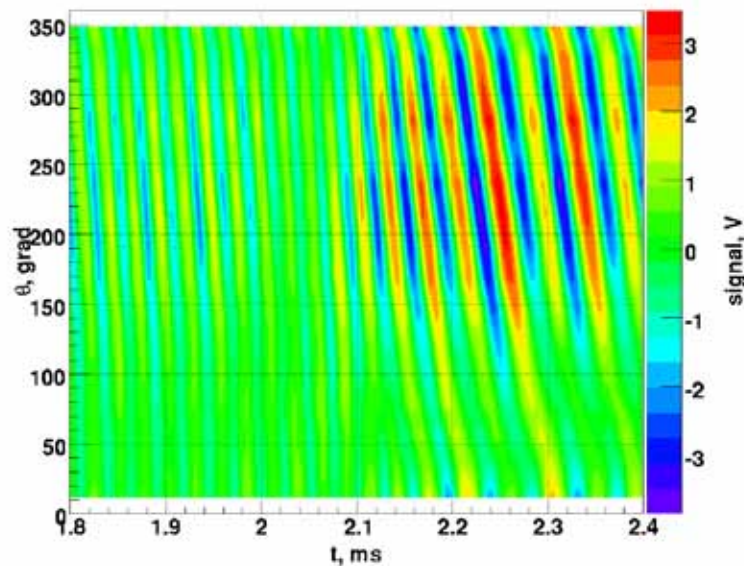


Fig.(4.1)3. The characteristic signal form from azimuthal set of probes (oscillations of the magnetic field radial component). Key stages: 0-1 ms – no large-amplitude oscillations with a distinct frequency; 1-2 ms – oscillations with azimuthal number  $m = 1$ ; 2.4 ms – oscillations with azimuthal number  $m = 2$ ;  $> 4$  ms – plasma decay, oscillation frequency decreases significantly over the period of oscillations.

It was found that the fluctuations have a dominant mode at any time. However, in the regimes with a maximum parameters number of modes does not remain constant during the experiment. The usual scenario is as follows: during the first millisecond from the beginning of the atomic beams injection oscillations are observed, then in the range from 1 to 2 ms the first mode is dominated, at approximately 2 ms there is a sharp transition to the second mode, which remains dominant until the end of the experiment. Fig.(4.1) 3 shows a signal from the azimuthal assembly at the time of changing the mode number. The first mode in Fig. 3 dominates up to time  $t = 2.1$  ms, this time nearby maximum stripes pass one to another. After  $t = 2.15$  ms the second mode becomes dominant, the slope angle of maximum stripes is changing and stripes pass next but one. Fig.(4.1)4 shows the spectra of the signal. The spectra show that in period of 1 – 2 ms the first mode is dominated with a frequency around 40 kHz, and between 2 and 4 ms the second mode plays the central role with frequency close to 20 kHz.

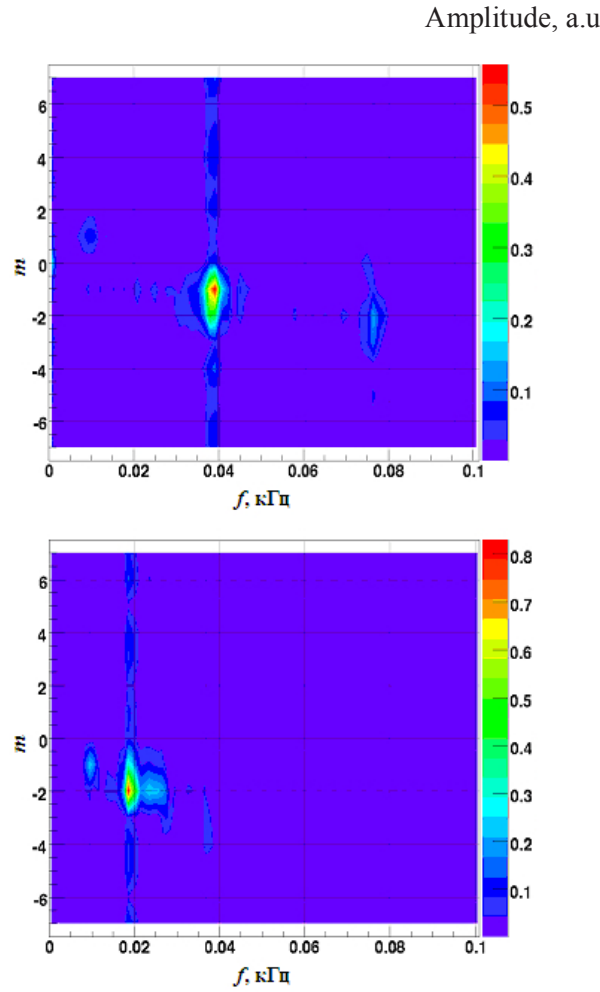


Fig.(4.1)4. Spectra of signals 1-2 ms (top) and 2-4 ms (bottom).

For the results interpretation let's note two things. First, the transition from  $m = 1$  to  $m = 2$  is fast and global plasma parameters that determine the confinement do not have time to change. Secondly, the measured frequency is the repetition rate of peaks by the probe, i.e. the measured frequency is the product of the frequency of plasma rotation on the mode number. According to the findings of the frequency of plasma rotation defined by the applied potential on the periphery is inversely proportional to the number of mode  $f_m = f_1 / m$ . Note also the rotational speed  $f_{amb}$  appearing in the plasma by the "natural" way – by the ambipolar potential that decreases on the plasma periphery. Considering these two terms, we obtain

$$f = m \cdot (f_m - f_{amb}) = f_1 - m \cdot f_{amb}. \quad (1)$$

Note that without the ambipolar plasma rotation measured frequency should not depend on the mode number. Using (1) for the transition from  $m = 1$  to  $m = 2$ , we can calculate the characteristic frequencies:  $f_1 \approx 60$  kHz and  $f_{amb} \approx 20$  kHz.

Longitudinal wavelengths were studied using a linear assembly of Mirnov probes and detectors of the passed beams. Fig.(4.1)5 shows a signal from a linear probes assembly of the same experiment that the signal from the circular assembly in Fig.(4.1)3. The signals from all probes of the linear assembly have the same phase. This means that the wavelength exceeds the size of the linear assembly which is 1 m. And allows us to assume that the fluctuations have a flute character. Additional measurements of the fluctuations of a linear plasma density in the central section and correlation analysis showed that the azimuthal position of the flute in the central section (measured by the detector of the passed beams) and a turning point (measured by Mirnov probes) coincide with accuracy up to  $10^\circ$ . In other words the longitudinal wavelength is longer than the GDT device. This finally proves the flute nature of the oscillations.

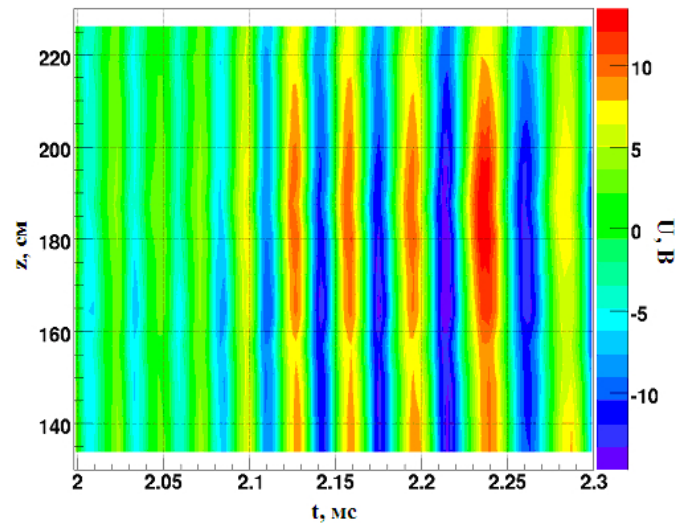


Fig.(4.1)5. The signal from the Mirnov probe depending on the longitudinal coordinate  $z$  and time  $t$ .

According to the results of this series of experiments we can draw two important conclusions:

1. Demonstrated that in the regime with the differential rotation the motion of the plasma column in transverse direction has a vortex character;
2. Perturbation of the plasma equilibrium in this case have character of flutes with the azimuthal wave number  $m = 1$  or  $m = 2$ , which is in agreement with the theoretical model.

#### 4.1.3 The maximum achievable electron temperature and energy balance

In parallel with experiments on the study of plasma motion at the vortex confinement there was the optimization of experimental parameters in order to achieve maximum electron temperature, which is one of the main parameters determining the energy lifetime of the hot ions in GDT. In addition measurements allowed to analyze the energy balance at optimized parameters were carried out.

The highest values of the electron temperature has been achieved in the regime with injection of 4.8 MW of deuterium beams into a deuterium plasma. Figure 6 shows the time dependence of the electron temperature. The origin corresponds to the beginning of the atomic injection.

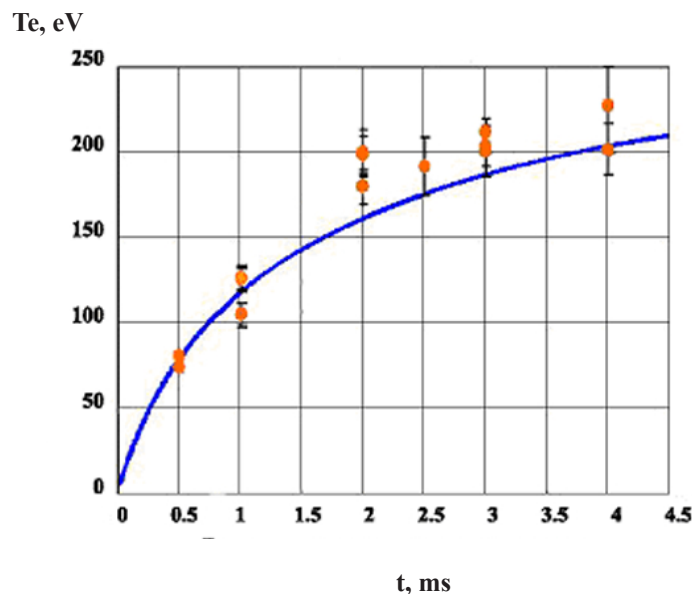


Fig.(4.1)6. Electron temperature vs time in the regime with injection of 4.8 MW deuterium beams into deuterium plasma: points - result of measurement, the line - result of "zero-dimensional" model taking into account the longitudinal losses in the gas-dynamic regime.

For comparison there are results of numerical simulation of plasma heating by atomic injection using a model of a collisionless Maxwellian plasma flow through the mirrors, which is adequate to the experimental conditions at the GDT. Good coincidence of the results of this simulation with measurements indicates a small value of the transverse heat loss power compared with power of longitudinal losses.

Numerical estimation of the transverse losses power ratio to the power of longitudinal ones was obtained in a special series of measurements, where we used the pyroelectric bolometer allowed us to measure the distribution of power density on the plasma absorbers surface. These measurements were carried out in the closest to a stationary regime with injection of hydrogen beams into hydrogen plasma. Power of plasma heating (the power captured by of the atomic beams, less power of charge-exchange neutrals flux from the plasma) was  $1.4 \pm 0.05$  MW and the measured power of longitudinal losses -  $1.3 \pm 0.2$  MW. Thus, in this regime the power of the transverse energy losses did not exceed 20% of the power of longitudinal ones.

#### 4.1.4 High-frequency electromagnetic oscillations

Analysis of previous investigations shows that Alfvén ion cyclotron instability can appear with today's plasma parameters in GDT. The main parameters determining the threshold of this type of microinstability:

$$\beta = 8\pi n_j \langle \varepsilon_j \rangle / B^2 - \text{relative pressure};$$

$$A \approx \pi / \Delta\theta - \text{degree of anisotropy},$$

where  $n_j, \langle \varepsilon_j \rangle$  - density and mean energy of hot ions,  $B$  - magnetic field,  $\Delta\theta$  - the characteristic angular width of hot ions distribution. An approximate criterion of the instability threshold is the inequality

$$A \cdot \beta > k, \text{ where } k \approx 1 \div 10.$$

For today's GDT parameters:  $A \gg 1, \beta \approx 0.5$ .

For registration of electromagnetic waves in the range of the ion cyclotron frequency resonance ( $\omega_{ci} = 2.7$  MHz) magnetic probe able to measure fluctuations of the three components of the magnetic field ( $B_z, B_r, B_\phi$ ) was mounted near the plasma. The characteristic features of Alfvén waves in the plasma during the development of Alfvén ion cyclotron instability are the following:

1. the direction of wave polarization vector rotation coincides with the direction of the ion cyclotron rotation;
2.  $B_z \ll B_r, B_\phi$  - amplitude of magnetic field z-component oscillations is much smaller than the corresponding amplitudes of r and  $\phi$  components.

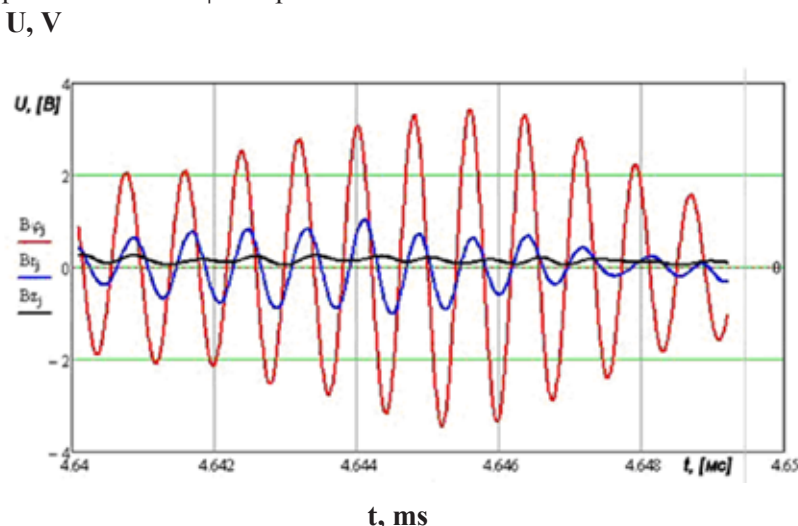


Fig.(4.1)7. Three components of the magnetic field oscillogram fragment: the amplitude of the z-component is small compared with the amplitudes of the other two components.

Figure (4.1)7 shows a fragment of magnetic field three components oscillogram, obtained in one of the experimental "shots". It is seen that the amplitude of z-component is small compared with the amplitudes of the other two components. Correlation analysis of fluctuations showed that the direction of wave polarization vector rotation coincides with the direction of the ion cyclotron rotation. Thus, we can conclude that with high probability we deal with the Alfvén ion cyclotron instability.

Analysis of the results of additional measurements made by the Mirnov coils system and energy analyzer of ions left the trap through the mirrors, allowed us to make following conclusions:

1. At the instability development there is an increase of the width of hot ions density peak in its turning points (the degree of anisotropy decreases).
2. At the instability development oscillations amplitude saturation is observed and losses of particles and energy through the mirrors increases insignificantly. According to the results of measurements of the ions leaving the trap average energy is as follows:

$$\langle E \rangle = 1 \pm 0.03 \text{ keV} \quad - \text{ without the instability;}$$

$$\langle E \rangle = 1.1 \pm 0.03 \text{ keV} \quad - \text{ with the same parameters of plasma but in presence of instability.}$$

Thus, we have shown that GDT is a good tool for further studies of a number of extremely important issues related to microinstabilities:

1. specification the theoretical models describing the thresholds of microinstabilities and the processes of saturation (the level of theoretical predictions accuracy today is not satisfactory);
2. studying the microinstabilities influence on plasma confinement and equilibrium.

## 4.2 Plasma theory

### 4.2.1 Plasma equilibrium and stability

Within paraxial approximation it is shown that in anisotropic plasma confined in an open-ended system with  $\beta$  above the mirror instability threshold a «magnetic hole» is formed near the turning point of the sloshing ions.

### 4.2.2 Dynamic plasma confinement

In 2010 we continued to study theory of the dynamic plasma confinement near unstable axially symmetric equilibria in open traps. Qualitative agreement of predicted theoretical scalings of the vortex confinement was established with data from dedicated experiments on GDT. A new feedback control method, based bending of the plasma discharge by external transverse magnetic field was proposed. In contrast to the vortex confinement it can be useful at a weak conductance to the end-plates as well.

### 4.2.3 Terahertz radiation

A phenomenological theory of generation of electromagnetic radiation of a laser spark in the frequency range 1-20 THz in the atmosphere was developed. Probability of multiquantum and tunnel ionization in a bichromatic electromagnetic field is calculated by using imaginary time method.

### 4.2.4 Nonneutral plasmas

A theory of equilibrium of a nonneutral plasmas under the effect of various perturbations of the magnetic and electrostatic fields has been elaborated

### 4.2.5 Theory of plasma dust formation

The size distribution of dust particles in nuclear fusion devices is close to the power function. It is shown that function of this kind can be the result of brittle destruction. From the similarity assumption it follows that the size distribution obeys the power law with the exponent between -4 and -1. The model of destruction has much in common with the fractal theory. The power exponent can be expressed in terms of the fractal dimension. An additional assumption about the structure of fragmentation offers that the exponent is close to -3. The exponent for the case of the biggest ball removing equals -3.4.

### 4.2.6 Theory of plasma wakefield acceleration

Proton beam driven plasma wakefield acceleration is further analyzed as a way to bring electrons to TeV energy range in a single plasma section. Several factors that could limit accelerator performance are considered: an external quadrupole focusing, the optimum choice of the plasma density profile, and the

long-term driver dynamics. The optimum conditions for acceleration are found, and the consequences of deviations from the optimum conditions are analyzed.

A model for the self-modulation instability of a long relativistic proton bunch propagating in uniform plasmas is developed. The self-modulated proton bunch resonantly excites a large amplitude plasma wave (wakefield), which can be used for acceleration of plasma electrons. It is shown that the self-modulation of the proton bunch competes with the hosing instability which tends to destroy the plasma wave. A method is proposed and studied through simulations to circumvent this problem, which relies on the seeding of the self-modulation instability in the bunch.

To verify the novel idea of proton beam driven plasma wakefield acceleration, a proof-of-principle demonstration experiment is now being planned. The idea is to use the available high energy proton beams either from the Proton Synchrotron (PS) or the Super Proton Synchrotron (SPS) at CERN, to shoot the beam into a plasma cell and to excite the plasma wakefield. Long proton beams are to be self-modulated due to the instability. The interactions between the plasma and the proton beam are simulated as a part of collaborative efforts. Similar effect of electron beam self-modulation can be experimentally tested at the PWFA facility currently under construction at the Budker INP.

Earlier studies on resonant excitation of plasma wakefields by long trains of short electron bunches are published.

#### **4.2.7 Simulation of turbulent plasma heating by a powerful electron beam**

Basic mechanisms of turbulent plasma heating by powerful electron beams are studied using numerical simulations. Both particle-in-cell and hybrid codes are used to investigate how beam-plasma instability evolves and saturates in the case of continuously injected electron beam. It was found that for sufficiently high plasma temperature beam driven turbulence is subjected to the constant pump, when the saturation level of heating power is determined solely by the nonlinear interaction of beam particles with resonant waves and does not depend on the turbulence structure in the nonresonant part of the spectrum.

The efficiency of plasma heating by low-energetic electron beams is investigated using 1D hybrid code. We determined how the relaxation efficiency depends upon beam parameters at the stage of turbulence excitation. It is shown that relaxation of a low-energetic beam appears to be more efficient compared to the beam with the same power, but higher beam energy. It is also shown that plasma density inhomogeneities shift the peak of energy release to the locally uniform region.

## **4.3 Beam Injectors of Hydrogen Atoms and Ions**

### **4.3.1 Beam Injectors of Hydrogen Atoms**

For plasma heating in the FRC device (Tri Alpha Energy Inc., USA) two injectors of focused beams of hydrogen atoms with 20 keV energy, 0.7 MW beam power, 5 ms pulse duration were developed and commissioned. Ion sources are based on the power arc discharge plasma generators with discharge current of 1.2 kA.

Modernization of four heating neutral beam injectors commissioned in TAE in 2008 year is finished. Now the injectors operate with energy of 20 keV, ion current of 45 A, pulse duration of 100 ms. For the injectors new ion optical systems with enlarged ion beam emission diameter were fabricated. RF plasma generators are without modification from the previous version.

On contract with EMC2 company (Energy Matter Conversion Corporation, San-Diego, USA) heating injector was developed and commissioned. Deuterium beam energy is 25 keV, ion current is 30 A, pulse duration is 3 ms. Ion source is based on the power arc discharge plasma generator. Design of the plasma generator is the same as mentioned above for the TAE injectors.

### 4.3.2 Project of powerful continuous injector of beam of fast hydrogen atoms

Project of powerful continuous injector of beam of fast hydrogen atoms with 500-1000 keV energy of atoms on the basis of negative ions is developed. The project is based on separate formation and acceleration of negative ion beam. Detailed designing of the basic elements of the injector is carried out. Variant of placing of the injector in the radiation protected hall of the DOL building is drawn. Experimental test stand for acceleration of hydrogen negative ion beam with current  $\sim 5$  A and energy 120 keV is prepared. Manufacturing drawings of negative ion source prototype are arranged.

## 4.4 GOL-3 Facility

### 4.4.1 Introduction

GOL-3 is a unique electro-physical facility intended for studies of physics of fast collective plasma heating by a high-current relativistic electron beam of microsecond duration and for studies of physics of multiple-mirror confinement of high-temperature plasma in corrugated magnetic field. The main feature of plasma behavior in the facility is the key role of collective and non-linear processes. Scientific program of 2010 was targeted to several specific tasks of physics and technology of multiple-mirror confinement systems for a high-temperature plasma. Development of experimental base was continued in 2010 in parallel with experiments under scientific programs. New advances in a technology of generation of long-pulse electron beams with the plasma emitter were achieved. The diagnostic complex of GOL-3 was improved with several new diagnostics which will be described later in the text.

General view of the facility is presented in Fig.(4.4)1. The 12-meter-long solenoid consists of 103 coils with an independent feed. In the regular multimirror configuration the magnetic field has 52 corrugation periods (cells of multimirror system) with 22 cm length, the field in maxima is 4.8 T, in minima is 3.2 T. The mirror ratio of the corrugated field is 1.5. This means that the operating mode of GOL-3 corresponds to a “weak corrugation regime”. The solenoid terminates in single magnetic mirrors with the field of 8-9 T. The exit unit consists of the plasma creation system and exit expander tank with the end beam collector. Magnetic field strength decreases to 0.05 T at the collector surface reducing therefore specific heat flux at the surface. Metals therefore can be used as material for the collector plate.



Fig.(4.4)1. Multiple-mirror trap GOL-3.

Typical experimental scenario is the following. Several gas-puff valves create required axial deuterium density distribution in a metal vacuum chamber Ø10 cm, placed inside the solenoid. Then a special linear discharge creates a start plasma with length-averaged density of  $(1\div 30)\cdot 10^{20} \text{ m}^{-3}$  and temperature  $\sim 2 \text{ eV}$ . After that the relativistic electron beam is injected into this plasma with the following parameters in a standard regime: electron energy is  $\sim 0.8 \text{ MeV}$ , current is  $\sim 25 \text{ kA}$ , duration is  $\sim 12 \mu\text{s}$ , energy content is  $\sim 120 \text{ kJ}$ , the beam diameter is  $\sim 4.1 \text{ cm}$  (this value corresponds to  $3.2 \text{ T}$  magnetic field as in minima of corrugated magnetic field). Such a beam is formed in a slit relativistic diode of the beam generator U-2 and then it is transformed to a circular shape and compressed by a magnetic system of U-2. As a result of collective heating the plasma gets ion temperature  $2\div 3 \text{ keV}$  (in the hottest part of the plasma column). Use of the multiple-mirror confinement scheme (the corrugated magnetic field) allows to confine the hot plasma much longer, than in a simple solenoidal trap.

#### 4.4.2 Experiments on injection of a beam with smoothly increasing power

In the experimental campaign of 2010 the new mode of formation of the relativistic electron beam for the first time has been tested at GOL-3. The essence of the work was that operation of spark-gaps of the high voltage generator of the U-2 accelerator has been reprogrammed to provide smooth growth of diode voltage from  $0.15$  to  $0.7 \text{ MV}$  during approximately  $8 \mu\text{s}$  (unlike earlier standard mode in which starting voltage was  $\sim 0.5 \text{ MV}$ ). Thus the current of the beam and its power also had the prolonged front, see Fig. (4.4)2. Full duration of the beam and its energy content remained practically without changes in comparison with the standard mode.

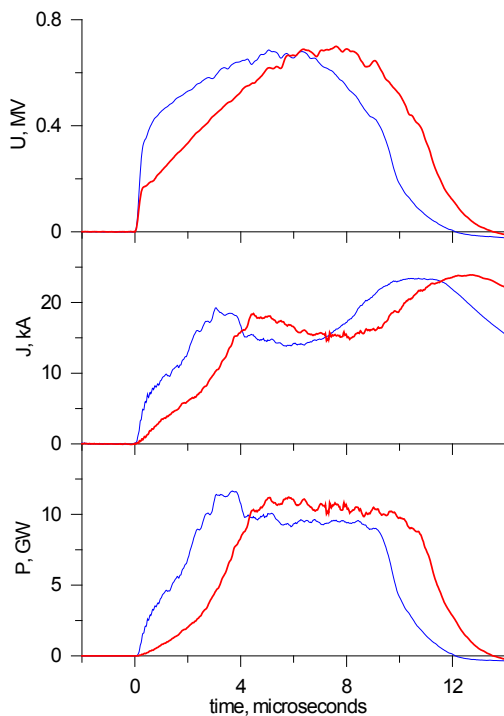


Fig.(4.4)2. Main parameters of the electron beam for two cases: the standard mode (thin lines) and the mode with smoothly increasing cathode voltage (thick lines). Typical waveforms of the diode voltage (top), the beam current (middle) and the beam power (bottom) are shown.

From the point of view of fusion prospects of the scheme of plasma heating by an electron beam in open traps, study of interaction of a less powerful beam with plasma (that is study of beam-plasma interaction with reduced beam to plasma density ratio) is essential. The reason is that interaction process of a high-current relativistic electron beam with plasma is nonlinear, and optimal beam power can be found that should provide collective heating of plasma electrons and maintain heat axial heat losses suppression with minimal energy consumption.

In the experiments we demonstrate that growth of the plasma energy content occurs almost linearly during injection of the electron beam even in spite of the fact that in first half of pulse beam power was essentially lowered in comparison with a standard mode, see Fig. (4.4)3. The resulting value of plasma energy content is close to that achieved in the standard mode. This result is positive from the point of view of prospects of planned transition to operation with a long-pulse electron beam of lowered power.

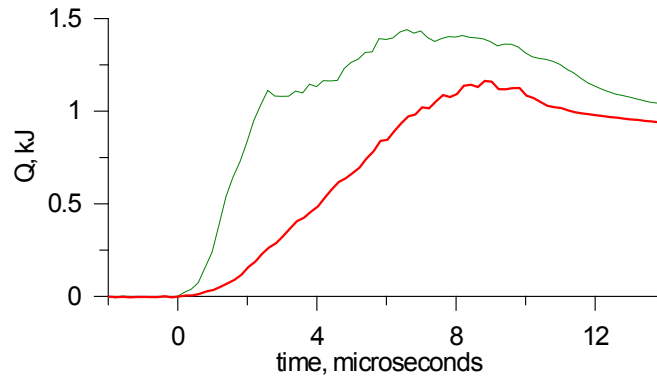


Fig.(4.4)3. Dynamics of the full plasma energy content by diamagnetic measurements. The standard operating mode is shown by the thin line, the mode with smooth increase in energy of electrons by the thick line.

#### 4.4.3 Measurement of electron distribution function

Thomson scattering system was upgraded in 2010. The main target for operation was to enable observation of dynamics of axial variation of plasma heating. The axial variability of plasma parameters is inherent feature of mirror machines that distinguishes them from tokamaks where plasma parameter depends practically only on normal to magnetic field coordinates. Another characteristic feature of GOL-3 device in contrast to other magnetic confinement systems is a strongly non-Maxwellian electron distribution function, which is the result of high power plasma heating and of turbulent mechanism of the heating. Moreover, plasma heating at GOL-3 is far much faster than in other modern magnetic confinement devices so it requires diagnostics with high temporal resolution. Due to the above mentioned features the upgrading required approaches that are different from those routinely used in toroidal devices. In particular, for observation in additional axial plasma cross-section (2 m from the input magnetic mirror) the laser beam was re-used and directed through plasma second time as it is shown in figure (4.4)4 where the layout of Thomson scattering system is depicted. Here the laser input is shown by the arrow. Detailed measurement of dynamics of high energy tails of electron distribution function requires two laser pulses with variable timing (0.1-100  $\mu\text{s}$ ) between them and with the energy of each pulse several times larger than typically used in devices with near Maxwellian plasmas. Two laser pulses are generated by new two-module oscillator system. The following amplifiers increase the energy of each pulse by a factor  $10^3$ .

Despite the amplification is strongly nonlinear the output laser pulses with nearly equal energy can be produced for varied time delay between them by tuning pump power and timing of the amplifiers. An example of the use of new Thomson scattering system is shown in Fig. (4.4)5 where plasma density and temperature (mean energy of non-Maxwellian plasma electrons) measured at two time instants (5.5  $\mu\text{s}$  and 8  $\mu\text{s}$  after the heating start) within a single shot are shown. Measurements are performed at two axial positions along the plasma column - 2 m and 4 m from the input of heating electron beam into plasma. The data points in the Figure have summarized from several plasma discharges. As can be seen from these measurements respectively dense plasma flows along magnetic field from input plug to the end of facility. So after 2.5  $\mu\text{s}$  the plasma density decreases at  $z = 2$  m but slightly increases at  $z = 4$  m. The mean energy of plasma electrons generally increases at both locations after 2.5  $\mu\text{s}$  however large spread of temperature at this time is noticeable. The more detailed examination of dynamics of plasma electron energy within one shot shows that electron temperature sometimes decreases on the period from 5.5 to 8  $\mu\text{s}$  while heating relativistic electron beam continues passing through plasma until 11  $\mu\text{s}$ . Such a behavior is basically consistent with the model of collective energy transfer from plasma electrons to ions. According to this model this mechanism starts just near 7-9  $\mu\text{s}$  since the start of plasma heating.

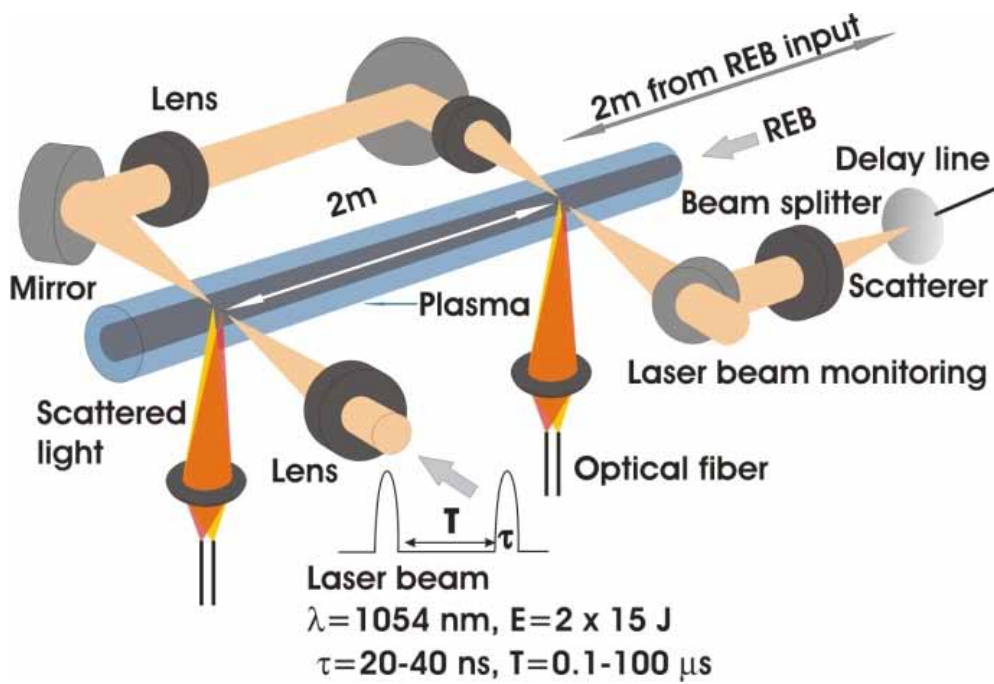


Fig.(4.4)4. The layout of upgraded Thomson scattering system for measurement at two spatial points and at two time instants within a single plasma discharge.

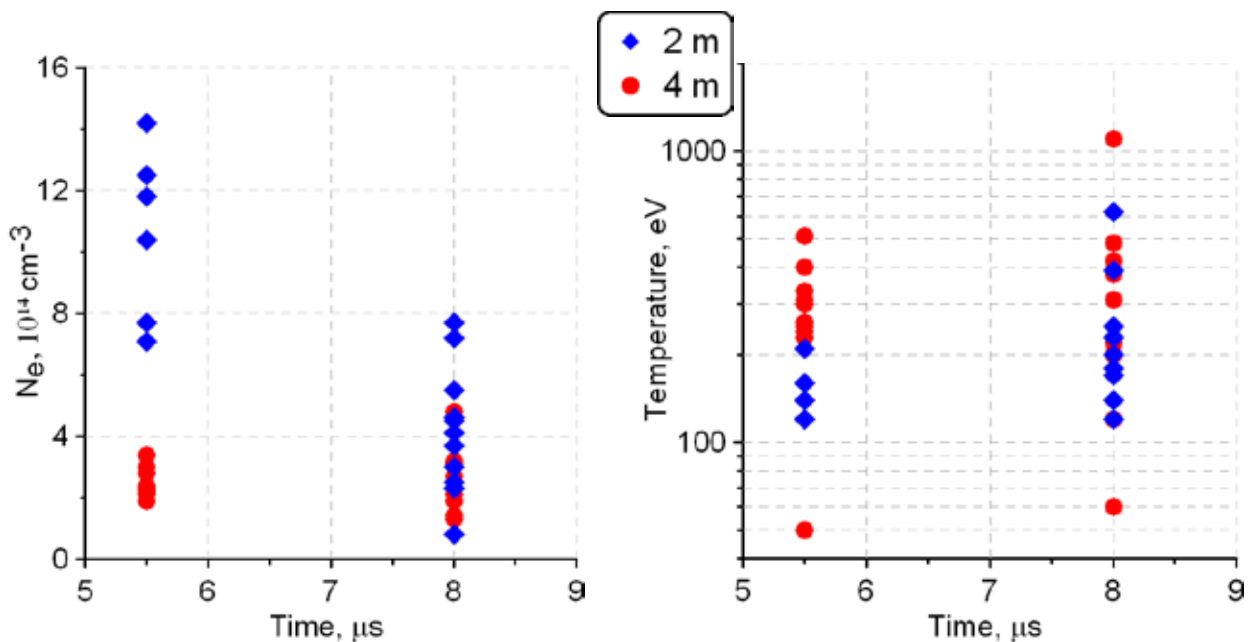


Fig. (4.4)5. Dynamics of density and mean energy of plasma electrons during the plasma heating at distance of 2 m and 4 m from input plug. Data are obtained from Thomson scattering measurements during several plasma discharges.

#### 4.4.4 Studies of sub-Terahertz plasma emission

In the conditions of turbulent plasma heating by a high-power relativistic electron beam there is a possibility of coupling of two Langmuir waves into an electromagnetic wave. Thus frequency of the electromagnetic wave approximately corresponds to double plasma frequency. For plasma density in a range  $10^{20} \div 10^{21} \text{ m}^{-3}$  the doubled linear plasma frequency is within the range  $180 \div 565 \text{ GHz}$ . Therefore investigation of spectrum and dynamics of emission of plasma in terahertz region provide information about beam-plasma interaction and processes that accompany relaxation of the electron beam in the plasma.

In the year 2008 a four-channel radiometric diagnostics has been developed for measurements of radiated power and spectrum of plasma emission in the vicinity of double plasma frequency. It is based on quasi-optical elements in which spectral selectivity is provided by use of anisotropic mesh filters.

In 2010 the experimental research of plasma terahertz radiation generated by the mentioned mechanism proceeded. The special attention was given to features of radiation dynamics. One of possible mechanisms of terahertz waves generation is concerned with occurrence in the plasma localized areas with raised density of Langmuir fluctuations. In this case radiation power dynamics should consist of a large number of short spikes. The similar structure of the signal is observed in the experiment, see Fig. (4.4)6.

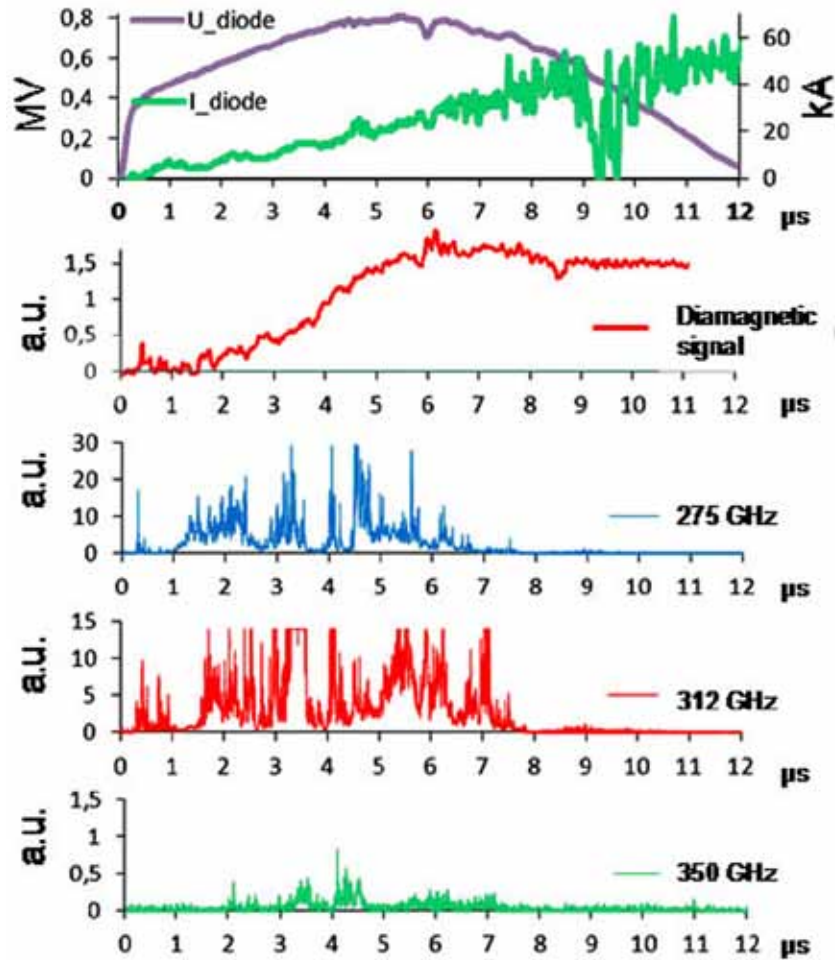


Fig. (4.4)6. Typical waveforms which characterize the stage of collective plasma heating by the relativistic electron beam in GOL-3. Shown from top to bottom are: the cathode voltage of the beam generator and the beam current; diamagnetic plasma pressure at coordinate  $z = 77$  cm; signals of detectors of terahertz radiation located at coordinate  $z=83$  cm. Central wavelengths of the bandpasses of the spectral system are designated for each detector.

It is clearly seen that terahertz radiation exists only at the stage of intensive heating of the plasma. After 7<sup>th</sup> microsecond radiation disappeared despite beam injection still proceeds and the plasma energy content is close to its maximum. This circumstance testifies that generation of terahertz radiation isn't connected directly with cyclotron rotation of electrons, but it is the plasma process.

#### 4.4.5 Results of plasma magnetic activity measurements

Magnetic activity of the plasma was found both at the stage of plasma heating and at a long time after the end of the beam injection. In the last case (at the stage of plasma cooling) transient magnetic disturbances occur. These events correspond to short (several oscillation periods, in some cases one pulse) bursts of oscillations with the main frequency  $10^5 \div 10^6$  Hz. Integral of the magnetic field amplitude along the whole burst duration equals to zero, i.e. the observed event doesn't lead to generation of the mean current along the plasma but corresponds to generation or vanishing of the opposite axially asymmetric current filaments. In some cases bursts of neutron and gamma emission observed by local radiation detectors strongly correlate in time with the magnetic activity of the plasma (Fig. (4.4)7). Statistical analysis of  $\sim 8000$  events in  $\sim 1200$  shots was conducted.

Fourier analysis of the magnetic disturbances has shown three statistically dissimilar groups of events with the main frequencies of about 0.38, 0.86 and 1.4 MHz. The least of them agrees well with the two-way Alfvén wave propagation through the whole length of the device. The disturbance was found to start on the one end of the plasma column and propagate through the plasma with the local Alfvén velocity (Fig. (4.4)8). Its decay time corresponds to the characteristic lifetime of a short (comparable to the length of one cell of the magnetic field) improper magnetic disturbance.

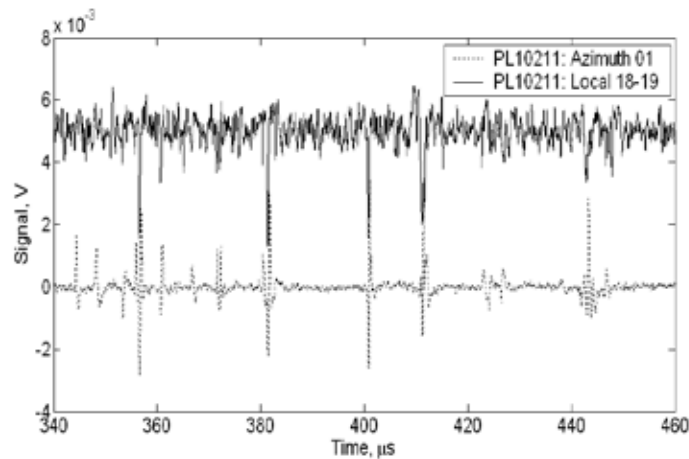


Fig.(4.4)7. Correlation of pulsed magnetic activity and neutron/gamma emission. Above: local neutron/gamma radiation detector data; below: azimuthal magnetic probe data.

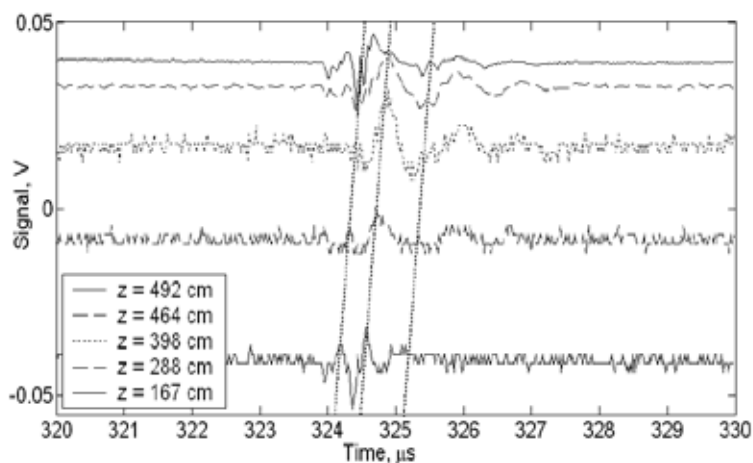


Fig.(4.4)8. Longitudinal correlation of the bursts. Zero lines are shifted proportionally to the coordinates of probes (from bottom to top: 167, 288, 398, 464, and 492 cm), slope of dotted lines corresponds to the mean Alfvén velocity.

Final interpretation of these bursts could be given as follow. At the stage of the turbulent heating a complex structure of opposite currents is formed in the plasma. After the end of the beam injection such structure could not disappear instantly because of its inductance. At the stage of plasma cooling filamentation of these structure could occur forming separate threads of current up to 50 A (estimation is based on the observed amplitudes of the bursts, amplitude distribution has a power law with the power -1.87). Observed signal could correspond to the annihilation of these threads, duration of the reconnection process conforms to theoretical predictions.

#### 4.4.6 Experimental investigations of tungsten erosion after powerful plasma stream irradiation

Experimental study of tungsten behavior under plasma loads relevant to ITER divertor were performed at the GOL-3 device. Experiments were performed in GOL-3 exit unit where energy density in the exhaust plasma stream decreases correspondingly with the broadening of the magnetic flux tube in the exit expander. Target energy loads in experiments were varied in range (0.3÷12) MJ/m<sup>2</sup>.

Investigations of tungsten surfaces after irradiations demonstrated the following.

At power loads less than threshold of melting (less 0.5 MJ/m<sup>2</sup>) surface changes are small. Changes of surface roughness were observed. Rising of power loads lead to strong melting of the surface and also evaporation. Boiling bubbles with diameter 50-300 microns and formation of crack networks with typical cell sizes 0.3 μm are observed with microscopy.

At moderate loads (5 pulses with energy density 2 MJ/m<sup>2</sup> per shot) corresponding to ELM type I in ITER divertor formation of three different crack networks with typical cell sizes of 1000, 10 and 0.3 μm are identified. Bubbles are also observed. Fig. (4.4)9 shows bubble on tungsten surface. Figure is taken by SEM Jeol JCM-5700. Using of SEM stereopairs with MeX software allow us to reconstruct 3D view of surface and measure depth of bubble. Fig. (4.4)10 shows bubble depth profile with typical depth 22 microns.

Fig. (4.4)11 shows SEM pictures with big magnification that allow to see structure of crack networks with cell sizes 0.3 μm.

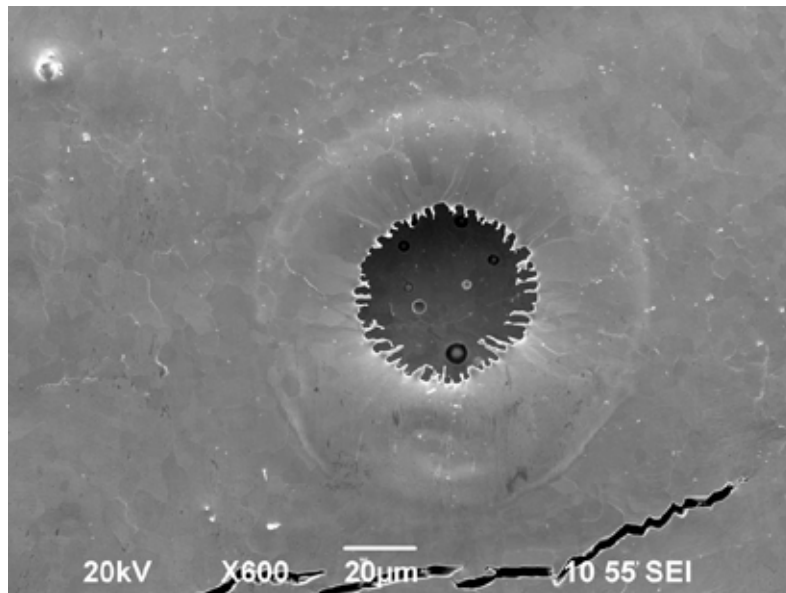


Fig.(4.4)9. Even moderate energy loads (5 pulses with energy density 2 MJ/m<sup>2</sup> per shot) leads to tungsten surface strong melting and formation of deep bubbles and cracks.

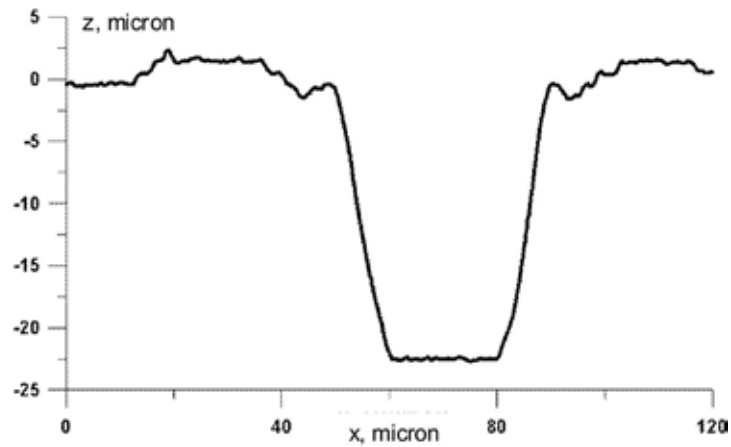


Fig.(4.4)10. Depth profile of bubble on tungsten surface. Measured by MeX software by using of SEM stereopair.

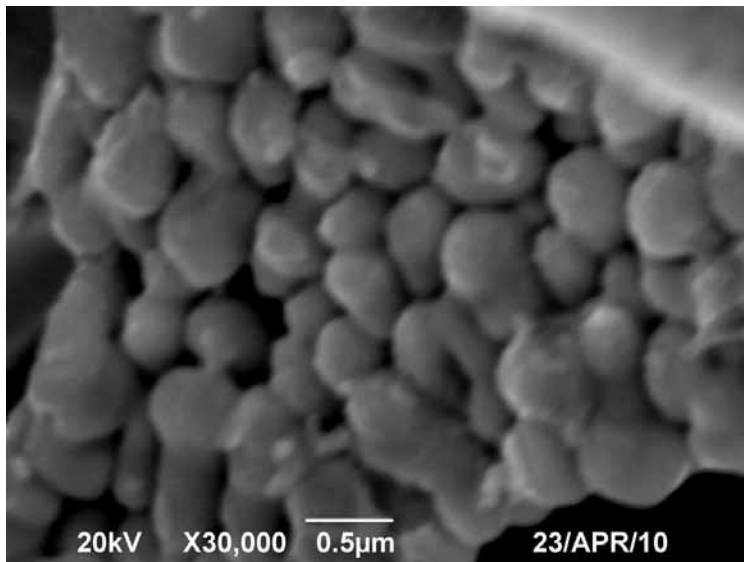


Fig.(4.4)11. Crack pattern with cell sizes 0.3  $\mu\text{m}$  on tungsten surface after irradiations.

It was shown that at energy loads corresponding to biggest ELM type I in ITER divertor (expected  $10^3$  ELM per ITER shot) tungsten erosion depth will be unacceptable strong: only after 9 GOL-3 pulses with energy density  $4 \text{ MJ/m}^2$  per shot erosion depth was hundreds of microns. Surface have form of frozen melt with waves with vertical changes of hundreds  $\mu\text{m}$ . Only crack network with cell sizes  $10 \mu\text{m}$  is observed. Fig. (4.4)12 shows typical view of surface after irradiations. Height of round object in right lower corner was  $280 \mu\text{m}$ . Altitude of upper object was  $100 \mu\text{m}$ , fig. (4.4)13 shows 3D view of object like this.

At energy loads  $12 \text{ MJ/m}^2$  tungsten erosion depth was more than  $150 \mu\text{m}$  per shot.

Comparative irradiations by powerful plasma stream of different tungsten grades was performed. Different tungsten grades shows different behavior under irradiations.

Experimental results set more severe limitation on tungsten surface maximal energy loads under plasma stream irradiations than previous ones.

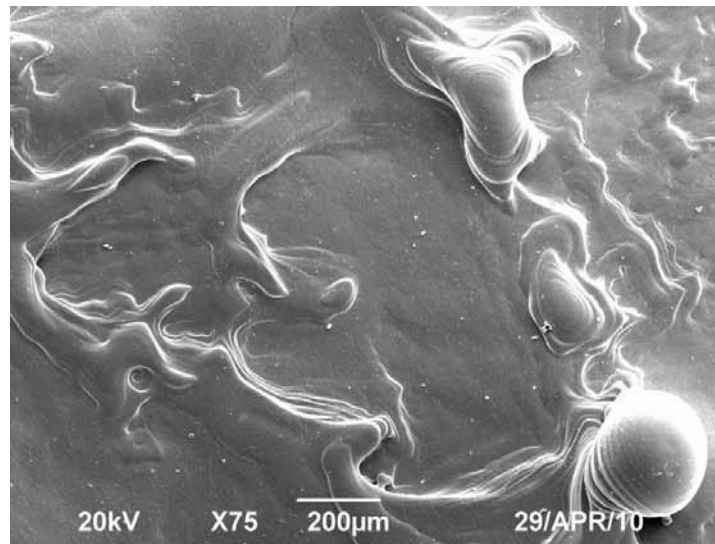


Fig.(4.4)12. SEM image of tungsten surface after 9 GOL-3 pulses with energy density  $4 \text{ MJ/m}^2$  per shot corresponding to biggest ELM type I in ITER divertor (expected  $10^3$  ELM per ITER shot).

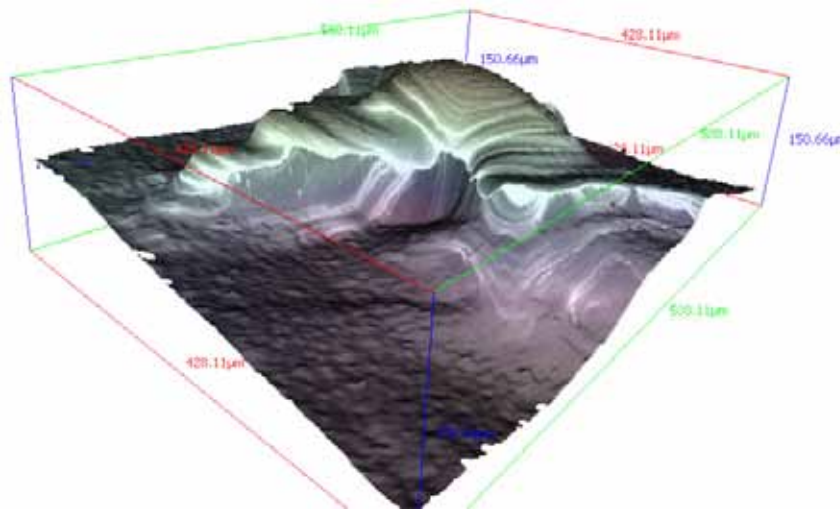


Fig.(4.4)13. 3D view of tungsten surface after 9 GOL-3 pulses with energy density  $4 \text{ MJ/m}^2$  per shot. Hills height is more than hundred  $\mu\text{m}$ .

#### 4.4.7 Development of diagnostic capabilities

Quality of the obtained physical information is limited by capabilities of a diagnostic complex of GOL-3. As well as during the previous periods considerable efforts were put into this subsystem of GOL-3 in 2010.

Macroscopical stability of the plasma column and variations in its size and position in regimes with injection of the beam of the reduced diameter was investigated by means of imaging VUV spectrometer. Comparison of spatial structure of VUV spectral lines of impurity ions with numerical calculation of dynamics of ionization balance resulted in the upper estimate of transverse diffusion coefficient in specified regimes  $\sim 2 \text{ m}^2/\text{s}$ . The low value of transverse diffusion coefficient that was confirmed in these experiments means that transverse losses aren't dominant even at reduction of diameter of the plasma column to  $\sim 1 \text{ cm}$  scale.

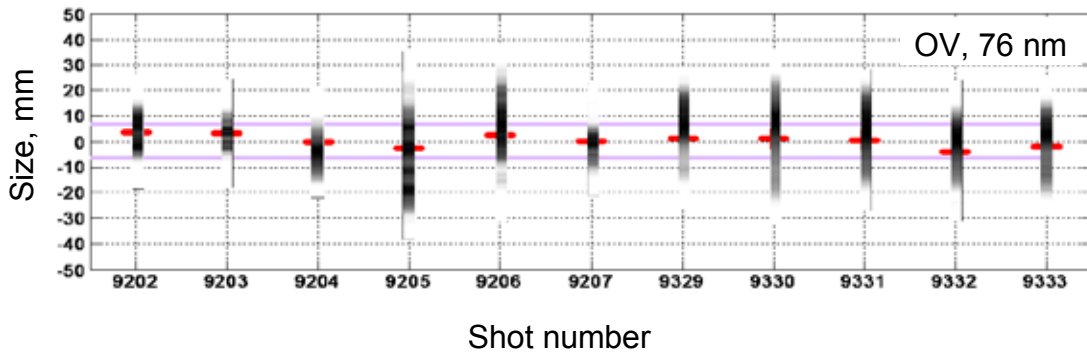


Fig.(4.4)14. Size and position of VUV-emitting plasma in a sequence of shots with the beam injection into a non-ionized deuterium. Shades of gray shows brightness and position of the plasma, its center is marked by a thick dash, expected beam diameter is shown as horizontal solid lines.

A new fast CCD camera VIDEOSPRINT by VIDEOSCAN company was put into regular operation at GOL-3. This camera produces monochrome images of transient processes. Peak frame rate reaches 250000 fps at  $1280 \times 2$  arrays with full resolution  $1280 \times 1024$  at lower speeds. At GOL-3 this camera is used for studying of processes of creation, heating and cooling of the plasma. External triggering of the camera and its remote control were made. In September, 2010 the first results were produced with this diagnostics and since that the camera is in operation.

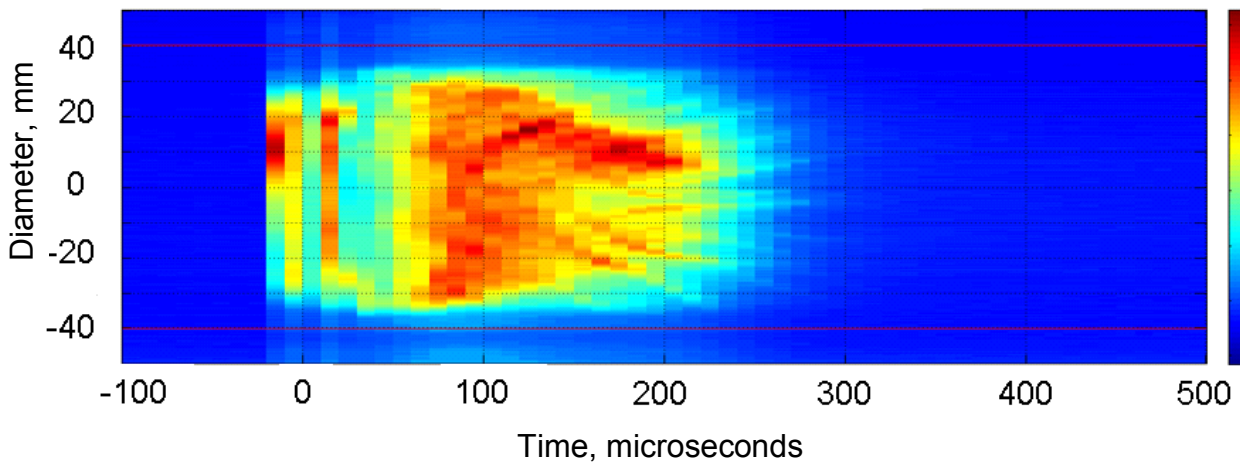


Fig.(4.4)15. Dynamics of plasma brightness (slit scan). Preliminary plasma starts at  $-35 \mu\text{s}$ , the beam starts at  $0 \mu\text{s}$ .

Passage to an essentially new synchronization system became an important infrastructural improving. Earlier for this purpose ГВИ-8М units connected under the complicated tree-like chart were used. New multichannel independent 32-bit synchronization system «Pulse» has been developed and made for their replacement in the Lab. 9 (by group of A. D. Khilchenko). It communicates with client computer with 100BaseTX. The «Pulse» System has up to 48 output channels in 3U 84HP IEC 60297 crate. It can be completed with drivers having an electrical output (which is compatible on parameters and connectors with earlier ГВИ-8М), or an optical output. In total 6 crates of a different set of drivers for control of GOL-3 and its major subsystems were made.

#### 4.4.8 Development of technology of creation of a long-pulse intensive electron beams based on plasma emitters

In 2010 the first series of experiments was done on generation of intense electron beam of submilli-second duration with injector based on arc plasma emitter. The injector was installed in exit tank (plasma expander) of GOL-3. The aim of experiments was to test reliability of power and control systems of the injector, as well as provide the beam generation with following parameters: accelerating voltage in the range of  $40 \div 120$  kV, emission current to up to 100 A and the beam duration  $0.1 \div 0.5$  ms. Emitting plasma was generated by pulsed arc discharge with cold cathode and hollow anode. The hydrogen serves as working gas. An arc generator was fed by an autonomous power source floated under the full accelerating potential.

Accelerating voltage pulse of quasi-rectangular form was obtained by means of partial discharge of high-voltage capacitor bank using two multigap spark switches. An electron beam was extracted from the plasma and accelerated in the diode-type EOS with 36 emission apertures of 4 mm in diameter, arranged in a hexagonal order. Then the beam was transported in a metallic drift tube at a residual gas pressure of  $\sim 1 \cdot 10^{-4}$  Torr at a distance of approximately 0.5 m and is absorbed in the end cap collector.

In the experiments the beam stored energy of 600 J and average beam power of about 4 MW were obtained. The experiments were performed in the absence of an external magnetic field. Maximally achieved (not simultaneously) in the first series of experiments, the beam parameters were: 110 keV, 70 A, 0.5 ms. Typical waveforms of voltage and emission current are shown in Fig. (4.4)16. Thus, the first experiments demonstrate the functionality of the chosen design of injector and the prospect of further improving the beam parameters.

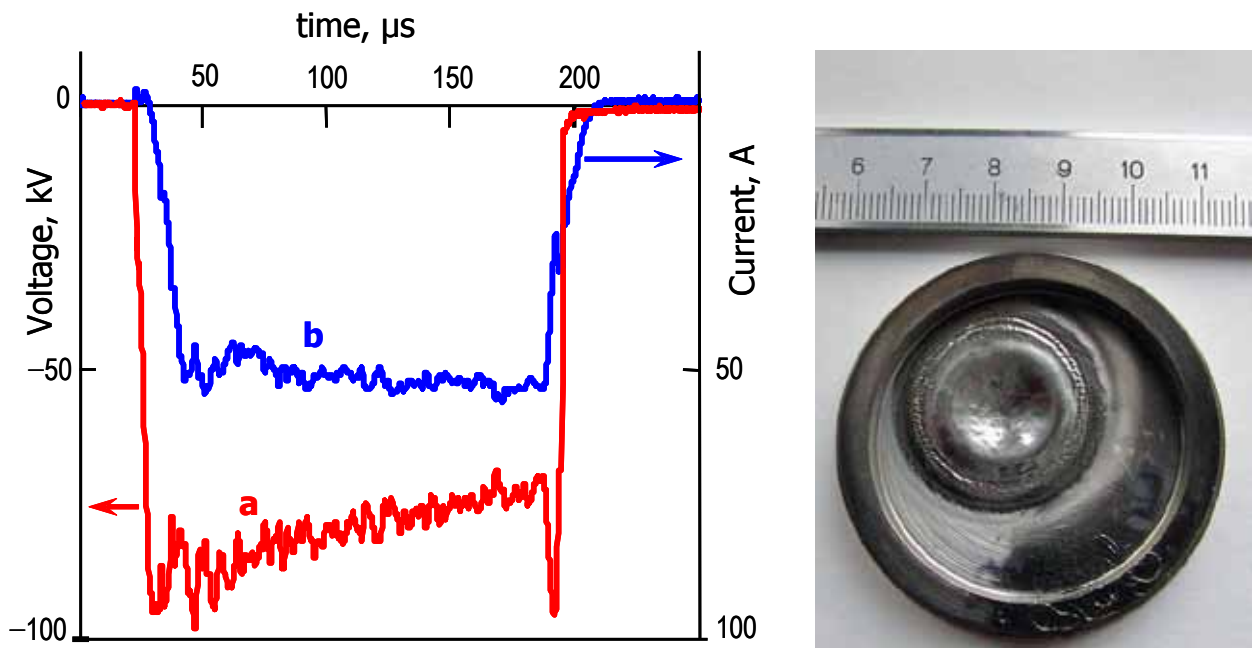


Fig.(4.4)16. Typical waveforms of the beam and imprint on the end cap of the drift tube (50 cm from the EOS).

#### 4.4.9 Summary

Experiments aimed at the development of a physical knowledge base for a mutimirror-trap-based fusion reactor are continued at the multimirror trap GOL-3. Physical data quality is improved both due to improvements of diagnostic equipment and due to dedicated experimental runs. New plasma heating technologies are developing in order to improve plasma parameters. Development of analytical and numerical

models of plasma in GOL-3 is in progress. Applied research contracted by outer organizations was carried out.

Third Workshop on program of GOL-3 was held in November, 2010. More than 30 reports that discussed current activities and future plans were made by involved scientists.

Participants of this work: A.V.Burdakov, A.P.Avrarov, A.V.Arzhannikov, V.T.Astrelin, V.I.Batkin, A.D.Beklemishev, V.B.Bobylev, V.S.Burmasov, P.V.Bykov, G.E.Derevyankin, V.G.Ivanenko, I.A.Ivanov, M.V.Ivantsivsky, P.V.Kalinin, I.V.Kandaurov, I.A.Kotelnikov, K.N.Kuklin, S.A.Kuznetsov, A.G.Makarov, M.A.Makarov, K.I.Mekler, S.V.Polosatkin, S.S.Popov, V.V.Postupaev, A.F.Rovenskih, A.A.Shoshin, S.L.Sinitsky, V.F.Sklyarov, N.V.Sorokina, V.D.Stepanov, A.V.Sudnikov, Yu.S.Sulyaev, I.V.Timofeev, A.V.Terekhov, Yu.A.Trunev, L.N.Vyacheslavov, V.A.Yarovoy.

5

ELECTRON-POSITRON  
COLLIDERS



## 5.1 VEPP-2000 in 2010

To begin with we will remind that the first bunch in VEPP-2000 has been received in September, 2007. The first measurements of luminosity and scanning  $\phi$ -meson resonance have been spent with detector SND in 2008. In 2009 detector CMD-3 has been established on the store, and VEPP-2000 has taken the present form.



Fig.(5.1)1. VEPP-2000 with SND and CMD-3 detectors.

### 5.1.1 First experimental work with SND and CMD-3 detectors $2 \times (500-950 \text{ MeV})$

In the end of 2009 CMD-3 was ready to the beginning of measurements. Naturally, it was necessary to begin a season calibration of CMD-3 systems in area of  $\phi$ -meson resonance. Simultaneously this measurement has served as a starting point for calibration of a scale of bunches' energy in VEPP-2000. After that the decision to pass energy area above  $\phi$ -meson with step of 50 MeV and with a set in each point of luminosity integral of an order  $500 \text{ nb}^{-1}$  was accepted. This work should allow to calibrate systems of particles' identification in both detectors, to check up working capacity of all power supply systems of the store, to fulfill details of operating programs and interaction of three computer clusters (the accelerator and two detectors). Experiment proceeded 6 months.

Measurement of luminosity of the store was carried out on both detectors by elastic scattering of electrons and positrons. By the season end the total integral of the luminosity which has been written down by detector SND, has made nearby  $7000 \text{ nb}^{-1}$ . Distribution of the luminosity integral on energy is presented in Fig.(5.1)2.

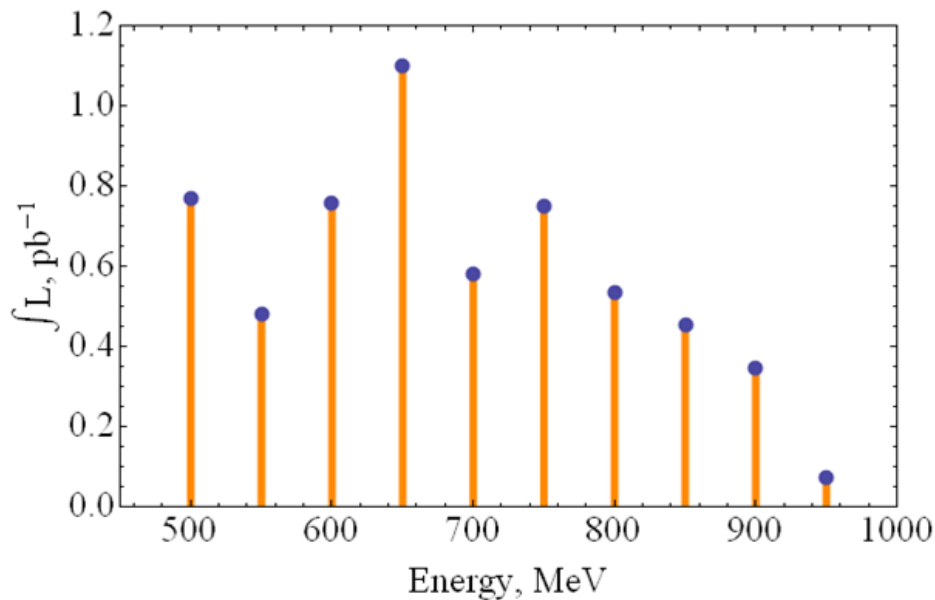


Fig.(5.1)2. Luminosity integral (SND data).

Decrease of the gathered luminosity in the high energy region is connected with limitation of particles' injection energy from booster storage ring BEP. In spite of the fact that the maximal magnetic field in BEP is sufficient to accelerate the beams up to 900 MeV, real limitations of boosting high currents (50–60 mA) have arisen because of not enough voltage of RF cavity and weak sextupole correctors. Above 800 MeV acceleration was performed into collider VEPP-2000. The absence of beams separation system in interaction points has considerably complicated this process. Besides, eddy currents induced in nitrogen screens of superconducting solenoids due to energy change led to sufficient betatron tunes shifts (up to  $\pm 0.02$ ). This effect reduced as boost speed from injection energy to experimental one, and duration of opposite descent, that led to the big loss of time and currents of colliding beams.

Thus, the first experimental work has shown with all evidence necessity of increasing the booster BEP energy up to 1 GeV that VEPP-2000 on any energy could work in “a factory mode”. The first study of this idea, considering transition to bunches from an injection complex, indicates that BEP modernization to 1 GeV is not very expensive (see chapter “BEP modernization”).

### 5.1.2 Radiative polarization and energy calibration

In the end of the first experimental season week attempt of calibrating VEPP-2000 energy by a method of a resonant depolarization has been undertaken. First of all, it is necessary to tell that presence of strong solenoids in magnetic structure of the store leads to considerable restrictions for radiating polarization of bunches. Polarization is possible only at opposite polarity of solenoids in each experimental drift. Moreover, the result depends as well on sequence of solenoids' polarities on a ring as a whole. If arrangement of solenoids underlines the first orbital harmonic of a longitudinal field radiative polarization is possible in energy range from 0.6 to 1 GeV with rather small polarization time. In Fig.(5.1)3 the computations with ASPIRRIN code of degree (top) and time (in the middle) of radiative polarization are shown in dependence on energy.

Ideally, when integral of solenoids' field is equal to zero (left) the integer resonance (spin tune is  $\nu = 2$ ) as well as betatron ones ( $\nu = 4 - \nu_1$  и  $\nu = \nu_2 - 2$ ) are absent. However, these resonances immediately arise at symmetry break of longitudinal field.

The bottom part of Fig.(5.1)3 presents a situation, when solenoids' layout creates the second orbital harmonic. Here polarization can exist only in low energy range 200–600 MeV. Large polarization time in this region does not allow one using radiative polarization in VEPP-2000. However, resonant depolarization is possible in this case with the beam preliminary polarized on high energy in booster BEP.

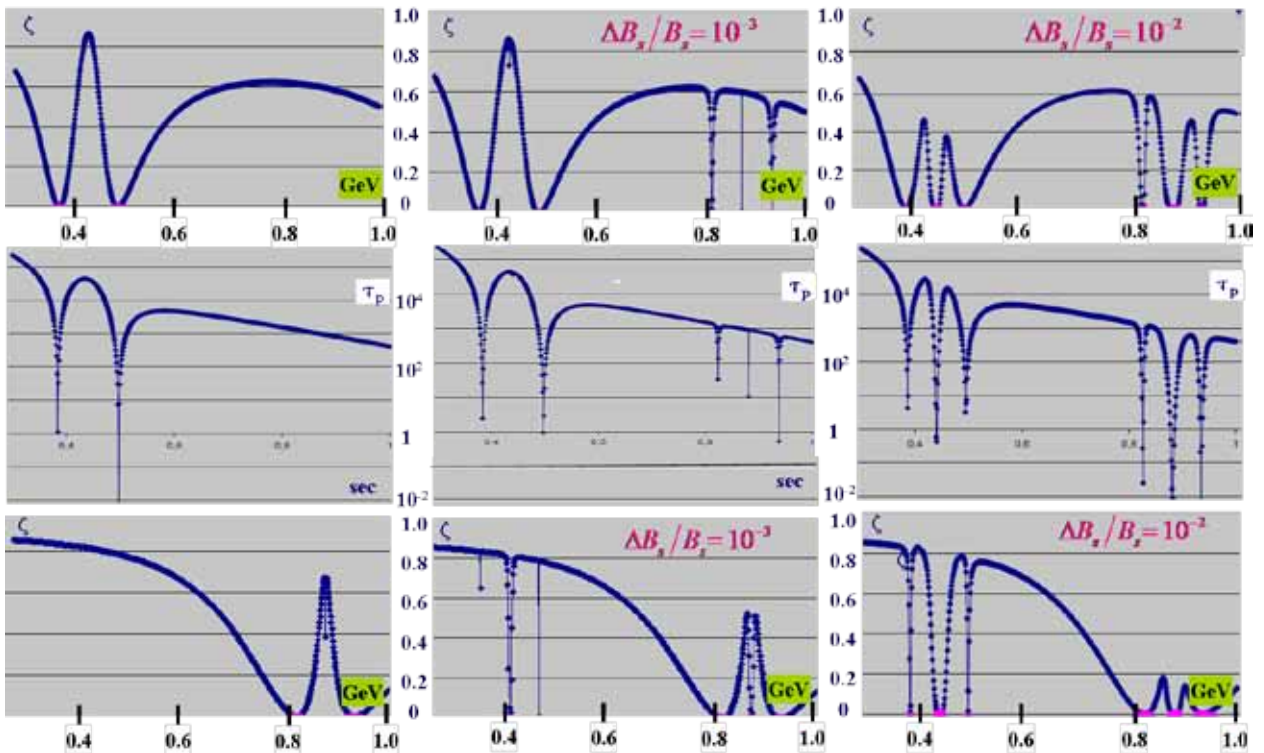


Fig.(5.1)3. Calculations of radiative polarization in VEPP-2000.

To register an effect of beam depolarization by measuring counting rate of particles scattered inside a bunch two mobile scintillation counters have been put in one technical drift of VEPP-2000 (Fig.(5.1)4). Besides, we have developed 2-channel RF multiplier feeding depolarizer, which consists of 4 short (10 cm) plates in the storage ring vacuum chamber. Plates' layout allows one to excite magnetic field of any direction in the plane transversal to the beam orbit.



Fig.(5.1)4. Probes for particles counters.

For the first measurement the energy of 750 MeV has been chosen, at which polarization time is about half an hour and there are no strong depolarizing resonances, even in the assumption of solenoids' symmetry break to level of 1%.

The depolarizer worked on frequency  $f_d = f_0 \cdot (2 - \nu)$ . Originally depolarizer frequency scan was performed in frequency range of about  $\Delta f_d \simeq 0.01 f_d$  with a rate of 10 Hz/s. After observation of first jumps in counting rate, normalized to square of beam current, the frequency range has been narrowed in two times and scanning rate — in 10 times. The data of these measurements is presented in Fig.(5.1)5.

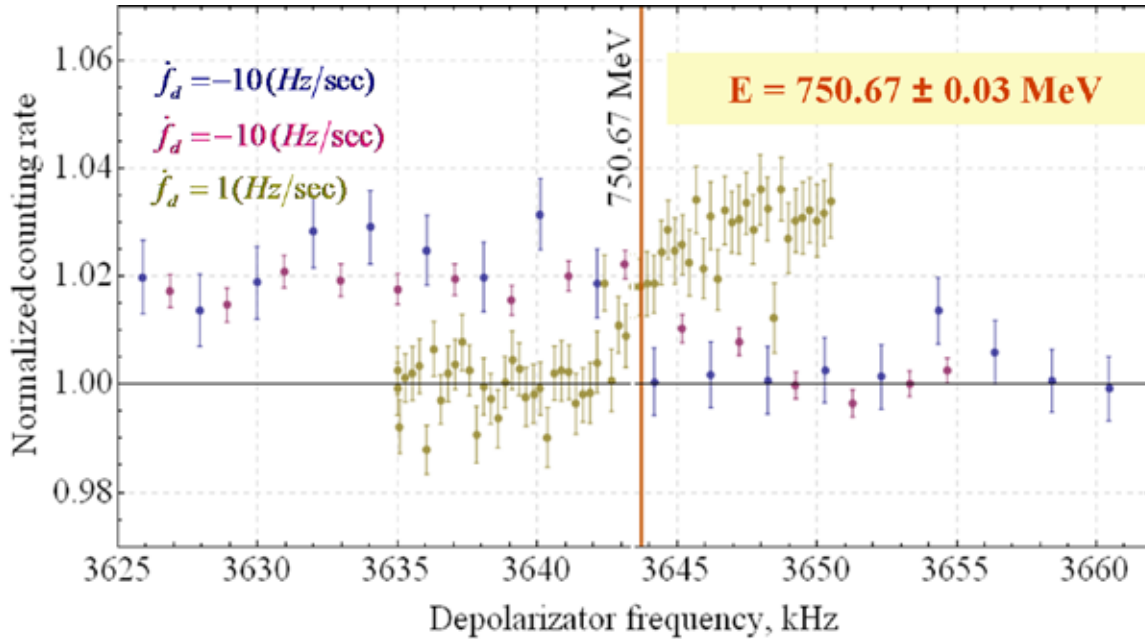


Fig.(5.1)5. Measurement of energy by method of resonant depolarization.

As one can see from Fig.(5.1)5 a jump of the counting rate occurs in narrow region of depolarizer frequencies, so we can determine beam energy as  $E=750.67 \pm 0.03$  MeV. The energy value obtained is in good agreement with expected one, which is based on magnetic measurements and energy calibration by mass of  $\phi$ -meson resonance.

### 5.1.3 Correcting the orbit and magnetic structure of VEPP-2000

While energy of VEPP-2000 change in wide range for a long time of work the need of correcting equilibrium particles' orbit and tuning optical system of storage ring arises inevitably. For VEPP-2000 it is especially actual, considering work of magnets at strong saturation.

The main task at correction of the closed orbit (CO) in VEPP-2000 is minimizing its deviation from magnetic axes of chosen elements. After correction of closed orbit, it is possible store position of the beam in all the beam position monitors (BPM), and to use these data for further orbit corrections. As BPM on VEPP-2000 we use 16 CCD, which detect synchrotron radiation of electrons and positrons from dipoles, and 4 image current monitors (pick-ups). CCDs are not fixed tightly, therefore from time to time their position changes, hence one need to make regular calibrations for orbit correction by data from BPM.

First method of orbit correction (OC), which has been automated on VEPP-2000, is method of correction relative to magnetic centers of quadrupoles. If a particle has an error  $\delta \vec{l} = (\delta x, \delta y)$  in quadrupole, then variation of gradient in this quad on  $\delta G$  will lead to CO shift equal to one from dipole corrector with the field  $\delta \vec{H} = (\delta x \delta G, \delta y \delta G)$ . Measuring orbit deviations in BPMs, caused by gradients errors in quadrupoles, it is possible construct response vectors  $\delta \vec{X}_{exp,i}$ .

As the accelerator structure is known, we can calculate theoretical responses  $\delta \vec{X}_{mod,i}$  to dipole correctors in corresponding quads. To find absolute coordinate of CO in a quadrupole number  $i$ ,  $\vec{X}_{err,i}$ , one

should minimize following functional:

$$F(\lambda_i) = (\vec{\chi}_{\text{mod},in} \lambda_i - \vec{\chi}_{\text{exp},in})^2 \rightarrow \min$$

Here  $\vec{\chi}_{\text{mod},in}$  и  $\vec{\chi}_{\text{exp},in}$  — are measured and model response vectors, normalized to accuracy of measurements  $\sigma_{in}$ :

$$\vec{\chi}_{\text{mod},in} = \left\{ \frac{\delta x_{\text{mod},i1}}{\sigma_{i1}}, \dots, \frac{\delta x_{\text{mod},iN}}{\sigma_{iN}} \right\}$$

$$\vec{\chi}_{\text{exp},in} = \left\{ \frac{\delta x_{\text{exp},i1}}{\sigma_{i1}}, \dots, \frac{\delta x_{\text{exp},iN}}{\sigma_{iN}} \right\}$$

Functional has minimal value with the next parameters:

$$\lambda_{\text{min},i} = \frac{(\vec{\chi}_{\text{mod},i} \cdot \vec{\chi}_{\text{exp},i})}{\vec{\chi}_{\text{mod},i}^2}$$

Now absolute coordinates of the beam in quadrupoles are calculated with these equations:

$$\delta x_{\text{err},i} = \frac{\delta H_{y,i} \lambda_{\text{min},i}}{\delta G_i}, \quad \delta y_{\text{err},i} = \frac{\delta H_{x,i} \lambda_{\text{min},i}}{\delta G_i}$$

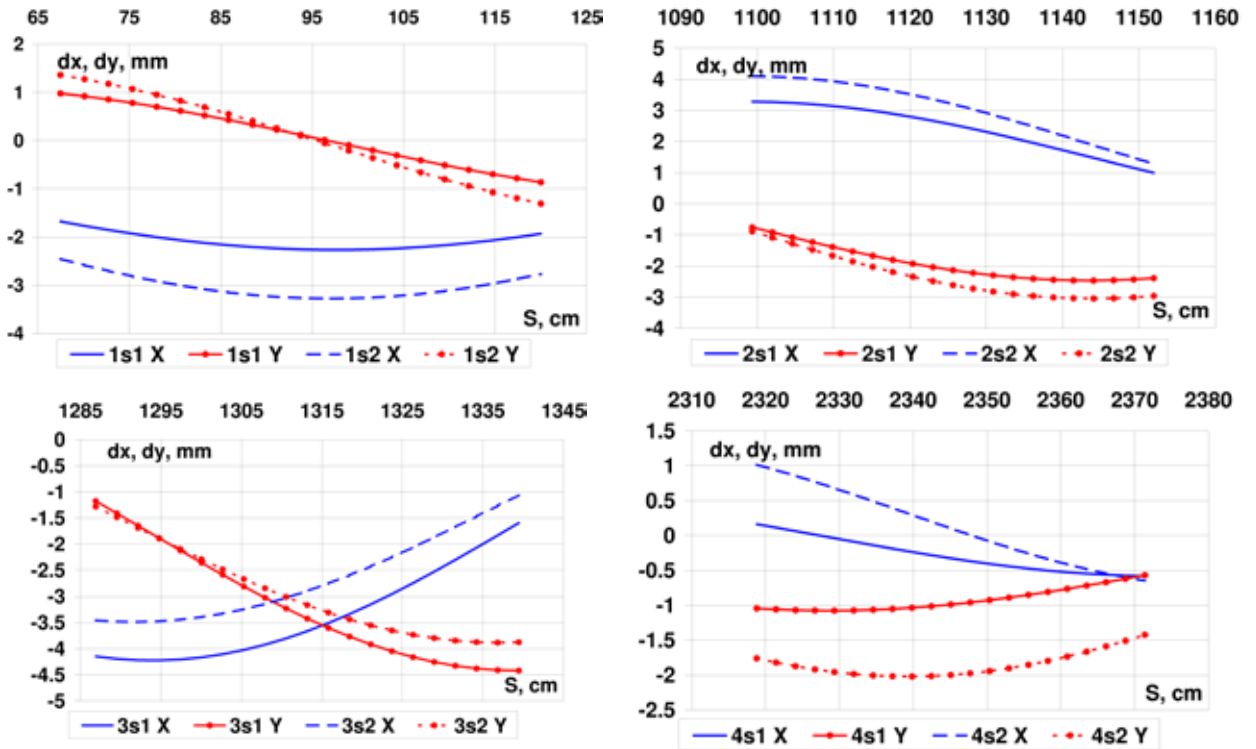


Fig.(5.1)6. An example of restored orbit deviation.

For some elements, such as long solenoids of final focus in VEPP-2000, it is necessary to know the exact information on passage of CO trajectory concerning magnetic axis of the element. Fig.(5.1)6 shows recovered orbit inside VEPP-2000 final focus solenoids relatively to their magnetic axes. Solenoids xS1 and xS2 are coils of one solenoid and should be coaxial. Apparently, the huge stresses arising in solenoids and errors at manufacturing have caused distinctions in the measured shifts. The big synchronous orbit shift is a consequence of intended distortion of the orbit, which purpose was to reduce background noise in detectors.

To repair CO distortions  $X_i$  we need to calculate response matrix  $M_{ij}$  consisted of CO shifts, caused by unit currents in correctors from the chosen group. Then one should find such currents  $I_j$ , which would minimize  $\|F\|$ :

$$F_i = \frac{X_i}{\sigma_i} - \frac{M_{ij}}{\sigma_i} I_j, \quad \sigma_i^2 = \sigma_{stat,i}^2 + \sigma_{syst,i}^2.$$

Code for correctors' optimization in VEPP-2000 uses SVD decomposition to inverse rectangular matrices:

$$I_j = \left( \frac{M_{ij}}{\sigma_i} \right)_{SVD}^{-1} \frac{X_i}{\sigma_i}.$$

Discrepancies of theoretical model lead to errors at orbit correction, so we need several iterations.

Fig.(5.1)7 shows the decrease of CO distortion from magnetic centers of quadrupoles after correction.

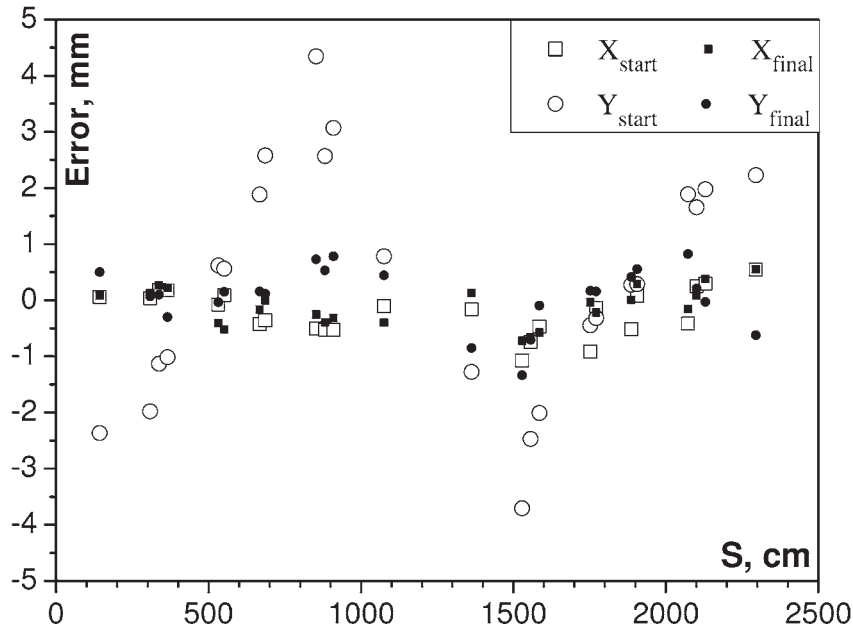


Fig.(5.1)7. An example of orbit correction.

#### 5.1.4 Optimizing the correctors strength

Some times there is a situation when some correctors work against each other, so we can significantly reduce their currents almost without changing the CO. On VEPP-2000 complex a special program has been developed, which allows one easily optimize correctors' strength. At the first stage the program collects data about strength of chosen correctors and computes CO distortion induced by them:

$$X_{dist} = \sum_{corr} X_i = M_{corr} I_{corr,i}.$$

After that the code calculates optimal currents making CO distortion differ from initial to acceptable value:

$$I_{optimal,i} = (M_{corr})_{SVD}^{-1} X_{dist}$$

$$\Delta X_{CO} = M_{corr} (I_{corr,i} - I_{optimal,i}).$$

Operator controls the difference between CO before and after optimization by selecting the quantity of singular values participating in inverse matrix calculation  $(M_{corr})_{SVD}^{-1}$ . After adjustment of the correctors strength, one should make orbit correction as the theoretical model of accelerator is slightly differs from

real. In Table(5.1)1 the results of described procedure are presented.

Table(5.1)1. Correctors strength tuni.

	Before tuning	After tuning	After correction
$\frac{\sum I_{corr}}{N_{corr}}$	0.52 A	0.22 A	0.28 A

### 5.1.5 Correcting the accelerator structure

One of the major problems when an accelerator is put into operation as well as its regular work is detection and eliminating the errors in linear magnetic structure of the machine. To correct the magnetic structure of VEPP-2000 the program has been written, which realizes algorithms from publisher papers.

The main idea of the method consists in minimizing the value of  $\chi^2$  by selection of the chosen parameters:

$$\chi^2 = \sum_{i,j} \frac{(M_{mod,ij} - M_{mes,ij})^2}{\sigma_{ij}^2} = \sum_{ij} V_{k(ij)}^2.$$

Here  $M_{exp,ij}$  и  $M_{mod,ij}$  — are experimental and theoretical response matrices of CO in  $i$ -th BPM depending on variation of  $j$ -th corrector,  $\sigma_{ij}$  — accuracy of appropriate measurements. The main feature of this code is that it uses 6D phase space when making calculations of responses on dipole correctors.

Table(5.1)2. Avaraged changes of currents in quadrupoles in 4 sequential iterations

Iteration	1	2	3	4
$100 \times \frac{\sum \Delta I_{quad} / I_{quad}}{N_{quads}}$	6.17	3.24	0.85	0.24

After improvement of the code "sixdsimulation" the procedure of correcting accelerator structure is made automatically. Interaction of operator with the program is organized through a sequence of dialog boxes, in which is possible to set necessary parameters. One iteration takes about 60 minutes. 50 minutes are needed to measure the CO response matrices on dipole correctors, betatron tunes and dispersion function. The next 10 minutes one spends to go through series of dialog boxes and to tune correction parameters. Table 2 and Fig.(5.1)8 illustrate successive correcting strong distortion of VEPP-2000 magnetic structure.

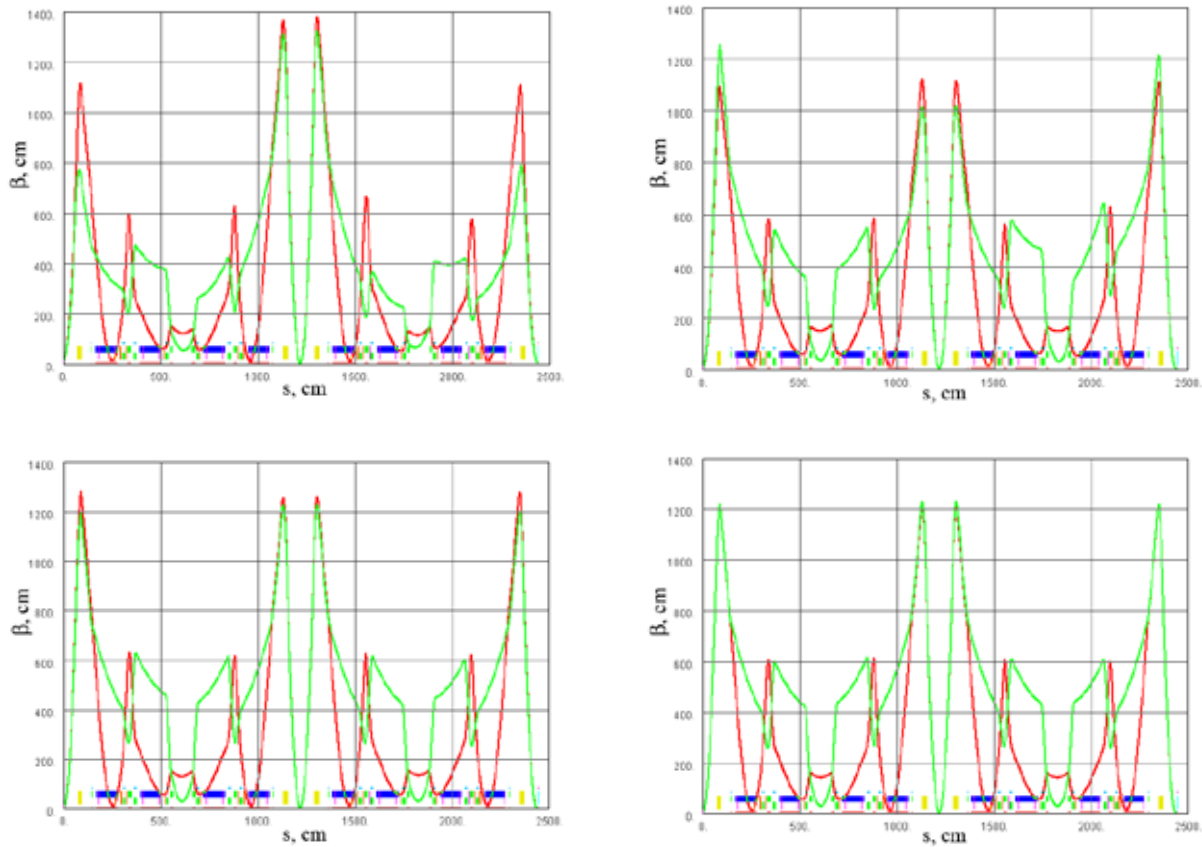


Fig.(5.1)8. An example of correcting the VEPP-200 structure.

For operational management of storage ring so called “adjustment knobs” have appeared very useful for changing betatron tunes along and across to coupling resonance; for correcting the value of coupling between X and Z oscillations; for repairing the leading orbit’s distortion harmonics; for making local orbit shifts (“bumps”), etc. The main tool is the program “ORBIT”, which combines optical measurements from CCDs in 16 points along the ring and data from 4 pick-ups placed in triplet drifts.

The same program is used for studying beam-beam effects. In Figures below calculated and measured envelopes of transverse beam sizes are shown for two cases. Fig.(5.1) 9 shows “natural” sizes with small beam currents, when beam-beam effects are absent. One can see good agreement of values that was obtained after correcting optics as described above. However in a case of interacting high electron current  $I^- = 45$  mA with small positron one  $I^+ = 3$  mA the sizes of the last are increased significantly outside the interaction region (Fig.(5.1) 10).

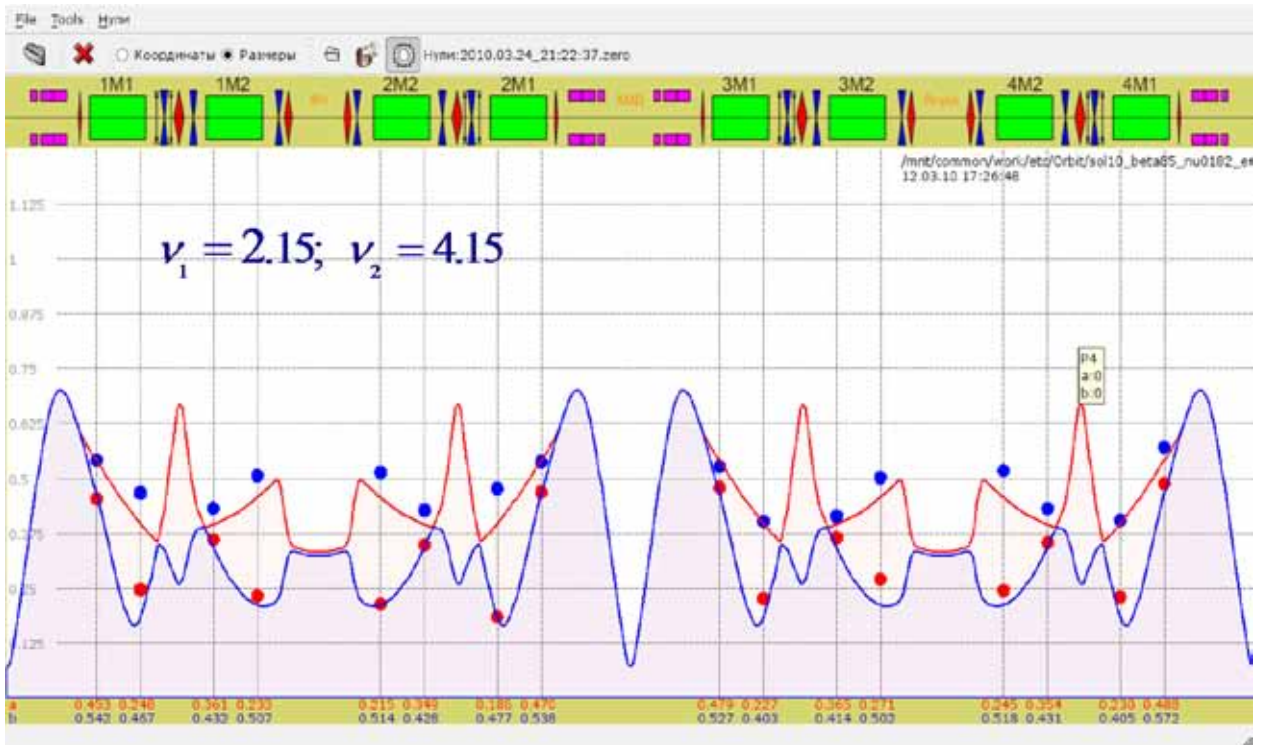


Fig.(5.1) 9. Beam sizes and envelopes.

$I^+ = 3 \text{ MA}; \quad I^- = 45 \text{ MA}; \quad \xi^+ = 0.1$

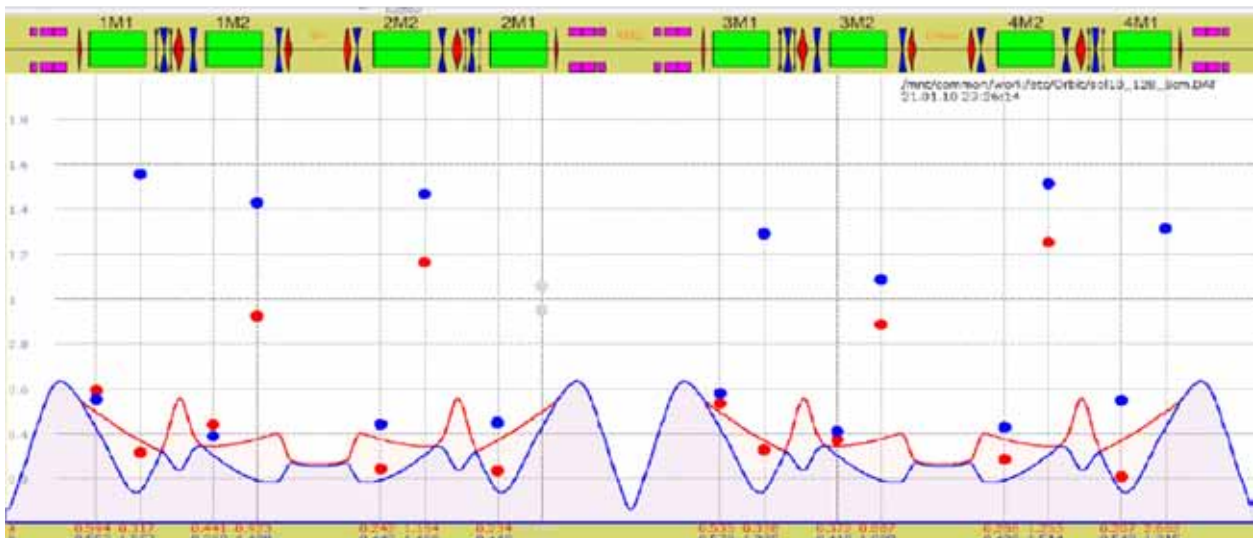


Fig.(5.1)10. Strong-weak beam-beam effects.

### 5.1.6 Luminosity measurements

Luminosity measurements on VEPP-2000 are performed since 2007 based on data from detectors SND and CMD-3. However, such measurements are slow enough (one procedure takes 30 s) and have large statistical error leading to their fluctuations, which is inconvenient to tune the accelerator. As an alternative tool independent luminosity measurement based on beams' sizes has been realized. Actually to calculate the luminosity one has to know sizes at interaction point and intensities of colliding bunches. Even in a machine with one ring the sizes of electron and positron beams are different because of beam-beam effects:

dynamical emittance  $\varepsilon$  and beta function  $\beta^*$  depend on current of opposite beam. And besides linear effects there is stochastic gain of emittance due to linear betatron and generated by beam-beam effects nonlinear resonances. This does not allow one to predict a dependence of luminosity on current in the case of strong colliding bunches.

Measuring beam sizes directly in interaction point is technically impossible. However, we have 16 points along the ring for measuring beam sizes with CCD cameras using synchrotron radiation from bending magnets: 8 points for each beam. In case of no opposite beam the optics and transfer matrices between points of measurement are known very well, so all the sizes can be recalculated to one azimuth for comparison and analysis. Beam-beam effects change beam emittances and introduce focusing distortion, but this disturbance is localized at interaction point (IP), so all transfer matrices outside the IP are unchanged.

Calculation of sizes and luminosity is made with such assumptions:

1. Optics of unperturbed ring is known, including transfer matrices, dispersion function and momentum spread in the beam.

2. Two arcs between IPs are always identical to each other, mirror symmetry is kept.

3. Optics is uncoupled, so we can use independent transfer matrices  $2 \times 2$ .

For transferring beam sizes to IP through focusing solenoid that is not true: solenoid makes rotation of betatron oscillation plane on a certain big angle. But total rotation has no value, therefore in a transport matrix focusing by the solenoid is considered only.

It is convenient to make fitting unknown parameters ( $\varepsilon$  and  $\beta_0$ ) in mirror symmetry point of the ring, e.g. in the middle of the technical drift, where Twiss parameter  $\alpha = 0$ . A transfer from mirror symmetry point with  $\alpha = 0$  to the  $i$ -th point of the ring can be done very simple:

$$\beta_i = \beta_0 \cdot (t_{11})_i + \beta_0^{-1} \cdot (t_{12})_i$$

here  $t_{ij}$  — elements of transfer matrix  $2 \times 2$ . Fitting the emittance  $\varepsilon$  and beta function  $\beta_0$  in mirror symmetry point by using measured sizes  $\sigma_i$  in  $i$ -th points is performed by procedure of minimizing sum of squared residuals:

$$S = \sum_i \frac{(\sqrt{\varepsilon \cdot \beta_i} - \sigma_i)^2}{\sigma_i^2 + o_i^2} = \sum_i \frac{(\sqrt{\varepsilon (\beta_0 \cdot t_{11i}^2 + \beta_0^{-1} \cdot t_{12i}^2)} - \sigma_i)^2}{\sigma_i^2 + o_i^2}$$

where  $o_i$  — error of sizes determination, and  $\sigma_i$  — measured size minus dispersion part  $\sigma_\beta = \sigma - D \cdot \frac{\sigma_E}{E}$

Pairs of ( $\varepsilon$ ,  $\beta_0$ ) are adjusted for horizontal and radial motion, for electrons and positrons independently. After fitting, the received parameters are transferred to IP and the luminosity is calculated:

$$L = \frac{N_1 N_2 f_0}{2\pi \sqrt{(\sigma_{1x}^2 + \sigma_{2x}^2)(\sigma_{1y}^2 + \sigma_{2y}^2)}}$$

where  $N$  — number of particles in a bunch,  $f_0$  — revolution frequency.

The described method of measuring luminosity is in good agreement (at level of 10 %) with readouts of luminosity monitors from detectors SND and CMD-3 at rather low currents. At limiting values of currents (beam-beam parameter  $\xi \sim 0.1-0.15$ ) there is a strong deformation of transverse distribution of particles, so that distribution becomes significantly non-Gaussian. Determination of beam sizes by pictures from CCD cameras as well as fitting emittances and beta functions become incorrect.

### 5.1.7 Booster BEP modernization

Magnetic structure of booster BEP consists of 12 periods, each of them contains dipole magnet, two quadrupoles and two sextupoles to compensate for residual chromaticity of focussing. The main part of

chromaticity is suppressed by sextupole part of quadrupoles' field, because poles of quads are made of special shape. Initially this ring was designed to have large energy and transverse acceptance for accumulation of positrons. The other task of BEP working is obtaining beams with small transverse phase-space volume. This BEP property allowed us to build small-aperture channels of injection into VEPP-2M and VEPP-2000.

With the transition to the use of quality beams from injection complex this large BEP acceptance becomes useless. It is logical to take an advantage of this condition to increase maximal booster energy up to 1 GeV by decreasing pole gaps in dipoles and quadrupoles. We will keep the whole ring optics and won't change commutation of dipoles' and quadrupoles' coils, which are fed in series from power rectifier with current of 10 kA.

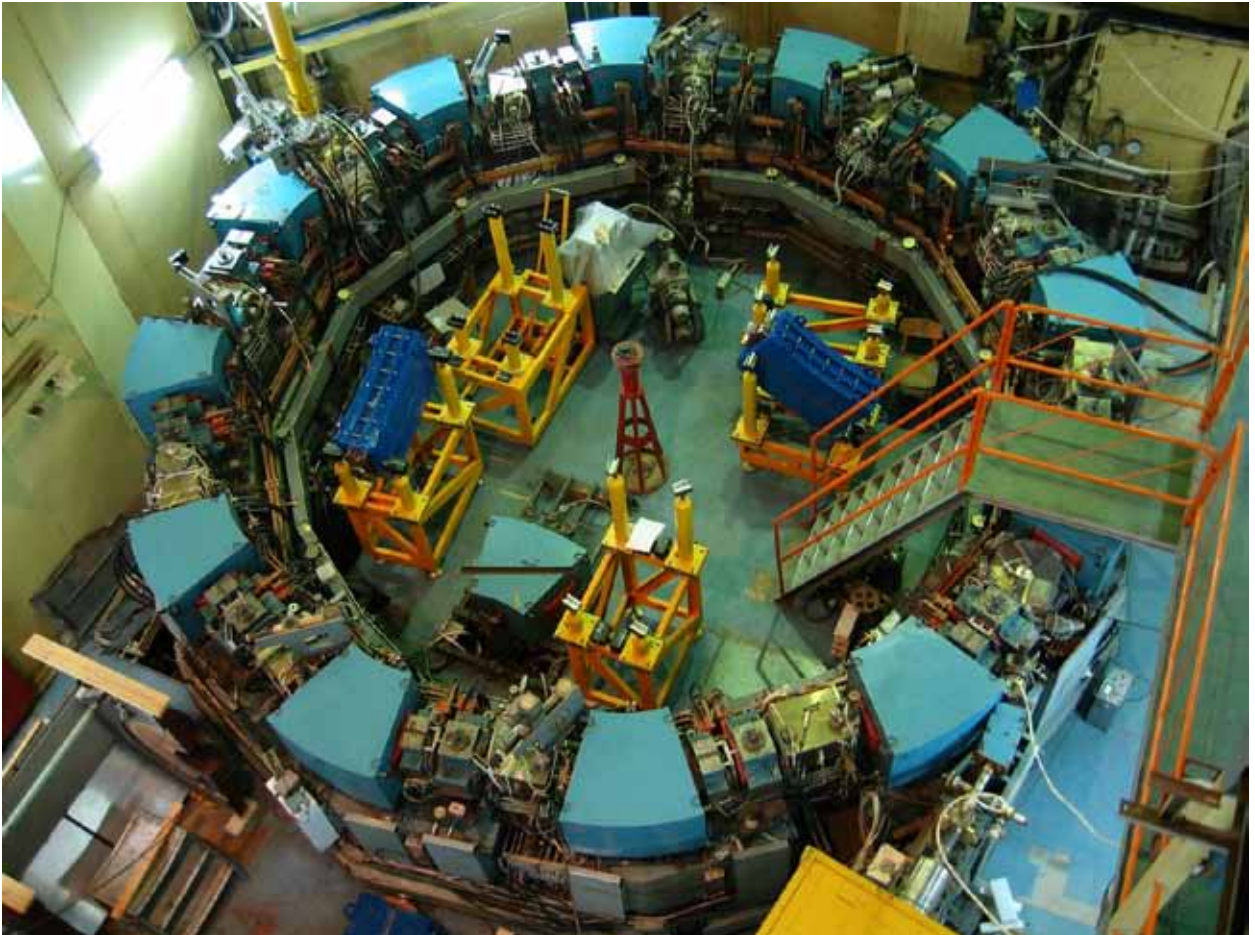


Fig.(5.1)11. Booster BEP.

To approve this idea we have carried out calculations of magnetic fields of dipoles and quads. Some improvements in pole shapes required to achieve this goal are shown in Fig.(5.1)12.

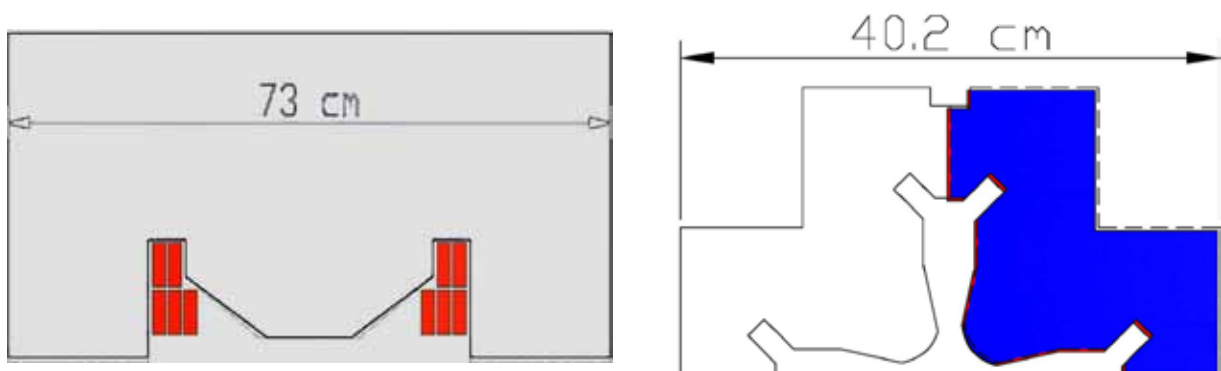


Fig.(5.1)12. Improvements in dipoles (left) and quads (right) of BE.

The saturation curve of magnetic field in dipole with a gap of 32 mm is presented in Fig.(5.1)13. Required field of 26 kGs needed for working at 1 GeV can be achieved with rectifier current of 9.5 kA, that is provided by existing rectifier.

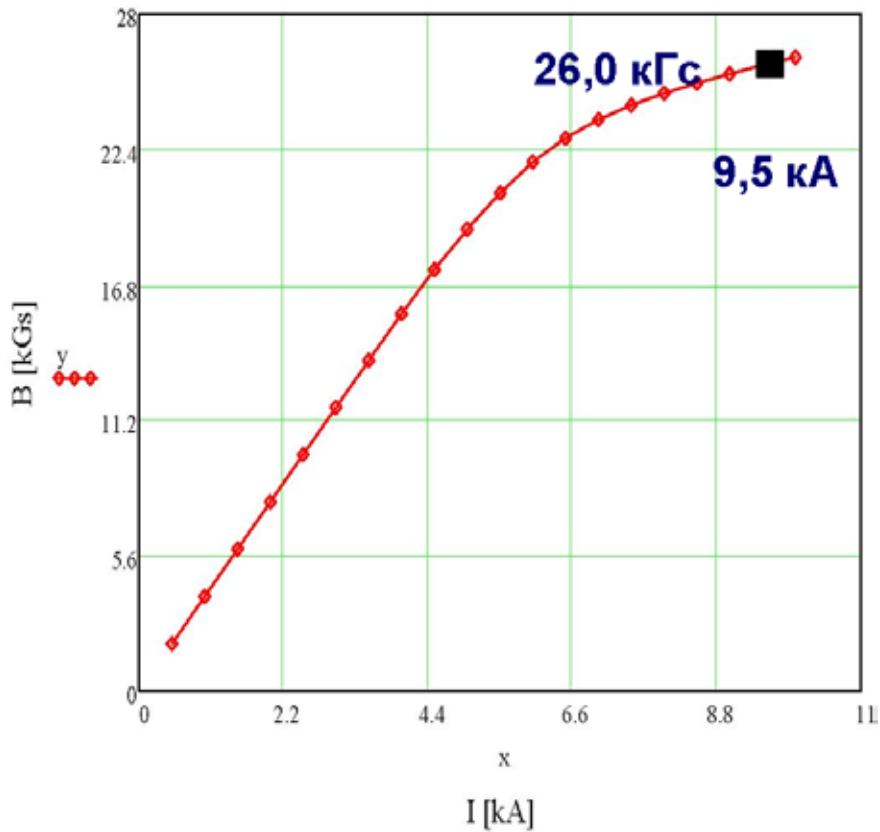


Fig.(5.1)13. Calculated saturation curve of BEP magnetic field in gap of 32 mm.

Vacuum system of BEP consists of 12 drifts, two of them are occupied with injection and ejection magnets, one rooms RF cavity. Remaining drifts have pumping including two with kicker plates. In new configuration all drifts are kept unchanged except RF cavity and injection magnet for particles from injection complex at energy 500 MeV. New injection magnet is ready. New RF cavity with frequency 174.4 MHz and accelerating voltage 110 kV is designed (Fig.(5.1)14) and put into manufacturing.

Vacuum chamber in dipoles and quadrupoles represents an oval profile from aluminum alloy with longitudinal hole for water cooling and welded flanges from stainless steel on the ends. Test improvement of such chamber to new configuration of dipoles and quads is already made in BINP manufacture. As it is shown in Fig.(5.1)15 chamber's shape is flattened to 31.5 mm in a dipole magnet and slightly changed in defocusing quadrupole. The remaining part of vacuum chamber keeps original cross-section.

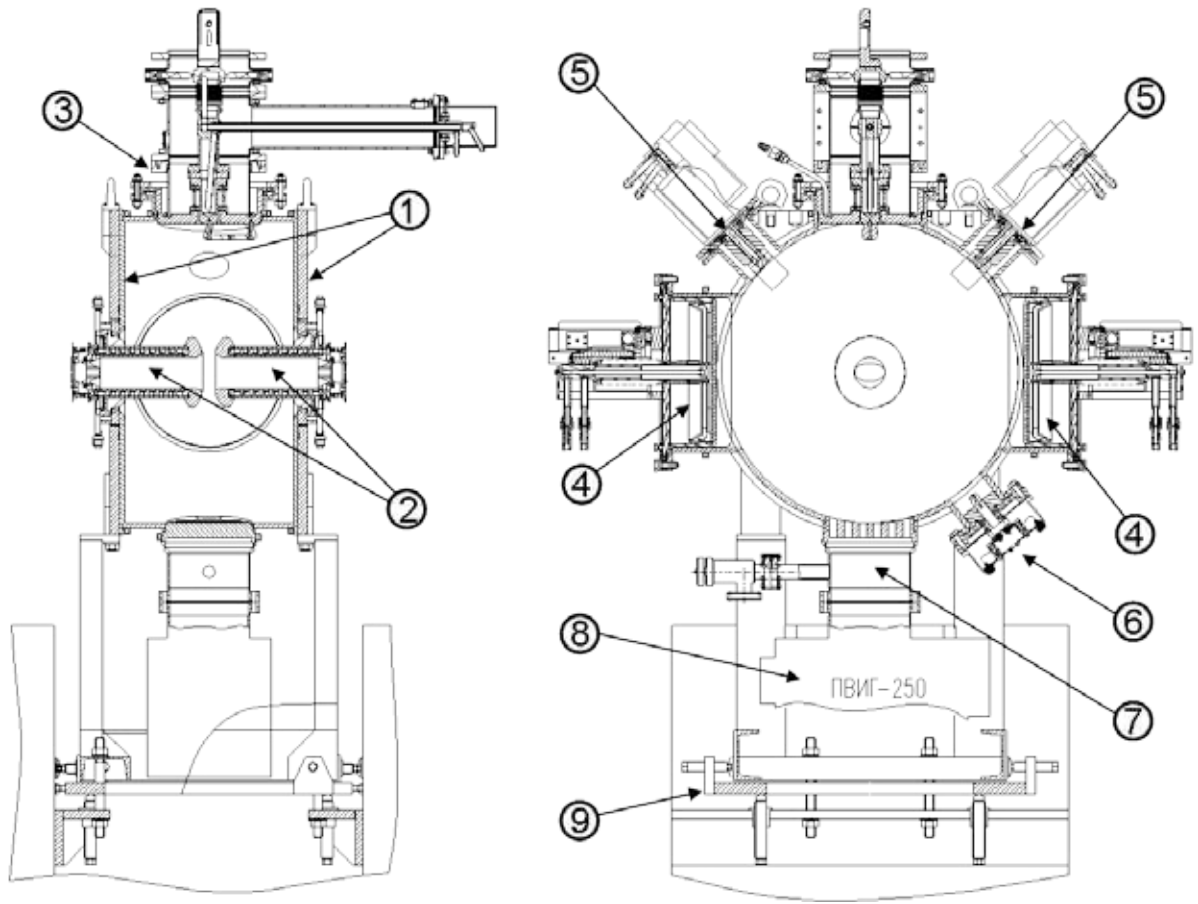


Fig.(5.1)14. New RF cavity for BEP.

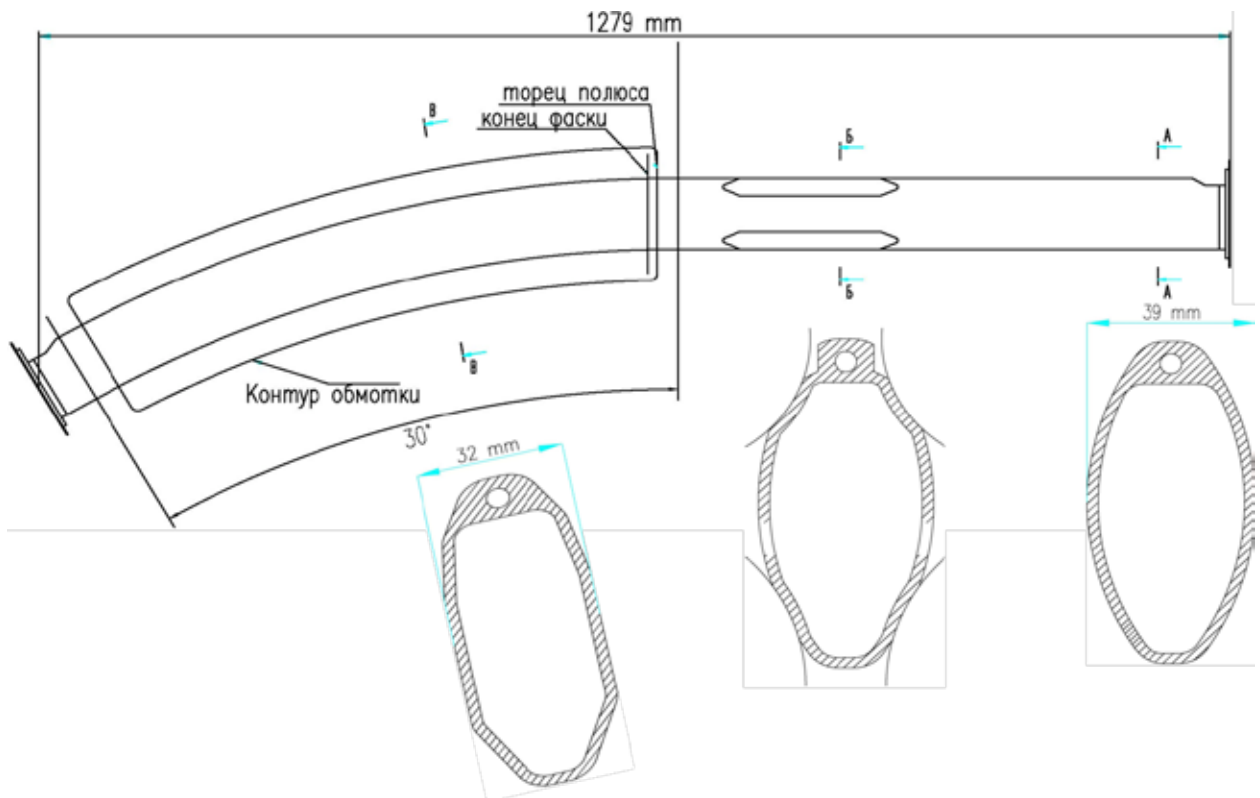


Fig.(5.1)15. Improvements in vacuum chamber of BEP.

## 5.2 The accelerator complex VEPP-4

The accelerator complex VEPP-4 is a unique facility for experiments with colliding electron-positron beams of high energy. The complex includes the injector «Positron», the multifunctional storage ring VEPP-3 and the electron-positron collider VEPP-4M with the universal magnetic detector KEDR. The main goal of the collider VEPP-4M is the experimental study of properties of elementary particles and parameters of the resonance and cross sections of electron-positron annihilation.

### 5.2.1 Distribution of working time

In 2010, the staff and users of the electron-positron collider VEPP-4M continued the experiments on high energy physics with the KEDR detector. The following experiments were prepared and conducted:

- measurement of the R parameter in the beam energy range of 0.9 - 1.5 GeV;
- scanning of the  $\psi(2s)$  meson.

In addition to the high-energy physics research, the users of the facility carried out experiments using synchrotron radiation beams extracted from the VEPP-3 and VEPP-4M storage rings.

A series of works was carried out to upgrade the VEPP-4 facility:

- the system for measuring the VEPP-4M beam energy by the method of inverse Compton back-scattering (CBS) was upgraded;
- the operation mode with a frequency of 1.5 Hz was perfected on the «Positron» facility to improve the speed of positron injection;
- a longitudinal feedback system was put into regular operation on VEPP-4M;
- a new system for temperature monitoring was adjusted in the mode of locking the magnet power supplies in case of overheating.

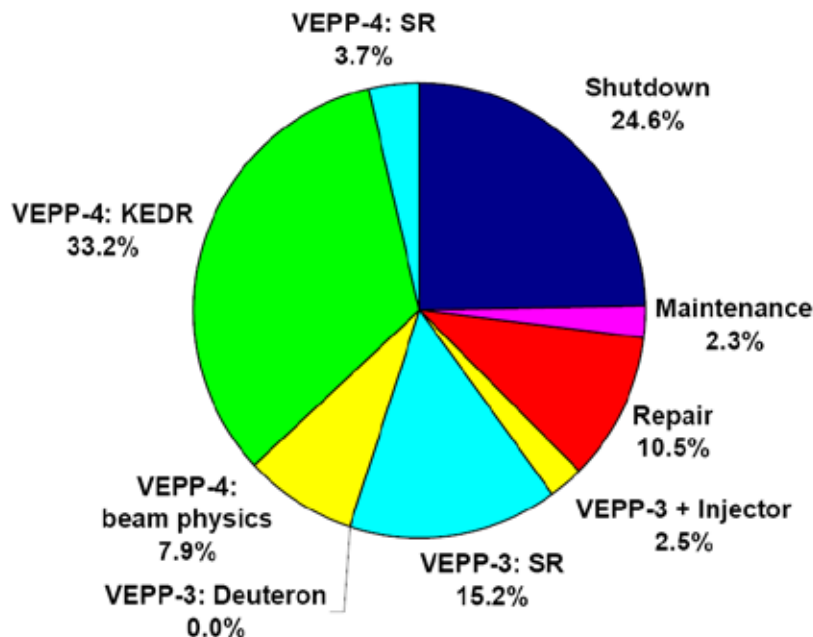


Fig. (5.2)1. Distribution of VEPP-4 working time.

Fig.(5.2)1 shows the distribution of VEPP-4 time for different tasks in 2010. It can be seen from the figure that the working time of the complex was distributed in main between the high energy physics experiments with the KEDR detector (33.2%) and those using synchrotron radiation (15.3% of the VEPP-3 time + 3.7% of the VEPP-4M time). The time allocated for the study of beam and accelerator physics (7.9%) is necessary both to keep the facilities in the operation mode required for experiments and to conduct topical beam physics research. Routine maintenance work (2.3%) is performed weekly. Time loss due to failures (10.5%) and repair is caused by the variety, complexity, and depreciation of the equipment, most of which has operated for decades.

### 5.2.2 High Energy Physics

Experiments on high energy physics with the KEDR detector continued in 2010. Currently, the main experiment is the measurement of the cross section of the  $e^+e^-$  annihilation into hadrons over a wide range of energy of 1.8 GeV to 8 GeV in the center of mass frame (the energy of particle beams is 0.9 GeV to 4 GeV). In addition, the scanning of  $\psi(2s)$  meson was carried out.

The cross section of the  $e^+e^-$  annihilation into hadrons is usually characterized by the  $R$  parameter, which equals the ratio of this cross section to the calculated cross section of the annihilation into muons. The  $R$  value is one of the most important characteristics in the physics of quarks, which defines, in particular, the hadron contribution to the anomalous magnetic moment of muon and renormalization of the electromagnetic coupling constant. Measuring  $R$  in the range of 5 to 7 GeV in the center of mass frame seems to be the most interesting. This interval has been studied only in the experiments with the MARK-I and Crystal Ball detectors. However, the results of MARK-I are now considered erroneous and the Crystal Ball result has not been published in journals, so there are no reliable data included in the PDG.

Statistics for beam energy of 0.9 - 1.5 GeV was being accumulated in 2010 as part of the experiment on  $R$  measurement. The system for determination of the beam energy and energy distribution from the CBS of laser photons was applied to the monitoring of beam parameters at scanning. Besides, several high-precision measurements of beam energy by the resonant depolarization method were carried out in order to calibrate the CBS system.

The main problem in this experiment is a significant drop in luminosity with decreasing beam energy; theoretical calculations give the dependence  $L \sim E^4$ . In addition, since the VEPP-4M was not planned for use at such low energies, there are some problems contributing to the luminosity loss. In particular, the negative impact of the collective effects of beam dynamics and the collision effects, lowering the limit beam currents, increases significantly at low energies.

Fig.(5.2).2 shows the luminosity measured for the year 2010 as a function of beam energy in comparison with the calculated curve. As can be seen in the figure, generally, the maximum luminosity agrees well with the theoretical curve.

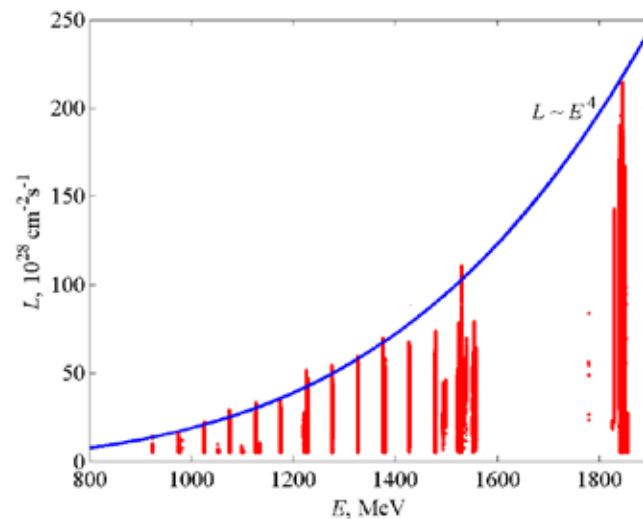


Fig. (5.2).2. Measured and calculated luminosity as a function of beam energy.

### 5.2.3 Modernization of the CBS system

The method of measuring the absolute beam energy by the CBS was implemented on VEPP-4M in 2005, for the first time for colliding beam facilities. Since then it has been a routine tool for monitoring beam energy.

Before the upgrade, the zone of interaction of laser radiation with electron beam was at the place of collision of the electron and positron beams. In this case, luminosity is a source of the large background

of high-energy gamma quanta from the  $e^+/e^-$  scattering through small angles. So, the luminosity monitor was inserted when the statistics data were acquired and removed when the energy was calibrated, which led to losses in the effective time of the experiment.

In 2010, the zone of interaction of the laser and electron beams for energy measurement by the CBS method was moved to the gap between magnets NEM1 and NEM2, as shown in Fig. After the removal of the interaction zone from the collision place and the corresponding relocation of the detector, the operation of the system for energy measurement does not depend on the operation mode of VEPP-4M: with or without luminosity. Now the HPGe detector is continuously, with a constant speed, acquiring a set of CBS spectra; the beam energy is measured in 15 minutes with a statistical error of 50 keV.

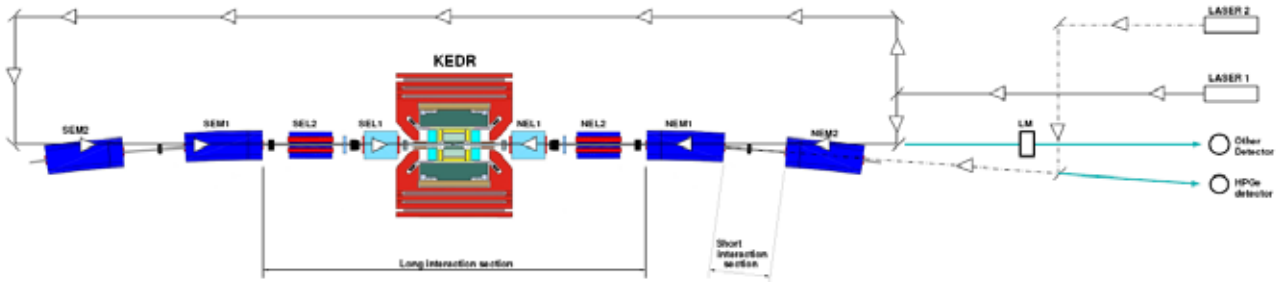


Fig.(5.2)3. The setup for measuring the beam energy by CBS.

Such a modification of the system allowed us

- to avoid hard gamma quanta from the  $e^+/e^-$  scattering through small angles getting into the HPGe detector. Now the energy measurement is carried out continuously and in parallel with acquiring statistics using the KEDR detector, and there is no need in moving the luminosity monitor;
- to restore the scheme of laser calibration of the system for registration of scattered electrons of the KEDR detector.

In 2010, in addition, the calibration of the energy scale of the HPGe detector was supplemented with the 6.13 MeV line from the Pu-C13 source. This allowed reducing the systematic error of the method to in the energy range of  $J/\psi - \psi$  ( $2s$ ) (1.55 – 1.85 GeV). Fig.(5.2).4 (top graph) shows an example of joint measurement of the energy of the VEPP-4M beam during 24 hours by the CBS and resonant depolarisation (RD) methods. The bottom graph presents the beam energy spread as measured by the CBS method for the same period of time.

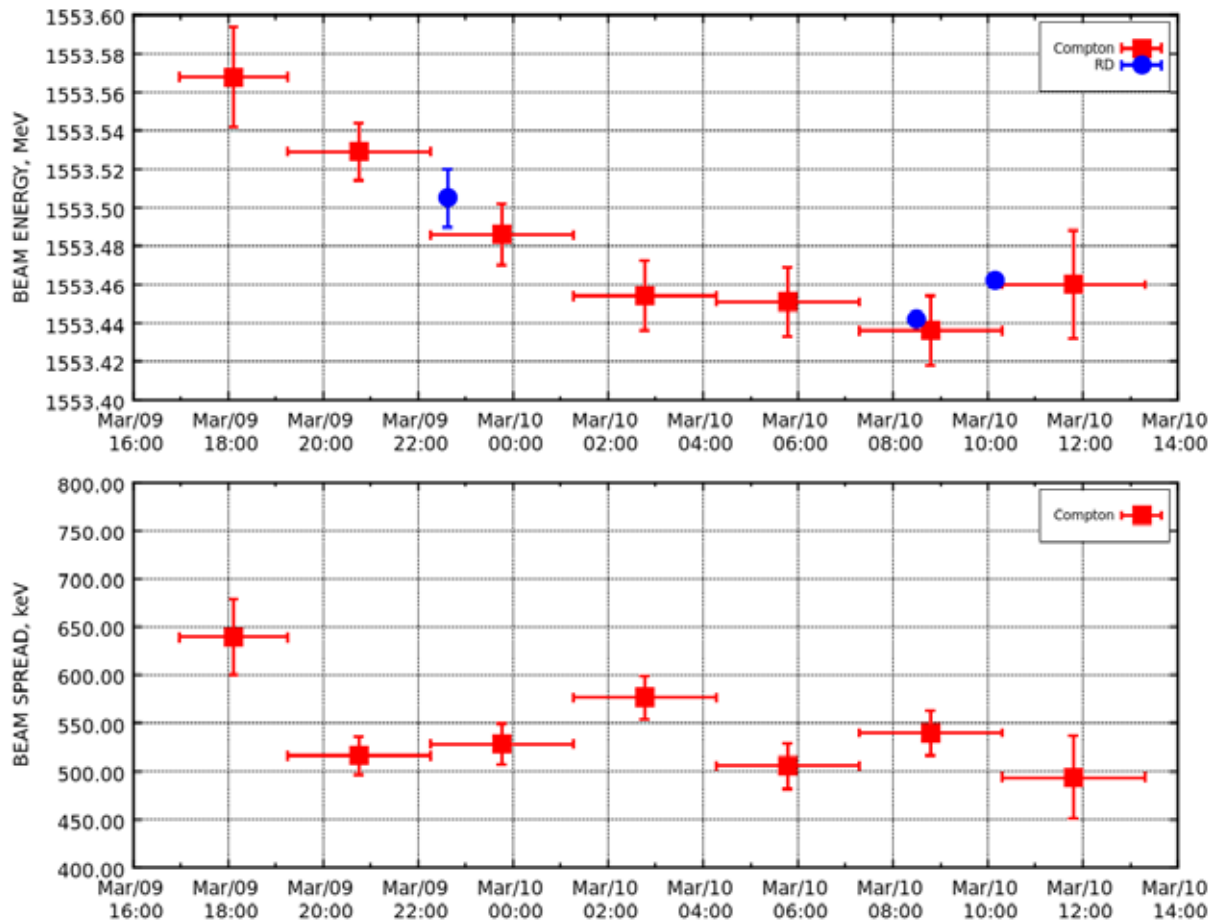


Fig.(5.2)4. Measurement of the VEPP-4M beam energy by the CBS and RD methods.

In 2010, the applicability of the Compton backscattering (CBS) to calibration of beam energy above 2 GeV was studied experimentally. For a beam energy of 3 GeV, the accuracy of the method – 500 keV – is sufficient for the experiment on the R measurement in this energy region.

#### 5.2.4 Upgrade of the “Positron” injector

To a large extent, the effectiveness of VEPP-4 operation in experiments on high energy physics is determined by the rate of accumulation of positrons in the VEPP-3 booster storage ring. To increase the speed of injection of positrons we refined the operation mode on the “Positron” facility at a frequency of 1.5 Hz. For this end, we conducted a number of preparatory works during the scheduled shutdown in the summer 2010:

- the charging circuits of the high-power pulse generators feeding the magnetic elements of the B-4 synchrotron and beam transport line were upgraded as well as all the pulse generators feeding the low-voltage correction magnets;
- a system for additional cooling of the B-4 commutator was designed and implemented;
- spare blocks control units for B-4 commutation were designed and fabricated;
- the thermal regime of the facility loads was investigated and a long run of all pulsed power sources of the «Positron» facility was performed.

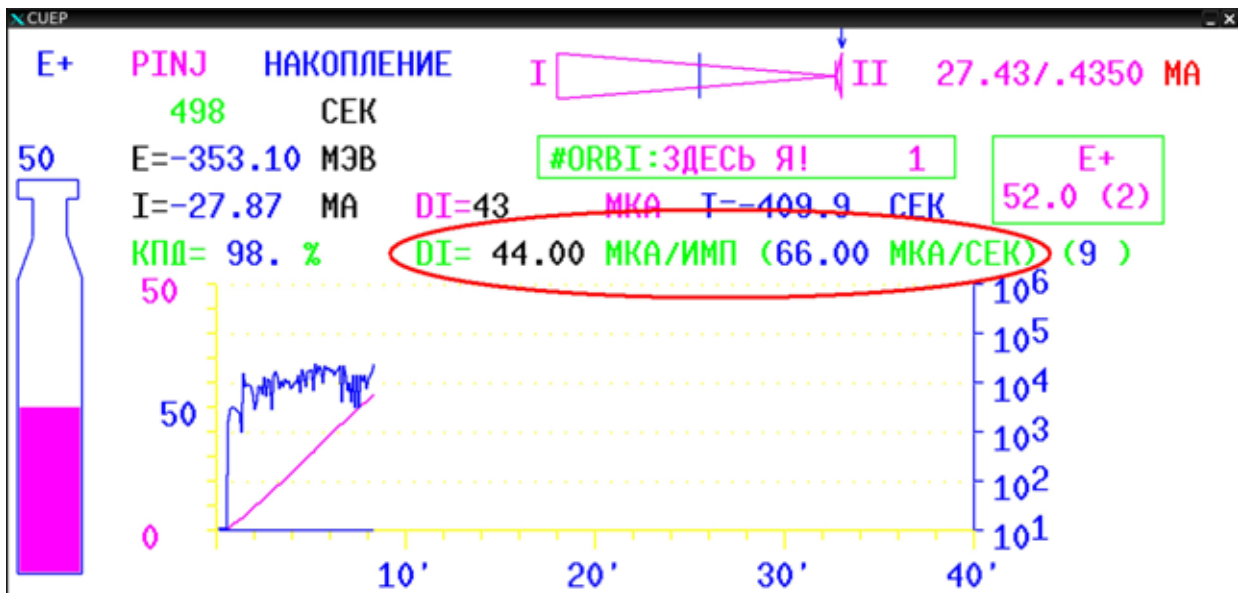


Fig.(5.2)5. Accumulation of positrons in the VEPP-3 booster storage ring.

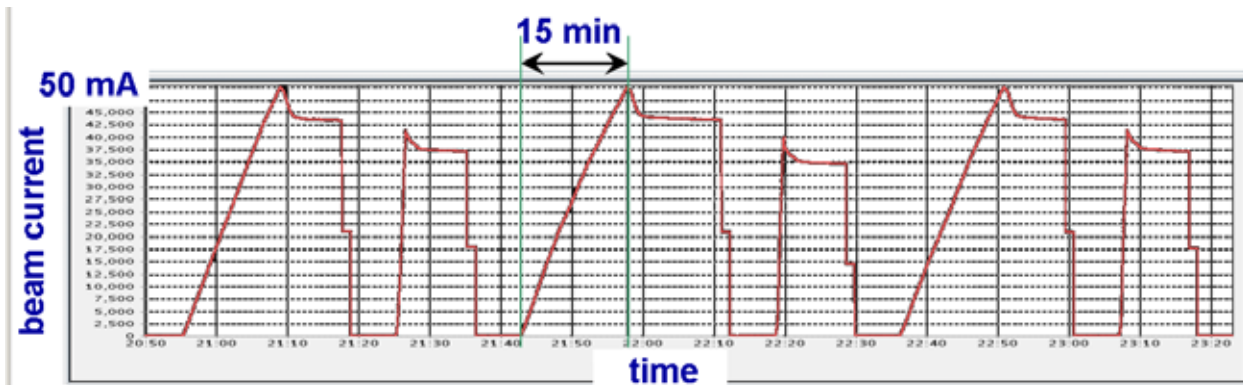


Fig.(5.2)6. VEPP-3 beam current as a function of time.

Fig.(5.2).5 illustrates the accumulation of positrons in the VEPP-3 booster storage ring; an average accumulation rate of 66  $\mu\text{A/s}$  was attained; Fig.(5.2).6 shows the VEPP-3 beam current as a function of time. As one can see, accumulation of a positron beam with a current of 50 mA in two bunches takes about 15 minutes.

A significant contribution to improving the reliability of the facility was made due to the installation of the multicell cathode of the ELIT-3A gun (electron source) and software-aided reduction in the heating of the ELIT-3A gun and the linear accelerator in modes without beam accumulation in VEPP-3. As a result,

- ELIT-3A has worked for two years with no opening required;
- the number of breakdowns at operation in the 900 J mode declined about 50 times;
- a kind of record was set in the electric strength of the ELIT-3A accelerator: 1 breakdown for 1 000 000 pulses.

Fig.(5.2).7 illustrates the operation of the complex at an experiment on high energy physics; the top chart shows the VEPP-3 beam current as a function of time; the lower plot presents the measured luminosity of the VEPP-4M electron-positron collider. It is evident that reliable operation of the “Positron” injector and VEPP-3 booster storage ring allows reaching luminosity above  $1.5 \cdot 10^{30} \text{ cm}^{-2} \text{ s}^{-1}$  at a VEPP-4M energy of 1.8 GeV in a durable run.

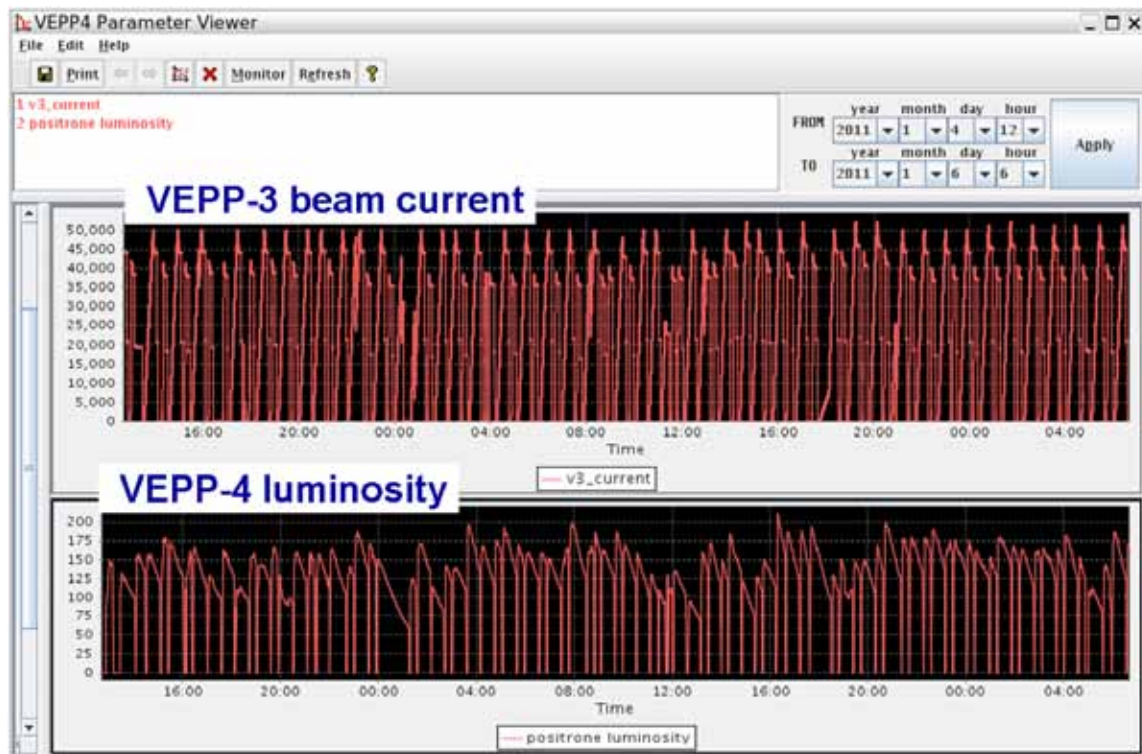


Fig.(5.2)7. VEPP-4 operation in the experiment mode.

Work on the improvement of the reliability of the facility is going on. We take measures on the improvement of the forced cooling of the high-current pulse generators feeding the powerful source of electrons ELIT-3A, magnets of the B-4 synchrotron, and the beam transport lines, as well as the thyristor block of the power supply systems of the B-4 synchrotron. The air conditioning of the room for the pulse power supply of “Positron” and the system controlling the starts of the low-voltage pulse power sources (shutdown of the injector in modes without beam storage in VEPP-3) were upgraded.

### 5.2.5 VEPP-4M longitudinal feedback system

An operation mode with two electron bunches and two positron ones, which drastically increases the luminosity, was implemented for conduction of experiments on high energy physics on the VEPP-4M electron-positron collider. A side effect of the increase in the number of bunches is the instability in the longitudinal motion of beams, which leads to large-amplitude phase oscillations. Phase oscillations lead to a sharp decrease in the luminosity and lifetime of beam. Moreover, the hit of the beam particles to the drift chamber of KEDR detector can trigger a high-voltage breakdown and damage the chamber itself. The instability is caused by the resonant excitation of higher modes in the accelerating cavities by the beam.

Three controllable mechanisms are provided to suppress higher modes in each of the five cavities of VEPP-4M. Certain areas of stable beam motion correspond to particular settings of the suppression mechanisms. However, when the temperature of the cavities changes, their geometrical dimensions vary, withdrawing the cavities out of the area of stable beam motion.



modulate the RF voltage applied to the kicker by means of two balanced modulators. The circuit has two built-in carrier-frequency generators: one tuned to the even 398th harmonic of the revolution frequency for suppression of the in-phase mode and second tuned to the odd 397th harmonic for suppression of the antiphase mode. The output signals of the balanced modulators are summed and delivered to the power amplifier.

Two RF kickers are used in the system: one for electrons and the other for positrons (Fig.(5.2).9, right). Each kicker consists of a pair of cavities, the resonant frequency of which  $f_c = 325.5$  MHz is midway between the 397th and 398th harmonics. The distance between the cavities of each pair was chosen to equal the wavelength quarter 230 mm. The frequencies of higher modes of the kicker cavities are above the critical frequency of the vacuum chamber (2500 MHz), which minimizes possible problems with wake-fields. The output power of the RF amplifier is divided by a directional coupler and transferred to the cavities through cables of equal length. The cavities are connected so that for particles of a certain polarity ( $e^+$  or  $e^-$ ) moving in their direction the phase of the RF voltage in the second cavity is shifted by  $\pi/2$  relative to the voltage phase in the first cavity. Thus, the particles of this polarity receive a double kick, while the kicker has no virtual influence on particles moving in the opposite direction.

Practical tests of the feedback system were carried out with a real multibunch instability excited via restructuring the higher modes of the accelerating RF cavities. The tests showed that the feedback system can suppress the oscillations with amplitude by an order of magnitude higher than the maximum permissible level of safe operation of the KEDR detector.

The longitudinal feedback system was put into regular operation and is used to suppress phase oscillations in the mode of experiments with the KEDR detector.

### 5.2.6 The temperature monitoring system

The new temperature monitoring system uses sensors that measure the temperature of the cooling water, magnets, tunnel walls, and air in the tunnel and sensors that lock the magnet power supply in case of overheating. The system is based on high-accuracy temperature sensors.

Currently, VEPP-4 is equipped with 283 measuring and 206 interlock sensors. 25 controllers control the sensor and pick up data. All measurements are stored in the VEPP-4 database. Fig.(5.2).10 shows a photograph of a controller and a temperature sensor.

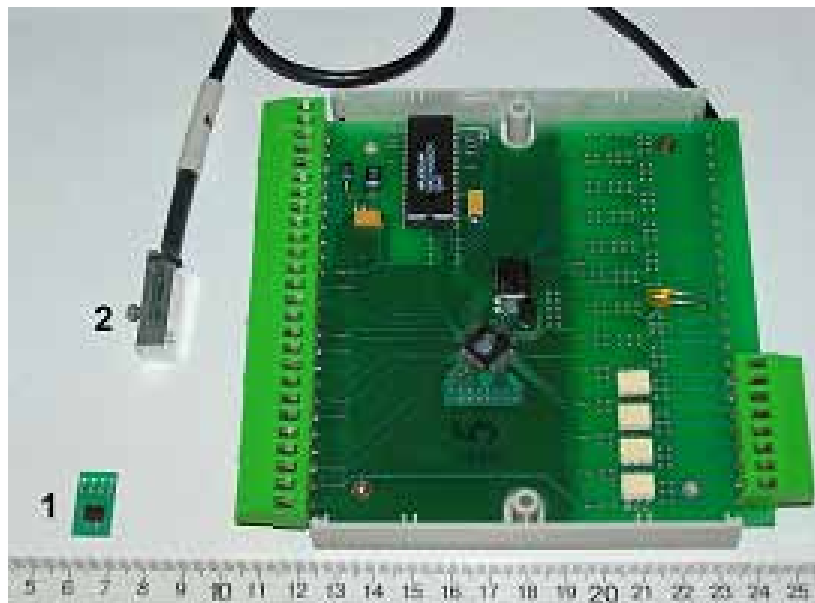


Fig.(5.2).10. A controller and a temperature sensor.

The fragment of the system (6 controllers) responsible for switching off the power sources of the magnets in case of overheating was put into operation in the experiment section of VEPP-4M in 2010.

Controllers that take data from the temperature sensors can have several controlled relays. The temperature threshold and type of operation – opening or closure of circuit – can be set for each relay. A

specific relay that will switch to the opposite state according to the specified temperature threshold can be assigned to each temperature sensor. The memory of controller stores actual temperature values, which are updated every second, and control parameters of the sensors – the temperature thresholds and the numbers of relay contacts that are closed when temperature goes beyond a specified range.

Settings for the temperature controllers are stored in the VEPP-4 database and used by the thermal control system programs.

Two relays of each controller are involved in blocking powering of the magnets. One relay is to switch on the audible alarm when the first temperature threshold (set to 55 °C) is reached at least on one blocking sensor. The other relay is to turn off the corresponding power supply circuit when the second temperature threshold (set to 60 °C) is reached at least on one blocking sensor.

Temperature measurements are recorded to the database every 5 seconds. The latest temperatures values are displayed in descending order. The following color code is foreseen: the yellow color is for the precautionary temperature threshold; red color lights up simultaneously with the audible alarm; the red indicator is flashing at operation of the relay disconnecting the power supply (the audible alarm goes on).

If necessary, the duty operator can disable the audible alarm. As the overheated magnet has cooled, each relay returns to its original state and the power supply of the corresponding magnet is switched on manually.

### **5.3 VEPP – 5 injection complex**

In 2010 construction of Injection Complex (IC) has been very dynamic. The IC can provide with electrons and positrons already existing in BINP electron – positron colliders VEPP – 2000 and VEPP – 4M as well as future Charm – Tau Factory simultaneously and ample. The operation of these installations is crucial for basic program of investigation of BINP SB RAS in High Energy Physics.

The Injection Complex is unique in Russian Federation and stays among the best installations of this kind all over the world. Moreover, some of its parts and subsystems have record-breaking characteristics and no analogues.

In the current year a construction of positron linear accelerator (see Fig. (5.3)1) that is the last required elements of new VEPP – 5 IC has been completed. The last module 4, which consists of 4 accelerator sections, has been assembled, pumped up to working vacuum and is in process of training and adjusting.



Fig.(5.3)1. Linear positron accelerator of VEPP – 5 IC.

During the year we've received the last fifth klystron for klystron preinjector gallery (see Fig. (5.3).2) and have prepared it for operation.



Fig. (5.3).2. Klystron preinjector gallery of IC VEPP – 5 with all klystrons.

In the frame of work for improvement and finishing IC the following steps were performed:

1. Master generator of IC was moved to radio-control room from klystron gallery.
2. The system of positron inlet-outlet for storage ring is prepared for operation.
3. The assembling of cable routing has been finished.
4. Sewage system of IC channels was assembled.
5. Fire alarm system for IC channels was mounted.
6. The reverse power supplies for downtake channel were mounted.
7. New racks of pulse power supplies for the IC channels were assembled.
8. The rack of ion pumps power supplies for IC channels was mounted.
9. The cooling system of downtake channel to VEPP – 3 was mounted.

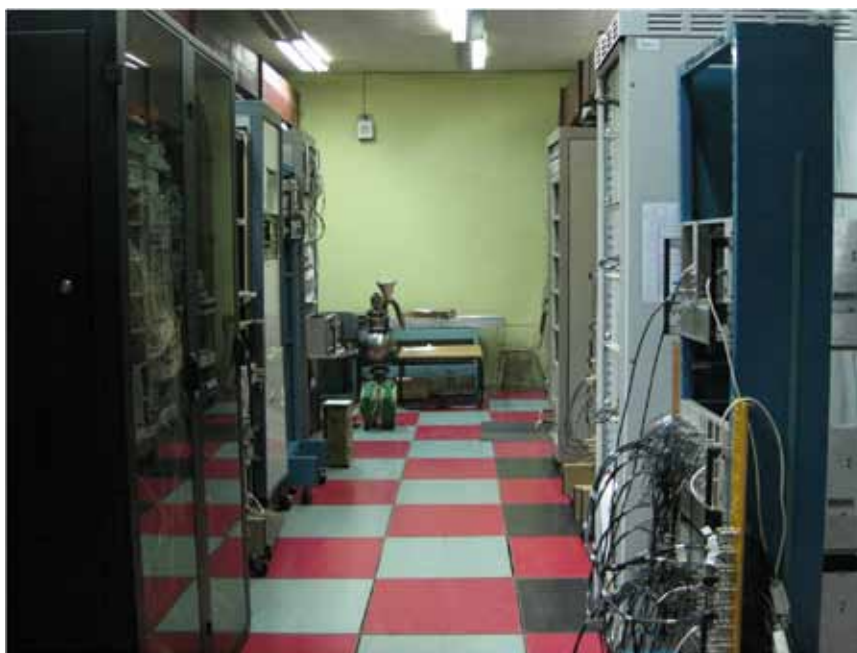


Fig. (5.3).3. Master oscillator-power amplifier at radio equipment room of IC.



Fig. (5.3)4. The system of positron inlet-outlet for storage ring is prepared for operation.



Fig. (5.3)5. General view of channel to VEPP – 2000 with magnetic elements, cable trays and ground loop.



Fig. (5.3)6. Elements of downtake channel to VEPP – 3 with coolant circuit.



Fig. (5.3)7. The elements of fire alarm system at the channel of IC.



Fig. (5.3)8. Cable trays and ground loop at IC channel.



Fig. (5.3)9. New rack of ion pumps power supplies.



Fig. (5.3)10. Reversible current power supplies IST for IC channels.



Fig. (5.3)11. New racks of pulse power supplies for the IC channels.

## 5.4 Linear inductive accelerator LIA - 2

In the frame of R&D work under the Contract No. 07-96 from 01.01.2008 “Design of injector of linear inductive accelerator for Russian Federal Nuclear Centre - All-Russian Research Institute of Technical Physics (RFNC – ARRITP)” a linear inductive accelerator LIA-2 has been designed, constructed, tested, and delivered to customer. Before the shipping in BINP SB RAS its full test was carried out.

The tests were performed from 21.10.2010 till 29.10.2010. Injector (LIA – 2) presented to customer is completed and stuffed with controlling system (see photos in Fig. (5.4).1 – (5.4).3). All injector assemblies are up to quality of technical standards according to test certificate No. 040-19/4544 from 27.07.2010.

During tests 20 of adjusting and 10 of working startups with gamma-burst were performed. For each pulse the following parameters were registered: electron beam energy, beam current in pulse, pulse duration, diameter of electron beam on the target and X-ray radiography ability. The test results are presented in Table (5.4)1.

Table (5.4)1. Base parameters of LIA – 2.

Parameter	Required data	Experiment results
Electron energy, MeV	2	1.9
Electron current in pulse, kA <sup>1</sup>	2	2
Electron beam current pulse duration, ns	200	180
Diameter of electron beam on the target, mm <sup>2</sup>	1 ÷ 2	1.8
Radiography ability at 1 meter from the target, mm Pb <sup>3</sup>	-	~ 90

<sup>1</sup> – Measuring of electron current and pulse duration was by means of current transformer with amorphous iron. A typical current pulse oscillogram is presented in Fig. (5.4)4;

<sup>2</sup> – Electron beam diameter is a diameter of a hole in tantalum target. One can see the photo in Fig. (5.4)5;

<sup>3</sup> – Transparent ability was not stipulated and presented for reference.

Tests performed proved LIA – 2 to be fully operational and meet our customer’s requests.

Been tested installation was dismantled, shipped from BINP SB RAS to the Russian Federal Nuclear Centre - All-Russian Research Institute of Technical Physics in November and assembled there in December 2010. During 2011 LIA-2 will be tested, adjusted, and put to operational regime, simultaneously with local staff training.



Fig. (5.4)1. High voltage modulators of LIA – 2 accelerator.



Fig. (5.4)2. Accelerator target assembly and front part of accelerator.



Fig. (5.4)3. General view of accelerator (rear view).

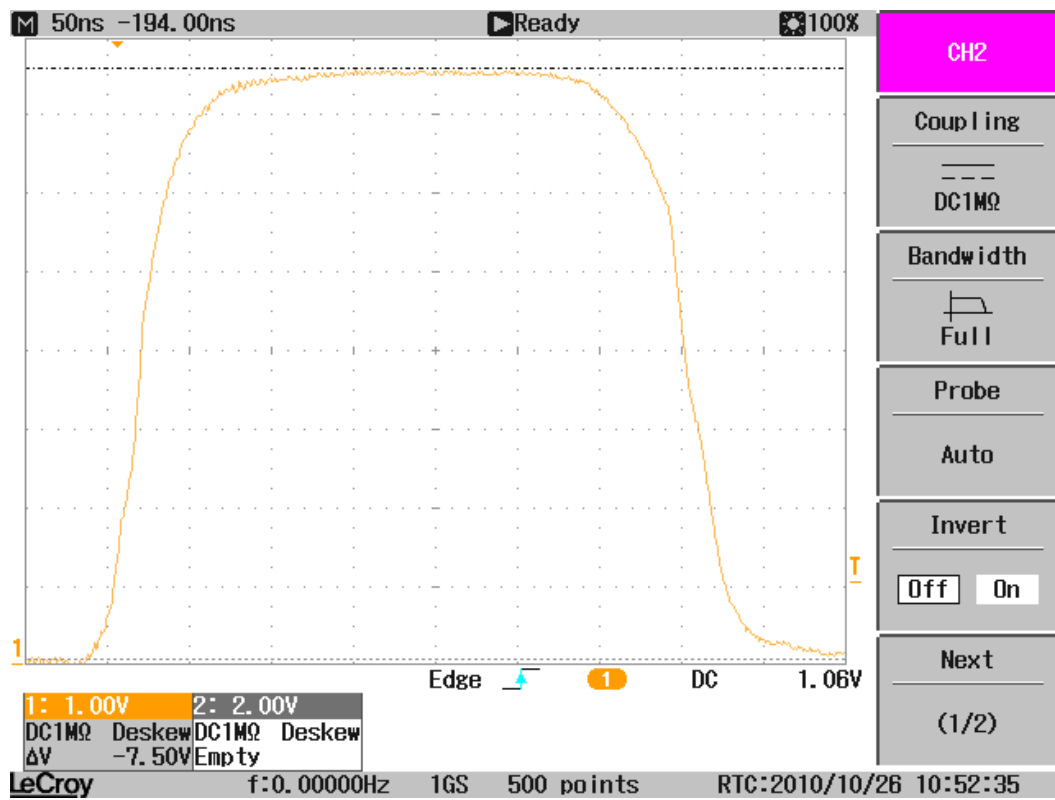


Fig. (5.4)4. Oscillogram of current pulse.

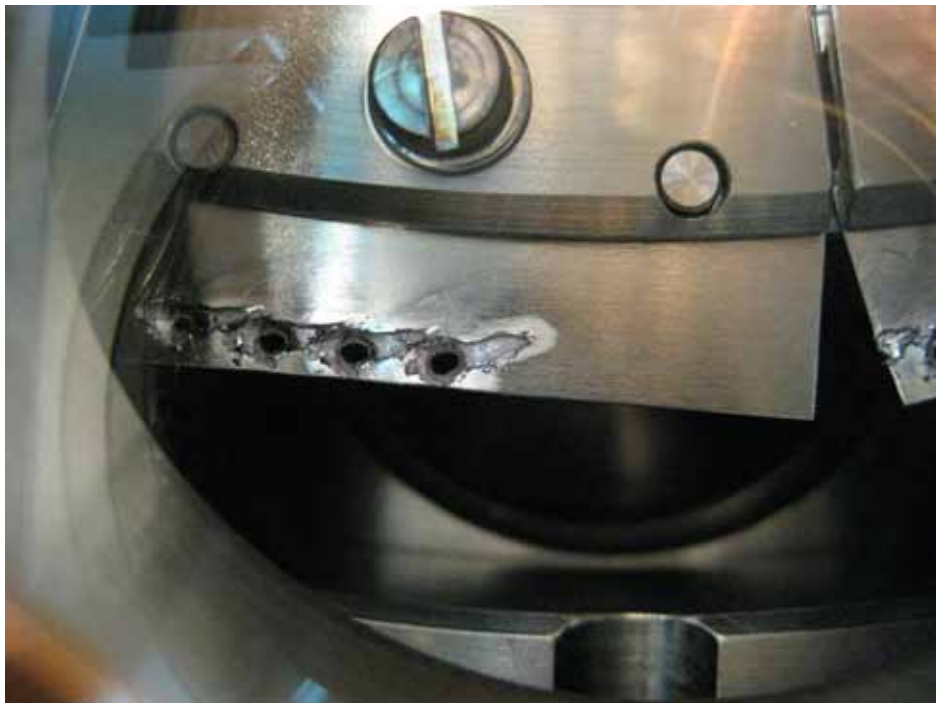


Fig. (5.4)5. Target of LIA – 2 with holes burned up by an electron beam.

## 5.5 Electron beam welding

Electron beam facilities for electron-beam technology have been produced and tested with success in BINP for Scientific Research Technological Institute “Progress”, Izhevsk, Russia. At present time they have been installed on technological equipments at six plants of Russia. These facilities operate in electron beam technological complex.

Electron beam facility can be used for electron-beam technology. Firstly, in case of sharp focused electron beam – for welding and cutting metals and alloys including refractory alloys. The power density can achieve 100 kW/mm<sup>2</sup> on the center of sharp focused beam. In case of smearing focusing, the beam can be used for warming up to high temperature and melting including thick layer on the substrate.

Electron – optic column can be installed on the outside of vacuum chamber as well as inside the chamber by the handler.

Table (5.5)1. Basic technical parameters.

Maximal electron beam power	30 kW
Accelerating voltage	60 kV
Beam current	0.5 – 500 mA
Accelerating voltage instability, not more	± 0.5%
Beam current instability, not more	± 2 %;
Parallel displacement of beam	done
Stored energy in reactive element of high voltage circuit, less	10 J
Power consumption, not more	36 kW
Weight, not more	1200 kg

In the current year the electron gun was upgraded to improve its reliability and to increase the cathode life time:

- Electron beam guide was made from the metal in order to avoid rubber gaskets;
- Cross section of electron beam guide was expanded;
- In order to improve breakdown strength, the shapes of driving electrode and anode were changed;
- New cathode unit with indirect heating (by electron beam) was developed and fabricated (see

Figure (5.5)1).

Also in current year electron beam facility unit for Scientific Research Technological Institute “Progress”, Izhevsk, Russia (see Figure (5.5)2) was upgraded.

Electron beam facility was exhibited on XIII International Siberian industrial exhibition “MANUFACTURING. METAL-WORKING. WELDING. METALLURGY” at Novosibirsk from 23.03.10 to 26.03.10 and was awarded Small Golden Medal.

The experiment with shielding window system on the base of liquid lead was carrying out during summer 2010 by using electron gun.



Fig. (5.5)1. The electron – optic column with indirect cathode heating (by electron beam) on the experimental chamber.



Fig. (5.5)2. Modified electron – optic column for Scientific Research Technological Institute “Progress”, Izhevsk, Russia on experimental chamber.



Fig. (5.5)3. Awards of Siberian industrial exhibition.



Fig. (5.5)4. Welding gun on the shielding window test stand with liquid lead.

In the current year, a development of the electron beam facility was began in the frame of ISTC project No. 4022 «Development of vacuum system and production technology for high luminosity electron-positron colliders». At present electron positron collider (KEKB, Japan) is in process of upgrading in order to increase its luminosity for several orders. That will increase thermo-mechanical stress of vacuum chamber due to huge power of synchrotron radiation and in turn will cause additional problems with the impedance of vacuum chamber and emission of secondary electrons and photoelectrons that will lead to the beam instability. The technology under consideration should provide accelerator with vacuum chamber to meet with hard conditions mentioned above.



Fig. (5.5)5. Vacuum chamber of welding facility which develop in frame of ISTC project “Development of vacuum system and production technology for high luminosity electron – positron colliders”.

## 5.6 Design and construction of electron guns

In 2010 electron gun group kept on designing and producing wide range of cathode units for different installations at BINP as well as for our contractors overseas.

In the frame of the contract with BNL, USA, electron gun units with  $\text{LaB}_6$  and IrCe-alloy emitters were produced and tested. They will be used in existing EBIS RHIC, and future electron lens of RHIC. You can see the samples in the photo below.

A contract for design and production electron guns for EBIS CARIBU, Argonne National Laboratory, CIHA, was signed. Some preliminary simulations of electron optics and engineering calculations were performed.



Fig. (5.6)1. General view of the cathodes for BNL (USA).

The group produced and tested about 150 cathode units 10 mm and 6 mm in diameter for industrial accelerator ELV-type. In Fig.(5.6)2 one can see the heating characteristics as well as dependence of surface temperature from the heating power for this cathodes. Their lifetime depends on vacuum conditions and can achieve 10 thousand hours. The cathodes permit up to 30 thousand of instantaneous switchings.

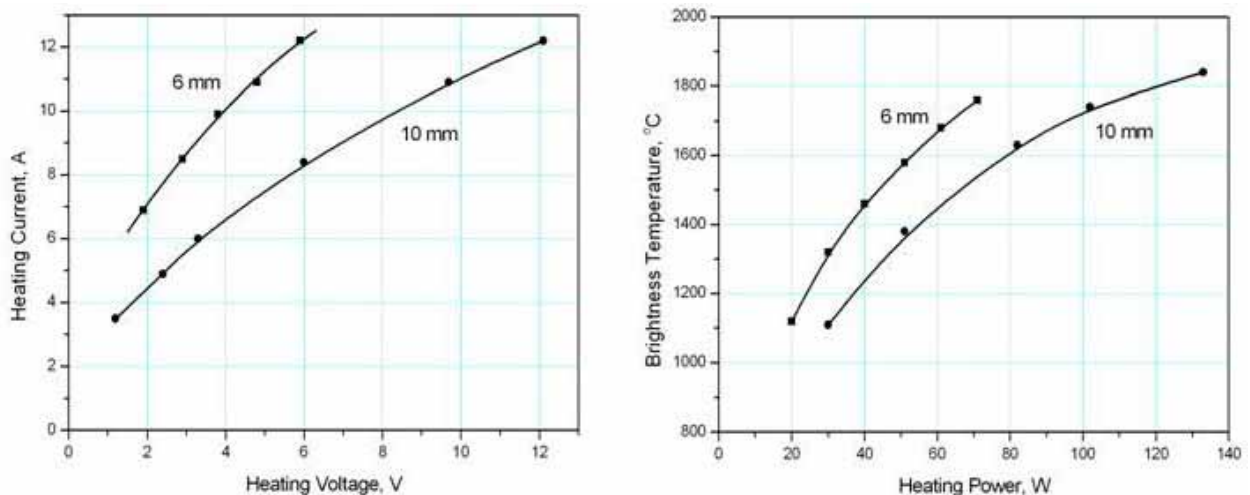


Fig. (5.6)2. Heating and temperature characteristics of the ELV-type cathodes.

The group continued to produce electron gun units with LaB<sub>6</sub> emitters 17 and 20 mm in diameter for industrial accelerators ILU – type. They have two types of heaters made from 0.8 and 1 mm in diameter tungsten wire, and can have spherical as well as plate emitting surface. The characteristics of the cathode with heater of 1 mm wire presented in Fig. Z.Z.3. Their lifetime at current density from the cathode 5 A/cm<sup>2</sup> is 10000 hours.

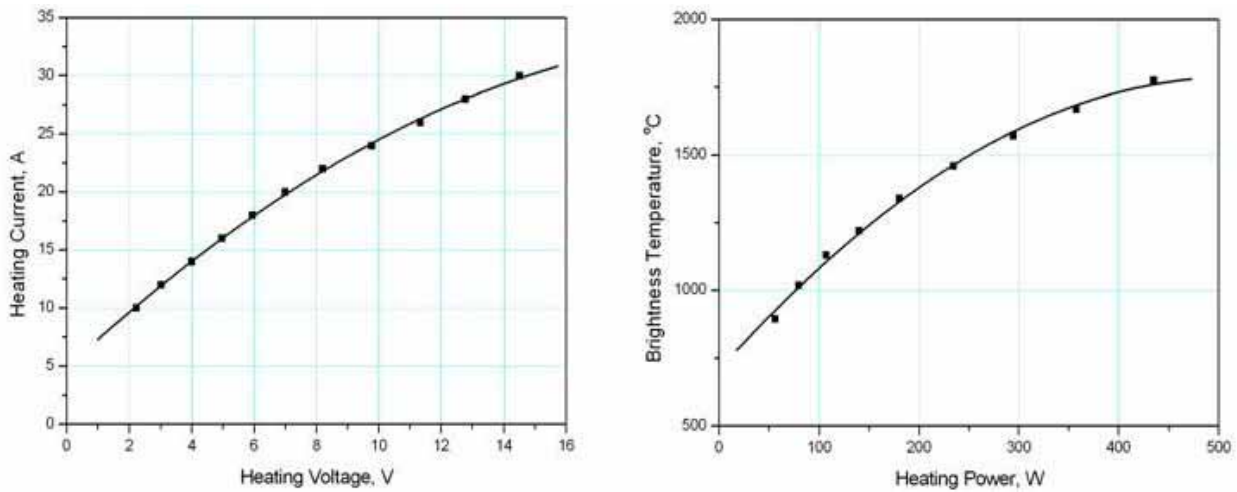


Fig. (5.6)3. Heating and temperature characteristics of the cathode unit ILU – type 20 mm in diameter.

In the picture (5.6)4 below one can see the unique cathode gun for linear induction accelerator LIU – 2. Its dispenser emitter has diameter 180 mm and was made in Thorium, Moscow while all the rest including the heater and cathode electrode at the BINP. The heater made of tantalum band fixed on insulators inside heater’s tank and allows having difference in temperature along the emitter surface less than 5 degrees. In Fig. (5.6)5 its heating and temperature characteristics are presented. The cathode emission corresponds to the best results for dispenser cathodes and turned to be higher in the installation compare to test vacuum chamber due to better vacuum conditions in the actual induction accelerator (10<sup>-9</sup> torr in LIU – 2 и 10<sup>-8</sup> torr in test chamber with the cold cathode).



Fig. (5.6)4. General view of the LIA – 2 cathode prepared for testing.

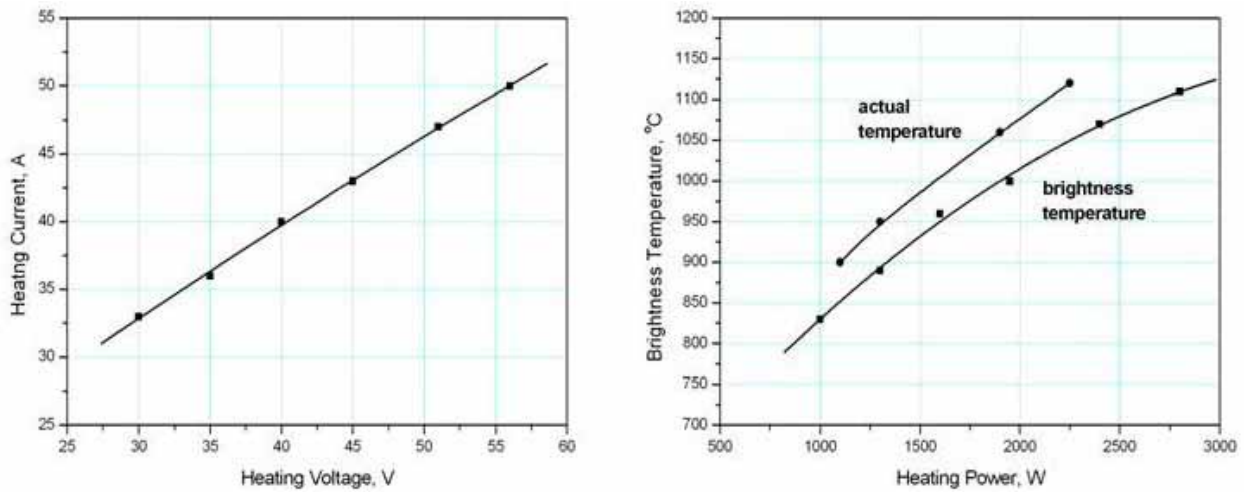


Fig. (5.6)5. Heating and temperature characteristics of the cathode of LIA – 2.

## 5.7 Creating electron cooling for a beam energy of up to 2 MeV

In 2010, the main task of laboratory 5-2 was the scientific support of the designing and manufacturing of the electron cooler for the COSY storage ring. The key elements were designed and manufactured by the end of the year. Their assembly and testing started. Experiments at COSY for better understanding of the processes of electron cooling were conducted in collaboration with the BINP staff.

The development and creation of the new electronic cooler for the German accelerator complex COSY are now in full swing. New scientific and technological solutions for high-rate cooling of proton beam interacting with the internal target were developed. The creation of the facility is to be completed in 2011.



Fig.(5.7)1. Mounting the cooler in the hall for tests.

For generation of a high-quality magnetic field in the cooling section of the electron cooler, it was proposed to use a magnetic field sensor located in the vacuum chamber of the accelerator. For this purpose, a prototype sensor similar to a compass placed in a gimbal suspension was made. For higher stability of measurements after heating of the vacuum chamber, the compass needle was made of special material, which reduces the sensitivity of the instrument to temperature as compared with a design with permanent magnets based on NdFeB. The first experiments on the stand showed a sufficient sensitivity of the compass in a field of 100 G but revealed insufficient repeatability due to a lacking precision in the manufacturing of the gimbal suspension.

For high-voltage power transmission to the accelerator column sections, a cascade transformer was designed and its prototype consisting of 3 sections was made.



Fig.(5.7)2. Transformer section under testing.

## **5.8 Work with the accelerator mass spectrometer**

The following results were obtained with the accelerator mass spectrometer created at BINP:

- stable operation of the accelerator mass spectrometer with the accelerating voltage of 1 MV was achieved;
- beam of stripped three-charged carbon ions with a current of 2  $\mu\text{A}$  and energy of 4 MeV was generated;
- 1% agreement in the measured concentrations of radiocarbon in pressed carbon filaments (modern sample) was demonstrated. The concentration of radiocarbon in MPG graphite (dead specimen) is approximately 1% of the modern level;
- the automated process of measuring the concentration of radiocarbon in samples was demonstrated with a drum fully loaded by samples (23 pieces);
- the first measurements of radiocarbon in tree rings from Akademgorodok were conducted. The radioactive carbon concentration matches the worldwide values as shown in Fig.(5.8)1.

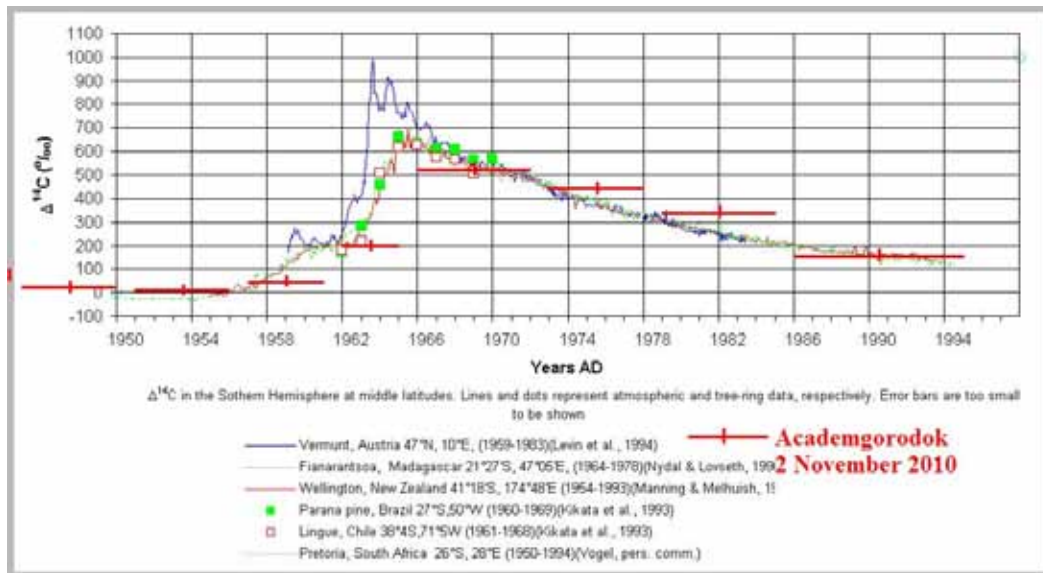


Fig.(5.8)1. The measured concentration of radiocarbon in tree rings. Each sample was made of several tree rings (the line width in the figure) at the collective research centre "Geochronology of Cenozoic".

## 5.9 Developing of hadron cancer therapy

The development of hadron cancer therapy continued at BINP in 2010. The development of prototype tandem accelerator was completed; a carbon ions current up to 3  $\mu\text{A}$  was achieved at a 1.25 MV nominal voltage in the high-voltage terminal. A prototype dipole magnet for the booster synchrotron with the measurement system was assembled; magnetic measurements for the determination of the shape of the transition region and the edge chamfer began. A vacuum of  $2 \cdot 10^{-10}$  Torr was achieved on the measurement stand with a pickup and prototypes of the vacuum chamber of main synchrotron, and pumping port. Prototypes of the electrostatic septums for injection into the booster and extraction from main synchrotron were produced.

An R&D work "Development of a physical design of an accelerator complex for medical treatment on the basis of the C-230 synchrotron" was performed for Konstantinov PNPI.

A contract for the manufacturing of dipole magnets for the synchrotron accelerator complex for ion cancer therapy MedAustron, Austria, was started.

## 5.10 Vacuum systems

### 5.10.1 High-vacuum infrared optical window

In 2010, BINP continued the development of soldering technology for infrared crystal windows.

A SeZn polycrystal was soldered to a titanium ring with lead solder (see Fig.(5.10)1). The advantage of this window type in comparison with the GaAs window (developed in 2009) is a broader spectral range  $0.45 \div 20$  microns, which allows using this window in the visible range, too. The transmission spectrum of the window is shown in Fig.(5.10)2.

A setup for measuring the energy by the Compton backscattering of a  $\text{CO}_2$  laser beam on relativistic particles in the accelerator complex BEPC-II (IHEP, Beijing) was working during 2010. The spectrum of the residual gas is shown in Fig.(5.10)3. The pressure in the vacuum chamber is about  $P=1 \times 10^{-10}$  Torr. No turbidity of the copper mirror was revealed during this period.

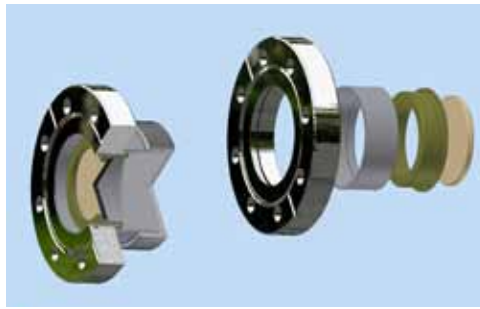


Fig.(5.10)1. Design of the high-vacuum SeZn window.

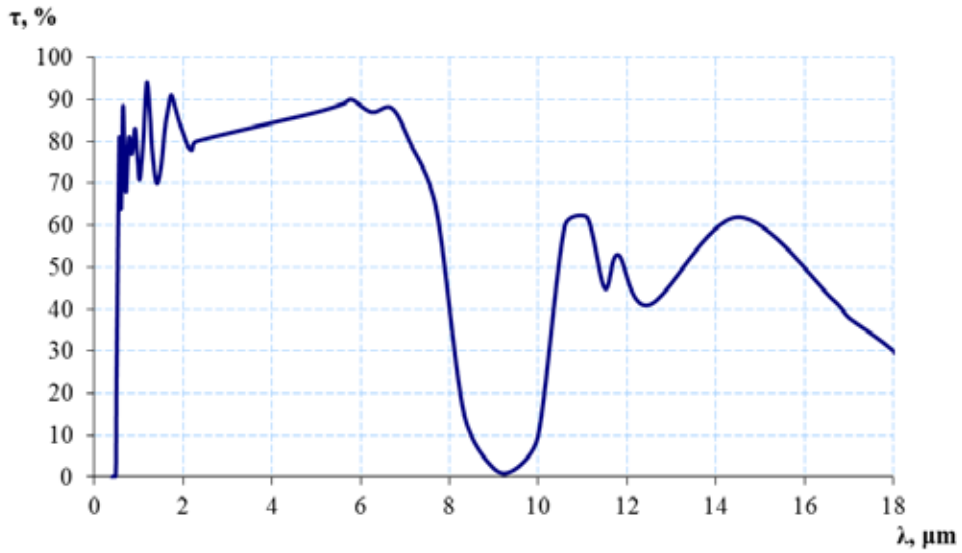


Fig.(5.10)2. Transmission spectrum of the ZnSe window, with duplitized  $\text{SiO}_2$  film 0.6  $\mu\text{m}$  thick.

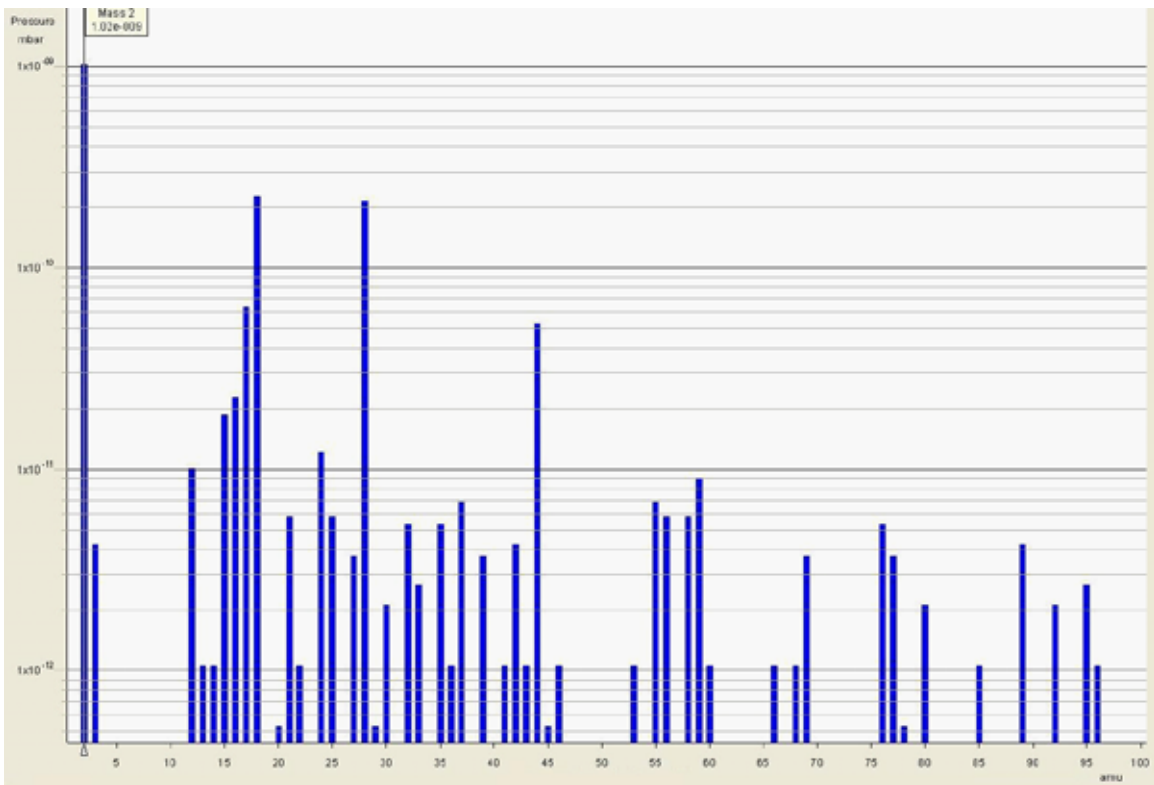


Fig.(5.10)3. Residual gas spectrum in the vacuum chamber with the GaAs window in the accelerator complex BEPC-II.

This work was partially supported by RFBR grants 08-02-00328-a, 08-02-00251-a, and RFBR-NNSF-08-02-92200-a and SB RAS fundamental research projects No.32, carried out jointly with the China Academy of Sciences.

### 5.10.2 Cryogenic equipment for testing the accelerating modules XFEL (DESY)

In 2010, BINP members were designing the cryogenic equipment for the XATB test bench (XFEL AMTF Test Bench).

The performance of the accelerating modules will be tested on test benches. The tests include examination of the cryogenic performance and performance characteristics of the resonators. The cryogenic tests include integral check of the tightness of all vacuum systems, cryogenic pipelines, current leads and devices and measurement of static thermal load at different temperatures.

In the course of the tests of the performance of the resonators of the module at 1.9 K, the maximum accelerating field of the resonators and the corresponding quality factor  $Q_0$  without load will be assessed, as well as X-rays and corresponding dark currents. The Q factor will be monitored by measuring dynamic cryogenic heat loads.

In total, 100 units must be inspected within two years.

Tests of a fully assembled resonator at high energy should be carried out at 1.9 K in order to evaluate the effectiveness of the cavity, including all its characteristics, such as the main energy of RF matching, quality factor, tuning and testing the volume for LHe. The test conditions are identical to the operating conditions in the accelerator, except for the electron beam parameters. Tests at high energy will be carried out in horizontal cryostat adapters, which will be connected to a cryogenic supply system of one of the bench.

Each facility for testing the accelerating modules consists of the test bench itself and the pipeline connecting the test bench with the distribution box. Each test facility will be surrounded with a concrete shielding and covered with a protective roof for the sake of radiation safety in all parts of the test building of the AMTF (Accelerator Module Test Facility). The module, or, respectively, the horizontal cryostat adapter, can be moved with the platform in the room for mounting/testing and back into the main hall of the test building.

The main pipeline connecting the stand with the distribution box supplies helium to the 4.5 K and 40 K circuits.

A specific feature of the distribution box stand is the usage of two heat exchangers: sub-cooler and countercurrent heat exchanger. 1.9 K helium is obtained using the Joule-Thompson valve with subsequent pumping-out to  $P = 31$  mbar.

Various-temperature flows of one bench are controlled using 13 cold pneumatic valves, including 3 Joule-Thompson valves and 11 warm air vents.

Dynamic heat loads on one bench are supposed to be measured with 12 pressure meters, 29 low-temperature TVO sensors for the ranges of  $1.5 \div 300$  K,  $4 \div 300$  K and  $40 \div 300$  K, 7 low-temperature platinum Pt1000 sensors for the range of  $40 \div 300$  K, and 3 Coriolis flow meters.

The vertical legs of the platform and fixed support withstand a load of about 100 kN in the compression operating mode and a tear load of about 120 kN in the event of an accident.

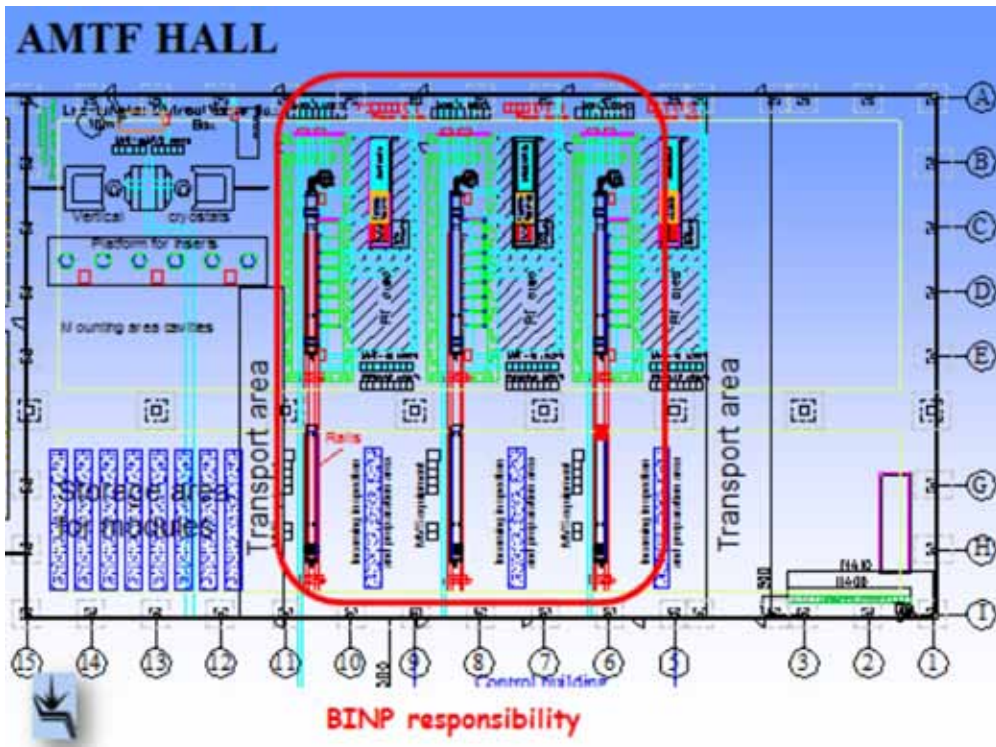


Fig.(5.10)4. AMTF hall and zone of the BINP equipment.

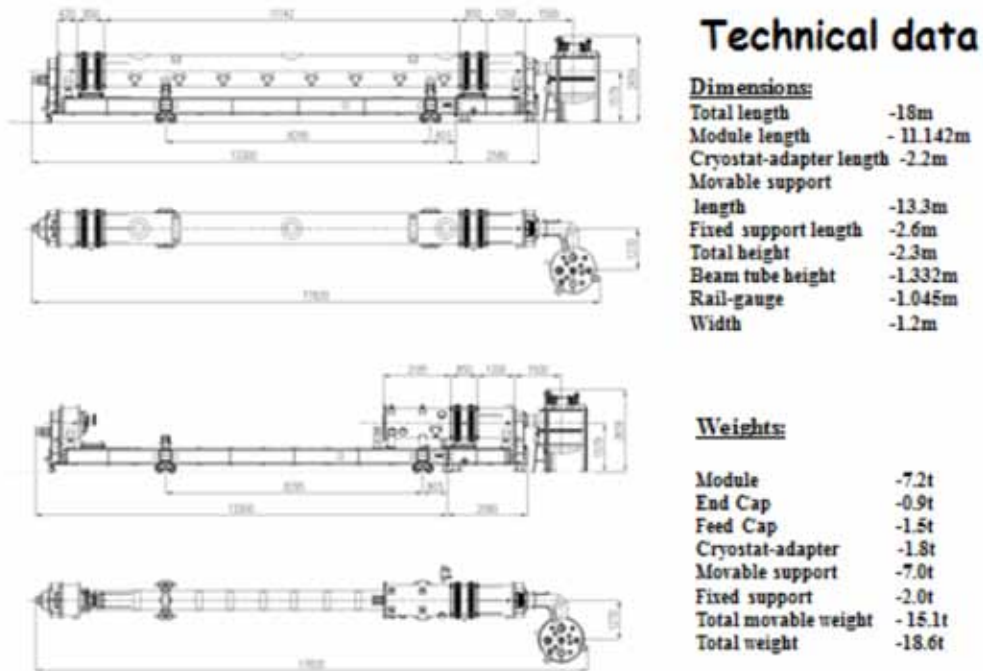


Fig.(5.10)5. Technical specifications of the BINP equipment.



Fig.(5.10)6. End unit.

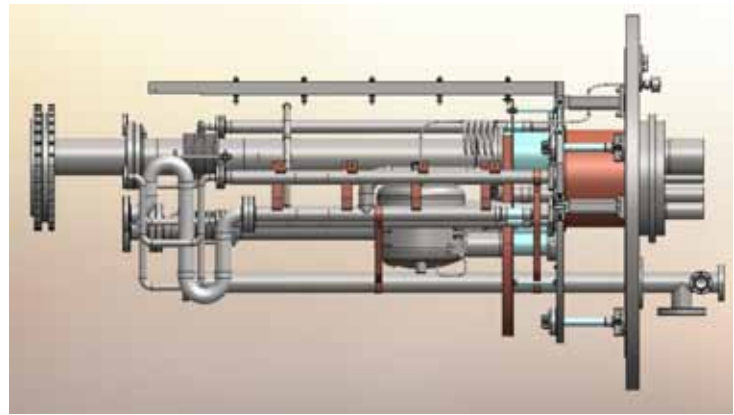


Fig.(5.10)7. Cold part of the distribution unit.

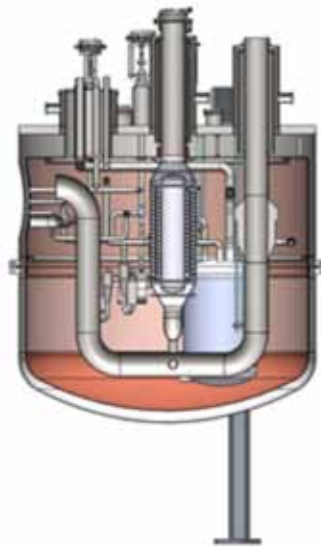


Fig.(5.10)8. Cross section of the distribution box with two heat exchangers.

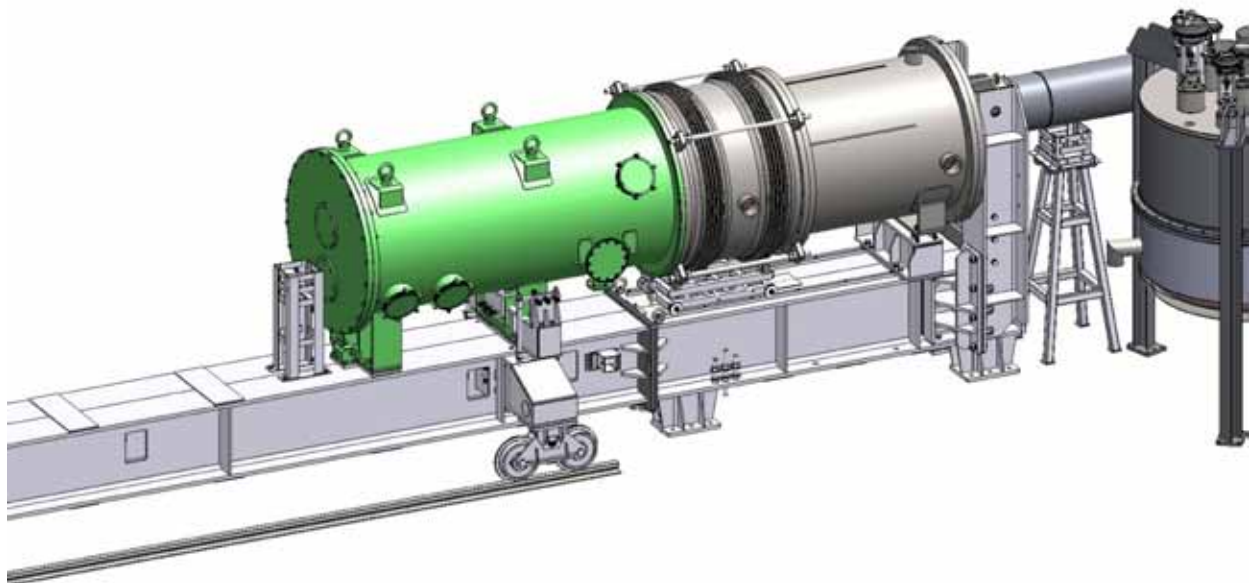


Fig.(5.10)9. Testing an individual resonator with a cryostat adapter.

### 5.10.3 Vacuum system of the NSLS-II booster

The booster for NSLS-II ensures accumulation of 200 MeV electron bunches and beam energy rise to 3 GeV. The total charge is around 10 nC, which corresponds to an average beam current of 20 mA. The perimeter of the booster is 158.4 meters. The residual gas pressure after acquiring an integral current of about 1 A-h should be no worse than  $10^{-7}$  Torr. The vacuum is ensured by means of ion pumps (70 pumps in total) from Gamma Vacuum Company with a pumping-out speed of 45 l/s. The pumps are located, on average, at a distance of 2.3 meters from each other.

Calculations showed that, despite the pulse operation of the booster (the duty factor in the intensity of synchrotron radiation is 1/7 at a repetition rate of 2 Hz), desorption of gas under SI influence will exceed the thermal desorption. Fig.(5.10)10 shows an example of calculation for one of the straight sections.

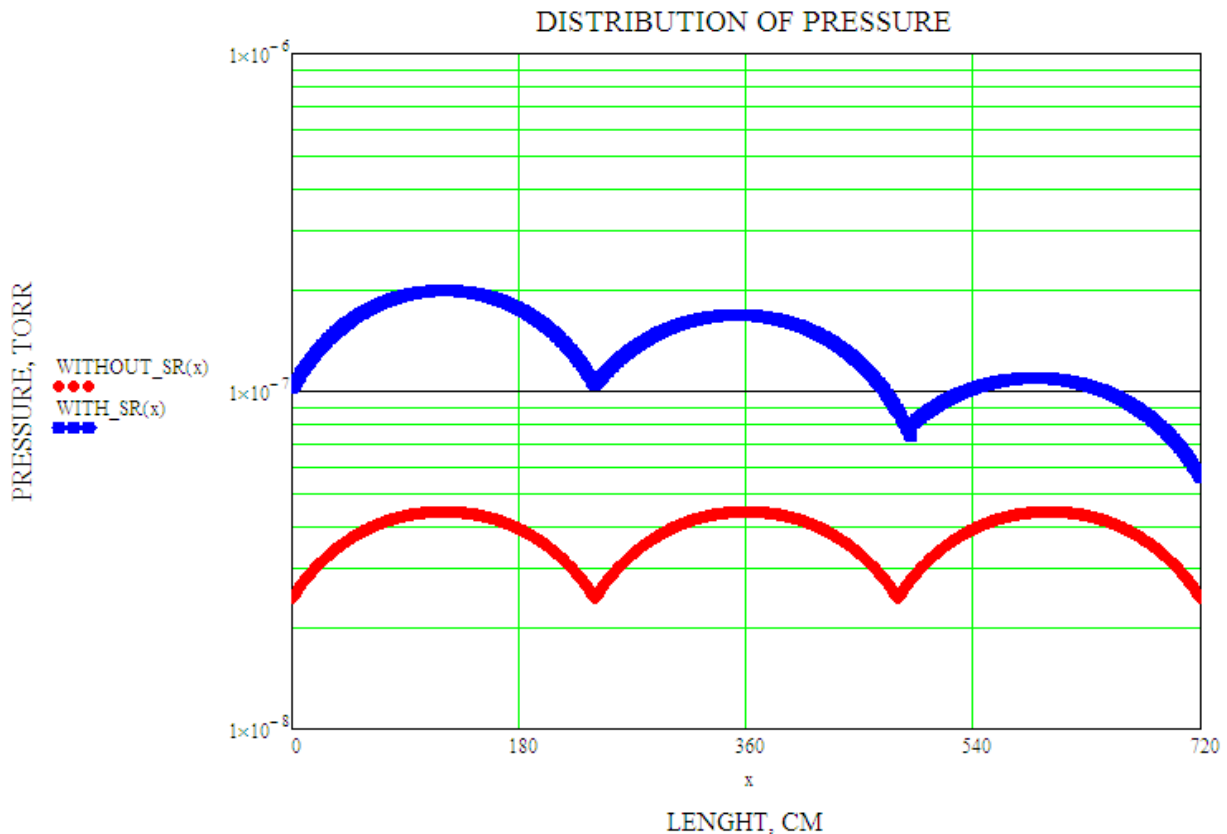


Fig.(5.10)10. Pressure distribution in the straight section.

One of the important parameters of the vacuum chamber is its resistance to various external factors such as atmospheric pressure.

Because of the relatively power of SR (the maximum power is equal to 44 W/m in the bending magnets BD) no special radiation dumps are required. However, such radiation can cause stresses in the vacuum chamber.

It was found that a synchrotron radiation with a power of about 44 W/m falls on the wall of the vacuum chamber, which leads to uneven heating of the chamber at the place of falling, by 60 degrees Celsius ( $\Delta T = 62^\circ\text{C}$ ).

Current was applied to the chamber under the atmospheric pressure, which was closed so as to prevent convective heat exchange with the environment. We measured the heating not only of the chamber itself but also of the magnet yoke. At a power of about 41.7 W/m, the average heating of the chamber was  $40^\circ\text{C}$ , which agrees well with the calculations. The coefficient of convective heat transfer  $\approx 8.6 \text{ W/m}^2\cdot\text{K}$  was found. Fig.(5.10)11 shows the dependence of the heating on the power.

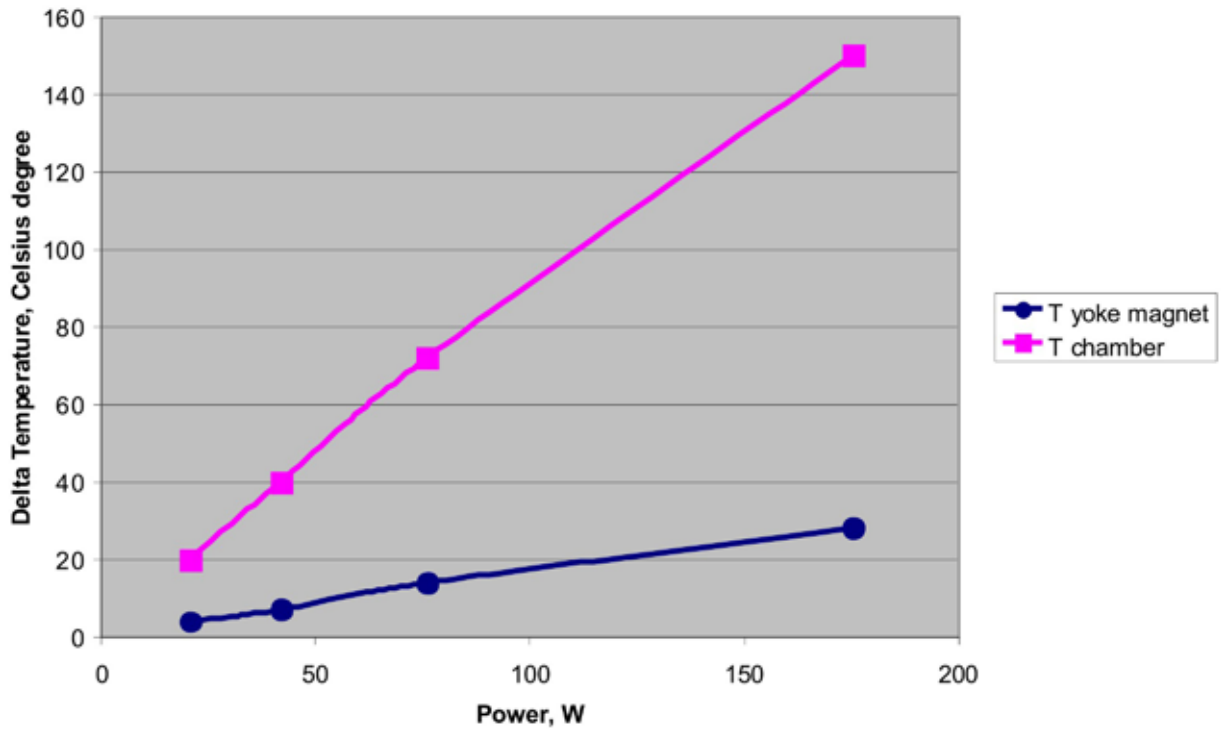


Fig.(5.10)11. Dependence of heating on power.

The second part of our experiments was to determine not the average temperature of the chamber heating and the coefficient of convective heat transfer but the heating throughout the cross section of the chamber. For this purpose, we created a prototype of the vacuum chamber with a 41x24 mm aperture. The Institute of Hydrodynamics SB RAS performed deposition of aluminum oxide ( $Al_2O_3$ ) about 100 microns, over which a nichrome strip 200  $\mu m$  thick and 5 mm wide was applied.

Imitation of SR beam was carried out using a conductor with current of a corresponding value equal to the SR power.

Fig.(5.10)3. shows the location of the thermocouples on the prototype of the vacuum chamber. The experimental data are presented in Table (5.10) 1.

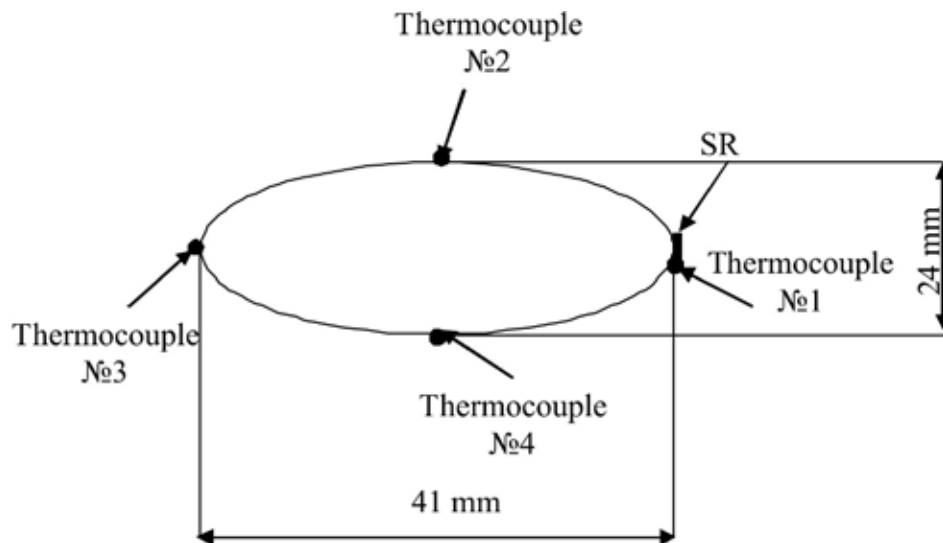


Fig.(5.10)12. Arrangement of thermocouples on the prototype vacuum chamber.

Table (5.10) 1. Experimental and theoretical data on the measurement of the temperature of heating.

	Power, W	$\Delta T$ , thermocouple 1, °C	$\Delta T$ , thermocouple 2, °C	$\Delta T$ , thermocouple 3, °C	$\Delta T$ , thermocouple 4, °C
Experiment	41.7	60	37	30	39
Calculation	41.7	62	39	32	39

Heating of a narrow strip ( $\approx 1$  mm) of the chamber makes the chamber undergo mechanical stresses of about of 114.5 MPa, while up to 150 MPa is allowable.

## 5.11 Electron-beam source of multicharge ions MIS-1

All functional units and systems of the electron-beam source of multicharge ions MIS-1, including the supply and control systems, were installed and adjusted in 2010. The installation was prepared for the test and commission phase in 2011.

A particular attention was paid to the high reliability of the equipment and functional units.

The time of the installation work-cycle and the electron beam operation time, including ionization and ion beam extraction time, ranges from 100 microseconds to 2.5 seconds (in the future, if the vacuum conditions allow, the work-cycle time can be increased).The duty factor exceeds 10.

During the operation, the electron beam at a current of 1 to 20 A and an energy of 50 keV goes along the axis of the drift structure. The electron beam current density  $J_e$  can be as high as 2 kA/cm<sup>2</sup> (the electron beam diameter is  $\sim 1.1$  mm). The beam power reaches 1 MW, and the power density is as high as 100 MW/cm<sup>2</sup>.

Any mismatch in the electric and magnetic fields of the electron-optical system (EOS) from the electron gun cathode to the electron collector may lead to a serious accident. To ensure the required level of reliability of the MIS-1 installation it is necessary to provide two levels of protection.



Fig.(5.11)1. Drift structure of MIS-1.



Fig.(5.11)2. System for dosed injection of atoms of solids and the inner part of the gas system.



Fig.(5.11)3. Anode modulator.



Fig.(5.11)4. High voltage regulable rectifier with a capacity of 100 kVA.

The first level of protection is ensured by the power supply system of the installation, which provides for the sequence of turning on and off all the functional systems of power supply as well as the overload protection and guaranteed availability of necessary locks: for the distillate cooling system, the air cooling system, the required vacuum in the vacuum chamber, and the nominal focusing field of 3 T within the drift structure.

The second level of protection is provided by the electronic control system. It ensures the required high-speed locks, matching parameters of the EOS and magnetic focusing system, and control of the parameters of the other systems.

In the near future, the installation will be mounted and mechanically adjusted, and the mutual alignment of the electron-beam system and the magnetic focusing system of MIS-1 will start in a safe mode with an electron-beam current of 1.5 A or less, the pulse duration of 100  $\mu$ s to 1 ms and a focusing magnetic field of 1 to 3 T.

This should secure the minimum possible electron beam losses. In the electron gun area, the current precipitation is to be  $\sim 10^{-3}$  on the anode and  $10^{-5}$  Je in the area of the drift structure and the ion trap.

The vacuum chamber and the internal-pumpdown system based on an internal non-evaporable getter (NEG) will be pre-heated.

Upon completion of the adjustment of the EOS and the magnetic focusing system, there will start a commissioning of all the installation working systems as well as preparation for carrying out experiments on multicharge ion beams production and their analysis.

Two samples of solid elements, niobium and graphite, with a system of pulsed dosed injection of their atoms are installed in the ion trap; there are internal components of the gas system mounted, which should provide a dosed injection of gaseous elements in the area of the ion trap.

## **5.12 Works on the electron-positron factories and beam physics**

In 2010 there were two commitments made in this field.

In the course of lectures on “Collective effects in the beam physics” there has been felt a certain incommodity due to a contracted presentation of the issues dealing with dephasing of beams and bunches, and Landau damping of coherent oscillations in the tutorial by D.V.Pestrikov on coherent oscillations. Initially it was meant that the students would learn the missing material when solving the tasks and doing exercises. The presentation of these issues in the monograph "Physics of intense beams in storage rings" (Science, 1989) by N.S. Dikansky and D.V.Pestrikov had a similar drawback. To eliminate these shortcomings, N.S. Dikansky and D.V. Pestrikov released a new tutorial "Landau damping and dephasing of coherent oscillations of beams in storage rings" (NSU, 2010). Along with a more systematic and detailed exposition of these issues, the tutorial helps to familiarize the students with a practical application of common methods of linear coherent oscillations to solving these problems.

The other work was devoted to the study of the effect of variations in the vibration frequencies of particles on the development of fast instabilities of transverse coherent oscillations of single bunches in storage rings. We were interested in instabilities with a large number of overlapped synchro-betatron modes of coherent oscillations of the bunch. These instabilities are observed in the up-to-date storage rings of charged particles (such as the ESRF in Grenoble, France). These storage rings tend to unavoidably memorize the bunch-induced fields on the orbit. In contrast to the LINACs, this memorizing leads to dividing the coherent signal of the bunch into the self-consistent part and the part, describing the effect of the bunch interruption. If the memorizing of induced fields does not lead to resonant instabilities, the self-consistent and non- self-consistent parts of the coherent signal develop in the same way in the bunch without a frequency spread. Due to the multifrequency modes of the beam, their total contribution to the signal increases with time slower than the amplitudes of individual modes. The spread in frequencies leads to the Landau damping of the self-consistent modes and dephasing of the non- self-consistent part of the oscillations. The effect of the Landau damping sets thresholds of the instability development. This occurs when the increment of the most unstable mode reaches the boundary of stability of the bunch coherent oscillations. In this case, the effect of interruption of the bunch consists in that the amplitudes of coherent oscillations at the instability threshold increase until they reach a steady value. Above the threshold, the amplitude oscillations increase; and below it, they decay. The dependences of the threshold effects on the parameters of the problem were studied.

## **5.13 Pulse magnet for the positron source of the KEK Super-B Factory**

In the framework of the international cooperation in 2010 there was developed and manufactured a conversion (pulsed) magnet, and improved the power supply (Fig. (5.13)1) for KEKB factory. These items were delivered to Japan. In the course of this project there was completed a comprehensive layout modification of the magnet power supply to remove structural drawbacks and improve the system reliability. As a result, there was attained a considerable power supply noise reduction, and improved the energy efficiency due to the replacement of the saturation choke with snubber elements in each thyristor assembly, as well as to the replacement of high-voltage commutation elements. This work was carried out in the first half of 2010. In the summer period the power supply was scheduled to reach its rated parameters (the maximum longitudinal magnetic field of 100 kG, and the pulse repetition frequency of 50 Hz), it was also planned to remove minor drawbacks resulting from the noise induced by high voltage elements of the power supply in the control circuits.

In autumn 2010, the knocked-down power supply, the conversion magnet (Fig.(5.13)2) and the vacuum chamber were shipped to Japan for further endurance tests and magnetic field measurements. In Japan, the magnet power supply was assembled and the entire system was tested for performance. With the cover of the vacuum chamber removed, the magnetic field value of 60 kG was reached at a repetition rate of 50 Hz.



Fig.(5.13)1. Power supply of the conversion magnet.

A further increase of the magnetic field seemed unfavorable because of the threat of an electrical breakdown in the air.

Later on, the conversion magnet was placed at the test bench of BINP, where comprehensive measurements of magnetic fields at a low field were carried out for 3 weeks together with Japanese collaborators. A three-dimensional map of the magnetic field was made based on the results of the measurements. It will be used for computer simulation of the capture of positrons, and for comparison of the simulation results with those obtained in the real experiments at the positron source of the KEK-B LINAC.

Later on, the jacket of the vacuum chamber was replaced and the conversion target was installed. The magnet in the vacuum chamber and the power supply were transferred to the klystron gallery of the KEK Linac for further endurance tests.

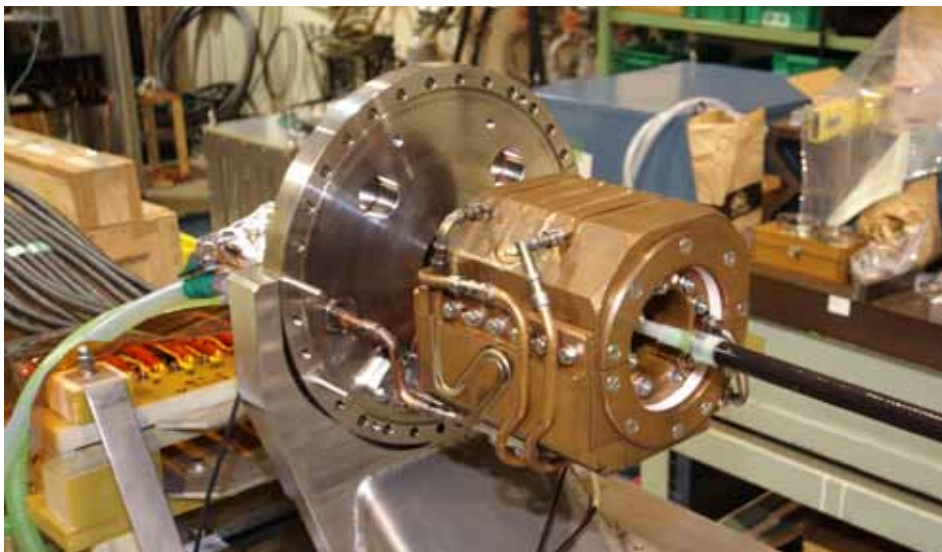


Fig.(5.13)2. Pulsed magnet for the positron source of the KEK Super-B Factory.

## 5.14 Works on the injection-extraction systems

A new source of high-voltage pulses on the TPI thyratrons (Fig. (5.14) 1) was developed for powering the VEPP-2000 kickers. Unlike the earlier-used TGI1000/25 with oxide cathode, these thyratrons have a hollow cathode allowing to work with large pulse currents (TPI1-1k/35 for up to 4 kA in the pulse mode). As the experience of working with TGI1000/25 shows, a current exceeding 2 kA leads with time to irreversible changes in the structure of the cathode and is caused by an unstable operation and self-breakdowns when high voltage pulses are applied to the anode. In addition, the small glow power of the new thyratrons allows using the power supply built in the start unit instead of a bulky filament transformer. The glow power in operation is 2 W or less, which is approximately 60 times lower than that of the TGI1000/25 thyatron, and a year's work makes a difference of more than 1 MW h per thyatron. A higher operating voltage (up to 35 kV) allows reaching an output voltage higher by 30% without a significant change in the scheme, except for other elements of the generator circuit (capacitors for higher voltage and decoupling chokes). To achieve 1 GeV on VEPP-2000, apart from alterations in the BEP ring and VEPP, it is necessary to increase the kicker impact by 25%.

In view of the small dimensions it is impossible to do without a sealed, Carbogal-filled enclosure for the thyatron, with terminals for the grid and anode. In the air, the operating voltage is limited by the breakdown in ceramics at a voltage of 23 kV or less.

A new thyatron control unit will be a significant change required for the replacement of the TPI thyatron in the generators. The reason is that other parameters of the pre-ionisation and running signals are needed.

Besides, additional kicker plates are fabricated for the injection at an energy of 1 GeV. They will be installed in the VEPP ring and powered from generators based on the new TPI thyratrons. There were manufactured 50-ohm loads (Fig.(5.14)1) for the VEPP-2000 complex, done under a contract with Kharkov Institute.

The switches in the circuit for switching the polarity and sending a pulse to the plates of the VEPP-2000 inflector turned out to be a weak point in the transmit path. The block comprised and involved one 16-contact and two 8-contact switches for the RK50-24-17 cable, the whole system together with the cable conductors being under an insulating gas pressure of 2 kg/cm<sup>2</sup>. The contact areas in the switch were not designed for a current exceeding 2.5 kA in a pulse mode and got out of order. After that, the technology for manufacturing the contacts was improved. In addition, the switching circuit was simplified: one large switch was left, and the connection of the kicker plates to the ballast resistors for harmonization in the switching mode was discarded. This made it possible to free up two 8-contact switches, one of which would be included in the layout of the power supply for two additional plates of the inflector. The injection mode of the complex is less than 1 Hz. Therefore, it was decided to upgrade the high-power charging system for the high-power supply of the generators of the injection system: accord – high-voltage transformer – the working capacity of the generator, replacing it with a compact inverter with voltage multiplication, located right in the casing of the generator.



Fig.(5.14)1. Thyratrons TPI1-1k/35 and TGI1000/25 and a 50 ohm load (from left to right).

The power consumed by the source is 6 W, which allows not only to mount two extra power generators for the new plates in the high-voltage unit but also omit cable lines and bulky transformers, which provides space for maintenance and a more rational arrangement of the equipment in the unit. Currently, the charging source prototype is being tested at the test bench with the parameters similar to those of the working generators (Fig.(5.14)2).



Fig.(5.14)2. Test bench for testing the charging source.

Long-term operation studies of bulk resistors for the kicker loads were carried out at the injection complex. The problem with the distillate quality causes degradation of resistors at an operation with high voltage. A significant increase in resistor rating occurs, sometimes even with physical destruction (burning) of the contact areas down to the inner layers of ceramics. Thus, a dozen of resistors were replaced during the operation of the complex, which is unacceptable for the operation mode. One of the ways to solve this problem is to replace the cooling system of distillate with an air one. Tests show that at a pressure of the air supply to the load of up to 2 kg/cm<sup>2</sup> and a power, equivalent to operation at 50 Hz, and the maximum voltage, the resistor is heated up to a temperature of 110 °C without changes in conductivity parameters. It was decided to replace the cooling of the loads at the injection complex to the air one. Besides, there were made some modifications in the loads themselves.



# 6

## SYNCHROTRON RADIATION SOURCES AND FREE ELECTRON LASERS



## Introduction

The share-use Siberian Center of Synchrotron and Terahertz Radiation (SRSTR) at BINP has worked for over thirty years. Works at the STSSTI are conducted in two directions: with synchrotron and terahertz radiation.

The "Synchrotron radiation" direction includes works on synchrotron radiation (SR) beams from VEPP-3 and VEPP-4, designing and construction of accelerators and special magnetic systems for SR generation for Russian and foreign centers and creation of experimental equipment for work with SR beams (radiation extraction beam lines, monochromators, detectors, etc.).

The "Terahertz radiation" direction includes works using radiation from Novosibirsk free electron laser (FEL) (in the range of 110-240  $\mu\text{m}$  and 40-120  $\mu\text{m}$ ), further development of Novosibirsk FEL and participation in international projects in this research area.

Besides, the program of the Center includes education and training of undergraduate and graduate students.

In 2010, 1,220 and 294 hours were allocated for work on SR beams from VEPP-3 and VEPP-4M, correspondingly. The experiments engaged 10 stations on 7 beamlines for SR extraction from VEPP-3 and 2 stations on radiation from VEPP-4M. Research groups from 55 institutes and other organizations conducted their experiments on SR in 2010. Work with terahertz radiation was organized on 6 user stations. An important task for 2010 was the commissioning of the second stage of Novosibirsk FEL and installation of the third stage systems.

About 750 hours of the working time was allocated for research on beams from Novosibirsk terahertz FEL. Research staff from 8 SB RAS institutes as well as teachers, students and graduates of Novosibirsk State University (NSU) and Novosibirsk State Technical University (NSTU) worked at the stations.

Work of the Siberian Center for Synchrotron and Terahertz Radiation in 2010 was supported by a large number of integration projects of SB RAS, RAS, RFBR and other funding sources, which are indicated below. The Siberian Center for Synchrotron and Terahertz Radiation was also involved in the following federal target programs: "Research and development in the priority directions of the scientific-technological complex of Russia for 2007-2012", contract 02.552.12.7001 the theme "Development of the Center of share-use of scientific equipment for provision of comprehensive research in the field of nanotechnology, environmental management, and living systems using synchrotron and terahertz radiation" (2008-2009); "Research and development in the priority directions of scientific-technological complex of Russia for 2007-2012", contract 02.552.11.7081, the theme "Carrying out exploration using synchrotron and terahertz radiation in the field of living systems, the industry of nanosystems and materials, ecology and environmental management at the center of share-use of scientific equipment "Siberian Center for Synchrotron and Terahertz radiation (SCSTR)"(2009-2010).

In 2010, Nikolai Vinokurov was awarded the State Prize of the Russian Federation in Science and Technology in 2009 for achievements in the development and creation of free electron lasers. The State Prize of the Novosibirsk region for participation in the development of free electron lasers was awarded to G.N. Kulipanov, A.N. Skrinsky, V.V. Kubarev, O.A. Shevchenko, M.A. Shcheglov, and V.V. Petrov.

## 6.1 Work on SR beams VEPP-3

### 6.1.1 Station "Explosion" (Extreme states of matter)

The station "Explosion" (Extreme states of matter) is intended for recording transmitted radiation and small angle X-ray scattering (SAXS) in the study of detonation and shock-wave processes.

Participating organizations in 2010:

- Russian Federal Nuclear Center All-Russian Research Institute of Technical Physics (VNIITF), Snezhinsk;
- Budker Institute of Nuclear Physics SB RAS, Novosibirsk;
- the Federal Nuclear Center of Russia, Russian Research Institute of Experimental Physics, Sarov (VNIIEF);
- the Institute of Hydrodynamics SB RAS, Novosibirsk;
- the Institute of Solid State Chemistry and Mechanochemistry (ISSCM) SB RAS, Novosibirsk.

In 2010, the work was carried out with financial support from the following projects:

1. SB RAS Integration project No. 11 "Study of the behavior of the crystal lattice of explosives and condensed nanoparticles during detonation by the methods of synchrotron radiation diffractometry";
2. RFBR grant 10-08-00859-a "Study of the shock wave front in nanostructured SiO<sub>2</sub> aerogel using synchrotron radiation";
3. RFBR grant 09-03-01155-a "Synchrotron radiation application to the study of model mechan chemical processes with nanosecond time resolution";
4. RFBR grant 08-03-00588-a "Investigation into the dynamics and kinetics of detonation processes using a improved method of synchrotron diagnostics";
5. RFBR grant 07-02-01079-a "Exploring the application of synchrotron radiation with energies of 30-60 keV to the study of detonation and shock-wave processes in explosive charges to 1500 g –development of the station "Detonation" on VEPP-4.

### Themes of works in 2010

One of the priorities of the Russian Federal Nuclear Center is the safe use of products containing explosives, which includes a wide range of issues, namely:

1. Safe use of products at higher temperatures. Existing fighting explosives withstand temperatures below 200° C. The skin of aircraft flying at low altitude can get as warm as 300° C. Munitions suspended outside shall endure until reaching the goal.
2. Safety during emergency situations (collision, fire, etc.). Explosives in products should be insensitive to shock and high temperatures.
3. Safety during prolonged storage. Explosives should keep their properties during prolonged (over 20 years) storage in the temperature range from -50° to +50° C.

Of all existing explosives, TATB (1,3,5-triamino-2,4,6-trinitrobenzene)-based compounds are the most promising. TATB is characterized by low sensitivity (lower than that of TNT) and good fire safety. It retains its properties at of up to 300° C and does not explode at temperatures above 320° C (it decomposes). Therefore, the study of TATB-based compositions is a priority for the RFNC.

Investigation of explosives by conventional methods requires a lot of experimentation and time. Therefore, the use of new, up-to-date techniques, some of which were developed by BINP, ISSCM, and LIH, is topical.

1. Technique for measuring the density distribution behind the detonation front. The density of matter is one of the main parameters in the physics of explosion. Our technique enables simultaneous measurement of the detonation velocity and mass velocity of the products, which allows one to compare data obtained with other techniques. Until now, there have been no other methods for rapid density measurement. The existing sensors for measuring pressure influence parameters of the medium. This is especially true for charges of small diameters.

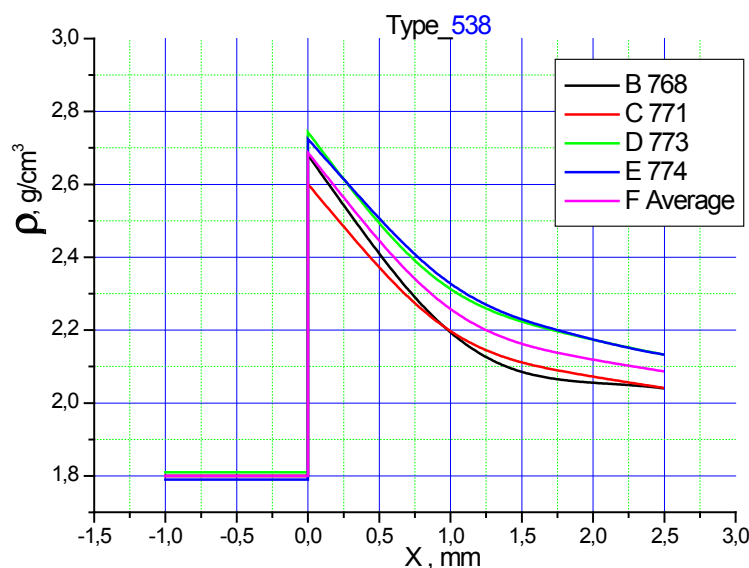


Fig.(6.1)1. Density distribution behind the TATB detonation front.

2. Technique for reconstruction of fields of pressure and velocities from a known density distribution. Using only the continuity equations and momentum conservation equations, we managed to obtain the distribution of pressure and mass velocity behind the detonation front.

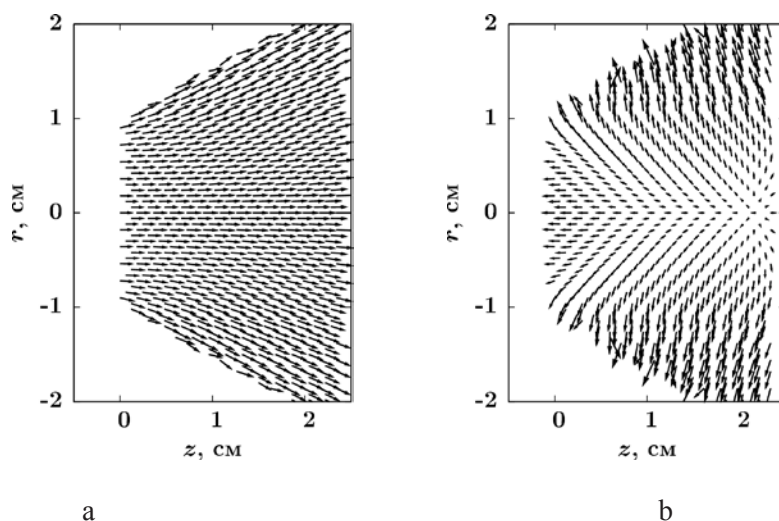


Fig.(6.1)2. The velocity field in the system associated with the detonation wave front (a) and in a fixed system (b) behind the TATB detonation front.

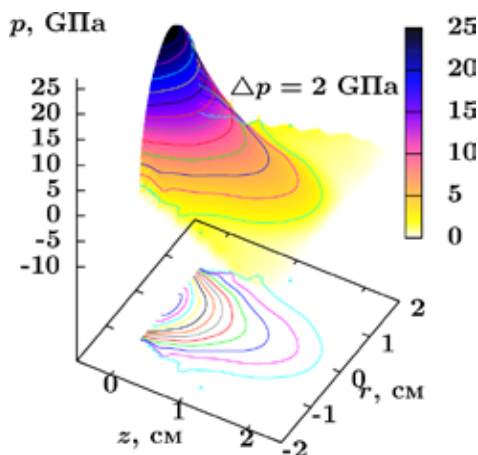


Fig.(6.1)3. Spatial distribution of pressure in TATB.

3. Technique for measuring SAXS behind the detonation front. Now there is no way to measure evolution of diffraction signals. This is the only technique of determination of the size of particles of the condensed phase of carbon. 10 to 30% of energy is released behind the detonation front due to the particle condensation.

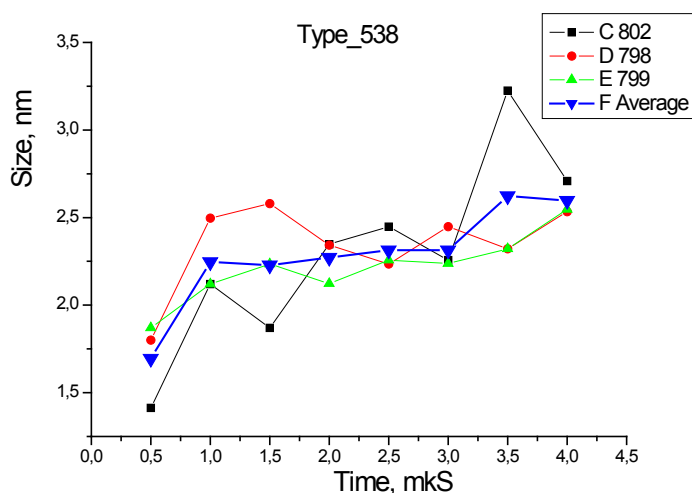


Fig.(6.1)4. Evolution of the growth of nanoparticle size over time at TATB detonation. The mean particle size is shown in curve F.

4. The method of X-ray microtomograms. Detonation velocity stability is one of the main parameters. This can be achieved by controlling the uniformity of density (the size of inhomogeneities should not exceed 10 microns). The installation on beamline 5 is Russia's the only facility that allows seeing inhomogeneities of about 5 microns inside a sample. (In the U.S. there are facilities measuring inhomogeneities to 10 nm in size).

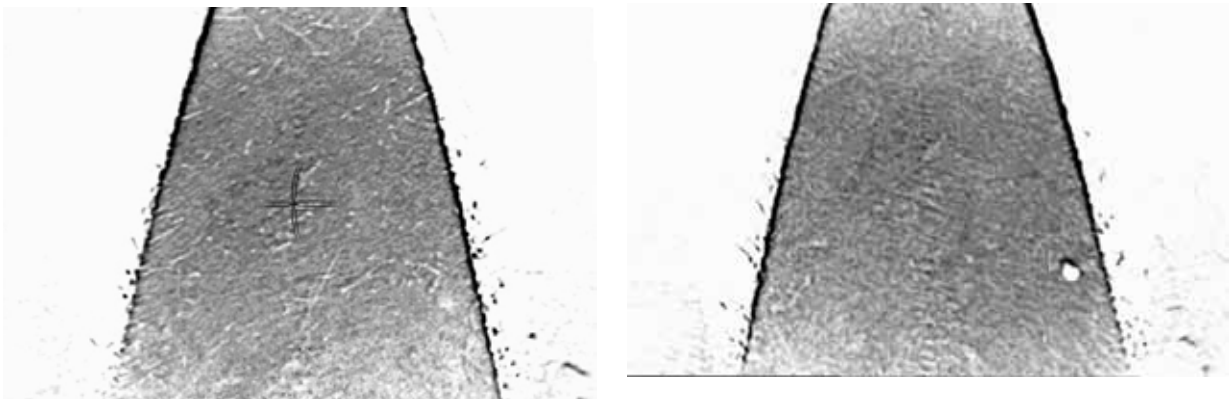


Fig.(6.1)5. Plasticized TATB. Room temperature (left). A temperature of 200° C (right). A 60 µm cavity can be seen.

5. Technique for measuring lattice parameters at temperature changes. The method of heating and cooling explosives is essential to controlling the stability of parameters during prolonged storage. Cyclical changes in temperature can mimic a long-term storage of explosives. Measurement of the positions of diffraction peaks allows controlling lattice parameters. Together with microtomography, this technique allows better control of explosive stability.

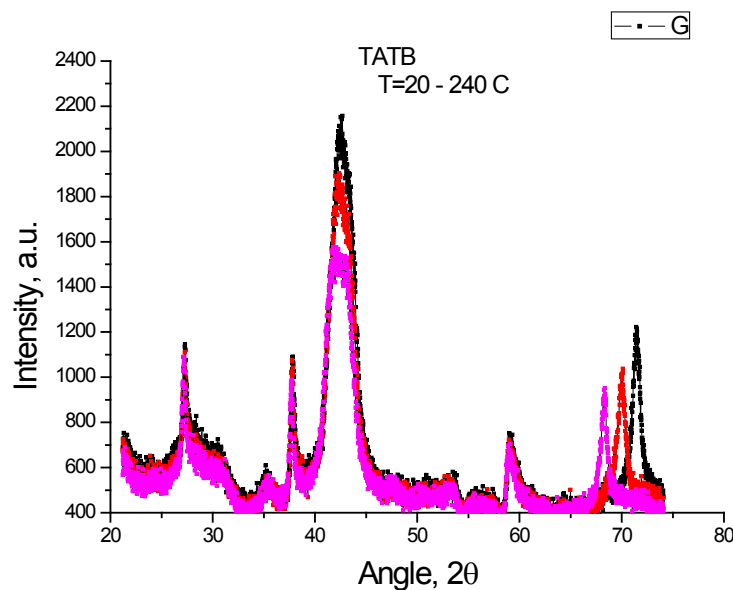


Fig.(6.1)6. Dynamics of the positions of diffraction peaks in TATB heated from 20° to 240° C.

### 6.1.2 Station “LIGA-technology and X-ray lithography”

The station is intended for experiments on X-ray lithography in thick resistive layers for manufacturing of microstructures including X-ray masks.

Participating organizations:

- Budker Institute of Nuclear Physics SB RAS, Novosibirsk;
- the Institute of Cytology and Genetics SB RAS, Novosibirsk;

- the Institute of Solid State Chemistry and Mechanochemistry SB RAS, Novosibirsk;
- the Institute of Automation and Electrometry SB RAS, Novosibirsk;
- Novosibirsk State University.

Works in 2010 were carried out with financial support from the following projects:

1. SB RAS interdisciplinary integration project No. 55 "X-ray LIGA technology for synthesizing 3D diffraction structures";
2. State contract No. 02/04, dated November 30, 2010, for the needs of the Russian Research Centre "Kurchatov Institute" "Conducting research in the field of hybrid microfluidic systems in the following directions: "basic elements of hybrid microfluidic systems for bio-sensing and other technologies" and "biosensors for detection and analysis of very low concentrations of biologically active compounds".

Themes of works in 2010:

1. Modernization of the SR station "LIGA" – design, assembly and testing of the X-ray generator of images for direct formation of microstructures (Budker Institute of Nuclear Physics, SB RAS).
2. Development of the methods for fabrication and testing X-ray masks for deep X-ray lithography (Budker Institute of Nuclear Physics, SB RAS and the Institute of Solid State Chemistry and Mechanochemistry SB RAS).
3. Design, manufacture and testing of selective elements of the THz range. Thin films of mesostructured silicate materials (Budker Institute of Nuclear Physics, SB RAS, the Institute of Solid State Chemistry and Mechanochemistry SB RAS, and Novosibirsk State University).
4. Development of basic elements of hybrid microfluidic systems for bio-sensing and other technologies (the Institute of Cytology and Genetics SB RAS, Budker Institute of Nuclear Physics SB RAS and the Institute of Solid State Chemistry and Mechanochemistry SB RAS).

Examples of works in 2010

#### 1. Development of methods for fabrication and testing X-ray masks for deep X-ray lithography.

BINP together with ISSCM SB RAS developed and implemented a technological process for manufacturing X-ray masks with a gold absorbing pattern on glassy-carbon substrate without using the expensive stages of electron beam lithography, fabrication of an intermediate X-ray mask and X-ray lithography in the soft SR spectrum for making a working pattern.

A microfluidic system layout pattern (developed by ICG SB RAS) was formed using the Direct-LIGA method, based on the principle of vector formation of a micropicture immediately in a thick layer of X-ray resist on a conducting radiotransparent substrate with a needle-like SR microbeam at the station "LIGA".

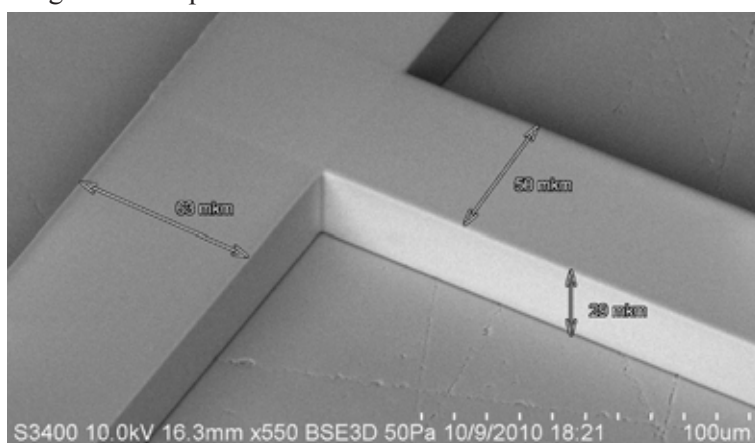


Fig.(6.1)7. Fragment of a work-piece for X-ray mask – a microstructure of the SU-8resist 29  $\mu\text{m}$  high on a glassy-carbon substrate.

A gold layer 20  $\mu\text{m}$  thick was electrochemically deposited on the work-piece for fabrication of a high-contrast X-ray mask. The fabricated X-ray mask was checked with optical and electron microscopes. The X-ray contrast was checked using synchrotron radiation at the station "X-ray Microscopy and Tomography" by a specially developed technique.

## 2. Development of basic elements of hybrid microfluidic systems for bio-sensing and other technologies.

Micro/nanofluidic systems (MNFS) are integrated devices – laboratories placed on chips and formed by a system of channels with a laminar flow of fluids, which creates the best and easy-to-control conditions for running of transport and diffusion processes; functioning of bacterial and eukaryotic cells; and running of biomolecular, molecular genetic, biochemical, and chemical reactions. The main advantage of MNFS is that they enable work with extremely small volumes of reagents –  $10^{-9}$ - $10^{-15}$  l and picograms of substances.

Microfluidic modules of two types were developed - for the immunodiffusion reaction (detection of antigens or antibodies in a fluid to test) and to automatically obtain the concentration gradient of an analyte.

10 disposable replaceable microfluidic modules of PMMA were made to conduct the immunodiffusion reaction as well as 10 disposable replaceable microfluidic modules - gradientators for positioning cells of genosensors. A high-contrast X-ray mask was made via electrochemically depositing a gold layer 20  $\mu\text{m}$  thick on the work-piece.

Rapid control of the manufacturing of X-ray mask and microfluidic modules was carried out using the optical microscope MII-4 and the scanning electron microscope HITACHI S3400N.

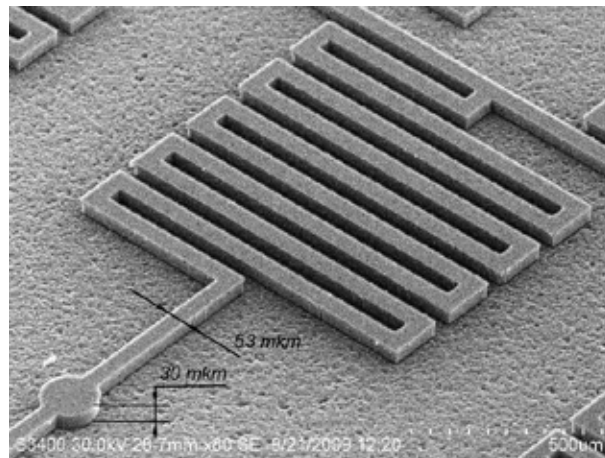


Fig.(6.1)8. Fragment of a work-piece of X-ray mask (an SU-8 structure before the galvanic deposition of gold).

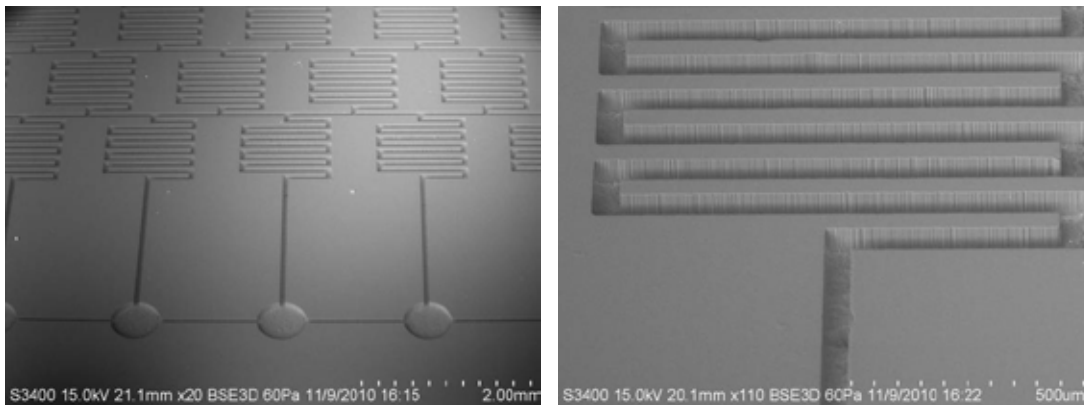


Fig.(6.1)9. SEM photos of fragments of the microchannel module.

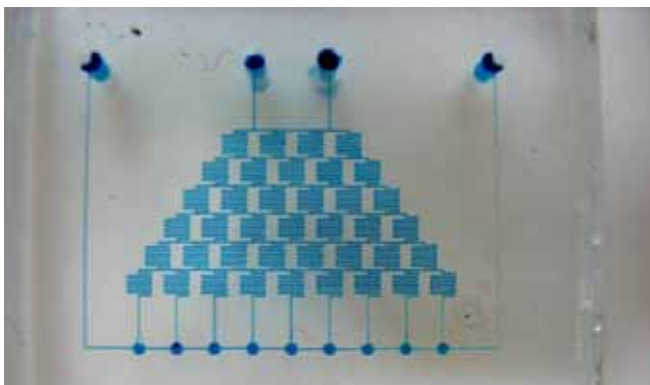


Fig.(6.1)10. Photo of a disposable replaceable microfluidic module – gradientator for positioning cells of genosensors. For clarity, the channels are filled with ink.

These measurements showed that microfluidic modules fabricated by the LIGA technology fully correspond to the topology, design documentation, and specification requirements. The width of channels of different modules is 55 microns to 60 microns. The roughness was less than 3%.

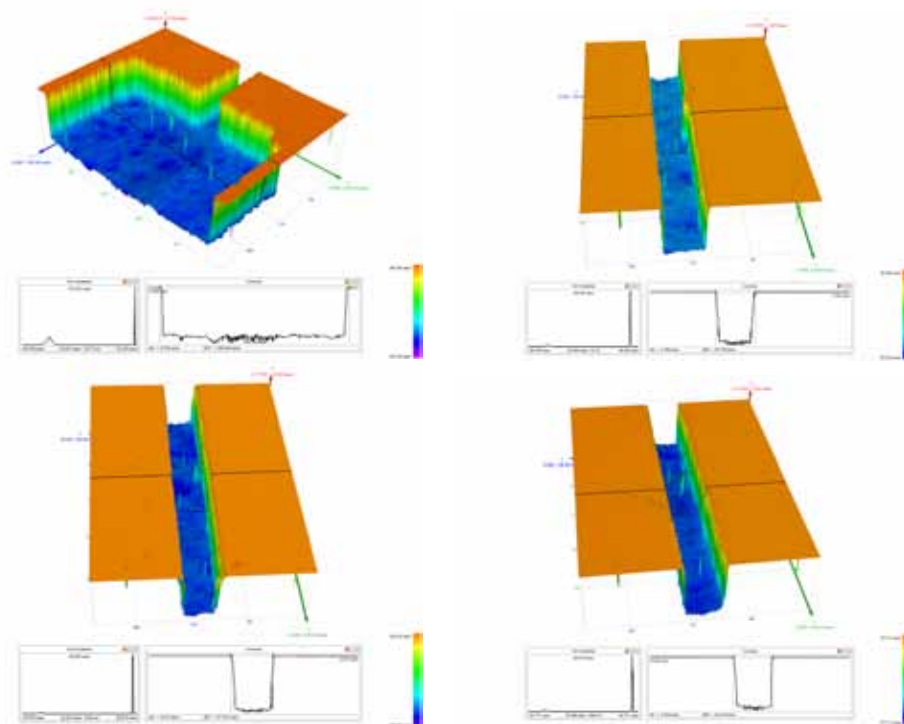


Fig.(6.1)11. Quality control of manufacturing of microfluidic modules using the profilometer Profile (TDI DT SB RAS).

Specimens of microfluidic systems were successfully tested at IC&G SB RAS.

### 6.1.3 Station “Anomalous Scattering”

The station is intended for precision studies of the structure of polycrystalline materials by the methods of X-ray diffraction with high angular resolution.

Participating organizations:

- Borekov Institute of Catalysis SB RAS, Novosibirsk;
- Nikolaev Institute of Inorganic Chemistry SB RAS, Novosibirsk;
- the Institute of Semiconductor Physics SB RAS, Novosibirsk;
- the Institute of Solid State Chemistry and Mechanochemistry SB RAS, Novosibirsk;
- the Institute of Chemistry and Chemical Technology SB RAS, Krasnoyarsk;
- Tomsk Polytechnic University;
- Tomsk State University;
- Institute of Strength Physics and Materials Science, Tomsk.

Works in 2010 were carried out with financial support from SB RAS and RFBR:

1. SB RAS interdisciplinary integration project No. 82 "Oxygen permeability of massive and applied membranes based on perovskites of mixed conductivity";
2. RFBR grant No. 09-03-90424-Ukr\_f\_a "Development and study of metal-oxide catalysts for heterogeneous catalytic processes of production and purification of hydrogen".

Themes of works in 2010:

1. Mesoporous alumina-silicate materials, variation in the size of mesopores with different temperature of hydrothermal treatment (the Institute of Catalysis SB RAS and the Institute of Chemistry and Chemical Technology SB RAS, Krasnoyarsk).
2. Heterostructures based on germanium and silicon. Quantum dots (the Institute of Semiconductor Physics SB RAS and the Institute of Catalysis SB RAS).
3. Oxygen-conducting materials based on perovskite-like oxides (Boreskov Institute of Catalysis SB RAS and the Institute of Solid State Chemistry and Mechanochemistry SB RAS).
4. Strengthening of coatings based on titanium nitride (Tomsk Polytechnic University).
5. Copper-cerium catalysts for hydrogen production and purification from CO impurities (the Institute of Catalysis SB RAS).
6. Relaxation processes in zirconium during plastic deformation (the Institute of Strength Physics and Materials Science, Tomsk).
7. Catalysts based on nickel-aluminum intermetallic compounds for the processes of carbon dioxide conversion of methane (the Institute of Catalysis SB RAS and Tomsk State University).
8. Oxide catalysts of perovskite-like structure for the processes of carbon dioxide conversion of methane (the Institute of Catalysis SB RAS).
9. Heterostructures based on cadmium sulfide (the Institute of Semiconductor Physics SB RAS and Institute of Inorganic Chemistry SB RAS).
10. Thin films of silicon carbonitrides of different composition and origin (the Institute of Inorganic Chemistry SB RAS).

Examples of works in 2010:

Mesoporous silica and the silicate-containing materials. Currently, more than 90% of industrial chemical processes are carried out on adsorbents and heterogeneous catalysts. Effectiveness of their use depends on the chemical and phase composition and structural features and textural characteristics of the material: specific surface area, pore volume and distribution on the effective size. Therefore, directed regulation of textural parameters of catalysts and adsorbents seems to be a topical task. From the viewpoint of catalysis, large specific surface area (up to 1000 m<sup>2</sup>/g or more), large porosity (over 1 cm<sup>3</sup>/g) and narrow pore size distribution are attractive and unique properties of silicate and silicate-containing mesoporous mesophase materials (MMMs). A typical example of MMM is the SBA-15 silicate, which has two-dimensional hexagonal packing of uniform-size pores with shape close to cylindrical. Textural parameters of such materials can be regulated by varying the hydrothermal treatment temperature (HTT) in the course of synthesis to remove the structure-forming agent (surface-active agent (surfactant) Pluronic P123). Introduction of impurity cations to the structure of mesoporous silicate on the stage of MMM synthesis allows making catalytic systems with catalytically active hetero-elements embedded in the silicate wall. The textural characteristics (specific surface area of mesopores, specific mesopore volume, distribution of mesopores and micropores by size) of materials to synthesize are determined by the method of low-temperature nitrogen adsorption; the structural ones (the two-dimensional unit cell parameter and the degree of structure regularity) are found using X-ray diffraction at the station "Anomalous Scattering" at the Siberian Center for Synchrotron Radiation.

The synthesis of mesoporous silicates and aluminosilicates was realized in 2010 with thermostating of the synthetic mixture during synthesis in the range of 20 - 150° C. MMMs were synthesized by deposition of SiO<sub>2</sub> and Al precursors in the presence of the surfactant Pluronic P123. The synthesis was carried out at pH of 1-3 because exactly under these conditions hetero-elements are precipitated from soluble forms. Aluminum sulfate (Al<sub>2</sub>(SO<sub>4</sub>)<sub>3</sub>) was used as a source of aluminum in aluminosilicate mesophases. After the HTT, the resulting material was filtered, washed with distilled water and dried in air. Then the material was calcined in order to remove the surfactant.

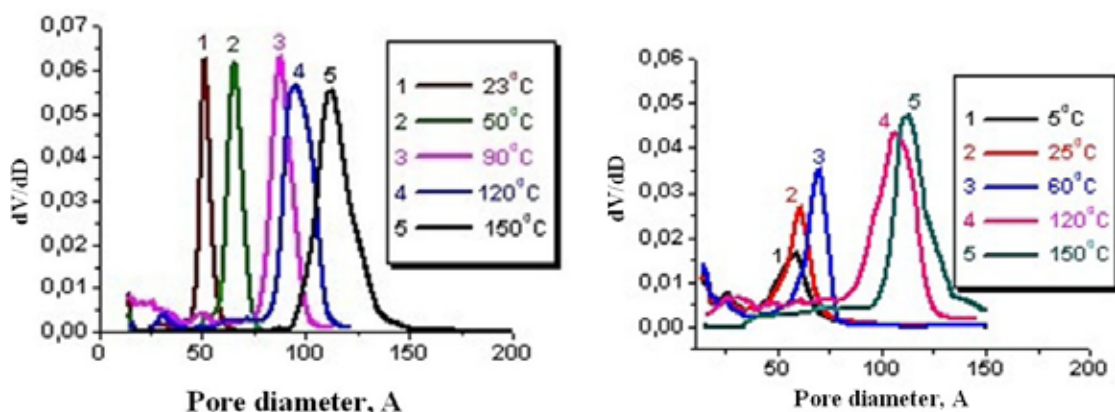


Fig.(6.1)12. Shows the distributions of pore volumes on sizes for silicon oxide and alumina-silicate material, calculated from nitrogen adsorption isotherms at 77 K which were measured on the automated adsorption unit ASAP - 2400 (Micromeritics). With increasing temperature of hydrothermal treatment the size of material pore also increases due to the surfactant thermal expansion prior to polycondensation of the silicate wall.

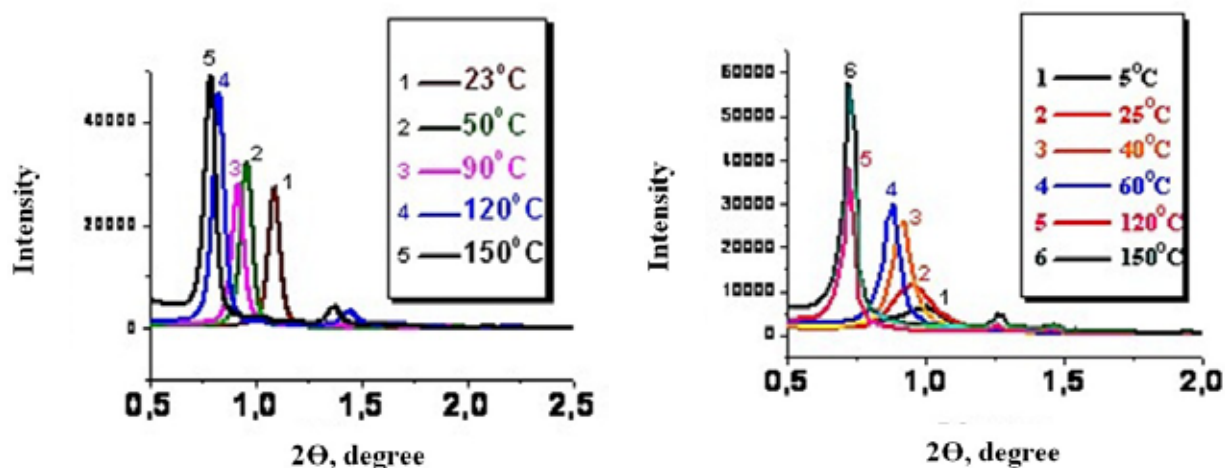


Fig.(6.1)13. Shows radiographs of the silicate and aluminosilicate materials, measured in the small-angle region. All the materials are characterized by diffractograms corresponding to a two-dimensional hexagonal packing of pores of identical size. With increasing temperature of hydrothermal treatment, the reflections are shifted towards the area of smaller angles and, correspondingly, the unit cell parameters increase. In addition, with increasing temperature the degree of structural perfection of MMM also increases, as evidenced by the appearance of reflections of higher orders in the diffraction patterns.

The textural characteristics of the materials calculated from the adsorption and X-ray data are presented in Table (6.1)1

Table (6.1)1. Textural and structural characteristics of silicate and aluminosilicate MMMs obtained at different temperatures of hydrothermal treatment.

HTT	Specific surface area, m <sup>2</sup> /g		Pore volume, m <sup>3</sup> /g		Cell parameter, a <sub>0</sub> , nm		Pore diameter, nm	
	SiO <sub>2</sub>	Al-SiO <sub>2</sub>	SiO <sub>2</sub>	Al-SiO <sub>2</sub>	SiO <sub>2</sub>	Al-SiO <sub>2</sub>	SiO <sub>2</sub>	Al-SiO <sub>2</sub>
23°C	456	720	0.49	0.59	9.26	10.7	5.1	6.1
50°C	460	696	0.67	0.65	10.61	11.1	6.5	6.9
90°C	648	-	0.99	-	12.13	-	8.7	-
120°C	578	843	0.95	0.85	12.43	11.7	9.5	10.6
150°C	391	700	1.01	0.66	12.74	14.2	11.,2	11.3

The studies have shown that thermal treatment of aluminosilicate mesophase materials makes it possible to adjust the pore size in the range of 6 - 11 nm, which is slightly less than was expected. X-ray dif-

fraction showed the presence of only one two-dimensional hexagonal phase, which was expected when planning the experiments. However, reducing the treatment temperature leads to a broadening of the diffraction peaks.

#### **6.1.4 Station “Precision Diffractometry”**

The station is intended for exploration of the change in the structure of polycrystalline materials under the influence of high temperature and reactive media by the methods of X-ray diffraction with time resolution.

Participating organizations:

- Boreskov Institute of Catalysis SB RAS, Novosibirsk;
- Nikolaev Institute of Inorganic Chemistry SB RAS, Novosibirsk;
- Institute of Solid State Chemistry and Mechanochemistry SB RAS, Novosibirsk;
- Tomsk Polytechnic University;
- Tomsk State University;
- Institute of Strength Physics and Materials Science SB RAS, Tomsk.

Works in 2010 were carried out with financial support from SB RAS:

SB RAS interdisciplinary integration project No.82 "Oxygen permeability of massive and coated membranes based on perovskite-like oxides of mixed conductivity".

Themes of works in 2010:

1. Oxygen-conducting materials based on perovskite-like oxides (Boreskov Institute of Catalysis SB RAS and the Institute of Solid State Chemistry and Mechanochemistry SB RAS).
2. Catalysts based on nickel-aluminum intermetallic compounds for the processes of carbon dioxide conversion of methane (the Institute of Catalysis SB RAS and Tomsk State University).
3. Oxide catalysts with a perovskite-like structure for the processes of carbon dioxide conversion of methane (the Institute of Catalysis SB RAS).
4. Structural changes and relaxation processes in palladium at introduction of hydrogen (Tomsk Polytechnic University).
5. Reduction of noble metal complexes (the Institute of Inorganic Chemistry SB RAS).
6. Aluminium-cobalt catalysts for the Fischer-Tropsch process (the Institute of Catalysis SB RAS).
7. Copper-nickel catalysts for the growth of nitrogen-containing carbon nanofibers (the Institute of Catalysis SB RAS).
8. Reduction of nanodispersed bismuth from oxides (the Institute of Solid State Chemistry and Mechanochemistry SB RAS).

Examples of works in 2010:

1. *In-situ* X-ray diffraction study of Ni-Cu catalyst in the growth of nitrogen-containing carbon nanofibers. Carbon nanofibers (CNFs) are used in various fields of science and technology, from electronics and materials science to catalysis and absorption. CNFs with inclusion of nitrogen are synthesized to be used as catalyst supports for ensuring better adhesion of the active component on the support surface. The synthesis is usually carried out from the gas phase by decomposition of hydrocarbons on catalysts – transition metals and their alloys. When different metals are used, CNFs of different morphology are produced.

This work studied the changes in the phase composition of the nickel-copper catalyst for the growth of nitrogen-containing CNFs (N-CNFs) in the process of the reaction of decomposition of ethylene/ammonia mixture under high temperature. The sample was placed in an X-ray reactor chamber Anton Paar XRK-900. The flow of gas was passed through the sample at a rate of 0.5 cm<sup>3</sup>/s and temperatures from ambient to 550° C. The initial sample was reduced directly in the reactor chamber in the hydrogen flow at 550° C in 15 min. Radiographs were recorded sequentially, by frames with an exposure time of 0.5-1 min.

The initial sample is a mixture of two components, containing primarily copper and nickel, correspondingly. According to the estimates and the Vegard law, the amount of nickel dissolved in copper and copper dissolved in nickel is about 15-20%. In the process of catalyst activation and subsequent decomposition of the ethylene-ammonia mixture the catalyst undergoes a series of transformations. Judging

by the nature of the radiographs, the main changes in the catalyst involve the nickel-containing component, whereas the copper-containing component is weakly transformed. Our experiments show that in the course of the reaction the lattice parameter of the nickel-rich alloy increases presumably due to dissolution of carbon and nitrogen, resulting from thermolysis of the initial reagents (Fig.(6.2)14). When the catalyst is cooled to a temperature of 440-450° C, formation of a new phase of unknown composition is observed. Re-heating of this phase to a temperature of 550° C leads to its disappearance and return of the catalyst to its former state. In this case, there is no formation of the nickel carbide phase. If pure nickel is used as a catalyst for CNF growth, a shift of reflections of nickel towards large angles is observed at a temperature of 550° C, which indicates formation of the unordered nickel carbide phase. Cooling of the catalyst in the reaction medium leads to the ordering and formation of the stoichiometric nickel carbide phase.

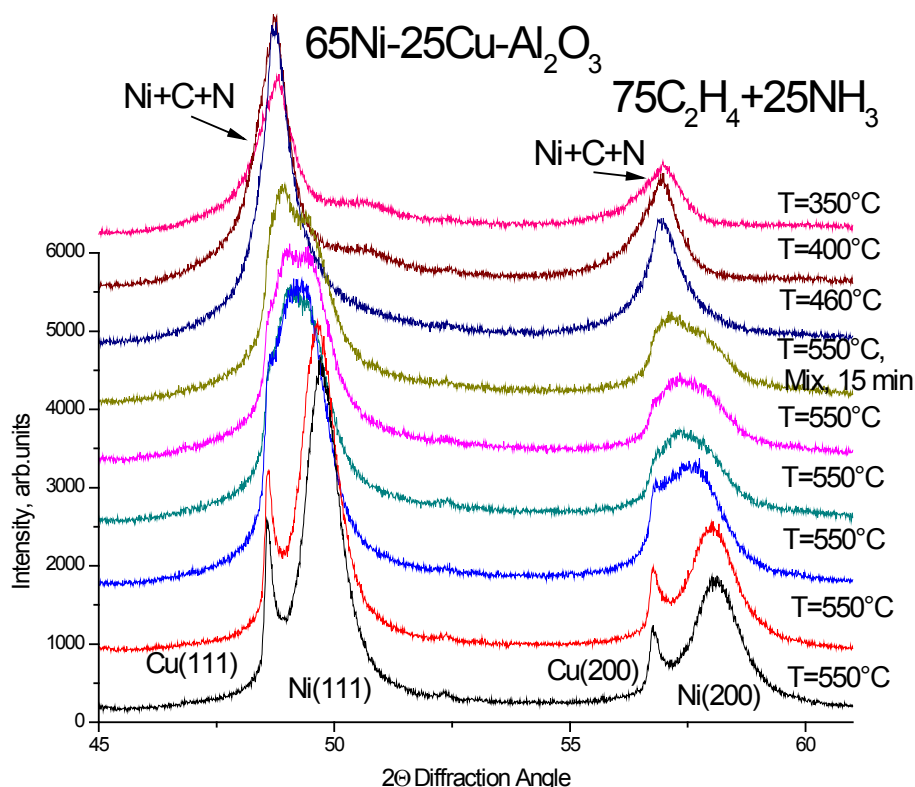


Fig.(6.1)14. Phase transformations of the nickel-copper catalyst for CNF synthesis in the course of reaction at different temperatures.

2. Study of hydrogen reduction of solid solutions of  $\text{Co}_{3-x}\text{Al}_x\text{O}_4$ . Deposited cobalt systems are of interest as catalysts for the Fischer-Tropsch synthesis. The precursor of the active component of the catalyst is cobalt oxide  $\text{Co}_3\text{O}_4$ , which is activated via reduction in an industrial reactor. Investigation into the process of  $\text{Co}_3\text{O}_4$  reduction is of interest for clarification of the regularities of formation of the active state of the catalyst. The behavior of cobalt-containing catalysts at reduction is often studied using model systems – bulk samples of  $\text{Co}_3\text{O}_4$  and solid solutions of  $\text{Co}_{3-x}\text{Al}_x\text{O}_4$ .

Using *in situ* X-ray diffraction, we studied reduction of the  $\text{Co}_{3-x}\text{Al}_x\text{O}_4$  (at  $x = 0 - 0.5$ ) and  $\text{Co}_3\text{O}_4/\gamma\text{-Al}_2\text{O}_3$  catalyst in a hydrogen flow at temperatures of up to 450° C. It was shown that reduction of solid solutions occurs in 2 stages:  $\text{Co}_3\text{O}_4$  is reduced to CoO and then to metallic Co (Fig.(6.2)5.). The same two-phase reduction is characteristic to the catalyst  $\text{Co}_3\text{O}_4/\gamma\text{-Al}_2\text{O}_3$ . With increasing aluminum content in the solid solution, the temperature of the transition  $\text{Co}_3\text{O}_4 \rightarrow \text{CoO}$  also increases. Thus, the introduction of aluminum prevents reduction of cobalt oxide.

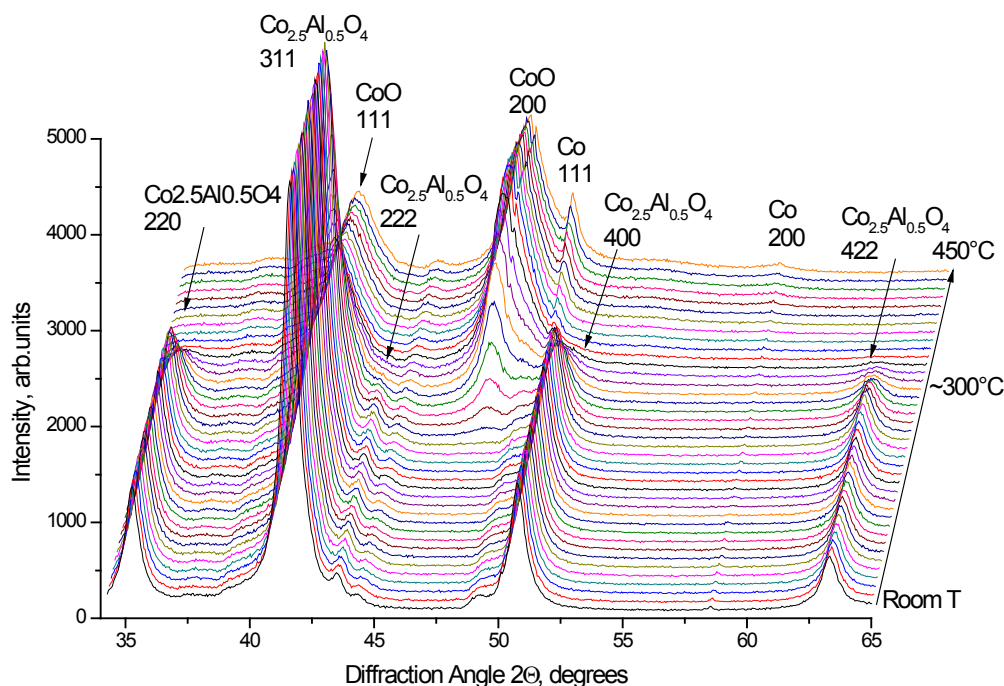


Fig.(6.1)15. The process of cobalt reduction from the solid solution of  $\text{Co}_{2.5}\text{Al}_{0.5}\text{O}_4$  in a hydrogen flow.

### 6.1.5 Station “X-ray fluorescent elemental analysis”

The station is intended for determination of the elemental composition of samples of different origin: geological rocks, biological tissues, aerosols, etc., by the method of X-ray fluorescence elemental analysis using synchrotron radiation (SR XRF). The elemental analysis can be carried out both in a local and in a scanning mode.

Participating organizations:

- the Institute of Theoretical and Experimental Biophysics, Pushchino;
- the Institute of General and Inorganic Chemistry RAS, Moscow;
- Indian Institute of Technology, Kharagpur, India;
- the Institute of Cell Biophysics RAS, Pushchino;
- the Institute of Archaeology and Ethnography SB RAS, Novosibirsk;
- Nikolaev Institute of Inorganic Chemistry SB RAS, Novosibirsk;
- the Regional Institute of Pathology and Pathomorphology SB RAMS, Novosibirsk;
- Sobolev Institute of Geology and Mineralogy SB RAS, Novosibirsk;
- the Institute of Earth Crust SB RAS, Irkutsk;
- Vinogradov Institute of Geochemistry SB RAS, Irkutsk;
- the Institute of Water and Environmental Problems (IWEP) SB RAS, Barnaul;
- the Institute of Biophysics SB RAS, Krasnoyarsk;
- the Institute of Cytology and Genetics SB RAS, Novosibirsk;
- the Institute of Chemical Kinetics and Combustion SB RAS, Novosibirsk;
- Budker Institute of Nuclear Physics SB RAS, Novosibirsk.

In 2010, work was carried out under the following projects (grants):

SB RAS interdisciplinary integration project No. 38, SB RAS interdisciplinary integration project No.120, Project No.16-17 of the Fundamental Research Program of the RAS Presidium “The environment in a changing climate: extreme natural events and disasters”, RFBR Project No. 08-05-00680 - a, and RFBR Project No. 09-05-90210-Mong-a.

Themes of some works in 2010:

*Urban ecology: analysis and evaluation with the help of XRF-SR on the example of Novosibirsk.* This work was supported by RFBR grant 09-05-00839 and SB RAS integration project No.84.

Conclusions of the work:

- Composition of aerosols reflects the aerosol pollution during winter; the elemental composition of birch and poplar leaves, for the vegetative season. Snow survey in late winter and sampling vegetation in autumn will make it possible to maintain a year-round urban environmental monitoring.
- The tin plant is a source of intense urban pollution with compounds of As, Sn, Tl, Cd, Cu, Zn, Pb, Sb, Bi, Ag, Br, and Hg, which is reflected in the composition of soil, vegetation and snow cover of surrounding areas.

*Comprehensive instrumental examination of the orientation and periodicity of global and regional climate changes and the environment in the geological history of the Late Cenozoic of Siberia to predict their changes in the near future.*

Due to the sharp fluctuations in the climate of the planet, taking place in recent decades, and unpredictable threatening, perhaps even catastrophic consequences for the nature and man, the research of the climate of past eras has a particular significance. For identification of the geological, mineralogical and geochemical features of these changes chemogenic sediments are studied by a complex of methods, including XRF-SR. Studying the elemental composition of lake sediments is necessary to determine patterns of variation in the relative concentrations of elements in dependence on the ambient temperature. The identification of these patterns and comparing them with other indicator traits can decipher "paleoclimatic records", determine the boundaries of climatic changes and identify fluctuations of lower order in separate periods of cooling/warming. Such systematic studies of small lakes in Central Asia have been performed for the first time.

Over 350 samples from the sedimentary sequences of four lakes in the Baikal region, Chita region and Baraba Lowlands were analyzed using X-rays in 2010. Series of analyses were carried out with a step of 1-2 cm. The content of the following elements were determined: Ca, K, Ti, V, Cr, Mn, Fe, Ni, Cu, Zn, Ga, Ge, Br, Rb, Sr, Y, Zr, Nb, Mo, Pb, As, Th, and U. The data obtained are now being processed and systematized.

*Reconstruction of the absolute values of average annual temperatures of the Altai region in the annual scale in the last 1500 years from data of scanning XRF microanalysis of the bottom sediments of Lake Teletskoye. The work was carried out under SB RAS interdisciplinary integration project No.92 "Forecast of climate changes in Central Asia based on analysis of annual records in lake sediments, tree rings and glaciers of the region."*

Box samples and a new core 2 m long were taken in 2010 in the deep area of Lake Teletskoye (Gorny Altai) from a motor ship belonging to the IWEP SB RAS. The core was opened and documented; its humidity and magnetic susceptibility were measured; solid preparations were made and analyzed with an SR XRF scanner with a step of 0.1-0.5 mm. The initial data were normalized to the one-year timescale using isotope chronology by  $^{137}\text{Cs}$  and  $^{14}\text{C}$  together with an estimate of the rate from a series of determinations in the Radiocarbon Laboratory of Poznan, Poland. The reconstruction was performed by multiple linear regression with function training from meteorological data of Barnaul station for the years 1840-2004. Fig.(6.1)17 presents the resulting climatic reconstruction of the regional average annual temperature in the interval of 1500 years ago in comparison with a set of reconstructions for the Northern Hemisphere. It is in good agreement with the global trends and presents regional characteristics.

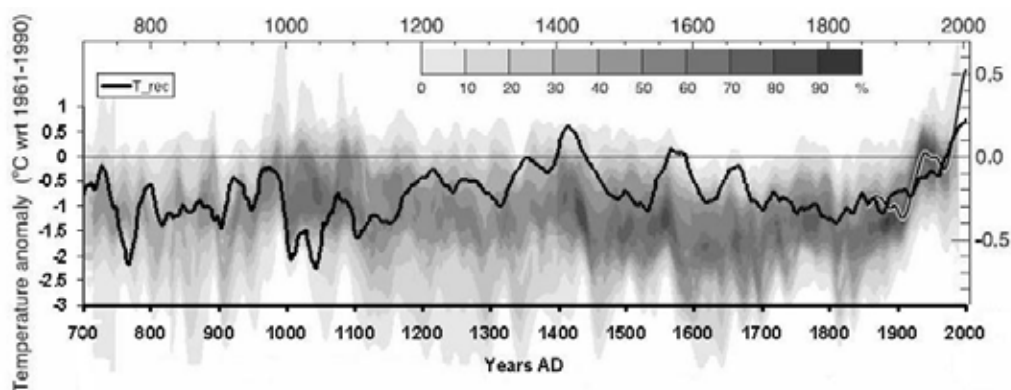


Fig.(6.1)16. Graph of reconstructed temperature (as deviation from the mean regional value for the period of 1961-1990, solid line, left scale) smoothed by the moving average method on 30 points is superimposed

on the temperature reconstruction for the Northern Hemisphere for 1300 years (deviation from the mean, shades of gray, right scale ). The separate line in the interval of 1856-2005 years presents instrumental data.

Wavelet (Fig.(6.1)17) and Fourier analysis revealed the following main periodicities: 750, 480, 250, 72, 58, 40, 22, 13 and 8 years.

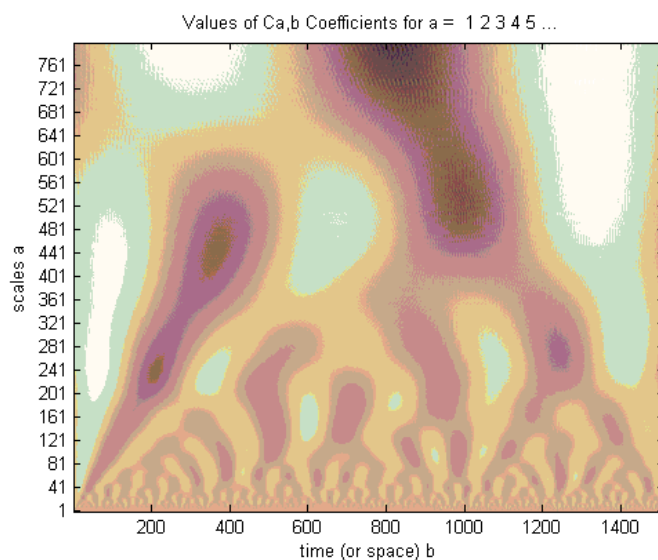


Fig.(6.1)17. Continuous wavelet transform of the reconstructed temperatures.

*Exploratory research in the field of assessment of biosafety of nanoobjects in dependence on elemental composition and size at the center of share use of scientific equipment “Genepools of laboratory animals” of the Institute of Cytology and Genetics SB RAS. State contract with the FASI: 2009-07-5.2-00-09-027.*

As a result, a comprehensive approach consisting of tools and techniques to pre-assess and predict the likely consequences of exposure of the human body and other living objects to nanocomponents was developed. The integrated approach included analysis of the distribution of nanoparticles in mice by the methods of atomic emission spectroscopy, X-ray fluorescent analysis, magnetic resonance tomography and laser scanning confocal microscopy. Various methods of exposure of animals to nanoparticles – intravenous and intraperitoneal injections, skin and intranasal applications, and by aerosols with different concentrations of nanoparticles – were developed.

Accumulation of gold and Tarkosil nanoparticles was revealed in the spleen of experimental animals, which agrees well with the newly emerging concepts that nanoparticles are not biologically neutral and are involved in immunoregulatory processes. It was shown that the use of atomic emission spectroscopy and X-ray analysis allows high-efficiency singling out organs and tissues that are potential targets for nanoscale materials.

A short list of other most important works that had been executed and are performed at the station SR XRF:

*Development of scientific and technological grounds for monitoring and modeling climatic processes in the area of Greater Vasyugan swamp.* The work was carried out under interdisciplinary integration project IP-66.

*X-ray fluorescent study of natural and bio-technology silk structures.* The work was done under RFBR grant No. 09-04-92663-IND\_a "Study of extracellular fibrillar biopolymers – natural silk fibers, protein network of silk and proteoglycan fibrils of both mucus and extracellular matrix of tissue."

*Study of macro- and microelement composition of archaeological samples (fragments of textiles, wool, hair, plants, and soil from the burials of Knyazhiy Gori (the Princely mountains) and Noin-Ula (Mongolia)).* The work was done under RFBR grant No. 10-06-00406-a "Hair from ancient tombs as an object of interdisciplinary research (study of the remains of the Xiongnu culture)".

*Regional climate changes during the Holocene and late Pleistocene and their indicators. Geochemical indicators of changes in depositional environment and climate during the Holocene and Late Pleistocene.*

Core of sediments of Lake Hovsgol GC-46 was studied in the course of the project. The content of

biogenic silica in the core varies from 1.42 to 7.24% in the range of 47-75 cm, whereas from 9.00 to 24.52% in the range of 0-47 cm. Judging by the content of biogenic silica in the sediments, the upper 48 cm of core GC-46 can be attributed to the Holocene; and the interval of 48-75 cm of it, to the Sartan stage of the late Pleistocene glaciation. Comparison of the elemental composition data with the  $\text{SiO}_{2\text{bio}}$  content showed a series of elements reflecting the transition from the Holocene to the glaciation.

Besides, to assess the accuracy of the results of the study of sediments we carried out elemental analysis of the following reference materials: bottom silt of Lake Baikal (BIL-1), sediments of Lake Baikal (BIL-2), carbonate background silt (SGH-1), background terrigenous silt (SGH-3), meadow grass mixture (Tr-1), and Canadian pondweed (EK-1). The work was conducted under RFBR grants No. 09-05-90710 and No. 08-05-98108-r\_sibir\_a.

*Biogeochemistry of stratified organogenic marsh and lake sediments (peat and sapropel) and geochemical barriers to flows of chemical elements from the atmosphere.* The work was done under RFBR grant No. 08-05-000392.

*Creation of a time model of the sedimentary records of climate in Lake Shira (Khakassia) based on counting the annual layering and isotopic determinations of global and regional developments.* This work was supported by RAN project 16.17. "Reconstruction of the sequence of events of climate aridization in Central Asia and Siberia in the late Cenozoic on the basis of a comprehensive study of lake sediments and peat".

### 6.1.6 Station "Diffraction using hard X-rays"

The station is intended for *in situ* diffraction studies of the structure of materials under physical and chemical influence.

Participating organizations:

- the Institute of Solid State Chemistry and Mechanochemistry SB RAS, Novosibirsk;
- Borekov Institute of Catalysis SB RAS, Novosibirsk;
- Nikolaev Institute of Inorganic Chemistry SB RAS, Novosibirsk;
- the Institute of Geology and Mineralogy SB RAS, Novosibirsk;
- the Institute of Metal Physics UB RAS, Ekaterinburg;
- the Physico-Technical Institute, Izhevsk.

The work in 2010 was carried out with financial support from the SB RAS and RFBR:

1. SB RAS project collaboration No. 138 "Finding fundamental principles of the influence of activations on the regulation of interaction of solid metals and their compounds with melted metals to create functional materials of desired structure and properties".
2. RFBR grant No. 10-08-00945-a "Materials; phases and states with improved thermoelectric properties at ultrahigh compression."
3. RFBR grant No. 08-03-00738-a "Selective oxygen permeability of nanostructured nonstoichiometric perovskites."

Themes of works in 2010:

1. Investigation into high-temperature interaction processes in metals and alloys in the solid (Cu, Ni, and Co) and liquid (Sn, In, Bi, and their eutectic melts) states.
2. Investigation into the processes of contact melting and eutectic crystallization on the basis of two- and three-component systems between Sn, In, and Bi.
3. Investigation into the morphology of explosives as well as changes in their structure under static high pressure.
4. Studies of phase transformations in microporous silicates at high pressures and temperatures.
5. Investigation into the structure and physicochemical properties of fine-grained paracetamol in the process of production of frozen solutions in the acetone-water-paracetamol system via vacuum drying.
6. Study of metastable high-pressure phases in the glycine-water system.
7. Study of changes in the crystal structure of crystals based on bismuth telluride under a pressure of  $10^{20}$  GPa.

8. Study of the formation of the structural-phase composition of the Fe(Fe<sub>3</sub>C, Fe<sub>5</sub>SiC) SiO<sub>2</sub> nanocomposites in the course of mechanosynthesis.

9. Investigation into the structural transformations at cycling of electrode materials in the lithium-ion cells (LICs) by the method of *in situ* SR diffraction.

1. Investigation into the structural transformations at cycling of electrode materials in LICs by the method of *in situ* SR diffraction

In the course of cycling of LICs, different mechanisms of introducing/extraction of lithium ions to from the structure of the electrode materials, determining their electrochemical properties, are realized. Changes in the size of the particles, modification, etc. vary the mechanism of the processes. So, lithium iron phosphate (LiFePO<sub>4</sub>) is characterized by a biphasic mechanism (there are both the initial and final phases at each point of charge-discharge). The biphasic mechanism restricts the movement of the interface, which is a consequence of the low mutual solubility and slow migration of the charge carriers, which adversely affects the technical characteristics of LICs. Reduction in the size of the particles leads to an increase in the areas of formation of solid solutions. As shown by diffraction studies, in the course of charging the LICs, the two-phase mechanism is partially replaced by the single-phase one due to partial substitution of Mn<sup>2+</sup> for Fe<sup>2+</sup>.

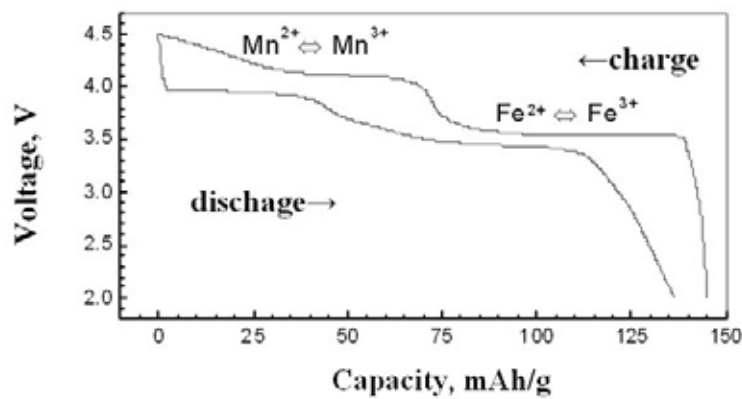


Fig.(6.1)18. Charge-discharge curve.

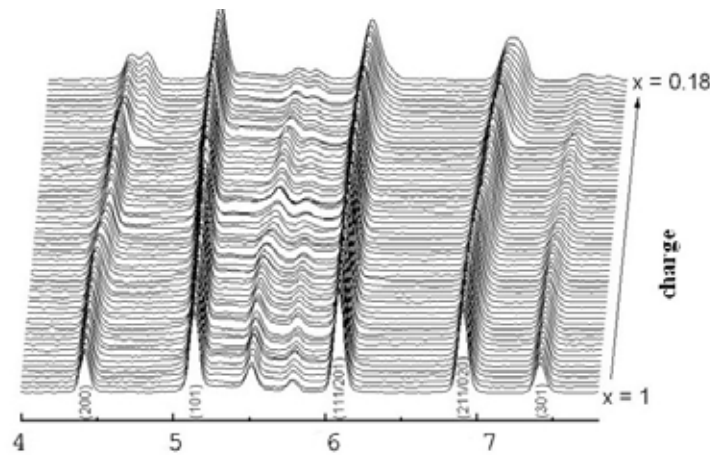


Fig.(6.1)19. Diffraction patterns obtained in the course of charging LICs.

2. Investigation into the contact melting and the eutectic crystallization and development of the technology of contact thermosetting melting with lead-free solders

Contact melting and eutectic crystallization have been used in engineering practice for a long time. Nevertheless, there is no consistent, predictive theory of these phenomena. It is obvious that processes occurring at the interface between the solid and liquid phases are reversible and hence they are different manifestations of the same phenomenon. Most of the research process of contact melting and especially eutectic solidification was conducted using various microscopic techniques on frozen samples. Diffraction studies are also mostly conducted either on frozen samples or on melts near the melting point. In so doing, the process of contact melting and eutectic solidification remained outside the experiment. Improvement

of the experimental techniques, especially development of high-intensity synchrotron radiation sources and two-coordinate detectors enabled *in situ* diffraction studies. Contact melting and subsequent eutectic solidification in the In-Sn and Bi-In systems were studied.

Fig.(6.1)20 presents fragments of diffraction patterns obtained at melting of crystallization in the Bi-In system.

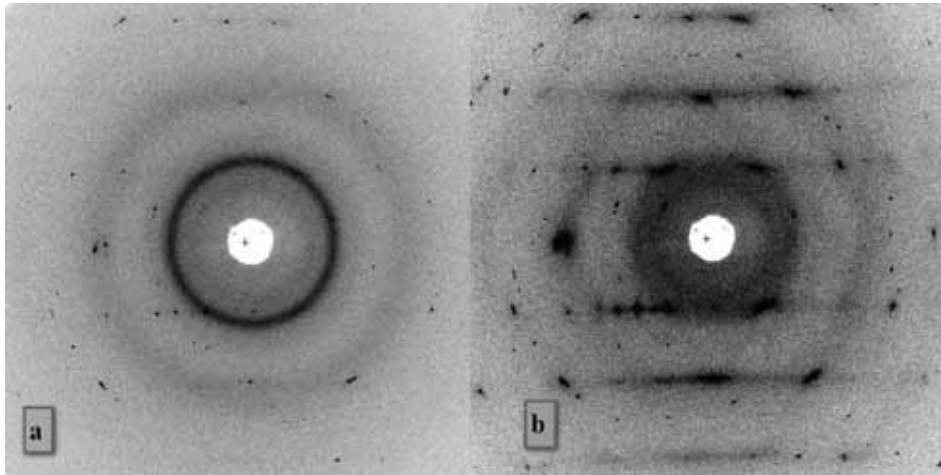


Fig.(6.1)20. Fragments of diffraction patterns obtained in the course of eutectic crystallization: (a) 5 minutes after the onset of crystallization; (b) 12 minutes after the onset of crystallization.

From the form of diffraction patterns we can conclude that a bicrystal formed in the crystallization zone. The phase of the indium in this crystal seems to be in the form of plates; and the phase of  $\text{BiIn}_2$ , in the form of needles or inclusions. Bragg reflections in the diffuse scattering bands indicate coherent boundaries between the phases.

From the results of research, one can see that eutectic alloys are natural composite materials, which differ in their physicochemical properties from other alloys. Using temperature-time exposure and chemical interaction with other substances, one can develop a technology of contact thermosetting soldering.

Replacing the traditional types of solders with leadless materials is not only an order of the day but also a requirement of numerous international committees on ecology. The In-Sn system is an eutectic-type system with an eutectic temperature of  $119^\circ\text{C}$ . Two intermetallic phases,  $\text{In}_3\text{Sn}$  and  $\text{InSn}_4$ , with wide homogeneity areas were revealed in it. When tin and indium are made to contact at temperatures above  $119^\circ\text{C}$ , the liquid phase forms in the contact zone (the melt points of indium and tin are  $156^\circ\text{C}$  and  $232^\circ\text{C}$ , respectively). Using coating of indium and tin with a thickness ratio of 1:4 on parts to connect, one can make a soldered joint at temperatures from  $120$  to  $150^\circ\text{C}$ . In this case, after a required exposure, unsoldering can be performed at temperatures above  $180^\circ\text{C}$ .

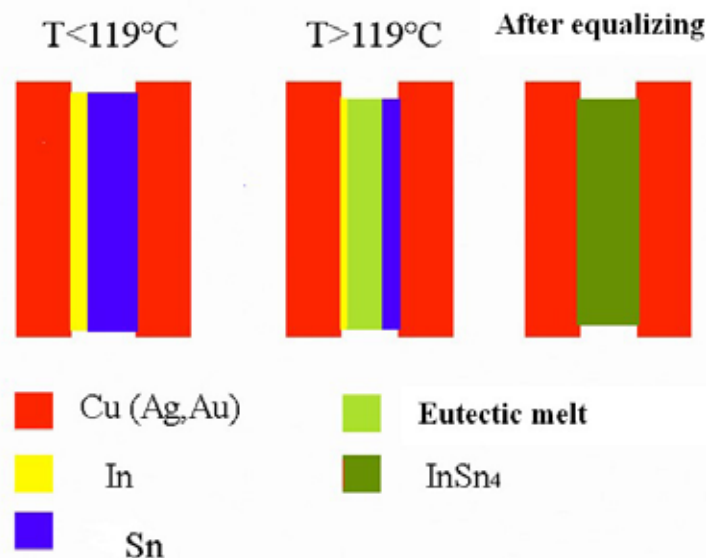


Fig.(6.1)21. Scheme of the contact thermosetting soldering using the In-Sn system.

It should be noted that soldering will be made only at the places of contact; no liquid phase forms at other places. In some cases, contact thermosetting soldering may be more feasible than wave soldering.

### **6.1.7 Station "X-ray Microscopy and Tomography"**

The station "X-ray Microscopy and Tomography" is intended for the study of the three-dimensional structure of samples with high spatial resolution.

Participating organizations:

- Budker Institute of Nuclear Physics SB RAS, Novosibirsk;
- Sobolev Institute of Geology and Mineralogy SB RAS, Novosibirsk;
- Lavrientiev Institute of Hydrodynamics SB RAS, Novosibirsk;
- the Institute of Chemical Kinetics and Combustion SB RAS, Novosibirsk;
- the Institute of Archaeology and Ethnography SB RAS, Novosibirsk.

Themes of works in 2010:

- Investigation into the morphology of natural diamonds by the method of X-ray topography.
- Study of growth dislocations in synthetic diamonds by the method of X-ray topography.
- Obtaining data on the three-dimensional structure of samples of explosives and propellants by the method of computer X-ray tomography (CXT) with high spatial resolution.
- Study of archaeological findings by the non-destructive method of CXT.
- Quality Control of X-ray patterns for LIGA technology.

The works were carried out under the following:

1. RFBR grant No. 09-05-00985-A "Zone-sectorial structure of diamonds from kimberlite deposits in Yakutia as reflecting the evolution of the formation conditions."
2. SB RAS interdisciplinary integration project No. 51 "The influence of environment on the morphology, actual structure and isotope composition of carbon in diamond".

Monochromatic X-rays with a wavelength  $\lambda = 1.13 \text{ \AA}$  extracted from the continuous SR spectrum with a monochromator based on single silicon crystal with the working plane [111] are used at the station. A collimator facing the sample cuts off spurious reflections of the monochromator and forms a beam with geometric dimensions of  $2 \times 2 \text{ mm}^2$ . Precision mechanics aligns a sample, which provides linear movement with an accuracy of  $1 \text{ }\mu\text{m}$  or better and angular travel with an accuracy of  $0.001^\circ$ . "Bragg magnifier" based on the increase in the linear dimensions of an X-ray beam reflected from crystals with an asymmetrical cut, is used for improvement of the spatial resolution of the images. The enlarged image is recorded by a highly sensitive X-ray detector on the basis of CCD matrix. The matrix ( $4008 \times 2670$ ) with a  $15.5 \times 15.5 \text{ }\mu\text{m}^2$  pixel size ensures detection of signal with a dynamic range of 16 bits, allowing high-quality images at a second-scale exposure.

Together with the Institute of Geology and Mineralogy SB RAS we continue investigating the morphology of natural diamonds from kimberlite pipes and placers of the Yakutsk diamond province. Using the method of X-ray topography (XT), we obtain information on defects due to disorders in the structure of the diamond crystal lattice. The possibilities of the topographic facility allow capturing images of diamond both in the passed beam and in radiation reflected at the Bragg angle (Fig.(6.1)22).

Extremely low absorption of X-rays in diamond due to the low atomic weight of carbon and selected operating wavelength makes it possible to obtain high-quality images of crystal structure defects in the transmitted radiation. When registering the passed radiation, we get a mixture of images caused by X-ray absorption in the crystal and intensity weakening due to the Bragg reflection (Fig.(6.1)23).

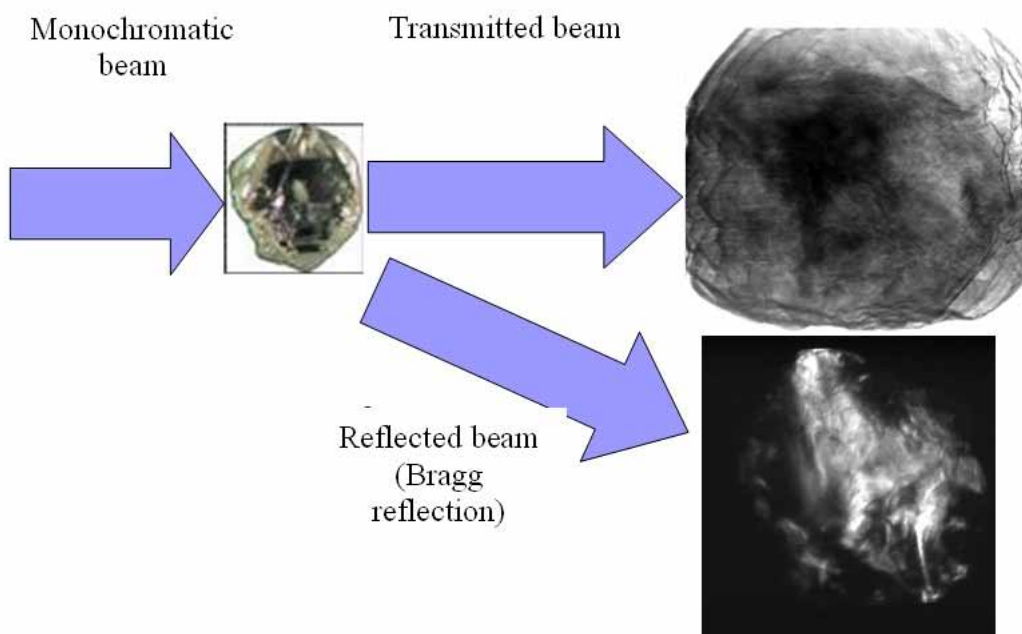


Fig.(6.1)22. Images of diamond in the passed beam and in radiation reflected at the Bragg angle.

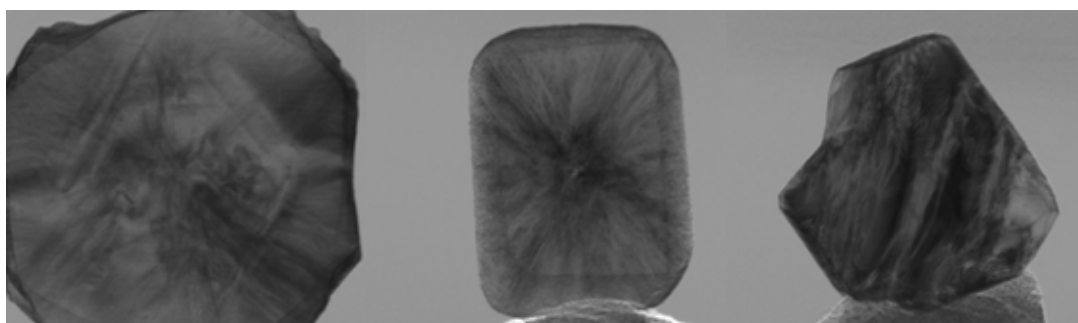


Fig.(6.1)23. Topographs of diamonds with different morphology, made in transmitted radiation.

In this case, we can well correlate the internal heterogeneity of the crystal lattice with the geometry of the crystal. However, for a more thorough characterization of the morphology of the crystal it may be necessary to obtain information not misrepresented by surface defects and the size of the crystal. In this case, registration in the reflected radiation makes it possible to record an image determined only by defects in the diamond crystal structure (Fig.(6.1)24).



Fig.(6.1)24. Topographs of diamond of different morphology made in reflected radiation.

It should be noted that recording in reflected radiation is associated with a number of difficulties arising from the alignment of the facility and takes quite a long time, unlike previous scheme, which requires a few seconds. Therefore, recording in the reflected beam is conducted primarily for unique patterns of interest.

Together with the group working at the station “LIGA technology and X-ray lithography” we conduct research on the characterization of X-ray patterns manufactured at our institute (Fig.(6.1)25).

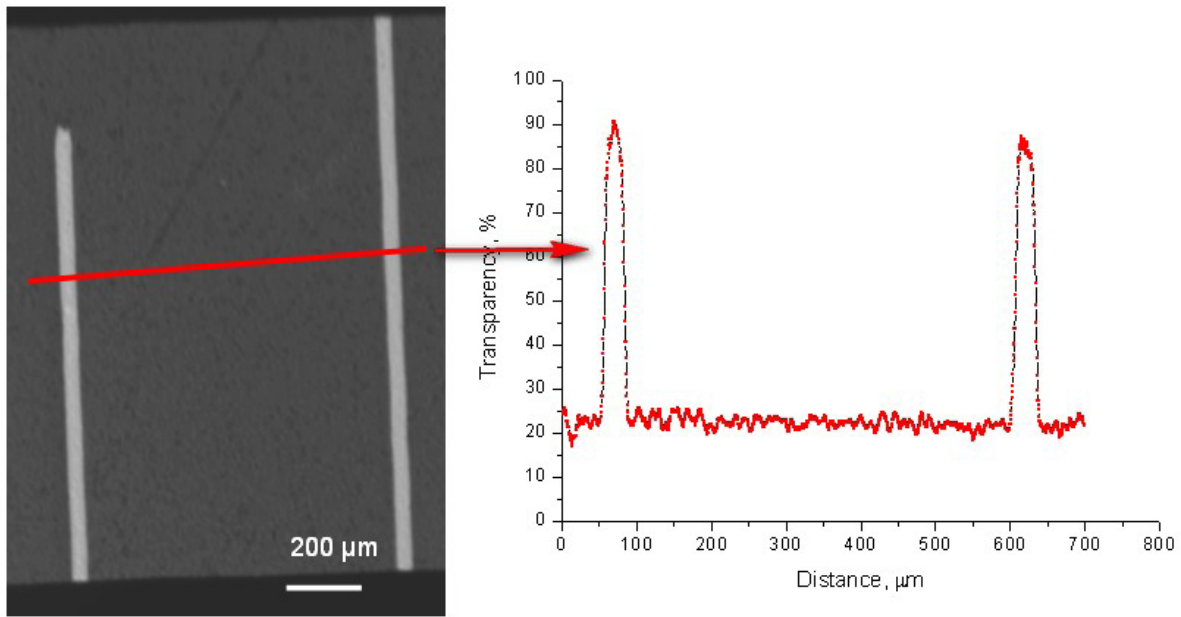


Fig.(6.1)25. Image of an X-ray pattern and profile of X-ray intensity along the line.

Study of the three-dimensional structure of energetic materials (EMs) using the method of computer X-ray tomography (CXT) allows assessing their manufacture quality from bulk density distribution in an objects to study. The presence of inhomogeneities and pores affects the rate of combustion and propagation of detonation front, which is an important parameter in the production of EMs.

Fig.(6.1)26 shows tomographic slices (3 μm thick) of EM specimens, obtained at different temperatures of crystallization.

These data clearly show that sample M1, made at +20° C, has a more porous structure in comparison with sample M2, made at a lower temperature.

Using the CXT, we explored the determination of the age of complexes containing timber of acceptable preservation. A variety of wooden objects (ornaments, harness decoration, weapons, utensils etc.) was accumulated in the course of archaeological research. Timber is often represented by small wooden articles rather than large samples from burials.

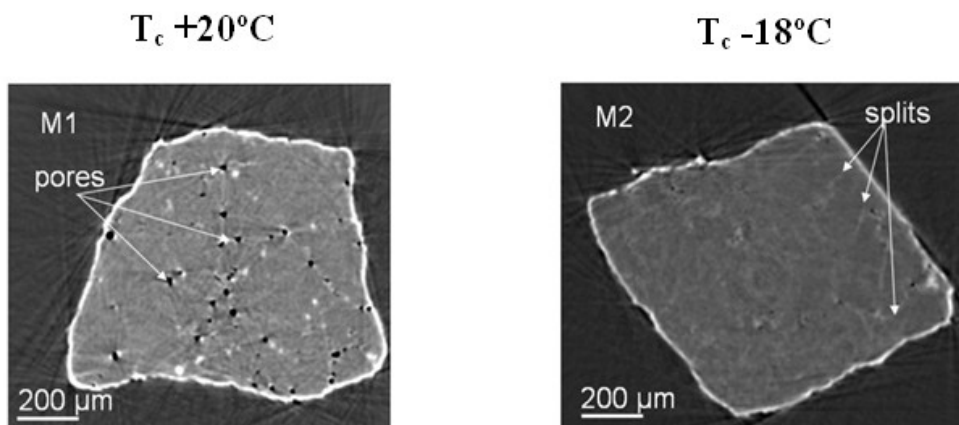


Fig.(6.1)26. EM samples based on the FTDO/DNP mixture, obtained at various temperatures of crystallization.

One of the main obstacles is the impossibility of investigating wooden articles by conventional methods, which are applicable in dendrochronology and first of all involve sampling in the form of transverse saw cuts or cores or preparing a plane and hence are associated with damaging the object of study. For obvious reasons, is impossible for archaeological objects due to their uniqueness and museum value.

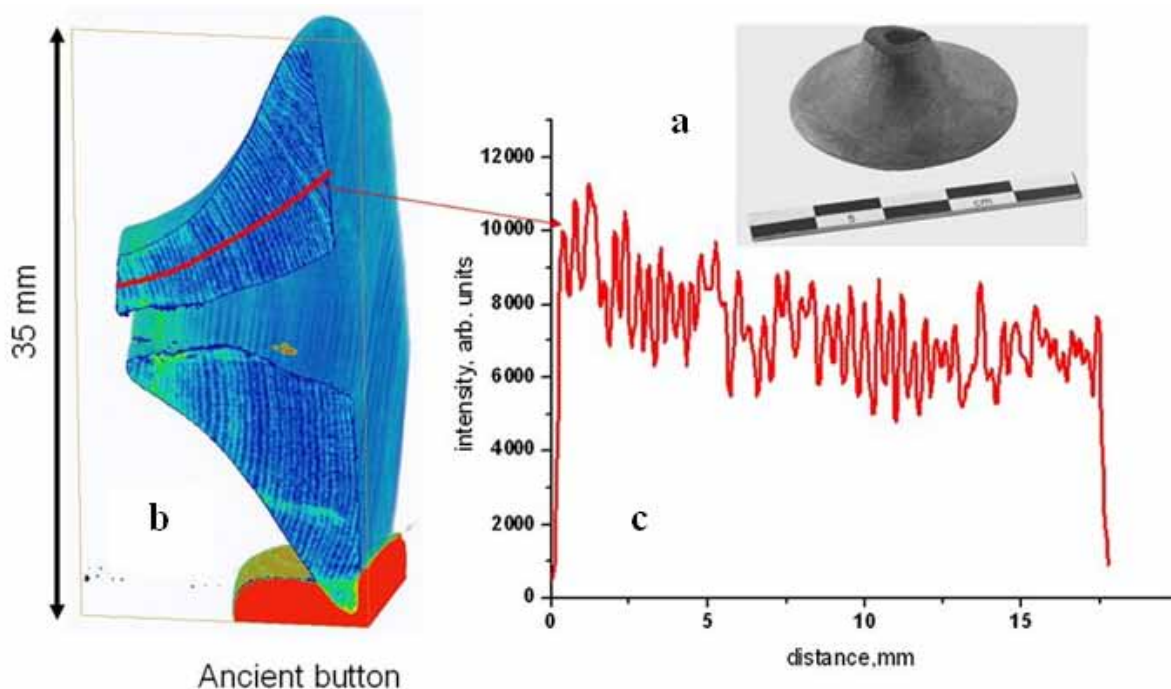


Fig.(6.1)27. Examination of a wooden article by the method of computer X-ray tomography: (a) general view of a quiver plate, (b) cross-section of the object with the radius of measurement, (c) density curve, reflecting the variability of the width of tree rings.

A three-dimensional image obtained by CXT allows making a virtual cut in an object in any desired plane (Fig.(6.1).27), including a cross-section, which is usually used to fix the width of tree rings. The available software makes it possible to measure the width of the rings and finally obtain data required for tree-ring analysis in their usual format - a series of numbers or a graphical curve. All further procedures with these data are then performed using already familiar tools of dendro-chronological research: individual series are compared with one another and then cross-dated by generalized tree-ring chronologies of monuments or prolonged absolute dendro-scales.

### 6.1.8 Station “Diffractive Movie”

The station is intended for the X-ray diffraction studies of structural and phase transformations in solids in the process of chemical reactions. After installation of the two-coordinate detector MarCCD, the station is also used for research by the method of diffractometry of mono-crystals. The application of a 2D detector makes it possible to study small amounts of substances as well as samples with a pronounced texture.

Participating organizations:

- Borekov Institute of Catalysis SB RAS, Novosibirsk;
- Nikolaev Institute of Inorganic Chemistry SB RAS, Novosibirsk;
- the Institute of Hydrocarbons Processing SB RAS, Omsk;
- the Institute of Solid State Chemistry and Mechanochemistry SB RAS, Novosibirsk.

Works in 2010 were carried out with financial support from SB RAS and RFBR:

1. SB RAS interdisciplinary integration project No. 13 “Development of the X-ray diffraction analysis of biologically important objects.”
2. RFBR grants 08-03-00335-a, 10-03-00451-a, and 08-03-00119-a.

Themes of works in 2010:

1. Development of the X-ray diffraction analysis of biologically important objects (the Institute of Catalysis SB RAS).
2. Study of formation of the phase composition of supported Pd and Ag catalysts prepared by the method of surface self-propagating thermosynthesis (the Institute of Hydrocarbons Processing SB RAS, Omsk)

3. Pd/ $\gamma$ -Al<sub>2</sub>O<sub>3</sub>/ glass fabric catalysts prepared by the method of surface self-propagating thermosynthesis in the reaction of selective hydrogenation of C<sub>2</sub>H<sub>2</sub> to C<sub>2</sub>H<sub>4</sub> (the Institute of Hydrocarbons Processing SB RAS, Omsk).

### 1. Supported catalysts

Activity of catalysts is defined by both their composition and the method of preparation; and their hydrodynamic properties depend on their geometry. The appearance of supports on the basis of glass fabrics (GF) and method of surface self-propagating thermosynthesis (SST) opens the possibility of obtaining samples with improved catalytic and hydrodynamic properties.

Unfortunately, *in situ* study of the dynamics of phase composition is not always possible at SST of catalysts. That is why a method was developed for determination of phase transitions, based on the rapid quenching of solid combustion front with subsequent scanning of the front region while the sample is moved under a beam of collimated synchrotron radiation.

Front of flameless combustion is an area of chemical, physical and physicochemical processes, which altogether provide the required heat release. The front consists of several zones, each having a certain extent: the zone of heating (ZH), where heat transfer and heating of the sample occur as well as partial-decomposition of the fuel additive; the main reaction zone (ZR); the zone of afterburning (ZA), where the chemical reactions continue, but they are no longer affecting the speed of the front; the zone of secondary physico-chemical transformations that define the composition and structure of the end products (ZST).

The purpose of this study is to investigate formation of the phase composition of the Pd/GF, Pd/Al<sub>2</sub>O<sub>3</sub>/GF, Ag/SiO<sub>2</sub>/GF and Ag/Al<sub>2</sub>O<sub>3</sub>/GF catalysts using the method of SR X-ray phase analysis.

KS-151-LA-grade GF, containing ~10% of ZrO<sub>2</sub>, and the same GF modified by  $\gamma$ -Al<sub>2</sub>O<sub>3</sub> (14% of the mass of the support) were used as supports for Pd catalysts. The reagents were Pd(NO<sub>3</sub>)<sub>2</sub> and citric acid or glucose. The content of Pd was 1% of the mass of the support.

A support of Ag-containing catalysts is an openwork-weaving silica glass fiber of the KS-11LA grade without special additives modified with SiO<sub>2</sub> and Al<sub>2</sub>O<sub>3</sub> oxides (10% of the mass of the support). During the preparation of the samples, the silver content varied (~ 7 to ~ 20% mass). In so doing, the Ag content per unit of surface area varied in the range of 0.01-0.03 g<sub>Ag</sub>/m<sup>2</sup>. The experiments were conducted with fragments of glass fiber (thread) fixed on a special holder. The scanning was performed with a step of 0.5-2.0 mm perpendicular to the front propagation. Signals were recorded by transmission. A point of registration was chosen and controlled with the goniometer "mardt" using a built-in camcorder. Diffraction patterns were registered with a two-coordinate detector MarCCD SX-165.

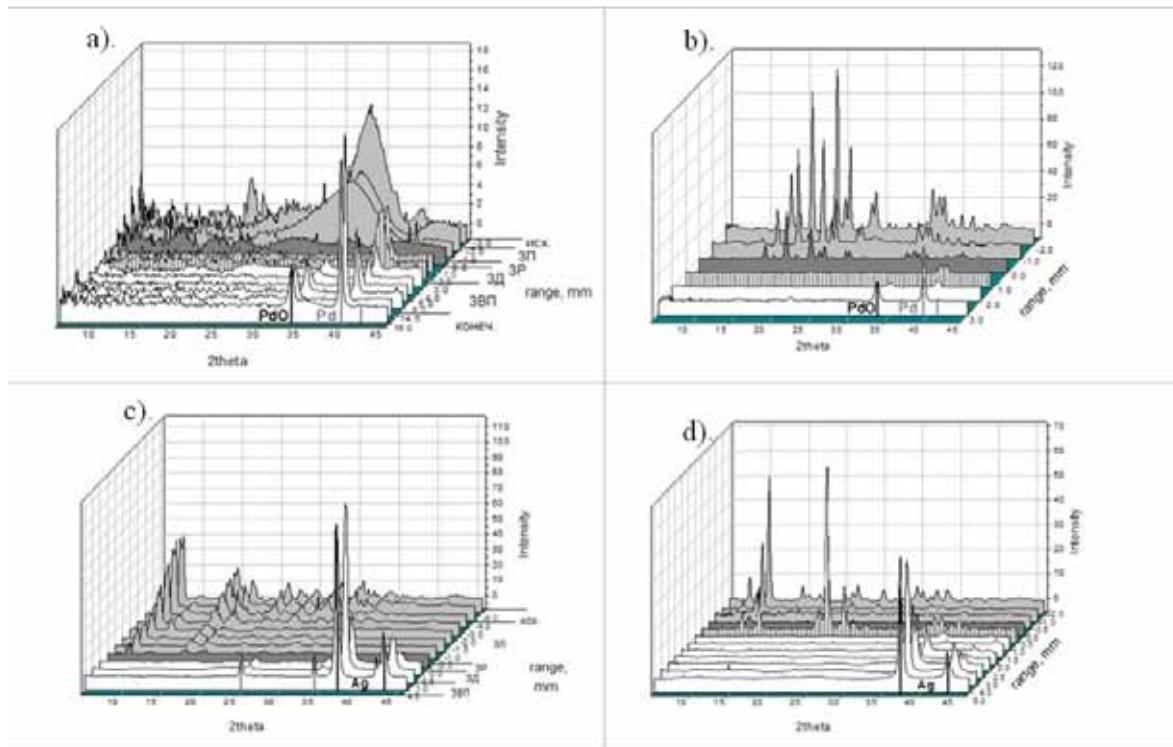


Fig.(6.1)28. shows a sequence of diffraction patterns for samples of Pd/GF(a, b), Ag/Al<sub>2</sub>O<sub>3</sub>/GF (c) and Ag/SiO<sub>2</sub>/GF (d).

The data allowed us to determine the length of the ZH, ZA and ZST, the phase composition in the ZA and ZST as well as the change in the size of the coherent-scattering region of the ZST phases. The corresponding areas of the front are indicated for the samples of Pd/GF (Fig.(6.2)28, a) and Ag/Al<sub>2</sub>O<sub>3</sub>/GF (Fig.(6.2)28, c). It was also found that for samples of Pd/GF the SST parameters depended on the nature of the fuel additive: for a sample where glucose was used the zone of secondary transformations is by order longer than for a sample with citric acid. For the samples of Pd/Al<sub>2</sub>O<sub>3</sub>/GF and Pd/Al<sub>2</sub>O<sub>3</sub>/GF the phases of PdO and Pd are not identified in the diffraction patterns, which is apparently associated with the very high dispersion of these phases. For the samples of Ag/SiO<sub>2</sub>/GF and Ag/Al<sub>2</sub>O<sub>3</sub>/GF, the diffraction patterns of the precursors are similar, suggesting that for them the precursors of the active ingredient are in the same form.

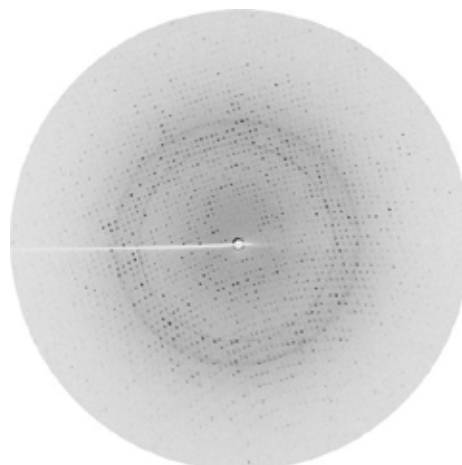
## 2. The first experiments with biological crystals

One of the challenges of modern crystallography is the determination of the spatial structure of both the initial proteins and their complexes with other proteins or molecules (receptors). It is necessary, for example, to reveal the mechanisms of action of drugs. Within the frameworks of the integration project, a unit consisting of the two-coordinate detector MarCCD SX-165 on the goniometer mardtb and cryogenic attachment was mounted on beamline 5b (Fig.(6.2)29). Biological objects are studied at 100 K, which is necessary to ensure their stability. In addition, low temperatures reduce the amplitude of thermal vibrations, which leads to an increase in the spatial resolution at structure reconstruction.

The technique is currently elaborated on test crystals. Fig.(6.2)29 presents a diffraction pattern from crystals of beta-galaktidazy. We are now mastering the software and processing the data.



a)



b)

Fig.(6.1)29. Photograph of the experimental station a) and a diffraction pattern from crystals of beta-galaktidazy.

### 6.1.9 Station “EXAFS Spectroscopy”

The station is intended for the study of the structure of the local environment of atoms of a selected chemical element (the coordination number and interatomic distance). Depending on the methodology, the object of analysis is the volume, surface or surface layers.

Over 200 samples were investigated and more than 500 spectra were recorded at the station EXAFS spectroscopy in 2010. More than 50 works were published and accepted for publication, including articles in refereed journals (over 20), conference proceedings and abstracts of conferences.

Participating organizations:

- the Institute of Catalysis SB RAS;
- the Institute of Inorganic Chemistry of SB RAS;
- the Institute of Chemical Physics RAS, Moscow;
- the IGIC RAS, Moscow;
- Rostov State University;

- the IOC RAS, Moscow;
- the Institute of Petrochemical Synthesis RAS, Moscow;
- the Institute of Hydrocarbons Processing SB RAS (IHP SB RAS);
- Saratov State University;
- the Institute of Chemical Kinetics and Combustion;
- the ISSCM SB RAS;
- the Limnological Institute SB RAS, Irkutsk;
- Hahn-Meitner-Institut, Berlin, Germany;
- the Institute for Semiconductor Physics SB RAS;
- Max-Planck-Institut für Kohlenforschung, Germany;
- the Institute of High Temperature Processes & Chemical Engineering, Patras, Greece;
- the Institute of Chemistry: Humboldt University, Berlin, Germany;
- Ohldeburg University, Ohldeburg, Germany;
- the Institute of Coal and Coal Chemistry, Kemerovo, Russia;
- Frumkin Institute of Electrochemistry, Moscow, Russia;
- the Institute of Geology and Mineralogy SB RAS;
- Institute of Metal Physics, UB RAS, Ekaterinburg;
- Åbo Akademi University, Turku, Finland;
- University of Oulu, Oulu, Finland;
- Udmurt State University, Izhevsk, Russia;
- the Physico-Technical Institute UB RAS, Izhevsk;
- Centro de Nanociencias y Nanotecnología, UNAM, Ensenada, BC, Mexico, Mexico;
- Instituto de Ciencia de Materiales de Sevilla, Spain;
- Centro Mixto CSIC-Universidad de Sevilla, Spain.

Works in 2010 were carried out with the support of the following projects

RFBR (08-03-00861a), RFBR (09-03-00369a), RFBR (09-03-00346a), RFBR (09-03-00780a), RFBR (08-02-00404a) Research (08-03-01016a), RFBR (08-03-00823a), RFBR (09-03-90424-Ukr\_f\_a) Research (09-03-00089a), RFBR (09-03-00133a), RFBR (09-03-00328a), RFBR (AF-080391758a), RFBR (08-03-92502-NTsNILa), FASI (No. 02.513.11.3203), TOTAL, RFBR (09-03-00514a), the Presidium of RAS (20, 21, 27), Research (09-05-98019a), RFBR (08-02-00404a), RFBR (08-03-00603a), RFBR (09-03-00780a), RFBR (09-03-00346a), RFBR (09-03-00540a), RFBR (08-03-00335a), RFBR (09-03-01013a), DGAPA-PAPIIT - IN 1207063.

The main directions and summary results of 2010:

*Development of methods for studying complex ultra-diluted and poly-component nanosystems.*

The possibilities of the method of fluorescence XAFS-spectroscopy using a new multi-element detection system for the study of complex nanoscale systems were shown. Energy-resolved registration of XAFS spectra by the fluorescence yield makes it possible to study samples of extremely low concentration (less than 0.1%) and nanometer-scale deposited system. The first results of the use of the detector and software for studying the hetero-metal nanostructured catalysts, geological samples, thin films and submonolayer coatings were obtained.

*Study of model mono- and bimetallic catalysts for the transformation of industrially important substrates (methane and ethylene)*

We investigated the genesis and structural features of the formation of the active ingredient for model bimetallic Pd-Me (Me = Co, Ce, Zn) catalytic nanosystems for methane reforming, deposited on oxide supports (membranes) via a complex of physical and chemical methods using synchrotron radiation (XAFS, XRD, XPS). The synthesis of palladium-containing catalysts was carried out by unorthodox methods based on mono- and bimetallic acetate and polycarboxylate metal complexes, at varying the processing conditions and using oxide supports of different nature. Possible models for structural stabilization of the palladium nanophase for bimetallic catalysts compared to monometallic analogues are discussed in detail.

XAFS spectroscopy, X-ray anomalous scattering and RFA were used for the comprehensive study of the genesis and structural features of model copper-nickel- $\text{Al}_2\text{O}_3$  catalyst in the process of decomposition of ethylene in the presence of ammonia. It was found that decomposition of ethylene, in this case, goes through formation of a complex nanophase "NiCuxCyNz". The prospects of application of this catalyst to

the synthesis of nitrogen-containing carbon nanomaterials with desired characteristics were shown.

*Studies of nanocomposite thin films and spatially correlated nanostructures based on semiconductor compounds of the Ge isoelectronic series*

A study of germanium thin films and nanostructures stabilized on various smooth and porous substrates ( $\text{SiO}_2$ , Si,  $\text{Al}_2\text{O}_3$ , etc.) was carried out. The samples were prepared by thermal evaporation of powder of the material in ultrahigh vacuum, which ensured high chemical purity of the samples in a wide range of temperatures of condensation. AFM, TEM, XRF-SR, and EXAFS studies of the surface morphology and local atomic structure of germanium films and nanostructures were performed. It was shown that continuous thin films have a mixed amorphous-nanocrystalline structure, whereas filamentous germanium nanostructures consist mainly of small amorphous clusters. It was found that the percentages of the amorphous and crystalline phases depend on the temperature of condensation. We found that the dependence of grain size for samples obtained at a condensation temperature of  $100^\circ\text{C}$  does not quite correspond to a classical linear relationship.

Methods of EXAFS, X-ray diffraction on synchrotron radiation and SEM were used for the study of the ZnS and ZnSe nanostructures created by depositing the material on porous films of anodic alumina. The temperature of the matrix during the deposition was  $0\text{--}150^\circ\text{C}$ . From a comprehensive analysis of data it was revealed that the nanostructures are composed of a mixture of wurtzite and sphalerite phases of the material, but a dominating growth occurs in the crystallographic direction (111) of the structure of the B3 type (sphalerite). With increasing pore diameter there was observed a growth of nanostructures in the form of "rings", which indicates a possible mechanism of filling the pores of the matrix from the wall to the center.

*Complex studies of low-percentage (from ~ 1%) new-generation nano-structured catalysts based on noble metals (Pt, Au, and Pd)*

Surface stabilized forms of Pt in low-percentage monodisperse platinum catalysts deposited on oxide supports of different nature (carbon,  $\text{Al}_2\text{O}_3$ ,  $\text{SiO}_2$ , and  $\text{TiO}_2$ ) were investigated by the methods of XAFS, XPS, and HRTEM. Currently, the supported platinum catalyst systems are widely used in the redox processes involving CO and/or hydrocarbons. It is obvious that reliable information on the active component and stabilization of its various surface forms will make it possible to optimize the methods of preparation and activation of catalysts with specific structural and functional characteristics, which would make the catalytic system more efficient. Supported monodisperse catalysts were prepared from non-chloride precursors via dry or wet impregnation of oxide supports. Control and regulation of the size of particles of the deposited metal were provided by pre-treatment of the supports and varied composition of the impregnating solutions. The charge state of the active component and the surface elemental composition of the catalysts were studied by the XPS method; the morphology and size of nanoparticles of platinum were defined from HRTEM data. XAFS was applied to the study of the structure of the local environment and the state of platinum in the samples. A technique was suggested for estimating the phase composition subject to the nano-size effects and changes in the oxidation of the metal active component from XAFS, XPS and TEM data. The effect of the support character on the morphology and phase composition of nanoparticles of the active ingredients, which are fine defective oxide or multi-phase metal-oxide systems, was shown.

A study of model low-gold catalyst systems promising for oxidation of CO and methane was carried out. The catalysts were prepared by Au deposition on nanoscale mixed oxides of aluminum, cerium and zirconium, prepared by the sol-gel method from organometallic compounds of these metals. Analysis of data obtained by a complex of the methods of XANES, EXAFS, HRTEM, ESDR, and XPS revealed that there might be various forms of stabilization of gold on the surface of the support, depending on the type of modifier and the sample history. It was shown that reduction in hydrogen at temperatures of  $150\text{--}200^\circ\text{C}$  does not lead to a significant contribution of Au(1+) ions and clusters of metallic gold. Apparently, practically all the gold in the initial samples and those reconstructed in the mild conditions is in the form of Au(3+) ions, localized on the surface of the support in a slightly distorted octahedral oxygen coordination. A further increase in the reduction temperature to  $400^\circ\text{C}$  leads to formation of metallic gold nanoparticles of about 1-3 nm.

An study of model low-percentage (less than ~ 0.5%) Pd/ $\text{Al}_2\text{O}_3$  catalysts was performed by the methods of XAFS and EPR. Currently, these catalysts are of considerable interest for neutralization of car exhaust and industrial emissions of gases. Using XANES it was revealed that palladium in the samples is mainly in the form of Pd(2+) ions in the nearest square-planar oxygen environment. No metallic phase of

Pd<sup>0</sup> was found within the accuracy of the method. EXAFS was used in a detailed study of the local structure peculiarities of the active component for samples with different prehistory. The possibility of purposeful variation of the state of oxide palladium nanostructures formed on the surface of Al<sub>2</sub>O<sub>3</sub>, from atomically dispersed to PdO nanoparticles, was shown and possible options for their structural models were considered. The EPR method showed the important role of donor centers in Al<sub>2</sub>O<sub>3</sub> surface in the stabilization of atomically dispersed ionic forms of palladium.

*Studies of promising catalysts for processing products of biomass fermentation into biofuel components*

A study of the state of metals and their local environment was carried out by the method of XAFS spectroscopy of promising catalytic nanosystems W-Re/Al<sub>2</sub>O<sub>3</sub> and Pd-Zn/Al<sub>2</sub>O<sub>3</sub>, which are used in production of fractions of alkanes and olefins C<sub>4</sub>-C<sub>12+</sub> – components of fuels – from biomass fermentation products. Considerable attention has been paid recently to the search for alternative, high-efficiency ways of development of the energy sector by means of renewable resources. Processing of renewable biomass energy may become one of the ways. A number of alcohols (ethanol, butanol, isopentanol, etc.), which are products of fermentation of biomass, can be components of fuels, both in pure form and after catalytic processing, which provides more effective and quality fuel components. Initial samples of catalysts were prepared by the sol-gel method based on mono- and bi-metal oxymethylates and carboxylates of metals of groups II-VII on the oxide support of  $\gamma$ -Al<sub>2</sub>O<sub>3</sub>. For all the systems under study there is a significant dispersion of the active component on the support surface. During the formation of the Pd-Zn system there appear surface mixed oxides ZnO-Al<sub>2</sub>O<sub>3</sub>, whereas Pd is predominantly in the form of nanoparticles of the oxide PdO, the size of which depends on the concentration and presence of the second Me. A strong interaction of the active ingredient with the support Al<sub>2</sub>O<sub>3</sub>, with the formation of distorted structures (WO<sub>x</sub>, W-O-Al, ReO<sub>y</sub>, (ReO<sub>3</sub>)<sub>ads</sub>-O-Al), was shown for the W-Re system. It was found that the local environment of the catalysts derived from bimetallic precursors has some differences from that in the case of samples synthesized based on mono-compounds. The genesis of the investigated nanosystems was described in detail; the correlation of their catalytic properties and structure was shown.

*Comprehensive study of supported gold catalysts used for fine organic chemicals and environmental catalysis*

The methods of EXAFS, XANES, TEM, EDX, and XPS were used for a comprehensive study of low-gold catalytic nanosystems deposited on alumina. A detailed study of the nature of various forms of gold stabilization is necessary to develop new efficient catalysts for various applications. These nanosystems are promising for industrial-important processes of fine organic synthesis and environmental catalysis –oxidation of secondary alcohols and CO. The synthesis of the catalysts was carried out with various methods of preparation (sol-gel, ion exchange, and impregnation), calcination temperature, and activation and modification of the support. It was found that the active ingredient consists essentially of a metal defective nanophase Au<sup>0</sup>. A correlation between the size and morphological and structural features of the gold nanoparticles and catalytic activity in selective oxidation of secondary alcohols was found.

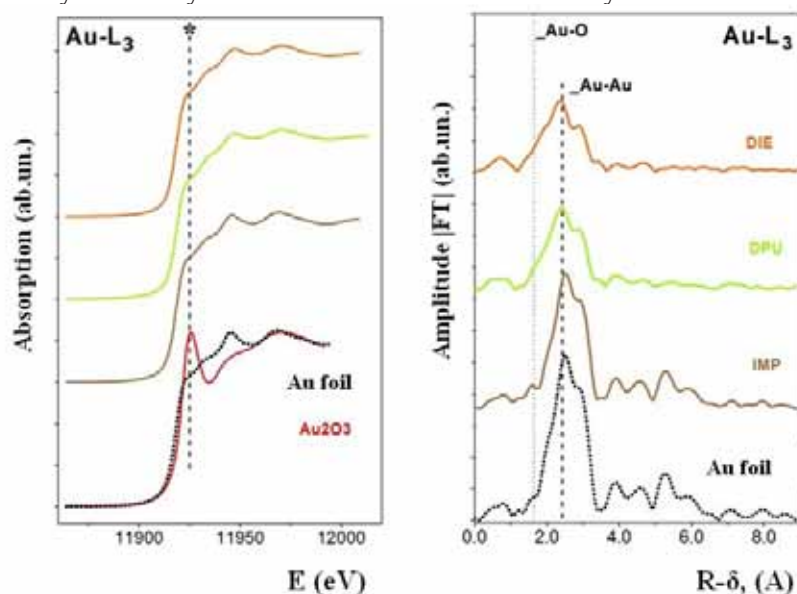


Fig.(6.1)30. XANES spectra (Au-L<sub>3</sub> edge; \* indicates the white line) and atomic radial distribution (ARD) functions of the local environment of gold for these samples and frames of reference.

### 6.1.10 Application of a 9-channel SCD to fluorescent XAFS-spectroscopy

For more than 20 years users of the SCSR have successfully registered XAFS spectra with the system for fluorescence signal detection, which cuts off the signal of elastically/inelastically scattered photons with the Z-1/Z-2 filter. However, in this case is impossible to investigate nanoscale systems of a rather complex elemental composition and low content of an element to study ( $\sim 0.5\%$  or less). For nanosystems including closely spaced chemical elements and/or containing a “heavy matrix” as well as ultradiluted samples it is necessary to use a detector with a sufficient energy resolution to separate the fluorescence signal namely of an element to study.

For a comprehensive solution to this problem, works on the commissioning of a unique 9-element detector made by Canberra (Fig.(6.1).31) were carried out at the station for EXAFS spectroscopy (beamline 8).

For the sake of better measurement parameters, we solved the problem of matching the detector with the fast digital spectrometric channel made by XIA. A software system was developed, allowing tuning the detection system and recording fluorescence XAFS spectra in the counting mode.

Studies of test samples were carried out for evaluation of the method of fluorescence XAFS-spectroscopy using the new detection system. The prospects of this approach were shown; the first results on the use of the detector and software to study supported catalysts of complex composition, ultra-diluted systems and geological samples were obtained.

Systems that were studied:

1)  $\sim 0.1$ - $0.2\%$  Pd model test catalysts supported by a “heavy Ce-Zr matrix” (cleaning of gas emissions). The prospects of the approach were shown; new information on the localization of Pd clusters on  $\text{CeO}_2$  was obtained (Fig.(6.1)32 and Fig. (6.1).33).

2) Model test low-percentage  $\text{Pt}/\text{Al}_2\text{O}_3$  samples. The possibility of obtaining reliable data on the local structure in diluted systems containing not more than  $\sim 0.05\%$  of an element under study was shown on the example of this nanosystem (Fig.(6.1)34 and Fig. (6.1)35).

3) A preliminary study of geologic samples (a conglomeration of bacteria and fungi that accumulate compounds of germanium) from geothermal sources (Lake Baykal,  $\sim 50$  ppm of Ge) was carried out. The prospects of the approach were shown; new data on the immediate environment of Ge were obtained (Fig. (6.1)36.).



Fig.(6.1)31. 9-element detector made by Canberra on beamline 8 (the EXAFS spectroscopy station).

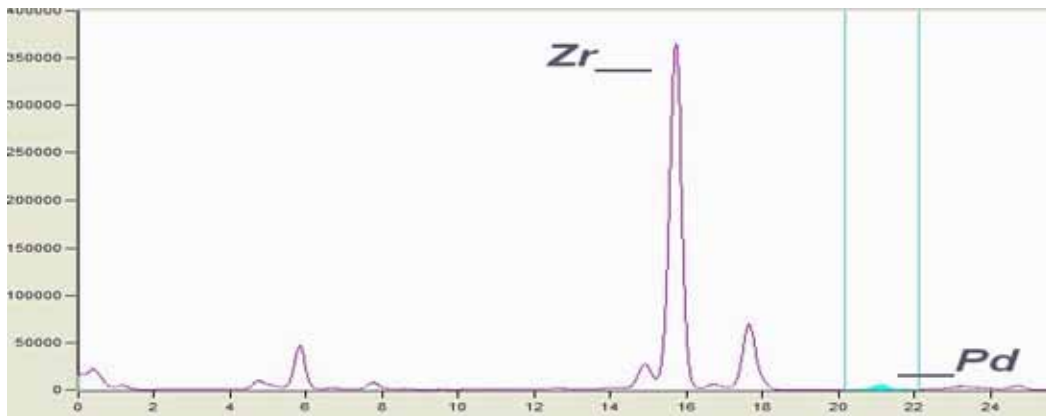


Fig.(6.1)32. Energy spectrum for the nanosystem of  $\sim 0.2$  Pd – 20% Ce-ZrO<sub>x</sub>/Al<sub>2</sub>O<sub>3</sub>.

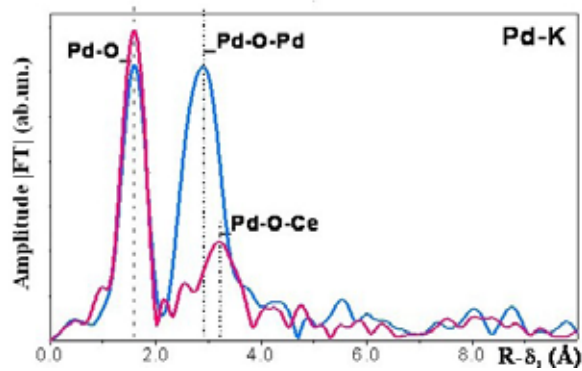


Fig.(6.1)33. Curves of atomic radial distribution in the local environment of palladium for the samples of  $\sim 0.2$  Pd-20%Ce-ZrO<sub>x</sub>/Al<sub>2</sub>O<sub>3</sub> and  $\sim 1\%$  Pd/Al<sub>2</sub>O<sub>3</sub> (frame of reference).

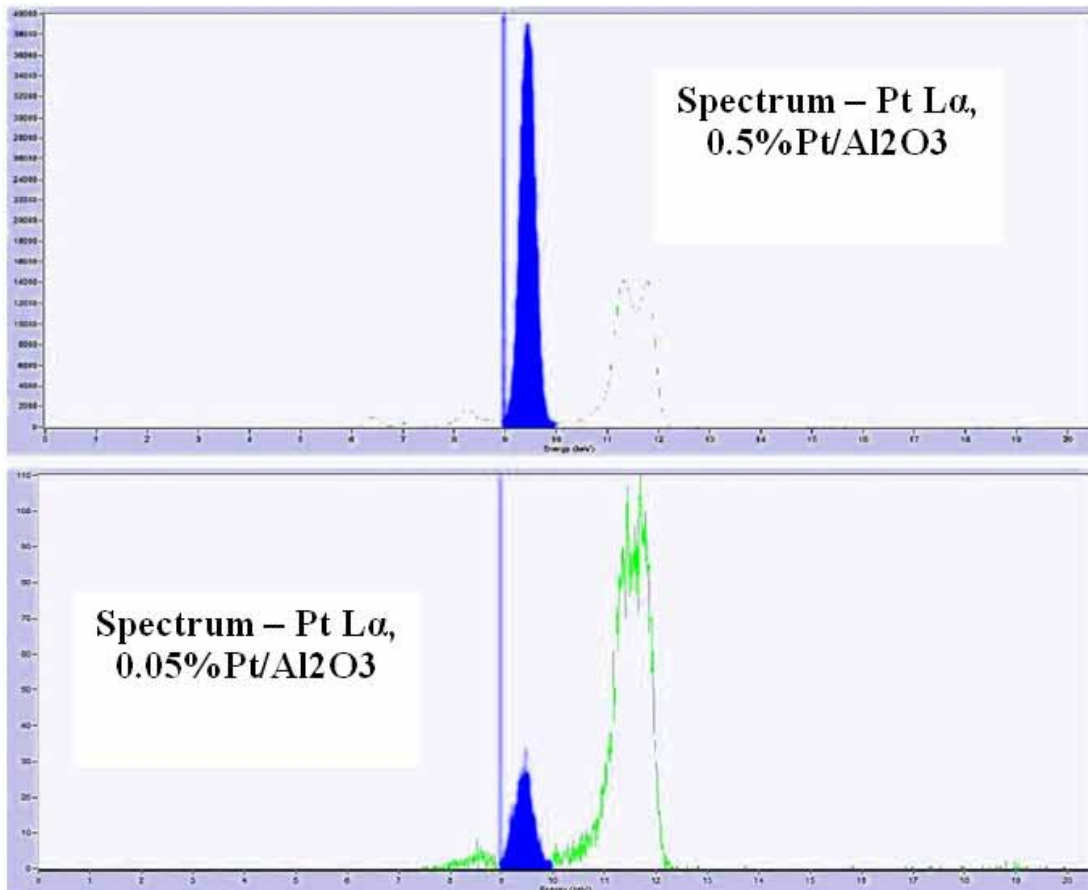


Fig.(6.1)34. Energy spectrum for the samples of  $\sim 0.5\%$  Pt/Al<sub>2</sub>O<sub>3</sub> and  $\sim 0.05\%$  Pt/Al<sub>2</sub>O<sub>3</sub>.

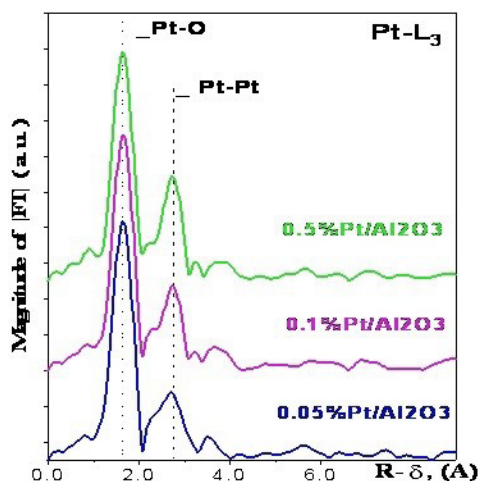


Fig.(6.1)35. Curves of atomic radial distribution in the local environment of platinum for the studied model test platinum samples.

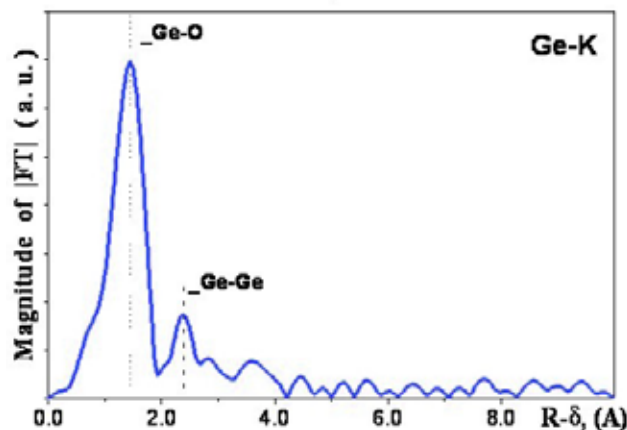


Fig.(6.1)36. Curves of atomic radial distribution in the local environment of germanium for the studied geologic samples (a conglomeration of bacteria and fungi, which accumulate germanium compounds) from geothermal sources (Lake Baykal, ~50 ppm of Ge).

## 6.2 Works on SR beams from VEPP-4M

### 6.2.1 Station “Cosmos”

The station is intended for metrology in the soft X-ray and VUV spectral ranges (10-1000 eV). The station is located in the SR bunker of VEPP-4 and receives radiation from bending magnet 3 in the northern inset of VEPP-4M (extraction beamline 10).

Participating organizations:

- Russian Federal Nuclear Center - All-Russian Research Institute of Experimental Physics, Sarov;
- Russian Federal Nuclear Center - Zababakhin All-Russian
- Research Institute of Technical Physics (VNIITF), Snezhinsk;
- Lebedev Physical Institute, RAS, Moscow;
- Ioffe Physico-Technical Institute named, St. Petersburg;
- Federal State Unitary Enterprise, Vavilov SOI, St. Petersburg.

Contract works on the calibration of silicon photodiodes in the spectral range of 100-1000 eV were carried out at the station for VNIITF, Snezhinsk, in 2010.

Examples of works in 2010:

#### 1. Building a model of the sensitivity function for a silicon photodiode

Since the 1990s, the development of the technology of manufacturing of silicon photodiode detectors has made it possible to create detectors of acceptable radiometric quality for the VUV and soft X-ray ranges. Commercial availability, temporal stability, sufficiently radiation resistance, and easiness of handling made these detectors the most convenient devices for detecting radiation in the soft X-ray spectral range. At photon energies of 100 - 1000 eV, however, the spectral sensitivity of the detectors requires regular calibration since it is affected by numerous factors – from the method of manufacturing of the detector to the thin films appearing on the receiving window during the operation. Calibration of the detectors in the soft X-ray range is a fairly complex task, requiring serious hardware and methodological support.

For this purpose, a technique was developed for construction of the analytic sensitivity function of a semiconductor detector from a set of calibration points. For objective reasons, any detector can be calibrated only from a finite number of points of the energy spectrum. Construction of an analytic function allows correct interpolation between the experimental points. The formula is based on a physical model of the detector, which takes into account its structure and manufacturing technology. A silicon photodiode calibrated at the German National Metrology Centre PTB is used as a reference detector at the station "Cosmos". The model sensitivity function of the diode is represented in the following parametric form:

$$S = \frac{1}{w} \exp\left(-\frac{d_c}{\lambda_c} - \frac{d_{SiO_2}}{\lambda_{SiO_2}} - \frac{d_B}{\lambda_B}\right) \left[ \exp\left(-\frac{d_{Si}}{\lambda_{Si}}\right) \left(1 - \exp\left(-\frac{d_{Si}}{\lambda_{Si}}\right)\right) + \sigma_s \left(1 - \exp\left(-\frac{d_{Si}}{\lambda_{Si}}\right)\right) \right]$$

where  $S$  is the sensitivity of the detector;  $w$  is the energy of formation of electron-hole pair in silicon (3.6 eV);  $d_i$  and  $\sigma_s$  are parameters by which the model is optimized to the experimental results;  $\lambda_c$ ,  $\lambda_{SiO_2}$ ,  $\lambda_B$ , and  $\lambda_{Si}$  are tabulated values of the optical constants of materials in the detector. A model function of this form describes the calibration data with an accuracy of 1% or better and allows a continuous interpolation of calibration data in the spectral region of 50-1800 eV:

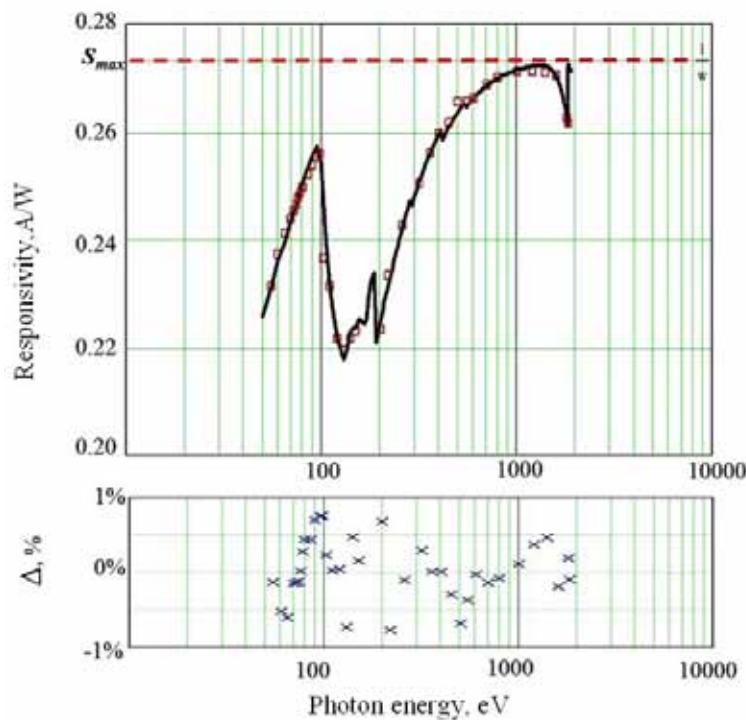


Fig.(6.2)1. *Upper graph*: experimental calibration data of the reference detector (squares) and approximation of the data (solid line). The horizontal dotted line marks the level of maximum achievable sensitivity for the silicon photodiode ( $S_{max}$ ). *Lower graph*: difference between the calibration data and the function approximation, %. All data are in the error corridor of  $\pm 1\%$ .

## 2.Exploration of the band characteristic of the secondary electron multiplier SEM-6

The band characteristic (distribution of the efficiency of the detector over the area of its entrance window) is a very important operating characteristic. The measurements were carried out via two-coordinate movement of the detector relative to the probing monochromatic beam. The transverse size of the probe beam was  $200 \times 200 \mu m^2$ . The measurements were performed for photon energies of 268 eV and two different supply voltages of the SEM-6 dynode system.

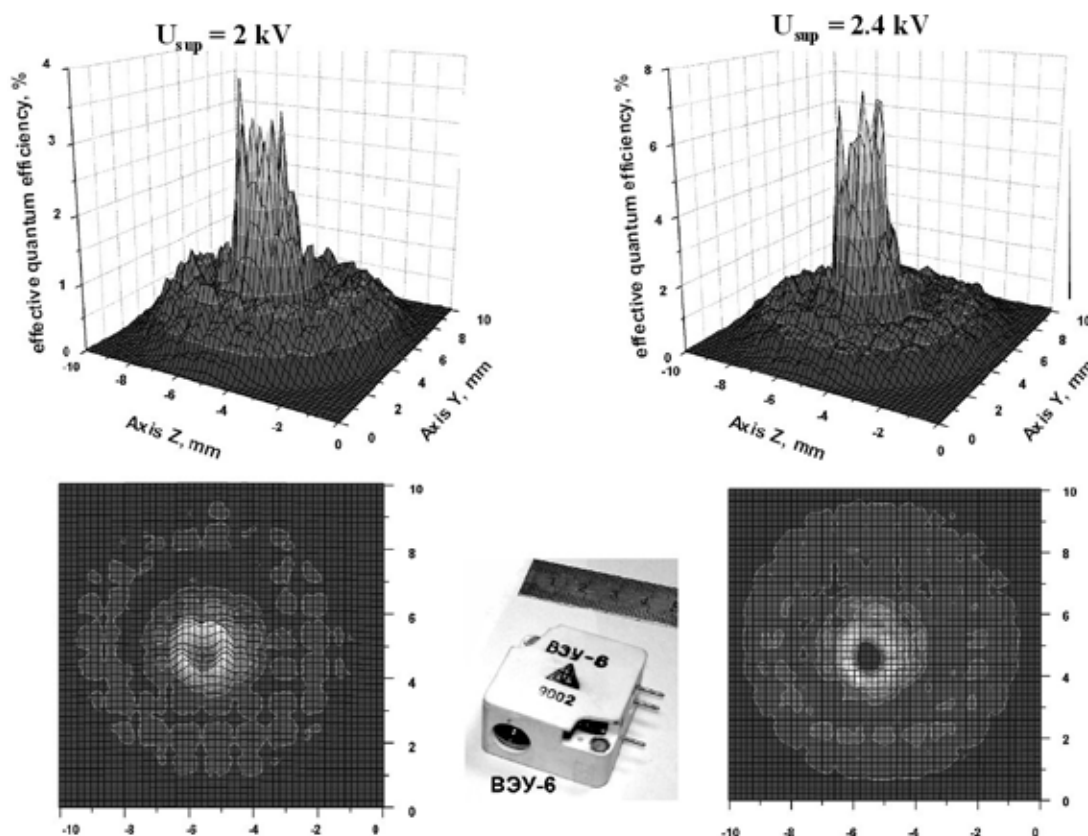


Fig.(6.2)2. Band characteristics of SEM-6 at a photon energy of 268 eV and dynode supply voltages of 2kV and 2.4 kV.

A strong heterogeneity of the band characteristic of the multiplier can be seen. It is funnel-shaped, with a sharp increase from the periphery to the center of the detector window. At the center of the window, on a site of about 1 mm<sup>2</sup>, again a sharp dip of sensitivity to almost zero can be seen. When the supply voltage of the dynode system increases, the overall detection efficiency grows, as well as heterogeneity. We should expect a strong dependence of the SEM-6 band characteristic on the angle of photon incidence. Thus, it would be reasonable to perform an absolute calibration of the SEM-6 only as part of a complete measuring device with rigidly fixed collimators of radiation, providing reproducibility of the measurement geometry.

### 3. Manufacturing of X-ray filters

A monochromat of high metrological quality is made at station “Cosmos” using loose-hanging thin-film filters. A filter is usually a thin (0.2 to 5 microns) film of metal glued on a special frame. Since such a filter is very fragile and ephemeral structure, there arose the problem of manufacturing such filters in-house. A technique of making single-component filters of several metals (Cu, Ti, Al, and Mo) 0.3 to 1.5 m thick with a working area of 5x10 mm<sup>2</sup> was elaborated in 2010. The metal film is sputtered on a specially prepared substrate (with a layer of carbon as an adhesive or a water-soluble salt on the surface) by means of the electron-beam or magnetron method, with subsequent separation and attaching to the frame.

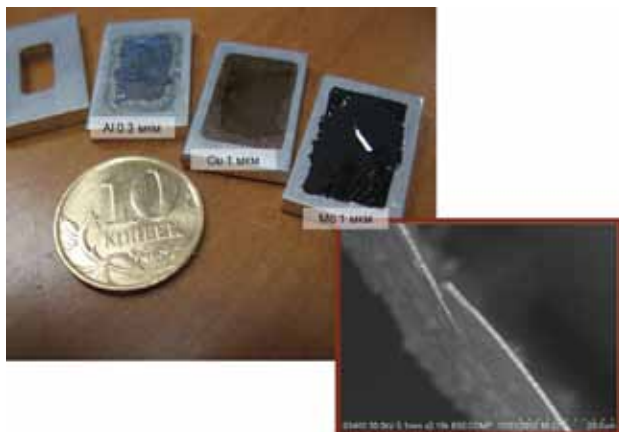


Fig.(6.2)3. General view of the filters and a micrograph of a cleavage of Mo film. The thickness is approximately 1 micron. Work is underway to improve the homogeneity and mechanical strength of the molybdenum filters.

The existing sputtering facility is being upgraded now, which will result in the opportunity to produce multi-layered loose-hanging films. The technique of making multi-layer films will result in filters with more diversified spectral properties and improved mechanical parameters. Increase in the mechanical strength is expected to allow manufacturing of filters to 0.2  $\mu\text{m}$  thick with an aperture of up to 30 mm.

## **6.3 Work with beams of terahertz radiation**

### **6.3.1 Novosibirsky terahertz free electron laser**

Novosibirsk free electron laser (FEL) is still the world's most powerful source of terahertz radiation. The maximum value of the average output power achieved at a pulse repetition frequency of 11.2 MHz is 500 W. In 2010, Novosibirsk FEL worked for users for about 750 hours. In the standard mode of operation for users at a repetition rate of 5.6 MHz, the average radiation power at the workstations depended on the wavelength and tuning of the accelerator system and was about 100 W. In this case, the FEL radiation is linearly polarized and fully spatially coherent; the wavelength is tunable in the range of 120 - 240  $\mu\text{m}$ ; the relative spectral width is less than 1% (FWHM); and the pulse duration is about 100 ps (FWHM).

In 2010, work on the FEL involved employees of Budker Institute of Nuclear Physics SB RAS, the Institute of Chemical Kinetics and Combustion SB RAS, the Institute of Cytology and Genetics SB RAS, the Institute of Inorganic Chemistry SB RAS, Rzhzanov Institute of Semiconductor Physics. SB RAS, the Institute of Theoretical and Applied Mechanics SB RAS, the Technological Design Institute of Scientific Instrument, and the Scientific-Technological Center of Unique Instrumentation RAS (Moscow) as well as teachers, students and graduates of Novosibirsk State University and Novosibirsk State Technical University.

One of the two major tasks in 2010 was the organization of regular work at the six user stations. The second task was to commission the second stage of Novosibirsk FEL.

### **6.3.2 Experimental station on THz radiation beams**

6.3.2.1. The "Metrology" station is intended for diagnostics, monitoring and optimization of the parameters of the FEL radiation and conducting physical experiments with the radiation.

Participating organizations:

- Budker Institute of Nuclear Physics SB RAS, Novosibirsk;
- the Institute of Semiconductor Physics SB RAS, Novosibirsk;
- Nikolaev Institute of Inorganic Chemistry SB RAS, Novosibirsk.

In 2010, the works were carried out with financial support from the RAS, SB RAS, and RFBR:

1. RAS Presidium Program No. 2720 "Creating highly sensitive photodetectors based on PbSnTe: In films for optical spectroscopy and spectroscopy in the terahertz range";
2. RAS Presidium Program No. 2734 "Study of the spectrum of electronic states in Si/CaF<sub>2</sub> BaF<sub>2</sub>/PbSnTe:In nanoheterostructures";
3. RFBR grant No. 09-02-12303-ofi\_m "Investigation into the interaction of terahertz radiation with new functional resonant metamaterials for devices controlling the polarization, phase, intensity and direction of propagation radiation";
4. SB RAS Interdisciplinary Integration Project No.24 "Metamaterials based on precision micro-and nanoshells for the terahertz and infrared ranges";
5. RFBR Grant No. 09-02-12121-ofi\_m "Development of methods for measuring and controlling parameters of high-power terahertz radiation"; and
6. RFBR Grant No. 10-02-90005-Bel\_a "Investigation into the interaction of terahertz electromagnetic radiation with materials based on carbon nanotubes."

Works in 2010

1) Lasing was attained at the third harmonics in the long-wave range of the terahertz FEL. The quality of radiation in this regime was no worse than that at the fundamental frequency. The laser was emitting a linearly polarized Gaussian beam with a wavelength of about 70 microns with an average power of about 30 W at a repetition frequency of electronic pulses of 5.6 MHz. There were three possible modes, switchable by certain manipulations with the optical resonator: pure first harmonic mode generation, pure third harmonic generation and generation at both harmonics simultaneously. Fig.(6.3)1 shows the spectra of FEL radiation in these three modes. Lasing at harmonics can extend the frequency range of the FEL.

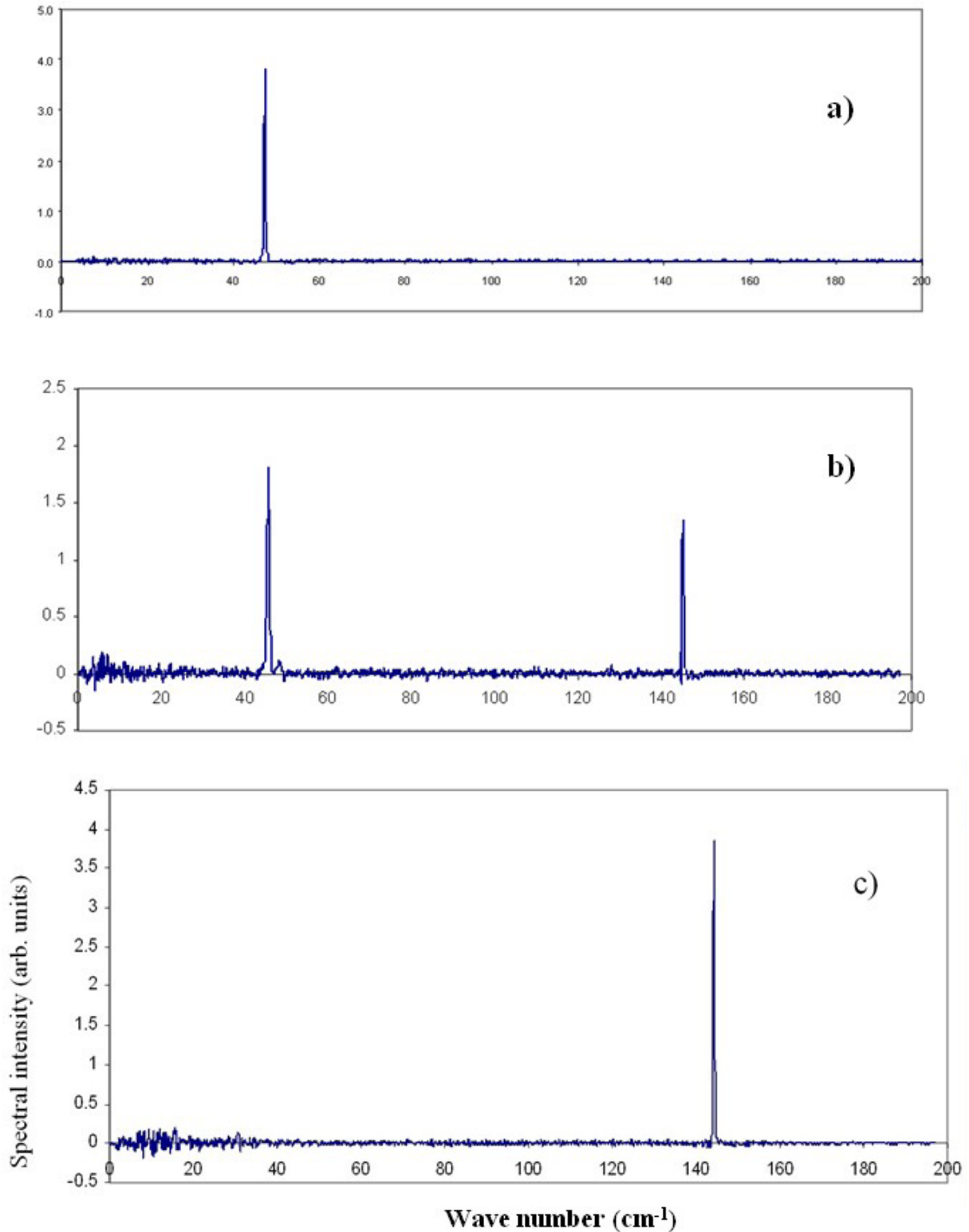


Fig.(6.3)1. Laser generation of the terahertz FEL at the first (a), first and third (b), and third (c) harmonics.

2) A fine structure was detected and studied in the optical-activity spectra of a lattice of microcoils on a GaAs substrate. According to calculations and control experiments, this structure is well explained by the interference of the zero and first orders of radiation diffraction on this lattice. The observed fine structure is shown in Fig (6.3)2.

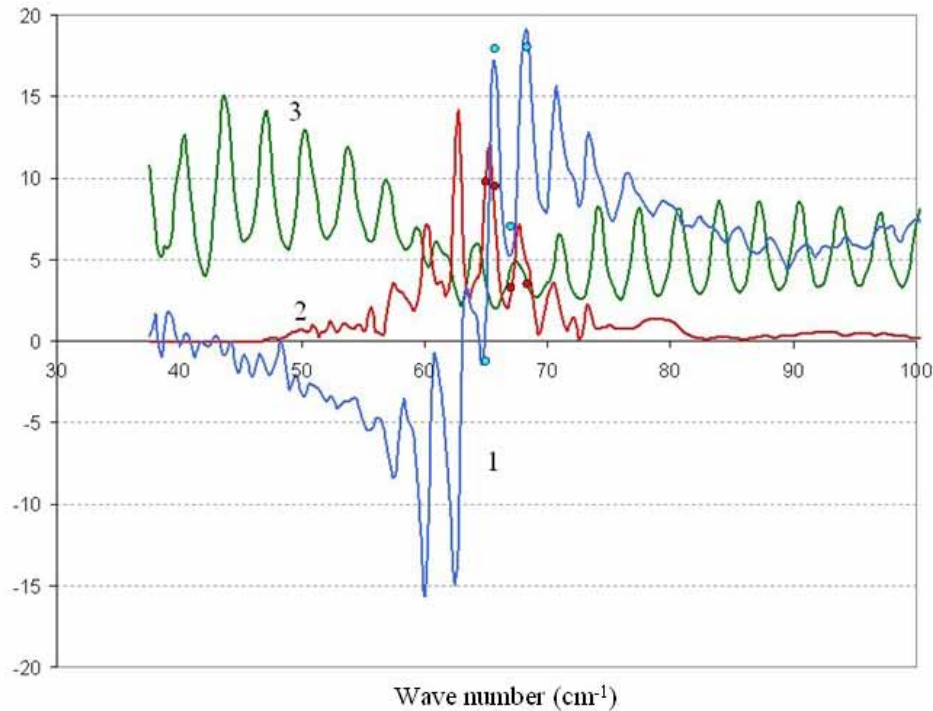


Fig.(6.3)2. Fourier spectra of rotation angles (1, degrees), circular dichroism (2, dichroism intensity  $\times 50$ ), and transmission (3, transmission  $\times 30$ ) and data of measurement on the FEL (dots) for a square grid of microcoils on a 400  $\mu\text{m}$  GaAs substrate. The FEL line width is 0.2  $\text{cm}^{-1}$ .

3) A large polarization effect was revealed on samples of oriented nanotubes in a polymer matrix in terahertz radiation. The antenna effect of these samples was apparently also discovered. It consists in a significant decrease in the polarization effect for wavelengths larger than twice the original length of the longest nanotubes. Fig.(6.3)3 shows the transmission spectra of one of the samples for two linear polarizations. Fig.(6.3)4 presents the polarization angle characteristics of this sample, measured on the FEL.

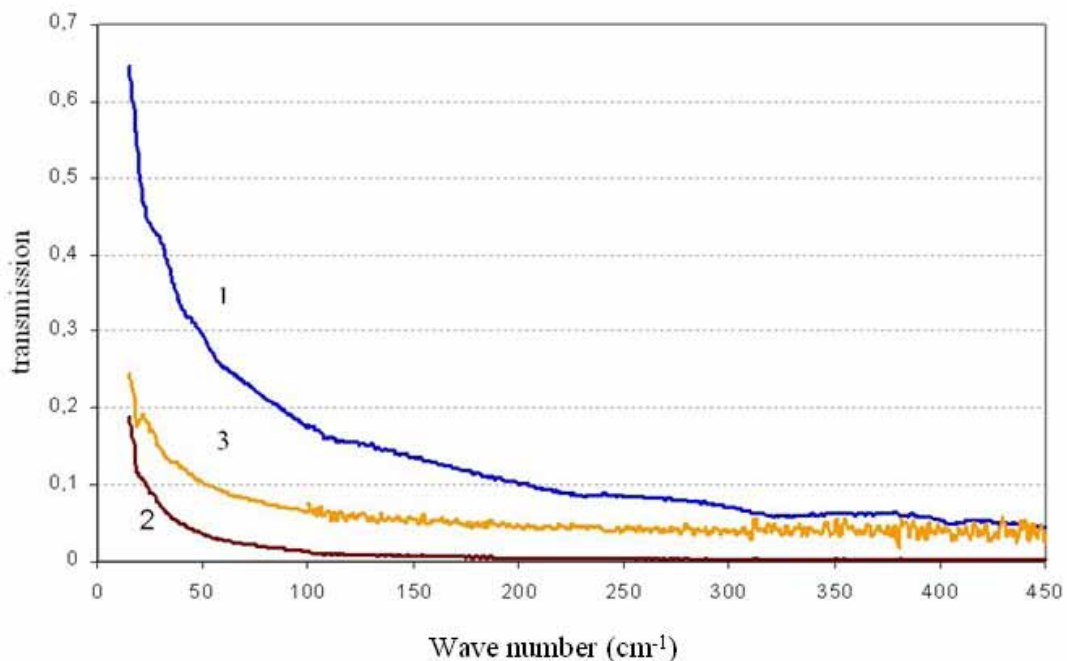


Fig.(6.3)3. The transmission spectra of samples of nanotubes for radiation polarized normally to the nanotube axes (1, upper curve) and along the nanotube (2, lower curve) and their ratios (3).

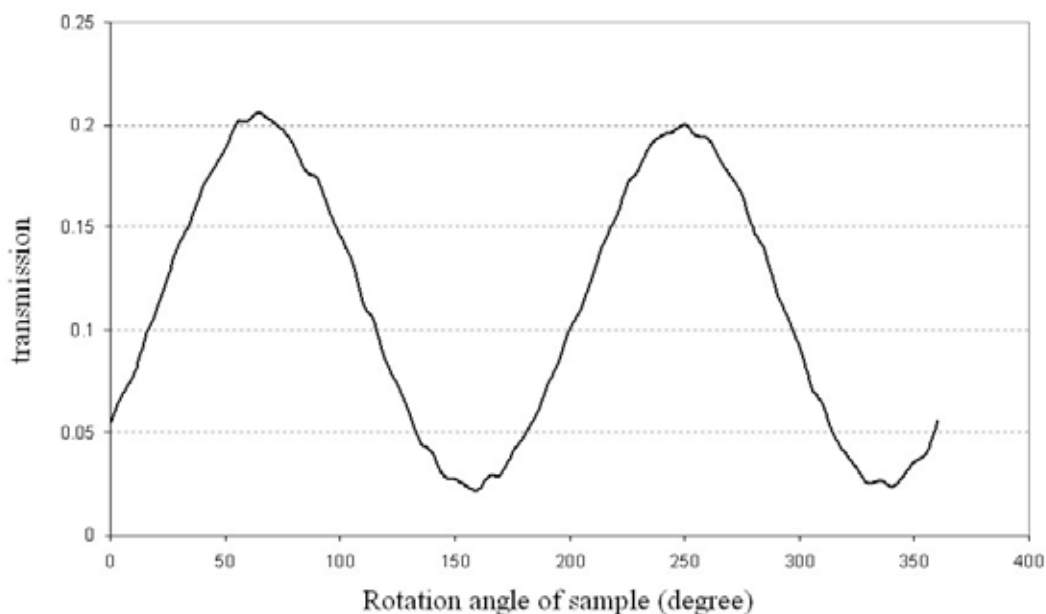


Fig.(6.3)4. Polarization angle characteristic of one of the samples with aligned carbon nanotubes.

6.3.2.2. Station for physicochemical and biological studies is intended for exploring the effects of radiation on micro- and nano-objects and products of ablation of nucleic acids, proteins, enzymes, polymers, and mineral clusters.

In 2010, works with biological objects were carried out with financial support of SB RAS interdisciplinary integration projects No. 39 and No. 52.

Participating organizations:

- Boreskov Institute of Catalysis SB RAS, Novosibirsk;
- the Institute of Solid State Chemistry and Mechanochemistry SB RAS, Novosibirsk;
- the Limnological Institute SB RAS, Irkutsk.

Themes of works in 2010:

1. Production of carbon nanostructures with the help of terahertz FEL (the Institute of Catalysis SB RAS).
2. Determination of the fractional composition of nanoproductions of mechanical activation of double oxides (the Institute of Solid State Chemistry and Mechanochemistry SB RAS, Novosibirsk).
3. Exploring composite silicon-polymer nanostructures (the Limnological Institute SB RAS, Irkutsk).

Preliminary results of the work in 2010:

### **1. Production of carbon nanostructures with the help of terahertz FEL**

Symmetrical polyhedral nanostructures (Fig.(6.3)5.) formed by monolayers of carbon (Fig.(6.3)6.) and carbon nanotubes of 6 nm in diameter and up to 1.5  $\mu\text{m}$  long (Fig.(6.3)7.) were produced under the influence of powerful focused FEL radiation (a wavelength of 130  $\mu\text{m}$ ) on samples of pure graphite in an atmosphere of dry nitrogen.

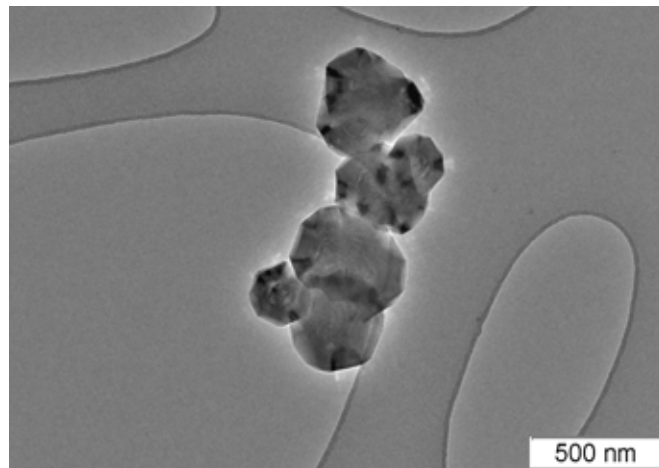


Fig. (6.3)5. Electron microscopy of particles produced by the powerful effect of FEL radiation on graphite.

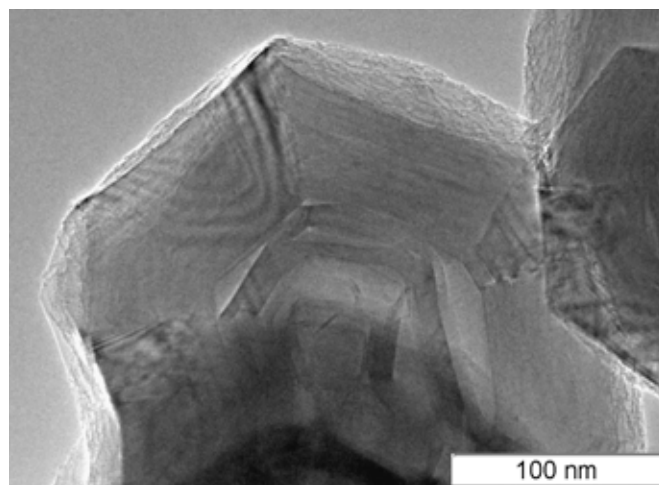


Fig.(6.3)6. The same as Fig. (6.3)5, lower scale.

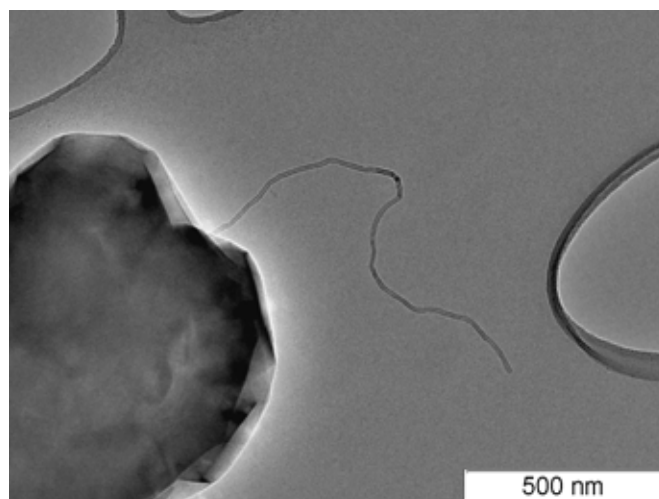


Fig.(6.3)7. The carbon nanotube.

Samples of pure graphite were provided by A.M. Volodin (BIC SB RAS); the electron microscopy was performed by V.V. Zaykovsky at the same institute. Optimal parameters for stable obtaining of such nanoscale particles are currently being selected and parameters of the crystal microstructure are being determined.

## 2. Determination of the fractional composition of nanoproducts of mechanical activation of double oxides

Soft terahertz ablation was used to find out the fractional composition of samples of spinel (Fig.(6.3)8.) The samples had been synthesized at ISSCM SB RAS (E. G.Avvakumov). The results obtained are consistent with the data of X-ray diffraction and electron microscopy.

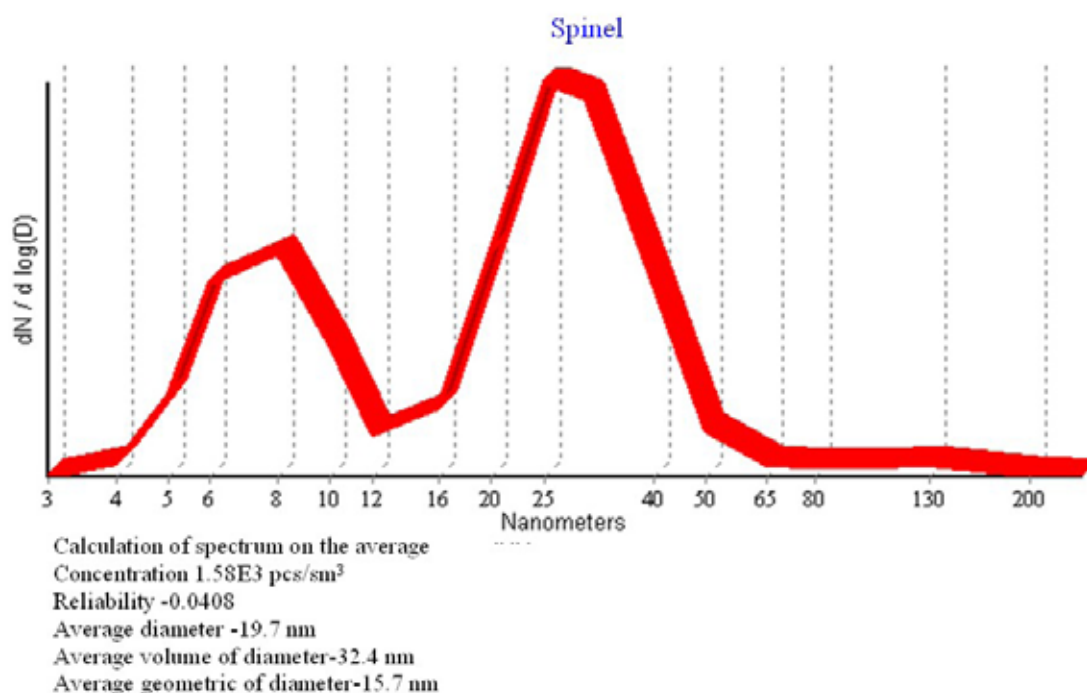


Fig.(6.3)8. Fractional composition of spinel from data of non-invasive ablation.

## 3. Exploration of composite silicon-polymer nanostructures

Laser ablation in combination with aerosol spectrometry was applied for finding out the structure of composite nanoparticles simulating the vesicles of transportation of silicon in diatoms. It was shown that particles of a radius of 20-100 nm, obtained at condensation of silicic acid in the presence of polyvinylamine and stable in the solution, contain silica fragments of a radius of 1.4 nm stabilized by organic polymer chains. These results indicate the unique possibilities of laser ablation in the study of the structure of composite nanoparticles.

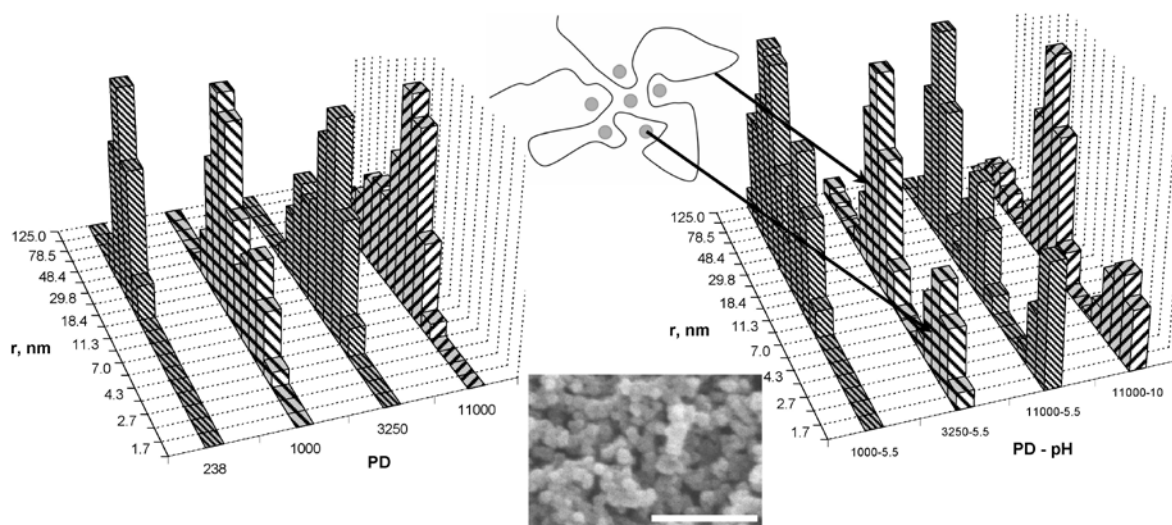


Fig.(6.3)9. The size distribution of particles produced by ablation of PVA samples of different polymerization degrees (PD) and composite particles formed at an equimolar ratio PVA/silicic acid and different pH values. A microphotography of the composite precipitate in the PVA - silicic acid system at an equimolar ratio of the components and pH = 10, a scale of 1 µm, and a schematic structure of the composite nanoparticles.

### 6.3.2.3. Station “Spectroscopy and introscopy (SpIn)”

The station is intended for the study of the absorption spectra of materials and substances as well as for multi-quasi-optical imaging experiments.

Participating organizations:

- Novosibirsk State University;
- Novosibirsk State Technical University;
- the Institute of Semiconductor Physics SB RAS, Novosibirsk;
- the Institute of Chemical Kinetics and Combustion SB RAS, Novosibirsk;
- the Technological Design Institute of Scientific Instrument Engineering SB RAS, Novosibirsk;
- the Scientific and Technological Center of Unique Instrumentation of RAS, Moscow;
- Patrice Lumumba Peoples’ Friendship University, Moscow;
- Korean atomic energy research institute, Daejeon, Korea;
- Terawave, Inc., Daejeon, Korea;
- Vieworks Co. ltd, Gyeonggi-do, Korea.

In 2010, works at the station were conducted with the support of the following grants:

1. RFBR grant 09-02-12121-ofi\_m “Development of methods for measuring and controlling parameters of high-power terahertz radiation”;
2. RFBR grant RFFI\_09-02-12158-ofi\_m “Development of physical foundations of tomography, holography and metrology using a source of coherent monochromatic terahertz radiation”;
3. SB RAS integration project No.89 “Development of the method of terahertz imaging spectroscopy of attenuated total internal reflection with the function of near-field microscopy”;
4. State contract No.02.740.11.0556 “Plasmon spectroscopy of materials, micro- and nanoparticles and biological objects in the terahertz range.”

Below are presented main results obtained.

#### **1. Spectroscopy of attenuation total reflection (ATR)**

Work continued on improving the quality of imaging in the ATR spectrometer. A system for recording images using a moving microbolometer array detector was created and put into operation. A scheme was proposed for holographic recording in real time. The Technological Design Institute of Scientific Instrument Engineering SB RAS developed and tested a confocal surface sensor using diffraction chromatic coding for the purposes of terahertz spectroscopy. The main element of the sensor is an unorthodox hybrid refractive-diffractive lens. The possibility of using a color video camera as a spectrum analyzer was shown.

#### **2. Recorders of images in the terahertz range**

Together with the Institute of Semiconductor Physics we continued exploring the mechanism of sensitivity of microbolometer array detectors to terahertz radiation. It was found that the structural elements of the receiving cells do not absorb terahertz radiation directly, and the sensitivity of the array depends strongly on the polarization of the electromagnetic wave (Fig.(6.3)10). It was concluded that the registration of wave occurs due to the antenna effect on the metal legs of each microbolometer, which causes ohmic heating of them and heat transfer to the corresponding element. Knowing the mechanism of operation of the existing arrays in the terahertz range allows a new approach to the development of the microbolometer arrays intended for image registration in the terahertz range and potentially increases their sensitivity by 1 - 2 orders of magnitude.

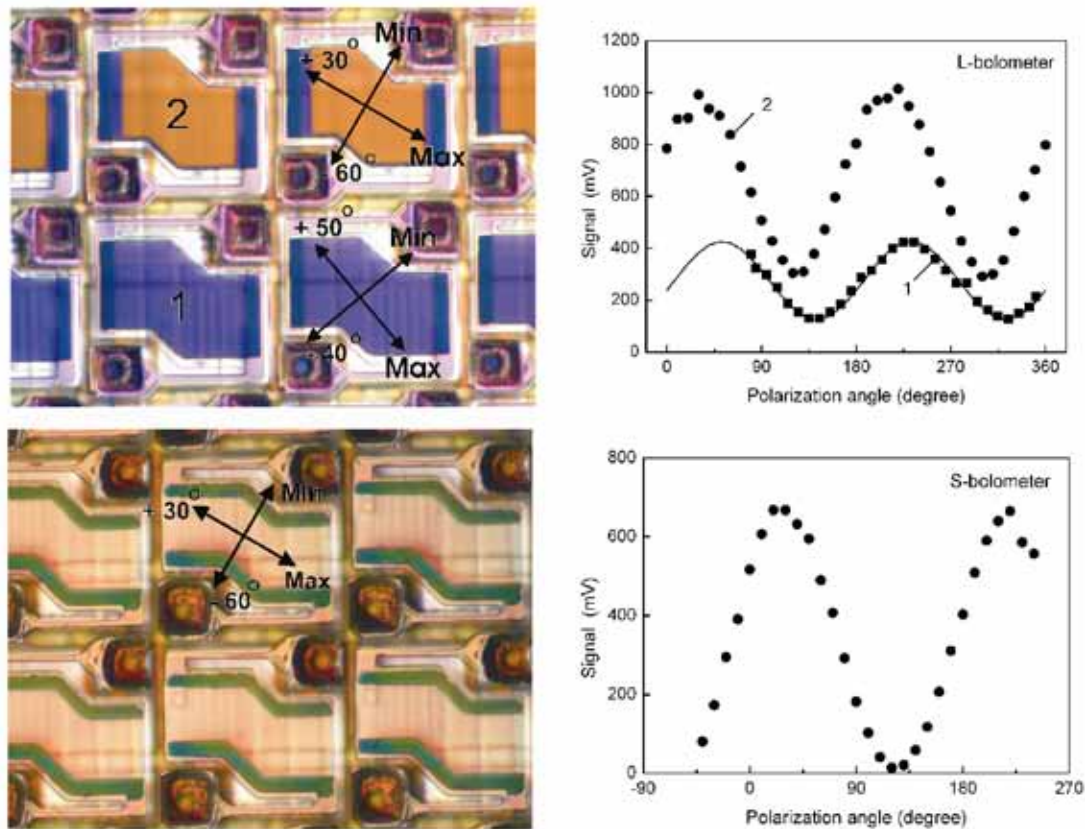


Fig.(6.3)10. Dependence of the sensitivity of microbolometer arrays of different types depending on the direction of terahertz radiation polarization. The sensitivity increases when a thin metal layer is applied to the surface of the sensor of the L bolometer (top graph).

### Plasmon spectroscopy of surfaces and films

A new method was tried for the capture of a free electromagnetic wave to a surface mode in the terahertz range using a slotted waveguide element instead of a "knife". The capture efficiency was shown to increase at least by an order of magnitude. Images of the surface wave intensity distribution on the end of a sample were obtained for the first time in real time using the microbolometer array. It was found that the intensity distribution is different from the distribution predicted by Drude. The dependences of the path length on the composition of the surface were studied.

### 3. Talbot effect in the terahertz range

The Talbot effect has recently caused great interest in X-ray measurement systems and passage of atomic beams through crystals. There has also been a surge of publications on this subject for the visible range. We do not know any experiment conducted in the terahertz range. We registered this effect for the first time in the terahertz range at wavelengths of 126 and 54 microns. We studied the manifestations of the effect when the characteristic size of the periodic structures was only a few wavelengths (up to three  $\lambda$  on the diameter of the hole) of the electromagnetic radiation (Fig.(6.3).11). The practical application of the effect to the FEL wavelength measurement, distance measure and investigation into the dynamics of optical inhomogeneities in condensed and gaseous media was demonstrated. The application of the effect to solving the problem of phase uncertainty in terahertz holography was considered.

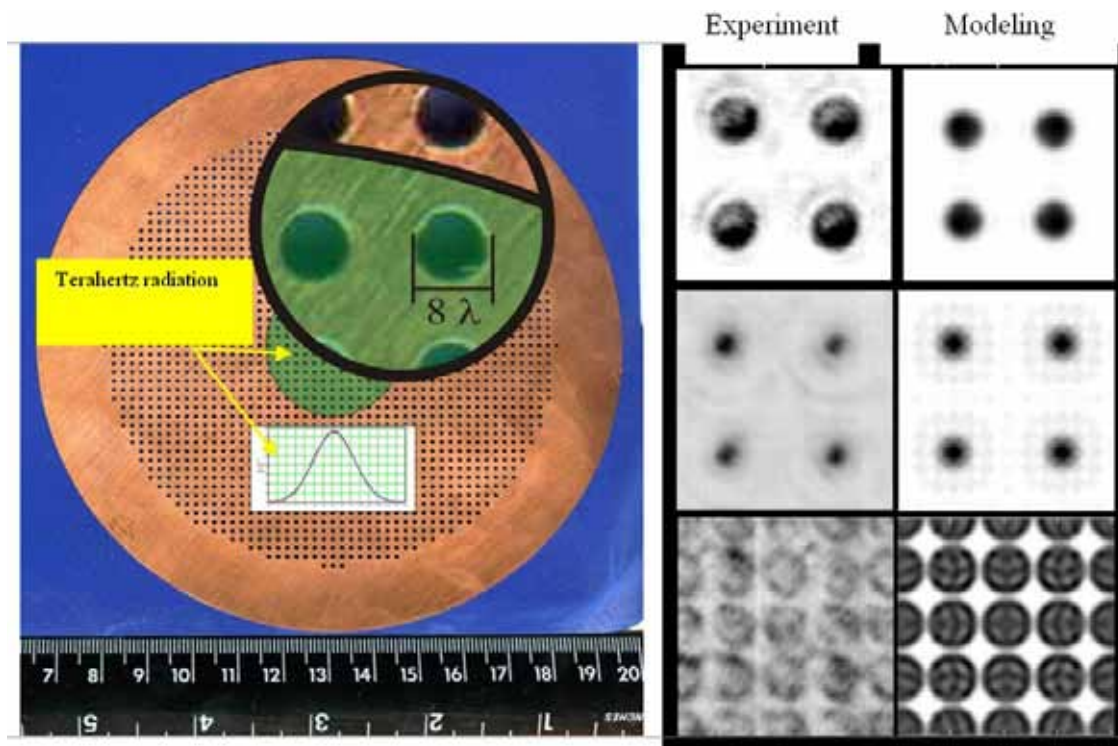


Fig.(6.3)11. Left: one of the periodic structures used to study the Talbot effect in the terahertz range. Right: comparison of numerical simulation and images recorded from some characteristic planes using a microbolometer array.

#### 4. Registration of images of objects illuminated with terahertz radiation

Model experiments on recording images of smooth and rough objects illuminated with radiation of the terahertz free-electron laser were carried out using the matrix microbolometer. The research was conducted in real time. The objects could be hidden behind a screen not transparent to visible and near infrared radiation. It was shown that rough objects are well imaged from their speckle pattern, and one can identify their shape with a thought-out organization of the optical system. Smooth conducting objects are visible only from their Fresnel reflections, which almost always occur at the boundaries and can be artificially hidden at a specially chosen orientation of large planes (see Fig.(6.3)12.). Dielectric objects are the most difficult to see, although there are some dynamic changes in vision. All objects, however, can be reliably detected if there is a background textured surface reflecting the terahertz radiation. In this case, the visualizing camera clearly records shadows of objects on the background of the speckle pattern. The results are of interest for industrial control systems and security systems.

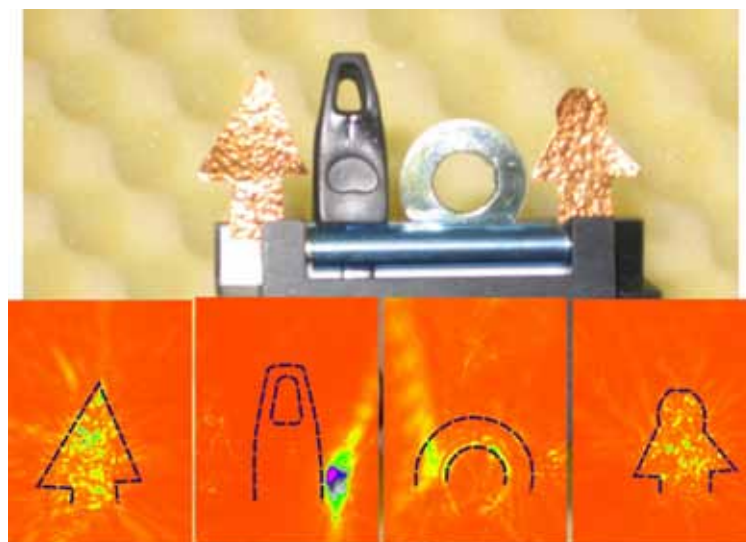


Fig.(6.3)12. Images of objects in the terahertz region, taken with the Fresnel lens and a microbolometer array.

## 6.3.2.4. Station for molecular spectroscopy

The station is intended for research of molecular spectra of chemical compounds important for combustion processes by means of FEL-radiation.

Participating organizations:

- the Institute of Chemical Kinetics and Combustion SB RAS, Novosibirsk;
- Budker Institute of Nuclear Physics SB RAS, Novosibirsk;
- the Institute of Atmospheric Optics SB RAS, Tomsk.

Works in 2010 were carried out with financial support from the following grants: SB RAS interdisciplinary integration project No. 102 "Development of the Faraday LMR spectrometer of the terahertz range using the free electron laser." SB RAS interdisciplinary integration project No. 52 "Commissioning of the second stage FEL and development and fabrication of the elements of the third stage FEL."

Themes of works in 2010:

1. Improvement of the sensitivity of the method for detecting paramagnetic molecules.
2. Development of methods for flame diagnostics using the terahertz FEL.

Examples of works in 2010:

**A study of absorption at the  $\text{H}_2\text{O}$  line of at high temperature was conducted for evaluation of the possibility of using the FEL radiation to measure the concentration of water vapor in a flame.**

Water vapor is the main absorbing component of THz radiation in a flame. Direct use of the FEL radiation for determination of the water vapor concentration is, however, greatly complicated by the absorption in the lead-in optical paths, which contain water vapor at room temperature. The length of a lead-in optical path is usually much greater than that in the flame; the absorption coefficient generally decreases with increasing temperature. These factors make it almost impossible to use the strong lines of water vapor for flame diagnostics. A particular selection of the absorption line for which the absorption coefficient at room temperature is small and increases with the temperature could be a solution.

The  $\text{H}_2\text{O}$  absorption line at  $77.3\text{ cm}^{-1}$  was chosen for the experiments. For it, the energy of the lower state is relatively large,  $E_1 = 1282.9\text{ cm}^{-1}$ , which is about 6 kT at room temperature. For this reason, the absorption coefficient for this line is small at room temperature (Fig.(6.3)13). As the temperature increases, the population of the lower state increases, which leads to an increase in the absorption coefficient. Fig. (6.3)14 shows how, as a result of redistribution of the population of rotational levels at heating, the relative intensity of four water-vapor absorption lines is changing in the range of  $77 - 80\text{ cm}^{-1}$ .

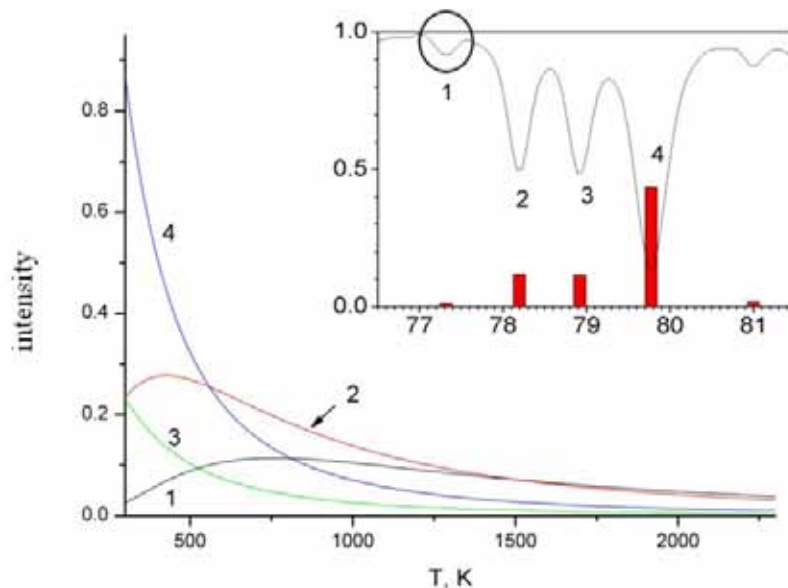


Fig.(6.3)13. Change in the relative intensity of four water-vapor absorption lines in the interval of  $77 - 80\text{ cm}^{-1}$ . The inset shows the corresponding portion of the spectrum of water vapor at room temperature. The circle indicates the line chosen for the measurement.

Calibration measurements of the absorption coefficient for FEL radiation at the absorption line of  $77.3\text{ cm}^{-1}$  were carried out in an open tube furnace 50 cm long, which was filled with water vapor.

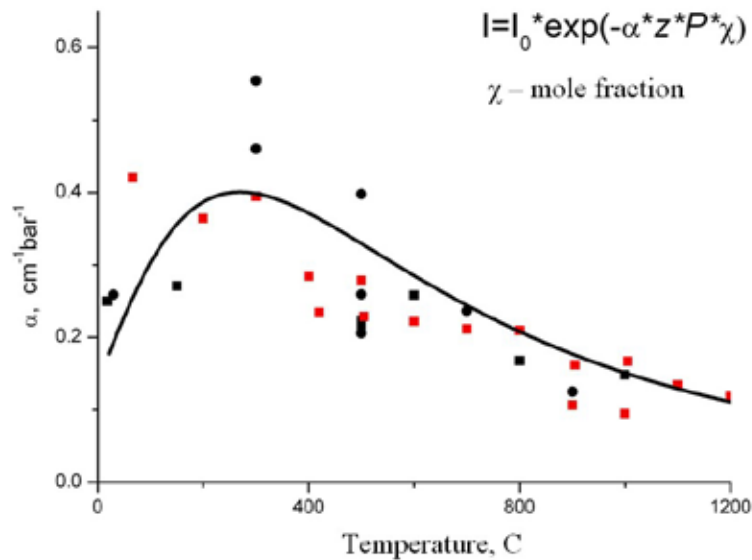


Fig.(6.3)14. Results of measurement of the coefficient of FEL radiation absorption by water vapor at different temperatures. The FEL was tuned to the absorption line of  $77.3 \text{ cm}^{-1}$ . The solid line presents a calculation subject to the real spectrum of the FEL and integrated intensity of the line (taken from the base of NASA).

The obtained calibration data were applied to the measurement of the concentration of water vapor in a soot-rich  $\text{C}_2\text{H}_4/\text{O}_2/\text{Ar}$  flame as a function of distance from the burner surface. Comparison of the experimental results and calculation showed that the  $\text{H}_2\text{O}$  vapor concentration measured at a distance of 20-25 mm from the burner ( $\text{CH}_2\text{O}$ , exp. =  $0.088 \pm 0.010$ ) are in satisfactory agreement with the results of calculations ( $\text{CH}_2\text{O}$ , calc. = 0.095). Thus, using the rotational terahertz spectroscopy with sufficient accuracy, one can measure the concentration of water vapor in soot flames and in flames of two-phase flows, which are difficult to measure by conventional optical methods.

**A submillimeter-range monochromator was fabricated to reduce the spectral width of the FEL radiation.**

The spectral resolution of the monochromator is about  $0.1 \text{ cm}^{-1}$ . This value is approximately equal to the width of the absorption lines in the rotational spectrum in a flame at atmospheric pressure. Fig.(6.3)15 presents an example of the FEL spectrum recorded with the monochromator as well as the lines of  $\text{D}_2\text{O}$  vapor absorption inside the spectral profile of the FEL.

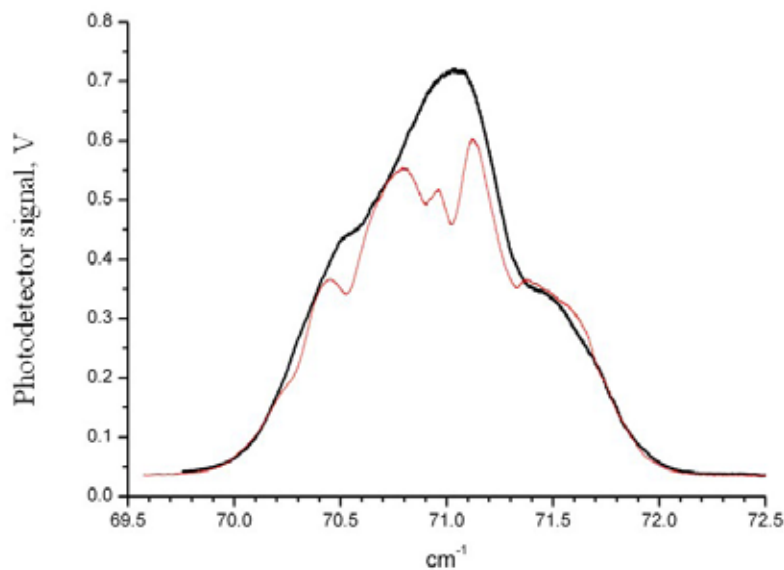


Fig.(6.3)15. FEL emission spectrum obtained with the monochromator (black line). The spectrum was recorded after the passage of radiation through the evacuated cuvette. The red line shows the change in the spectrum when the cuvette was filled with  $\text{D}_2\text{O}$  vapor at a pressure of 3 Torr.

## 6.3.2.5. Station "Heterogeneous deposition of thin layers"

Station was put into operation in 2010. It is intended for the study of physicochemical processes of induced deposition of thin layers on solid surfaces.

The work is part of the scientific program of the Institute of Inorganic Chemistry V.36.5. "Development of the chemistry of complex, cluster, and supramolecular structures and synthesis of new materials based on them."

Research Project: Chemistry of volatile metal complexes with organic ligands and the processes of their thermal and photostimulated transformations on various types of surfaces as a basis for the formation of nanostructured materials by the MO CVD method.

Scientific project leader: Prof. K. Igumenov

Participating organizations:

- Nikolaev Institute of Inorganic Chemistry SB RAS, Novosibirsk;
- Boreskov Institute of Catalysis SB RAS, Novosibirsk;
- Rzhanov Institute of Semiconductor Physics SB RAS, Novosibirsk.

Theme of the work in 2010:

Investigation into the process of induced deposition of thin layers of copper using combined synthesis-transport of small volatile metal complexes.

Brief description of the theme:

New physicochemical processes of precipitation of metal nanostructures on solid surfaces are the basis for development of a number of advanced technologies in microelectronics, catalysis, synthesis of new optoelectronic materials, etc. One of the promising methods of conformal metallization of surfaces with complex working relief is our method of combined synthesis-transfer (CST) as extension of the conventional MO CVD technology. The essence of this approach is bringing together two processes in one reactor volume: the **synthesis** of a volatile metal complex and its **transfer** onto the substrate with subsequent formation of a layer on its surface. The CST method has shown its effectiveness in forming metal layers of a variety of small-size copper complexes arising when volatile precursors are passed through fine filling of copper-containing solids (non-volatile precursors).

The choice of precursors, methods of their activation, and layer deposition conditions in the MTP process determines the characteristics of the target material. A significant advantage is the possibility of application of nonequilibrium processes of activation of precursors and the synthesis zone of the layer as well as the possibility of generation and application of metastable volatile metal complexes, which are difficult to produce and extract in pure form. Moreover, the CST principle makes it constructively possible to place and alternately involve several combinations of reagent precursors in one reaction volume, thus forming structures of layers of different destination in one technological operation.

The best-quality thin layers of copper on quartz and silicon substrates were produced at generation of formate complexes with fumes of formic acid and filling of a fine-dispersed mixture of metallic copper and copper oxide with a 1:1 ratio. Thermal activation of the substrate was combined with plasma activation of the synthesis zone of the layer using a microwave discharge. Typical examples of the synthesized layers of copper were analyzed in detail using the methods of optical spectroscopy, scanning electron microscopy (SEM), X-ray spectroscopy (XRS) and diffraction of synchrotron radiation (DSR). It was revealed that the deposited layer has a characteristic densely-packed grain structure with a predominant content of copper in the metallic state  $\text{Cu}^0$  in the form of nanosized grains.

It should be noted that similar CST processes with deposition of thin layers of different functionality can be arranged for a number of refractory, coin and precious metals such as W, Ti, Ta, Ru, etc.

Moreover, also under RFBR grant No. 09-02-12100 "Study of the fundamentals of the selective action of terahertz radiation on the spatial organization of biological objects" we studied the non-thermal effects of electromagnetic radiation on different levels of organization of living systems. The terahertz range of the electromagnetic spectrum was selected for these studies. The objects of the impact were the following biological systems: pUC18 plasmid DNA and artificial genosensor structures based on stress-responsive promoters and proteomes of *E. coli* M13 cells. The workstation was upgraded; a model system was developed for studying the direct effects of terahertz radiation on DNA. The effect of THz radiation on stress-sensitive cell systems that respond to oxidative stress was explored. Within the frameworks of the study of

the integral proteomic response of *E. coli* cell to exposure to terahertz radiation, two-dimensional maps of *E. coli* proteomes were constructed and individual proteins that change their expression under the influence of terahertz radiation were identified.

The station was upgraded for the purpose of controlling the exact irradiation dose. Terahertz radiation is delivered to the workstation via a standard module for radiation distribution among the workstations. A general view of the station after the upgrade is shown in Fig.(6.3)16.



Fig.(6.3)16. Station after the upgrade.

The upgrade included the following:

1) Installation and adjustment of the flat bending and focusing mirrors. The flat mirror is intended for changing the direction of parallel rays. The angle of incidence on the focusing mirror was  $40^\circ$ ; its focus was 12 cm. Correspondingly, the focal length for one coordinate was 9.2 cm and for the other, 15.6 cm.

2) A shutter consisting of two copper disks with a diameter of 20 cm with a common rotation axis and rotated by a motor was fabricated for adjusting the average output power at a constant peak power. Each disk has one sector-shaped hole occupying 1:30 of its area. Turning the disks relative to each other allows regulating the area of the open hole, changing the average output power and leaving the peak power unchanged. For changing the density of the average and peak power, the sample was positioned at various points of radiation focusing after the shutter.

3) A special cuvette was made for exposure of biological samples. A sample is placed in the cuvette between two stretched polypropylene films 40  $\mu\text{m}$  thick. The volume of the cuvette is 50  $\mu\text{l}$ ; the distance between the films is 25  $\mu\text{m}$ ; the diameter of the cuvette is 50 mm;

4) The cross section of the radiation beam in the plane of the cuvette is an elongated ellipse. For the exposure of sample to be uniform throughout the volume, a special mechanism rotated the cuvette. The axis of rotation passed through the edge of the ellipse.

The temperature of liquid samples was controlled with a highly sensitive thermal imager TKVr-SVIT101 made by the Institute of Semiconductor Physics SB RAS. It has a sensitivity of  $0.027^\circ\text{C}$  or better and allows dynamic registration of changes in temperature fields.

### **Study of the impact of terahertz radiation on genetic material**

pUC18 plasmid DNA was used as a model object in the study of the impact of terahertz radiation on genetic material. Irradiation of the plasmid with terahertz radiation may lead to denaturation of the molecule as a result of destruction of hydrogen bonds on certain sites in the double-stranded DNA structure under the influence of the radiation. At a molar excess of complementary oligonucleotides, there will occur hybridization with formation of a corresponding triplex structure. Using fluorochrome-labeled oligonucleotides will allow imaging the triplex structure at electrophoretic analysis. Hybridization of the labeled

oligonucleotides with the pUC18 plasmid DNA indicates destruction of hydrogen bonds in the DNA when exposed to terahertz radiation. Site selection in pUC18 plasmid was carried; the technique of electrophoretic analysis of the products of hybridization of denatured sites was developed and tested.

The reaction mixture was placed in a specially designed cuvette for the purpose of studying the effects of THz radiation on the secondary structure of the DNA. The reaction mixture contained 500 ng/ $\mu$ l of pUC18 plasmid DNA and 5 ng/ $\mu$ l of the fluorochrome-labeled oligonucleotide. The temperature of the medium in the cuvette was controlled with the thermal imager “TKVr-SviT-101” and maintained between 12 to 14 °C. 50  $\mu$ l of the reaction mixture was placed in the experimental cuvette and irradiated with terahertz radiation with a power density of 1.4 W/cm<sup>2</sup> at different wavelengths waves for 5 - 20 min. The reaction mixture was then collected and applied on a gel for conduction of electrophoresis with voltage applied and a gel temperature of ~ 37 - 40° C. A series of experiments was carried out by this scheme at various wavelengths and exposure times. The wavelengths and irradiation times are shown in Table (6.3)1.

Table (6.3)1. Conditions of the experiment on the effects of THz radiation on the secondary structure of DNA.

No	1	2	3	4	5	6	7	8
Wavelength, $\mu$ m	125.1	128.7	138.5	141.4	130	130	130	140
Time, minutes	10	10	5	5	5	10	20	10

In all the experiments, no formation of triplexes of the corresponding oligonucleotide and pUC18 plasmid DNA was observed under exposure to terahertz radiation. The results can be explained by three factors:

- 1) Terahertz radiation does not provide denaturation of the secondary structure of DNA.
- 2) The hydrogen bonds of the secondary structure have a narrow resonance-absorption band, which had not been found in experiments by that time.
- 3) A shorter time of relaxation of denatured DNA as compared with the mobility of the oligonucleotide in the reaction mixture.

#### **Exploration of the impact of terahertz radiation on stress-sensitive cell systems**

Exploration of the impact of terahertz radiation on living objects is of interest in connection with the planning of using this range of wavelengths for development of security systems. The emergence of powerful sources of terahertz radiation also poses the problem of studying the response of living organisms to terahertz radiation. In this project, a task to explore the effect of radiation on the individual links in cell metabolism was posed. A series of stress-sensitive genosensors created in ICG SB RAS was used as model objects. Fig.(6.3)17 shows the general scheme of the work of genosensor structures based on *E.coli* cells. A stress-sensitive promoter (highlighted in red) is attached to the reporter gene (green). The *gfp* gene, encoding the Green Fluorescent Protein (GFP) (fluorescent protein) is used as the reporter gene.

The resulting recombinant plasmid is introduced into the bacterial cell. When the cell gets in adverse conditions, the stress-sensitive promoter attached to the regulatory element goes off. The reporter gene allows visualizing the work of the promoter – the cell produces the fluorescent protein and turns green, which can be seen with a conventional fluorescence microscope or registered with a spectrophotometer.

Several genosensor structures with different stress-sensitive promoters were developed: *katG*, *yfiA*, and *dps*.

#### **Terahertz radiation influence on the expression of the *katG* and *E. coli dps* genes**

Since the LB medium, in which genosensor cells are generated preparatively, has intrinsic fluorescence in the range of Gfp fluorescence, cells of the *E.coli/pKat-gfp* genosensor were transferred to basal medium M9 of the following composition: 0.4% glucose, 0.2% casamino acids, 48 mM Na<sub>2</sub>HPO<sub>4</sub>, 22 mM KH<sub>2</sub>PO<sub>4</sub>, 18.7 mM NH<sub>4</sub>Cl, 8.5 mM NaCl, 1 mM MgSO<sub>4</sub>, and 0.1 mM CaCl<sub>2</sub>. Then the cells were transferred into a specially designed cuvette. The temperature of the medium in the cuvette was controlled with the thermal imager TKVr SVIT-101 and maintained at 35 ± 2 °C. The cells were exposed for 10 min. The efficiency of genosensors was controlled via the induction of Gfp synthesis by 8 mM of hydrogen peroxide. The response of the cells of *E.coli/pKat-gfp*, *E.coli/pDps-gfp* and *E.coli/pYfi-gfp* was evaluated from the fluorescence level (irradiation: 485 nm, 0.1 s; emission: 535 nm) at a cultivation temperature of 37° C. The fluorescence was measured with the fluorometer Perkin Elmer VICTOR3 in relative units.

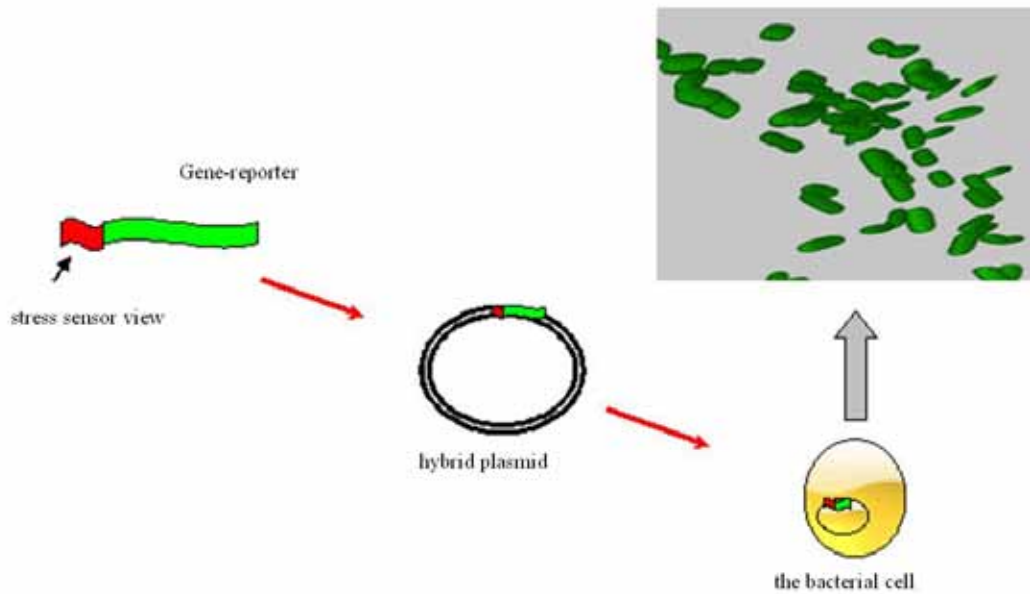


Fig.(6.3)17. Schematic diagram of the genosensor organization.

Signals of individual *E.coli/pKat-gfp* cells in response to terahertz radiation were recorded with the laser scanning microscope LSM500META manufactured by ZEISS. The GFPvaa molecules were excited using the 488 nm line of the argon laser. Laser scanning microscope makes it possible to select a signal from a narrow optical fiber (about 0.7  $\mu\text{m}$ ) containing the biological entities. Background signals above and below this plane were excluded from registration. Signals were registered in a range of 505 nm to 525 nm using a 63-fold lens. The data obtained were processed with the “LSM Image Examiner” software of ZEISS. *E.coli/pKat-gfp* genosensor cells were registered via simultaneous microscopy of the preparations, carried out by a method giving an image similar to that of differential contrast. The software used makes it possible to superimpose images obtained from analysis of optical sections and light microscopy. This method allowed registering individual cells producing GFPvaa.

Fig.(6.3)18 presents the results of the microscopy of *E.coli/pKat-gfp* genosensor cells after 10 min of exposure to terahertz radiation with a power density of 1.4 W/cm<sup>2</sup> and a wavelength of 130  $\mu\text{m}$ .

Joint analysis of cell images obtained in the differential contrast and at excitation of the fluorescent signal showed that approximately 80% of *E.coli/pKat-gfp* cells respond to a 40 min irradiation with GFPvaa synthesis. Cells of the same genosensor without exposure to terahertz radiation were a negative control in this series of experiments. As can be seen from the Fig.(6.3)18, bottom, only a few *E.coli/pKat-gfp* genosensor cells, for random reasons, showed the ability to synthesize GFPvaa. Thus, we can conclude that terahertz radiation with a wavelength of 130 microns induces synthesis of GFP in *E.coli/pKat-gfp* genosensor cells.

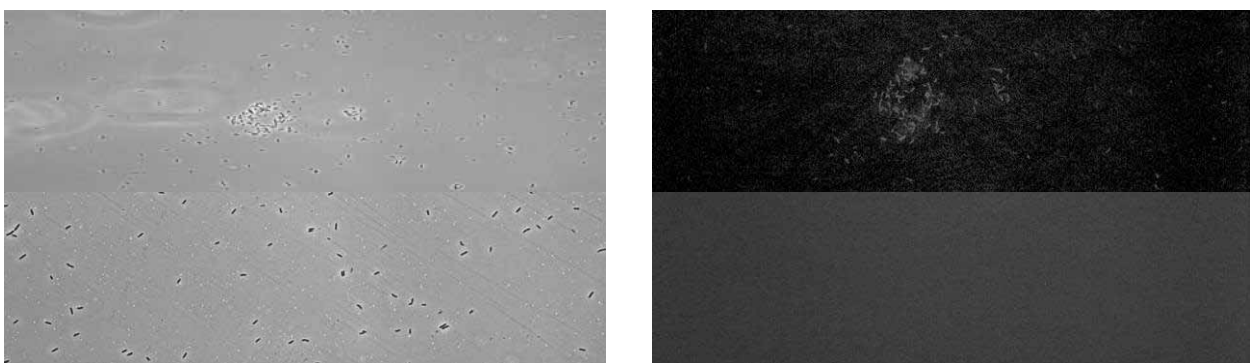


Fig.(6.3)18. Top: *E.coli/pKat-gfp* cells after exposure to the 130  $\mu\text{m}$  FEL radiation. Top left: the phase contrast image; top right: fluorescent microscopy. Bottom: control (without irradiation). Bottom left: the phase contrast image; bottom right: fluorescent microscopy.

Later on, the induction of GFP synthesis in the cells of genosensors was recorded with the fluorimeter Perkin Elmer VICTOR3. Fig.(6.3)19 presents the values of the level of GFP expression at the induction of *E.coli/pDps-gfp* genosensor cells with terahertz radiation with a power density of 1.4 W/cm<sup>2</sup> and a wavelength of 130 microns.

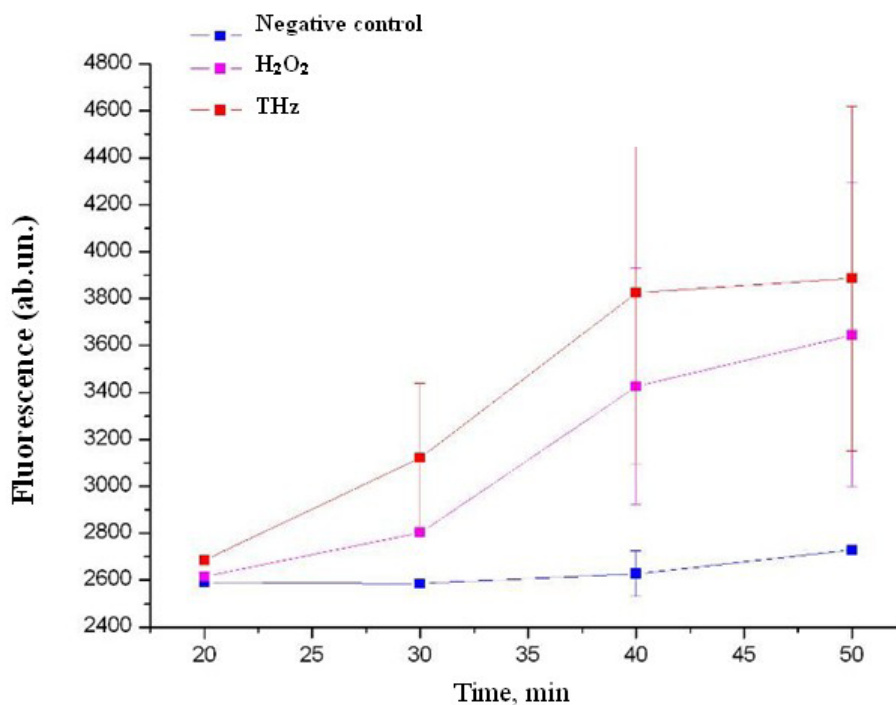


Fig.(6.3)19. Level of expression of Gfp in the *E.coli/pDps-gfp* genosensor cells at the induction with terahertz radiation (THz) and hydrogen peroxide (H<sub>2</sub>O<sub>2</sub>) and without induction.

It is seen from Fig.(6.3)19 that the level of expression of GFP in the *E.coli/pDps-gfp* genosensor cells at the induction with terahertz radiation and hydrogen peroxide was significantly different from that in non-induced cells.

#### Study of the integrated proteomic response of *E.coli* cells to exposure to terahertz radiation

A clone of *E.coli* strain M13 was evolved for the research. 50 µl of cells was transferred into a specially designed cuvette. The cells were exposed to terahertz radiation with a power density of 1.4 W/cm<sup>2</sup> and a wavelength of 130 microns; the temperature in the chamber was maintained at 35 ± 2° C via regulating the flux with the shutter as described above. The temperature of the medium in the cuvette was controlled with the thermal imager TKVr SVIT-101. The exposure lasted for 10 minutes. Then the culture was taken from the chamber and transferred to a thermostat for 37° C and incubated for 5 min for the response to develop, after which the cells were fixed with 50% ethanol. The procedure was repeated with several portions of the culture to a final volume of the irradiated culture of about 300 ml. The control group were *E.coli* M13 cells, which were fixed in portions with the corresponding times of cultivation until obtaining a final volume of 300 ml.

Analysis of the *E.coli* proteome was carried out by modern methods of proteomic analysis including two-dimensional electrophoresis with subsequent protein identification by MALDI-TOF mass spectrometry (UltraFlex III, Bruker). Standardization of the experiment was provided with a modern system developed by BioRad, which allows a significant increase in the reproducibility of two-dimensional proteomic maps. The high resolution of the applied methods and techniques of proteome research provided the first identification of the impact of terahertz radiation on *E.coli* cells.

Fig.(6.3)20 presents an electrophoregram of the total *E.Coli* protein after exposure to terahertz radiation. The arrows indicate electrophoretic protein fractions with significant differences (the Student criterion, 95%) in the levels of expression (two-fold). 8 protein fractions of *E.coli* proteome protein that alter their expression under the influence of terahertz radiation were found.

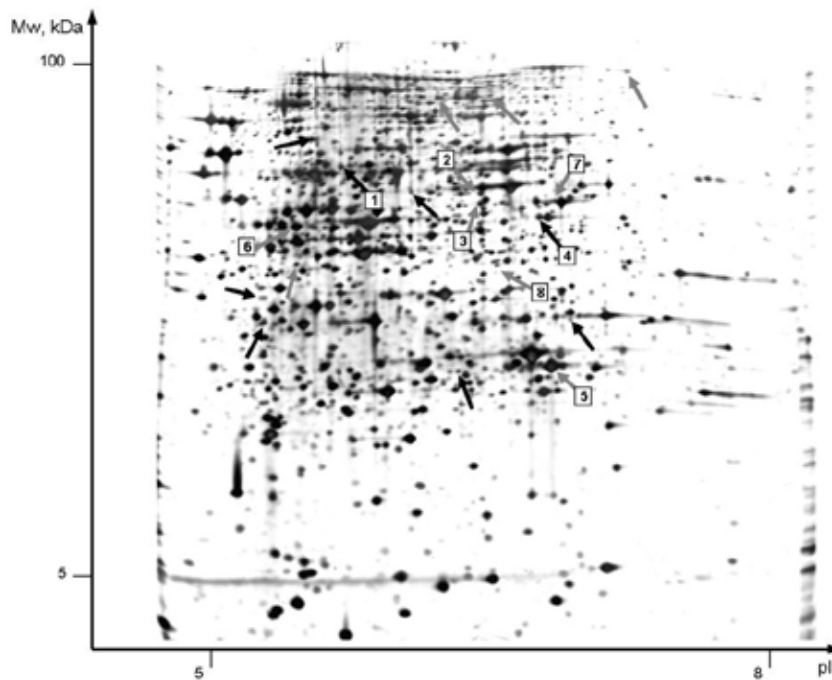


Fig.(6.3)20. Electrophoretogram of the E.Coli total protein after exposure to terahertz radiation. The black arrows indicate fractions with increased expression in the experiment as compared with the control sample and the gray arrows are for fractions with reduced expression. Numbers 1-8 designate identified fractions the expression of which differed more than two-fold as compared with the fractions of the control sample.

Mass-spectrometric identification

Mass spectrometric identification of peptides obtained for each fraction was performed with Ultraflex ToF ToF (Bruker Daltonics) by the MALDI method using  $\alpha$ -Cyano-4-hydroxycinnamic acid (CHCA) as a matrix. The identification of the composition of tryptic hydrolysates was performed using the MASCOT software and NCBI database. The identified proteins are listed in Table (6.3)2.

Table (6.3)2. Identified protein fractions of the E.Coli culture, the expression of which changed more than two-fold (increased or decreased) when the bacteria were exposed to THz radiation.

Fraction No.	Identified protein	Expression variance	Mw, Da	pI	Sequence Coverage	Score
1	Glutamine synthetase	increase	51871	5.26	47 %	77
2	Phosphoglucosamine mutase	decrease	47487	5.71	35 %	70
3	Glucarate dehydratase	decrease	49110	5.69	30 %	63
4	Cysteine desulfurase	increase	45061	5.94	48 %	95
5	Uridine phosphorylase	decrease	27142	5.81	76 %	142
6	Phosphopentomutase	decrease	44342	5.11	38 %	96
7	Serine hydroxymethyltransferase	decrease	45316	6.03	52 %	111
8	Threonine dehydratase catabolic	decrease	35210	5.75	69 %	116

*E.coli* has several systems that provide cell response to changes in environmental conditions. Signals coming from outside activate the corresponding gene network, which results in reprogramming of the transcription and development of an adaptive response, which in turn leads to correction of metabolism; in some cases, systems of the stress response are activated. At least five ways of response to external signals are described for *E.coli*: Bae, Cpx, Psp, Rcs, and sE, which provide a response to physical, chemical or biological (viral infection) influence and specific gene networks of stress responses: to heat shock, oxidative stress, etc. The identified changes in the *E.coli* proteome indicate both the activation and repression of certain metabolic fates under exposure of a living system to terahertz radiation. Bioinformatics analysis of changes in the *E.coli* proteome under the influence of terahertz radiation will make it possible to determine which gene networks are activated, and thus the targets influenced by terahertz radiation.

### 6.3.3 The second stage of Novosibirsk FEL

The creation and commissioning of the second stage of Novosibirsk FEL carried out with financial support from SB RAS integration Project No. 6/2006 “Development and creation of the second stage FEL”, RAS “Basic” Project for Basic Research No. 2.6.6.4 “Creation of the FEL for the terahertz and infrared ranges with an average power of up to 50 kW”, SB RAS integration Project No. 52 “Commissioning of the second stage FEL and development and fabrication of the elements of the third stage FEL”, State R&D Contract No. 02.740.11.0430 “Commissioning of the second stage of high-power free electron laser and the development of the elements of the third stage”, and RFBR Initiative project No. 09-02-12121-ofi\_m “Development of methods for measuring and controlling parameters of high-power terahertz radiation.”

The second stage of the free electron laser (FEL) is created for movement toward higher frequencies in the terahertz range. The world's first accelerator-recuperator (AR) with two tracks (i.e. with a four-fold passage of electron beam through the high-frequency cavities) was built and commissioned for creation of an FEL operating in the frequency range of 3 - 10 THz.

The full-scale AR uses the same accelerating RF structure as the AR of the first stage, but is situated, unlike the latter, in the horizontal plane (Fig.(6.3)21). Thus, it is not necessary to demount one to build up the other. Operation mode is selected via simply switching the bending magnets.

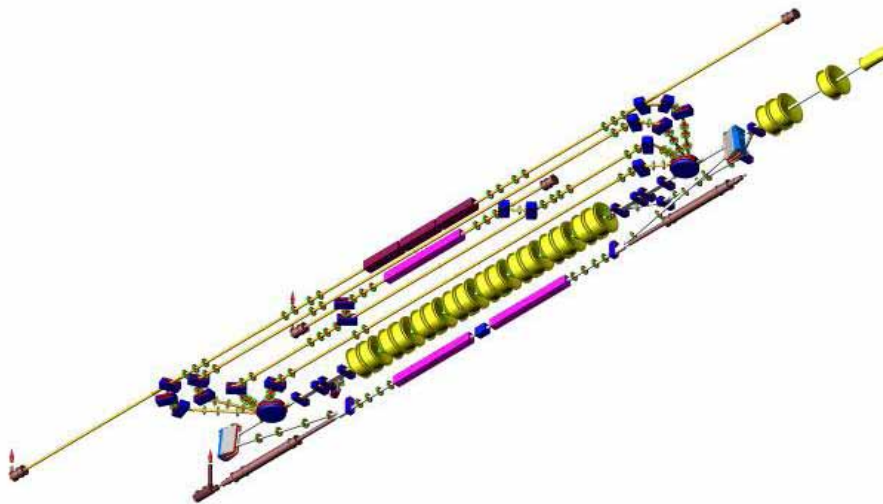


Fig.(6.3)21. Scheme of the full-scale 4-track accelerator-recuperator (plus one track in the vertical plane with the FEL for the THz range of 110-240 microns).

The second stage FEL is placed on the second track of the AR. We plan to install a high-power FEL for the near infrared wavelength range of 5 - 12 microns on the last (40 MeV) track of the AR.

The free electron laser operating in the wavelength range of 40 - 80 microns was created in 2009. The maximum average output power is about 500 W, which is a world record in that range. In 2010, radiation from the new free electron laser was delivered to the user stations, and experiments with its use began.

Because of the strong absorption of radiation in air it is necessary to pass radiation through pipes filled with dry nitrogen or evacuated to low pressure. The first variant is preferable because of the ease of extraction of broad beams of radiation to the user stations through thin polypropylene windows. The beamline for extraction of radiation from the second stage FEL (middle part) is shown in the figure. Radiation coming from below is reflected from two mirrors, gets into the “old” part of the beamline (in a distance) through the movable mirror assembly. Through the old part of the beamline, the radiation is delivered to the user stations. The emission spectra, pulse duration and average radiation power were measured. Radiation of the second stage FEL will be used in research in physics, chemistry and biology. In addition, the beamline that distributes radiation among the stations is additionally equipped with an extraction unit for installation of one station more.



Fig.(6.3)22. Radiation extraction beamline of the second stage FEL (middle part). Radiation coming from below is reflected from two mirrors and gets into the “old” part of the beamline (in a distance) through the movable mirror assembly.

The optical cavity for the FEL third stage was designed in 2010. The fabrication of the elements of the FEL third stage was completed.

### 6.3.4 Results of the year 2010 and plans for the year 2011

The main results of 2010:

1. Regular work of users was provided on the first stage THz FEL.
2. The radiation extraction beamline and users stations were upgraded; work on the creation of new user stations continued.
3. The radiation extraction beamline of the second stage FEL was commissioned.
4. The installation of the vacuum chamber of the third and fourth tracks of the accelerator-recuperator was completed.
5. The optical cavity for the FEL on the fourth track was designed.
6. A room was prepared for the test bench for the RF injector.
7. One RF generator of the AR was upgraded.

Plans for the year 2011:

1. Commissioning of the AR with four tracks.
2. Designing of the beamline for radiation extraction from the FEL on the fourth track.
3. Continuation of the work on the creation of new stations.
4. Continuation of the work on the designing and manufacturing of units of the test bench for the RF injector.
5. Continuation of the work for users.

## 6.4 Development and creation of specialized generators of SR

### 6.4.1 Superconducting wigglers

In June 2010, within the frameworks of the contract, the 119-pole wiggler with a period of 31 mm, magnetic field of 2.2 T and pole gap of 12.6 mm was delivered and assembled in the area of the ALBA-CELLS (Spain) storage ring under construction. Final tests of the cryogenic and control systems were carried out as well as a cycle of magnetic measurements of the wiggler. The spectral properties of the wiggler radiation at energies of up to 10 keV have an undulator radiation structure due to the low value of the undulator parameter, which equals 6. With increasing photon energy the spectrum turns into the synchrotron radiation spectrum.

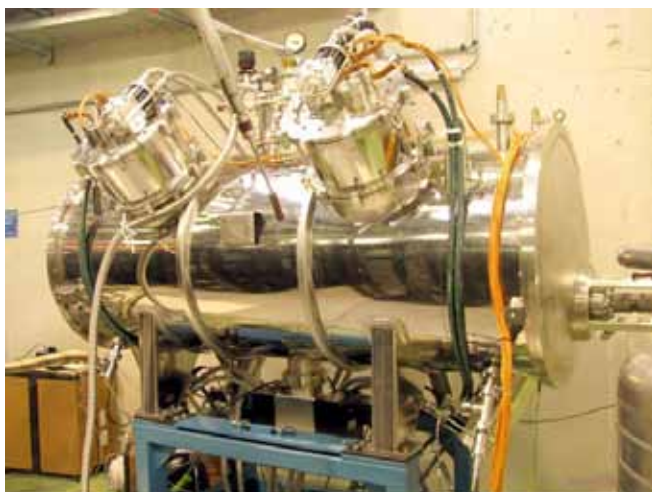


Fig.(6.4)1. Testing the 119-pole wiggler with a field of 2.2 T and a period of 31 mm on the ALBA-CELLS (Spain) storage ring.

Another distinctive feature of the wiggler is the use of a thin superconducting wire with a diameter of 0.55 mm with current characteristics that are unique for such a cross section (240 A in a field of 7 T). With such thin wire used, special attention was paid to the protection of the superconductor from burning and the output of energy in case of a superconductivity breakdown. The point is that the ultimate current parameters of the wire are achieved by reducing the cross section of copper, which is necessary for stabilization of the superconductor. A large number of superconducting coils connected in series imposed stringent additional requirements to the production quality and control procedures for each superconducting coil as well as the quality of electrical contacts between them. All 238 wiggler coils are connected in series so that the total heat release in the junctions does not exceed 50 mW at a current of 450 A.

The cryogenic system of the wiggler also has some particularities. The usage of gold-plated copper heat exchangers increased recondensation of gaseous helium and contributed to the supercooling of the liquid helium and the magnet to about 3.5 K. This is expected to provide as many as two years of reliable operation of the wiggler without servicing with zero consumption of helium. Besides, the pressure in liquid-helium vessel, which was reduced to about 0.5 bar, allows withstanding as many as three superconductivity breakdowns without helium release into the atmosphere.

The wiggler is planned to be installed and commissioned directly on the ALBA-CELLS storage ring in June 2011. Radiation from the wiggler will be used at the MSPD (Materials Science and Powder Diffraction) experimental station, working with radiation in the energy range of 10-50 keV. This energy range covers most experiments on powder diffraction measurement, scattering and diffraction at high pressures.

#### 6.4.2 Radiation-resistant dipole magnet for the ion accelerator under construction at GSI (Germany)

The international research accelerator center GSI is under construction in Germany. Russia actively participates in this center. BINP had designed and is constructing a dipole magnet for the Super-FRS, which is intended for extraction of secondary ion beams (secondary ions are obtained a target is bombarded with accelerated ions or protons) to the user stations. Since the dipole magnet is located after the target, the secondary ions have a large spread in angles and coordinates.

The dipole magnet has a pole gap of 0.18 m, effective magnetic length of 2.4 m, and bending radius of 12.5 m. The weight of the magnet is about 100 tons. The dipole magnet will be located in a zone of strong induced radiation and thus it must have no structural elements containing organic compounds.

The contract work on the development and manufacturing of the first (of three) radiation-resistant dipole magnet for the accelerator center GSI (Germany) was started in 2007 and completed in 2010.

The magnet was assembled as a whole by 2010. Magnetic measurements were conducted in 2010, by the results of which the poles of the magnet were finalized, which allowed us to attain the design field parameters. The dipole magnet retunes the magnetic field from 0.15 T to 1.6 T in 120 seconds. The magnetic field nonuniformity does not exceed  $\pm 2 \cdot 10^{-4}$  in the horizontal aperture of  $\pm 20$  cm throughout this range.



Fig.(6.4)2. Radiation-resistant dipole magnet at the bench for magnetic measurements.

### **6.4.3 Technological storage ring complex (TSC “Zelenograd”)**

A long training of the linear accelerator was completed by early 2009. That made it possible to increase the energy of electrons at the output of the linear accelerator (Linac) to 65 MeV and enlarge one-time capture of electrons into the small storage ring (SSR). After optimization of parameters of the power and control systems and debugging the software, the operation mode was achieved that allows accumulating up to 70 mA electrons in the SSR. Further increase in the accumulated current is associated with long-time degassing of the walls of the vacuum chamber with an SR beam. The regimes of raising the energy of electrons accumulated in the SSR to an energy of 450 MeV and bypassing electrons from the SSR to the beamline EOB-2 to the main ring were refined. The injection complex is ready to start work for the large storage ring.

Simultaneously with the works on the injection complex, the installation of the magnetic elements on the large storage ring (LSR) and the upgrade of the high-power sources were continued and completed.

In 2009, the vacuum system of the large storage ring was fabricated and assembled and its pumping out started. In addition, BINP fabricated an RF generator on new oscillating tubes as well as 180 MHz bi-metal cavities. Commissioning of the entire complex is planned for late 2010.



Fig.(6.4)3. Mounting the vacuum system of the large storage ring of SR source “Zelenograd”.

#### 6.4.4 Development of the new synchrotron radiation source for the Siberian Centre for Synchrotron and Terahertz Radiation

Works on the conceptual development of a dedicated SR source continued in 2010. Special attention was paid to the following issues:

- overall arrangement of the complex and engineering and user infrastructure;
- optimization of the magnetic structure of the main ring;
- development of a scientific program and research directions on this source.

Works on a preliminary design of the buildings and engineering and user infrastructure were carried out in 2009. It included the main specifications, layout of the buildings, and required amounts of resources as well as estimates of the construction cost.

The work on the designing of buildings within the unified concept of the Institute development continued in 2010. Previous drafts were slightly modified, which made it possible to effectively fit the complex in the BINP development concept and to avoid conflicts with construction plans of other complexes, while maintaining the overall functionality. The general view of the buildings for the new SR source is presented in Fig.(6.4)4.



Fig.(6.4)4. General view of the buildings of the new center for synchrotron radiation within the unified BINP development concept.

Besides, further optimization of the magnetic structure of the main ring of the SR source was underway in 2010. At the level of linear elements, the magnetic structure had been defined earlier. The main parameters of the ring are presented in Table (6.4)1 and the optical functions of superperiod are in Fig.(6.4)5.

The superperiod consists of three TBA cells; a superconducting dipole with a field of 8.5 T is the central magnet in the central cell. All other magnets are normal, with a field of 1.6 T. In total, there are 4 superperiods in the ring. This approach allows using magnets of different types in the main structure and provides a sufficient number of straight sections with a small dispersion function for accommodation of multi-pole devices for radiation generation (wigglers or undulators).

Table (6.4)1. The main parameters of the SR source storage ring.

Parameter	Value
Electron energy	2.2 GeV
Field in the bending magnets	8.5 T in the SC magnets 1.6 T in the normal magnets
Transition energy of SR quanta	30 keV for SR from the SC magnets 6 keV for beams from the normal magnets
Amount of the bending magnets	4 SC magnets 32 normal magnets
Angle of bending in the magnets	15° in the SC magnets and central 7.5° in the side normal magnets
Phase volume of beam(horizontal equilibrium emittance)	~ 5 nm · rad
Beam current	500 – 1000 mA

Beam lifetime	8 – 10 hours
Orbit circumference	214 m
Injection type	at full energy with the possibility of maintaining the working current of beam

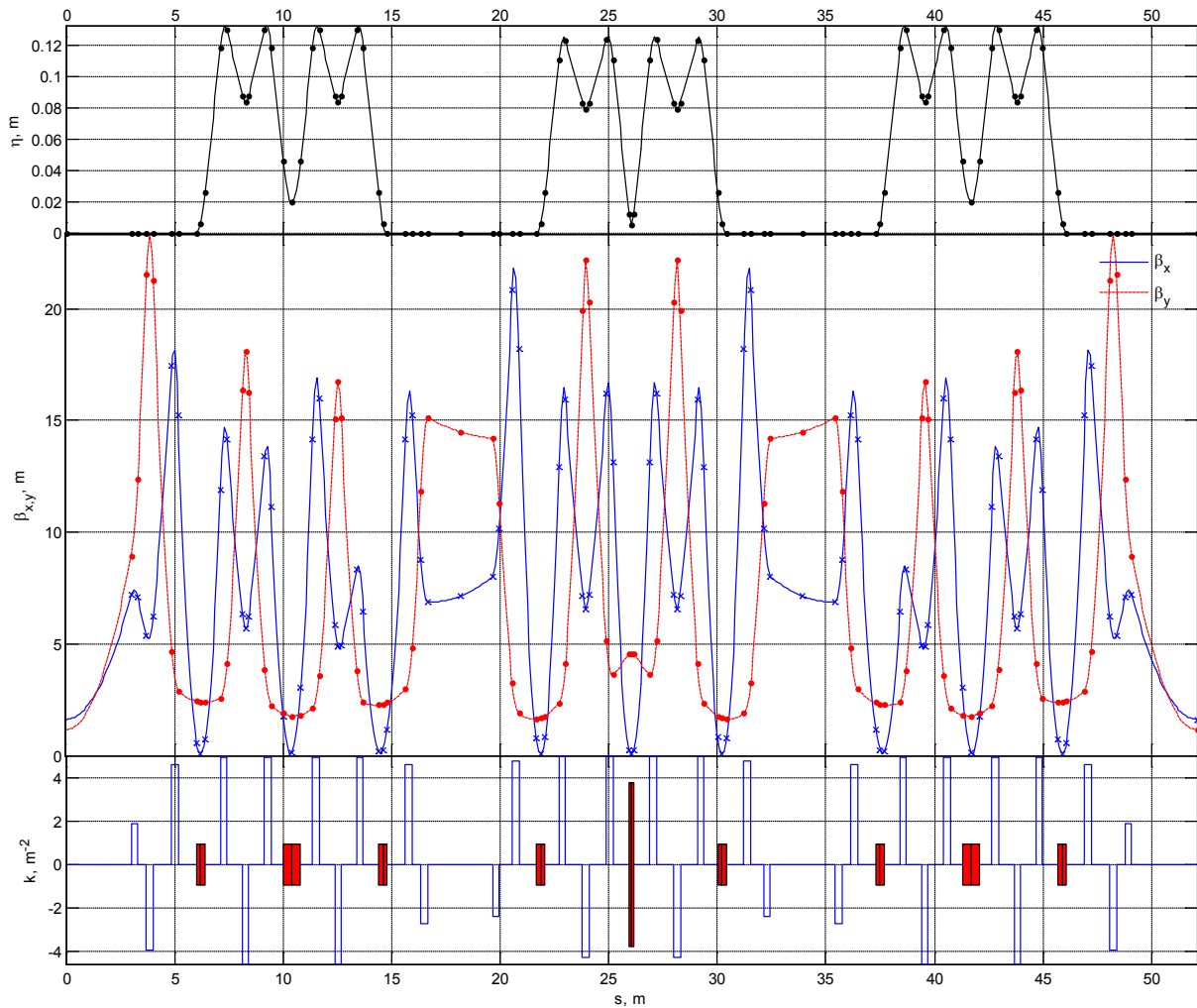


Fig.(6.4)5. Optical functions of the superperiod of the SR source.

The main goal of the optimization in 2010 were the nonlinear elements of the magnetic structure, which reduce the natural chromatism of the low-emittance structure while maintaining a sufficient dynamic aperture.

Standard approaches to chromatism suppression using sextupole lenses in this case do not provide effective suppression for technologically attainable values of sextupole gradients. This is due to the high rigidity of the system of quadrupole focusing and overall compactness of the structure, i.e. the lack of space for accommodation of a sufficient number of sextupoles.

In the course of the optimization it was proposed to use combined quadrupole-sextupole lenses. In this case, the efficiency of suppression increases substantially because the sextupole gradients are at the places of maxima of the beta functions. Thus, the values of sextupole gradient may be smaller than in the case of isolated sextupoles with the same degree of suppression. This, in turn, makes it possible to save a sufficient dynamic aperture.

The results of simulation of this approach give a hope for obtaining the required sextupole harmonics using small iron-free coils in the quadrupoles. It is also supposed to use a small number of isolated sextupoles for general correction. Optimization of the scheme is ongoing.

With the conceptual design of the source and new directions of scientific research on it in mind, a series of survey lectures on the SR application to different research areas was given at the SR-2010 conference. Based on these lectures review reports were formed that will be included in the scientific part of the conceptual design of the source.

#### **6.4.5 MARS at the RRC “Kurchatov Institute”**

In 2010 a decision was taken on the realization of the project "MARS" in the area of the RRC "Kurchatov Institute (KI)"; the project was discussed in detail within the frameworks of the Russian-German Workshop "Kurchatov Centre of Synchrotron Radiation and Nanotechnology" (18-19 February 2008, RRC KI, Moscow) and at the RSNE conference (2009).

There are plans to develop a project of the creation of a fourth-generation SR source "MARS" for the RRC "Kurchatov Institute" (under a contract with the RRC "Kurchatov Institute").

## **6.5 Conferences, meetings, seminars**

### **6.5.1 XVIII International Conference on Synchrotron Radiation application “SR-2010”**

XVIII International Conference on Synchrotron Radiation application SR-2010 was conducted on 19 to 22 July at BINP (such conferences have been held since 1975, once every 2 years). The conference was held with financial support from RFBR. The conference was attended by about 150 people. 45 of them came from different cities of Russia (Zelenograd, Irkutsk, Krasnoyarsk, Moscow, Pushchino, Rostov-on-Don, Snezhinsk, Tomsk, Russia, and Chernogolovka). 35 participants were representing institutions of Novosibirsk and Akademgorodok (besides BINP). The conference was also attended by 35 BINP members. 9 participants represented organizations from Germany (Institute for Synchrotron Radiation, Institute for Microstructure Technology, and DESY) and France (ESRF). 62 oral reports for about 25 hours in total were presented at the conference as well as 71 posters.

Traditionally, the conference covers all the issues associated with the generation and application of synchrotron and terahertz radiation. Scientific topics of SR-2010 are reflected in the list of sections: "SR sources and free electron lasers", "Apparatus for experiments with SR application", "Diffraction and Scattering", "Spectroscopy", "X-ray fluorescent analysis with SR application". A workshop dedicated to the discussion of the project of the fourth-generation SR source "MARS" was conducted within the frameworks of the conference.

That year the theme of the conference was formulated in accordance with the "Concept of SB RAS till the year 2020". According to this document it is planned to create at Novosibirsk Scientific Center a new up-to-date synchrotron radiation source, which should become an important element of the development of various branches of science. Therefore, a significant part of the plenary sessions of the conference was devoted to the formation of the scientific program of the future synchrotron radiation source, imposing additional requirements to the source, increasing the number of potential user groups, and providing support to the project. Leading scientists from different RAS institutes presented plenary talks about the most exciting developments in various fields of science, scientific tasks and possible use of synchrotron radiation to solve these tasks. Such approach to the conference program had fully justified itself – SB RAS members, which had free access to the BINP during the conference, were very active during the plenary sessions.

In addition, exhibitions and workshops of manufacturers and suppliers of scientific equipment were held during the conference. The following companies were presented: LeCroy Corp. (USA), MSH Techno (Russia), Scientific Equipment (Russia), and MICOS (Germany). These actions allowed the conference participants to become acquainted with the equipment and establish contacts with the companies.

The conference proceedings are being prepared for publication in an installment of the journal "Poverkhnost" ("Surface"). Articles submitted for publication are reviewed by experts engaged by the Organizing Committee. The oral reports are made public on the conference website: <http://ssrc.inp.nsk.su/SR2010/presentations/>.



Fig.(6.5)1. Opening of the Conference SR-2010.

### **6.5.2 International Symposium on the generation and application of terahertz radiation**

The International Symposium "Terahertz radiation: generation and application", combined with the School of young professional, was conducted in Akademgorodok on 26 to 28 July 2010. It was devoted to the fundamental and applied problems of terahertz radiation generation, recording and coherent interaction with different media. In fact, it was the first scientific forum in Russia completely devoted to this science area, which had started only in the last 15 years of the last century. Due to the known events, in Russia it was delayed by nearly 20 years.

This international symposium became possible due to the Russian terahertz community, which was initiated by both the "terahertz" sections of various laser and optical conferences and the first workshop "Generation and application of terahertz radiation", held 24 - 25 November 2005 in Novosibirsk. To a extent, the community appeared due to the financial support of this research area within the Fundamental Research Program of the RAS Presidium "Electromagnetic waves of the terahertz range"(2006 – 2009) and the Program for RFBR targeted basic research for 2009 - 2010 "Coherent interaction of X-ray, synchrotron and terahertz radiation with condensed media".

92 specialists took part in the symposium, including 12 participants from Germany, Britain, Japan, Korea, China, Netherlands and Ukraine. Its program consisted of a one-day plenary session, two oral sessions in parallel, a poster session and excursion to the free electron laser. Eleven 40-minute plenary lectures, six 40-minute keynote reports, twenty-eight 30-minute invited talks, seventeen 20-minute oral presentations and fourteen poster presentations were made.

An exhibition of the company TYDEX (St. Petersburg), manufacturing optical components and detectors for the terahertz range, was held during the symposium.

The poster session was held at the share-use center "Synchrotron and terahertz radiation" and combined with the excursion to the free electron laser. This laser, located at the Siberian Center for Photochemical Research, is the most powerful source of terahertz radiation in the world. Currently, there are six workstations. The participants of the symposium got acquainted with the accelerator-recuperator with two active laser cavities and equipment of the workstations available to users.



Fig.(6.5)2. Excursion to Novosibirsk free electron laser.

A collection of abstracts (ISBN 978-5-904968-03-8) had been published by the beginning of the Symposium. Selected articles based on papers presented at the Symposium are published in a special issue of *Vestnik NSU*, series Physics, as well as in the *International Journal of Infrared, Millimeter and Terahertz Waves* (Springer). After the Symposium a four-day tour to the Altai Mountains was organized, which was attended by about thirty people.

All the participants said the Symposium was a success. It allowed the researchers working in the field of terahertz radiation to obtain sufficient information about the research carried out at Russian and some foreign centers, to discuss these works in detail and to contact with people whose work seemed to be interesting. By the Symposium results it was decided to hold such forums in Russia every other year. The next symposium will be held at Moscow University in 2012.

### 6.5.3 School for Young Professionals “Synchrotron radiation in the Earth sciences”

The third Russian school for Young Professionals on synchrotron radiation was held at BINP on 11 to 15 October 2010. The previous schools were focused rather on the application of individual methods implemented at our share-use center: EXAFS-spectroscopy and X-ray analysis (2008) and diffraction methods (2009). This year we tried to concentrate on applying these methods to a specific area of science – “Synchrotron radiation in the Earth sciences”, in particular, to geochronology, petrology, and archaeology.

Schools for Young Professionals on synchrotron radiation are carried out for presenting the essence and possibilities of X-ray diffraction and spectroscopic techniques using synchrotron radiation. It is very important that interdisciplinary scientific contacts are started, which are especially necessary in younger years. Practical training within the frameworks of the school presents the experimental and methodological base of the Siberian Center for Synchrotron and Terahertz radiation (SCSTR). Synchrotron radiation has long been an integral part of the research infrastructure, providing the necessary knowledge for breakthrough technologies. The schools give young scientists working in various fields of science a new look at the object of their research. Regular schools allow young people to install reliable contacts with many scientists from leading research institutions of the Ural-Siberian region.

The schools students were 75 people, including 69 young professionals from Dubna, Ekaterinburg, Irkutsk, Krasnoyarsk, Novosibirsk, Snezhinsk, and Tomsk.

The school program included 23 academic hours of lectures and 40 hours of practical training. The lectures were delivered by 20 lecturers from among the senior research staff of the SCSTR, the Institute of Geology and Mineralogy SB RAS, and Siberian Federal University (Krasnoyarsk). Based on the materials presented by the lecturers, a collection of detailed abstracts of lectures was prepared, published, and distributed to all participants of the school.



Fig.(6.5)3. Students and lecturers of the School on synchrotron radiation.

#### **6.5.4 Conference of students and graduates working at the SCSTR**

The 9th Annual Conference of undergraduate and graduate students working at the Siberian Center for Synchrotron and Terahertz Radiation was held on April 26, 2010. The purpose of the conference was to familiarize the scientific community with the activities of the younger generation and train students and graduates in presenting their results. At the same time, the conference is part of the competition for BINP young professionals (Section of synchrotron radiation).

16 reports were presented, including 13 reports of NSU and NSTU students, 2 reports of BINP graduates I, and 1 report of a graduate of the Institute of Catalysis. The committee of the competition included both BINP members and representatives of other institutes participating in the Siberian center for SR. The committee noted the common high level of the submitted papers and awarded one first, two second and two third places (with diplomas and prizes). The conference participants were presented mugs inscribed with the symbols of the SCSTR.

#### **6.5.5 Participation of SCSTR members in other academic activities**

Scientific Session "BINP – 2010". BINP SB RAS, Novosibirsk, 15-16 January 2010.

The 4th European XFEL Users' Meeting, DESY, Hamburg, Germany, January 27-29, 2010.

Theoretical and practical conference: "Centers of share use of scientific equipment in the modern sector of research and development", Moscow, February 19, 2010.

THz-bio workshop, THz-Bio Application System Center at Seoul National University (SNU), Seoul, Korea, 9 March 2010.

X International Conference "Zababakhin scientific readings", "Russian Federal Nuclear Center – VNI-IEF", Snezhinsk, 15-19 March, 2010.

XFEL Working Group Meeting, Kurchatov Institute, Moscow, April 15, 2010.

European XFEL MAC meeting, 5-6 May 2010, Hamburg.

Workshop on the 50 Anniversary of DESY, Hamburg, Germany, 18-22 May 2010.

International particle accelerator conference IPAC 2010, Kyoto, Japan, 23-28 May 2010

International conference "Fundamentals of laser assisted micro-and nanotechnologies". (FLAMN-10), St. Petersburg - Pushkin, Russia, July 5-8, 2010.

New perspectives of high energy physics, 13th ISTC SAC seminar, Novosibirsk, Russia, 1-5 September, 2010.

35th International conference on infrared, millimeter and terahertz waves IRMMW-THz 2010, Rome, Italy, 5-10 September 2010.

VII Forum on the Interregional Cooperation of the Republic of Kazakhstan and the Russian Federation with the participation of the Heads of the States on "Cooperation in the field of sustainable development of high technology", Ust-Kamenogorsk, 7-8 September 2010.

Workshop "X-ray Optics – 2010", Chernogolovka, 20-23 September 2010.

VIII International Conference "Actual Problems of Electronic Instrument Proceeding" APEIE - 2010, Novosibirsk, September 22-24, 2010.

XXII Russian particle accelerator conference, RuPAC-2010, Protvino, Russia, 2010, Sept. 27 - Oct. 1.

Strategy of the development of large-scale research infrastructures of the Russian Federation and cooperation with the European Union: Third Intern. workshop, October 29, 2010, Nancy, France.

The 17th international symposium on laser spectroscopy, SOLS 2010, November 4-5, 2010, KAERI Daejeon, Korea.

3rd meeting of the European XFEL Machine Advisory Committee (MAC), Hamburg, Germany, November 11-12, 2010.

2nd JAAWS at PAL, Pohang, Korea, 28-29 November 2010.

Scientific session of the SB RAS General Meeting, Novosibirsk, December 10, 2010.

Scientific session of the RAS General Meeting of Sciences, Moscow, 13-15 December 2010.



7

RADIOPHYSICS  
AND  
ELECTRONICS



## Introduction

BINP work in the field of radiophysics and electronics is concentrated mainly at the Radiophysics Laboratory. The main tasks of the laboratory are associated with the development and research of radio-physical systems for accelerators and charged-particle storage rings, which, in turn, are developed by the Institute in accordance with the state programs “Colliding beams,” “High-energy physics,” “Synchrotron radiation,” “Physics of microwaves”, and “Plasma Physics”.

Under these programs, the laboratory staff is engaged in the development of various electronics: power, control, diagnostics, and computer control systems, RF accelerating systems and RF and SHF energy sources. We also study the behavior of charged particle beams in conjunction with accelerating systems and other elements and devices of accelerators and storage rings of charged particles. It is obvious that the main results of the activity of the laboratory are part of the common research results and works carried out on the existing complexes: VEPP-4, VEPP-2000, FEL, and the injection complex, as well as works in the field of plasma physics.

Due to the universal nature of some developments of the laboratory, some of them become a basis for the instruments and devices of independent scientific or technological value. Some developments are applied to and used in the Institute studies on other themes or in contracts with Russian and foreign scientific centers in the U.S., Germany, Switzerland, Japan, China, and South Korea.

Of particular interest are the contract works for CERN on the manufacture of LHC elements, which ended in 2008 – 2009; works for Zelenograd on the manufacture of the synchrotron radiation source, which will continue for another few years; works on the creation of the injectors of neutral atoms for the Tri Alpha Energy institution (TAE, USA). The activity on the TAE facility commissioning has already moved into a research stage, bringing new interesting contracts to BINP.

Below are briefly presented some results of the works conducted in 2010 and the key points of the works that will continue in 2011 and beyond.

## 7.1 Power supplies of electrophysical facilities

### 7.1.1 Stabilized current sources

Development of stabilized current sources for various electrical installations and some of their elements is one of the main tasks of the Radiophysics Laboratory. Devices of this class include, above all, DC power supplies for electromagnets for charged-particle storage rings. Depending on the task, the output current of such sources has a value of a few amperes to tens of kA. Correspondingly, the output power is tens of watts to hundreds of kilowatts and a few megawatts. The power sources usually have a wide range of current adjustment (up to 60 dB) and high accuracy of control and stabilization (an error of 0.01% or less). The current sources are complicated electrophysical devices with computer control, monitoring, and testing; with a complex system of locks and devices for internal control. The Russian industry produces no analogues.

In recent years, after long operation of power supplies and test equipment in the physical systems (accelerators and storage rings of charged particles), the electronics have become physically outdated and lost their features, which used to be the best. This inevitably leads to higher operating costs and forced outages of facilities, which has to be taken into account at planning the research and financial costs.

- The long-term work on the upgrade of the electronics of precise stabilized current sources (SCS) for powering electromagnets continued in 2010. Those are devices for a power of 50 kW, 100 kW and 200 kW with a thyristor regulator and a ripple damping channel. The power supplies are controlled by means of integrated single-channel 16-digit DACs (CEAC121); the current is measured with noncontact current transformers (DCCTs). Five stabilized current sources were upgraded in 2010. The upgrade included replacement of the electronics, intra-cabinet cabling and capacitor banks. 18 sets of control electronics for stabilized current sources were manufactured and adjusted in 2011, which provides upgrade of several stabilized current sources and thirteen sources of the B-1000 type (1000 A/ 20 V).

- The development, manufacturing and testing of the electronics and power units for devices for load current reverse in the stabilized current sources of the K-500 line continued in 2010 because the line is

designed to transport electrons and positrons to VEPP-2000 and VEPP-4. The electronics and power units have been installed in the stabilized current sources of the line and are waiting for their turn in the plan of start-up and mounting works at the complex.

- In 2010, the Low-Voltage Equipment Plant (Rasskazovo, the Tambov region) delivered to BINP four current sources (350A, power ranging from 50 to 200 kW) for powering the magnetic system of the facility for electron cooling of ions (the contract with COSY, Germany). The power sources were tested and prepared for work on the COSY stand at BINP. These sources are made in the Euromechanics racks. BINP designed and manufactured five sets of control electronics, also in Eurostandard, specifically for this program. The plant is to produce two other sources (2 kA, 60 and 120 kW) for BINP in 2011, also with our control and measurement electronics.

- The routine upgrade and maintenance of the main power supplies for BEP and VEPP-2000, which are megawatt-power devices with a current of up to 10 kA, continued in 2010. Besides, a stabilized current source (800A/23V) (manufactured in Rasskazovo) was put into operation on the magnetic measurement stand. Moreover, a current source with an output current up to 2.5 kA appeared on the stand as a result of the upgrade.

- The “Reverse” mode in the BEP power supply was refined.
- It should also be noted that the designing of the power supplies for the NSLS-II Booster dipoles began. This work will be performed in 2011 in cooperation with Danfysik, Denmark.

The development and commissioning of current sources with an output power of up to 10kW made by the Switch Mode Technology continued:

- Under a contract, reverse current sources for powering superconducting solenoids were supplied to the CryoMagnet company: two sources for  $\pm 300\text{A}/8\text{V}$ , and one source with current up to  $\pm 1000\text{ A}/5\text{ V}$ .

- The adaptation of the newly made power sources for VEPP-2000 continued. Those are 12 sources for 300A/8V for powering superconducting solenoids. Besides, in accordance with the needs of the complex, four dual current sources were used to increase the powering of four quadrupole lenses.

- Unipolar current sources with the maximum parameters of 300A/18V, designed to power the elements of the FEL magnetic system, had successfully fed the first stage of the FEL magnets, so in 2010 we continued the production of such sources for powering the magnetic system of the FEL second stage. It is worth recalling that five sources of this series were delivered to JINR (Dubna) in 2008 and had successfully operated at the complex IREN.

Note that each of these Switch Mode sources is equipped with two noncontact current transducers: one for stabilization and the other for independent measurements. Each current source is in turn equipped with a built-in control DAC/ADC module. The long-term instability of the output current of the sources does not exceed 50 - 100ppm.

- As part of the Switch Mode technology we continued developments extending the scope of application of the power unit designed for electron-beam welding. As a result, variants of 20-kilohertz converters with an output power of 10 kW, 15 kW, 40 kW and 60 kW appeared at the laboratory. These converters in conjunction with the output rectifiers and matching transformers provided the basis for the following developments, which started in 2009 and are in plans for future years:

- a bench for testing and adjustment of the column (COSY) power supplies was assembled;

- the COSY column power supply for 60 kW, 500 V, and 20 kHz was assembled and tested. The source was tested at an output power of up to 60 kW. It allows a long term work at power up to 50 kW. It is under elaboration for operation at a power of 60kW and more. The source is made in a 5-level 19 Euromechanics rack by a modular principle. The source will be installed on the COSY cooler at BINP in 2011, with subsequent delivery to Germany.

- 2 current sources for 1000A and 30 kW, which also operate at a frequency of 20 kHz, were developed and are under assembling now. Tests of them are planned for 2011.

- Under the contract with BNL (USA) we designed and submitted to the workshop elements of the power supplies for the quadrupole lenses for the booster.

- New developments of power supplies for relatively «low-power» (50 kV, 15 kW and 30 kW) ion injectors were begun: the design was completed and parts were ordered.

The development, improvement and manufacture of small series of relatively low-power current sources feeding correcting magnets or special devices continued.

- The manufacturing and adjustment of a complete set of current sources for powering the correctors of the technological storage-ring complex (TSC) were completed. About 40 channels (two cabinets) were delivered to Zelenograd in 2010, which completes the supplies (about 200 channels for 5A/30V). The system is waiting for the installation of the TSC magnetic system and cabling.
- A set of 11 MPS-20-100 current sources ( $\pm 20\text{A}/100\text{V}$ ) for powering the TSC multipole lenses and 3 MPS-20-50 current sources ( $\pm 20\text{A}/50\text{V}$ ) were also sent to Zelenograd in 2010.
- About ten channels of 20A sources are to be delivered to the Injection Complex in 2011, which will begin the replacement of the morally and physically outdated current sources TIR-25.
- Power supplies for the correcting magnets for the COSY project were designed and manufactured and are being tuned now. Those are MPS (6A) sources for about 50 channels and eight current sources with an output current of up to 20A, six of them being «shunt» sources.
- Power supplies for correctors for the K-500 beam line were put into production.
- About 20 channels of bipolar power sources of the UM-1, UM-3 and UM-10 types with output currents of 1A, 3A, and 10A, respectively, were manufactured and put into operation. The sources are installed on the FEL, EBW, and LIA complexes. About 50 channels more for powering the correctors were put into production and will be installed on the cooling storage ring and linac of the injection complex in 2011.

### 7.1.2 High-voltage sources. Electronics for diagnostic and heating injectors of neutral atoms

Recent developments in the field of diagnostic and heating injectors of neutral atoms created a significant demand for them from foreign centers engaged in plasma physics. This, in turn, intensified the development, manufacturing and supply of injectors with the complete powering system and the computer control and monitoring system.

Below is given a partial list of such works in 2010.

1. It is sometimes difficult to separate the development of electronics and the designing of the injector itself. Two sets of power and control electronics for the “heating” injectors for the tokamak “Compass-D” (IPP, Prague, Czech Republic) were made and transferred to the customer for operation. Parameters of the main power supplies are given below:

High-voltage power supply: 40kV/15A/500 ms.

Power supply for the lock grid: 500V/10A/500 ms.

Current source for the bending magnet: 400V/500A/25 ms.

2. The electronics of the high-voltage power supply for the four “heating” injectors at TAE (U.S.) were commissioned and upgraded. The main goal of the upgrade was ensuring operation of atomic injectors without expensive motor generator. The duration of the injector duty cycle was reduced from one second to eight milliseconds, which allowed us to use the already existing energy storage units.

achieved after the upgrade: 20kV/60A/8 ms.

3. A conceptual design of a high-voltage power supply for an injector of negative ions was developed in 2010.

Energy of negative ions: up to 1 MeV

Beam power: up to 3 MW

4. The designing and manufacturing of a high-voltage power system for a stationary injector of negative ions started.

Ion energy: up to 120 keV

Current: up to 30 mA

### **7.1.3 High-voltage sources. Power electronics for electron beam welding (EBW)**

In 2010, we together with the NITI “Progress” (Izhevsk) continued the implementation of energy units and EBW modules at enterprises of the country. Currently, six EBW modules with our power-generating units operate at Russian enterprises. One unit is in use on a BINP stand.

At the same time, we continued developing and manufacturing components and assemblies as well as their power supply systems, and monitoring and control systems for electron beam welding modules and associated applications.

- A high-voltage power supply for a new injector of the FEL (100mA/150kV) was designed and assembled. The high-voltage column was made on the basis of multiplier with a working frequency of 20 kHz. The source will be installed on the FEL in the first half of 2011.

- We continued the upgrade of EBW modules with an output power of 60 kW, 30 kW, and 15 kW for future contract works. In particular, we started developing a 5 kW energy unit.

- In 2010, under the contract with COSY, we developed a power supply for the electron collector in the high-power column of the cooler. The power supply for 3A/5kV is in the high-voltage terminal of the high-voltage column. The power supply is made as five sections with an output voltage of 1 kV; the sections are connected in series at the exit. At the entry, all the sections are fed in parallel from the transformer line of the column. Four of the sections are unregulated converters, which can be enabled or disabled, and one section is a regulated converter. Control is realized through an optical channel. The power supply was assembled and tested and will be put into operation in 2011.

- An upgraded high-voltage power system for the source of negative ions was put into operation. That is several controlled precision stabilizers with a voltage of up to 40 kV and a power of up to 2 kW. The work will continue in 2011, aiming at optimal beam parameters.

- In the late 2009 and early 2010, we continued the developments for K-500 (electron and positron transport lines), which resulted in the production of 25 switched power supplies (generators) for the magnetic components of the lines. The power supplies work with a cumulative capacitance of 100 microfarad, a maximum voltage of 700 V and pre-selection of the current pulse polarity. The operating frequency is 1 Hz. The monitoring and control are realized via the CEAC124 controller. The electronics are realized in the “Euromechanics” standard.

- Another variant of pulse generator was designed for the LIA focusing system. Six generators were manufactured and installed on the LIA.

It should also be mentioned that in 2010 we continued the maintenance of earlier manufactured systems and their components in use on facilities of the Institute and outside it.

## **7.2 Development of measuring systems and devices for automation of physical experiments**

The contribution of the laboratory to the automation of facilities, stands and large physical complexes consists in the following:

- development and delivery of complete systems (monitoring, control, diagnostics, and computer systems) with subsequent participation of the authors in the adaptation to physical facilities;

- development of elements for control, monitoring, and timing of power systems with subsequent comprehensive delivery of these systems to accelerators and storage rings of charged particles and study of their effect on the complex as a whole;

- delivery of standardized individual modules (CAMAC, VME, «Vishnya», Euromechanics) to existing or new installations and stands;

- development of new approaches, techniques, and, thus, new devices that address physical experimental tasks at a new level;

- upgrade of the existing systems for automation, control and diagnostics on operating physical facilities;

- repair and maintenance of several thousand units of electronics and complete systems designed and in use.

The equipment designed and manufactured at BINP is widely used both at the SB RAS and at many scientific organizations in Russia and abroad. The nomenclature of the manufactured devices makes up a few dozen types of digital, analog and digital-analog mixed signal devices, units or modules.

- 100 various units with the CAN-BUS interface for control and monitoring systems for electro-physical facilities were fabricated, adjusted and put into operation. Two new modules appeared in 2010: VSDC2, a two-channel meter of instantaneous values and shapes of pulsed magnetic fields, and IVI1811, a two-channel meter of nanosecond time intervals. A detailed description of the modules is available on the site of the laboratory.

- It should be noted that devices of this family are widely used in contract works. In recent years, more than half of the modules produced (900 pieces in total) along with various power sources and measurement and control systems were supplied to JINR (Dubna), KISR (Moscow), TSC (Zelenograd), NITI “Progress” (Izhevsk), KAERI (South Korea), and IMP (China).

- The Institute intensely exploits several systems for different magnetic measurements based on the new-generation equipment that enables high-precision measurements of fields both with Hall-probe matrices and movable coils. A measurement set includes the following:

- a precision ADC with a built-in analog switch;
- a 32-channel switch with a switching error of 1  $\mu\text{V}$ . For work with Hall sensors, the module is equipped with a high-precision (0.001%) current generator;
- a precise digital-output integrator.

Table (7.1) 1. The family of devices with the CAN-BUS interface.

Name	Brief characteristics
CANDAC16	16-channel, 16-digit DAC; 8-bit input/output registers
CANADC40	40-channel, 24-digit DAC (of the 0.03% class); 8-bit input/output registers
CDAC20 CEDAC20	20-digit DAC; 5-channel, 24-digit ADC (of the 0.003% class); 8-bit input/output registers (“Vishnya” and Euromechanics)
CEAC51	20-digit DAC; 5-channel, 24-digit ADC (of the 0.003% class), 8-bit input/output registers (Euromechanics 3U standard)
CAC208 CEAC208	8-channel, 16-digit DAC; 20-channel, 24-digit ADC (of the 0.003% class); 8-bit input/output registers (“Vishnya” and Euromechanics)
CEAC124	4-channel, 16-digit DAC; 12-channel, 24-digit ADC (of the 0.003% class); 4-bit input/output registers (Euromechanics 3U standard)
CEAC121	1-channel, 16-digit DAC; 12-channel, 24-digit ADC (of the 0.003% class); 4-bit input/output registers (Euromechanics 3U standard), designed to control fast power supplies
CEAD20	20/40-channel, 24-digit ADC (of the 0.003% class); 4-bit input/output registers (Euromechanics 3U standard)
CGVI8	8-channel, 16-digit generator of delayed pulses; 8-bit input/output registers
CPKS8	8-channel, 16-digit code-duty factor converter
SLIO24	CANbus interface: a 24-digit two-directional bus and built-in board
CKVCH	Commutator of RF signals 8-1, 2*(4-1), 4*(2-1)
CANIPP	CANbus interface: 2 branches of the BPM type
CANIVA	16-channel vacuum meter (ion pump current)
CURVV	multi-purpose input/output register (2 output and 4 input 8-bit registers)
CIR8	register of discrete signals (interruption register, BSI, input/output registers)
CAC168	8-channel 16-digit DAC; 16-channel, 24-digit ADC (of the 0.03% class); input/output registers; built-in board
CAN-DDS	the CAN-DDS module is a divider of input clock frequency with remotely tunable fractional coefficient
CAN - ADC3212	for closing the feedback circuit in the thermal adjustment scheme of RF cavities
CANGW	Ethernet-CAN/RS485 gateway
VME-CAN	VME-CAN interface
CEDIO_A	multiport input/output register
GZI-CAN	4-channel generator of delayed pulses, 80 ns – 10.28 $\mu\text{s}$
VSDC2	module for precise measurement of magnetic fields by the induction method, 2 channels
IVI1811	time interval meter with a resolution of 0.5 ns

- The electronics for the stand for magnetic measurements of the NSLS-2 quadrupole lenses were designed, manufactured and put into operation. The new software was created for the stand. Unlike previous designs, the stand equipment allows making the error of measurement of the multipole components better than  $10^{-5}$ .
- Magnetic measurements of the GSI radiation-resistant magnet manufactured in 2009 were carried out. For the first time, the coordinates of the carriage were found using a laser interferometer and specially designed electronics.
- A batch of VSDC2 modules intended for the measurement of instantaneous values of pulsed magnetic fields in the lines of the accelerator storage complexes of BINP was made. Now they are being tested on VEPP-2000. This device is to replace the outdated BIIP-4 module.
- The control system for the linear induction accelerator (LIA) for pulsed radiography was put into operation. This control system, made on the basis of the up-to-date Compact PCI standard, ensured the successful commissioning of the accelerator in November 2010.
- PCI modules of 5 types for control of the linear induction accelerator were designed and manufactured in the required quantities.
- For replacement of the high-cost carriers of PMC boards needed in large quantities for the LIA control system, we developed our own module, which is fully compliant with the Compact PCI standard. The required quantity of the modules was produced, adjusted and installed in the LIA control system.
- The software of the power supply control units on VEPP-2000 was upgraded, which allowed us to simplify the process of current alteration in the magnetic elements of the storage ring.
- The control system for the electron gun and beam line was delivered to the customer and put into operation under the contract on the upgrade of the ion cooler on the IMP (Lanzhou, China). The system comprises about 20 electronic modules, including fast high-voltage formers (3 kV) with adjustable amplitude. The new electronics modulate the energy of the cooling electron beam.
- A set of modules of control electronics for the electron gun of the ion cooler for COSY was made and tuned.
- A prototype electronic system for tuning the magnetic field of the ion cooler for COSY was manufactured and tested. The development of two variants of the electronics – with manual and computer-aided control – was begun.
- As part of contract work, the laboratory participated in the designing of the control system for the NSLS-II booster.
- Works on the creation of the control system for the 4-track FEL were continued.
- The development of the timer (90 MHz) for the new modulator of the injector gun started.
- The development of the new generation of power supplies and modulator for the electron gun of the free electron laser injector was continued.
- The work on the implementation of up-to-date intelligent controllers in control systems for physical setups was continued. Another batch of controllers and CAN-Ethernet gateways for various installations of the Institute was made.
- Using up-to-date hardware components, we designed a precise (0.002%) interpolating DAC with the MIL-STD-1553B Interface to replace the outdated power equipment of the main magnetic elements of VEPP-4. The software and hardware of the module are compatible with the previous outdated design. The required quantity of modules was manufactured, adjusted and installed.
- The firmware of the port multiplexers for the data acquisition system on the CMD-3 detector was tested under actual operating conditions and corrected.
- 3 sets of control systems for neutral beam injectors (the diagnostic and heating variants of injectors) were delivered and commissioned. The systems are based on commercially available components. The software is unified for both versions of injector and enables integration into the overall control.
- A new power supply was developed for electron beam welding modules, with the possibility of indirect electron-beam heating of the cathode. The aim of this development is to create a cathode with a significantly larger lifetime.
- The first experiments on the measurement of the transverse beam size in electron beam welding modules were conducted. The results showed that the measurement system is stable and can be used for the operational control of the electron beam parameters.
- The matrix TC237 CCD was tested in the modes of rapid accumulation of images (0.25 - 1  $\mu$ s per image). A special optical bench was developed for testing the temporal and spatial resolution in these

modes.

- A high-voltage (10 kV) linear amplifier on transistors was developed and tested. This development greatly simplifies the control electronics of electrostatic devices of physical facilities (BINP Preprint 2010-32).
- The time interval meter in the nanosecond range with the CAN-BUS interface was put into operation on VEPP-2000. The device is designed to monitor the performance of the “injection-extraction” systems.
- The development of the two-channel meter of ultra-low currents for ionization chambers was continued.
- The development of the system for monitoring the main parameters of the heat pump used in the cooling system of accelerator complexes started.
- Three sets of new electronics for VEPP-4 pickups with specially-designed software were manufactured and put into operation. The new electronics can distinguish bunches near the site of meeting and measures bunch displacement with high accuracy.
- A full set of electronics for the measurement of the orbit and betatron frequencies for the TSC was made. Part of the equipment was sent to the TSC.
- Prototypes of all of the electronic units for the COSY pickups were designed, manufactured and tested. A series of units for 12 pickups is under production. The pickups are being measured on the stand.
- A prototype unit for signal processing for the betatron frequency measuring system for the NSLS-II booster (BNL) was designed and manufactured.
- The development and manufacture of the RF power amplifier (4 MHz) for plasma heating were completed. The amplifier was tested at a purely resistive load and an “antenna”. With an 8 kW output power of the amplifier at purely resistive load we received 5 kW, which is estimated as a rather good result.
- A prototype of a new precise, “pickup”, electronics for VEPP-3 and other storage rings was designed and manufactured. VEPP-3 is supposed to be equipped with it in 2011.
- Equipment for selective depolarization of individual electron bunches for VEPP-4 was manufactured and put into operation.
- The electron and positron beam lines for the transverse feedback system designed to suppress betatron oscillations of beams on VEPP-4 were put into operation. The equipment was tested on all the available beam currents at energies up to 2 GeV. The elaboration of various operation modes of the system will continue – at rising energy, at betatron frequency measurement, and at operation with a large number of bunches (up to 8). The creation of the software interface of the system started late in 2010, with the participation of the complex staff.
- The second block for amplitude-phase measurements at the injection complex was tuned. At the end of the year, we participated in the resumed work on the upgrade of the elements of the existing RF system scheme.
- We continued the adjustment of the FEL beam diagnostics systems for the third and fourth tracks, and, subject to the beam orbit measurements, of the whole complex.
- New blocks for signal matching and fast protection for the modulator of klystron 5045 were developed and are now being installed on the injection complex.
- 12 capacitive and 12 ultrasonic hydrostatic sensors, upgraded from the previous version, were manufactured and delivered to the University of Montana (USA). The system is equipped with its own software. 10 capacitive hydrostatic sensors were delivered to KEK (Japan) under a contract.
- A large part of the work on the manufacturing of 18 hydrostatic capacitive vertical displacement detectors for SLAC (U.S.) was completed. The detectors will be sent to the customer in 2011.
- The development of the laboratory site <http://www.inp.nsk.su/activity/automation/index.ru.shtml> continued. This site should contribute to a fuller and more correct use of the laboratory developments. For this purpose, manuals (application notes) were added to the descriptions of various modules. The site is updated regularly.

## 7.3 Research related to the modeling and solution to electrostatic and electrodynamic problems of accelerator physics

1. Work on the further development of programs for calculation of electrostatic and magnetostatic fields and electron and ion guns continued, including the following:

- The algorithms of the ExtraSAM program, which allows calculations of axially symmetric electron- and ion-optical systems taking into account the space charge and thermal spread of the transverse velocity of beam particles, were upgraded. Besides, the emission of an intense beam of charged particles in RF fields was simulated in a low-frequency approximation.
- The MAGEL3B program for the calculation of three-dimensional beam transportation systems with pre-calculation with the ExtraSAM and MAGEL3D programs and taking into account the space charge and thermal spread of the transverse velocity of beam particles was improved.

2. Works on the numerical calculations, modeling and designing of electron guns, electron and ion beams, and magnetic systems were conducted including the following:

- Under a contract with the TAE laboratory (U.S.), using the ExtraSAM, MAGEL3D and MAGEL3B program we continued the calculation of the system for formation, acceleration and transport of a 10 A quasi-stationary ion beam with a power of 10 MW, taking into account the transverse temperature and beam space charge. The system includes a large number of magnets and electron-optical elements of complicated design.
- In the framework of the BNCT project and using MAGEL3B, we selected parameters of the magnetic elements of the high-energy proton-beam transport channel. We achieved a good agreement between the results of calculation and measurement of the size of non-scanned and scanned beam on the neutron target of the installation.
- In the framework of the contract on the supply of 100 kW industrial RF accelerator ILU-14, using the ExtraSAM program we simulated the internal injection and dynamics of electron beam in the accelerator, taking into account the beam space charge. We showed the possibility of injecting and passing beams with an energy of 7.5 MeV and 10 MeV and the required capacity of 100 kW through the accelerator structure.
- Under the contract on the creation of a powerful source of neutral particles, we carried out simulation and optimization of magnetic field in a plasma charge-exchange target.
- Under the contract on the creation of the high-voltage electron-cooling installation for COSY, we developed the electron gun and collector. The electron gun is able to control the current density distribution for optimization of the electron cooling process, while maintaining a moderate transverse temperature of the beam.

## 7.4 RF generator for the resonance electron accelerator based on a coaxial resonator

Within a few recent years the Federal State Enterprise Russian Federal Nuclear Physics Center All-Russian Research Institute of Experimental Physics (RFNC-VNIIEF) has worked on the designing and development of a high-power irradiation complex on the basis of a resonance electron accelerator with a wide range of output electron beam energy (1 to 8 MeV) and an average power of 300 kW. A half-wave coaxial resonator is the accelerating structure of the projected facility. At the stage of prototyping the facility for attaining electron beams in the given energy range with currents around 1 mA, the high-frequency generator that was designed and manufactured at BINP will be used as the RF power system.

### The main technical parameters of the RF generator

Operating frequency range	98 ... 102 MHz
Maximum output power	180 kW

Output power adjustment	0 ... 100%
Operation mode	continuous
Wave impedance of the output feeder	50 Ohm
Diameters of the coaxial feeder	160 x 70 mm
Net efficiency of the generator	40% or more
Parameters of the supply mains	3-phase voltage 380V/50 Hz

The RF generator includes a three-stage power amplifier, the power supplies of the anodes, screen and control grids, and heating of the tubes and the system controlling the accelerating voltage amplitude. The output stage of the amplifier is made on the powerful generator tetrode GU-101A; the GU-92A tetrode is used in the intermediate stage. The first amplification stage is a semiconductor one. Each stage is a separate shielded module of open mounting, i.e. without cabinets. Excitation for the output stage up to 10 kW comes from the intermediate stage by a hard coaxial feeder. The anode power supply of the RF generator consists of three sections integrated in one unit. The rest power supplies of the tube stages are mounted in the control rack of the RF generator. The control system is located in the crate of the control rack.

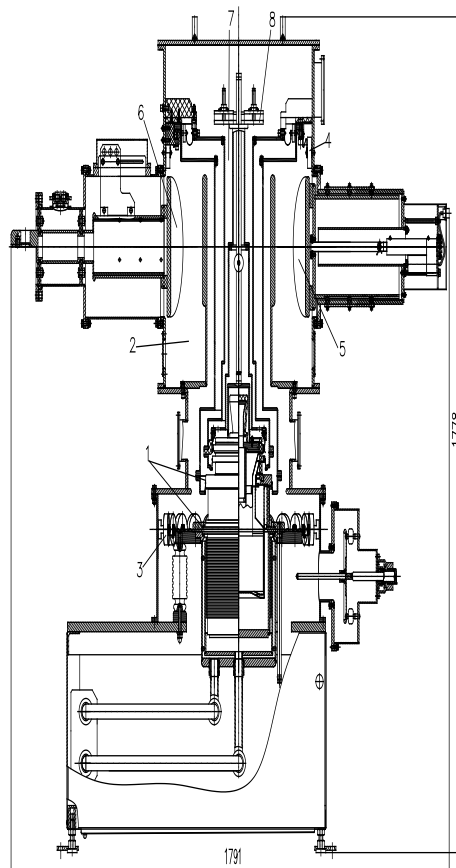


Fig.(7.4)1. The structural scheme of the output stage of the RF generator.

The output stage of the RF generator is assembled on the GU-101A tetrode in a common-grid circuit. The structural scheme of the output stage is shown in Fig.(7.4) 1. Output cavity (2) is a single parallel oscillatory circuit (anode circuit) designed as a long line with a TEM-type wave generated by the series connection of coaxial line segments with a total length of  $\frac{3}{4}$  of the wavelength. One end of the line is connected to the leads of the anode and screen grid of tube (1) and the second end is short-circuited. The characteristic impedance of the equivalent resonant circuit is 3.9 Ohm. The unloaded Q factor of the circuit is around 3000. The loaded Q factor is 85. Blocking capacitors (3) and (4) separate the constant potentials of the anode and screen grid of the tube from the grounded housing.

Plunger (5) tunes the anode circuit to resonance with the working frequency. A remote-controlled mechanism moves the plunger, which changes the capacitance introduced in the anode circuit. The coupling with the load is a capacitive one. Moving plunger (6), one can change the coupling capacitance. The coefficient of coupling of load with the anode circuit is set such that the tube operates within allowable modes at actual values of load resistance and output power. The absence of sliding contacts in the plunger increases the reliability of the generator operation.

Input cavity (7) is also a single parallel oscillatory circuit consisting of segments of coaxial lines that are loaded from one end with the capacitor between the cathode and control grid of the tube and from the other, with the structural capacitor of plate (8). The equivalent length of the cavity formed by these elements is equal to  $\frac{1}{2}$  of the wavelength. The electrodes of the tube are fed through RF filters.

A directional coupler (DC) for measuring the coefficient of reflection from the generator load is installed in the output coaxial feeder.

For efficient control of the build quality of the assemblies connecting the tube with the resonant circuits of the stage, the stage is structurally divided into two main parts. The first part, which includes the tube with the contact spring crowns, water tank and some of the RF units, is assembled outside the body of the stage. This provides a good visual monitoring of the contacts that are adjacent to the electrodes of the tube. When this part has been assembled, a lifting mechanism descends it into the second, stationary, part, and the stage is assembled as a whole.

The pre-exit stage is equipped with the GU-92A tetrode, also in a common-grid circuit. The stage is excited from a semiconductor amplifier with a maximum capacity of up to 500 Watt through a RK50-9-12 flexible coaxial cable. The stage is equipped with a mechanism for tuning of its resonant frequency and has the option of adjusting the coupling of the stage with the load, i.e. with the input circuit of the output stage of the generator. Both the adjusting elements are operated manually.

The semiconductor amplifier is used to excite the intermediate tube stage. The amplifier includes two stages; both the stages use a push-pull circuit. The first amplification stage is collected on domestic field-effect transistors (FET) KP923A; the output stage uses an IXZ2210N50L dual FET made by the IXYS Semiconductor company. At a maximum input signal power of 3 W and a frequency of 100 MHz, the amplifier output power is 500 W at a load of 50 Ohms. The excitation to the input of the amplifier comes from the controlled amplifier in the control rack with the crate for the electronics controlling the cavity RF voltage. The semiconductor amplifier is cooled with water.

The power supplies of the control grids and tube heating, electronics units of the run/stop system, interlocks, protection, control of operation (locking and signaling control, LSC) and the RF excitation of the generator are placed in a cabinet installed next to the tube stage. The LSC circuit is realized on the programmable logic and has the option of remote monitoring and control. The high-voltage power supply applies voltage to the anodes and screen grids of the amplification tubes (tetrodes) of the RF generator and provides rapid de-energization of the tetrodes in case of breakdown in the tubes and circuits of the RF generator.

#### Parameters of high-voltage power supply:

Limit values		GU-101 anode	GU-92 anode	Screen grids
Output no-load voltage	V	14000	7000	1200
Rated voltage	V	12600	6000	1120
Maximum average output current	A	28	4	2
Maximum effective value of the output voltage ripple	%	1	2	0.5

The anode rectifier is a controllable high-voltage source with the input controlled by a thyristor regulator. The source works at the supply-line frequency. Adjustable voltage arrives at the input of the step-up transformer. From the output of the transformer, high voltage is supplied to the diode rectifier connected in the Larionov circuit. Supply-line ripple of the rectified voltage is filtered by LC filters. An in-series RC chain suppressing the spill-out of the filter at a resonant frequency of 30 Hz is connected to the filter of the 14 kV source.

For prevention of destruction of the generator tubes at breakdowns, the 14 kV anode rectifier is equipped with protection, which de-energizes the anode of the tube in less than 50 microseconds.

The power supplies of the anodes and screen grids of both the tubes are housed in four cabinets, which

are mechanically interlinked to provide air cooling from the built-in fan. The anode transformer TSGL 400 – a supply dry-type three-phase transformer with Geafoil cast insulation – is installed inside these cabinets.

The generator is powered from a three-phase supply line of 380V/50Hz. At a maximum output power, consumption is 400 kW and current in each phase is 600A. The built-in fan cools the anode power supply. The heat release is  $\sim 9$  kW at an output power of 400 kW. The overall dimensions of power supply are (W  $\times$  D  $\times$  H) 3300  $\times$  800  $\times$  2100 mm. The weight is  $\sim 3000$  kg.

The RF control system stabilizes the amplitude of the accelerating voltage of the cavity, retunes the master oscillator of the system so that the cavity is tuned to resonance and provides safe operation of the generator by means of locks and protections. The feedback circuit provides stabilization of the amplitude of the RF voltage of the cavity. The signal Urez from the measurement circuit of the cavity (Fig. 2) comes to the amplitude detector of the modulator. The rectified voltage is compared in the modulator with the external constant reference voltage. The amplified error signal controls the gain of the controllable amplifier. Parameters of the error signal amplifier and feedback circuit are selected so as to ensure a relative stability of the amplitude of the accelerating voltage of the cavity of at least 0.1%.

The second amplitude detector converts the RF signal I<sub>feed</sub> from the current sensor of the power-input circuit of the cavity installed in the feeder line to a constant voltage. This voltage is used in the modulator if for some reason the cavity is detuned. In so doing, the modulator limits the increase in the current of the power-input circuit and power of the RF generator to a safe level.

The second feedback circuit controls the frequency of the master oscillator of the system (50 MHz exciter). To this end, signals from the measurement circuit of the cavity together with a signal proportional to the current of the cavity circuit are transferred to the input of 100 MHz phase-meter. The output of the phase-meter controls the input of the electronics tuning the exciter frequency so that the cavity is tuned to resonance. The error of the cavity tuning does not exceed 5% of its bandwidth. An operation mode is foreseen in which the feedback is broken and the frequency of the exciter can be retuned manually from the front panel of the unit or from the external control unit.

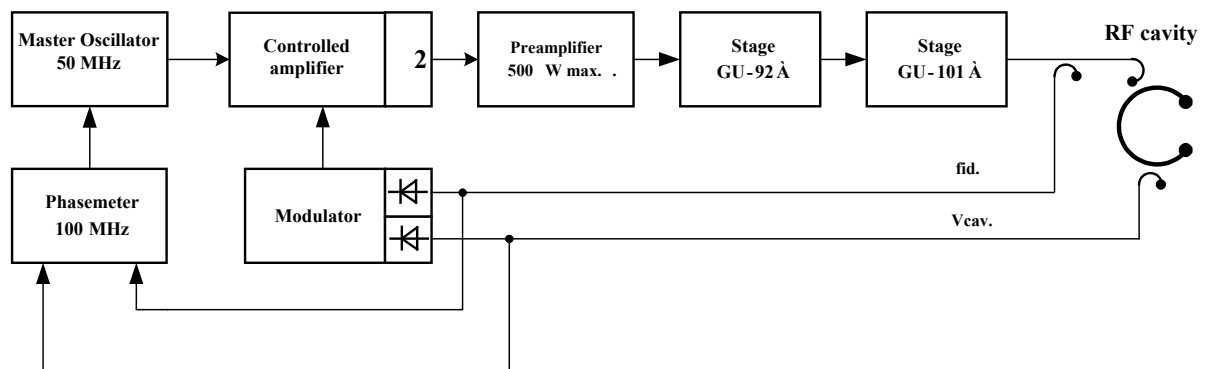


Fig.(7.4) 2. Block diagram of the RF control system

A bench for testing the generator was assembled, including all the elements that are intended for delivery. The output stage of the generator was connected to a load equivalent scattering a power of 200 kW with an SWR of 1.33 at 100 MHz. Parameters for a load power of 180 kW were measured at 100 MHz.

#### Parameters of the test of the output stage in a mode close to critical.

№	Parameter	Units	Value
1	RF load power	kW	181
2	RF power of incident wave (DC output reading)	W	1.85
3	RF power of reflected wave (DC output reading)	W	0.038
4	RF input power	kW	4.5
5	Anode voltage	kV	+12.5
6	Anode current	A	22.5
7	Voltage of grid 2	V	+1100
8	Current of grid 2	A	0.9
9	Voltage of grid 1	V	-290
10	Current of grid 1	A	0.3

---

11	Filament voltage	V	12.8
12	Filament current	A	594
13	Water consumption for cooling the anode	l/min	170
14	Water pressure in the delivery pipe	atm	2.2
15	Water pressure in the drain connection	atm	0.5

After successful completion of the tests in July 2010, the manufactured equipment was sent to the customer.

The work was performed under a contract with the Federal State Enterprise "Russian Federal Nuclear Center - All-Russian Research Institute of Experimental Physics" ("VNIIEF") 607190 Russia, Sarov, the Nizhny Novgorod region.

The work was carried out with the participation of V.S. Arbuzov, Yu.A. Biryuchevsky, E.I. Gorniker, E.V. Kozyrev, A. A. Kondakov, S.A. Krutikhin, G.Ya. Kurkin, S.V. Motygin, V. N. Osipov, G.V. Serdobintsev, K.N. Chernov.

## **7.5 Manufacturing and tuning of the elements of the accelerating structure for the modular industrial linear electron accelerator for 10 MeV/100 kW**

Works under the project of the complex for sterilization of medical products and decontamination of hazardous hospital wastes using the ILU-14 accelerator were continued. After the manufacturing of the elements of the accelerating structure a series of cold measurements was conducted for tuning the cells of the structure to the operating frequency. For the purpose of measuring the partial frequencies of the cells, separate sections of the structure were mounted in an upright position on a special stand; the measurement of the partial frequency of a cell was conducted after short-circuiting the apertures of adjacent cavities with specially made copper cylinders. The measurement results showed that the partial frequencies of the accelerating cells are within the permissible accuracy immediately after the manufacturing and no tuning is required. The cups of the coupling cavities were turned in accordance with the calculated sensitivity of partial frequency to the geometric dimensions of the cell, and then control measurements were performed in the upright position. When all the coupling cells were tuned, the accelerating structure was assembled entirely in a horizontal position. The results of measuring the distribution of the amplitudes of the accelerating field in the accelerating cells by the method of pulling a small perturbing body along the axis of the structure showed sufficient homogeneity within 10%.

The electron source is a triode electron RF gun consisting of the cathode-grid unit placed in the gap of the first accelerating cavity of the accelerating system and the resonant system for applying an additional RF voltage to the grid-cathode gap. The cavity was tuned to the operating frequency of  $176.2 \pm 0.2$  MHz using tuning elements and shunted with an external load to a load Q value of 15, which is necessary to increase the broadbandness of the device. A general view of the electron source is shown in the figure.

The RF power is applied to the accelerating structure through four coaxial power inputs. At operation with beam the power loss caused by reflection must not exceed 4% (a reflection coefficient of 0.2 or less). The power inputs are matched by a special technique where an individual input is coordinated with the structure without beam until the VSWR in the power feeder is 1.2 or less. This provides the necessary matching of the power inputs when the accelerator is operated with an electron beam. The coupling coefficient is adjusted via rotation of the coupling element – a loop.



Fig.(7.5)1. Section of the accelerating structure in an upright position.



Fig.(7.5)2. View of a coupling cell.

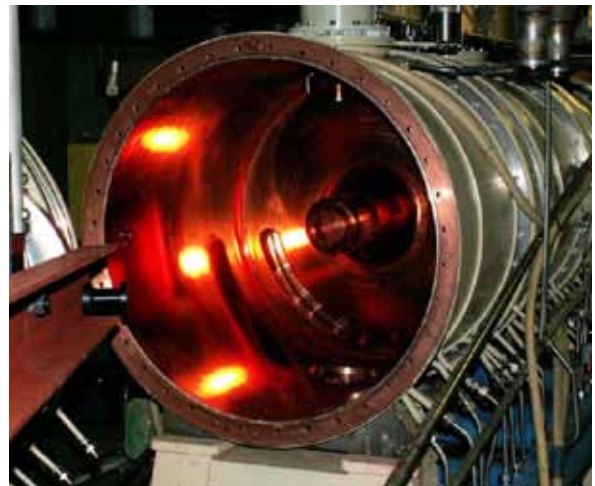


Fig.(7.5)3. View of the accelerating cell during the assembly of the structure.



Fig.(7.5)4. Source of electrons at the measurement stand.

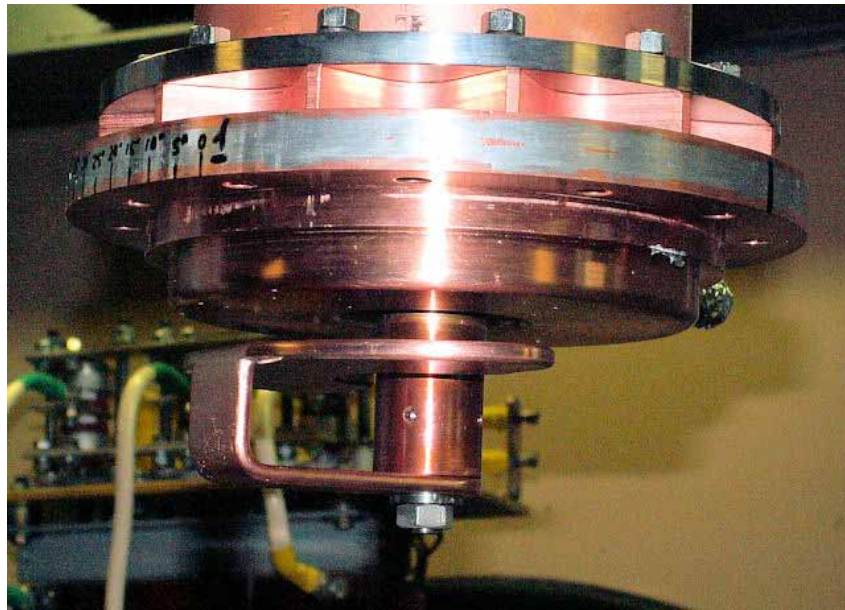


Fig.(7.5)5. Coupling loop of the power input.



Fig.(7.5)6. Accelerating structure after matching of the power inputs.

Currently, they at the accelerator facility are working to reach the design parameters of electron beam.

The works were carried out with the participation of I.G. Makarov, G.N. Ostreiko, A.D. Panfilov, G.V. Serdobintsev, V.V. Tarnetsky, M.A. Tiunov, K.N. Chernov

## 7.6 Project of 100 MHz continuous wave RF generator with an output power of 540 kW

### RF section of the generator

Within a few years they at the Federal State Unitary Enterprise Russian Federal Nuclear Center-VNIIEF (RFNC-VNIIEF), Sarov, have worked on the design and creation of a powerful resonance electron accelerator with the wide range of output electron beam energy of 1 to 8 MeV and average power of 300 kW. Under a contract with the RFNC-VNIIEF, BINP developed an RF generator with an output of 540 kW in continuous operation at 100 MHz.

Since there is no RF generating equipment with power over 200 kW in continuous operation at 100 MHz, the required power of 540 kW can only be obtained by summing the powers of several oscillating tubes.

The scheme of summed powers proposed in this paper was used at BINP in the designing of 180 MHz generators for the accelerator of the free electron laser. Summing powers of three tube modules is carried out by directly attaching them to the output coupling line in cross-sections of this line, those cross-sections spaced by a multiple of the half-wavelength. Each generator unit must provide an output power of 180 kW.

For summing the powers and maximizing the efficiency of each tube it is necessary to correctly balance the amplitude and phases of the excitation currents of the output generator modules.

The tube module was designed on the basis of the power amplification stage on the GU101A tube. This power amplification stage was developed at BINP and tested at an output power of 180 kW and frequency of 100 MHz. Now it is the output stage of the RF generator delivered to RFNC-VNIIEF, Sarov, in July 2010.

Each generator comprises a semiconductor pre-amplifier with an input power of up to 3 W and output power of 500 W or more. Power from the pre-amplifier arrives at the input of the intermediate amplifier stage, made on a single GU-92A tetrode. The output power of this stage of 12 kW excites the output module of the generator in which one GU-101A tetrode is used.

For the purpose of attaining a power of 540 kW three identical GU-101A tube modules, for tuning the resonance frequency of the anode circuit and controlling coupling with the load, are set in the output stage.

The places of connection of the modules to the coupling line are spaced by a distance equal to the half-wavelength in this line. For the summing of the powers of the modules to be possible the middle unit must excite the line in antiphase to the extreme ones. In this scheme, the voltages and currents in the cross sections where the modules are included (and, consequently, the loads of the current sources) are always equal to one another, regardless of the load magnitude. Therefore, the powers output by each current source are also equal.

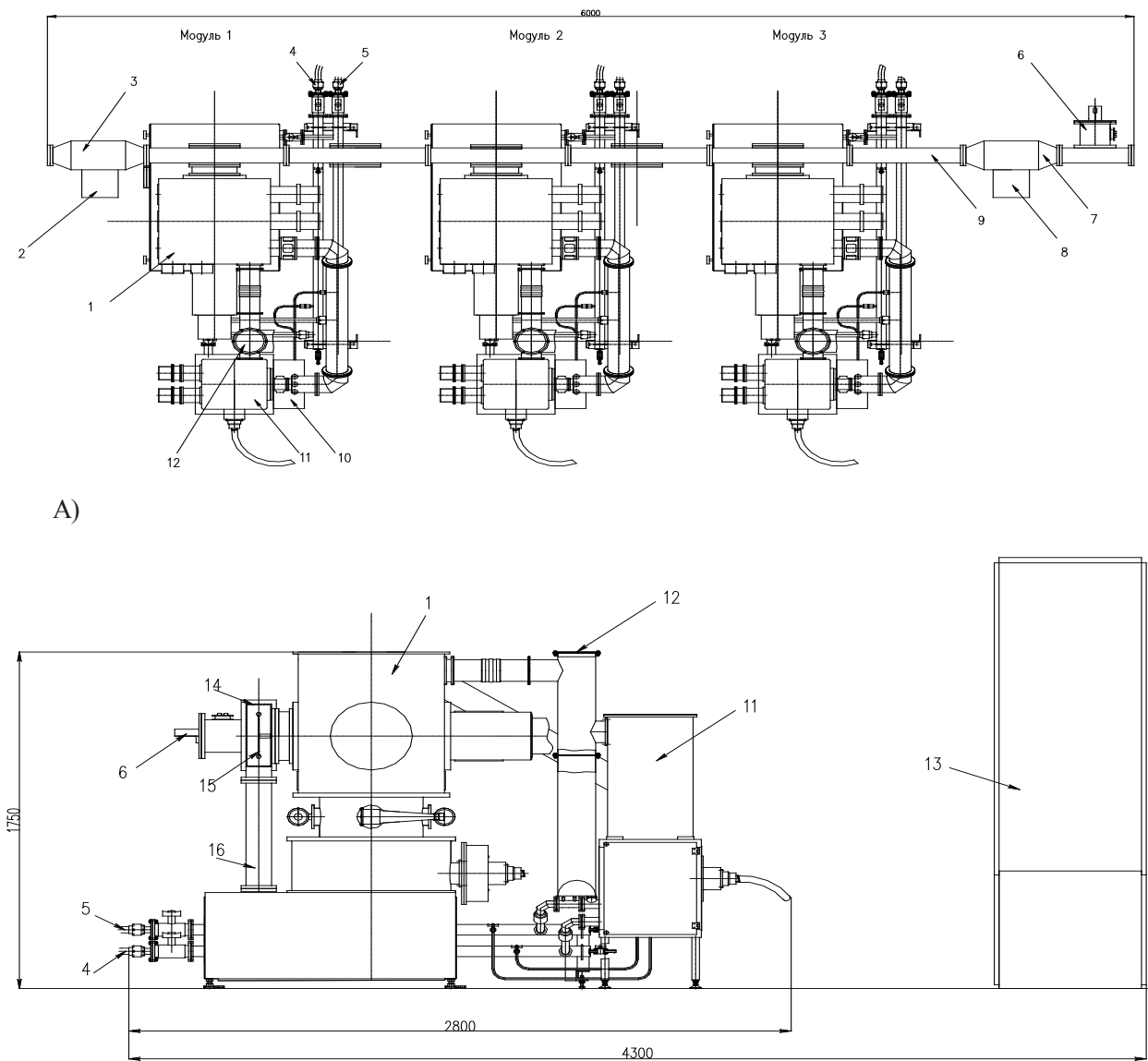
The input circuits of each tube module are excited independently from individual pre-amp stages.

The optimum balance of the phases and amplitudes of the excitation voltages is achieved through a system of control of the amplitude and phase signals on the inputs of the generators.

In the frequency range of  $100 \pm 1$  MHz the system does not require any retuning, except for setting to resonance, common for the three tubes of the anode circuit.

Coupling with the load is controlled by varying the wave impedance of the  $\frac{1}{4}$  wavelength segment of the line on the output of the generator.

The input circuit of the module does not require in-line tuning. The input circuits of the tube modules are not joined in this version. Each module is excited from a separate channel, which consists of a GU92A tube amplifier and a semiconductor amplifier. All the stages are assembled in common-grid circuits. Both tubes require forced water and air cooling. The summing channel of the output stage also requires forced air cooling. The general view of the generator is shown in Fig.(7.6)1 (A, B).



A)

B)

Fig.(7.6)1. A) the 540 kW RF generator. Top view. 1 – the output module of the generator with the GU-101A tube; 2, 3 – the tuning unit; 4, 5 – the inputs of the water cooling; 6 – the coaxial output of RF power; 7, 8 – the quarter-wavelength transformer with a variable wave impedance; 9 – the quarter-wavelength transformer with an impedance of 30 Ohm; 10, 11 – the RF power amplification stage with the GU-92A tetrode; 12 – the input of the air-cooling of the tube stages of the generator.

B) the 540 MHz RF generator. Side view. 4, 5 – the inputs of the water cooling; 6 – the coaxial output of RF power; 11 – the RF power amplification stage with the GU-92A tetrode; 13 – the cabinet for the low-voltage power supplies and control; 14 – the summing communication line; 15 – the centre conductor of the summing communication line; 16 – the inductive stub.

Each tube module on the GU101A tetrode provides power up to 200 kW in load when operating in the output stage of the 3 modules. The system controlling the coupling of the three-module stage with the load allows attaining a power of 540 kW at a VSWR less than 1.3 in the frequency range of 99 - 101 MHz. The output of the generator is designed for connection of a hard copper coaxial feeder with an impedance of 50 Ohm and the diameter of the inner and outer conductors, respectively, 70 mm and 160 mm.

### Power system of the generator

Each of the three channels of the generator has its own power supply. The power supply of the line of the generator is located in two racks:

- a. Rack for low-voltage power supplies (the filament, tube grids and pre-amplifier) and controls.
- b. High-voltage (14 kV) power supply of the anodes.

The rack for the low-voltage power supplies and controls comprises power supplies for the filaments of the tetrodes, the bias rectifier for the control grids of the tetrodes and the generator control unit. The Euro-mechanics rack size is  $600 \times 800 \times 2100$  mm. The rack for the controls and low-voltage supplies is placed near the stages of the RF generator.

The high-voltage power supply transfers voltage to the anode and screen grids of the amplification vacuum tubes (tetrodes) of the RF generator and provides a smooth rise at switching-on and quick de-energization of the tetrodes in case of breakdowns in the tubes and circuits of the RF generator.

The anode power supply is an adjustable high-voltage source with the input controlled by a thyristor regulator and operating at the supply-line frequency. Adjustable voltage arrives at the input of the step-up transformer with an overall capacity of 400 kW. The transformer is a commercial, three-phase, dry-type transformer TSGL with natural air cooling. The (linear) voltage of the high-voltage winding is 10000 V, and the (linear) voltage of the low-voltage one is 380 V.

High voltage from the output of the transformer arrives at the diode rectifier, connected in the Lari-onov circuit. The supply voltage of the anode of the first tube stage is taken from the common-coupling point of the secondary winding of the transformer.

On the output of the 14 kV supply there is installed a circuit for fast protection of the GU101A oscillating tube in case of breakdown and overload. The response time of the fast protection is less than 50 microseconds.

The power supply of the screen grids is an unregulated three-phase dry-type transformer of the TS type with natural air cooling and overall power of 2.5 kVA.

The anode power supply is cooled by the built-in fan. The heat release is  $\sim 9$  kW at an output power of 400 kW.

The overall dimensions of the power supply are (W  $\times$  D  $\times$  H)  $3300 \times 800 \times 2100$  mm; the weight is  $\sim 3000$  kg.

### Control system of the RF generator power

The control system provides the required parameters of high-voltage on the accelerating cavity and protects the generator from overloads and emergency situations.

Requirements to the RF system:

1. Instability of the amplitude of the accelerating voltage of the cavity of  $\pm 0.1\%$  or less.
2. Adjustment of the output power level in the range of 0 ... 100%.
3. The basic operating mode is continuous.
4. Phasing of the RF currents of the output tubes with an accuracy of  $\pm 5$  degrees or better at 100 MHz and alignment of their amplitudes.
5. An exciter which provides frequency tuning in the operating frequency range of the cavity is used as the master oscillator. In the working mode, the exciter frequency is tuned by the natural frequency of the cavity. The adjustment error must not exceed  $\pm 0.05$  of the cavity bandwidth.

The block diagram of the RF system is shown in Fig.(7.6)2. The system consists of three independent channels for power control and amplification, which are arranged identically. The RF power from the output stages of the channels is summed in the RF summator. The RF summator is connected to the accelerating cavity.

A signal to the input of the preamplifier and further to the high-power stages in each channel passes through a circular electronic phase shifter (PSh1) and adjustable RF signal amplifier (AA). The AA gain is regulated by a constant voltage.

There are two common external feedback circuits. One of them regulates the frequency of the 100 MHz exciter – the RF master oscillator – of the system so that the cavity is always tuned to resonance. To this end, RF signals from the sensor of the accelerating-voltage amplitude and sensor of the cavity loop current are transferred to input 1 of the 100 MHz phase meter. The output of the phase meter controls the frequency of the exciter.

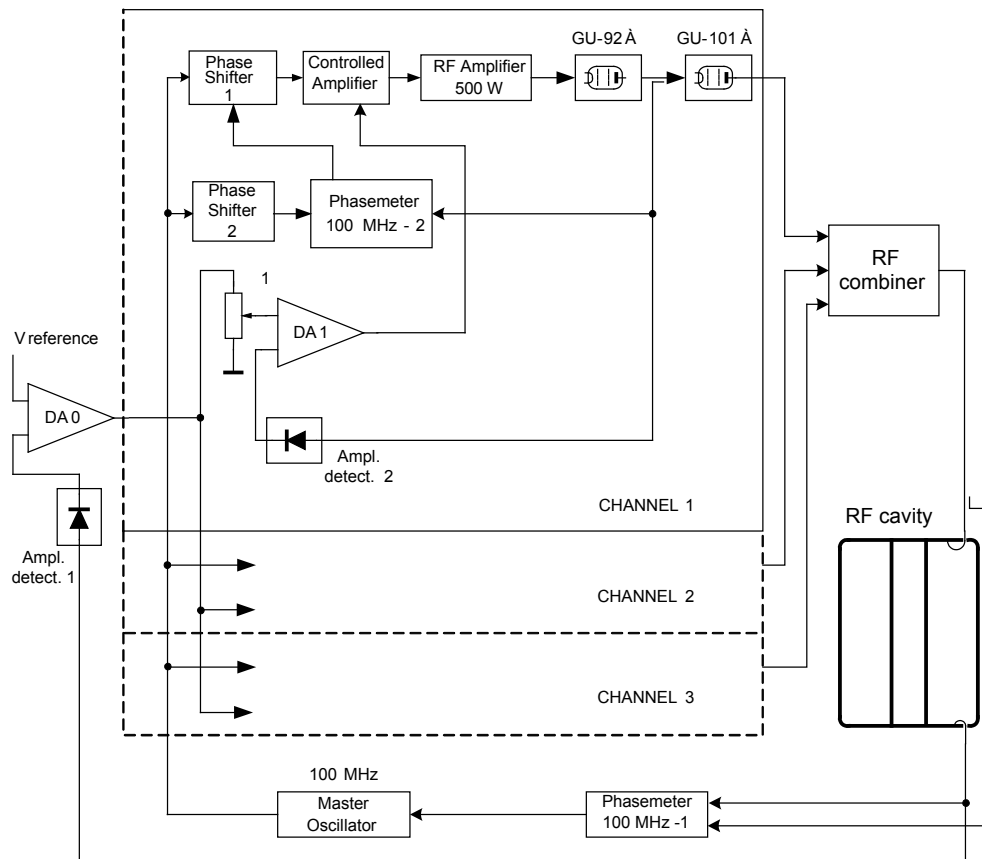


Fig.(7.6)2. Block diagram of the RF control system.

The second feedback circuit stabilizes the amplitude of the accelerating voltage of the cavity. For this end, the RF signal voltage from the measurement loop of the cavity arrives at Amplitude detector 1. Differential amplifier DA0 compares the output dc voltage with the reference voltage. The error signal output from DA0 is a common reference signal for the internal feedback circuits that regulate the amplitude of the excitation of the output stages for RF power amplification.

In each of the internal feedback circuits there is an amplitude detector (Amplitude detector 2 for the first channel) that generates a voltage proportional to the amplitude of the RF voltage in the cathode circuit of the output tube. Differential amplifier DA1 compares this voltage with the internal reference voltage from the DA0 output. The DA1 output signal controls the adjustable amplifier AA. Adjusting resistance R1 (for the first channel) is used to align the operation modes of the output stages subject to the difference in amplification parameters of the tubes and coupling coefficients of the signal voltage sensors in the cathode circuit of the tubes.

Each channel has a second feedback circuit, which regulates the phase of the RF voltage in the cathode circuit of the output tube. For this purpose, the signal from the RF voltage sensor on the GU-101A input is also delivered to input 2 of the 100 MHz phase meter. The common reference RF voltage from the 100 MHz exciter is transferred to the second input of this phase meter. The output of the phase meter controls the electronic circular phase shifter PSh1 (for the first channel). This provides a strict correlation of the RF voltage phase at each input of the GU-101A with the reference voltage.

Phase shifter PSh2, made on switchable manually-operated strip lines, initially sets the voltage phase on the GU-101A input. The phase shifter will be set so as to provide identical phases of the RF currents of the output tubes relative to the reference voltage and, therefore, to each other.

The control system has circuits for locks and protection of the RF generator and cavity in emergency situations.

The fast-acting protection is triggered when the cavity voltage and feeder current exceed threshold values. In this case, the excitation is removed from the inputs of the preamplifiers of the RF generator channels. The operating speed of the channels is about 100 microseconds.

The work was done by V.S. Arbuzov, E.I. Gorniker, E.V. Kozyrev, S.A. Krutikhin, G.Ya. Kurkin, V.N. Osipov, A.M. Pilan, G.N. Serdobintsev, and K.N. Chernov.

## 7.7 Upgrading the RF continuous-power generators for the FEL

BINP designed and built 600 kW continuous-power generators for a frequency of 181 MHz for the excitation of the RF cavities of the FEL microtron-recuperator. The required output power of the generator is obtained by summing the powers generated by the 4 tubes in the output stage. The principle of constructing such multi-tube output stages of generators was given in the earlier editions of the annual reports. Currently, powerful GU101A tetrodes of the VHF range are used in these generators. The total number of the GU101A tubes installed in the FEL generators is 12. From the experience of generator operation, at a tube-generated power less than 120 kW the tube life exceeds 4000 hours at low filament voltage (to 12.6 V). At the same time, at a higher RF power from a tube (120 to 150 kW) the service life is reduced to 1000 hours, or less in some cases. When the GU101A tubes were under development, it was assumed that in the future, for extension of the service life of tubes in the generators, they will be replaced with tubes with pyrographite grids, GU105A, the service life of which is several times longer. Unfortunately, production of pyrographite grids in Russia had been stopped. So, it was decided to develop and manufacture RF generators on TH781 tubes with pyrographite grids, produced by THALES (France). The warranty service life of these tubes is 3500 hours. The tube manufacturer thinks that at 180 MHz and an output power of 150 kW the tubes can operate at a reduced filament voltage for 7000 hours at least.

Table (7.7) 1. The main parameters of the TH781 tubes and, for comparison, GU101A.

Parameter	TH781	GU101A	Units
Anode dissipation power	250	250	kW
Screen grid dissipation power	4	3	kW
Control grid dissipation power	1.5	1.5	kW
Anode voltage	22	14	kV
Anode voltage at operation at a frequency of 180 – 200 MHz	10	8	kV
Screen grid voltage	1800	1200	kV
Control grid voltage	- 800	- 600	V
Anode pulse current	140	100	A
Filament voltage	10	15	V
Filament current	340	660	A
Transconductance	0.12	0.2	A/V
Anode-grid 2 capacitance	54	108	pF
Cathode-grid 1 capacitance	230	350	pF
Grid 1-grid 2 capacitance	270	400	pF
Anode-cathode capacitance	0.32	1.1	pF
Anode-grid q capacitance	2.2	12	pF
Cathode-grid 2 capacitance	14	28	pF
Maximum diameter	168	295	mm
Maximum length	425	525	mm

The table shows that the diameter and interelectrode capacitances of TH781 are approximately 2 times smaller. The filament power of TH781 is 3 times less and the transfer capacitances are 2-4 times smaller.

On the basis of generators that use the GU101A tubes a structure was designed that allows rather fast (in 40 hours or less) adjusting a four-tube generator both to TH781 tubes and to the combined use of these and Russian tubes. This solution allowed minimizing the cost of the manufacturing, assembling and tuning of the generators while maintaining the previous principles of power summation, tuning of RF systems and coupling with accelerating cavities. In addition, the combined use of tubes of different types allowed continuous FEL operation, with gradual replacement of tubes as new ones become available.

Fig.(7.7)1 sketches out the TH781 arrangement in the generator module. The joint operation of tubes of different types was possible due to the fact that the size of the anode circuit of the module with TH781 provides equal amplitudes of the RF voltage on the TH781 and GU101A anodes.

Since purchasing a required number of tubes takes a considerable time, the operation of the generator for the FEL must be ensured during this time via gradual replacement of the tubes of the four-tube stage. Therefore, we assembled and tuned several variants of the amplifier stages:

1. One-tube stage with a TH781 tube for an output power of 150 kW.
2. Four-tube stage with one TH781 and three GU101A tubes for an output power of 600 kW.
3. Four-tube stage with two TH781 and two GU101A tubes for an output power of 600 kW.
4. Four-tube stage with four TH781 tubes for an output power of 600 kW.

The power dissipated on the anodes of the tubes was calculated by the calorimetric method. We measured the difference in the water temperature on the inlet and outlet of the tanks for cooling the anodes of the tubes, as well as water consumption.

Variation 1, which is necessary to study the properties of a stage with one tube module, was assembled in the output stage of the generator which excites the accelerating cavity of the injector to the FEL microtron. At tests with a load equivalent of 50 Ohms we attained a power of 150 kW and showed that the filament voltage can be decreased to 8.5 V. The filament current was 315 A. The gain of the stage was 11 dB at an anode voltage of 7.9 kV.

The one-tube stage loaded on the accelerating cavity in the RF system of the FEL injector was also tested. Certain work was executed to provide suppression of self-excitation of the generator throughout the range of tuning of the stage and vary the input power level. We verified if the stable stage operation for a narrow-band load with full reflection was possible without using a circulator.

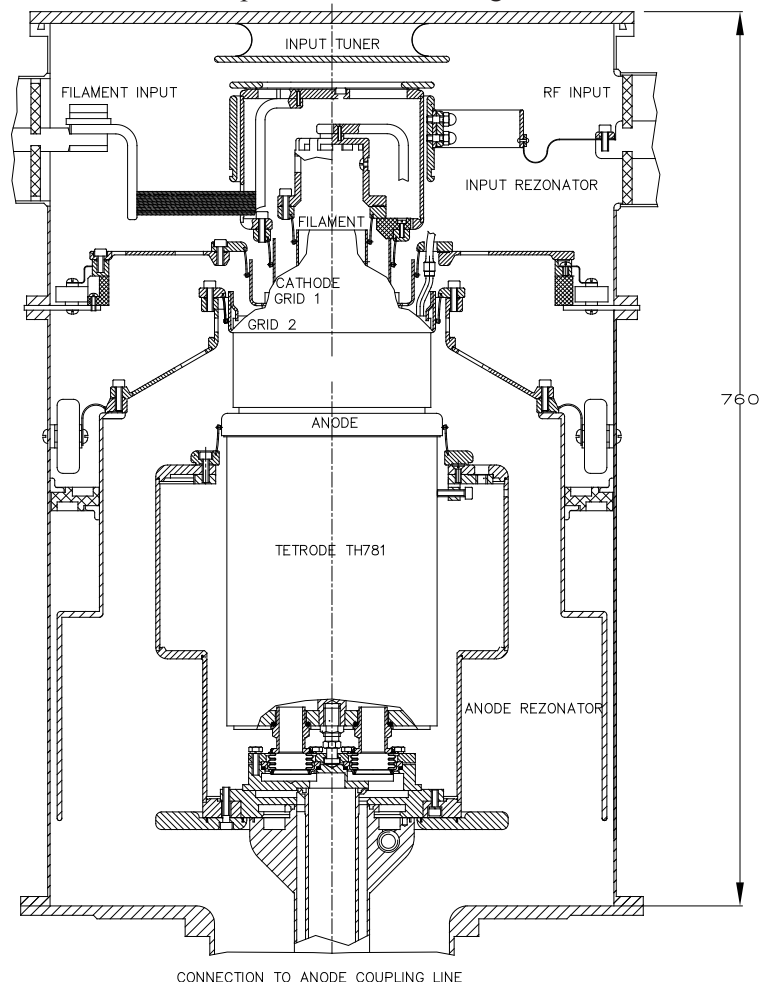


Fig.(7.7)1. Arrangement of a TH781 tetrode in the body of the tube module of the generator.

Variants 2 and 3 were used in one of the generators and were successively working on the FEL for about a year.

The four-tube stage with one TH781 module and three GU101A modules was loaded directly on the divider waveguide to 8 accelerating cavities of the microtron-recuperator. The difference in the power generated by the TH781 and GU101A modules did not exceed 10%.

Variant 3. Two TH781 modules and two GU101A modules were installed in the four-tube stage of the generator. The stage was also tested in the FEL RF system on the 8 accelerating cavities of the microtron-recuperator. At an output power of 500 kW, the maximum difference in the powers generated by each module was less than 20 kW. Further tuning, which improves the distribution of the powers generated by the tubes, was postponed as the operation results met the FEL requirements.

Variant 4 was realized in September 2010. All tubes in the four-tube stage were replaced by TH781 ones. Currently, the generator is operating in the FEL RF system and simultaneously being tested for determination of its maximum capacity and efficiency and provision of its stable operation in different modes. Results of the measurements and calculation of the stage parameters at a total voltage on the cavities of 6500 kV are shown in Table (7.7) 2.

Table (7.7) 2.

Parameter	1-TH781	2-TH781	3-TH781	4-TH781	Units
Operation frequency	180.4				MHz
Output RF power	507				kW
Filament voltage	8.0	8.0	8.1	8.2	V
Filament current	325	310	312	306	V
Anode voltage	8.4				kV
Screen grid voltage	960				V
Control grid voltage	- 200	- 200	- 200	- 190	V
Anode current	23.6	23.1	22.2	20.9	A
Screen grid current	0.7	0.8	0.7	0.8	A
Control grid current	0.5	0.6	0.6	1.0	A
Anode power supply power	198	194	187	176	kW
Power scattered on the anode	75	68	74	73	kW
RF power on the module input	~8	~8	~8	~8	kW
RF power generated by a tube	137	140	124	114	kW
RF power lost in the walls	2	2	2	2	kW
Tube efficiency	69	72	66	65	%
Stage efficiency (electron)	67				%

The work was executed by V.S. Arbuzov, E.I. Gorniker, E.V. Kozyrev, A.A.Kondakov, A. Pilan, and V.G. Cheskidov.

## 7.8 Defining parameters of the RF system of the storage ring Siberia-2 for ensuring the stability of longitudinal motion of electrons for in-phase dipole oscillations

In 2010, the laboratory completed a research work on the analysis of current restrictions that are imposed by the new accelerating RF system for the synchrotron radiation source Siberia-2 (Kurchatov Institute, Moscow). This system was commissioned in 2009. The power of the RF system must be sufficient for acceleration of a current of 300 mA. This value has not been reached yet. Studies were conducted on how the RF system should be tuned for its limitations on current to exceed 300 mA. It was shown that parameters of the feedback circuits that stabilize the amplitude (automatic gain control, or AGC), accelerating voltage phase (phase lock, or PL), and the length of feeders by which power is transferred from the generators to the cavities substantially influence in-phase dipole oscillations. We found parameters of the feedback circuits and the length of the feeders at which no in-phase dipole oscillations occur for currents up to 300 mA throughout the energy range. The results are expounded in BINP preprint 2010-6.

The work was performed with the participation of V.M. Petrov and N.V. Mityanina.

## 7.9 Status of the RF system of the 2.2 GeV storage ring in Zelenograd

The RF system of the storage ring operates at a frequency of 181.33 MHz and consists of two bi-metal cavities, a 300 kW feeding generator with an output stage on two TH781 tubes, the power transfer channel, and the control system. The RF system was described in the Institute report for the year 2008.

In 2010, the pumped-off cavities were delivered to Zelenograd. The ion pumps of the cavities were switched on and a vacuum of  $7 \cdot 10^{-8}$  Pa was immediately attained. The measured intrinsic Q factors of the cavities are 42600 and 42700. These values correspond to the Q factor measurements performed at BINP.

The cavities were installed on the storage ring (Fig.(7.9) 1). The distance between the centers of the accelerating gaps is  $827 \text{ mm} \pm 1 \text{ mm}$ , which equals a half of the working wavelength. We had to fabricate a 22 mm insert between the cavities. The aperture flanges of the cavities were aligned relative to the flanges of the vacuum chamber using the four geodetic beacons mounted on each cavity.

Removable units and mechanisms for tuning the frequency of the fundamental and higher modes were mounted on the cavities. The water-cooling system for the two cavities was fully assembled. All four collectors of the cavities are connected to the outlet shut-off valves with stainless steel pipes.

It took a long time to start powering the two ion pumps, after which a vacuum better than  $1 \cdot 10^{-8}$  Pa was reached in the cavities. This exceeds the vacuum of  $1 \cdot 10^{-7}$  Pa that is required by the specifications. Vacuum in the cavities was measured using a special tube installed in each cavity.



Fig.(7.9)1. Two accelerating cavities in the 2.2 GeV storage ring.

BINP members inspected the high-voltage power cabinets for the generator that had been installed in Zelenograd earlier.

All generator elements that were manufactured anew by BINP (the RF stages, elements of the wave-guide-feeder system and power cabinets) were delivered to Zelenograd. Before the shipment, the assemblage had been checked and cold measurements of the output stages on the TH781 tube had been performed.

The radorack with the required set of instruments was also made and dispatched.

The work was executed with the participation of V.S. Arbutov, M.I. Vlasenko, A.V. Golovin, V.L. Golovin, E.I. Gorniker, S.A. Krutikhin, G.Ya. Kurkin, I.V. Kuptsov, L.A. Mironenko, V.N. Osipov, A.M. Pilan, I.K. Sedlyarov, V.S. Stepanov, and M. Yu.Fomin.

## 7.10 RF system of the neutral beam injectors of the COMPASS tokamak

In 2010, we continued the work under the contract between BINP and the Institute of Plasma Physics (IPP) on the development and fabrication of two heating neutral-beam injectors. Gas ionization in the plasma chamber of these injectors is performed by means of high-frequency discharge.

The RF system of the power supplies was described in the report for the last year. The electronic components, the stage of the power amplifier on the 4CW50000E tube and the decoupling RF transformer were manufactured in 2010.

The amplification stage on the 4CW50000E tube is a new product, so it was subjected to the auto-excitation resistance test. For this purpose, the tube, with no plasma loading, was unlocked up to a cathode current of 5 A. No stray excitation was observed. A power of about 26 kW was reached under loading with a gas discharge. This power is quite sufficient to ensure the required beam current, so it was decided not to raise its level to the maximum design parameters.

System settings:

Operation frequency	MHz	3.8...4.2
Load power	kW	26
Pulse/pause duration	s	0.3 / 900
DC voltage on the «antenna»	kV	40

Both the RF systems were mounted and tuned at the IPP as part of the neutral beam injectors. Beams of hydrogen and deuterium atoms with an energy of 40 keV and a current of 12A were generated. The design parameters of the beams were demonstrated to the customer.

The work was performed with the participation of A.A. Kondakov, N.L. Kondakova, S.A. Krutikhin, S.V. Motygin, and V.N. Osipov.

## 7.11 New RF system for the electron-positron storage ring BEP

One of the points in the upgrade of BEP is the replacement of the existing RF system, operating on the second harmonic, with a new one. It is necessary to make a new accelerating cavity and an RF power generator for feeding it and change the control system.

The main requirements to the BEP new cavity are as follows: the operational frequency is the thirteenth harmonic of the BEP turnover frequency – 174.4 MHz; the operational accelerating voltage is about 110 kV; the maximum RF power transmitted into the beam is about 14 kW. The overall dimensions of the new cavity should not exceed those of the existing one. In 2010, this cavity was under designing.

The cavity has a cylindrical body consisting of the copper shell and bi-metal (copper- stainless steel) walls (Fig.(7.11)1, pos.1). The bi-metal structure of the walls increases their hardness and reduces the influence of the atmospheric pressure on the geometry of the cavity. There are symmetrically arranged coaxial inserts at the center of the walls (pos. 2). Such a structure allows decreasing the operating mode frequency and reducing the number of higher modes (HMs) of the cavity, thereby reducing their influence on the beam. The symmetry and small size of the accelerating gap provide additional reduction in the influence for HMs with an odd number of variations along the cavity axis. The areas where the coaxial inserts are jointed with the walls have a radius of curvature. That was done to minimize the possibility of a multipactor discharge in these areas. The cavity frequency is varied by means of two plungers connected with the

tuning mechanisms (pos. 4). In addition, the structure allows tuning the HM frequency at a given operating frequency using the HM tuning mechanisms (pos.5).

The power input (pos. 3) is designed to transfer about 20 kW of RF power into the cavity. Parameters of the power input loop are calculated so that the input resistance in the plane of the connecting flange is equal to 75 Ohms at the rated beam loading.

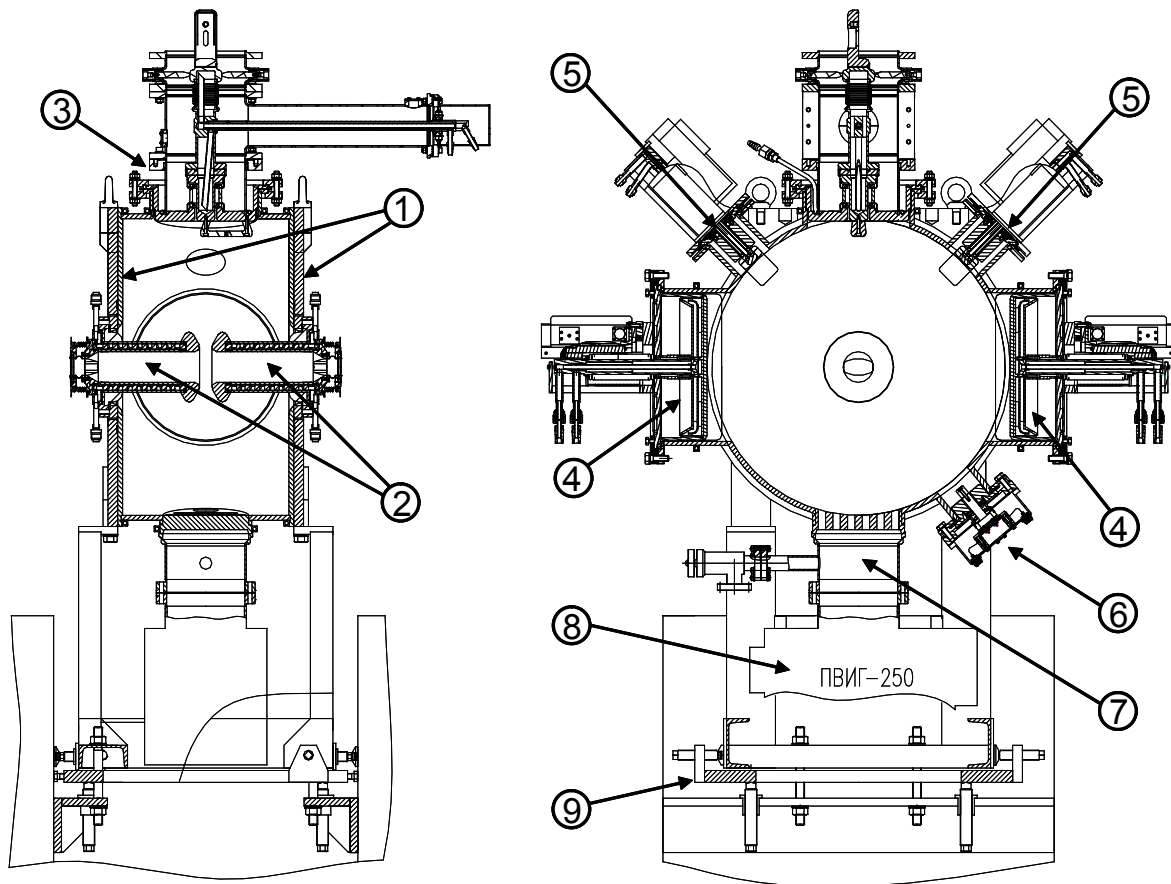


Fig.(7.11)1. The resonator structure: 1 – the bi-metal walls, 2 – the coaxial inserts, 3 – the power input, 4 – the mechanisms for frequency retuning, 5 – the mechanisms for HM retuning, 6 – the measuring loop, 7 – the vacuum pumping port, 8 – the vacuum pump, 9 – the stand .

Table (7.11)1: Parameters of the BEP cavity

Parameter	BEP
Turnover frequency, MHz	13.4135
Harmonic number	13
Operation frequency, MHz	174.3755
Frequency retuning, kHz	$\pm 130$
$R\tau_{\text{cavity}}^2$ , MOhm	1.4
Beam current, A	0.2
Bunch quantity	1
Beam energy, GeV	1000
Energy loss per revolution, keV	69.2
Accelerating voltage, kV	112
Beam length ( $\sigma_z$ ), mm	45.5
Power into the beam, kW	13.8
Power loss in the cavity, kW	4.5
Total power, kW	18.3

A full design study of the resonator was made. The power input and the body of the cavity were put into production.

## 7.12 Preparation of the VEPP-4M RF system for work at an energy of 4 GeV

Lately the VEPP-4M storage ring was working at low energy (1.5-2 GeV). The storage ring is equipped with 4 cavities connected to the generator via a waveguide power divider. The facility operates with two cavities detuned down in frequency and a total voltage of 600 kV fed only to two cavities. The output stage of the generator is made on 2 GU101A tubes. Only one tube is in operation. The heating of the second tube is switched off.

The total voltage of the cavities required at operation at 4 GeV is 1.6 MeV, the power consumed by cavities being 32 kW. The electron energy loss at 4 GeV is 710 keV per revolution. The power consumed by the beam at a current of 15 mA is 11 kW.

In the course of preparation of the RF system of the storage ring for operation at an energy of 4 GeV the mode with a total voltage of 2 MV on the four cavities was tested, the power from the generator being 50 kW in this case. Adjusting the transfer characteristic of the waveguide system without beam, we set the coupling of the generator with the waveguide and thus provided normal operation of the output tube. In this mode, the generator can operate both at an energy of 4 GeV and at a low energy without additional tuning. When the second tube is connected, the maximum output power of the generator can be increased up to 200 kW.

Because of a leak in the plunger for detuning the higher modes and deterioration of vacuum in the cavity the unit was replaced in the course of preventive maintenance. The cavity was pumped off, and a vacuum of  $10^{-8}$  Torr was achieved in it without heating. The vacuum keeps improving with further pumping off.

The cooling system was inspected; minor faults were eliminated. The possibility of operation at 4 GeV without reconnection of water and with the same system of thermal stabilization is supposed.

The voltage on the VEPP-4 cavities was re-calibrated by the frequency of beam synchrotron oscillation with accuracy better than 1%. Gauge readings on all informative devices were brought to conformity with the calibration.

Workshop 1 keeps finalizing one of the cavities for VEPP-4.

The work was performed with the participation of V.S. Arbuzov, E.I. Gorniker, I.V. Kuptsov, G.Ya. Kurkin, I.K. Sedlyarov, S.D. Gurov, V.N. Erokhov, S.E. Karnaev, V.A. Kiselev, L.A. Mironenko.

## 7.13 CCDTL accelerating structures for Linac4, CERN

The works on the fabrication of accelerating structures for linear accelerator Linac4 – a new injector of the LHC, CERN – were continued in 2010. BINP together with RFNC-VNIITF (Russian Federal Nuclear Center - Russian Institute of Technical Physics, Snezhinsk) is to make 7 CCDTL accelerating modules (Coupled Cavity DTL, a linear accelerator with drift tubes and coupling cells) for a frequency of 352 MHz for acceleration of H<sup>-</sup> ions in the energy range of 50-100 MeV (see Fig.(7.13) 1 and Fig(7.13)2).

In 2010 a set of working drawings for the drift tubes was released; the work study was performed; the tooling was made; the prototypes were fabricated (Fig.(7.13)2 and Fig.(7.13)3). One of the difficult points of the manufacturing process is the electron-beam welding (EBW) of the suspension rod and the body of the drift tube. The targeting system of the ELW device of the BINP experimental workshop was upgraded for accurate aiming at the junction. Before welding, as a low-current electron beam scans across the junction, the reverse current is measured. The smallest reverse current indicates the junction. Appropriate hardware and software were developed. Testing on samples showed that the new system provides aiming accuracy better than 0.2 mm.

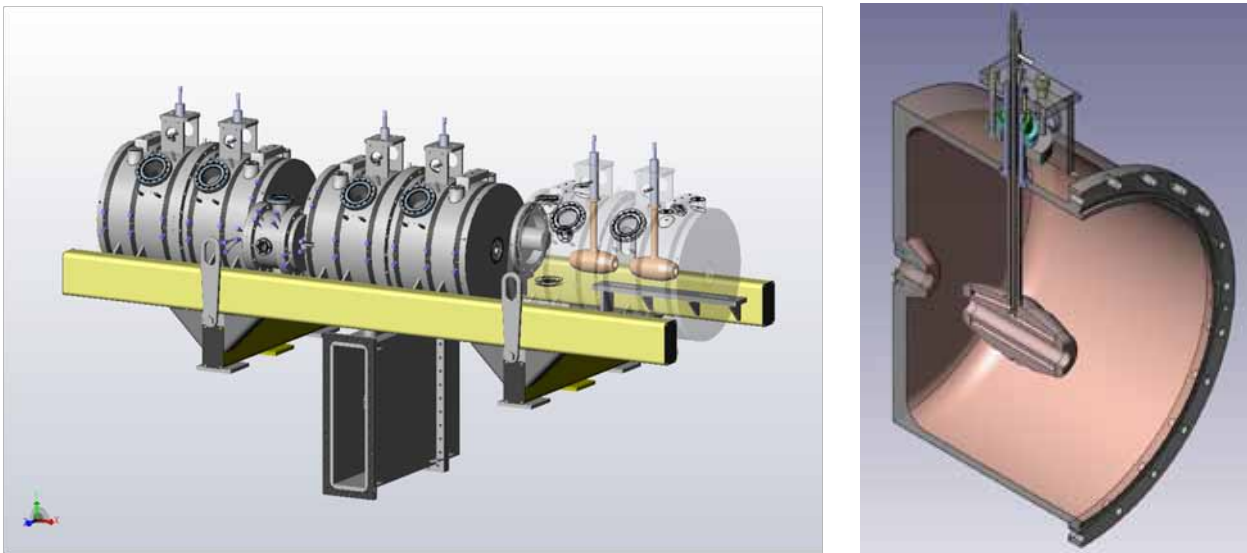


Fig.(7.13)1. Left: the CCDTL accelerating module. Right: half of the CCDTL accelerating cavity with the drift tube inside (cross section).



Fig.(7.13)2. Pilot sample of the drift tube.

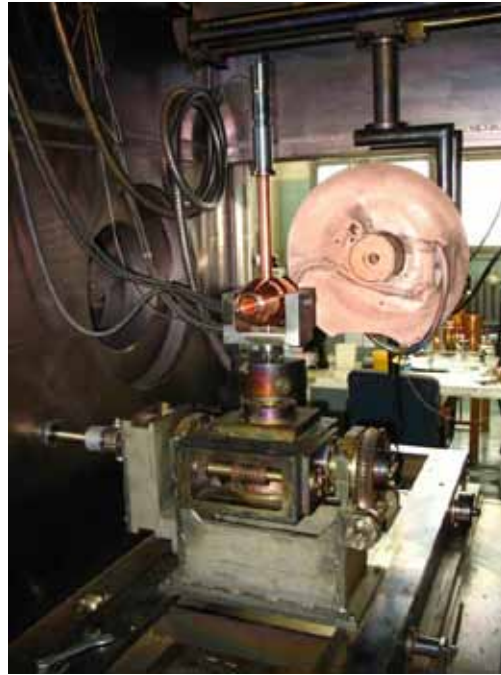


Fig.(7.13)3. Drift tube in the chamber of the EBW device.

10 sets of suspension rods were made completely; another 40 sets are ready to some extent (final machining is required for keeping the possibility of adjusting the rod length subject to the actual size of the seat on the body cavity). 50 drift tubes are partially ready: the cooling ducts in the parts were made; the parts were welded together; the unit is ready for finishing. The finishing is performed after accurate determination of the drift tube dimensions from measurements of the ready body of the cavity.

The bodies of the cavities of the 1st unit were manufactured (3 accelerating cavities and 2 coupling cavities, see Fig.(7.13)4 and Fig.(7.13)5). The application of the copper coating on the inner surface of the cavities was completed. The bodies of the cavities of 2nd and 3rd modules were partially processed.



Fig.(7.13)4. The body of the cavity of the 1st module is prepared for vacuum tests.



Fig.(7.13)5. Coupling cell of the 1st module after application of the copper coating.

Tuning and measuring the 1st module on the BINP site is scheduled for January 2011.

The work was carried out with the financial support from ISTC (International Science and Technology Centre, Moscow).

The work was performed with the participation of A.G. Tribendis, E.K. Kenzhebulatov, E.A. Rotov, N.V. Matyas, E.A. Cooper, A.N. Selivanov, M.G. Fedotov, A.G. Chertovskikh, Ya.G. Kryuchkov, Yu.A. Biryuchavsky.



8

POWERFUL  
ELECTRON ACCELERATORS  
AND  
BEAM TECHNOLOGIES



## 8.1 Radiation technology and ELV series electron accelerators

In 2010, the laboratory № 12 had supplied nine accelerators, carried out contract supervision of 4 accelerators delivered to the customers earlier and had signed over 20 contracts for accelerators supply in 2011 – 2012. The stock of orders for these years is completely formed. Such a demand growth for our accelerators is explained by several factors. First: the demand was increased due to the completion of the economic crisis. Second, that is also significant, is the improvement of operational parameters, providing the power of 100 kW in the range of 1.0 - 1.5 MeV. In that case the cost and price of the accelerator were changed insignificantly.

It is quite interesting to see the statistics of demand for accelerators. We compare the last 30 contracts.

Power, kW	100	50	<50
Qty of accelerators	27	2	1

The shift toward higher power capacities is visible. The only accelerator of less than 50 kW power is a mobile accelerator, which should not be included in the statistics.

Energy, MeV	2.5	1.5	1.0
Qty of accelerators	9	11	10

The accelerators requested by the customers by energies are distributed uniformly.

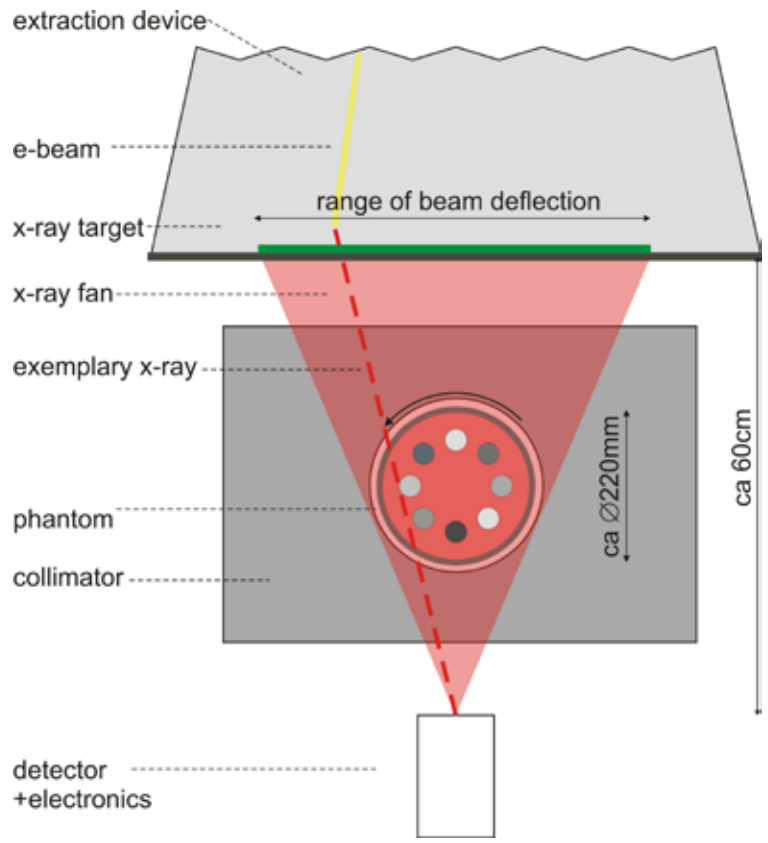
In 2010, together with the staff of the Institute of Safety Research (Germany), the experiments on modeling of electron-beam computed tomography using ELV accelerator electron beam were carried out.

Normally, in CT the cross-sections of objects are reproduced by means of moving X-ray source with subsequent reconstruction of forms using a computer. The German party proposed to use a scanning electron beam instead of the moving source. Previously, in Dresden, on the basis of electron gun of 150 kV voltage, the computed tomographic scanner allowing to produce up to 7000 object forms per second with a resolution of 1 mm had been designed and developed. The main application of this technology is visualization of gas-liquid flows in pipelines.

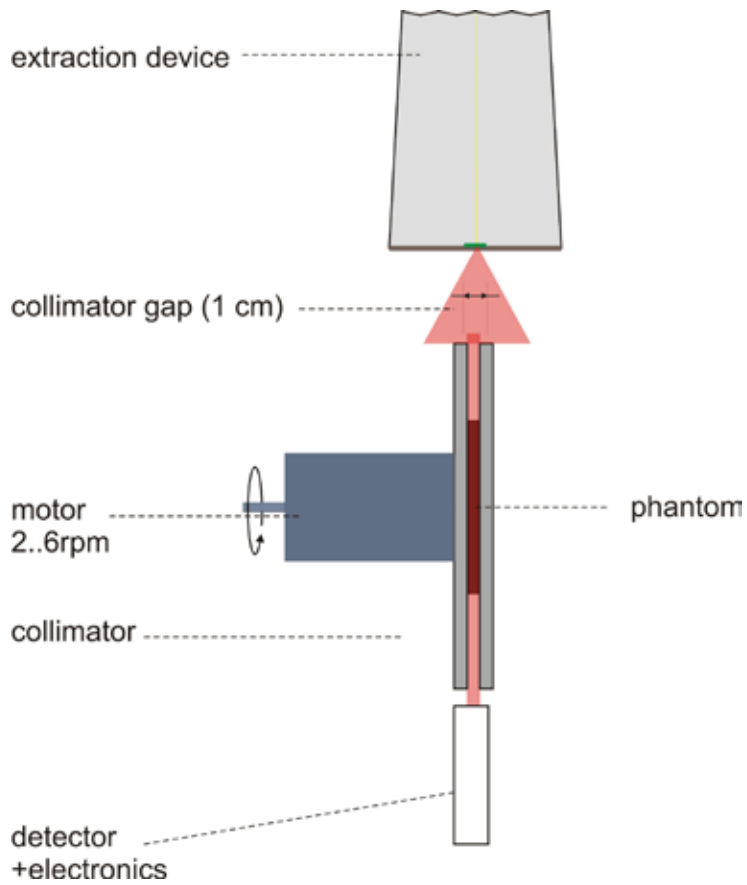
To increase the resolution and capabilities of this technology the German party proposed to use the ELV accelerator scanning electron beam focused to a minimum at the location of tantalum target. General view of the experimental facility is shown in Fig.(8.1)1, the converter cross-section is shown in Fig.(8.1)2.

The output window of ELV accelerator extraction device has been modified. Instead of commonly used titanium foil the water-cooled aluminum target was installed. To reduce the heating of the walls of extraction device the heat shields welded to the target from vacuum side of the target were mounted. In the slot between heat shields and target body a tantalum sheet of 0.4 mm thickness and 600 x 18 mm dimensions, used as a converter, was placed. Cooling of the converter occurred exclusively due to thermal radiation. Minimum cross-section beam size in the experiments was  $0.7 \pm 0.1$  mm. Maximum beam current did not exceed 2 mA and was determined by the temperature of sublimation of tantalum converter.

Under the target the steel collimator with a slit width of 1 cm was mounted. In the collimator body the phantom driven in rotation by an electric motor with a rotary speed of 2 to 6 revolutions per second to simulate the tomographic image with a circular radiation source was installed. Under the collimator the radiation detector with an amplifier was placed. The signal from the detector was processed on a computer installed in the control room of the accelerator.



a)



b)

Fig.(8.1)1. Longitudinal (a) and cross-section (b) view of simulation computed tomography installation

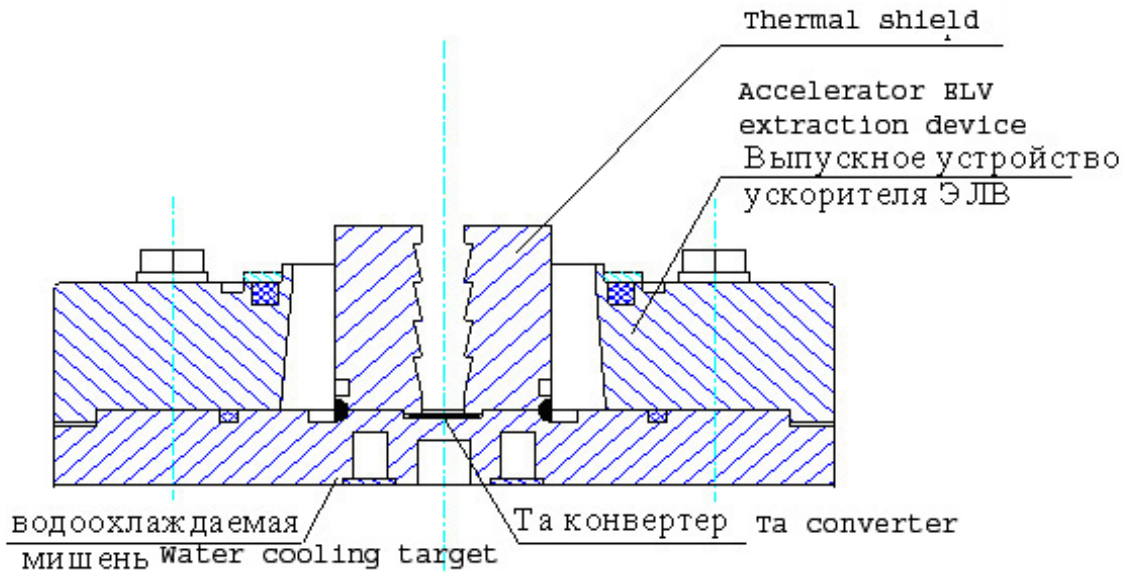


Fig.(8.1)2. Cross-section of bremsstrahlung converter

As a result of successful experiments the phantom tomograms with the resolution up to 2 mm were obtained. That is enough satisfactory when using one detector.

After complete experimental data processing the German party decided to sign a contract for delivery the ELV accelerator with the following parameters:

- Accelerated electron energy – 1 MeV
- Beam current – up to 100 mA
- Value of energy pulsation – should not exceed  $\pm 5\%$ .

The singularity of this delivery for us is that accelerator tube should have the possibility of 90° rotation relatively to horizontal axis.

The only one possible variant of development of such accelerator is to use remote accelerator tube installed in a separate tank and connected with high-voltage rectifier by means of feeder as it is shown Fig. (8.1)3.

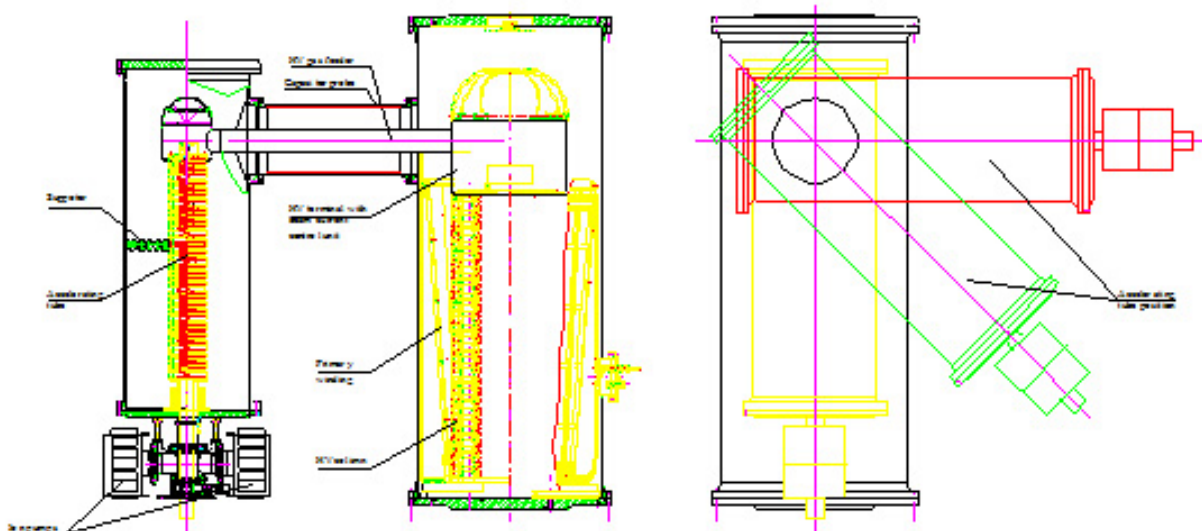


Fig.(8.1)3. Variant of assembly of accelerator with remote accelerator tube

The experiments at the laboratory bench equipped with ELV-6 accelerator with focused electron beam extracted into air were continued.

Most of the experiments were related to nanopowders production.

1. In cooperation with the Institute of Solid State Chemistry and Mechanochemistry SB RAS the series of works on obtaining the fine powders of bismuth and bismuth oxide ( $\text{Bi}_2\text{O}_3$ ) for medical applications at the manufacture of drugs, particularly DeNol, were carried out. In 2009 the productivity of these powders was obtained: 150 – 250 g / h using only 20% of nominal power of electron beam. However, the average particle size was large, i.e. about 0.5 microns. In 2010, the principle possibility of reducing the average particle size was shown (Fig.(8.1)4). Thereto, at the preliminary stage we had to decrease the process productivity considerably.

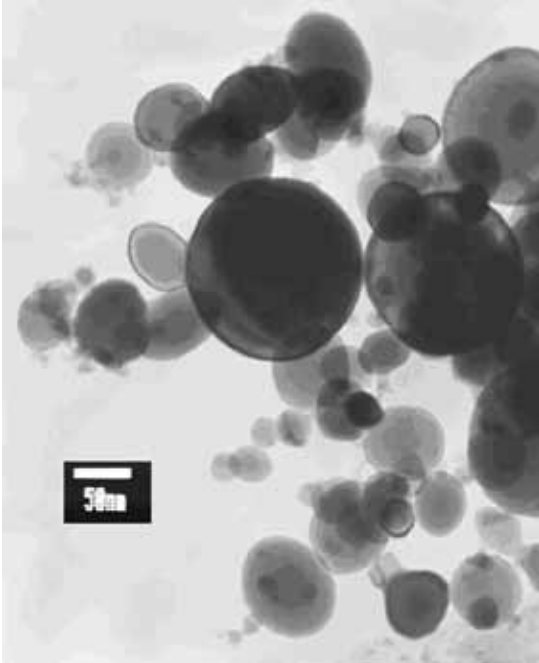


Fig.(8.1)4. Nanopowder Bi

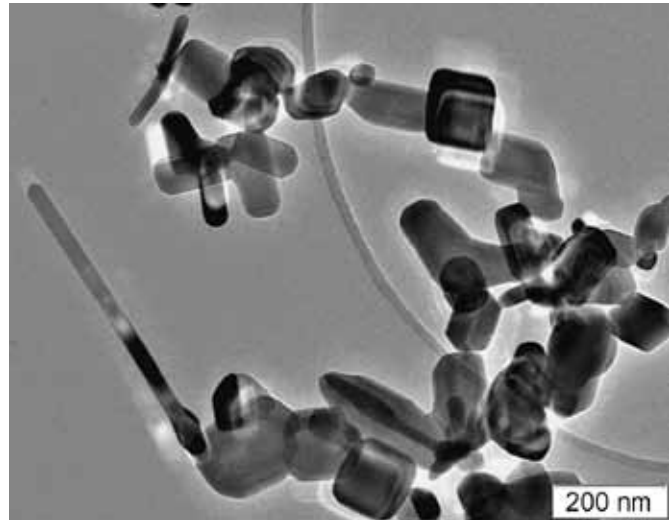


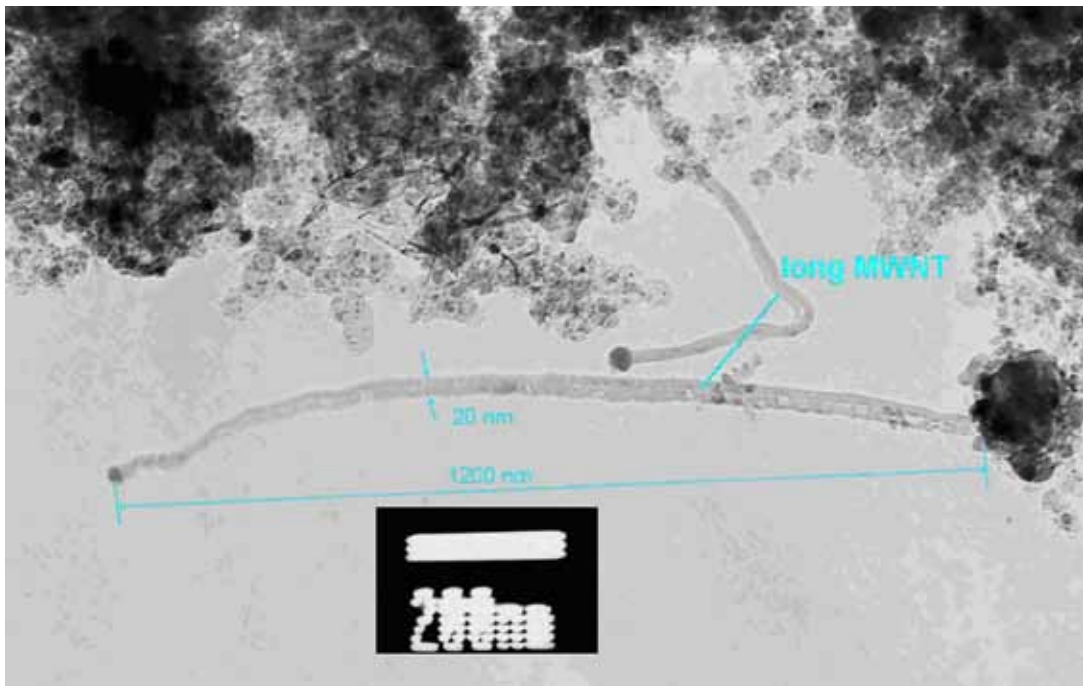
Fig.(8.1)5. Crystals of ZnO

2. In cooperation with Khristianovich Institute of Theoretical and Applied Mechanics of the Siberian Branch of the RAS the investigations of the possibility of obtaining zinc oxide ( $\text{ZnO}$ ), which can be applied in medicine, solar cells, photocatalysis, cosmetics, gas sensors creation, paint and varnish industry, as well as in several other perspective high-tech industries had been held. The experiments were carried out directly on demand of the export-oriented enterprise, researching the possibility of creating an alternative technology for industrial production of nano-sized powders of zinc oxide for use in industrial rubber applications. To get this matter the source material in the form of zinc metal was placed in a sublimator, and then was heated by an electron beam in air, respectively, the pairs of zinc were oxidized with the formation of zinc oxide. As a result a powder of complex structure was obtained. The results of transmission electron microscopy are shown in Fig.(8.1)5.

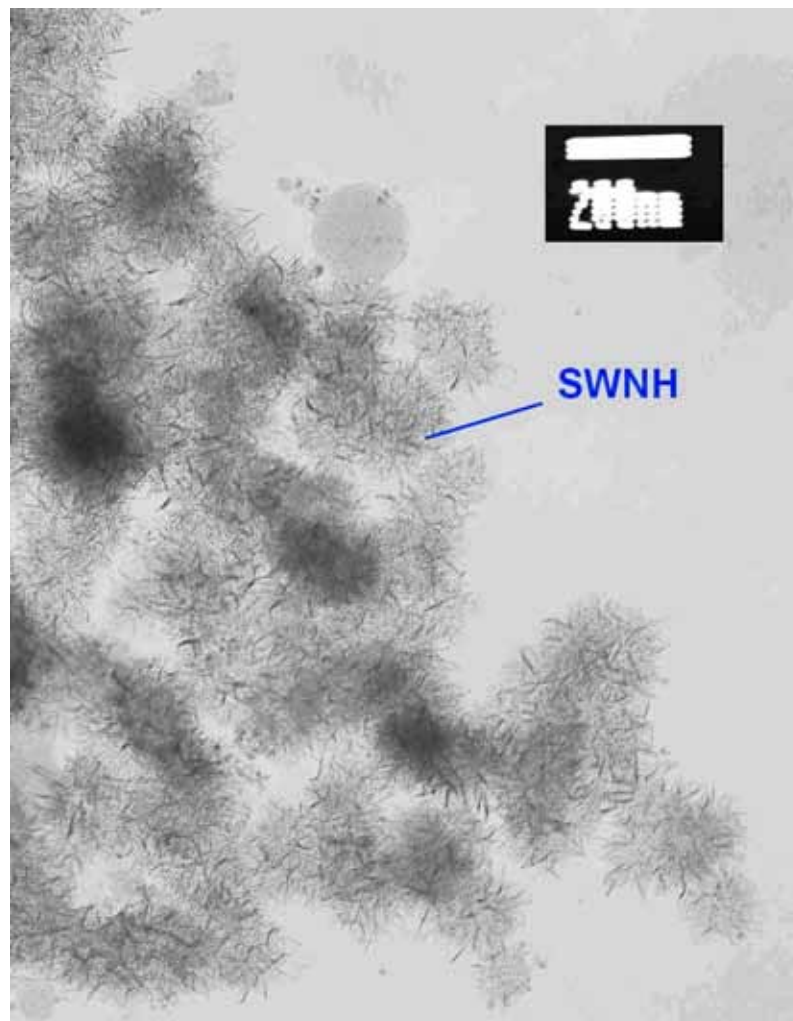
The crystals have different shapes. There are needle-shaped, round and prismatic, with the sizes range from 50 nm up to micron. There are particles splices. Mainly, the surface of the particles is smooth. There is also a mesoporous fraction of the size of blocks and mesopores of about 5 nm.

Integrally, the results of experiments confirmed the possibility of obtaining zinc oxide at the facility for nano-sized powders production. The samples were given to industrial enterprises being the initiator of the work to evaluate the properties of the material obtained.

3. By means of evaporation technique of basic carbon target in inert gas medium the carbon nanostructures like nanohorns and nanotubes were obtained. To obtain multiwall (MWNT) and single-wall (SWNT) nanotubes the graphite powder tablets prepared by means of pressing were added into catalyst. To obtain nanohorns evaporation of pure graphite sample were held. Fig.(8.1)6(a) shows an example of a long multiwall nanotube, Fig.(8.1)6(b) presents accumulation of single-wall nanotubes, which are of great scientific and practical interest in comparison with multiwall ones. Fig.(8.1)7 shows nanopowder consisting of nanohorns.



a)



b)

Fig.(8.1)6. Multiwall nanotubes (a) and single-wall nanotubes (b)

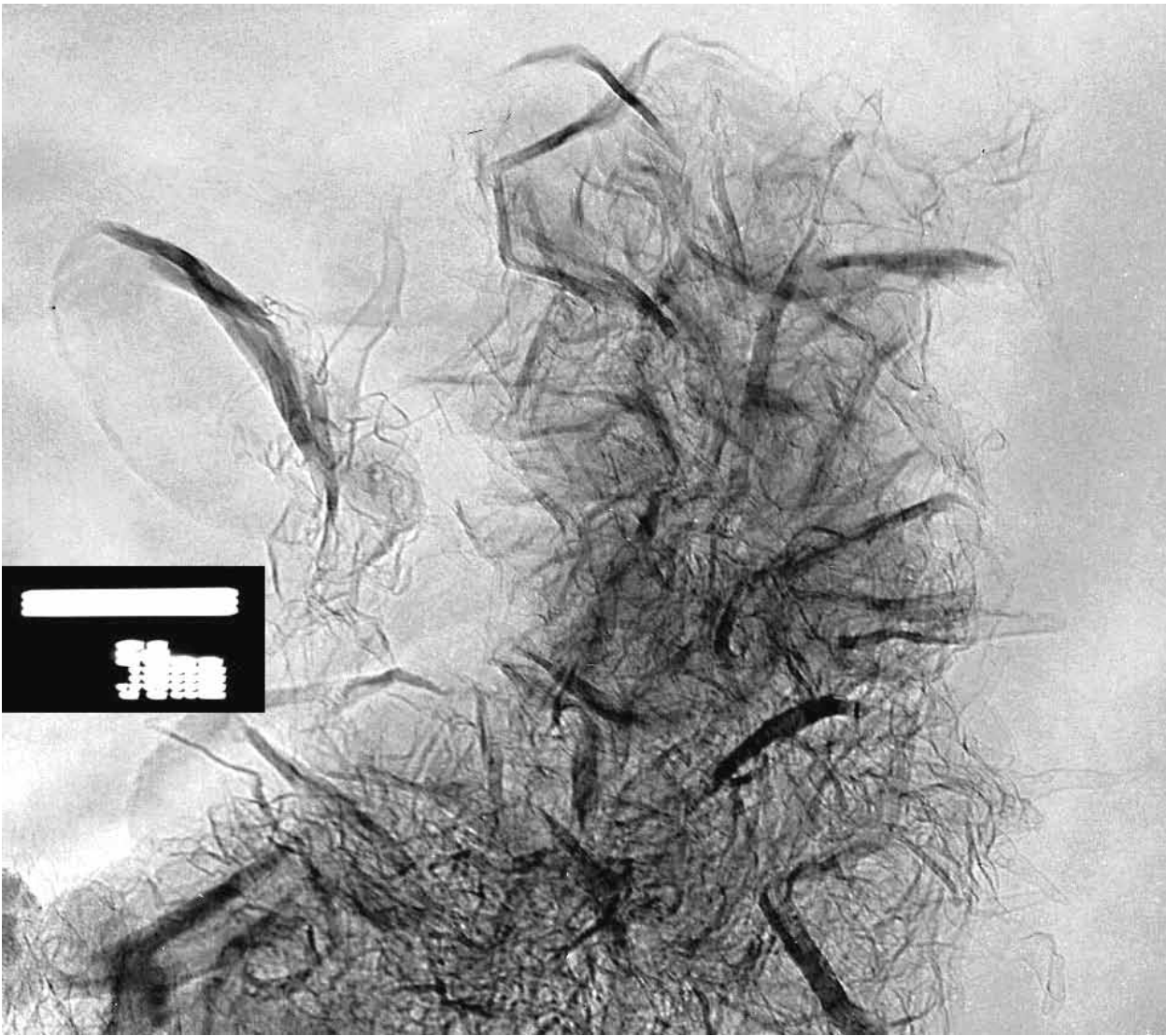


Fig.(8.1)7. Accumulation of nanohornes

Another part of the experiments at the stand was related to the formation of coatings at the metal by welding.

The coatings of Ti-Ta-Nb, performed in collaboration with the Novosibirsk State Technical University were continued to be studied. Alloys of this system are of interest in sight of their anti-corrosion properties as the best current biocompatible materials and as a material for lining of chemical reactors meant for nuclear power plants waste treatment. The concentration of alloying elements like tantalum and niobium was varied from 3 to 35% by weight at 1 - 2 mm coating thickness. Two types of structures such as martensitic at a low concentration of alloying elements (up to 10%) and dendritic at higher concentrations were obtained. The composition and structure of coatings are uniform in thickness. Basically, X-ray analysis of coatings surfaces shows just presence of one phase. It is  $\alpha$ -titanium. However, when increasing the speed of coating formation it is noticed the presence of incompletely dissolved particles of tantalum closer to the bottom of the melting bath. The hardness of coatings is 60% higher than the hardness of the basis due to solid solution hardening.

## 8.2 ILU accelerators and their applications

### 8.2.1 Accelerator supplies

Since 1983 the ILU accelerators are supplied abroad where they are used for researches and are working in the industrial lines. Some of these machines are working round the clock for years. The reliability and technical level of these machines is confirmed by the new supplies.

The accelerator ILU-6 that was continuously working since 1983 in the firm “RadPol”, Człuchow, Poland, was modernized and put into operation March 2010. The maximum energy before modernization was 2 MeV, after modernization the machine is working at energy of 2.5 MeV with beam current up to 10 mA. The accelerator control system was modernized and moved into the control room of the ILU-10 accelerator, and now one operator is controlling 2 machines – ILU-6 and ILU-10 – commonly working on the plastic goods production line.

The ILU-8 machine with local biological shield was put into operation on the “Chuvashkabel” plant, Cheboksary, Russia. The line for wire irradiation is working since March 2010.

The second ILU-10 machine with energy up to 5 MeV and beam current up to 10 mA was manufactured and commissioned according the contract with Siberian Center for Pharmacology and Biotechnology.

Works on the modular linear electron accelerator prototype

The accelerator prototype block diagram is given in Fig. 1. During 2010 its elements were tuned and the accelerator prototype was tested.

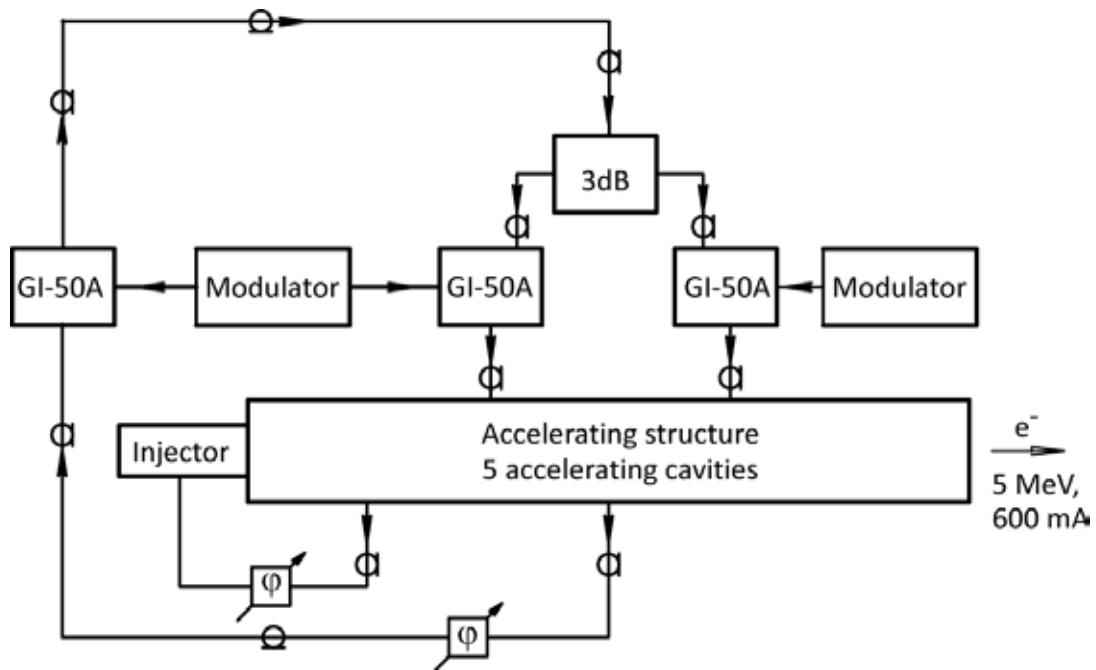


Fig.(8.2)1. Accelerator prototype block diagram.

The results of these works – the principally new RF system was worked out. This new RF system comprises the 2-staged RF generator with preliminary stage, 2 final stages and 2 RF power inputs into accelerating cavity. The electron injector with RF control was tested. The measured beam energy spectrum corresponds the calculated values.

The accelerating structure of the prototype comprised 5 accelerating cells (3 full cells and 2 half-cells at both end of the structure) and 4 coupling cells. The RF power was inputted into 2 side full accelerating cells, the feedback signal was fed from the middle accelerating cell.

The energy of 5 MeV and pulse beam power of 600 mA were achieved, it corresponds the pulse beam power of 3 MW. The energy losses in the structure were 0.8 MW, pulse RF power supplied by each of the 2 final stages was 1.8 MW. So the RF system provided the pulse RF power required to reach the design parameters of the ILU-14 machine that have the RF generator with 4 final stages.

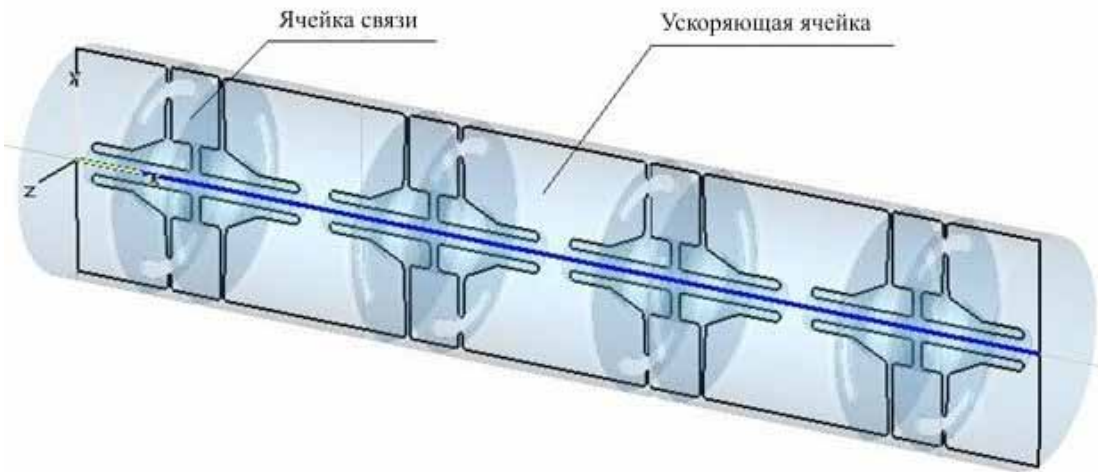


Fig.(8.2)2. Accelerating structure of the prototype.

### 8.2.2 Fabrication and testing of the modular electron accelerator ILU-14

After the completion of the works on the accelerator prototype 2 full accelerating and 2 coupling cells were added to the accelerating structure of the prototype. The new accelerating structure has the 5 full accelerating cells and 2 accelerating half-cells. This accelerating cell is shown in Fig.(8.2)3.

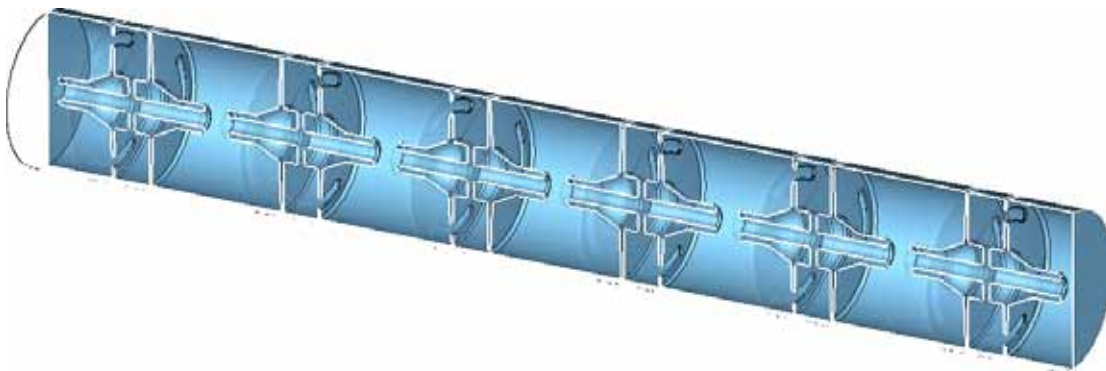


Fig.(8.2)3. ILU-14 accelerating structure.

The feedback signal in the ILU-14 is taken out from the central accelerating structure, and RF power input is done into other 4 full accelerating cells. The accelerating half-cells are placed on the both ends of the structure as in the prototype, see Fig.(8.2)1 and Fig.(8.2)2.

The ILU-14 is the new powerful (up to 100 kW) multi-gap multi-cavity machine for energy range of 7.5-10 MeV, the accelerating structure design is shown in Fig.4. The main elements are: bi-periodical accelerating structure with coaxial coupling cavities consisting of 7 accelerating cells, RF autogenerator comprising 1 preliminary and 4 final stages on GI-50A triodes, 4 RF power inputs, triode RF electron gun having the option to apply the additional RF bias voltage on grid-cathode gap and 3 modulators.

The new modulators' synchronization system was developed. The energy accumulation in the inductive energy storages of each modulator are spaced in time and the resulting loading unevenness of the feeding 3-phase net ( $P_{peak}/P_{average}$ ) was decreased from 2 to 1.3. The modulators are mounted and their common work was checked.

The power supply for magnets of the ILU-14 machine was mounted using the units UM produced by Lab 6-0.

The bunker for ILU-14 testing was prepared in 2010. The energy of this accelerator is up to 10 MeV, and the beam is accelerating and extracting horizontally. The bunker was initially designed for the accelerators with beam extracting vertically down, and maximum energy of 2.5 MeV.

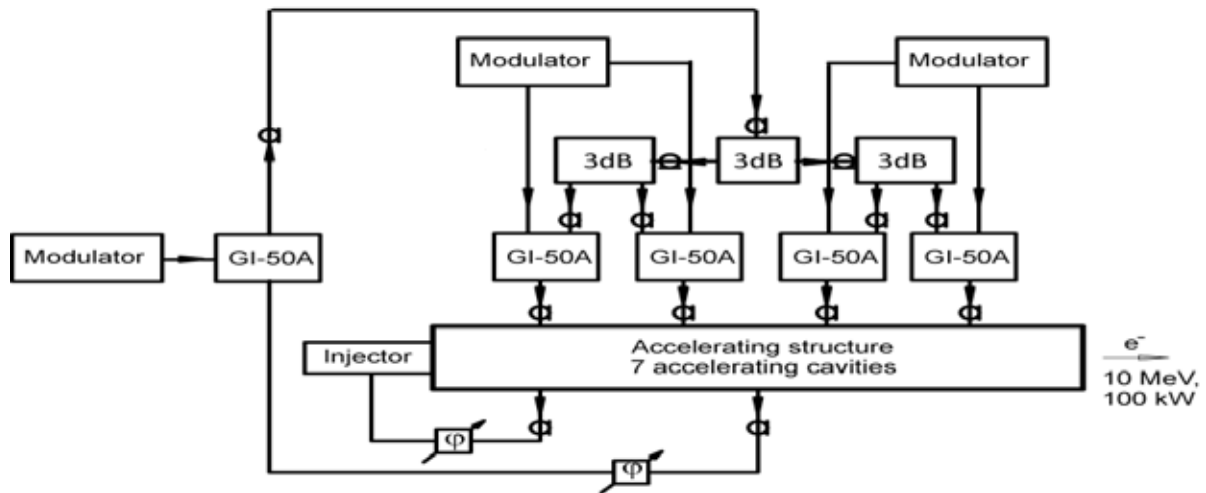


Fig.(8.2)4. ILU-14 block diagram.

To ensure the radiation safety during the testing the required local radiation shielding reinforcements were calculated. Basing on the calculation results 3 local radiation shielding reinforcements were fabricated and mounted – one reinforcement is made of steel and 2 reinforcements are mounted from the lead bricks. The efficiency of these reinforcements will be checked later during the accelerator testing.

The testing of the ILU-14 started in 2010. The tuning of its accelerating structure and RF power inputs was done together with Lab 6-2.

The new RF generator with preliminary stage and 3db bridges on its output was tuned and the first hot testing (with beam) of the accelerator were carried out.

The effective accelerating voltage of 10 MV was reached on the accelerating structure without beam. The accelerator generated electron beam in the energy range of 7-10 MeV. The testing and tuning of the accelerator is going on.

The complex for medical goods sterilization and decontamination of medical wastes based on ILU-14 machine is under development.

The common work of Lab 14 and Lab 6-2 on ILU-14 development will be continued in 2011.

### 8.2.3 New technologies development

The research works were performed to develop the radiation-thermal synthesis of complex oxide compounds. The perovskite-like compounds for membrans were sintered under the Interdisciplinary Project of Siberian Branch №82 “Oxide permeability of the massive and deposited membranes based on perovskites with mixed conductivity”.

The pilot works on radiation-thermal sintering of the fuel elements cells were carried out in collaboration with Borskov Institute of Catalysis, Novosibirsk.

The research activities in radiation treatment of the oil products were carried out under the Integration Project №5 of the Siberian Branch Presidium. The work was carried out in collaboration with Institute of Solid State Chemistry and Mechanochemistry, Novosibirsk, and Institute of Oil Chemistry, Tomsk.

The test irradiations to study the radioresistivity of the microbes were carried out.

Various medical goods were subjected to electron beam treatment on the contract basis. The works were carried out on the ILU-6 and ILU-10 accelerators.

Participants of the works:

A.A. Bryazgin, V.V. Bezuglov, A.Yu. Vlasov, V.A. Gorbunov, I.V. Gornakov, B.A. Dolzhenko, A.M. Molokoedov, L.A. Voronin, M.V. Korobeynikov, A.N. Lukin, I.G. Makarov, S.A. Maximov, V.E. Nekhaev, G.N. Ostreyko, A.D. Panfilov, V.V. PodobaeV, G.V. Serdobintsev, A.V. Sidorov, V.V. Tarnetsky, M.A. Tjunov, V.O. Tkachenko, B.L. Faktorovich, V.G. Cheskidov, E.A. Shtarklev, A.M. Yakutin.



9

PHYSICS  
FOR  
MEDICINE



## 9.1 Status of BNCT

Several works have been carried out to optimize the transportation of high-power stationary proton beam onto the lithium target and to protect and enhance the reliability of vulnerable parts of high-energy beam line. As a result, the technical condition of the accelerator complex attains a level that allows us to carry out long-term, stable generation of neutrons. Applying additional beam diagnostics a stable generation of neutron beam achieved with proton current of 0.7 mA for 5 hours, and highest current of protons on the lithium target increased to 1.8 mA. All the problems with exposure and storing of activated targets were solved. All works carried out helped us to start the first biological experiments on neutron capture therapy.

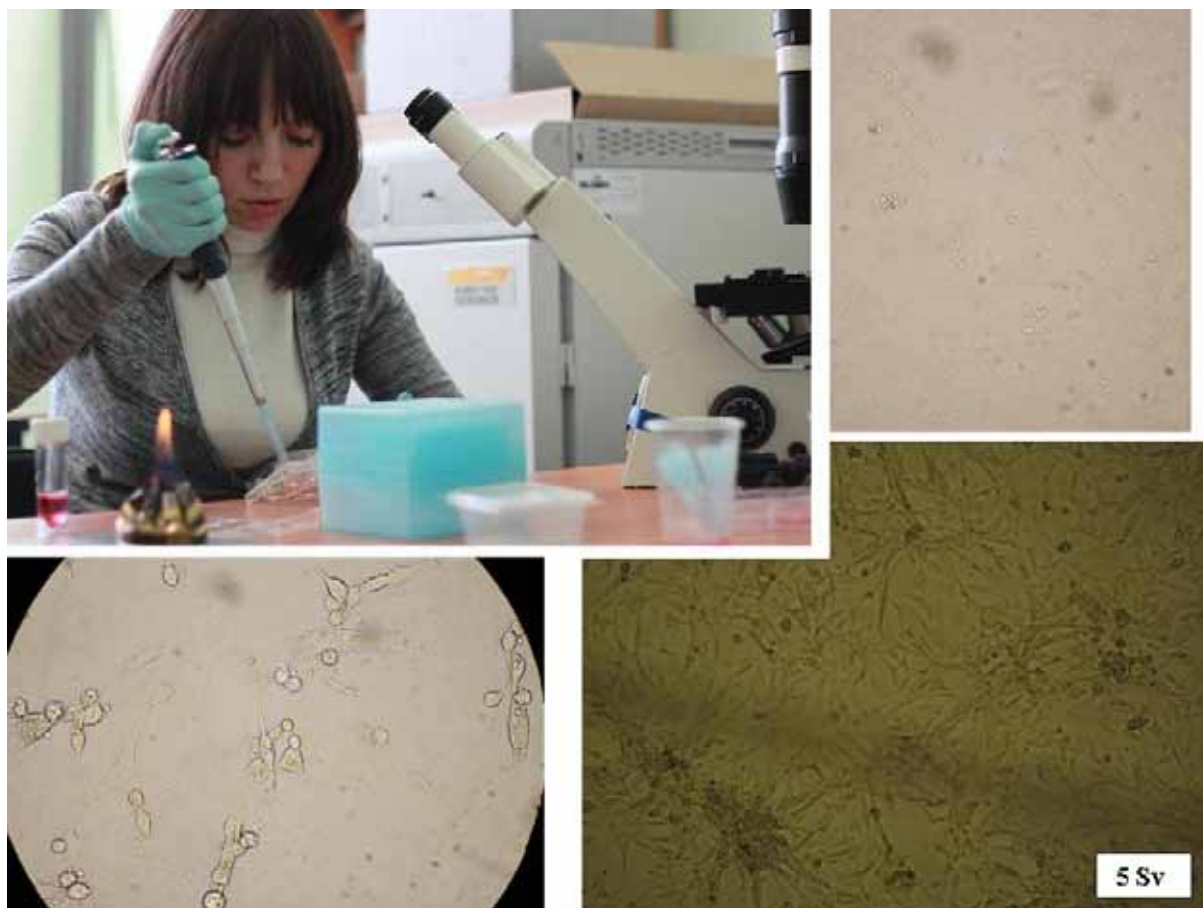


Fig. (9.1)1. The first in vitro experiments on BNCT.

To study the neutron spectrum a unique TOF diagnostics was designed and manufactured. The idea consists in the fact that the accelerator complex operates in a stable regime of generation of the proton beam with energy below the threshold of the  ${}^7\text{Li}(p,n){}^7\text{Be}$ . At the same time short pulses of negative voltage are transmitted on the lithium target, that is isolated electrically from the body of the installation. The voltage impulses make protons to raise the energy higher than the reaction threshold and generate short pulses of neutrons (Fig.(9.1)2).

In experiments on the generation of resonant gamma rays with help of  ${}^{13}\text{C}(p,\gamma){}^{14}\text{N}$  reaction the intensities of the weak spectral lines and branching ratios were measured with previously unattained accuracy, which became possible using the new high speed gamma-spectrometer.

The long-time stabilization of proton energy was achieved in the near-threshold regime of resonant gamma rays generation. Automatic adjustment of accelerating voltage according to measured gamma rays yield allowed us to get the long-time proton energy accuracy better than 0.15% for 2.5 hours.

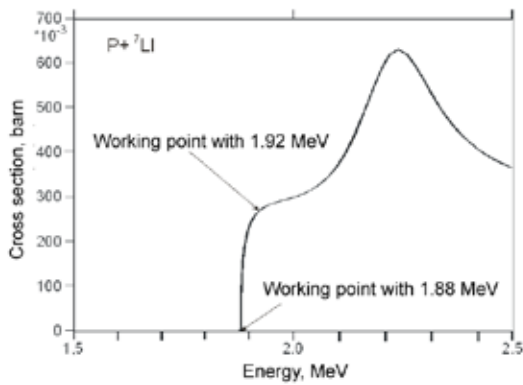


Fig.(9.1)2. Dependence of neutron generation cross section on proton energy.

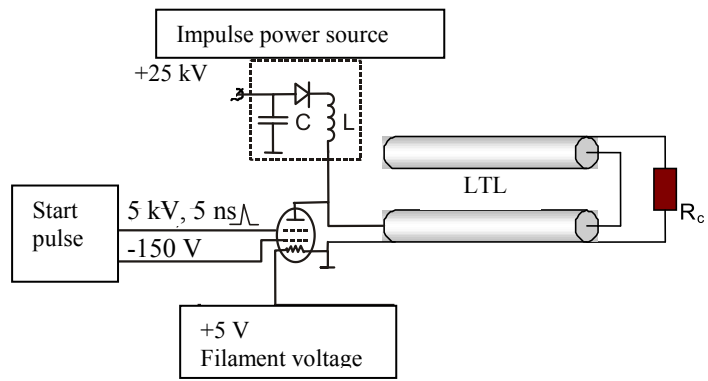


Fig.(9.1)3. Scheme of the high voltage short pulses generator.

## 9.2 X-ray detectors for medicine and examination of people

### 9.2.1 Medical Radiography

BINP produced 13 1536-channel detectors for ZAO "Nauchpribor" (Orel), which were supplied to medical institutions of Russia as part of digital scanning fluorographs.

### 9.2.2 X-ray Inspection System "Sibscan" for examination of people

For the purpose of improving anti-terrorist protection, a second plant "Sibscan" was installed in the international terminal of the airport Tolmachevo and commissioned.

In 2010, based on the experience of previous years, a new version of the XIS plant was developed. One major advantage of the new version is the reduced dimensions. The volume occupied by the plant decreased from 15 m<sup>3</sup> to 9.5 m<sup>3</sup>. This eases the requirements to premises for the plant and thus expands the possibilities of its application. A pilot plant is under being fabricated. It is to be completed in 2011.

### 9.2.3 Works for High Energy Physics

The electronics of coordinate chambers for an extracted beam of tagged positrons or electrons were designed, manufactured and commissioned. As part of the new detector CMD-3 The endcap calorimeter is running in full in the new KMD-3 detector. The BINP members actively participated in conducting experiments with the detector ATLAS, CERN, and another experiment on the search for neutrinoless muon decay, MEG, at PSI, Switzerland.

## BIBLIOGRAPHY

### List of publications

- [1] Golubenko Yu.I., Kuksanov N.K., Salimov R.A., Nemytov P.I. Extraction of a powerful electron beam into the atmosphere through two parallel titanium foils. // *J. of Applied Mechanics and Technical Physics*. - 2010. - Vol.51. - N2. - P.145-147.
- [2] Anchugov O.V., Blinov V.E., Bogomyagkov A.V., Volkov A.A., Zhuravlev A.N., Karnaev S.E., Kiselev V.A., Levichev E.B., Meshkov O.I., Mishnev S.I., Morozov I.I., Muchnoi N.Yu., Nikitin S.A., Nikolaev I.B., Petrov V.V., Piminov P.A., Simonov E.A., Sinyatkin S.V., Skrinsky A.N., Smalyuk V.V., Tikhonov Yu.A., Tumaikin G.M., Tsukanov V.M., Shamov A.G., Shatilov D.N., Shvedov D.A. Use of the methods of accelerator physics in precision measurements of particle masses on the VEPP-4 complex with the KEDR detector. // *Instruments and Experimental Techniques*. - 2010. - Vol.53. - N1. - P.15-28; *PTE*. - 2010. - N1. - P.20-33.
- [3] Aruev P.N., Kolokolnikov Yu.M., Kovalenko N.V., Legkodymov A.A., Lyakh V.V., Nikolenko A.D., Pindyurin V.F., Sukhanov V.L., Zabrodsky V.V. Preliminary characterization of semiconductor detectors in the soft X-ray range using synchrotron radiation from the VEPP-4 storage ring. // *Surface Investigation-X-Ray Synchrotron and Neutron Techniques*. - 2010. - Vol.4. - N1. - P.99-103; *Poverhnost*. - 2010. - N2. - P.19-24.
- [4] Pakhlova G.V., Pakhlov P.N., Eidelman S.I. Exotic charmonium. // *Physics Uspekhi*. - 2010. - Vol.53. - N3. - P.219-241.
- [5] Erokhin A., Medvedko A., Skorobogatov D., Selivanov P. A four quadrant voltage converter (600 V, 500 A). // *Instruments and Experimental Techniques*. - 2010. - Vol.53. - N2. - P.240-245; *PTE*. - 2010. - N2. - P.90-96.
- [6] Polosatkin S.V., Grishnyaev E.S., Davydenko V.I., Ivanov I.A., Podyminogin A.A., Shikhovtse I.V. Optical spectroscopy of plasma of the radio frequency emitter of a powerful fast neutral beam injector. // *Instruments and Experimental Techniques*. - 2010. - Vol.53. - N2. - P.253-257; // *PTE*. - 2010. - N2. - P.104-109.
- [7] Dimov G.I. Emelev I.S. Plasma potential distribution in tandem surface-plasma source of negative ions. // *Technical Physics Letters*. - 2010. - Vol.36. - N3. - P.254-257; *JTP*. - 2010. - T.36. - N6. - P.15-21.
- [8] Kozyrev E.V. Microwave devices. // *Textbook*. - Novosibirsk: NSTU Publishing house, 2010. - 156p. (in Russian).
- [9] Vostretsov A.G., Burdakov A.V., Radchenko S.E., Kuznetsov A.S., Sulyaev Yu.S. Method of detect of gamma-quant absorption passed nitrogen-containing matter. // *Avtometriya*. - 2010. - Vol.46. - N3. - P.22-29.
- [10] Bondarenko A.V., Vinokurov N.A., Miginsky S.V., Ostreiko G.N. Bondarenko A.V., Miginsky S.V., Vinokurov N.A., Ostreiko. A novel extraction scheme from a synchrotron using a magnetic shield. // *Problems of Atomic Science and Technology. Ser.: Nucl. Phys. Investigations*. - 2010. - N3. - P.31-34.
- [11] Matveev V.A., Sisakyan A.N., Skrinsky A.N. Large Hadron Collider - a new step to the knowledge of the depths of matter. The contribution of physicists in Russia is the largest international project at the turn of the XX and XXI century (in Russian). // *Vestnik RAN*. - 2010. - V.80. - N3. - P.204-217.
- [12] Zhmurikov, E.I., Bolkhovityanov D.Yu., Blinov M.F., Ishchenko A.V., Kot N.Kh., Titov A.T., Tsybulya S.V., Luigi Tecchio. On the problem of reactor graphite lifetime. // *Surface: Investigation-X-Ray Synchrotron and Neutron Techniques*. - 2010. - Vol.4. - N3. - P.442-451; (*Poverhnost* - 2010. - N5. - P.89-99).

- [13] Anikeev A.V., Bagryansky P.A., Beklemishev A.D., Lizunov A.A., Maksimov V.V., Murakhtin S.V., Prikhodko V.V., and Solomakhin A.L. Suppression of longitudinal losses in a Gas Dynamic Trap by using an ambipolar mirror. // *Plasma Physics Reports*. - 2010. – Vol.36. - N5. - P.381-389.
- [14] Barnyakov A.M. A cavity microwave load. // *Instruments and Experimental Techniques*. - 2010. - Vol.53. - N3. - P.385-388.
- [15] Kolmogorov V.V., Abdrashitov G.F. A high voltage power source based on a distributed capacitive energy storage. // *Instruments and Experimental Techniques*. - 2010. - Vol.53. - N3. - P.381-384.
- [16] Aulchenko V.M., Zhulanov V.V., Shekhtman L.I., Evdokov O.V., Zhogin I.L., Tolochko B.P., Prueel E.R., Ten K.A.. A detector for imaging of explosions on a synchrotron radiation beam. // *Instruments and Experimental Techniques*. - 2010. - Vol.53. - N3. - P.334-349.
- [17] Peltek S.E., Goryachkovskaya T.N., Rubtsov N.B., Khlebodarova T.M., Kolchanov N.A., Popic V.M., Pindyurin V.F., Goldenberg B.G., Scheglov M.A., Kulipanov G.N. Microfluidic systems in biology and engineering of genosensors. // *NANO. Technology. Ecology. Manufacturing*. - 2010. - N2(4). - P.84-87.
- [18] Barkov L.M., Gauzshtein V.V., Dmitriev V.F., Lazarenko B.A., Levchuk M.I., Loginov A.Yu., Mishnev S.I., Nikolenko D.M., Osipov A.V., Rachek I.A., Sidorov A.A., Stibunov V.N., Toporkov D.K., Shestakov Yu.V., Zevakov S.A. Tensor asymmetry of  $\pi$  meson photoproduction on polarized deuterons. // *Bulletin of the Russian Academy of Sciences: Physics*. - 2010. - Vol. 74, - N6. - P.743-746.
- [19] Gerasimov V.V., Knyazev B.A., Cherkassky V.S., Obtaining spectrally selective images of objects in attenuated total reflection regime in real time in visible and terahertz ranges. // *Optics and Spectroscopy*. - 2010. - Vol.108. - N6. - P.859-865.
- [20] Gauzstein V.V., Loginov A.Yu., Nikolenko D.M., Osipov A.V., Sidorov A.A., Stibunov V.N. Virtual photons in the reaction  $d(e, pp)e'\pi^{-1}$ . // *Bulletin of the Russian Academy of Sciences: Physics*. - 2010. - N5. - P.14-19.
- [21] R.E. Gerasimov, V.S. Fadin. Scalar contribution to the BFKL kernel. // *Physics of Atomic Nuclei*. - 2010. - Vol.73. - N7. - P.1214-1228.
- [22] Kamenschik A.Yu., Pokrovsky V.L., Khriplovich I.B. On the 90th anniversary of Academician Khalatnikov. Physical Sciences Division of Russian Academy of Sciences, 21 October 2009. // *Physics Uspekhi*. - 2010. - Vol.180. - N3. - P.328-330.
- [23] Ivanov A.V., Reva V.B. Calculation of the variable-profile electron beam for electron coolers. // *Instruments and Experimental Techniques*. - 2010. - Vol.53. - N4. - P.539–544.
- [24] Chernousov Yu.D. Ivannikov V.I., Shebolaev I.V., Levichev A.E., Pavlov V.M. Bandpass characteristics of coupled resonators. // *Technology and Electronics*. - 2010. - Vol.55. - N8. - P.923-929.
- [25] Knyazev B.A., Nikitin A.A., Cherkassky V.S. Automatic registration of movement of objects by the speckle method in the terahertz range. // *Optoelectronics, Instrumentation and Data Processing*. - 2010. - Vol.46. - N4. - P.78-83.
- [26] Vedernikov V.M., Dutov P.M., Kokarev A.I., Kiriyanov V.P., Knyazev B.A., Nikitin V.G., Pal'chikova I.G., Sametov A.R., Stupak M.F., Chugui Yu.V., Chukanov V.V. Diffractive elements for free-electron laser. // *Optoelectronics, Instrumentation and Data Processing*. - 2010. - Vol.46. - N4. - C.84-97.
- [27] Terekhov A.V., Timofeev I.V., Lotov K.V. Two-dimensional numerical model for studies of collective beam-plasma interaction. // *Vestnik NSU. Ser.: Physics*. - 2010. - Vol.5. - N2. - P.85-97.
- [28] Silagadze Z.K., Chaschina O.I. Comment on «Note on the dog-and-rabbit chase problem in introductory kinematics». // *Vestnik NSU*. - 2010. - Vol.5. - N2. - P.111-115.
- [29] Nikolenko D.M., Barkov L.M., Gramolin A.V., Dmitriev V.F., Zevakov S.A., Karnakov I.V., Lazarenko B.A., Mishnev S.I., Muchnoi N.Y., Rachek I.A., Sadykov R.S., Toporkov D.K., Shestakov Y.V., Shekhtman L.I., Arenhövel H., Arrington J., Potterveld D.H., Holt R.J., Belostotski S.L., Nelyubin V.V., et al. Experiments with internal targets at the VEPP-3 electron storage ring. //

- Physics of Atomic Nuclei. - 2010. - Vol.73. - N8. - P.1322-1338.
- [30] Achasov M.N., Beloborodov K.I., Berdyugin A.V., Bogdanchikov A.G., Bukin D.A., Vasil'ev A.V., Golubev V.B., Dimova T.V., Druzhinin V.P., Koop I.A., Korol' A.A., Koshuba S.V., Pakhtusova E.V., Serednyakov S.I., Silagadze Z.K., Skrinsky A.N., Shatunov Yu.M., Shtol' D.A. Measurement of the  $e^+e^- \rightarrow \eta\pi^+\pi^-$  cross section in the root  $\sqrt{s}=1.04-1.38$  GeV energy range with a Spherical Neutral Detector at the VEPP-2M Collider. // JETP Letters. - 2010. - Vol.92. - N2. - P.80-84.
- [31] Kiselev V.A., Smaluk V.V. Experimental investigation of coupling impedances of the VEPP-4M electron-positron collider. // JTP. - 2010. - Vol.55. - N8. - P.1175-1182.
- [32] Pal'chikov E.I., Kondrat'ev V.I., Golikov E.V., Cheremisin A.N. Experimental study of a BaFBr:Eu image plate detector depending on dose, spectrum of pulse X-ray source, and scan number. // J. of Surface Investigation X-Ray Synchrotron and Neutron Techniques. - 2010. - Vol.4. - N4. - P.622-629.
- [33] Valeev R.G., Deev A.N., Romanov E.A., Kriventsov V.V., Beltyukov A.N., Mezentsev N.A., Eliseev A.A., Napol'skii K.S. Synthesis and structure study of ordered arrays of ZnSe nanodots. // J. of Surface Investigation X-Ray Synchrotron and Neutron Techniques. - 2010. - Vol.4. - N4. - P.671-674.
- [34] Ivanov V.Yu., Pustovarov V.A., Kruzhalov A.V., Tausenev D.S., Zinin E.I. Time-resolved spectroscopy of natural and synthetic BeO crystals. // J. of Surface Investigation X-Ray Synchrotron and Neutron Techniques. - 2010. - Vol.4. - N4. - P.645-648.
- [35] Kuznetsov S.A., Arzhannikov A.V., Gelfand A.V., Zorenko A.V., Gorshunov B.P. Multi channel radiometric system for registration of sub-millimeter radiation generated by beam-plasma interaction. // Bulletin of NSU. Ser.: Physics. - 2010. - Vol.5. - Issue 3. - P.5-19.
- [36] Bryzgunov M.I., Bublei A.V., Vostrikov V.A., Panasyuk V.M., Parkhomchuk V.V., Reva V.B. Compact storage ring with longitudinal magnetic field and electron cooling. // Vestnik NSU. Ser.: Physics. - 2010. - V.5. - N3. - P.79-89.
- [37] Tsidulko Yu.A., Chernoshtanov I.S. Nonlinear stage of Alfvén ion cyclotron instability. // Vestnik NSU. Ser.: Physics. - 2010. - V.5. - N3. - P.90-94.
- [38] Batrakov A.M., Logatchev P.V., Pavlenko A.V., Sazanskiy V.Ya., Fatkin G.A.. Control system of linear induction accelerator for X-ray system. // Vestnik NSU. Ser.: Physics. - 2010. - Vol.5. - N3. - P.98-105.
- [39] Kuksanov N.K., Nemytov P.I., Golubenko Y.I. Small-sized rotary voltmeter in systems measurement and stabilization accelerating voltage for industrial electron accelerators. // Bulletin of NSU. Ser.: Physics. - 2010. - Vol.5. - N3. - P.95-97
- [40] Lotov K.V., Maslov V.I., Onishchenko I.N. Transformer ratio in a plasma wakefield accelerator driven by trains of relativistic electron bunches. // Problems of Atomic Science and Technology. - 2010. - Vol.4. - P.85-89.
- [41] Dar'in A.V., Rakshun Ya.V. Scanning X-ray fluorescent microanalysis of natural samples using synchrotron radiation (SR) from the VEPP-3 (BINP SB RA) and focusing x-ray optics. // School for young professional, "Synchrotron radiation in the Earth Sciences", Novosibirsk, 11-15 October 2010: Lecture bank. - Novosibirsk: BINP, 2010. - P.8-15 (SCSTR: 3rd School for young professionals, "Synchrotron radiation in advanced technology") (in Russian).
- [42] Zolotarev K. Foundations of X-ray fluorescence analysis (XRF), features of XRF using synchrotron radiation (SR). XRF at the world's synchrotron radiation centers. // School for young professional, "Synchrotron radiation in the Earth Sciences", Novosibirsk, 11-15 October 2010: Lecture bank. - Novosibirsk: BINP, 2010. - P.16-20 (SCSTR: 3rd School for young professionals, "Synchrotron radiation in advanced technology") (in Russian).
- [43] Kulipanov G.N. Synchrotron radiation: generation and application (in Russian). // School for young professionals, "Synchrotron radiation in the Earth Sciences, Novosibirsk", 11-15 October 2010: Lecture bank. - Novosibirsk: BINP, 2010. - P.28-49 (SCSTR: 3rd School of for young professionals "Synchrotron radiation in advanced technology").
- [44] Kuper K.E. X-ray microscopy and microtomography using synchrotron radiation. // School for young

- professionals, "Synchrotron radiation in the Earth Sciences, Novosibirsk", 11-15 October 2010: Lecture bank. - Novosibirsk: BINP, 2010. - P.50-53 (SCSTR: 3rd School for young professionals "Synchrotron radiation in advanced technology") (in Russian).
- [45] Mezentsev N.A. SR source on superconducting magnets. // School for young professionals, "Synchrotron radiation in the Earth Sciences", Novosibirsk, 11-15 October 2010: Lecture bank. - Novosibirsk: BINP, 2010. - p.81-85 (SCSTR: 3rd School for young professionals "Synchrotron radiation in advanced technology") (in Russian).
- [46] Nikolenko A.D. Space weather. The study of solar activity in the range of 10 to 2000 eV. Remote sensing. // School for young professionals, "Synchrotron radiation in the Earth Sciences", Novosibirsk, 11-15 October 2010: Lecture bank. - Novosibirsk: BINP, 2010, p.86-89.
- [47] Vladimirov V.M., Zapryagaev I.A., Konnov V.G., Kurkin G.Ya., Tarnetski V.V., Chernov K.N. Low-noise source of microwave signals, // PTE. - 2010. - N5. - P.93-94.
- [48] Batkin V.I. Charges on the surface of a lens cavity in a two-dimensional homogeneous conductor. // JTP. - 2010. - Vol.55. - N9. P. 1386-1387.
- [49] Avdeeva E.G., Bogdanchikov A.G., Botov A.A., Bukin D.A., Vasiljev A.V., Vesenev V.M., Golubev V.B., Dimova T.V., Druzhinin V.P., Korol A.A., Koshuba S.V., Obrazovsky A.E., Pakhtusova E.V., Serednyakov S.I., Sirotkin A.A., Surin I.K., Usov Yu.V., Filatov P.V., and Kharlamov A.G. New tracking system of the SND detector. // Phys. Atom. Nucl. - 2010. - Vol.73. - N11. - P.1931-1934.
- [50] Gilev O.N., Vikhlyaev D.A., Legkodymov A.A., Nikolenko A.D. Absolute calibration of X-ray optical elements and detectors at a wavelength of 46.9 nm. // J. Instruments and Experimental Techniques. - Nov. 2010. - Vol.53. - N6. - P.873-876.
- [51] Bayanov B.F., Kandiev Ya.Z., Kashaeva E.A., Malyshkin G.N., Taskaev S.Yu., Chudaev V.Ya. A protective subsurface container for holding and temporary storage of activated targets. // J. Instruments and Experimental Techniques. - Nov. 2010. - Vol.53. - N6. - P.883-885.
- [52] Gerasimov V.V., Knyazev B.A., Nikitin A.K., Nikitin V.V. Method for identifying diffraction satellites of surface plasmons in terahertz frequency range. // J. Technical Physics Letters. - Nov. 2010. - Vol.36. - N11. - P.1016-1019.
- [53] Gerasimov V.V., Zhizhin G.N., Nikitin A.K., Knyazev B.A. The excitation of terahertz-range surface plasmons by frustrated total internal reflection through the substrate. // J. of Optical Technology. - 2010. - Vol.77. - N8. - P.465-468.
- [54] Achasov M.N., Beloborodov K.I., Berdyugin A.V., Bogdanchikov A.G., Bukin, D.A., Vasil'ev A.V., Golubev V.B., Dimova T.V., Druzhinin V.P., Koop I.A., Korol' A.A., Koshuba S.V., Pakhtusova E.V., Serednyakov S.I., Silagadze Z.K., Skrinsky A.N., Shatunov Yu.M. Searching for the process  $e^+e^- \rightarrow K^+K^-\pi^0$  in experiments with the spherical neutral detector at VEPP-2M. // JETP. 2010. - Vol.110. - N1. - P.26-33.
- [55] Onuchin A.P. Experimental methods of nuclear physics: a tutorial. // Novosibirsk: NSTU, 2010. - 219p. (Ser. " Textbooks NSTU").
- [56] Levichev E.B. Lectures on nonlinear dynamics of particles in a circular accelerator: a tutorial. // Novosibirsk: NSTU, 2010. - 222p. (Ser. " Textbooks NSTU").
- [57] Dikansky N.S., Pestrikov D.V. Landau damping and dephasing of coherent oscillations of beams in storage rings. // Textbook. - Novosibirsk: NSU, 2010. - 82p. (in Russian)
- [58] Belikov O.V., Veremeenko V.F., Chupyra A.G. Fundamentals of electronics. // Textbook. - Novosibirsk: NSU, 2010. - 112p (in Russian).
- [59] Kwan T.J.T., Morgado R.E., Wang Tai-Sen.F., Vodolaga B., Terekhin V., Onischenko L.M., Samsonov E.V., Vorozhtsov A.S., Alenitsky Yu.G., Perpelkin E.E., Glazov A.A., Novikov D.L., Parkhomchuk V., Reva V., Vostrikov V., Mashinin V.A., Fedotov S.N., Minayev S.A. The development of enabling technologies for producing active interrogation beams. // RSI. - 2010. - Vol.81. - N10. - P.103304-1-13.
- [60] Khrebtov I.A., Malyarov V.G., Zerov V.Yu., Nicolenco A.D., Pindyurin V.F., Legkodymov A.A., Lyah V.V. Test of model of absolute measuring instrument of synchrotron radiation power. // Key

- Engineering Materials. - 2010. - Vol.437. - P.636-640.
- [61] Fadin V.S., Fiore R., Grabovsky A.V. Matching of the low-x evolution kernels. // Nucl. Phys. B. - 2010. - Vol.831. - N1/2. - P.248-261; JETP. - 2010. - Vol.110. - P.383-405.
- [62] Chernyak V.L. Mass spectrum in supersymmetric QCD and problems with the Seiberg duality. Equal quark masses. // ЖЭТФ. - 2010. - Vol.137. - N3. - C.437-459; JETP. - 2010. - Vol.91. - N5/6. - P.383-405.
- [63] Chernyak V.L. A three-loop check of the "a-maximization" in SQCD with adjoint(s). // Письма в ЖЭТФ. - 2010. - Vol.91. - N5/6. - C.237-239; JETP. - 2010. - Vol.91. - N5/6. - P.219-221.
- [64] Evsyukova M.A., Yalovega G., Balerna A., Menushenkov A.P., Rakshun Ya.V., Teplov A.A., Mikheeva M.N., Soldatov A.V. Crystal-quasicrystal transition in the Al-Cu-Fe system: Analysis of the local atomic structure. // Physica Condensed Matter B. - 2010. - Vol.405. - N8. - P.2122-2124.
- [65] Aubert B., BABAR Collab., Blinov V.E., Bukin A.D., Buzykaev A.R., Druzhinin V.P., Golubev V.B., Onuchin A.P., Serebnyakov S.I., Skovpen Yu.I., Solodov E.P., Todyshev K.Yu., et al. Searches for lepton flavor violation in the decays  $\tau^{+-} \rightarrow e^{+-} \gamma$  and  $\tau^{+-} \rightarrow \mu^{+-} \gamma$ . // Phys. Rev. Lett. - 2010. - Vol.104. - N2. - P.021802-1-7; [arXiv:0908.2381 [hep-ex]].
- [66] Uehara S., Belle Collab., Eidelman S., Epifanov D., Gabyshev N., Kuzmin A., Shwartz B., Zyukova O., et al. Observation of a Charmoniumlike enhancement in the  $\gamma\gamma \rightarrow \omega J/\psi$  process. // Phys. Rev. Lett. - 2010. Vol.104. - N9. - P.092001-1-6.
- [67] Urquijo P., Belle Collab., Arinstein K., Eidelman S., Gabyshev N., Kuzmin A., Shwartz B., Zhilich V., Zhulanov V., Zyukova O., et al. Measurement of  $|V_{ub}|$  from inclusive charmless semileptonic B decays. // Phys. Rev. Lett. - 2010. - Vol.104. - N2. - P.021801-1-5.
- [68] Shen C.P., Belle Collab., Eidelman S., Epifanov D., Gabyshev N., Shwartz B., Zyukova O., et al. Evidence for a new resonance and search for the Y(4140) in the  $\gamma\gamma \rightarrow \phi J/\psi$  process. // Phys. Rev. Lett. - 2010. Vol.104. - N11. - P.112004-1-5.
- [69] Aubert B., BABAR Collab., Blinov V.E., Bukin A.D., Buzykaev A.R., Druzhinin V.P., Golubev V.B., Onuchin A.P., Serebnyakov S.I., Skovpen Yu.I., Solodov E.P., Todyshev K.Yu., et al. Measurement of  $|V_{cb}|$  and the form-factor slope in anti B  $\rightarrow D\ell^+ \text{ anti } \nu_l$  decays in events tagged by a fully reconstructed B meson. // Phys. Rev. Lett. - 2010. - Vol.104. - N1. - P.011802-1-7.
- [70] Vladimir Nikolaevich Baier 1930-2010. // CERN Courier. - 2010. - Vol.50. - N3. - C.33, photo.
- [71] Sanchez P. del Amo., BABAR Collab., Blinov V.E., Buzykaev A.R., Druzhinin V.P., Golubev V.B., Onuchin A.P., Serebnyakov S.I., Skovpen Yu.I., Solodov E.P., Todyshev K.Yu., Yushkov A.N., et al. Test of lepton universality in Y(1S) decays at BABAR. // Phys. Rev. Lett. - 2010. - Vol.104. - N19. - P.191801-1-7; [E-print: arXiv:1002.4358 [hep-ex]].
- [72] Fujikawa M., Belle Collab., Arinstein K., Aulchenko V., Bondar A., Shebalin V., Sokolov A., Usov Y., Vinokurova A., et al. Measurement of CP asymmetries in  $B^0 \rightarrow K^0 \pi^0$  decays. // Phys. Rev. D. - 2010. - Vol.81. - N1. - P.011101-1-7.
- [73] Aushev T., Belle Collab., Bondar A., Eidelman S., Gabyshev N., Shwartz B., Usov Y., Zhulanov V., Zyukova O., et al. Study of the  $B \rightarrow X(3872) \rightarrow (D^* D^0) K$  decays. // Phys. Rev. D. - 2010. - Vol.81. - N3. - P.031103-1-7.
- [74] Joshi N.J., Belle Collab., Arinstein K., Aulchenko V., Bondar A., Eidelman S., Gabyshev N., Kuzmin A., Poluektov A., Shwartz B., Usov Y., Zhilich V., Zyukova O., et al. Measurement of the branching fractions for  $B^0 \rightarrow D_s^{*+} \pi^-$  and  $B^0 \rightarrow D_s^{*-} K^+$  decays. // Phys. Rev. D. - 2010. - Vol.81. - N3. - P.031101-1-6.
- [75] Petric M., Belle Collab., Arinstein K., Eidelman S., Gabyshev N., Kuzmin A., Shebalin V., Shwartz B., Vinokurova A., Zhulanov V., et al. Search for leptonic decays of  $D^0$  mesons. // Phys. Rev. D. - 2010. - Vol.81. - N9. - P.091102-1-6.
- [76] Aubert B., BABAR Collab., Blinov V.E., Bukin A.D., Buzykaev A.R., Druzhinin V.P., Golubev V.B., Onuchin A.P., Serebnyakov S.I., Skovpen Yu.I., Solodov E.P., Todyshev K.Yu., et al. Observation of inclusive  $D^{*\pm}$  production in the decay of Y(1S). // Phys. Rev. D. - 2010. - Vol.81. - N1. - P.011102-1-8.
- [77] Aubert B., BABAR Collab., Blinov V.E., Bukin A.D., Buzykaev A.R., Druzhinin V.P., Golubev V.B., Onuchin A.P., Serebnyakov S.I., Skovpen Yu.I., Solodov E.P., Todyshev K.Yu., et al. Observation of

- the  $\chi_{c2}/(2P)$  meson in the reaction  $\gamma\gamma \rightarrow D$  anti  $D$  at BABAR. // *Phys. Rev. D.* - 2010. - Vol.81. - N9. - P.092003-1-16; [E-print: arXiv:1002.0281 [hep-ex]].
- [78] Achasov M.N., Beloborodov K.I., Berdyugin A.V., Bogdanchikov A.G., Bukin A.D., Bukin D.A., Dimova T.V., Druzhinin V.P., Golubev V.B., Koop I.A., Korol A.A., Koshuba S.V., Lysenko A.P., Pakhtusova E.V., Serednyakov S.I., Shatunov Yu.M., Silagadze Z.K., Skrinsky A.N., Vasiljev A.V. Search for lepton flavor violation process  $e^+e^- \rightarrow e\mu$  in the energy region radical  $\sqrt{s} = 984\text{-}1060$  MeV and  $\phi \rightarrow e\mu$  decay. // *Physical Review D.* - 2010. - Vol.81. - N5. - P.057102-1-4.
- [79] Lees J.P., BABAR Collab., Blinov V.E., Buzykaev A.R., Druzhinin V.P., Golubev V.B., Onuchin A.P., Serednyakov S.I., Skovpen Yu.I., Solodov E.P., Todyshev K.Yu., Yushkov A.N., et al. Search for charged lepton flavor violation in narrow  $Y$  decays. // *Phys. Rev. Lett.* - 2010. - Vol.104. - N15. - P.151802-1-7; [E-print: arXiv:1001.1883 [hep-ex]].
- [80] Aubert B., BABAR Collab., Blinov V.E., Bukin A.D., Buzykaev A.R., Druzhinin V.P., Golubev V.B., Onuchin A.P., Serednyakov S.I., Skovpen Yu.I., Solodov E.P., Todyshev K.Yu., et al. Measurement and interpretation of moments in inclusive semileptonic decays anti  $B \rightarrow X_c$   $l^-$  anti  $\nu$ . // *Phys. Rev. D.* - 2010. - Vol.81. - N3. - P.032003-1-25.
- [81] Khriplovich I.B. Strict upper limits on electric dipole moment of  $W$  boson. // *Physics of Atomic Nuclei* . - 2010. - Vol.73. - N4. - P.634-635.
- [82] Knyazev B.A., Kulipanov G.N., Vinokurov N.A. Novosibirsk terahertz free electron laser: instrumentation development and experimental achievements. // *Measurement Science and Technology.* - 2010. - Vol.21. - N5. - P.054017-1-29.
- [83] Ko B.R., Belle Collab., Aulchenko V., Eidelman S., Pakhlov P., Pakhlova G., Shebalin V., Sokolov A., Zhilich V., Zyukova O., et al. Search for CP violation in the decays  $D^+_{(s)} \rightarrow K^0_S \pi^+$  and  $D^+_{(s)} \rightarrow K^0_S K^+$ . // *Phys. Rev. Lett.* 2010. - Vol.104. - N18. - P.181602-1-6.
- [84] Chiang C. - C., Belle Collab., Arinstein K., Aulchenko V., Bondar A., Eidelman S., Gabyshev N., Sokolov A., Usov Y., Zyukova O., et al. Search for  $B^0 \rightarrow K^{*0}$  anti- $K^{*0}$ ,  $B^0 \rightarrow K^{*0} K^{*0}$  and  $B^0 \rightarrow K^+ \pi^- K^\pm \pi$  decays. // *Phys. Rev. D.* - 2010. - Vol.81. - N7. - P.071101-1-7.
- [85] Ablikim M., BESIII Collab., Achasov M.N., Muchnoi N.Yu., et al. Branching fraction measurements of  $\chi/\text{sub } c0/$  and  $\chi/\text{sub } c2/$  to  $\pi^0 \pi^0$  and  $\eta \eta$ . // *Phys. Rev. D.* - 2010. - Vol.81. - N5. - P.052005-1-8.
- [86] Aubert B., BABAR Collab., Blinov V.E., Bukin A.D., Buzykaev A.R., Druzhinin V.P., Golubev V.B., Onuchin A.P., Serednyakov S.I., Skovpen Yu.I., Solodov E.P., Todyshev K.Yu., et al. Measurement of branching fractions of  $B$  decays to  $K_1(1270)\pi$  and  $K_1(1400)\pi$  and determination of the CKM angle  $\alpha$  from  $B^0 \rightarrow a_1(1260)^+ \pi^-$ . // *Phys. Rev. D.* - 2010. - Vol.81. - N5. - P.052009-1-16.
- [87] Aubert B., BABAR Collab., Blinov V.E., Bukin A.D., Buzykaev A.R., Druzhinin V.P., Golubev V.B., Onuchin A.P., Serednyakov S.I., Skovpen Yu.I., Solodov E.P., Todyshev K.Yu., et al. Search for  $B^+ \rightarrow l^+ \nu/\text{sub } l/$  recoiling against  $B^- \rightarrow D^0 l^-$  anti  $\nu$   $X$ . // *Phys. Rev. D.* - 2010. - Vol.81. - N5. - P.051101-1-9.
- [88] Ablikim M., BESIII Collab., Achasov M.N., Muchnoi N.Yu., et al. Measurements of  $h^1_c(1P_1)$  in  $\psi'$  decays. // *Phys. Rev. Lett.* - 2010. - Vol.104. - N13. - P.132002-1-6.
- [89] Ivanov A.A., Beklemishev A.D., Kruglyakov E.P., Bagryansky P.A., Lizunov A.A., Maximov V.V., Murakhtin S.V., Prikhodko V.V. Results of recent experiments on GDT device after upgrade of heating neutral beams. // *Fusion Science and Technology.* - 2010. - Vol.57. - N4. - P.320-325.
- [90] Beklemishev A.D., Bagryansky P.A., Chaschin M.S., Soldatkina E.I. Vortex confinement of plasmas in symmetric mirror traps. // *Fusion Science and Technology.* - May 2010. - Vol.57. - N4. - P.351-360.
- [91] Molvik A., Ivanov A., Kulcinski G.L., Ryutov D., Santarius J., Simonen T., Wirth B.D., Ying A.A. GAS dynamic trap neutron source for fusion material and subcomponent testing. // *Fusion Science and Technology.* - 2010. Vol.57. - N4. - P.369-394.
- [92] Zobov M., Alesini D., Biagini M.E., Biscari C., Bocci A., Boni R., Boscolo M., Bossi F., Buonomo B., Clozza A., Delle Monache G.O., Demma T., Di Pasquale E., Di Pirro G., Drago A., Gallo A., Ghigo A., Guiducci S., Ligi C., Marcellini F., Mazzitelli G., Milardi C., Murtas F., Pellegrino L.,

- Preger M.A., Quintieri L., Raimondi P., Ricci R., Rotundo U., Sanelli C., Serio M., Sgamma F., Spataro B., Stecchi A., Stella A., Tomassini S., Vaccarezza C., Schioppa M., Esposito M., Branchini P., Iacoangeli F., Valente P., Levichev E., Piminov P., Shatilov D., Smaluk V, et al. Test of "Crab-Waist" collisions at the DAFNE  $\Phi$  factory. // *Phys. Rev. Lett.* - 2010. - Vol.104. - N17. - P.174801-1-5.
- [93] Khriplovich I.B., Lamoreaux S.K., Sushkov A.O., Sushkov O.P. Comment on "Rovibrational quantum interferometers and gravitational waves". // *Phys. Rev. A.* - 2010. - Vol.81. - N6. - P.067601-1-3.
- [94] Avilov M.S., Tecchio L.B., Titov A.T., Tsybulya V.S., Zhmurikov E.I. Design of the 50 kW neutron converter for SPIRAL2 facility. // *NIM. A.* - 2010. - Vol.618. - N1-3. - P.1-15.
- [95] Actis S., Arbuzov A., Balossini G., Beltrame P., Bignamini C., Bonciani R., Carloni Calame C.M., Cherepanov V., Czakov M., Czyz H., Denig A., Eidelman S., Fedotovich G.V., Ferrogliola A., Gluza J., Grzelinska A., Gunia M., Hafner A., Ignatov F., Jadach S., Jegerlehner F., Kalinowski A., Kluge W., Korchin A., Kuhn J.H., Kuraev E.A., Lukin P., Mastrolia P., Montagna G., Muller S.E., Nguyen F., Nicosini O., Nomura D., Pakhlova G., Pancheri G., Passera M., Penin A., Piccinini F., Placzek W., Przedzinski T., Remiddi E., Riemann T., Rodrigo G., Roig P., Shekhovtsova O., Shen C.P., Sibidanov A.L., Teubner T., Trentadue L., Venanzoni G., Van der Bij J.J., Wang P., Ward B.F.L., Was Z., Worek M., Yuan C.Z. Quest for precision in hadronic cross sections at low energy: Monte Carlo tools vs. experimental data. // *Eur. Phys. Journal. C.* - 2010. - Vol.66. - N3/4. - P.585-686; [E-print: arXiv:0912.0749 [hp-ph]].
- [96] Aamodt K., The ALICE Collab., Frolov A., Pestov Y, et al. First proton-proton collisions at the LHC as observed with the ALICE detector: measurement of the charged-particle pseudorapidity density at  $\sqrt{s} = 900$  GeV. // *Eur. Phys. Journal. C.* - 2010. - Vol.65. - N1/2. - C.111-125.
- [97] Zhang X.L., Shiltsev V., Valishev A., Kamerzhiev V., FZ-Julich, Romanov A. Tevatron electron lens and its applications. // *Proc. of Workshop on Beam Cooling and Related topics 2009, Aug.31 - Sept.4, 2009, Lanzhou, P.R.China / Ed. by Y. Yuan, X. Yang.* - Lanzhou: Atomic Energy Press, 2010. - P.103-106.
- [98] Bryzgunov M.I., Panasyuk V.M., Reva V.B. Calculation of electron beam motion in electron cooling system for COSY. // *Proc. of Workshop on Beam Cooling and Related topics 2009, Aug.31 - Sept.4, 2009, Lanzhou, P.R.China / Ed. by Y. Yuan, X. Yang.* - Lanzhou: Atomic Energy Press, 2010. - P.134-137.
- [99] Parkhomchuk V.V., Reva V.B., Bublely A.V., Panasyuk V.M. Electron cooling for the therapy accelerator complex. // *Proc. of Workshop on Beam Cooling and Related topics 2009, Aug.31 - Sept.4, 2009, Lanzhou, P.R.China / Ed. by Y. Yuan, X. Yang.* - Lanzhou: Atomic Energy Press, 2010. - P.168-172.
- [100] Yang X.D., Mao L.J., Li G.H., Ma X.M., Yan T.L., Yuan Y.J., Song M.T., Yang J.C., Liu Y., Zhao T.C., Xia J.W., Zhang W., Gao D.Q., Zhou Z.Z., Yan H.B., Mao R.S., Han S.F., Zheng J.H., Yang X.T., Zhao H.W., Xiao C., Yin D.Y., Li P., Jia H., Parkhomchuk V.V., Reva V.B., Skorobogatov D.N. Commissioning of electron cooling in CSRe. // *Proc. of Workshop on Beam Cooling and Related topics 2009, Aug.31 - Sept.4, 2009, Lanzhou, P.R.China / Ed. By Y. Yuan, X. Yang.* - Lanzhou: Atomic Energy Press, 2010. - P.173-177.
- [101] Dietrich J., Kamerzhiev V., Juelich F.Z.J, Bryzgunov M.I., Goncharov A.D., Parkhomchuk V.V., Reva V.B., Skorobogatov D.N. Status of the 2 MEV electron cooler for COSY Juelich. // *Proc. of Workshop on Beam Cooling and Related topics 2009, Aug.31 - Sept.4, 2009, Lanzhou, P.R.China / Ed. by Y. Yuan, X. Yang.* - Lanzhou: Atomic Energy Press, 2010. - P.178-180.
- [102] Aamodt K., Belikov I., Frolov A., Gorbunov S., Gorbunov Y., Grigoriev V., Ivanov A., Ivanov M., Ivanov V., Kaplin V., Kiselev S., Nikolaev S., Pestov Yu., Vasiliev A., et al. (ALICE Collab.). Charged-particle multiplicity measurement in proton-proton collisions at radical  $\sqrt{s} = 0.9$  and 2.36 TeV with ALICE at LHC. // *The Eur. Phys. J. C.* - 2010. - Vol.68, N1/2. - P.89-108.
- [103] Kuznetsov S.A., Arzhannikov A.V., Kubarev V.V., Kalinin P.V., Sorolla M., Navarro-Cia M., Aznabet M., Beruete M., Falcone F., Goncharov Yu.G., Gorshunov B.P., Gelfand A.V., Fedorina N.I. Development and characterization of quasi-optical mesh filters and metastructures for subterahertz and terahertz applications. // *Key engineering materials.* - 2010. - Vol.437. - P.276-280.

- [104] Shen C.P., Belle Collab., Eidelman S., Gabyshev N., Kuzmin A., Shwartz B., Zhulanov V., Zyukova O, et al. Search for charmonium and charmoniumlike states in  $Y(1S)$  radiative decays. // Phys. Rev. D. - 2010. - Vol.82. - N5. - P.051504-1-6.
- [105] Das A., Belle Collab., Arinstein K., Aulchenko V., Bondar A., Eidelman S., Gabyshev N., Shebalin V., Shwartz B., Usov Y., Zhilich V., Zhulanov V., Zyukova O, et al. Measurements of branching fractions for  $B^0 \rightarrow D_s^+ \pi^-$  and anti- $B^0 \rightarrow D_s^- \pi^+$ . // Phys. Rev. D. - 2010. - Vol.82. - N5. - P.051103-1-7.
- [106] Sanchez P. del Amo., BABAR Collab., Blinov V.E., Buzykaev A.R., Druzhinin V.P., Golubev V.B., Onuchin A.P., Serednyakov S.I., Skovpen Yu.I., Solodov E.P., Todyshev K.Yu., Yushkov A.N, et al. Measurement of CP observables in  $B^+ \rightarrow D_{CP}^+ K^+$  decays and constraints on the CKM angle  $\gamma$ . // Phys. Rev. D. - 2010. - Vol.82. - N7. - P.072004-1-20; [E-print: arXiv:1007.0504 [hep-ex]].
- [107] Sanchez P. del Amo., BABAR Collab., Blinov V.E., Buzykaev A.R., Druzhinin V.P., Golubev V.B., Onuchin A.P., Serednyakov S.I., Skovpen Yu.I., Solodov E.P., Todyshev K.Yu., Yushkov A.N, et al. Search for  $b \rightarrow u$  transitions in  $B^- \rightarrow DK^-$  and  $D^* K^-$  decays. // Phys. Rev. D. - 2010. - Vol.82. - N7. - P.072006-1-18; [E-print: arXiv:1006.4241 [hep-ex]].
- [108] Sanchez P. del Amo., BABAR Collab., Blinov V.E., Buzykaev A.R., Druzhinin V.P., Golubev V.B., Onuchin A.P., Serednyakov S.I., Skovpen Yu.I., Solodov E.P., Todyshev K.Yu., Yushkov A.N, et al. Evidence for the decay  $X(3872) \rightarrow J\psi\omega$ . // Phys. Rev. D. - 2010. - Vol.82. - N1. - P.011101-1-8; [E-print: arXiv:1005.5190 [hep-ex]].
- [109] Lees J.P., BABAR Collab., Blinov V.E., Buzykaev A.R., Druzhinin V.P., Golubev V.B., Onuchin A.P., Serednyakov S.I., Skovpen Yu.I., Solodov E.P., Todyshev K.Yu., Yushkov A.N, et al. Limits on tau lepton-flavor violating decays into three charged leptons. // Phys. Rev. D. - 2010. - Vol.81. - N11. - P.111101-1-8; [E-print: arXiv:1002.4550 [hep-ex]].
- [110] Sanchez P. del Amo., BABAR Collab., Blinov V.E., Buzykaev A.R., Druzhinin V.P., Golubev V.B., Onuchin A.P., Serednyakov S.I., Skovpen Yu.I., Solodov E.P., Todyshev K.Yu., Yushkov A.N, et al. Search for CP violation using T-odd correlations in  $D^0 \rightarrow K^+ K^- \pi^+ \pi^-$  decays. // Phys. Rev. D. - 2010. - Vol.81. - N11. - P.111103-1-8; [E-print: arXiv:1003.3397 [hep-ex]].
- [111] Wedd R., Belle Collab., Arinstein K., Aulchenko V., Eidelman S., Epifanov D., Gabyshev N., Kuzmin A., Poluektov A., Shebalin V., Shwartz B., Usov Y., Vinokurova A., Zhilich V., Zhulanov V., Zyukova O, et al. Evidence for  $B \rightarrow K \eta' \gamma$  decays at Belle. // Phys. Rev. D. - 2010. - Vol.81. - N11. - P.111104-1-7.
- [112] Sanchez P. del Amo., BABAR Collab., Blinov V.E., Buzykaev A.R., Druzhinin V.P., Golubev V.B., Onuchin A.P., Serednyakov S.I., Skovpen Yu.I., Solodov E.P., Todyshev K.Yu., Yushkov A.N, et al. Observation of the rare decay  $B^0 \rightarrow K^0 K^- \pi^+$ . // Phys. Rev. D. - 2010. - Vol.82. - N3. - P.031101-1-8; [E-print: arXiv:1003.0640 [hep-ex]].
- [113] Drutskoy A., Belle Collab., Aulchenko V., Bondar A., Eidelman S., Gabyshev N., Kuzmin A., Poluektov A., Shwartz B., Usov Y., Zhulanov V, et al. Measurement of  $Y(5S)$  decays to  $B^0$  and  $B^+$  mesons. // Phys. Rev. D. - 2010. - Vol.81. - N11. - P.112003-1-7.
- [114] Aubert B., BABAR Collab., Blinov V.E., Bukin A.D., Buzykaev A.R., Druzhinin V.P., Golubev V.B., Onuchin A.P., Serednyakov S.I., Skovpen Yu.I., Solodov E.P., Todyshev K.Yu., et al. Observation of the decay  $\text{anti } B^0 \rightarrow \Lambda_c^+ \text{ anti } \pi \tau^0$ . // Phys. Rev. D. - 2010. - Vol.82. - N3. - P.031102-1-8; [E-print: arXiv:1007.1370 [hep-ex]].
- [115] Lee M.J., Belle Collab., Arinstein K., Aulchenko V., Bondar A., Eidelman S., Epifanov D., Gabyshev N., Garmash A., Kuzmin A., Poluektov A., Shebalin V., Shwartz B., Usov Y., Vinokurova A., Zhilich V., Zhulanov V., Zhyukova V, et al. Measurement of the branching fractions and the invariant mass distributions for  $\tau \rightarrow h^- h^+ h^- \nu_\tau$  decays. // Phys. Rev. D. - 2010. - Vol.81. - N11. - P.113007-1-13.
- [116] Sanchez P. del Amo., BABAR Collab., Blinov V.E., Buzykaev A.R., Druzhinin V.P., Golubev V.B., Onuchin A.P., Serednyakov S.I., Skovpen Yu.I., Solodov E.P., Todyshev K.Yu., Yushkov A.N, et al. Exclusive production of  $D^+ D_s^-$ ,  $D^{*+} D_s^-$ , and  $D^{*+} D_s^{*-}$  via  $e^+e^-$  annihilation with initial-state radiation. // Phys. Rev. D. - 2010. - Vol.82. - N5. - P.052004-1-10; [E-print: arXiv:1008.0338 [hep-ex]].
- [117] Bozek A., Belle Collab., Arinstein K., Aulchenko V., Eidelman S., Shwartz B., Zhulanov V., et al. Observation of  $B^+ \rightarrow \text{anti } D^{*0} \tau^+ \nu_\tau$  and evidence for  $B^+ \rightarrow \text{anti } D^0 \tau^+ \nu_\tau$  at Belle. // Phys. Rev. D. -

2010. - Vol.82. - N7. - P.072005-1-6.
- [118] Poluektov A., Belle Collab., Bondar A., Arinstein K., Aulchenko V., Eidelman S., Epifanov D., Gabyshev N., Garmash A., Kuzmin A., Shebalin V., Shwartz B., Vinokurova A., Usov Y., Zhilich V., Zhulanov V., Zyukova O, et al. Evidence for direct CP violation in the decay  $B \rightarrow D^{(*)}K$ ,  $D \rightarrow K_S \pi^+ \pi^-$  and measurement of the CKM phase  $\varphi_3$ . // Phys. Rev. D. - 2010. - Vol.81. - N11. - P.112002-1-12.
- [119] Anisyonkov A., Klimentov A., Krivashin D., Titov M., et al. (ATLAS Collab.). ATLAS distributed computing. // Proc. of NEC 2009 Conference. - Dubna: JINR, 2010. - P.45-48.
- [120] Talyshev A., et al. (ATLAS Collab.). Commissioning of the ATLAS liquid argon calorimeter. // Proc. of NEC 2009 Conference. - Dubna: JINR, 2010. - P.265-272.
- [121] Milstein A.I., Terekhov I.S. Induced charge generated by a potential well in graphene. // Phys. Rev. B. - 2010. - Vol.81. - N12. - P. 125419-1-5.
- [122] Di Piazza A., Milstein A.I. High-energy electron-positron photoproduction cross section close to the end of the spectrum. // Phys. Rev. B. - 2010. - Vol.82. - N4. - P. 042106-1-9; arXiv:1003.5816 [physics.acc-ph].
- [123] Kumar N., Pukhov A., Lotov K. Self-modulation instability of a long proton bunch in plasmas. // Phys. Rev. Lett. - 2010. - Vol.104. - N25. - P.255003-1-4.
- [124] Louvot R., Belle Collab. Arinstein K., Eidelman S., Poluektov A., Shebalin V., Zyukova O, et al. Observation of  $B^0 \rightarrow D^0 \pi^+$  and  $B^0 \rightarrow D^0 \pi^0$ . // sub s/  $\pi^+$  and  $B^0 \rightarrow D^0 \pi^0$ . // sub s/  $\rho^+$  and measurement of the  $B^0 \rightarrow D^0 \pi^+$  longitudinal polarization fraction. // Phys. Rev. Lett. - 2010. - Vol.104. - N23. - P.231801-1-6.
- [125] Sakai K., Belle Collab., Arinstein K., Bondar A., Eidelman S., Kuzmin A., Shwartz B., Zyukova O, et al. Search for CP-violating charge asymmetry in  $B^\pm \rightarrow J/\psi K^\pm$  decays. // Phys. Rev. D. - 2010. - Vol.82. - N9. - P.091104-1-7.
- [126] Aubert B., BABAR Collab. Blinov V.E., Bukin A.D., Buzykaev A.R., Druzhinin V.P., Golubev V.B., Onuchin A.P., Serebnyakov S.I., Skovpen Yu.I., Solodov E.P, et al. Correlated leading baryon-antibaryon production in  $e^+e^- \rightarrow c \text{ anti } c \rightarrow \Lambda_c^+ \text{ anti } \Lambda_c^- X$ . // Phys. Rev. D. - 2010. - Vol.82. - N9. - P.091102-1-8; [E-print: arXiv:1006.2216 [hep-ex]].
- [127] Sanchez P. del Amo., BABAR Collab., Blinov V.E., Buzykaev A.R., Druzhinin V.P., Golubev V.B., Onuchin A.P., Serebnyakov S.I., Skovpen Yu.I., Solodov E.P., Todyshev K.Yu., Yushkov A.N, et al. Search for  $B^+ \rightarrow D^+ K^0$  and  $B^+ \rightarrow D^+ K^{*0}$  decays. // Phys. Rev. D. - 2010. - Vol.82. - N9. - P.092006-1-11 [E-print: arXiv:1005.0068 [hep-ex]].
- [128] Sanchez P. del Amo., BABAR Collab., Blinov V.E., Buzykaev A.R., Druzhinin V.P., Golubev V.B., Onuchin A.P., Serebnyakov S.I., Skovpen Yu.I., Solodov E.P., Todyshev K.Yu., Yushkov A.N, et al. Search for  $B^+$  meson decay to  $\alpha_1^+(1260) K^{*0}(892)$ . // Phys. Rev. D. - 2010. - Vol.82. - N9. - P.091101-1-8.
- [129] Sanchez P. del Amo., BABAR Collab., Blinov V.E., Buzykaev A.R., Druzhinin V.P., Golubev V.B., Onuchin A.P., Serebnyakov S.I., Skovpen Yu.I., Solodov E.P., Todyshev K.Yu., Yushkov A.N, et al. Observation of new resonances decaying to  $D\pi$  and  $D^*\pi$  in inclusive  $e^+e^-$  collisions near radical  $\sqrt{s} = 10.58$  GeV. // Phys. Rev. D. - 2010. - Vol.82. - N11. - P. 111101-1-9; [E-print: arXiv:1009.2076 [hep-ex]].
- [130] Dudnikov V., Chapovsky P., Dudnikov A. Cesium control and diagnostics in surface plasma negative ion sources. // RSI. - 2010. - Vol.81. - N2. - P.02A714-1-3.
- [131] Listopad A.A., Coenen J.W., Davydenko V.I., Deichuli P.P., Ivanov A.A., Mishagin V.V., Savkin V.Ya., Schalt W., Schweer B., Shulzhenko G.I., Stupishin N.V., Uhlemann R. Operation and upgrade of diagnostic neutral beam injector RUDI at TEXTOR tokamak. // RSI. - 2010. - Vol.81. - N2. - P.02B104-1-3.
- [132] Sorokin A., Belov V., Davydenko V., Deichuli P., Podyminogin A., Shikhovtsev I., Shulzhenko G., Stupishin N., Tiunov M. Characterization of 1 MW, 40 keV, 1 s neutral beam for plasma heating. // RSI. - 2010. - Vol.81. - N2. - P.02B108-1-4.
- [133] Aamodt K., (ALICE COLLAB.), Belikov I., Frolov A., Gorbunov S., Gorbunov Y., Grigoriev V.,

- Ivanov A., Ivanov M., Ivanov V., Kaplin V., Kiselev S., Nikolaev S., Pestov Yu., Vasiliev A., et al. Charged-particle multiplicity measurement in proton-proton collisions at radical  $s = 7$  TeV with ALICE at LHC. // *Eur. Phys. J. C.* - 2010. - Vol.68. - N3/4. - P.345-354.
- [134] Amelino-Camelia G., Eidelman S., Fedotov G.V., Lukin P, et al. Physics with the KLOE-2 experiment at the upgraded DAFNE. // *Eur. Phys. J.C.* - 2010. -Vol.68. - N3/4. - P.619-681; [E-print: arXiv: 1003.3868 [hep-ph]].
- [135] Fadin V.S., Fiore R., Grabovsky A.V., Papa A. Low-x evolution equations in Möbius representation. // *Physics of Particles and Nuclei.* - 2010. - Vol.41. - N6. - P.935-938.
- [136] Fadin V.S. Möbius representation of the BFKL kernel. // In: *Subtleties in Quantum Field Theory.* / Ed. D.Diakonov, Gatchina, 2010.
- [137] Ioffe B.L., Fadin V.S., Lipatov L.N. Quantum Chromodynamics: Perturbative and Nonperturbative aspects. // Cambridge University Press, 2010.
- [138] Dmitriev V.F., Milstein A.I., Salnikov S.G. Spin-dependent part of  $p\bar{p}$  interaction cross section and Nijmegen potential. // *Physics Letters B.* - 2010. - Vol.690. - N4. - P.427.
- [139] Di Piazza A., Lotstedt E., Milstein A.I., Keitel C.H. Effect of a strong laser field on  $e+e$ -photoproduction by relativistic nuclei. // *Phys. Rev. A.* - 2010. - V.81. - N6. - P.062122.
- [140] Di Piazza A., Milstein A.I., and Müller C. Polarization of the electron and positron produced in combined Coulomb and strong laser fields. // *Phys. Rev. A.* - 2010. - V.82. - P.062110.
- [141] Bekavac S., Grozin A.G., Marquard P. Matching QCD and HQET heavy-light currents at three loops. // *Nucl. Phys. B.* - 2010. - V.833. - N1-2. - P.46-63.
- [142] Grozin A.G. Matching heavy-quark fields in QCD and HQET at three loops. // *Phys. Lett. B.* - 2010. - V.692. - P.161-165.
- [143] Grozin A.G. Matching QCD and HQET at three loops. // *Nucl. Phys. B. (Proc. Suppl.)*.- 205-206. - (2010). - P.301-307.
- [144] Chernyak V.L. On mass spectrum in SQCD. Unequal quark masses. // *ЖЭТФ.* - 2010. -Т.138. - N6(12). - C.1076-1087; *JETP.* - 2010. - Vol.111. - P.949-961.
- [145] Chernyak V.L. Exclusive  $\gamma\gamma$  processes. // *Chinese Physics C.* - 2010. Vol. 34. - N6. - P.822-830.
- [146] Sokolov Valentin V. Electron Quantum Transport Through a Mesoscopic Device: Dephasing and Absorption Induced by Interaction with a Complicated Background. // *World Scientific.* - 2010. - P.309-319.
- [147] Sokolov Valentin V. Ballistic electron Quantum transport in a presence of a disordered background. // *J. Phys. A: Math. Theor.* - 2010. - V.43. - P.265102.
- [148] Kharkov Ya.A., Sokolov V.V., and Zhirov O.V. Quantum chaos versus noisy environment. // *J. Sib. Fed. Univ. Math. Phys.* - 2010. - Vol.3. - N3, P.303-310.
- [149] Rudenko A.S., Khriplovich I.B. Can CP-violation be observed in heavy-ion collisions? // *Canadian Journal of Physics.* - 2010. - V.89. - P.63.
- [150] Berengut J.C., Dmitriev V.F., Flambaum V.V. Effect of quark-mass variation on big bang nucleosynthesis. // *Phys. Lett. B.* - 2010. - Vol.683. - N2-3. - P.114.
- [151] Shepelyansky D.L., Zhirov O.V. Google matrix, dynamical attractors and Ulam networks. // *Phys. Rev. E.* - 2010. - Vol.81. - N3, Part2. - P.036213.
- [152] Shepelyansky D.L., Zhirov O.V. Towards Google matrix of brain. // *Phys. Lett. A.* - 2010. - Vol. A374. - P.3206; [E-print: arXiv:1002.4583v2 [cond-mat.dis-nn]] (2010).
- [153] Lee R.N. Space-time dimensionality  $\mathcal{D}$  as complex variable: Calculating loop integrals using dimensional recurrence relation and analytical properties with respect to  $\mathcal{D}$ . // *Nucl. Phys. B.* - 2010. - Vol.830. - N3. - P.474-492.
- [154] Lee R.N., Smirnov A.V., Smirnov V.A. Analytic results for massless three-loop form factors. // *JHEP.* - Apr 2010. - N4. - P.020.
- [155] Lee R.N., Smirnov A.V., Smirnov V.A. Dimensional recurrence relations: an easy way to evaluate

- higher orders of expansion in  $\epsilon$  Nucl. Phys. Proc. Suppl. 205-206 (2010) 308-313.
- [156] Lee R.N. Calculating multiloop integrals using dimensional recurrence relation and  $\mathcal{D}$ -analyticity. // Nucl. Phys. Proc. Suppl. 205-206 (2010) 135-140.
- [157] Baier V.N., Katkov V.M. Pair creation by a photon in an electric field. // Phys. Lett. A. - 2010. - Vol.374. - N22. - P.2201-2206.
- [158] Khatsymovsky V.M. Integration over connections in the discretized gravitational functional integrals. // Mod. Phys. Lett. A. - 2010. - Vol. 25. - N5. - P.351-368.
- [159] Khatsymovsky V.M. Defining integrals over connections in the discretized gravitational functional integrals. // Mod. Phys. Lett. A. - 2010. - Vol. 25. - N17. - P.1407-1423.
- [160] Khatsymovsky V.M. A version of the connection representation of Regge action. // Classical and Quantum Gravity. - 2010. - Vol.27. - N6. - P.065003.
- [161] Artru X., Chehab R., Chevallier M., Kamitani T., Omori T., Rinolfi L., Strakhovenko V.M., Suwada T., Variola A., Vivoli A.A positron source using channeling in crystals for linear colliders. // Int. J. Mod. Phys. A. - 2010. - Vol.25. - P.106.
- [162] Hagiwara Kaoru, Kirilin Grisha. Angular distribution of thrust axis with power-suppressed contribution in  $e^+e^-$  annihilation. // J. of High Energy Physics. - 2010. - N10. - P.093; ISSN 1126-6708.
- [163] Zhiron A.O., Zhiron O.V., Shepelyansky D.L. Two-dimensional ranking of Wikipedia articles. // European Physical Journal B. - 2010. - Vol.77. - N4. - P.523-531; [E-print: arXiv:1006.4270v1 [cs. IR] (2010)].
- [164] Petrenko A.V., Lotov K.V., Logatchov P.V. and Burdakov A.V. The facility for 500 MeV plasma wake-field acceleration experiments at Budker INP. // AIP Conf. Proc. - 2010. - Vol.1229. - P.467-471.
- [165] Xia G., Caldwell A., Lotov K., Pukhov A., Kumar N., An W., Lu W., Mori B.W., Joshi C., Huang C., Muggli P., Assmann R., Zimmermann F. Update of proton driven plasma wakefield acceleration. // AIP Conf. Proc. - 2010. - Vol.1229. - P.510-515.
- [166] Aamodt K., Belikov I., Frolov A., Gorbunov S., Gorbunov Y., Grigoriev V., Ivanov A., Ivanov M., Ivanov V., Kaplin V., Kiselev S., Nikolaev S., Pestov Yu., Vasiliev A., et al. (ALICE Collab.). Midrapidity antiproton-to-proton ratio in pp collisions root  $s=0.9$  and 7 TeV measured by the ALICE experiment. // Physical Review Letters. - 2010. - Vol.105. - N7. - P.072002.
- [167] Afonin A., Akimov A., Cheplakov A., Ershov V., Maslennikov A.L., Orlov I., Peleganchuk, S.V., Petrov V., Pivovarov S., Pospelov G.E., Prokopenko N., Talyshev A., Tikhonov Yu.A., Usov Y., et al. (HiLum ATLAS Endcap Collab.). Relative luminosity measurement of the LHC with the ATLAS forward calorimeter. // J. of Instrumentation. - 2010. - Vol.5. - P.P05005; [E-print: arXiv:1005.1784; 0036327, 2010, 16p].
- [168] Terekhov Andrew V., Parallel Dichotomy Algorithm for solving tridiagonal system of linear equations with multiple right-hand sides. // J. Parallel Computing. - 2010.- Vol.36. - N8. - P.423-438.
- [169] Fedotov G.V., Kuraev E.A., Sibidanov A.L. Monte-Carlo generator photon jets used for luminosity at  $e^+e^-$ . // Chinese Physics C. - 2010. - Vol.34. - N6. - P. 877-882.
- [170] Tikhonov Yu.A. (ATLAS Liquid Argon HiLum Grp). Operation of the ATLAS end-cap calorimeters at sLHC luminosities: An experimental study. // NIM: Sec. A: Accelerators Spectrometers Detectors and Associated Equipment. - 2010. - Vol.617. - N1-3. - P.115-117.
- [171] Yang X.D., Mao L.J., Li G.H., Ma X.M., Yan T.L., Yuan Y.J., Song M.T., Yang J.C., Liu Y., Zhao T.C., Xia J.W., Zhang W., Gao D.Q., Zhou Z.Z., Yan H.B., Mao R.S., Han S.F., Zheng J.H., Yang X.T., Zhao H.W., Xiao C., Yin D.Y., Li P., Jia H., Parkhomchuk V.V., Reva V.B., Skorobogatov D.N. Commissioning of electron cooling in CSRe. // Chinese Physics C. - 2010. - Vol.34. - N7. - P.998-1004.
- [172] Silagadze Z.K., Tarantsev G.I. Comment on «Note on the dog-and-rabbit chase problem in introductory kinematics». // European Journal of Physics. - 2010. - Vol.31. - N2. - P.L37-L38.

- [173] Logashenko I.B. (CMD-3 Collab. and SND Collab.). Measurement of R at VEPP-2000. // Chinese Physics C. - 2010. - Vol.34. – N6. - P.669-674.
- [174] Druzhinin V.P. Measurements of the  $\gamma\gamma^*\rightarrow\pi^0$  and  $\gamma\gamma^*\rightarrow\eta^c$  transition form factors at BABAR. // Chinese Physics C. - 2010. - Vol.34. - N6. - P.816-821.
- [175] Mo Xiao-Hu., Achasov M. N., Blinov V. E., Krasnov A.A., Muchnoi N.Yu., Nikolaev I.B., Pyata E.E., Shamov A.G., Zhukov A.A., et al. Beam energy measurement system at BEPC II. // Chinese Physics C. 2010. - Vol.34. - N6. - P.912-917.
- [176] Maziashvili Michael, Silagadze Zurab. Quantum gravitational corrections to the hydrogen atom and harmonic oscillator. // Intern. J. of Modern Physics D. - 2010. - Vol.19. – N2. - P.137-151;
- [177] Korneev V.N., Shlektarev V.A., Zabelin A.V., Aul'chenko V.M., Tolochko B.P., Lanina N.F., Medvedev B.I., Nayda O.V., Vazina A.A. Equipment for investigations of biological nanostructures by diffraction methods using synchrotron radiation. // Glass Physics and Chemistry. - 2010. - Vol.36. – N1. - P.100-109.
- [178] Ivanovskikh K.V., Meijerink A., Piccinelli F., Speghini A., Zinin E.I., Ronda C., Bettinelli M. Optical spectroscopy of Ca<sub>3</sub>Sc<sub>2</sub>Si<sub>3</sub>O<sub>12</sub>, Ca<sub>3</sub>Y<sub>2</sub>Si<sub>3</sub>O<sub>12</sub> and Ca<sub>3</sub>Lu<sub>2</sub>Si<sub>3</sub>O<sub>12</sub> doped with Pr<sup>3+</sup>. // J. of Luminescence. - 2010. - Vol.130. - N5. - P.893-901.
- [179] Meshkov O.I., Zhuravlev A.N., Smaluk V.V. Multi-pinhole camera for beam position and vertical angle stabilization. // Instrumentation. - 2010. - Vol.5. - P03004. - 1748-0221.
- [180] Abakumova E.V, Achasov M.N., Krasnov A.A, Kosarev A.N, Muchnoi N.Yu., Pyata E.E., Zhukov A.A. High vacuum infrared window. // Vacuum Technique and Technology. - 2010. - V.20. - N2. - P.77-81.
- [181] Akhmetshin R.R., Aulchenko V.M., Banzarov V.Sh., Barkov L.M., Baru S.E., Bashtovoy N.S., Bondar A.E., Bragin A.V., Eidelman S.I., Epifanov D.A., Fedotov G.V., Gabyshev N.I., Grebenuk A.A., Grigoriev D.N., Ignatov F.V., Karpov S.V., Kazanin V.F., Khazin B.I., Koop I.A., Krokovny P.P., Kuzmin A.S., Logashenko I.B., Lukin P.A., Lysenko A.P., Mikhailov K.Yu., Okhapkin V.S., Perevedentsev E.A., Popov A.S., Redin S.I., Ruban A.A., Ryskulov N.M., Shatunov Yu.M., Shwartz B.A., Sibidanov A.L., Snopkov I.G., Solodov E.P., Yudin Yu.V., Zaytsev A.S., et al. (CMD-2 and CMD-2 Collab.). Detectors and physics at VEPP-2000. // Nucl. Instrum. Meth. A. - 2010. - Vol.623. - P.353-355.
- [182] Grancagnolo F., Fiore G., Ignatov F.V., Karavdina A.V., Khazin B.I., Miccoli A., Okhapkin V.S., Pivovarov S.G., Popov A.S., Ruban A.A., Sibidanov A.L., Snopkov I.G., Grancagnolo F., Khazin B.I., et al. // Drift chamber for the CMD-3 detector. // Nucl. Instrum. Meth. A. - 2010. - Vol.623. - P.114-116.
- [183] Anisenkov A., Ignatov F., Pirogov S., Sibidanov A., Viduk S., Zaytsev A. CMD-3 detector offline software development. // J. Phys. Conf. - 2010. - Ser.219:032027.
- [184] Di Dominico A., ..., Sibidanov A.L., et al. (KLOE Collaboration). CPT symmetry and quantum mechanics tests in the neutral kaon system at KLOE. // Found. Phys. - 2010. - Vol.40. - P.852-866.
- [185] Sanchez P. del Amo., ..., Blinov V.E., Bukin A.D., Druzhinin V.P., Golubev V.B., Onuchin A.P., Serednyakov, S.I., Skovpen Yu.I., Solodov E.P., Todyshev K.Yu., et al. (BABAR Collab.). Search for the rare decay  $B\rightarrow K\nu\bar{\nu}$ . // Phys. Rev. D. - 2010. - Vol.82. - P.112002; [E-print: arXiv:1009.1529].
- [186] Sanchez P. del Amo., ..., Blinov V.E., Bukin A.D., Druzhinin V.P., Golubev V.B., Onuchin A.P., Serednyakov, S.I., Skovpen Yu.I., Solodov E.P., Todyshev K.Yu., et al. (BABAR Collab.). Measurement of the absolute branching fractions for  $D_s^- \rightarrow \ell^- \bar{\nu}_\ell$  and extraction of the decay constant  $f_{D_s}$ . // Phys. Rev. D. - 2010. - Vol.82. - P.091103; [E-print: arXiv:1008.4080 [hep-ex]].
- [187] Sanchez P. del Amo., ..., Blinov V.E., Bukin A.D., Druzhinin V.P., Golubev V.B., Onuchin A.P., Serednyakov, S.I., Skovpen Yu.I., Solodov E.P., Todyshev K.Yu., Yushkov A.N., et al. (BABAR Collab.). Search for  $f_1(2220)$  in radiative  $J/\psi$  decays. // Phys. Rev. Lett. - 2010. - Vol.105. - N17. - P.172001-1-7; [E-print: arXiv:1007.3526 [hep-ex]].
- [188] Sanchez P. del Amo., ..., Blinov V.E., Bukin A.D., Buzykaev A.R., Druzhinin V.P., Golubev V.B.,

- Onuchin A.P., Serednyakov, S.I., Skovpen Yu.I., Solodov E.P., Todyshev K.Yu., Yushkov A.N., et al. (BABAR Collab.). Study of  $B \rightarrow X\gamma$  decays and determination of vertical bar  $|V_{td}/V_{ts}|$  vertical bar. // Phys. Rev. D. - 2010. - Vol.82. - N5. - P.051101-1-8; [E-print: arXiv:1005.4087 [hep-ex]].
- [189] Sanchez P. del Amo., ..., Blinov V.E., Buzykaev A.N., Druzhinin V.P., Golubev V.B., Onuchin A.P., Serednyakov, S.I., Skovpen Yu.I., Solodov E.P., Todyshev K.Yu., et al. (BABAR Collab.). Evidence for direct CP violation in the measurement of the Cabibbo-Kobayashi-Maskawa angle gamma with  $B^+ \rightarrow D^{(*)} K^{(*)+}$  decays. // Phys. Rev. Lett. - 2010. - Vol.105. - N12. - P.121801-1-7; [E-print: arXiv:1005.1096 [hep-ex]].
- [190] Del Amo Sanchez P., ..., Blinov V.E., Buzykaev A.R., Druzhinin V.P., Golubev V.B., Onuchin A.P., Serednyakov, S.I., Skovpen Yu.I., Solodov E.P., Todyshev K.Yu., Yushkov A.N., et al. (BABAR Collab.). Measurement of  $D^0 - \bar{D}^0$  mixing parameters using  $D^0 \rightarrow K_S^0 \pi^+ \pi^-$  and  $D^0 \rightarrow K_S^0 K^+ K^-$  decays. // Phys. Rev. Lett. - 2010. - Vol.105. - N8. - P.081803-1-7; [E-print: arXiv:1004.5053 [hep-ex]].
- [191] Amo Sanchez P., ..., Blinov V.E., Bukin A.D., Druzhinin V.P., Golubev V.B., Onuchin A.P., Serednyakov, S.I., Skovpen Yu.I., Solodov E.P., Todyshev K.Yu., et al. (BABAR Collab.). B-meson decays to  $\eta\rho$ ,  $\eta'f_0$ , and  $\eta'K^*$ . // Phys. Rev. D. - 2010. - Vol.82. - P.011502; [E-print: arXiv:1004.0240 [hep-ex]].
- [192] Amo Sanchez P., ..., Blinov V.E., Bukin A.D., Druzhinin V.P., Golubev V.B., Onuchin A.P., Serednyakov S.I., Skovpen Yu.I., Solodov E.P., Todyshev K.Yu., et al. (BABAR Collab.). Observation of the  $Y1^3D_J$  bottomonium state through decays to  $\pi^+ \pi^- Y1S$ . // Phys. Rev. D. - 2010. - 2010. - Vol.82. - P.111102; [E-print: arXiv:1004.0175 [hep-ex]].
- [193] Lees J.P., ..., Blinov V.E., Bukin A.D., Druzhinin V.P., Golubev V.B., Onuchin A.P., Serednyakov, S.I., Skovpen Yu.I., Solodov E.P., Todyshev K.Yu., et al. (BABAR Collab.). Measurement of the  $\gamma\gamma^* \rightarrow \eta_c$  transition form factor. // Phys. Rev. D. - 2010. - Vol.81. - P.052010; [E-print: arXiv:1002.3000 [hep-ex]].
- [194] Bragin Alexey V., Barkov Lev M., Bashtovoj Nikolay S., Grebenuk Andrej A., Karpov Sergey V., Okhapkin Victor S., Pivovarov Sergey G., Popov Yuri S., Ruban Alexander A., Khazin Boris I. Performance of the thin superconducting solenoid of the CMD-3 detector. // IEEE Transactions on Applied Superconductivity. - Oct. 2010. - Vol.20. - N5. - P.2336-2340.
- [195] Stibunov V.N., Barkov L.M., Gauzshteyn V.V., Dmitriev V.F., Loginov A.Yu., Mishnev S.I., Nikolenko D.M., Osipov A.V., Rachek I.A., Sadykov R.Sh., Sidorov A.A., Shestakov Yu.V., Toporkov D.K., Fix A.I., Zevakov S.A. Study of tensor analysing component T21 for the  $\pi$  meson photoproduction on the deuteron. // Bulletin of the Russian Academy of Sciences: Physics. - 2010. - Vol.53. - N10/2. - P.18-24.
- [196] Gauzshteyn V.V., Zevakov S.A., Lazarenko B.A., Loginov A.Yu., Mishnev S.I., Nikolenko D.M., Osipov A.V., Rachek I.A., Sadykov R.Sh., Sidorov A.A., Stibunov V.N., Toporkov D.K., Shestakov Yu.V. Measurement of tensor analysing components  $T_{20^-}$ ,  $T_{21^-}$  и  $T_{22}$  for the  $\gamma d \rightarrow p p \pi$  meson photoproduction on the deuteron. // Bulletin of the Russian Academy of Sciences: Physics. - 2010 - Vol.53. - N10/2. - P.25-28 (76616598).
- [197] Riordan S., ..., Nikolenko D.M., Rachek I.A. and Shestakov Yu.V., et al. Measurements of the electric form factor of the neutron up to  $Q^2 = 3.4 \text{ GeV}^2$  using the rReaction  $3\text{He}^+(e^+en)pp$ . // Phys. Rev. Lett. - 2010. - Vol.105. - P.262302.
- [198] Di Benedetto Vito, Hauptman John, Mazzacane Anna, Ignatov Fedor. Dual-readout, particle identification, and 4th. // NIM in Physics Research A. Sec.: Accelerators Spectrometers Detectors and Associated Equipment. - Nov 1, 2010. - Vol.623. N1. - P.237-239.
- [199] Barnyakov A.Yu., Barnyakov M.Yu., Beloborodov K.I., Bobrovnikov V.S., Buzykaev A.R., Danilyuk A.F., Golubev V.B., Kirillov V.L., Kononov S.A., Kravchenko E.A., Onuchin A.P., Martin K.A., Serednyakov S.I., Vesenev V.M. Particle identification aerogel counter with  $n=1.13$  for  $\pi/K$  separation. // NIM in Physics Research A. Sec.: Accelerators Spectrometers Detectors and Associated Equipment. - Nov 1, 2010. - Vol.623. - N1. - P.336-338.
- [200] Achasov M.N., Beloborodov K.I., Berdyugin A.V., Botov A.A., Golubev V.B., Dimova T.V., Druzhinin V.P., Kardapoltsev L.V., Kharlamov A.G., Kovrizhin D.P., Koop I.A., Korol A.A.,

- Koshuba S.V., Obrazovsky A.E., Pakhtusova E.V., Shtol D.A., Serednyakov S.I., Silagadze Z.K., Skrinsky A.N., Tikhonov Yu.A., Shatunov Yu.M., Vasil'ev A.V. Study of the process  $e^+e^- \rightarrow \pi^+\pi^-\pi^0\pi^0$  at energies  $\sqrt{s} < 1$  GeV. // Chinese Physics C. - 2010. - Vol.34. - N6. - P.680-685.
- [201] Abreu H., Beloborodova O., Bobrovnikov V., Maslennikov A., Maximov D., Peleganchuk S., Pospelov G., Talyshev, A., Tikhonov Yu., Usov, Y., et al. Performance of the electronic readout of the ATLAS liquid argon calorimeters. // J. of Instrumentation. - Sep. 2010. - Vol.5. - P09003; [<http://iopscience.iop.org/1748-0221/5/09/P09003>].
- [202] Silagadze Z.K. Citation entropy and research impact estimation. // J. Acta Physica Polonica B. - 2010. - Vol.41. - N11. - P.2325-2333.
- [203] Aulchenko V.M., Baru S.E., Evdokov O.V., Leonov V.V., Papushev P.A., Porosev V.V., Savinov G.A., Sharafutdinov M.R., Shekhtman L.I., Ten K.A., Titov V.M., Tolochko B.P., Vasiljev A.V., Zhogin I.L., Zhulanov V.V. Fast high resolution gaseous detectors for diffraction experiments and imaging at synchrotron radiation beam. // NIM A. - 2010. - Vol.623. - P.600-602.
- [204] Adam J., ..., Grigoriev D.N., Ignatov F., Kiselev O., Popov A., Yudin, Yu.V., et al (MEG Collab.). A limit for the  $\mu \rightarrow e\gamma$  decay from the MEG experiment. // Nucl. Phys. B (Proc. Suppl.). 2010. - Vol.834. - N1-2. - P.1-12.
- [205] Grigoriev D.N., Kazanin V.F., Kuznetsov G.N., Shepelev S.N., V.N., Vasiliev Ya.V., et al. Alpha radioactive background in BGO crystals. // NIM A. - 2010. - Vol.623. - P.999-1001.
- [206] Babichev S.E., Baru S.E., Porosev V.V., Ukraintsev Yu.G. The new approach to maintenance of transport safety at examination of passengers and the personnel. // Special Technics. - 2010, N6. - P.22-27.
- [207] Ukraintsev Yu.G., Chernukha E.A., Puchko T.K. Diagnostics of a narrow basin in modern obstetrics. // Medical Business. 2010, N12(199). - P.24-26 (in Russian).
- [208] Baru S.E. X-rays to a terrorist. // Magazine «Defence order». - 2010, N2(15). - P.24-27 (in Russian).
- [209] Baru S.E. We help real. // Magazine «Military brotherhood». - 2010. - N5. - P.88-91 (in Russian).
- [210] Blinov V.E., Bukin A.D., Buzykaev A.R., Druzhinin V.P., Golubev V.B., Onuchin A.P., Serednyakov S.I., Skovpen Yu.I., Solodov E.P., Todyshev K., et al. (BaBar Collab.). Measurements of charged current lepton universality and  $|V_{us}|$  using tau lepton decays to  $e^- \bar{\nu}_e \nu_\tau$ ,  $\mu^- \bar{\nu}_\mu \nu_\tau$ ,  $\pi^- \nu_\tau$ , and  $K^- \nu_\tau$ . // Phys. Rev. Lett. - 2010. - Vol.105. - N5. - P.051602-1-8; [arXiv:0912.0242 [hep-ex]].
- [211] Bondar A., Buzulutskov A., Grebenuk A., Sokolov A., Akimov D., Alexandrov I., Breskin A. Direct observation of avalanche scintillations in a THGEM-based two-phase Ar avalanche detector using Geiger-mode APD. // J. of Instrumentation. - 2010. - Vol.5. - Paper P08002. - P.1-21.
- [212] Bondar A., Buzulutskov A., Grebenuk A., Pavluchenko D., Tikhonov Y. Further studies of two-phase avalanche detectors: Electron emission and gamma-ray detection properties. // NIM. A. - 2010. - Vol.A623. - P.102-104.
- [213] Antonelli M., Bondar A., Sibidanov A., et al. Flavor physics in the quark sector. // Phys. Rept. - 2010. - Vol.494. - N3-4. - P.197-414; [E-print: arXiv:0907.5386 [hep-ph]].
- [214] Miyazaki Y., ..., Arinstein K., Aulchenko V., Bondar A., Eidelman S., Epifanov D., Gabyshev N., Garmash A., Kuzmin A., Poluektov A., Shebalin V., Shwartz B., Sokolov A., Usov Y., Vinokurova A., Zhilich V., Zhilich V., Zhulanov V., Zyukova O., et al. (Belle Collab.), Search for lepton flavor and lepton number violating  $\tau$  decays into a lepton and two charged mesons. // Phys. Lett. B. - 2010. - Vol.682. - N4-5. - P.355.
- [215] Hayasaka K., ..., Arinstein K., Aulchenko V., Eidelman S., Epifanov D., Gabyshev N., Kuzmin A., Poluektov A., Shwartz B., Zyukova O., et al. (Belle Collab.). Search for lepton flavor violating  $\tau$  decays into three leptons with 719 million produced  $\tau^+\tau^-$  pairs. // Phys. Lett. B. - 2010. - Vol.687. - N2-3. - P.139-143.
- [216] Miyazaki Y., ..., Arinstein K., Aulchenko V., Eidelman S., Gabyshev N., Kuzmin A., Poluektov A., Shwartz B., Usov Y., Zhilich V., Zyukova O., et al. (Belle Collab.). Search for lepton flavor violating  $\tau$  decays into  $\ell\ell\bar{K}_s^0$  and  $\ell\ell\bar{K}_s^0K_s^0$ . // Phys. Lett. B. - 2010. - Vol.692. - N1. - P.4-9.
- [217] Hara K., ..., Aulchenko V., Bondar A., Eidelman S., Gabyshev N., Kuzmin A., Shwartz B.,

- Zhilich V., Zyukova O., et al. (Belle Collab.). Evidence for  $B^- \rightarrow \tau^-(\nu)\overline{\text{tau}}$  with a semileptonic tagging method. // Phys. Rev. D. - 2010.- Vol.82. - P.071101.
- [218] Peng C.-C., ..., Bondar A., Eidelman S., Gabyshev N., Shwartz B., Zhilich V., Zhulanov V., Zyukova O., et al. (Belle Collab.). Search for  $B_s^0 \rightarrow hh$  decays at the  $Y(5S)$  resonance. // Phys. Rev. D. - 2010.- Vol.82. - P.072007.
- [219] Nakahama Y., ..., Arinstein K., Bondar A., Eidelman S., Shwartz B., Zhilich V., et al. (Belle Collab.). Measurement of CP violating asymmetries in  $B^0 \rightarrow K^+ K^- K_s^0$  decays with a time-dependent Dalitz approach. // Phys. Rev. D. - 2010. - Vol.82. - P.073011.
- [220] Chen K.-F., ..., Bondar A., Eidelman S., Epifanov D., Gabyshev N., Shwartz B., Zhulanov V., Zyukova O., et al. (Belle Collab.). Observation of an enhancement in  $e^+e^-$  to  $Y(1S)\pi^+\pi^-$ ,  $Y(2S)\pi^+\pi^-$ , and  $Y(3S)\pi^+\pi^-$  production around  $\sqrt{s}=10.89$  GeV at Belle. // Phys. Rev. D. - 2010. - Vol.82. - P.091106(R).
- [221] Dungen W., ..., Eidelman S., Kuzmin A., Zhulanov V., et al. (Belle Collab.). // Measurement of the form factors of the decay  $B^0 \rightarrow D^{*+} l^+ \nu$  and determination of the CKM matrix element  $|V_{cb}|$ . // Phys. Rev. D. - 2010. - Vol.82. - P.112007.
- [222] Uehara S., ..., Arinstein K., Bondar A., Eidelman S., Shwartz B., Zhilich V., et al. (Belle Collab.). // Phys. Rev. D. - 2010. - Vol.82. - P.114031.
- [223] Louvot R., ..., Arinstein K., Bondar A., Eidelman S., Poluektov A., Shebalin V., Zyukova O., et al. (Belle Collab.). Observation of  $B_s^0 \rightarrow D_s^{*-} \pi^+$ ,  $B_s^0 \rightarrow D_s^{(*)} \rho^+$  decays and measurement of  $B_s^0 \rightarrow D_s^{*-} \rho^+$  polarization. // Phys. Rev. Lett. - 2010. - Vol.104. - P.231801.
- [224] Hyun H. J., ..., Arinstein K., Bondar A., Eidelman S., Gabyshev N., Kuzmin A., Shwartz B., Zhilich V., Zyukova O., et al. (Belle Collab.). Search for a low mass particle decaying into  $\mu^+\mu^-$  in  $B^0 \rightarrow K^0 X$  and  $B^0 \rightarrow \rho^0 X$  at Belle. // Phys. Rev. Lett. - 2010. - Vol.105. - N9. - P.091801-1-5.
- [225] Ishimura K., ..., Arinstein K., Bondar A., Eidelman S., Kuzmin A., Zhulanov V., Zyukova O., et al. (Belle Collab.). First measurement of inclusive  $B \rightarrow X_s \eta$  decays. // Phys. Rev. Lett. - 2010. - Vol.105. - N19. - P.191803-1-6.
- [226] Esen S., ..., Arinstein K., Aulchenko V., Bondar A., Eidelman S., Usov Yu., Zhilich V., et al. (Belle Collab.). Observation of  $B_s^0 \rightarrow D_s^{(*)+} D_s^{(*)-}$  using  $e^+e^-$  collisions and a determination of the  $B_s$  - anti- $B_s$  width difference  $\Delta\Gamma$ . // Phys. Rev. Lett. - 2010. - Vol.105. - N20. - P.201802-1-6.
- [227] Gershon T., and Poluektov A. Double Dalitz plot analysis of the decay  $B \rightarrow D K^+ \pi^-$ ,  $D \rightarrow K S \pi^+ \pi^-$ . // Phys. Rev. D. - 2010. - Vol. 81. - N1. - P.014025.
- [228] Bondar A., Poluektov A., and Vorobiev V. Charm mixing in a model-independent analysis of correlated  $D^0$  anti  $D^0$  decays. // Phys. Rev. D. - 2010. - Vol.82. - P.034033.
- [229] Aaij R., Bobrov A., Bondar A., Eidelman S., Poluektov A., Shekhtman L., et al. Prompt  $K_s$  production in pp collisions at  $\sqrt{s}=0.9$  TeV. // Phys. Lett. B. - 2010. - Vol 693. - P.69.
- [230] Aaij R., Bobrov A., Bondar A., Eidelman S., Poluektov A., Shekhtman L., et al. Measurement of  $\sigma(pp \rightarrow b \text{ anti-} b X)$  at  $\sqrt{s}=7$  TeV in forward region. // Phys. Lett. B. - 2010. - Vol 694. - P.209.
- [231] Schonning K., Kuzmin A., Shwartz B., et al. Production of  $\eta$  and  $3\pi$  mesons in the  $pd \rightarrow 3\text{He}X$  reaction at 1360 and 1450 MeV. // Eur. Phys. J. A. - 2010. - Vol.45. - N1. - P.11-21.
- [232] Schonning K., Shwartz B., et al. (by CELSIUS/WASA Collab.). The  $pd \rightarrow \text{He-3} \eta \eta^0$  reaction at  $T(p) = 1450$  MeV. // Phys. Lett. B. - 2010. - Vol.685. - P.33-37.
- [233] Kren F., Shwartz B., et al. (by CELSIUS/WASA Collab.). Exclusive measurements of  $pp \rightarrow d\pi^+\pi^0$ : double-pionic fusion without ABC effect. // Phys. Lett. B. - 2010. - Vol.684. - N2-3. - P.110-113.
- [234] Eidelman S. Tau lepton decays. // Chinese Physics C. - 2010. - Vol.34. - N6. - P.896-.
- [235] Nakamura K., ..., Eidelman S., et al. (Particle Data Group). Review of particle physics. // J. Phys. G. - 2010. - Vol.37. - N7A. - P.075021.
- [236] Eidelman S., et al.,  $e^+e^-$  annihilation to  $\pi^0\pi^0\gamma$  and  $\pi^0\eta\gamma$  as a source of information on scalar and vector mesons. // Eur. Phys. J. C. - 2010. - Vol.69. - N1-2. - P.103-118.
- [237] Telnov V.I. Lectures on mechanics and the theory of relativity. // NSU, 2010, 175p. - <http://www.inp.nsk.su/~telnov/mech/>.

- [238] Anashin V.V., Aulchenko V.M., Baldin E.M., Barladyan A.K., Barnyakov A.Yu., Barnyakov M.Yu., Baru S.E., Bedny I.V., Beloborodova O.L., Blinov A.E., Blinov V.E., Bobrov A.V., Bobrovnikov V.S., Bogomyagkov A.V., Bondar A.E., Buzykaev A.R., Eidelman S.I., Glukhovchenko Yu.M., Gulevich V.V., Gusev D.V., Karnaev S.E., Karpov S.V., Kharlamova T.A., Kiselev V.A., Kononov S.A., Kotov K.Yu., Kravchenko E.A., Kulikov V.F., Kurkin G.Ya., Kuper E.A., Levichev E.B., Maksimov D.A., Malyshev V.M., Maslennikov A.L., Medvedko A.S., Meshkov O.I., Mishnev S.I., Morozov I.I., Muchnoi N.Yu., Neufeld V.V., Nikitin S.A., Nikolaev I.B., Okunev I.N., Onuchin A.P., Oreshkin S.B., Orlov I.O., Osipov A.A., Peleganchuk S.V., Pivovarov S.G., Piminov P.A., Petrov V.V., Poluektov A.O., Popkov I.N., Prisekin V.G., Ruban A.A., Sandyrev V.K., Savinov G.A., Shamov, D.N. Shatilov A.G., Shwartz B.A., Simonov E.A., Sinyatkin S.V., Skovpen Yu.I., Skrinsky A.N., Smaluk V.V., Sokolov A.V., Sukharev A.M., Starostina E.V., Talyshev A.A., Tayursky V.A., Telnov V.I., Tikhonov Yu.A., Todyshev K.Yu., Tumaikin G.M., Usov Yu.V., Vorobiov A.I., Yushkov A.N., Zhilich V.N., Zhulanov V.V., Zhuravlev A.N. Measurement of  $D^0$  and  $D^+$  meson masses with the KEDR detector. // Phys. Lett. B. - 2010. - Vol.686. - Issue 2-3. - P.84-90.
- [239] Anashin V.V., Aulchenko V.M., Baldin E.M., Barladyan A.K., Barnyakov A.Yu., Barnyakov M.Yu., Baru S.E., Bedny I.V., Beloborodova O.L., Blinov A.E., Blinov V.E., Bobrov A.V., Bobrovnikov V.S., Bogomyagkov A.V., Bondar A.E., Buzykaev A.R., Eidelman S.I., Glukhovchenko Yu.M., Gulevich V.V., Gusev D.V., Karnaev S.E., Karpov S.V., Kharlamova T.A., Kiselev V.A., Kononov S.A., Kotov K.Yu., Kravchenko E.A., Kulikov V.F., Kurkin G.Ya., Kuper E.A., Levichev E.B., Maksimov D.A., Malyshev V.M., Maslennikov A.L., Medvedko A.S., Meshkov O.I., Mishnev S.I., Morozov I.I., Muchnoi N.Yu., Neufeld V.V., Nikitin S.A., Nikolaev I.B., Okunev I.N., Onuchin A.P., Oreshkin S.B., Orlov I.O., Osipov A.A., Peleganchuk S.V., Pivovarov S.G., Piminov P.A., Petrov V.V., Poluektov A.O., Popkov I.N., Prisekin V.G., Ruban A.A., Sandyrev V.K., Savinov G.A., Shamov A.G., Shatilov D.N., Shwartz B.A., Simonov E.A., Sinyatkin S.V., Skovpen Yu.I., Skrinsky A.N., Smaluk V.V., Sokolov A.V., Sukharev A.M., Starostina E.V., Talyshev A.A., Tayursky V.A., Telnov V.I., Tikhonov Yu.A., Todyshev K.Yu., Tumaikin G.M., Usov Yu.V., Vorobiov A.I., Yushkov A.N., Zhilich V.N., Zhulanov V.V., Zhuravlev A.N. Measurement of  $\Gamma(J/\psi) \cdot B(J/\psi \rightarrow e^+e^-)$  and  $\Gamma(J/\psi) \cdot B(J/\psi \rightarrow \mu^+\mu^-)$ . // Physics Letters B. - 2010. - Vol.685. - N2/3. - P.134-140; [E-print: arXiv:1012.1694, 2010 [Hep-ex]].
- [240] Shamov A.G., Anashin V.V., Aulchenko V.M., Baldin E.M., Barladyan A.K., Barnyakov A.Yu., Barnyakov M.Yu., Baru S.E., Bedny I.V., Beloborodova O.L., Blinov A.E., Blinov V.E., Bobrov A.V., Bobrovnikov V.S., Bogomyagkov A.V., Bondar A.E., Buzykaev A.R., Eidelman S.I., Glukhovchenko Yu.M., Gulevich V.V., Gusev D.V., Karnaev S.E., Karpov S.V., Kharlamova T.A., Kiselev V.A., Kononov S.A., Kotov K.Yu., Kravchenko E.A., Kulikov V.F., Kurkin G.Ya., Kuper E.A., Levichev E.B., Maksimov D.A., Malyshev V.M., Maslennikov A.L., Medvedko A.S., Meshkov O.I., Milstein A.I., Mishnev S.I., Morozov I.I., Muchnoi N.Yu., Neufeld V.V., Nikitin S.A., Nikolaev I.B., Okunev I.N., Onuchin A.P., Oreshkin S.B., Orlov I.O., Osipov A.A., Peleganchuk S.V., Pivovarov S.G., Piminov P.A., Petrov V.V., Poluektov A.O., Popkov I.N., Prisekin V.G., Ruban A.A., Sandyrev V.K., Savinov G.A., Shatilov D.N., Shwartz B.A., Simonov E.A., Sinyatkin S.V., Skovpen Yu.I., Skrinsky A.N., Smaluk V.V., Sokolov A.V., Sukharev A.M., Starostina E.V., Talyshev A.A., Tayursky V.A., Telnov V.I., Tikhonov Yu.A., Todyshev K.Yu., Tumaikin G.M., Usov Yu.V., Vorobiov A.I., Yushkov A.N., Zhilich V.N., Zhulanov V.V., Zhuravlev A.N. Measurement of  $J/\psi$  leptonic widths with the KEDR detector. // Chinese Physics C. - 2010. - Vol.34. - N6. - P.836-841.
- [241] Anashin V.V., Aulchenko V.M., Baldin E.M., Barladyan A.K., Barnyakov A.Yu., Barnyakov M.Yu., Baru S.E., Bedny I.V., Beloborodova O.L., Blinov A.E., Blinov V.E., Bobrov A.V., Bobrovnikov V.S., Bogomyagkov A.V., Bondar A.E., Buzykaev A.R., Eidelman S.I., Glukhovchenko Yu.M., Gulevich V.V., Gusev D.V., Karnaev S.E., Karpov S.V., Kharlamova T.A., Kiselev V.A., Kononov S.A., Kotov K.Yu., Kravchenko E.A., Kulikov V.F., Kurkin G.Ya., Kuper E.A., Levichev E.B., Maksimov D.A., Malyshev V.M., Maslennikov A.L., Medvedko A.S., Meshkov O.I., Mishnev S.I., Morozov I.I., Muchnoi N.Yu., Neufeld V.V., Nikitin S.A., Nikolaev I.B., Okunev I.N., Onuchin A.P., Oreshkin S.B., Orlov I.O., Osipov A.A., Peleganchuk S.V., Pivovarov S.G., Piminov P.A., Petrov V.V., Poluektov A.O., Popkov I.N., Prisekin V.G., Ruban A.A., Sandyrev V.K., Savinov G.A., Shamov A.G., Shatilov D.N., Shwartz B.A., Simonov E.A., Sinyatkin S.V., Skovpen Yu.I., Skrinsky A.N., Smaluk V.V., Sokolov A.V., Sukharev A.M., Starostina E.V., Talyshev A.A., Tayursky V.A.,

- Telnov V.I., Tikhonov Yu.A., Todyshev K.Yu., Tumaikin G.M., Usov Yu.V., Vorobiov A.I., Yushkov A.N., Zhilich V.N., Zhulanov V.V., Zhuravlev A.N. Measurement of  $J/\psi \rightarrow \eta_c \gamma$  at KEDR. // Chinese Physics C. - 2010. - Vol.34. - N6. - 831-835; [arXiv:1002.2071v2, 2010 [hep-ex]].
- [242] Anashin V.V., Aulchenko V.M., Baldin E.M., Barladyan A.K., Barnyakov A.Yu., Barnyakov M.Yu., Baru S.E., Bedny I.V., Beloborodova O.L., Blinov A.E., Blinov V.E., Bobrov A.V., Bobrovnikov V.S., Bogomyagkov A.V., Bondar A.E., Buzykaev A.R., Eidelman S.I., Glukhovchenko Yu.M., Gulevich V.V., Gusev D.V., Karnaev S.E., Karpov S.V., Kharlamova T.A., Kiselev V.A., Kononov S.A., Kotov K.Yu., Kravchenko E.A., Kulikov V.F., Kurkin G.Ya., Kuper E.A., Levichev E.B., Maksimov D.A., Malyshev V.M., Maslennikov A.L., Medvedko A.S., Meshkov O.I., Mishnev S.I., Morozov I.I., Muchnoi N.Yu., Neufeld V.V., Nikitin S.A., Nikolaev I.B., Okunev I.N., Onuchin A.P., Oreshkin S.B., Orlov I.O., Osipov A.A., Peleganchuk S.V., Pivovarov S.G., Piminov P.A., Petrov V.V., Poluektov A.O., Popkov I.N., Prisekin V.G., Ruban A.A., Sandyrev V.K., Savinov G.A., Shamov A.G., Shatilov D.N., Shwartz B.A., Simonov E.A., Sinyatkin S.V., Skovpen Yu.I., Skrinsky A.N., Smaluk V.V., Sokolov A.V., Sukharev A.M., Starostina E.V., Talyshv A.A., Tayursky V.A., Telnov V.I., Tikhonov Yu.A., Todyshev K.Yu., Tumaikin G.M., Usov Yu.V., Vorobiov A.I., Yushkov A.N., Zhilich V.N., Zhulanov V.V., Zhuravlev A.N. Recent results from the KEDR Detector. // Chinese Physics C. - 2010. - Vol.34. - Issue 6. - P.650-655.
- [243] Pestrikov D.V. Effect of the frequency spread on the transverse beam break-up instability of a bunch in storage rings. // NIM in Physics Research A. Sec.: Accelerators Spectrometers Detectors and Associated Equipment. - Dec 21, 2010. - Vol.624. - N3. - P.567-577.
- [244] Bochkov V.D., Bochkov D.V., Akimov A.V., Logatchev P.V., Dyagilev V.M., Ushich V.G. Application of TPI-thyratrons in a double-pulse mode power modulator with inductive-resistive load. // IEEE Transactions on Dielectrics and Electrical Insulation, 2010. - Vol.17. - N3. - P.718-722.
- [245] Bubnikov I.A., Sorokin A.I., Kotosonov A.S., Virgilev Yu.S., Kalyagina I.P., Zhmurikov E.I., Gubin K.V., Logatchev P.V. Specifics of the carbon graphitization on the base of isotope  $^{13}\text{C}$ . // Academy news. Chemistry and Chemical Engineering. - 2010, V.53. - P.64-68. (in Russian).
- [246] Vostrikov V.A., Levichev E.B., Parkhomchuk V.V., Petrichenkov M.V., Skrinsky A.N. - RF Patent: Model №93026 «The accelerator complex for cancer therapy by proton and ion beams». - Novosibirsk: Budker INP SB RAS.
- [247] Auslender V.L., Bryazgin A.A., Chernov K.N., Cheskidov V.G., Factorovich B.L., Gorbunov V.A., Gornakov I.V., Kuznetsov G.I., Makarov I.G., Matyash N.V., Ostreiko G.N., Panfilov A.D., Serdobintsev G.V., Tarnetsky V.V., Tiunov M.A. 100 kW modular linear accelerator for industrial applications with electron energy of 7.5-10 MeV. // Problems of Atomic Science and Technology. Ser.: Nuclear Physics. - 2010. - Vol.53. - N2. - P.9-13.
- [248] Sorokin A., Belov V., Davydenko V., Deichuli P., Ivanov A., Podyminogin A., Shikhovtsev I., Shilgenko G., Stupishin N., Tiunov M. Characterization of 1 MW, 40 keV, 1 s neutral beam for plasma heating. // RSI. - 2010. - Vol.81. - N2. - P.02B108-02B108-4.
- [249] Dement'ev E.N., Karnaev S.E., Krutikhin S.A., Kurkin G.Ya., Medvedko A.S., Motygin S.V., Oreshonok V.V., Osipov V.N., Petrov V.M., Rotov E.A., Smaluk V.V., Sukhanov D.P., Cherepanov V.P. Commissioning feedback systems at VEPP-4M electron-positron collider // Physics of Particles and Nuclei Letters. - 2010. - Vol.7. - N7. - P.466-472.
- [250] Volkov V. (BINP, Novosibirsk, Russia), J. Knobloch and A. Matveenko (HZB, Berlin, Germany). Monopole passband excitation by field emitters in 9-cell TESLA-type cavities. // Physical Review. - Special Topics: Accelerators and Beams, 2010. - Vol.13. - N8. - 19 August 2010. - DOI: 10.1103/PhysRevSTAB.13.084201.
- [251] Belikov O.V., Belozеров A.V., Becher Yu., Bulycheva Yu., Fateev A.A., Galt A.A., Kayukov A.S., Krylov A.R., Kobetz V.V., Logachev P.V., Medvedko A.S., Meshkov I.N., Minashkin V.F., Pavlov V.M., Petrov V.A., Pyataev V.G., Rogov A.D., Sedyshev P.V., Shabratov V.G., Shvec V.A., Shvetsov V.N., Skrypnik A.V., Sumbaev A.P., Ufimtsev A.V. and Zamrij V.N. Physical start-up of the first stage of IREN facility. // Journal of Physics Conference Series 205, 2010, doi: 10.1088/1742-6596/205/1/012053 (XVIII Intern. School on Nuclear Physics: Neutron Physics and Applications, 21-27 September, 2009, Varna, Bulgaria).

- [252] Simonen T.C., Anikeev A., Bagryansky P., Beklemishev A., Ivanov A., Lizunov A., Maximov V., Prikhodko V., Tsidulko Yu. High beta experiments in the GDT Axisymmetric Magnetic Mirror. // J. of Fusion Energy. - Dec. 2010. - Vol.29. - N6. - P.558-560.
- [253] Horton W., Fu X.R., Ivanov A., Beklemishev A. Parameter optimization studies for a Tandem Mirror Neutron Source. // J. of Fusion Energy. - Dec. 2010. - Vol.29. -N6. - Sp. Iss. SI. - P.521-526.
- [254] Sorokina N., Burdakov A., Ivanov I., Kuklin K., Polosatkin S., Popov S., Postupaev V., Rovenskikh A., Shoshin A., Schudlo I. Diagnostics of heavy impurities at GOL-3 facility. // NIM in Physics Research A. Sec.: Accelerators Spectrometers Detectors and Associated Equipment. - Nov. 11, 2010. - Vol.623. - N2. - P.750-753.
- [255] Burdakov A.V., Ivanov A.A., Kruglyakov E.P. Modern magnetic mirrors and their fusion prospects. // Plasma Physics and Controlled Fusion. - Dec. 2010. - Vol.52. - N12. - Part. 1. - P.124026.
- [256] Kotelnikov I., Rome M. Relativistic thermal equilibrium of non-neutral plasmas. // Physics Letters A. - Nov. 1, 2010. - Vol.374. - N48. - P.4864-4871.
- [257] Aamodt K., Ivanov A., Ivanov M., Ivanov V., Pestov Yu. Alignment of the ALICE inner tracking system with cosmic-ray tracks. // J. of Instrumentations. - March 2010. - Vol.5. - P.P03003.
- [258] Kabantsev A.A., Dubin Daniel H.E., Driscoll C.F., Tsidulko Yu.A. Chaotic transport and damping from theta-ruffled separatrices. // Physical Review Letters. - 2010. - Vol.105. - N20. - P.205001-1-4.
- [259] Kabantsev A.A., Dubin Daniel H.E., Driscoll C.F., Tsidulko Yu.A. Neoclassical transport caused by collisionless scattering across an asymmetric separatrix. // Physical Review Letters. - 2010. - Vol.105. - N18. - P.185003-1-4.
- [260] Aamodt K., Frolov, A., Grigoriev V., Ivanov A., Ivanov M., Ivanov V., Kiselev S., et al. (ALICE Collab.). Transverse momentum spectra of charged particles in proton-proton collisions at root s=900 GeV with ALICE at the LHC. // Physics Letters B. - 2010. - Vol.693. - N2. - P.53-68.
- [261] Beklemishev A.D., Bagryansky P.A., Prikhodko V.V. Application of electrode-driven shear flows for improved plasma confinement. // ВАНТ. Сер.: Физика плазмы (Problems of Atomic Science and Technology. Ser.: Plasma Physics). - 2010. - N6(70). - P.8-10.
- [262] Tanaka K, Vyacheslavov L.N., Mishchenko A., et al. (LHD Expt Grp). Particle transport of LHD. // Fusion Science and Technology. - Aug. 2010. Vol.58. - N1(Sp. Iss. SI). - P.70-90.
- [263] Kawahata K., Sanin A., Vyacheslavov L.N., et al. Overview of LHD plasma diagnostics. // Fusion Science and Technology. 2010. - Vol.58. - N1(Sp. Iss. SI). - P.331-344.
- [264] Akiyama T., Vyacheslavov L.N., Sanin A., et al. (LHD Expt Grp). Interferometer systems on LHD. // Fusion Science and Technology. - 2010. - Vol.58. - N1(Sp. Iss. SI). - P.352-363.
- [265] Balakin Alexey V., Borodin Alexander V., Kotelnikov Igor A., Savelev Andrey B., Shkurinov Alexander P. THz Emission from a femtosecond laser focus in a two-color scheme. // Journal of Optical Society of America B. Optical Physics. - 2010. - Vol.27. - N1. - P.16-26.
- [266] Romé Massimiliano, Kotelnikov Igor. Transport induced by symmetry breaking in a nonneutral plasma. // AIP Conf. Proc. - 2010. - Vol.1242. - P.175-182.
- [267] Kotelnikov I.A., Shkurinov A.P. Multiphoton ionization by a two-color laser pulse. // Vestnik NSU. Ser.: Physics. 2010. - Vol.5. - N4. - 2010.
- [268] Bayanov B., Burdakov A., Kuznetsov A., Makarov A., Sinitskii S., Sulyaev Yu., Taskaev S. Dosimetry and spectrometry at accelerator based neutron source for boron neutron capture therapy. // Radiation Measurements. - 2010. - Vol.45. - P.1462-1464.
- [269] Frolov A., Grigoriev V., Ivanov A., Ivanov M., Ivanov V., Kaplin V., Kondratiev V., Kondratyeva N., Vasiliev A., Vassiliev I., et al (Alice Collab.). Two-pion Bose-Einstein correlations in pp collisions at root s=900 GeV. // Physical Review D. - 2010. - Vol 82. - N5. - P.052001.
- [270] Ivanov A.V., Reva V.B. Calculation of the variable-profile electron beam for electron coolers. // Instruments and Experimental Techniques. - 2010. - Vol.53. - N4. - P.539-544.
- [271] Lotov K.V. Simulation of proton driven plasma wakefield acceleration. // Phys. Rev. ST - Accel. Beams. - 2010. - Vol.13. - N4. - P.041301(1-9).

- [272] Lotov K.V., Maslov V.I., Onishchenko I.N., and Svistun E.N. Resonant excitation of plasma wakefields by a non-resonant train of short electron bunches. // *Plasma Phys. Control. Fusion.* - 2010. - Vol.52. - N6. - P.065009.
- [273] Lotov K.V., Maslov V.I., Onishchenko I.N., Svistun E.N. 2.5d simulation of plasma wakefield excitation by a nonresonant train of relativistic electron bunches. // *Problems of Atomic Science and Technology. Ser.: Nuclear Physics Investigations.* - 2010. - Vol.2(53). - P.122-124.
- [274] Lotov K.V., Maslov V.I., Onishchenko I.N., Vesnovskaya M.S. 2d3v simulations of cylindrical relativistic electron beam instability in a plasma. // *Problems of Atomic Science and Technology.* - 2010. - Vol.4. - P.12-16 (in Russian).
- [275] Timofeev I.V., Terekhov A.V. Simulations of turbulent plasma heating by powerful electron beams. // *Physics of Plasmas.* - 2010. - Vol.17. - P.083111.
- [276] Kotelnikov A., Bagryansky P.A., Prikhodko V.V. Formation of a magnetic hole above the mirror-instability threshold in a plasma with sloshing ions. // *Physical Review E.* - 2010. - Vol.81. - N6, Part 2. - P.067402. -P.067402-1-4.
- [277] Astrelin V.T., Burdakov A.V., Bykov P.V., Ivanov I.A., Ivanov A.A., Jongen Y., Konstantinov S.G., Kudryavtsev A.M., Kuklin K.N., Mekler K.I., Polosatkin S.V., Postupaev V.V., Rovenskikh A.F., Sinitskiy S.L., Zubairov E.R. Blistering of the selected materials irradiated by intense 200 keV proton beam. // *Journal of Nuclear Materials.* - 2010. - Vol.396. - N1. - P.43-48.
- [278] Moiseenko V.E., Dreval N.B., Agren O., Stepanov K.N., Burdakov A.V., Kalinin P.V., and Tereshin V.I. Fast wave heating in a mirror during plasma build-up. // *Eur. Phys. Journal D.* - 2010. - Vol.56. - N3. - P.359-367.
- [279] Sadykov V.A., Usoltsev V.V., Fedorova Yu.E., Sobyenin V.A., Kalinin P.V., Arzhannikov A.V., Vlasov A., Korobeynikov M.V., Bryazgin A.A., Salanov A.N., Predtechensky M.P., Bobryenok O.F., Ulikhin A., Uvarov N.F., Smorygo O.L., Ilyushenko A.V., Ulyanitsky V.Yu., Zlobin S.B. Design of middle-temperature solid oxide fuel cells based on porous substrates of strain hardening Ni-Al alloy. // *Electrochemistry, 2010* (to be published).
- [280] Sadykov Vladislav, Mezentseva Natalia, Usoltsev Vladimir, Sadovskaya Ekaterina, Ishchenko Arkady, Pavlova Svetlana, Bepalko Yulia, Kharlamova Tamara, Zevak Ekaterina, Salanov Aleksei, Krieger Tamara, Belyaev Vladimir, Bobrenok Oleg, Uvarov Nikolai, Okhlupin Yury, Smorygo Oleg, Smirnova Alevtina, Singh Prabhakar, Vlasov Aleksandr, Korobeynikov Mikhail, Bryazgin Aleksandr, Kalinin Peter, Arzhannikov Andrei. Solid oxide fuel cell composite cathodes based on perovskite and fluorite structures. // *Journal of Power Sources, 2010*, (to be published).
- [281] Navarro-Cia M., Kuznetsov S.A., Aznabet M., Beruete M., Falcone F., and Sorolla Ayza M. A Route for ultramillimeter wave and terahertz metamaterial design. // *IEEE Journal of quantum electronics, 2010* (to be published).
- [282] Sorokina N., Burdako A.V., Ivanov I., Kuklin K., Polosatkin S., Popov S., Postupaev V., Rovenskikh A., Shoshin A., Schudlo I. Diagnostics of heavy impurities at GOL-3 facility. // *NIM in Physics Research A.* - 2010. - Vol.623. - P.750-753.
- [283] Bardakhanov S.P., Vasiljeva I.V., Kuksanov N.K. and Mjakin S.V. Surface functionality features of nanosized silica obtained by electron beam evaporation at ambient pressure. // *Advances in Materials Science and Engineering.* - 2010. - Article ID 241695, 5p, doi:10.1155/2010/241695. - Hindawi Publishing Corporation.
- [284] Kozlov A.S., Petrov A.K., Kulipanov G.N., Aseyev V. A novel method of probing the fractional composition of nanosystems // *KONA powder and particle journal.* - 2010. - N28. - P.219-226.
- [285] Levichev E., Vinokurov N. Undulators and other insertion devices. // *Reviews of Accelerator Science and Technology.* - 2010. - Vol.3. - N1. - P.203-220.
- [286] Vinokurov N. Low-gain free electron lasers. // *Reviews of Accelerator Science and Technology.* - 2010. - Vol.3. - N1. - P.77-91.3
- [287] Pickalov V.V., Balandin A.L., Rodionov D.G., Vlasenko M.G., Knyazev B.A. Terahertz tomography: algorithms and experimental setup. // *Vestnik NSU. Ser.: Physics.* - 2010. - Vol.5. - N4. - P.91-97.

- [288] Verkhoglyad A.G., Zavialova M.A., Knyazev B.A., Makarov S.N., Stupak M.F. Development of a confocal sensor for a 3D surface on the basis of diffraction chromatic coding for the purposes of terahertz spectroscopy (in Russian). // Vestnik NSU. Ser.: Physics. - 2010. - Vol.5, N4. - P.117-122.
- [289] Gerasimov V.V., Knyazev B.A., Nikitin A.K. Terahertz dispersive spectroscopy thin-film study via surface-plasmon. // Vestnik NSU. Ser.: Physics. - 2010. - Vol.5. - N4. - P.158-161.
- [290] Gerasimov V.V., Knyazev B.A., Nikitin A.K., Nikitin V.V. Noninterferometric methods for determining the complex refractive index of terahertz surface plasmons (in Russian). // Vestnik NSU. Ser.: Physics. - 2010. - Vol.5. - N4. - p.147-150.
- [291] Choporova Ju.Ju., Vlasenko M.M., Gerasimov V.V., Knyazev B.A., Nikitin A.A., Cherkassky V.S. Recording holograma in the terahertz range on the free electron laser (in Russian). // Vestnik NSU. Ser.: Physics. - 2010. - Vol.5. - N4. - P.98-102.
- [292] Demyanenko M.A., Esaev D.G., Ovsyuk V.N., Fomin B.I., Marchishin I.V., Aliev V.Sh, Knyazev B.A., Gerasimov V.V., Kulipanov G.N. Vinokurov N.A., Litvintsev V.I. Development and application of uncooled microbolometer matrices for the terahertz range (in Russian). // Vestnik NSU. Ser.: Physics. - 2010. - Vol.5. - N4. - P.73-78.
- [293] Gerasimov V.V., Knyazev B.A., Cherkassky V.S. Way to measure the distribution of the complex refractive index of strongly absorbing samples (in Russian). - RF Patent № 2396547 dated 04.05.2009. The decision on granting 25.03.2010.
- [294] Abramskii A.Yu., Goldenberg B.G., Zelinsky A.G., Kondratyev V.I., Korolkov V.P., Koronkevich V.P., Masliy A.I., Medvedev A.Zh. Development of electroless- and electroplating processes for lithographic production of 3D microstructures. // Electroplating & Superface Treatment. - 2010. - Vol.XVIII. - N2. - P.11. ISSN 0869-5326.
- [295] Kriventsov V.V., Valeev Z.G., Surnin D.V., Beltukov A.N., Vetoshkin V.M., Zubavichus Ya.V., Eliseev A.A., Mezentsev N.A. Synthesis and study of the structure of ordered arrays of Ge nanowires // Journal of Structural Chemistry. - 2010. - Vol.51. - P. S135-S139.
- [296] Valeev R., Romanov E., Deev A., Beltukov A., Napolski K., Eliseev A., Krylov P., Mezentsev N., Kriventsov V. Synthesis of ZnSe semiconductor nanodots arrays by templated PVD. // Physica Status Solidi. - 2010. - Vol. 7. - N6. - P.1539-1541.
- [297] Batrakov A.M. Control systems for scientific installations. // Novosibirsk: NSU, 2010, 24p.
- [298] Bekhtenev E.A., Batrakov A.M.. DAC's and ADC's. // Novosibirsk: NSU, 2010, 30p.
- [299] Raschenko V.V. Pulse techniques. // Novosibirsk: NSU, 2010, 130p.
- [300] Fatkin G.A., Ottmar A.V. Parallel data buses for control systems. // Novosibirsk: NSU: ИГУ, 2010, 56p.
- [301] Bekhtenev E.A., Serednaykov S.S. Reference Guide on C. // Novosibirsk: NSU, 2010, 26p.
- [302] Fatkin G.A., Panov A.N. Distributed control systems and serial data buses. // Novosibirsk: NSU, 2010, 32p.
- [303] Bryazgin A.A., Voronin L.A., Tkachenko V.O., Sidorov A.V., Gorbunov V.A., Kokin E.N., Lukin A.N., Nekhaev V.E., Panfilov A.D., Padchenko V.M., Faktorovich B.L., Shtarklev E.A., Bezuglov V.V., Vlasov A.Yu., Korobeinikov M.V. Application of accelerators of ILU types for sterilization purpose. // Medical Business. - 2010. - N12(199). - P.60-62.
- [304] Ablikim M., Achasov M.N., Muchnoi N.Yu., et al. (BESIII Collab.). Observation of a  $p(\bar{p})$ -over-bar mass threshold enhancement in  $\psi' \rightarrow \pi^+\pi^- J/\psi$  ( $J/\psi \rightarrow \gamma p(\bar{p})$ -over-bar) decay. // Chinese Physics C. - 2010. - Vol.34. - N4. - P.421-426.
- [305] Nayak Pranaba K., Gupta Sunil K., Jain Atul, Mazumdar Indranil, Raha Sibaji, Saha Swapan K., Bobrov Aleksandr V., Osipov Anton, Shwartz Boris. A study of the  $\gamma$ -ray flux during the total solar eclipse of 1 August 2008 at Novosibirsk, Russia. // J. Astroparticle Physics. - 2010. - Vol.32. - N6. - P.286-293.
- [306] Lotov K.V., Maslov V.I., Onishchenko I.N. Long sequence of relativistic electron bunches as a driver in wakefield method of charged particles acceleration in plasma. // ВАИТ. Сер.: Физика плазмы.- 2010. -N6(70). - P.103-107.

- [307] Lotov K.V., Maslov V.I., Onishchenko I.N., Svistun E.N., Vesnovskaya M.S. To the plasma wakefield excitation by a nonresonant sequence of relativistic electron bunches at plasma frequency above bunch repetition frequency. // ВАНТ. Сер.: Физика плазмы. - 2010. - N6(70). - P.114-116.
- [308] Aad G., ATLAS Collab., Kazanin V.A., Kolachev G.M., Korol A., Kotov K.Y., Malyshev V., Maslennikov A.L., Orlov I., Panin V.N., Peleganchuk S.V., Schamov A.G., Skovpen K., Soukharev A., Talyshev A., Tikhonov Y.A., Zaytsev A., et al. Search for new particles in two-jet final states in 7 TeV proton-proton collisions with the ATLAS detector at the LHC. // Phys. Rev. Lett. - 2010. - Vol.105. - N16. - P.161801-1-17; [E-print: arXiv:1008.2461, 2010].
- [309] Aad G., ATLAS Collab., Bobrovnikov V.B., Bogdanchikov A., Kazanin V.A., Kolachev G.M., Korol A., Malyshev V., Maslennikov A.L., Orlov I., Peleganchuk S.V., Shamov A.G., Skovpen K., Soukharev A., Talyshev A., Tikhonov Y.A., Zaytsev A., et al. Observation of a centrality-dependent dijet asymmetry in lead-lead collisions at radical  $\sqrt{s_{NN}}=2.76$  TeV with the ATLAS detector at the LHC. // Phys. Rev. Lett. - 2010. - Vol.105. - N25. - P.252303-1-18; [E-print: arXiv:1011.6182, 2010].
- [310] Aamodt K., ALICE Collab., Pestov Yu., et al. Centrality dependence of the charged-particle multiplicity density at midrapidity in Pb-Pb collisions at radical  $\sqrt{s_{NN}}=2.76$  TeV. // Phys. Rev. Lett. - 2010. - Vol.106. - N3. - P.032301-1-7.
- [311] Ablikim M., BESIII Collab., Achasov M.N., et al. Evidence for  $\psi'$  decays into  $\gamma\pi^0$  and  $\gamma\eta$ . // Phys. Rev. Lett. - 2010. - Vol.105. - N26. - P.261801-1-6.
- [312] Aamodt K., ALICE Collab., Pestov Yu., et al. Elliptic flow of charged particles in Pb-Pb collisions at radical  $\sqrt{s_{NN}}=2.76$  TeV. // Phys. Rev. Lett. - 2010. - Vol.105. - N25. - P.252302-1-11.
- [313] Aamodt K., ALICE Collab., Pestov Yu., et al. Charged-particle multiplicity density at midrapidity in central Pb-Pb collisions at radical  $\sqrt{s_{NN}}=2.76$  TeV. // Phys. Rev. Lett. - 2010. - Vol.105. - N25. - P.252301-1-11.
- [314] Aad G., ATLAS Collab., Malyshev V., Maslennikov A.L., Peleganchuk S.V., Kazanin V.A., Kotov K.Y., Orlov I., Soukharev A., Talyshev A., Tikhonov Y.A., Schamov A.G., Zaytsev A., et al. The ATLAS simulation infrastructure. // Europ. Phys. J. C. - 2010. - Vol.70. - N3. - P.823-874; [E-print: arXiv:1005.1784; 0036327.- 2010 - 16p].
- [315] Aad G., ATLAS Collab., Kazanin V.A., Kotov K.Y., Malyshev V., Maslennikov A.L., Orlov I., Peleganchuk S.V., Soukharev A., Talyshev A., Tikhonov Y.A., Shamov A.G., Zaytsev A., et al. Commissioning of the ATLAS muon spectrometer with cosmic rays // Europ. Phys. J. C. - 2010. - Vol.70. -N3. - P.875 - 916; [E-print: arXiv:1006.4384, 2010].
- [316] Aad G., ATLAS Collab., Kazanin V.A., Kotov V.A., Malyshev V., Maslennikov A.L., Orlov I., Peleganchuk S.V., Schamov A.G., Soukharev A., Talyshev A., Tikhonov Y.A., Zaytsev A., et al. Readiness of the ATLAS tile calorimeter for LHC collisions. // Europ. Phys. J. C. - 2010. -Vol. 70. - N4. - P.1193 -1236; [E-print: arXiv:1007.5423, 2010].
- [317] Aad G., ATLAS Collab., Kazanin V.A., Kotov K.Y., Malyshev V., Maslennikov A.L., Orlov I., Peleganchuk S.V., Schamov A.G., Soukharev A., Talyshev A., Tikhonov Y.A., Zaytsev A., et al. The ATLAS inner detector commissioning and calibration. // Europ. Phys. J. C. - 2010. - Vol.70. - N3. - P.787-821; [E-print: arXiv:1004.5293, 2010].
- [318] Aad G., ATLAS Collab., Kazanin V.A., Kotov K.Y., Malyshev V., Maslennikov A.L., Orlov I., Shamov A.G., Soukharev A., Talyshev A., Tikhonov Y.A., Peleganchuk S.V., Zaytsev A., et al. Readiness of the ATLAS liquid argon calorimeter for LHC collisions. // Europ. Phys. J. C. - 2010. - Vol.70. - N3. - P.723-753.
- [319] Aad G., ATLAS Collab., Kazanin V.A., Kotov K.Y., Malyshev V., Maslennikov A.L., Orlov I., Peleganchuk S.V., Shamov A.G., Soukharev A., Talyshev A., Tikhonov Y.A., Zaytsev A., et al. Drift time measurement in the ATLAS liquid argon electromagnetic calorimeter using cosmic muons. // Europ. Phys. J. C. - 2010. - Vol.70. - N3. - P.755-785; [E-print: arXiv:1002.4189, 2010].
- [320] Kulipanov G.N. Generation and application of terahertz radiation: history and prospects (in Russian). Vestnik NSU. Ser.: Physics. - 2010. - Vol.5. - N4. - P.24-27.
- [321] Kuznetsov S.A., Arzhannikov A.V., Gelfand A.V., Kubarev V.V., Navarro-Cia M., Beruete

- M., Falcone F., Sorolla M., Thumm M. Microstructured quasi-optical selective components for subterahertz and terahertz applications. // Vestnik NSU. Ser.: Physics. - 2010. - Vol.5. - N4. - P.79-90.
- [322] Arzhannikov A.V., Burdakov A.V., Kalinin P.V., Kuznetsov S.A., Makarov M.A., Mekler K.I., Polosatkin S.V., Postupaev V.V., Rovenskikh A.F., Sinitsky S.L., Sklyarov V.F., Stepanov V.D., Sulyaev Yu.S., Thumm M.K.A., Vyacheslavov L.N. Subterahertz generation by strong Langmuir turbulence at two-stream instability of high current 1-MeV REBs. // Vestnik NSU. Ser.: Physics. - 2010. - Vol.5. - N4. - P.44-49.
- [323] Abdulmanov V.G., Dikansky N.S. MIS-1 Electron-beam ion source MIS-1. // Physics of Particles and Nuclear Letters. - 2010. - Vol.7. - N7. - P.1-3.
- [324] Aad G., ..., Kazanin V.A., Kotov K.Yu., Malyshev V., Maslennikov A.L., Orlov I., Peleganchuk S.V., Schamov A.G., Soukharev A., Talyshev A., Tikhonov Yu.A., Zaytsev A., et al. (ATLAS Collab.). Charged-particle multiplicities in pp interactions at  $\sqrt{s} = 900$  GeV measured with the ATLAS detector at the LHC. // Phys Lett. B. - 2010. - Vol.688. - N1. - P.21-42; [E-print: arXiv:1003.3124, 2010].
- [325] Aad G., ..., Kazanin V.A., Kotov K.Yu., Malyshev V., Maslennikov A.L., Orlov I., Peleganchuk S.V., Schamov A.G., Skovpen K., Soukharev A., Talyshev A., Tikhonov Yu.A., Zaytsev A., et al. (ATLAS Collab.). Performance of the ATLAS detector using first collision data // J. High Energy Phys. - 2010. - Vol.09. - P.056; [E-print: arXiv:1005.5254, 2010].
- [326] Aad G., ..., Bobrovnikov V.B., Bogdanchikov A., Kazanin V.A., Kolachev G.M., Korol A., Kotov K.Yu., Malyshev V., Maslennikov A.L., Orlov I., Panin V.S., Peleganchuk S.V., Skovpen K., Schamov A.G., Soukharev A., Talyshev A., Tikhonov Yu.A., Zaytsev A., et al. (ATLAS Collab.). Measurement of the  $W \rightarrow l\nu$  and  $Z/\gamma^* \rightarrow ll$  production cross sections in proton-proton collisions at  $\sqrt{s} = 7$  TeV with the ATLAS detector. // JHEP 12 (2010) 060; [E-print: arXiv:1010.2130, 2010].
- [327] Silagadze Z.K. Schrodinger's cat versus Darwin. // Electronic J. Theor. Physics. - 2010. - Vol.7. - P.1-56.
- [328] Silagadze Z.K. Sliding rope paradox. // Latin American J. Phys. Educ. - 2010. - Vol.4. - P.294-302.

#### REPORTS ON THE CONFERENCES

- [329] Anashin V.V., Goncharova N.F., Semenov A.M., Ushakov V.A., Filipchenko A.V., Schegolev L.M. Review and status of TNK vacuum system. // XVIII Intern. Synchrotron Radiation Conference (SR-2010). 19 - 22 July 2010, Novosibirsk. - Theses 2010. Novosibirsk: BINP SB RAS. - P.16.
- [330] Batrakov A.M., Vagin P.V., Vobly P.D., Gurov D.S., Ilyin I.V., Ogurtsov A.B., Tischer M., Utkin A.V., Havin N.G., Kholopov M.A., Shichkov D.S. Wigglers on permanent magnets for reducing the emittance of the synchrotron radiation source Petra-III. // XVIII Intern. Conf. on the Application of Synchrotron Radiation: SR-2010, Novosibirsk, 19 - 22 July 2010. - Theses. Novosibirsk: BINP SB RAS, 2010. - P.2
- [331] Korneev V.N., Shlektarev V.A., Zabelin A.V., Lanina N.F., Aulchenko V.M., Tolochko B.P., Litvinov E.I., Vasina A.A. Status of the "Dixie" station on the synchrotron source SIBERIA-2 for studies of the nanostructured dynamics of natural and synthetic materials by means of SAXS/WAXS diffraction. // XVIII Intern. Conf. on the Application of Synchrotron Radiation: SR-2010, Novosibirsk, 19 - 22 July 2010. - Theses. Novosibirsk: BINP SB RAS, 2010. - P.24
- [332] Ivlyushkin D.V., Gorlovoi A.V., Kondratiev V.I., Lyah V.V., Nikolenko A.D., Pindyurin V.F., Ustinov A.A. Perfection of absolute calibration methods of semiconductor photodiodes. // XVIII Intern. Conf. on the Application of Synchrotron Radiation: SR-2010, Novosibirsk, 19 - 22 July 2010. - Theses. Novosibirsk: BINP SB RAS, 2010. - P.25
- [333] Rakshun Ya.V., Kholopov M.A., Chernov V.A. Experimental module of station for soft X-ray spectroscopy. // XVIII Intern. Conf. on the Application of Synchrotron Radiation: SR-2010, Novosibirsk, 19 - 22 July 2010. - Theses. Novosibirsk: BINP SB RAS, 2010. - P.27.
- [334] Gorlovoi A.V., Ivlyushkin D.V., Nikolenko A.D., Shestov S.V. Two-coordinate detector for the

- metrological station "Kosmos". // XVIII Intern. Conf. on the Application of Synchrotron Radiation: SR-2010, Novosibirsk, 19 - 22 July 2010. - Theses. Novosibirsk: BINP SB RAS, 2010. - P.29.
- [335] Kuper K.E. (Cooper), Zedgenizov D.A., Ragozin A.L., Shatsky V.S., Ten K.A., Prueel E.R., Zarko V.E., Kvasov A.A., Goldenberg B.G., Goldenberg E.L., Slusarenko I.Yu. Review of the works carried out at the SR station "X-ray microscopy and tomography" on VEPP-3. // XVIII Intern. Conf. on the Application of Synchrotron Radiation: SR-2010, Novosibirsk, 19 - 22 July 2010. - Theses. Novosibirsk: BINP SB RAS, 2010. - P.30-31.
- [336] Goldenberg B.G., Cooper K.E.(Kuper), Kondratiev V.I., Sorokoletov D.S., Golubtsov S.K. Express method for controlling X-ray masks for deep X-ray lithography. // XVIII Intern. Conf. on the Application of Synchrotron Radiation: SR-2010, Novosibirsk, 19 - 22 July 2010. - Theses. Novosibirsk: BINP SB RAS, 2010. - P.32.
- [337] Parkhomchuk V.V., Rastigeev S.A. Acceleration mass spectrometer of the sharing center "Geochronology of the Cenozoic era". // XVIII Intern. Synchrotron Radiation Conference (SR-2010). 19 - 22 July, 2010, Novosibirsk, Russia. - Proceedings, Novosibirsk: BINP SB RUS, 2010, P.19-22.
- [338] Kriventsov V.V., Chernov V.A., Zolotarev K.V. The first results of the multielement SCD for fluorescent XAFS spectroscopy at the Siberian SR center. // XVIII Intern. Conf. on the Application of Synchrotron Radiation: SR-2010, Novosibirsk, 19 - 22 July 2010. - Theses. Novosibirsk: BINP SB RAS, 2010. - P.37.
- [339] Timchenko N.A., Goldenberg B.G., Pindyurin V.F., Petrova E.V., Nikolenko A.D., Litvin S.V., Kanaev V.G. Yurchenko V.I. Templates for the production of regular microstructures by the LIGA-technology methods. // XVIII Intern. Conf. on the Application of Synchrotron Radiation: SR-2010, Novosibirsk, 19 - 22 July 2010. - Theses. Novosibirsk: BINP SB RAS, 2010. - P.3.
- [340] Aulchenko V.M., Golovizin A.V., Evdokov O.V., Zhogin I.L., Zhulanov V.V., Prueel E.R., Tolochko B.P., Ten K.A., Shekhtman L.I. Status of the DIMEX detector. // XVIII Intern. Conf. on the Application of Synchrotron Radiation: SR-2010, Novosibirsk, 19 - 22 July 2010. - Theses. Novosibirsk: BINP SB RAS, 2010. - P.38-39.
- [341] Kotelnikov A.I., Selivanov A.N., Fedotov M.G. CCD detector for the high time resolution experiments on the SR beams. // XVIII Intern. Synchrotron Radiation Conference: SR-2010, Novosibirsk, 19 - 22 June, 2010. - Digest reports. Novosibirsk: BINP SB RAS, 2010. - P.44.
- [342] Gentshev A.N., Kondratiev V.I., Pindyurin V.F., Zelinskii A.G. Manufacturing LIGA masks with thin brittle plates as carrier membranes. // XVIII Intern. Synchrotron Radiation Conference (SR-2010). 19 - 22 July 2010, Novosibirsk. - Theses 2010. Novosibirsk: BINP SB RAS. - P.45.
- [343] Gentshev A.N., Golubtsov B.G., Kondratiev V.I., Pindyurin V.F., Zelinskii A.G. LIGA masks based on epoxy graphite. // XVIII Intern. Synchrotron Radiation Conference (SR-2010). 19 - 22 July 2010, Novosibirsk. - Theses 2010. Novosibirsk: BINP SB RAS. - P.46.
- [344] Legkodymov A.A., Mashkovtsev M.R., Nikolenko A.D., Pindyurin V.F., Lyakh V.V. Avakian S.V., Voronin N.A. Comparative certification of secondary electron multipliers in the ultrasoft X-ray range. // XVIII Intern. Synchrotron Radiation Conference (SR-2010). 19 - 22 July 2010, Novosibirsk. - Theses 2010. Novosibirsk: BINP SB RAS. - P.47.
- [345] Gentshev A.N., Kondratiev V.I., Kuznetsov S.A., Pindyurin V.F., Zelinskii A.G. Manufacturing technology and testing of selective elements of terahertz radiation in the form of copper grid structures. // XVIII Intern. Synchrotron Radiation Conference (SR-2010). 19 - 22 July 2010, Novosibirsk. - Theses 2010. Novosibirsk: BINP SB RAS. - P.48.
- [346] Gentshev A.N., Golubtsov B.G., Kondratiev V.I., Pindyurin V.F. Zelinskii A.G. Manufacturing of bio-chips using LIGA technology. // XVIII Intern. Synchrotron Radiation Conference (SR-2010). 19 - 22 July 2010, Novosibirsk. - Theses 2010. Novosibirsk: BINP SB RAS. - P.49.
- [347] Gentshev A.N., Kondratiev V.I., Pindyurin V.F., Zelinskii A.G. Beryllium LIGA masks. // XVIII Intern. Synchrotron Radiation Conference (SR-2010). 19 - 22 July 2010, Novosibirsk. - Theses 2010. Novosibirsk: BINP SB RAS. - P.50.
- [348] Shmakov A.N., Ivanov M.G., Tolochko B.P. Sharafutdinov M.R., Ancharov A.I., Zhogin I.L.,

- Sheromov M.A. New possibilities for x-ray diffraction studies at the Siberian center of synchrotron and terahertz radiation. // XVIII Intern. Synchrotron Radiation Conference (SR-2010). 19 - 22 July 2010, Novosibirsk. - Theses 2010. Novosibirsk: BINP SB RAS. - P.68.
- [349] Yuriev G.S., Gentshev A.N., Kulakova I.I., Karpukhin A.V. The structure of hydrogenated DNDH nanoparticles. // XVIII Intern. Synchrotron Radiation Conference (SR-2010). 19 - 22 July 2010, Novosibirsk. - Theses 2010. Novosibirsk: BINP SB RAS.
- [350] Vasina A.A., Vasilieva A.A., Zabelin A.V., Lanina N.F., Majewski E.I., Korneev V.N., Kulipanov G.N., Kupriyanova T.A., Letyagin V.P., Stankevich V.G. X-ray diffraction and fluorescence studies of epithelial tissue in cancer pathology. // XVIII Intern. Synchrotron Radiation Conference (SR-2010). 19 - 22 July 2010, Novosibirsk. - Theses 2010. Novosibirsk: BINP SB RAS. - P.81.
- [351] Markova Yu.N., Maximovskaya V.V., Kerber E.V., Zolotarev K.V., Rakshun Ya.V. Reproducibility of XRF-SR on standard samples of sediments and vegetation of the Baikal region. // XVIII Intern. Synchrotron Radiation Conference (SR-2010). 19 - 22 July 2010, Novosibirsk. - Theses 2010. Novosibirsk: BINP SB RAS. - P.137.
- [352] Zarko V.E., Kvasov A.A., Simonenko V.N., Chesnokov E.N., Cooper K.E., Kalmykov P.I., Tsipilev V.P. Determination of the threshold of laser initiation of crystallized mixtures furazanotetrazin dioxide and dinitrodiazapentane. - Also in English. // Zababakhin readings: X Intern. Conf. 15 - 19 March 2010: Abstracts. - Snezhinsk: Russian Federal Nuclear Center - VNIIEF, 2010. - P.89-90.
- [353] Kuper K.E. (Cooper), Ten K.A., Pruel E.R., Aminov Ya.A., Loboyko B.G., Smirnov E.B., Muzyrya A.K. X-ray microtomography of TATB charges on SR beams. - Also in English. // Zababakhin readings: X Intern. Conf. 15 - 19 March 2010: Abstracts. - Snezhinsk: Russian Federal Nuclear Center - VNIIEF, 2010. - P.101.
- [354] Gilyov O.N., Vikhlyayev D.A., Legkodymov A.A., Nikolenko A.D. Absolute calibration of x-ray optical elements and detectors used in the diagnostic methods of laser X-ray emission of argon capillary discharge plasma ( $\lambda=46,9$  HM). - Also in English. // Zababakhin readings: X Intern. Conf. 15 - 19 March 2010: Abstracts. - Snezhinsk: Russian Federal Nuclear Center - VNIIEF, 2010. - P.158-159.
- [355] Choporova Yu.Yu., Knyazev B.A., Gerasimov V.V., Vlasenko M.G. Recording holograms using the free electron laser. // X Intern. Conf. on Actual Problems of Electronic Instrument Engineering (APEIE-2010), Novosibirsk, September 22 - 24, 2010. - Proc. Novosibirsk: IEEE Catalog Number CFP1-471-PRT, NSTU, 2010, Vol.5. - P.43-46.
- [356] Rudenko A.S., Khriplovich I.B. Can CP-violation be observed in heavy-ion collisions? // III All-Russia Meeting: Precision Physics and Fundamental Physical Constants, 7 - 10 December, 2010, St-Petersburg: Intern. Symposium "50 Years on the Road to Quantum Unit of SR", 6 December, 2010: Theses. - St-Petersburg, SPU, 2010. - P.5.
- [357] Eidelman S.I. High-precision tau lepton mass measurements. // III All-Russia Meeting: Precision Physics and Fundamental Physical Constants, 7 - 10 December, 2010, St-Petersburg: Intern. Symposium. "50 Years on the Road to Quantum Unit of SR", 6 December. 2010: Theses. - St-Petersburg, SPU, 2010. - P.54.
- [358] Akhmetshin R.R., Aulchenko V.M., Banzarov V.Sh., Barkov L.M., Bashtovoi N.S., Bondar A.E., Bragin A.V., Epifanov D.A., Gabyshev N.I., Grebenyuk A.A., Grigoriev D.N., Zaitsev A.S., Zverev S.G., Ignatov F.V., Karpov S.V., Kazanin V.F., Kuzmin A.S., Logashenko I.B., Lukin P.A., Mikhailov K.Yu., Nikulin M.A., Okhapkin V.S., Popov A.S., Redin S.I., Ruban A.A., Ryzhenkov A.E., Ryskulov N.M., Sibidanov A.L., Skriskiy A.N., Smakhtin V.P., Solodov E.P., Tikhonov Yu.A., Fedotov G.V., Khazin B.I., Shwarz B.A., Shemyakin D.N., Eidelman S.I., Yudin Yu.V. CMD-3 Detector. // III All-Russia Meeting: Precision Physics and Fundamental Physical Constants, 7 - 10 December, 2010, St-Petersburg: Intern. Symposium. "50 Years on the Road to Quantum Unit of SR", 6 December. 2010.: Theses. - St-Petersburg, SPU, 2010. - P.72.
- [359] Gentshev A.N., Goldenberg B.G., Zelinskii A.G., Kuznetsov S.A., Maslii A.I. LIGA application to creation of selective elements of the terahertz range - metal and thick pseudo-metal grid structures. // Working Meeting "X-ray Optics - 2010", Chernogolovka, 20 - 23 Sept. 2010, Chernogolovka:

- IMT RAS, 2010. - P.156-157.
- [360] Beklemishev A.D. On the applicability of the vortex holding the neutron source and other open traps // About vortex confinement applicability for the neutron source and other open traps. // XXXVII Zvenigorod Intern. Conference on Plasma Physics and Controlled Fusion, 8-12 February, 2010. - Abstracts. - M: "PLAZMAIOFAN", 2010, P.30 (in Russian).
- [361] Postupaev V.V., Astrelin V.T., Batkin V.I., Burdakov A.V., Burmasov V.S., Vyacheslavov L.N., Ivanenko V.G., Иванов I.A., Ivantsivsky M.V., Kuznetsov S.A., Kuklin K.N., Makarov M.A., Mekler K.I., Polosatkin S.V., Popov S.S., Rovenskikh A.F., Sinitsky S.L., Stepanov V.D., Sudnikov A.V., Sulyaev Yu.S., Sklyarov V.F., Sorokina N.V., Shoshin A.A., Experiments with "thin" electron beam at GOL-3. // XXXVII Zvenigorod Intern. Conference on Plasma Physics and Controlled Fusion, 8-12 February, 2010. - Abstracts. - M: "PLAZMAIOFAN", 2010, P.31 (in Russian).
- [362] Korzhavina M.S., Anikeev A.V., Maximov V.V., Pushkareva A.N., Myrakhtin S.V., Prikhodko V.V., Bagryansky P.A. Experimental study of longitudinal plasma confinement in the Gas Dynamic Trap. // XXXVII Zvenigorod Intern. Conference on Plasma Physics and Controlled Fusion, 8-12 February, 2010. - Abstracts. - M: "PLAZMAIOFAN", 2010, P.3.
- [363] Anikeev A.V., Bagryansky P.A., Zaitsev K.V., Kirillov K.Yu., Korzhavina M.S., Kotelnikov I.A., Lizunov A.A., Lvovsky A.V., Maximov V.V., Murakhtin S.V., Pinzhenin E.I., Prikhodko V.V., Pushkareva A.N., Solomakhin A.L. Confinement of fast ions in the GDL in the regime with high relative pressure. // XXXVII Zvenigorod Intern. Conference on Plasma Physics and Controlled Fusion, 8-12 February, 2010. - Abstracts. - M: "PLAZMAIOFAN", 2010, P.3.
- [364] Chirkov A.Yu., Ryzhkov S.V., Bagryansky P.A., Anikeev A.V. Thermonuclear regimes of the axially symmetric open system with high-power fast particles injection. // XXXVII Zvenigorod Intern. Conference on Plasma Physics and Controlled Fusion, 8-12 February, 2010. - Abstracts. - M: "PLAZMAIOFAN", 2010, P.40.
- [365] Solomakhin A.L., Bagryansky P.A., Biel W., Dreier H., Ivanenko S., Kvashnin A.N., Kovalenko Yu.V., Lambertz H.T., Lizunov A.A., Savkin V.Ya., Khilchenko A.D. Multi-channel dispersion interferometer for the density and position control of plasma. // XXXVII Zvenigorod Intern. Conference on Plasma Physics and Controlled Fusion, 8-12 February, 2010. - Abstracts. - M: "PLAZMAIOFAN", 2010, P.4.
- [366] Anikeev A.V. Numerical model of the neutron source based on Gas Dynamic Trap for the transmutation of long-life radioactive wastes. // XXXVII Zvenigorod Intern. Conference on Plasma Physics and Controlled Fusion, 8-12 February, 2010. - Abstracts. - M: "PLAZMAIOFAN", 2010, P.45.
- [367] Ivanov A.A., Maximov V.V., Pinzhenin E.I., Pchelyakov O.P., Tishkovsky E.G., Chistokhin I.B. Applying of silicon diodes for the particle flows registration on the GDT facility. // XXXVII Zvenigorod Intern. Conference on Plasma Physics and Controlled Fusion, 8-12 February, 2010. - Abstracts. - M: "PLAZMAIOFAN", 2010, P.55.
- [368] Sklyarov V.F., Burdakov A.V., Kuznetsov S.A., Mekler K.I., Polosatkin S.V., Postupaev V.V., Rovenskikh .F., Sinitsky S.L. Investigation of submillimetre radiation emission spectrum on the GOL-3 facility. // XXXVII Intern. (Zvenigorod) Conference on Plasma Physics and Controlled Fusion, Zvenigorod, 8-12 February, 2010: Abstracts. - M: "PLAZMAIOFAN", 2010, P.56.
- [369] Zubarev P.V., Donin A.S., Moiseev D.V., Murakhtin S.V. GDT modernization. New power supply system for the atomic injection. // XXXVII Zvenigorod Intern. Conference on Plasma Physics and Controlled Fusion, 8-12 February, 2010. - Abstracts. - M: "PLAZMAIOFAN", 2010, P.57.
- [370] Maximov V.V., Pinzhenie E.I. Measurement of DD reaction yield at GDT facility. // XXXVII Intern. (Zvenigorod) Conference on Plasma Physics and Controlled Fusion, Zvenigorod, 8-12 February, 2010: Abstracts. - M: "PLAZMAIOFAN", 2010, P.58.
- [371] Lvovsky A.V., Solomakhin A.L. Measurement of linear plasma density in Gas Dynamic Trap with the dispersion interferometer. // XXXVII Zvenigorod Intern. Conference on Plasma Physics and Controlled Fusion, 8-12 February, 2010. - Abstracts. - M: "PLAZMAIOFAN", 2010, P.60.

- [372] Sudnikov A.V., Burdakov A.V., Ivanov I.A., Makarov M.A., Mekler K.I., Polosatkin S.V., Postupaev V.V., Rovenskikh A.F., Sinitsky S.L. Pulse MHD plasma activity of the GOL-3 facility at a cooling down stage. // XXXVII Intern. (Zvenigorod) Conference on Plasma Physics and Controlled Fusion, Zvenigorod, 8-12 February, 2010: Abstracts. - M: "PLAZMAIOFAN", 2010, P.69.
- [373] Anikeev A.V., Bagryansky P.A., Donin A.S., Zaitsev K.V., Ivanov A.A., Kirillov K.Yu., Kovalenko Yu.V., Korzhavina M.S., Kruglyakov E.P., Lizunov A.A., Lvovsky A.V., Maximov V.V., Murakhtin S.V., Pinzhenin E.I., Prikhodko V.V., Pushkareva A.N., Savkin V.Ya., Solomakhin A.L. GDT facility: regular modernization stage and achieved results. // XXXVII Intern. (Zvenigorod) Conference on Plasma Physics and Controlled Fusion, Zvenigorod, 8 - 12 February, 2010: Abstracts. - M: "PLAZMAIOFAN", 2010, P.76.
- [374] Beklemishev A.D. Three-dimensional forceless equilibrium in the open axisymmetric trap with current. // XXXVII Intern. (Zvenigorod) Conference on Plasma Physics and Controlled Fusion, Zvenigorod, 8 - 12 February, 2010: Abstracts. - M: "PLAZMAIOFAN", 2010, P.8.
- [375] Skovorodin D.I., Beklemishev A.D. Numerical kinetic model of the plasma outflow from the mirror trap. // XXXVII Intern. (Zvenigorod) Conference on Plasma Physics and Controlled Fusion, Zvenigorod, 8 - 12 February, 2010: Abstracts. - M: "PLAZMAIOFAN", 2010, P.82.
- [376] Burdakov A.V., Ivanov I.A., Polosatkin S.V., Postupaev V.V., Rovenskikh A.F., Sorokina N.V., Shoshin A.A., Shchudlo I.M. Investigation of heavy impurities in the multimirror trap GOL-3. // XXXVII Intern. (Zvenigorod) Conference on Plasma Physics and Controlled Fusion, Zvenigorod, 8 - 12 February, 2010: Abstracts. - M: "PLAZMAIOFAN", 2010, P.89.
- [377] Burdakov A.V., Ivanov I.A., Ivanenko V.G., Makarov M.A., Mekler K.I., Polosatkin S.V., Postupaev V.V., Rovenskikh A.F., Sudnikov A.V., Sinitsky S.L., Shoshin A.A., Shudlo I.M. Stabilization of a relativistic electron beam by dense plasma cloud in the expander of the GOL-3 facility. // XXXVII International (Zvenigorod) Conference on Plasma Physics and Controlled Fusion, Zvenigorod, 8-12 February, 2010: Abstracts. - M: "PLAZMAIOFAN", 2010, P.93.
- [378] Astrelin V.T., Burdakov A.V., Grigoriev S.V., Kandaurov I.V., Koval N.N., Teresov A.D. Features of electron flows forming in a diode with grid stabilisation of a plasma emission surface. // XXVII International (Zvenigorod) Conference on Plasma Physics and Controlled Fusion, Zvenigorod, 8 - 12 February, 2010: Abstracts. - M: "PLAZMAIOFAN", 2010, P.328.
- [379] Miginsky S.V. Energy spread and efficiency of FEL. // XVIII Intern. Conf. on the Application of Synchrotron Radiation: SR - 2010, Novosibirsk, 19 - 22 July 2010: Theses - Novosibirsk: BINP SB RAS, 2010. - P.11.
- [380] Abakumova E.V., Anashin V.V., Balewski K., Boespflug R., Levichev E.B., Krasnov A.A., Kuzminykh V.S., Nagorny B., Semenov A.M., Smaluk k V.V., Tischer M., Wedekind H-P., Zapfe K., Zhukov A.A., Zolotarev K.V. Vacuum components performance for beam damping sections of PETRA III SR source. // XVIII Intern. Conf. on the Application of Synchrotron Radiation: SR - 2010, Novosibirsk, 19 - 22 July 2010: Theses - Novosibirsk: BINP SB RAS, 2010. - P.12.
- [381] Salikova T.V. Stabilization FEL lasing based on fuzzy logic. // XVIII Intern. Conf. on the Application of Synchrotron Radiation: SR - 2010, Novosibirsk, 19 - 22 July 2010: Theses - Novosibirsk: BINP SB RAS, 2010. - P.15.
- [382] Khrushev S.V., Lev V.K., Mezentsev N.A., Miginsky E.G., Shkaruba V.A., Syrovatin V.M., Tsukanov V.M. Superconducting 117-pole 2.2 T wiggler with period of 30 mm for ALBA storage ring. // XVIII Intern. Conf. on the Application of Synchrotron Radiation: SR - 2010, Novosibirsk, 19 - 22 July 2010: Theses - Novosibirsk: BINP SB RAS, 2010. - P.23.
- [383] Batrakov A., Ilyin I., Tischer M., Shichkov D., Utkin A., Vagin P., Vobly P. Hardware and software package for fine adjustment of PETRA-3 damping wigglers. // XVIII Intern. Conf. on the Application of Synchrotron Radiation: SR - 2010, Novosibirsk, 19 - 22 July 2010: Theses - Novosibirsk: BINP SB RAS, 2010. - P.26.
- [384] Goldenberg B.G., Gentshev A.N. Golubtsov S.K., Zelinskii A.G., Kondrat'ev V.I., Kuznetsov S.A., Cooper K.E., Maslii A.I., Medvedev A.J., Petrova E.V., Pindyurin V.F. Sorokoletov D.S., Timchenko N.A. LIGA-technology at the Siberian center for Synchrotron and Terahertz radiation.

- // XVIII Intern. Conf. on the Application of Synchrotron Radiation: SR - 2010, Novosibirsk, 19 - 22 July 2010: Theses - Novosibirsk: BINP SB RAS, 2010. - P.35.
- [385] Rakshun Ya.V., Legkodymov A.A., Maximovskaya V.V., Kholopov M.A., Dar'in A.V. RFA station upgrade. // XVIII Intern. Conf. on the Application of Synchrotron Radiation: SR - 2010, Novosibirsk, 19 - 22 July 2010: Theses - Novosibirsk: BINP SB RAS, 2010. - P.40.
- [386] Ivanov V.Yu., Pustovarov V.A., Kikas A., Kaambre T., Kuusik I., Kirm M., Zinin E.I. VUV and XUV luminescent spectroscopy of anion and cation excitons in oxide crystals. // XVIII Intern. Conf. on the Application of Synchrotron Radiation: SR - 2010, Novosibirsk, 19 - 22 July 2010: Theses - Novosibirsk: BINP SB RAS, 2010.
- [387] Burdakov A.V., Dimov G.I., Ivanov A.A., Kruglyakov E.P. Novosibirsk mirrors: past, present and future. // The 8th Intern. Conf. on Open Magnetic Systems for Plasma Confinement, Novosibirsk, Russia, 5 - 9 July 2010, Abstr., Novosibirsk: BINP SB RAS, 2010, P.12.
- [388] Almagri A.F., Anderson J.K., Chapman B.E., Deichuli P., Den Hartog D.J., Forest C.B., Fiksel G., Ivanov A.A., Liu D., Nornberg M.D., Sarff J.S., Stupishin N., Waksman J. Majority ion heating by neutral beam injection and confinement of fast ions in the Madison Symmetric Torus reversed field pinch. // The 8th Intern. Conf. on Open Magnetic Systems for Plasma Confinement, Novosibirsk, Russia, 5 - 9 July 2010, Abstr., Novosibirsk: BINP SB RAS, 2010, P.14.
- [389] Anikeev A.V., Bagryansky P.A., Beklemishev A.D., Donin A.S., Ivanov A.A., Kovalenko Yu.V., Korzhavina M.S., Kruglyakov E.P., Lizunov A.A., Lvovskiy A.V., Maximov V.V., Murakhtin S.V., Pinzhenin E.I., Prikhodko V.V., Pushkareva A.N., Savkin V.Ya., Solomakhin A.L., Zaytsev K.V. Confinement of hot ion plasma with  $\beta=0.6$  in the gas dynamic trap. // The 8th Intern. Conf. on Open Magnetic Systems for Plasma Confinement, 5 - 9 July 2010, Novosibirsk, Russia. - Abstr., Novosibirsk: BINP SB RAS, 2010, P.16.
- [390] Chirkov A.Yu., Ryzhkov S.V., Bagryansky P.A., Anikeev A.V. Plasma kinetics models for fusion systems based on the axially-symmetric mirror devices. // The 8th Intern. Conf. on Open Magnetic Systems for Plasma Confinement, 5 - 9 July 2010 Novosibirsk, Russia. - Abstr., Novosibirsk: BINP SB RAS, 2010, P.18.
- [391] Akhmetov T.D., Ivanov A.A., Prikhodko V.V. Possible further steps for upgrading the GDT device. // The 8th Intern. Conf. on Open Magnetic Systems for Plasma Confinement, Novosibirsk, Russia, 5 - 9 July 2010, Novosibirsk. - Abstracts, Novosibirsk: BINP SB RUS, 2010, P.19.
- [392] Kotelnikov I.A. Equilibrium of high-beta plasma with sloshing ions above the mirror instability threshold. // The 8th Intern. Conf. on Open Magnetic Systems for Plasma Confinement, Novosibirsk, Russia, 5 - 9 July 2010, Novosibirsk, Russia. - Abstracts, Novosibirsk: BINP, 2010, P.21.
- [393] Shoshin A.A., Arzhannikov A.V., Burdakov A.V., Chebotarev V.V., Garkusha I.E., Ivanov I.A., Kuklin K.N., Makarov M.A., Makhraj V.A., Marchenko A.K., Mekler K.I., Rovenskikh A.F., Polosatkin S.V., Postupaev V.V., Sinitsky S.L., Tereshin V.I. Plasma-surface interaction during ITER type I ELMs: comparison of simulation with QSPA Kh-50 and the GOL-3 facilities. // The 8th Intern. Conf. on Open Magnetic Systems for Plasma Confinement, 5 - 9 July 2010, Novosibirsk. - Abstracts, Novosibirsk: BINP SB RAS, 2010, P.25.
- [394] Anisyonkov A. ATLAS grid information system. // 13th ISTS SAC Seminar "New Perspectives of High Energy Physics", 1 - 5 Sept., 2010, Budker INP, Novosibirsk, Russia. - Book of Abstracts, Novosibirsk: 2010, P.7.
- [395] Blinov V. Liquid 1016-1019 system for high power neutron converter. // 13th ISTS SAC Seminar "New Perspectives of High Energy Physics", 1 - 5 Sept., 2010, Budker INP, Novosibirsk, Russia.- Book of Abstracts, Novosibirsk: 2010, P.11.
- [396] Berkaev D., Ostanin I., Kozak V., Cherepanov V., Repkov V., Bykov E. Beam measurement system of VEPP-2000 injection channels. // 13th ISTS SAC Seminar "New Perspectives of High Energy Physics", 1 - 5 Sept., 2010, Budker INP, Novosibirsk, Russia. - Book of Abstracts, Novosibirsk: 2010, P.10.
- [397] Bogomyagkov A.V. Interaction region of Super  $\tau$  factory. // 13th ISTS SAC Seminar "New Perspectives of High Energy Physics", 1 - 5 Sept., 2010, Budker INP, Novosibirsk, Russia. - Book

- of Abstracts, Novosibirsk: 2010, P.12.
- [398] Bryzgunov M.I., Bubley A.V., Vostrikov V.A., Panasyuk V.M., Parkhomchuk V.V., Reva V.B. Low energy proton storage ring with longitudinal magnetic field and electron cooling. // 13th ISTS SAC Seminar "New Perspectives of High Energy Physics", 1 - 5 Sept., 2010, Budker INP, Novosibirsk, Russia. - Book of Abstracts, Novosibirsk: 2010, P.13.
- [399] Epstein L.B. CMD-3 Liquid Xenon calorimeter's signals processing for timing measurements. // 13th ISTS SAC Seminar "New Perspectives of High Energy Physics", 1 - 5 Sept., 2010, Budker INP, Novosibirsk, Russia. - Book of Abstracts, Novosibirsk: 2010, P.15.
- [400] Getmanov Ya.V., Shevchenko O.A., Vinokurov N.A. Electron injection into a cyclic accelerator using laser wakefield acceleration. // 13th ISTS SAC Seminar "New Perspectives of High Energy Physics", 1 - 5 Sept., 2010, Budker INP, Novosibirsk, Russia. - Book of Abstracts, Novosibirsk: 2010, P.16.
- [401] Gramolin A.V. Proton form factors and two-photon exchange contribution to elastic electron-proton scattering. // 13th ISTS SAC Seminar "New Perspectives of High Energy Physics", 1 - 5 Sept., 2010, Budker INP, Novosibirsk, Russia. - Book of Abstracts, Novosibirsk: 2010, P.17.
- [402] Ignatov F. The hadronic cross-sections measurements at VEPP-2M and VEPP-2000 e<sup>+</sup>e<sup>-</sup> colliders. // 13th ISTS SAC Seminar "New Perspectives of High Energy Physics", 1 - 5 Sept., 2010, Budker INP, Novosibirsk, Russia. - Book of Abstracts, Novosibirsk: 2010, P.18.
- [403] Achasov M.N., Beloborodov K.I., Berdyugin A.V., Botov A.A., Golubev V.B., Dimova T.V., Druzhinin V.P., Kardapoltsev L.V., Kharlamov A.G., Kovrizhin D.P., Koop I.A., Korol A.A., Koshuba S.V., Obrazovsky A.E., Pakhtusova E.V., Serednyakov S.I., Silagadze Z.K., Skrinsky A.N., Tikhonov Yu.A., Shatunov Yu.M., Vasil'ev A.V. Study of the process  $e^+e^- \rightarrow \pi^+\pi^-\pi^0\pi^0$  at energies  $2E < 1$  GeV. // 13th ISTC SAC Seminar "New Perspectives of High Energy Physics", 1 - 5 Sept., 2010, Budker INP, Novosibirsk, Russia. - Book of Abstracts, Novosibirsk: 2010, P.20.
- [404] Obrazovskii A.E. Experimental study of higher order QED processes. // 13th ISTC SAC Seminar "New Perspectives of High Energy Physics", 1 - 5 Sept., 2010, Budker INP, Novosibirsk, Russia. - Book of Abstracts, Novosibirsk: 2010, P.26.
- [405] Okunev I. Superconducting final focus system for Super C-Tau Factory. // 13th ISTC SAC Seminar "New Perspectives of High Energy Physics", 1 - 5 Sept., 2010, Budker INP, Novosibirsk, Russia. - Book of Abstracts, Novosibirsk: 2010, P.27.
- [406] Petrozhitsky A.V. Time-of-flight detector for new accelerator mass spectrometer. // 13th ISTC SAC Seminar "New Perspectives of High Energy Physics", 1 - 5 Sept., 2010, Budker INP, Novosibirsk, Russia. - Book of Abstracts, Novosibirsk: 2010, P.28.
- [407] Piminov P. Super Tau Charm Factory Project. // 13th ISTC SAC Seminar "New Perspectives of High Energy Physics", 1 - 5 Sept., 2010, Budker INP, Novosibirsk, Russia. - Book of Abstr., Novosibirsk: 2010, P.29.
- [408] Khriplovich I.B., Rudenko A.S. Can CP-violation be observed in heavy-ion collisions? // 13th ISTC SAC Seminar "New Perspectives of High Energy Physics", 1 - 5 Sept., 2010, Budker INP, Novosibirsk, Russia. - Book of Abstr., Novosibirsk: 2010, P.30; [E-print: ArXiv:1003.3339 [hep-ex]].
- [409] Shebalin V. Upgrade of the electromagnetic calorimeter for the Belle II experiment. // 13th ISTC SAC Seminar "New Perspectives of High Energy Physics", 1 - 5 Sept., 2010, Budker INP, Novosibirsk, Russia. Book of Abstr., Novosibirsk: 2010, P.32.
- [410] Skovpen K. ATLAS sensitivity to left-right symmetry at 7 TeV. // 13th ISTC SAC Seminar "New Perspectives of High Energy Physics", 1 - 5 Sept., 2010, Budker INP, Novosibirsk, Russia. - Book of Abstr., Novosibirsk: 2010, P.33.
- [411] Sinyatkin S. Low emittance lattice for the CLIC damping ring. // 13th ISTC SAC Seminar "New Perspectives of High Energy Physics", 1 - 5 Sept., 2010, Budker INP, Novosibirsk, Russia. - Book of Abstr., Novosibirsk: 2010, P.35.
- [412] Tikhonov Yu. High energy physics in Budker INP. // 13th ISTC SAC Seminar "New Perspectives of High Energy Physics", 1 - 5 Sept., 2010, Budker INP, Novosibirsk, Russia. - Book of Abstr.,

- Novosibirsk: 2010, P.37.
- [413] Bogdanchikov A., Korol A., Zaytsev A. System administration of ATLAS TDAQ computing environment. // 13th ISTC SAC Seminar "New Perspectives of High Energy Physics", 1 - 5 Sept., 2010, Budker INP, Novosibirsk, Russia. - Book of Abstr., Novosibirsk: 2010, P.38.
- [414] Aulchenko V., Bondar A., Kuzmin A., Shebalin V., Shwartz B., Usov Yu., Zhulanov V. New electron for Belle II electromagnetic calorimeter. // 13th ISTC SAC Seminar "New Perspectives of High Energy Physics", 1 - 5 Sept., 2010, Budker INP, Novosibirsk, Russia. - Book of Abstr., Novosibirsk: 2010, P.39.
- [415] Kozyrev A.N. New DAQ CMD-3 detector. // 13th ISTC SAC Seminar "New Perspectives of High Energy Physics", 1 - 5 Sept., 2010, Budker INP, Novosibirsk, Russia. - Book of Abstr., Novosibirsk: 2010, P.40.
- [416] Kononov S. Development of the Focusing Aerogel RICH detectors. // 13th ISTC SAC Seminar "New Perspectives of High Energy Physics", 1 - 5 Sept., 2010, Budker INP, Novosibirsk, Russia. - Book of Abstr., Novosibirsk: 2010, P.41.
- [417] Burdakov A.V., Arzhannikov V., Astrelin V.T., Beklemishev A.D., Ivanov A.A., Ivantsivsky M.V., Kandaurov I.V., Kotelnikov I.A., Kruglyakov E.P., Polosatkin S.V., Postupaev V.V., Sinitsky S.L., Timofeev I.V., Zhukov V.P. Concept of fusion reactor based on multi-mirror trap. // The 8th Intern. Conf. on Open Magnetic Systems for Plasma Confinement, Novosibirsk, Russia, 5 - 9 July 2010. - Abstr., Novosibirsk: BINP SB RAS, 2010, P.28.
- [418] Kandaurov I., Astrelin V., Avrorov A., Burdakov A., Bykov P., Derevyankin G., Kapitonov V., Kurkuchekov V., Rovenskikh A., Sinitsky S., Trunev Yu., Yarovoy V. Submillisecond electron beam for plasma heating in multi-mirror trap GOL-3. // The 8th Intern. Conf. on Open Magnetic Systems for Plasma Confinement, Novosibirsk, Russia, 5 - 9 July 2010. - Abstr., Novosibirsk: BINP SB RAS, 2010, P.29.
- [419] Timofeev I.V., Terekhov A.V. Simulations of turbulent plasma heating by powerfull electron beams. // The 8th Intern. Conf. on Open Magnetic Systems for Plasma Confinement, Novosibirsk, Russia, 5 - 9 July 2010. - Abstr., Novosibirsk: BINP SB RAS, 2010, P.30.
- [420] Arzhannikov A.V., Burdakov A.V., Kuznetsov S.A., Makarov M.A., Mekler K.I., Polosatkin S.V., Postupaev V.V., Rovenskikh A.F., Sinitsky S.L., Sklyarov V.F., Sulyaev Yu.S., Vyacheslavov L.N. Subterahertz emission at strong REB-plasma interaction in multimirror trap GOL-3. // The 8th Intern. Conf. on Open Magnetic Systems for Plasma Confinement, Novosibirsk, Russia, 5 - 9 July 2010: Abstr., - Novosibirsk: BINP SB RAS, 2010, P.31.
- [421] Beklemishev A.D. Tail-waving system for active feedback stabilization of flute modes in open traps. // The 8th Intern. Conf. on Open Magnetic Systems for Plasma Confinement, Novosibirsk, Russia, 5 - 9 July 2010. - Abstr., Novosibirsk: BINP SB RAS, 2010, P.34.
- [422] Bagryansky P.A., Beklemishev A.D., Zaytsev K.V., Kotelnikov I.A., Maximov V.V., Prikhodko V.V., Pushkareva A.N., Soldatkina E.I. Low-frequency oscillations of plasma in the Gas Dynamic Trap. // The 8th Intern. Conf. on Open Magnetic Systems for Plasma Confinement, Novosibirsk, Russia, 5 - 9 July 2010, Novosibirsk. - Abstr., Novosibirsk: BINP SB RAS, 2010, P.35.
- [423] Anikeev A.V., Bagryansky P.A., Chernoshtanov I.S., Korzhavina M.S., Prikhodko V.V., Tsidulko Yu.A. Study of microinstabilities in anisotropic plasmoid of thermonuclear ions. // The 8th Intern. Conf. on Open Magnetic Systems for Plasma Confinement, Novosibirsk, Russia, 5 - 9 July 2010. - Abstr., Novosibirsk: BINP SB RAS, 2010, P.37.
- [424] Sidorov A.V., Bagryansky P.A., Beklemishev A.D., Izotov I.V., Prikhodko V.V., Razin S.V., Skalyga V.A., Zorin V.G. Non-equilibrium heavy gases plasma MHD-stabilization in axisymmetric mirror magnetic trap. // The 8th Intern. Conf. on Open Magnetic Systems for Plasma Confinement, Novosibirsk, Russia, 5 - 9 July 2010. - Abstr., Novosibirsk: BINP SB RAS, 2010, P.39.
- [425] Bagryansky P.A., Biel W., Dreier H., Ivanenko S.V., Khilchenko A.D., Kovalenko Yu.V., Kvashnin A.N., Lambertz H.T., Lizunov A.A., Lvovskiy A.V., Savkin V.Ya., Solomakhin A.L. Measurement of plasma density in modern fusion devices by dispersion interferometer. // The 8th Intern. Conf. on Open Magnetic Systems for Plasma Confinement, Novosibirsk, Russia, 5 - 9 July 2010. - Abstr.,

- Novosibirsk: BINP SB RAS, 2010, P.494.
- [426] Chernoshanov I.S., Tsidulko Yu.A. Alfvén ion-cyclotron instability in mirror trap with high-anisotropic plasma. // The 8th Intern. Conf. on Open Magnetic Systems for Plasma Confinement, Novosibirsk, Russia, 5 - 9 July 2010. - Abstr., Novosibirsk: BINP SB RAS, 2010, P.40.
- [427] Ivanov A.A., Davydenko V.I., Deichuli P.P., Belov V.P., Gorbovsky A.I., Mishagin V.V., Shikhovtsev I.V., Sorokin A.V., Stupishin N.V., Shulzhenko G.I., Fiksel G., Schweer B. Development of focused neutral beams with small angular divergence for plasma heating and diagnostics. // The 8th Intern. Conf. on Open Magnetic Systems for Plasma Confinement, Novosibirsk, Russia, 5 - 9 July 2010. - Abstr., Novosibirsk: BINP SB RAS, 2010, P.43.
- [428] Postupaev V.V., Arzhannikov A.V., Astrelin V.T., Batkin V.I., Burdakov A.V., Burmasov V.S., Ivanov I.A., Ivantsivsky M.V., Kuklin K.N., Kuznetsov S.A., Makarov M.A., Mekler K.I., Polosatkin S.V., Popov S.S., Rovenskikh A.F., Shoshin A.A., Sinitsky S.L., Sklyarov V.F., Sorokina N.V., Sudnikov A.V., Sulyaev Yu.S., Vyacheslavov L.N. Experiments with "Thin" electron beam at GOL-3. // The 8th Intern. Conf. on Open Magnetic Systems for Plasma Confinement, Novosibirsk, Russia, 5 - 9 July 2010. - Abstr., Novosibirsk: BINP SB RAS, 2010, P.49.
- [429] Anikeev A.V., Dagan R., Fischer U. Numerical model of the fusion-fission hybrid system based on Gas Dynamic Trap for transmutation of radioactive wastes. // The 8th Intern. Conf. on Open Magnetic Systems for Plasma Confinement, Novosibirsk, Russia, 5 - 9 July 2010. - Abstr., Novosibirsk: BINP SB RAS, 2010, P.54.
- [430] Driscoll C.F., Kabantsev A.A., Dubin D.H.E., Tsidulko Y.A. Overview of transport, damping, and wave-couplings from separatrix dissipation in an axisymmetric plasma. // The 8th Intern. Conf. on Open Magnetic Systems for Plasma Confinement, Novosibirsk, Russia, 5 - 9 July 2010. - Abstr., Novosibirsk: BINP SB RAS, 2010, P.56.
- [431] Beklemishev A.D. Three-dimensional force-free equilibria in open traps driven by electron beams. // The 8th Intern. Conf. on Open Magnetic Systems for Plasma Confinement, Novosibirsk, Russia, 5 - 9 July 2010. - Abstr., Novosibirsk: BINP SB RAS, 2010, P.60.
- [432] Sudnikov A.V., Burdakov A.V., Ivanov I.A., Makarov M.A., Mekler K.I., Polosatkin S.V., Postupaev V.V., Rovenskikh A.F., Sinitsky S.L. MHD activity in GOL-3 at the stage of plasma cooling. // The 8th Intern. Conf. on Open Magnetic Systems for Plasma Confinement, Novosibirsk, Russia, 5 - 9 July 2010. - Abstr., Novosibirsk: BINP SB RAS, 2010, P.61.
- [433] Ivanov I.A., Burdakov A.V., Ivanenko V.G., Makarov M.A., Mekler K.I., Polosatkin S.V., Postupaev V.V., Rovenskikh A.F., Sudnikov A.V., Sinitsky S.L., Shoshin A.A., Shchudlo I.M. Stabilization of relativistic electron beam by dense plasma cloud in GOL-3 expander. // The 8th Intern. Conf. on Open Magnetic Systems for Plasma Confinement, Novosibirsk, Russia, 5 - 9 July 2010. - Abstr., Novosibirsk: BINP SB RAS, 2010, P.64.
- [434] Skovorodin D.I., Beklemishev A.D. Numerical kinetic model of axial confinement in a mirror trap. // The 8th Intern. Conf. on Open Magnetic Systems for Plasma Confinement, Novosibirsk, Russia, 5 - 9 July 2010. - Abstr., Novosibirsk: BINP SB RAS, 2010, P.66.
- [435] Dimov G.I. Feasible scenario of creation and burning of fusion plasma in ambipolar D-T reactor. // The 8th Intern. Conf. on Open Magnetic Systems for Plasma Confinement, Novosibirsk, Russia, 5 - 9 July 2010. - Abstr., Novosibirsk: BINP SB RAS, 2010, P.70.
- [436] Dimov G.I., Emelev I.S., Vobly P.D., Kobets V.V., Tiunov M.A. Multicusp trap with circular geometry for confinement of low-temperature plasma. // The 8th Intern. Conf. on Open Magnetic Systems for Plasma Confinement, Novosibirsk, Russia, 5 - 9 July 2010. - Abstr., Novosibirsk: BINP SB RAS, 2010, P.71.
- [437] Volosov V. Problems of the ACT reactor (the P11B reaction). // The 8th Intern. Conf. on Open Magnetic Systems for Plasma Confinement, Novosibirsk, Russia, 5 - 9 July 2010. - Abstr., Novosibirsk: BINP SB RAS, 2010, P.72.
- [438] Anikeev A.V., Bagryansky P.A., Fischer U., Noack K., Tsidulko Yu.A. The GDT based neutron source as a driver in a sub-critical burner of radioactive wastes. // The 8th Intern. Conf. on Open Magnetic Systems for Plasma Confinement, Novosibirsk, Russia, 5 - 9 July 2010. - Abstr.,

- Novosibirsk: BINP SB RAS, 2010, P.74.
- [439] Bagryansky P.A., Maximov V.V., Pinzhenin E.I., Prikhodko V.V. DD product yield in the GDT central cell. // The 8th Intern. Conf. on Open Magnetic Systems for Plasma Confinement, Novosibirsk, Russia, 5 - 9 July 2010. - Abstr., Novosibirsk: BINP SB RAS, 2010, P.86.
- [440] Polosatkin S., Belykh V., Davydenko V., Fiksel G., Ivanov A., Kapitonov V., Khilchenko A., Khilchenko V., Mishagin V., Tiunov M. Advanced neutral particle analyzer for fusion plasma diagnostics. // The 8th Intern. Conf. on Open Magnetic Systems for Plasma Confinement, Novosibirsk, Russia, 5 - 9 July 2010. - Abstr., Novosibirsk: BINP SB RAS, 2010, P.87.
- [441] Arakcheev A.S., Lotov K.V. Formation of small dust particles by brittle destruction. // The 8th Intern. Conf. on Open Magnetic Systems for Plasma Confinement, Novosibirsk, Russia, 5 - 9 July 2010. - Abstr., Novosibirsk: BINP SB RAS, 2010, P.89.
- [442] Batkin V.I., Bobylev V.B., Burdakov A.V., Davydenko V.I., Ivanov A.A., Kapitonov V.A., Mekler K.I., Polosatkin S.V., Postupaev V.V., Rovenskikh A.F., Sorokina N.V., Sulyaev Yu.S., Trunev Yu.A. Development of new neutral beam injection system on GOL-3 facility. // The 8th Intern. Conf. on Open Magnetic Systems for Plasma Confinement, Novosibirsk, Russia, 5 - 9 July 2010. - Abstr., Novosibirsk: BINP SB RAS, 2010, P.88.
- [443] Listopad A.A., Davydenko V.I., Ivanov A.A., Schweer B. Characterization of RUDI neutral beam parameters by optical diagnostics. // The 8th Intern. Conf. on Open Magnetic Systems for Plasma Confinement, Novosibirsk, Russia, 5 - 9 July 2010. - Abstr., Novosibirsk: BINP SB RAS, 2010, P.92.
- [444] Shoshin A.A., Arzhannikov A.V., Burdakov A.V., Kuklin K.N., Ivanov I.A., Mekler K.I., Polosatkin S.V., Postupaev V.V., Raspopin K.S., Rovenskikh A.F., Simonov P.A., Sinitsky S.L., Snytnikov V.N. Structure modification of different graphite and glassy carbon surfaces under high power action by hydrogen plasma. // The 8th Intern. Conf. on Open Magnetic Systems for Plasma Confinement, Novosibirsk, Russia, 5 - 9 July 2010. - Abstr., Novosibirsk: BINP SB RAS, 2010, P.90.
- [445] Smirnov A., Krivenko A.S., Murakhtin S.V., Savkin V.Ya., Korepanov S.A., Putvinski S. Neutral beam dump with cathodic arc titanium gettering. // The 8th Intern. Conf. on Open Magnetic Systems for Plasma Confinement, Novosibirsk, Russia, 5 - 9 July 2010. - Abstr., Novosibirsk: BINP SB RAS, 2010, P.91.
- [446] Abdrashitov G.F., Abdrashitov A.G., Deichuli P.P., Donin A.S., Khilchenko A.D., Lizunov A.A., Moiseev D.V., Murakhtin S.V., Sorokin A.V., Zubarev P.V. Neutron beam systems of the Gas Dynamic Trap. // The 8th Intern. Conf. on Open Magnetic Systems for Plasma Confinement, Novosibirsk, Russia, 5 - 9 July 2010. - Abstr., Novosibirsk: BINP SB RAS, 2010, P.94.
- [447] Averbukh I.I., Belov V.P., Davydenko V.I., Deichuli P.P., Ivanov A.A., Kapitonov V.A., Podyminogin A.A., Sorokin A.A., Shikhovtsev I.V. A continuously operated 70mA, 50keV proton source for plasma diagnostic and other applications. // The 8th Intern. Conf. on Open Magnetic Systems for Plasma Confinement, Novosibirsk, Russia, 5 - 9 July 2010. - Abstr., Novosibirsk: BINP SB RAS, 2010, P.95.
- [448] Sorokina N., Burdakov A., Makarov M., Mekler K., Polosatkin S.V., Postupaev V., Rovenskikh A., Sinitsky S., Stepanov V. Study of plasma on the GOL-3 facility by imaging VUV spectroscopy. // The 8th Intern. Conf. on Open Magnetic Systems for Plasma Confinement, Novosibirsk, Russia, 5 - 9 July 2010. - Abstr., Novosibirsk: BINP SB RAS, 2010, P.96.
- [449] Popov S.S., Vyacheslavov L.N., Ivantsivskiy M.V., Burdakov A.V., Kasatov A.A., and the GOL-3 team. Upgrading of Thomson Scattering system for measurements of spatial dynamics of plasma heating in GOL-3. // The 8th Intern. Conf. on Open Magnetic Systems for Plasma Confinement, Novosibirsk, Russia, 5 - 9 July 2010. - Abstr., Novosibirsk: BINP SB RAS, 2010, P.98.
- [450] Lvovskiy A.V., Solomakhin A.L. Line plasma density measurement in the Gas Dynamic Trap with dispersion interferometer. // The 8th Intern. Conf. on Open Magnetic Systems for Plasma Confinement, Novosibirsk, Russia, 5 - 9 July 2010. - Abstr., Novosibirsk: BINP SB RAS, 2010, P.100.
- [451] Burmasov V.S., Bobylev V.B., Ivanova A.A., Ivanenko S.V., Kasatov A.A., Kasatov D.A., Kuklin

- K.N., Popov S.S., Puryga E.A., Rovenskikh A.F., Sklyarov V.F. CO<sub>2</sub> interferometer for GOL-3 multimirror trap. // The 8th Intern. Conf. on Open Magnetic Systems for Plasma Confinement, Novosibirsk, Russia, 5 - 9 July 2010, Novosibirsk. - Abstracts, Novosibirsk: BINP SB RUS, 2010, P.101.
- [452] Arzhannikov A.V., Makarov M.A., Sinitsky S.L., Stepanov V.D. Energy spectrum of electrons in flow from plasma column heated by REB at GOL-3 facility. // The 8th Intern. Conf. on Open Magnetic Systems for Plasma Confinement, Novosibirsk, Russia, 5 - 9 July 2010. - Abstr., Novosibirsk: BINP SB RAS, 2010, P.103.
- [453] Timofeev I.V., Terekhov A.V., Lotov K.V. Direct computation of the growth rate for the instability of a warm relativistic electron beam in a magnetized plasma. // The 8th Intern. Conf. on Open Magnetic Systems for Plasma Confinement, Novosibirsk, Russia, 5 - 9 July 2010. - Abstr., Novosibirsk: BINP SB RAS, 2010, P.105.
- [454] Astrelin V., Burdakov A., Kandaurov I., Postupaev V., Sinitsky S., Timofeev I. Physical basis for the use of long pulse electron beam in multi-mirror trap. // The 8th Intern. Conf. on Open Magnetic Systems for Plasma Confinement, Novosibirsk, Russia, 5 - 9 July 2010. - Abstr., Novosibirsk: BINP SB RAS, 2010, P.106.
- [455] Ivanov A.A. Perspectives of development of magnetic mirror traps in Novosibirsk. // The 8th Intern. Conf. on Open Magnetic Systems for Plasma Confinement, Novosibirsk, Russia, 5 - 9 July 2010. - Abstr., Novosibirsk: BINP SB RAS, 2010, P.110.
- [456] Astrelin V., Burdakov A., Vshivkov V., Vshivkov K., Medvedev S., Shvabl., Yakunkin N. Numerical modeling of plasma dynamic in non-uniform magnetic field. // The 8th Intern. Conf. on Open Magnetic Systems for Plasma Confinement, Novosibirsk, Russia, 5 - 9 July 2010. - Abstr., Novosibirsk: BINP SB RAS, 2010, P.108.
- [457] Vinokurov N.A., Knyazev B.A., Dementyev E., Dovzhenko B.A., Gerasimov V.V., Getmanov Ya.V., Kolobanov E.I., Kubarev V.V., Kulipanov G.N., Medvedev L.E., Miginsky S.V., Mironenko L.A., Ovchar V.K., Persov B.Z., Popik V.M., Salikova T.V., Scheglov M.A., Serebnyakov S.S., Shevchenko O.A., Skrinsky A.N., Tcheskidov V.G., Tokarev Yu.F., Vlasenko M.G., Vobly P.D., Zaigraeva N.S. Novosibirsk free electron laser: instrumentation development and experimental achievements. // Intern. Symp. "Terahertz Radiation: Generation and Application", July 26 - 28, 2010, Novosibirsk, Russia. - Digest Rep., Novosibirsk: BINP SB RAS, 2010, P.11.
- [458] Aliev V.Sh., Dem'yanenko M.A., Esaev D.G., Ovsyuk V.N., Fomin B.I., Knyazev B.A., Gerasimov V.V., Kulipanov G.N., Vinokurov N.A. Design and application of uncooled microbolometer array for terahertz spectral range. // Intern. Symp. "Terahertz Radiation: Generation and Application", July 26 - 28, 2010, Novosibirsk, Russia. - Digest Rep., Novosibirsk: BINP SB RAS, 2010, P.26.
- [459] Kubarev V.V. Drummond light of calcium oxide. // Intern. Symp. "Terahertz Radiation: Generation and Application", July 26 - 28, 2010, Novosibirsk, Russia. - Digest Rep., Novosibirsk: BINP SB RAS, 2010, P.31.
- [460] Vlasenko M.G., Cherkassky V.S., Choporova Yu.Yu., Gerasimov V.V., Knyazev B.A., Krutko V.V., Polschitsin A.A., Malykh N.Yu., Nikitin A.A. Talbot effect in visible and terahertz ranges: examination and application. // Intern. Symp. "Terahertz Radiation: Generation and Application", July 26 - 28, 2010, Novosibirsk, Russia. - Digest Rep., Novosibirsk: BINP SB RAS, 2010, P.38.
- [461] Pickalov V.V., Balandin A.L., Rodionov D.G., Vlasenko M.G., Knyazev B.A. Terahertz tomography: algorithms and experimental setup. // Intern. symp. "Terahertz Radiation: Generation and Application", July 26 - 28, 2010, Novosibirsk, Russia. - Digest Rep., Novosibirsk: BINP SB RAS, 2010, P.40.
- [462] Arzhannikov A.V., Burdakov A.V., Kalinin P.V., Kuznetsov S.A., Makarov M.A., Mekler K.I., Polosatkin S.V., Postupaev V.V., Rovenskikh A.F., Sinitsky S.L., Sklyarov V.F., Stepanov V.D., Sulyaev Yu.S., Vyacheslavov L.N. Subterahertz generation by strong Langmuir turbulence at two-stream instability of high current 1-MeV REBs. // Intern. Symp. "Terahertz Radiation: Generation and Application", July 26 - 28, 2010, Novosibirsk, Russia. - Digest Rep., Novosibirsk: BINP SB RAS, 2010, P.42.

- [463] Kotelnikov I.A. Multiphoton ionization by a two-color laser pulse. // Intern. Symp. "Terahertz Radiation: Generation and Application", July 26 - 28; Joined with Scientific School-Workshop, 29 July - 1 August, 2010, Novosibirsk, Russia. - Digest Rep., Novosibirsk: BINP SB RAS, 2010, P.56.
- [464] Peltek S.E., Mesheryakova I.A., Goryachkovskaya T.N., Demidova E.V., Demidov E.A., Khlebodarova T.M., Oschepkov D.Yu., Kolchanov N.A., Popik V.M., Scheglov M.A., Vinokurov N.A., Kulipanov G.N., Nikolaev E.N. E.coli proteom expression under terahertz irradiation. // Intern. Symp. "Terahertz Radiation: Generation and Application", July 26 - 28, 2010, Novosibirsk, Russia. - Digest Rep., Novosibirsk: BINP SB RAS, 2010, P.5.
- [465] Kuznetsov S.A., Arzhannikov A.V., Kubarev V.V., Paulish A.G., Gelfand A.V., Navarro-Cia M., Beruete M., Falcone F., Sorolla M., Goldenberg B.G. Microstructured quasioptical selective components for subterahertz and terahertz applications. // Intern. Symp. "Terahertz Radiation: Generation and Application", July 26 - 28, 2010, Novosibirsk, Russia. - Digest Rep., Novosibirsk: BINP SB RAS, 2010, P.63.
- [466] Klimov A.E., Kubarev V.V., Paschin N.S., Shumsky V.N. Photocurrent dynamics in PbSnTe: in films in the submillimeter spectral range. // Intern. Symp. "Terahertz Radiation: Generation and Application", July 26 - 28, 2010, Novosibirsk, Russia. - Digest Rep., Novosibirsk: BINP SB RAS, 2010, P.68.
- [467] Gerasimov V.V. Real-time imaging ATR spectrometer with tunable terahertz free electron laser as a radiation source. // Intern. Symp. "Terahertz Radiation: Generation and Application", July 26 - 28, 2010, Novosibirsk, Russia. - Digest Rep., Novosibirsk: BINP SB RAS, 2010, P.70.
- [468] Vedernikov V.M., Dutov P.M., Kokarev A.I., Knyazev B.A., Palchikova I.G., Stupak M.F., Chugui Yu.V., Gerasimov V.V. Transparent power diffractive lenses for FEL radiation. // Intern. Symp. "Terahertz Radiation: Generation and Application", July 26 - 28, 2010, Novosibirsk, Russia. - Digest Rep., Novosibirsk: BINP SB RAS, 2010, P.71.
- [469] Miginsky S.V. Compact submillimeter FEL project. // Intern. Symp. "Terahertz Radiation: Generation and Application", July 26 - 28, 2010, Novosibirsk, Russia. - Digest Rep., Novosibirsk: BINP SB RAS, 2010, P.72.
- [470] Assovskiy I.G., Berlin A.A., Gerasimov V.V., Obraztsova E.A. On terahertz non-destructive detection of energetic materials. // Intern. Symp. "Terahertz Radiation: Generation and Application", July 26 - 28, 2010, Novosibirsk, Russia. - Digest Rep., Novosibirsk: BINP SB RAS, 2010, P.74.
- [471] Verkhogliad A.G., Zavyalova M.A., Knyazev B.A., Makarov S.N., Stupak M.F. Development of confocal 3D surface sensor based on the diffraction - chromatic coding method for the purpose of spectroscopic measurements. // Intern. Symp. "Terahertz Radiation: Generation and Application", July 26 - 28, 2010, Novosibirsk, Russia. - Digest Rep., Novosibirsk: BINP SB RAS, 2010, P.75.
- [472] Choporova Yu.Yu., Cherkassky V.S., Gerasimov V.V., Knyazev B.A., Nikitin A.A., Vlasenko M.G. Approaching terahertz holography using the free electron laser. // Intern. Symp. "Terahertz Radiation: Generation and Application", July 26 - 28, 2010, Novosibirsk, Russia. - Digest Rep., Novosibirsk: BINP SB RAS, 2010, P.77.
- [473] Gerasimov V.V., Knyazev B.A., Nikitin A.K. Terahertz dispersive spectroscopy for thin-film study via surface-plasmon - bulk wave interference. // Intern. Symp. "Terahertz Radiation: Generation and Application", July 26 - 28, 2010, Novosibirsk, Russia. - Digest Rep., Novosibirsk: BINP SB RAS, 2010, P.78.
- [474] Gerasimov V.V., Knyazev B.A., Nikitin A.K., Nikitin V.V. Noninterferometric techniques to determine terahertz surface-plasmon complex refractive index. // Intern. Symp. "Terahertz Radiation: Generation and Application", July 26 - 28, 2010, Novosibirsk, Russia. - Digest Rep., Novosibirsk: BINP SB RAS, 2010, P.79.
- [475] Kubarev V.V., Kulipanov G.N., Shevchenko O.A., Vinokurov N.A. Third harmonic lasing on terahertz NovoFEL [Electronic resource]. // 35th Intern. Conf. on Infrared, Millimeter, and Terahertz Waves (IRMMW-THz 2010), Rome, Italy, 5 - 10 Sept. 2010. - 3p.
- [476] Klimov A.E., Kubarev V.V., Shumsky V.N. Terahertz imaging using intermediate thermal screen [Electronic resource]. // 35th Intern. Conf. on Infrared, Millimeter, and Terahertz Waves (IRMMW-

- THz 2010), Rome, Italy, 5 - 10 Sept. 2010. - 1p.
- [477] Knyazev B.A., Cherkassky V.S., Choropova Yu.Yu., Gerasimov V.V., Vlasenko M.G. The Talbot effect in the terahertz spectral range [Electronic resource. // 35th Intern. Conf. on Infrared, Millimeter, and Terahertz Waves (IRMMW-THz 2010), Rome, Italy, 5 - 10 Sept. 2010. - 2p.
- [478] Knyazev B.A., Balandin A.L., Cherkassky V.S., Choropova Yu.Yu., Gerasimov V.V., Dem'yanenko M.A., Esaev D.G., Nikitin A.A., Pickalov V.V., Vlasenko M.G., Rodionov D.G., Shevchenko O.A. Classic holography, tomography and speckle metrology using a high-power terahertz free electron laser and real-time image detectors [Electronic resource]. // 35th Intern. Conf. on Infrared, Millimeter, and Terahertz Waves (IRMMW-THz 2010), Rome, Italy, 5 - 10 Sept. 2010. - 3p.
- [479] Bekhtenev E.A., Karpov G.V., Shubin E.I. The TNK beam position monitor system [Electronic resource]. // XXII Russian Particle Accelerator Conf. (RUPAC-2010), IHEP, Protvino, Sept. 27 - Okt. 1, 2010. - Protvino, IHEP, 2010, P.110-112.
- [480] Bekhtenev E.A., Karpov G.V. Wideband BPM electronics for the VEPP-4M collider [Electronic resource]. // RuPAC XXII: Russian Particle Accelerator Conf. (RUPAC-2010), IHEP, Protvino, Sept. 27 - Okt. 1, 2010. - Protvino: IHEP, 2010, P.245-247.
- [481] Golubenko Yu.I., Medvedko A.S., Nemitov P.I., Pureskin D.N., Senkov D.V. Power source for high-voltage column of injector to proton synchrotron with output power up to 5 kW [Electronic resource]. // XXII Russian Particle Accelerator Conf. (RUPAC-2010), IHEP, Protvino, Sept. 27 - Okt. 1, 2010. - Protvino: IHEP, 2010, P.360-362.
- [482] Rogovsky Yu., Nesterenko I.N. Calibration of the electrostatic beam position monitor for VEPP-2000 [Electronic resource]. // XXII Russian Particle Accelerator Conf. (RUPAC-2010), IHEP, Protvino, Sept. 27 - Okt. 1, 2010. - Protvino: IHEP, 2010, P.98-100.
- [483] Rogovsky Yu.A., Bekhtenev E.A. Pickup beam measurement system at the VEPP-2000 collider [Electronic resource]. // XXII Russian Particle Accelerator Conf. (RUPAC-2010), IHEP, Protvino, Sept. 27 - Okt. 1, 2010. - Protvino: IHEP, 2010, P.101-103.
- [484] Senkov D.V., Gusev I.A., Medvedko A.S., Protopopov A.Yu., Pureskin D.N. High-voltage source with output voltage up to 60 kV with output current up to 1A [Electronic resource]. // XXII Russian Particle Accelerator Conf. (RUPAC-2010), IHEP, Protvino, Sept. 27 - Okt. 1, 2010. - Protvino: IHEP, 2010, P.357-359.
- [485] Rastigeev S.A., Frolov A.R., Goncharov A.D., Klyuev V.F., Konstantinov S.G., Konstantinov E.S., Kutnykova L.A., Parkhomchuk V.V., Petrichenkov M.V., Petrozhitskii A.V. First radiocarbon measurements at BINP AMS [Electronic resource]. // XXII Russian Particle Accelerator Conf. (RUPAC-2010), IHEP, Protvino, Sept. 27 - Okt. 1, 2010. - Protvino: IHEP, 2010, P.309-312.
- [486] Semenov A.V., Cherepkov V.G., Kluev V.F., Konstantinov E.S., Kuper E.A., Mamkin V.R., Medvedko A.S., Nemytov P.I., Repkov V.V., Reva V.B., Salimov R.A., Senkov D.V., Vostrikov V.A. Status of HITS injector [Electronic resource]. // XXII Russian Particle Accelerator Conf. (RUPAC-2010), IHEP, Protvino, Sept. 27 - Okt. 1, 2010, Protvino. - IHEP, 2010, P.376-378.
- [487] Sukhanov D.P., Cherepanov V.P., Oreshonok V.V., Smaluk V.V. Transverse bunch-by-bunch digital feedback for the VEPP-4M collider [Electronic resource]. // XXII Russian Particle Accelerator Conf. (RUPAC-2010), IHEP, Protvino, Sept. 27 - Okt. 1, 2010. - Protvino: IHEP, 2010, P.236-238.
- [488] Ivanov A.V., Bryzgunov M.I., Bubley A.V., Panasyuk V.M., Parkhomchuk V.V., Reva V.B. Electron gun and collector for 2 MeV electron cooler for COSY [Electronic resource]. // XXII Russian Particle Accelerator Conf. (RUPAC-2010), IHEP, Protvino, Sept. 27 - Okt. 1, 2010. - Protvino: IHEP, 2010, P.233-235. WECHZ05.
- [489] Nikitin S. Accelerator aspects of the precision mass measurement experiments at the VEPP-4M collider with the KEDR detector [Electronic resource]. // XXII Russian Particle Accelerator Conf. (RUPAC-2010), IHEP, Protvino, Sept. 27 - Okt. 1, 2010. - Protvino: IHEP, 2010, P.11-13.
- [490] Belikov O., Kozak V., Medvedko A. A family of twenty-amperes power supplies for multipole correctors for accelerators and storage rings [Electronic resource]. // XXII Russian Particle Accelerator Conf. (RUPAC-2010), IHEP, Protvino, Sept. 27 - Okt. 1, 2010. - Protvino: IHEP, 2010, P.306-308.

- [491] Rogovsky Yu.A., Berkaev D.E., Kyrpotin A.N., Nesterenko I.N., Romanov A.L. Beam measurements with visible synchrotron light on VEPP-2000 collider [Electronic resource]. // XXII Russian Particle Accelerator Conf. (RUPAC-2010), IHEM Protvino, Sept. 27 - Okt. 1, 2010. - Protvino: IHEM, 2010, P.104-106.
- [492] Talanov V., Dzhelyadin R., Bobrov A., Bondar A., Alessio F., Corti G., Lieng M.H. A beam loss scintillator system for background monitoring at the LHCb experiment. // XXII Russian Particle Accelerator Conf. (RUPAC-2010), IHEM Protvino, Sept. 27 - Okt. 1, 2010. - Protvino: IHEM, 2010, P.286-288.
- [493] Kuksanov N.K., Golubenko Yu.I., Nemytov P.I., Salimov R.A., Fadeev S.N., Lavruhkin A.V., Korchagin A.I., Kogut D.S., Semenov A.M. High power ELV accelerators for industries application. // XXII Russian Particle Accelerator Conf. (RUPAC-2010), IHEM Protvino, Sept. 27 - Okt. 1, 2010. - Protvino: IHEM, 2010, P.313-315.
- [494] Bohme C., Dietrich J., Kamerdzhev V., Julich F.Z.J., Bryzgunov M., Reva V., Kobets A., Meshkov I., Rudakov A., Shurkhno N., Sidorin A. Results of electron cooling beam studies at COSY [Electronic resource]. // XXII Russian Particle Accelerator Conf. (RUPAC-2010), IHEP, Protvino, Sept. 27 - Okt. 1, 2010. - Protvino: IHEP, 2010, P.156-160. WECHZ04.
- [495] Shwartz D., Berkaev D., Kirpotin A., Koop I., Lysenko A., Nesterenko I., Perevedentsev E., Rogovsky Yu., Romanov A., Shatunov P., Shatunov Yu., Skrinsky A., Zemlyansky I. Present status of VEPP-2000 [Electronic resource]. // XXII: Russian Particle Accelerator Conf. (RUPAC-2010), IHEP, Protvino, Sept. 27 - Okt. 1, 2010. - Protvino: IHEP, 2010, P.1-5.
- [496] Vinokurov N.A., Demytyev E.N., Dovzhenko B.A., Galt A.A., Getmanov Ya.V., Knyazev B.A., Kolobanov E.I., Kubarev V.V., Kulipanov G.N., Medvedev L.E., Miginsky S.V., Mironenko L.A., Ovchar V.K., Persov B.Z., Popik V.M., Salikova T.V., Scheglov M.A., Serebnyakov S.S., Shevchenko O.A., Skrinsky A.N., Tcheskidov V.G., Vlasenko M.G., Vobly P.D., Zaigraeva N.S. Status and prospects of the Novosibirsk FEL facility [Electronic resource]. // XXII Russian Particle Accelerator Conf. (RUPAC-2010), IHEP, Protvino, Sept. 27 - Okt. 1, 2010. - Protvino: IHEP, 2010, P.133-135.
- [497] Dietrich J., Kamerdzhev V., Julich F.Z.J., Bryzgunov M.I., Goncharov A.D., Parkhomchuk V.V., Reva V.B., Skorobogatov D.N. Progress with the 2 MeV electron cooler for COSY-Julich/HESR [Electronic resource]. // XXII Russian Particle Accelerator Conf. (RUPAC-2010), IHEP, Protvino, Sept. 27 - Okt. 1, 2010, Protvino. - IHEP, 2010, P.147-150. WECHZ02.
- [498] Dietrich J., Kamerdzhev V., Julich F.Z.J., Bryzgunov M.I., Bocharov V.N., Bublely A.V., Cheskidov V.G., Goncharov A.D., Kryuchkov A.M., Panasyuk V.M., Parkhomchuk V.V., Polukhin V.A., Putmakov A.A., Reva V.B., Skorobogatov D.N. Development of electron cooler components for COSY [Electronic resource]. // XXII Russian Particle Accelerator Conf. (RUPAC-2010), IHEP, Protvino, Sept. 27 - Okt. 1, 2010. - Protvino: IHEP, 2010, P.151-155. WECHZ03.
- [499] Podobaev V.S., Bezuglov V.V., Bryazgin A.A., Chernov K.N., Cheskidov V.G., Factorovich B.L., Gorbunov V.A., Gornakov I.V., Ivanov A.V., Kokin E.N., Korobeynikov M.V., Lukin A.N., Makarov I.G., Matyash N.V., Maximov S.A., Ostreiko G.N., Panfilov A.D., Radchenko V.M., Romashko N.D., Serdobintsev G.V., Sidorov A.V., Tarnetsky V.V., Tiunov M.A., Tkachenko V.O. Status of ILU-14 electron accelerator [Electronic resource]. // XXII Russian Particle Accelerator Conf. (RUPAC-2010), IHEP, Protvino, Sept. 27 - Okt. 1, 2010. - Protvino: IHEP, 2010, P.411-413. [<https://oraweb.cern.ch/pls/rupac2010/jacow.html>].
- [500] Boettcher Ju., Zamriy V.N., Kayukov A.S., Kobets V.V., Meshkov I.N., Minashkin V.F., Pyataev V.G., Skripnik A.V., Sumbaev A.P., Shabratov V.G., Shvets V.A., Shvetsov V.N., Logachev P.V., Pavlov V.M. The electron linear accelerator LUE-200 - driver the IREN facility [Electronic resource]. // XXII Russian Particle Accelerator Conf. (RUPAC-2010), IHEP, Protvino, Sept. 27 - Okt. 1, 2010. - Protvino: IHEP, 2010, P.346-348.
- [501] Yang X., Li G., Li J., Ma X., Mao L., Mao R., Yan T., Yang J., Yuan Yo., Parkhomchuk V.V., Reva V.B. Electron cooling experiments in CSR [Electronic resource]. // XXII Russian Particle Accelerator Conf. (RUPAC-2010), IHEP, Protvino, Sept. 27 - Okt. 1, 2010. - Protvino: IHEP, 2010, P.161-165.

- [502] Eidelman S. Status of muon g-2. // All-Russia Meeting «Precision Physics and Fundamental Physical Constants», 7 - 10 December, 2010, St-Petersburg, Russia; Intern. Symposium «50 Years on the Road to Quantum Unit of SR», 6 December. 2010: Theses. - St-Petersburg, SPU, 2010. - P.15.
- [503] Achasov M.N., Astigeevich P.M., Aulchenko V.M., Barnyakov A.Yu., Beloborodov K.I., Berdyugin A.V., Blinov V.E., Bogdanchikov A.G., Botov A.A., Bukin D.A., Golubev V.B., Grevtsov K.A., Dimova T.V., Druzhinin V.P., Kardapoltsev L.V., Kharlamov A.G., Kovrizhin D.P., Korol A.A., Koshuba S.V., Kravchenko E.A., Martin K.A., Obrazovsky A.E., Onuchin A.P., Pakhtusova E.V., Serednyakov S.I., Silagadze Z.K., Skovpen K.Yu., Skrinsky A.N., Surin I.K., Tikhonov Yu.A., Usov Yu.V., Shatunov Yu.M., Shtol D.A., Shukaev A.N., Vasiljev A.V., Vlasenko E.A. Spherical Neutral Detector for experiments at VEPP-2000 e+e- collider. //III All-Russia Meeting: Precision Physics and Fundamental Physical Constants, 7 - 10 December, 2010, St-Petersburg: Intern. Symposium "50 Years on the Road to Quantum Unit of SR", 6 December, 2010: Theses. - St-Petersburg, SPU, 2010. - P.71.
- [504] Beruete M., Navarro-Cia M., Kuznetsov S.A., Falcone F., Aznabet M., Sorolla M. Polypropylene films for millimeter-to-terahertz waves metasurfaces [Electronic resource]. // 35th Intern. Conf. on Infrared, Millimeter, and Terahertz Waves (IRMMW - THz 2010), Rome, Italy, 5 - 10 Sept. 2010.
- [505] Arzhannikov A.V., Burdakov A.V., Kuznetsov S.A., Makarov M.A., Mekler K.I., Postupaev V.V., Rovenskikh A.F., Sinitzky S.L., Sklyarov V.F. Generation of submillimeter radiation by strong plasma turbulence at electron beam - plasma interaction [Electronic resource]. // 35th Intern. Conf. on Infrared, Millimeter, and Terahertz Waves (IRMMW-THz 2010), Rome, Italy, 5 - 10 Sept. 2010. - Paper Fr-E.1-4.
- [506] Kuznetsov S.A., Navarro-Cia M., Gelfand A.V., Fedorinina N.I., Arzhannikov A.V., Beruete M., Falcone F., Sorolla M. Ultra-thin Mm-wave absorbers based on high-impedance metasurfaces [Electronic resource]. // 35th Intern. Conf. on Infrared, Millimeter, and Terahertz Waves (IRMMW-THz 2010), Rome, Italy, 5 - 10 Sept. 2010, Paper We-P.93.
- [507] Paulish A., Fedorinin V.N., Gelfand A.V., Kuznetsov S.A., Paulish A.G. Matrix micro-golay cell IR imager [Electronic resource]. // 35th Intern. Conf. on Infrared, Millimeter, and Terahertz Waves (IRMMW-THz 2010), Rome, Italy, 5 - 10 Sept. 2010, Paper Mo-P.75
- [508] Valishev A., Kuznetsov G., Shiltsev V., Strancari G., Zhang X., Romanov A. Progress with tevatron electron lens head-on beam-beam compensation [Electronic resource]. // The 1st Intern. Particle Accelerator Conf. (IPAC'10), 23 - 28 May, 2010, Kyoto, Japan. - Kyoto Intern. Conf. Center, 2010, P.2084-2086.
- [509] Biagini M.E., Raimondi P., Piminov P., Sinyatkin S., Nosoehkov Y., Wittmer W. Super-B lattice studies [Electronic resource]. // The 1st Intern. Particle Accelerator Conf. (IPAC'10), 23 - 28 May, 2010, Kyoto, Japan. - Kyoto Intern. Conf. Center, 2010, P.1521-1523.
- [510] Getmanov YA.V., Shevchenko O.A., Vinokurov N.A. Electron injection into a cyclic accelerator using laser wakefield acceleration [Electronic resource]. // The 1st Intern. Particle Accelerator Conf. (IPAC'10), 23 - 28 May, 2010, Kyoto, Japan. - Kyoto Intern. Conf. Center, 2010, P.1503-1505.
- [511] Vinokurov N.A., Demytyev E.N., Dovzhenko B.A., Getmanov Ya.V., Knyazev B.A., Kolobanov E.I., Kubarev V.V., Kulipanov G.N., Medvedev L.E., Miginsky S.V., Mironenko L.A., Ovchar V.K., Palagin K.V., Persov B.Z., Popik V.M., Salikova T.V., Scheglov M.A., Serednyakov S.S., Shevchenko O.A., Skrinsky A.N., Tcheskidov V.G., Tokarev Yu.F., Vobly P.D., Zaignraeva N.S. Novosibirsk free electron laser facility: two-orbit ERL with two FELs [Electronic resource]. // The 1st Intern. Particle Accelerator Conf. (IPAC'10), 23 - 28 May, 2010, Kyoto, Japan. - Kyoto Intern. Conf. Center, 2010, P.2427-2429. [<http://accelconf.web.cern.ch/AccelConf/IPAC10/papers/weoara03.pdf>].
- [512] Cherepkov V.G., Kluev V.F., Konstantinov E.S., Kuper E.A., Mamkin V.R., Medvedko A.S., Nemytov P.I., Repkov V.V., Reva V.B., Salimov R.A., Semenov A.V., Senkov D.V., Vostrikov V.A. Ion injector based on tandem accelerator [Electronic resource]. // The 1st Intern. Particle Accelerator Conf. (IPAC'10), 23 - 28 May, 2010, Kyoto, Japan. - Kyoto Intern. Conf. Center, 2010, P.717 - 719.
- [513] Vogel V., Cherepenko A., Choroba S., Hartung J., Bak P., Korepanov A., Evmenova N. Connection

- module for the european X-RAY FEL 10 MW horizontal multibeam klystron [Electronic resource]. // The 1st Intern. Particle Accelerator Conf. (IPAC'10), 23 - 28 May, 2010, Kyoto, Japan. - Kyoto Intern. Conf. Center, 2010, P.3978 - 3980.
- [514] Romanov A.L., Berkaev D.E., Kirpotin A.N., Koop I.A., Perevedentsev E.A., Rogovsky Yu.A., Shatunov P.Yu., Shwartz D.B. Round beam lattice correction using response matrix at VEPP-2000 [Electronic resource]. // The 1st Intern. Particle Accelerator Conf. (IPAC'10), 23 - 28 May, 2010, Kyoto, Japan. - Kyoto Intern. Conf. Center, 2010, P.4542-4544.
- [515] Bondarenko A.V., Miginsky S.V., Vinokurov N.A. A novel extraction scheme from a synchrotron using a magnetic shield [Electronic resource]. // The 1st Intern. Particle Accelerator Conf. (IPAC'10), 23 - 28 May, 2010, Kyoto, Japan. - Kyoto Intern. Conf. Center, 2010, P.1656-1658.
- [516] Dietrich J., Kamerzhiev V., Bryzgunov M.I., Goncharov A.D., Parkhomchuk V.V., Reva V.B., Skorobogatov D.N. Status of the 2 MeV electron cooler for COSY Juelich [Electronic resource]. // The 1st Intern. Particle Accelerator Conf. (IPAC'10), 23 - 28 May, 2010, Kyoto, Japan. - Kyoto Intern. Conf. Center, 2010, P.843-845. MOPD067.
- [517] Simonov E., Levichev E., Shatilov D. Application of frequency map analysis to beam-beam effects study in crab waist collision scheme [Electronic resource]. // The 1st Intern. Particle Accelerator Conf. (IPAC'10), 23 - 28 May, 2010, Kyoto, Japan. - Kyoto Intern. Conf. Center, 2010, P.4692-4694.
- [518] Chernousov Yu., Ivannicov V., Shebolaev I., Levichev A., Pavlov V. Characteristics of the parallel coupled accelerating structure [Electronic resource]. // The 1st Intern. Particle Accelerator Conf. (IPAC'10), 23 - 28 May, 2010, Kyoto, Japan. - Kyoto Intern. Conf. Centre, 2010, P.3764-3767.
- [519] Romanov A.L., Valishev A.A., Shiltsev V. Simplified approach to evaluation of beam-beam tune spread compression by electron lens [Electronic resource]. // The 1st Intern. Particle Accelerator Conf. (IPAC'10), 23 - 28 May 2010, Kyoto, Japan. - Kyoto Intern. Conf. Centre, 2010, P.4545-4547.
- [520] Drago A., Raimondi P., Zobov M., Shatilov D. Synchrotron oscillation damping due to beam-beam collisions [Electronic resource]. // The 1st Intern. Particle Accelerator Conf. (IPAC'10), 23 - 28 May 2010, Kyoto, Japan. - Kyoto Intern. Conf. Centre, 2010, P.3644-3646.
- [521] Wienands U., Nosochkov Yu., Sullivan M.K., Wittmer W., Barber D.P., Biagini M.E., Raimondi P., Koop I., Nikitin S., Sinyatkin S. Polarization in Super B [Electronic resource]. // The 1st Intern. Particle Accelerator Conf. (IPAC'10), 23 - 28 May 2010, Kyoto, Japan. - Kyoto Intern. Conf. Centre, 2010, P.1587-1589.
- [522] Variale V., Valentino V., Batazova M., Kuznetsov G., Skarbo B., Clauser T., Cosimo Raino A. Charge breeding test experiment with a hollow gun EBIS [Electronic resource]. // The 1st Intern. Particle Accelerator Conf. (IPAC'10), 23 - 28 May 2010, Kyoto, Japan. - Kyoto Intern. Conf. Centre, 2010, P.4167-169.
- [523] Papaphilippou Y., Levichev E., Sinyatkin S., Vobly P., Zolotarev K., et al. Design optimisation of the CLIC damping rings [Electronic resource]. // The 1st Intern. Particle Accelerator Conf. (IPAC'10), 23 - 28 May, 2010, Kyoto, Japan. - Kyoto Intern. Conf. Centre, 2010, P.3554-3556.
- [524] Zolotarev K., Malyshev O.B., Korostelev M., Wolski A., Lucas J.M., Collomb N., Postlethwaite S. SR power distribution along wiggler section of ILS DR [Electronic resource]. // The 1st Intern. Particle Accelerator Conf. (IPAC'10), 23 - 28 May, 2010, Kyoto, Japan. - Kyoto Intern. Conf. Centre, 2010, P.3569-3571.
- [525] Malyshev O.B., Lucas J.M., Collomb N., Postlethwaite S., Korostelev M., Wolski A., Zolotarev K. Mechanical and vacuum design of the wiggler section of the ILC damping rings [Electronic resource]. // The 1st Intern. Particle Accelerator Conf. (IPAC'10), 23 - 28 May, 2010, Kyoto, Japan. - Kyoto Intern. Conf. Centre, 2010, P.3563-3565.
- [526] Xia G., Caldwell A., Lotov K., Pukhov A., Assmann R., Zimmermann F. A proposed experiment on the proton driven plasma wakefield acceleration [Electronic resource]. // The 1st Intern. Particle Accelerator Conf. (IPAC'10), 23 - 28 May, 2010, Kyoto, Japan. - Kyoto Intern. Conf. Centre, 2010, P.4392-4394.
- [527] Sullivan M.K., Bertsche K., Vobly P., Bettoni S., Raimondi P., Paoloni E. A new interaction region design for the Super B factory [Electronic resource]. // The 1st Intern. Particle Accelerator Conf.

- (IPAC'10), 23 - 28 May 2010, Kyoto, Japan. - Kyoto Intern. Conf. Centre, 2010, P.1581-1583.
- [528] Kulipanov G. High-power THz NovoFEL: applications. // THz-Bio Workshop, March 9-10, SNU, Seoul, Korea. - Abstr., Seoul Nat. Univ, 2010, P.29-30. P.28: (Brief Biographies and Research Interests).
- [529] Knyazev B.A., Choporova Yu.Yu., Gerasimov V.V., Vlasenko V.G. Terahertz imaging devices and classic optical experiments at Novosibirsk free electron laser. // The 17th Intern. Symp. on Laser Spectroscopy (SOLS 2010), Nov. 4 - 5, 2010, Daejeon, Korea. - Daejeon: KAERI, 2010, P.IV-3 (Abstract Book of Sols. - 2010. - Vol.17, N1).
- [530] Miginsky S.V. Compact submillimeter FEL project. // The 17th Intern. Symp. on Laser Spectroscopy: SOLS 2010, Nov. 4 - 5, 2010, Daejeon, Korea. - Daejeon: KAERI, 2010, P.IV-4 (Abstract Book of Sols., 2010, Vol.17, N1).
- [531] Fadin V.S. BFKL pomeron in QCD and in N=4 SUSY. // The 3rd Intern. Workshop "High Energy Physics in the LHC Era", January 4 - 8, 2010, Valparaiso, Chile.
- [532] Fadin V.S. Möbius form of the BFKL kernel and the colour dipole model. // XLIV PNPI Winter School, March 9-14, 2010, Roschino, Russia.
- [533] Fadin V.S., Fiore R., Grabovsky A.V. and Papa A. Quasi-conformal shape of the BFKL kernel and impact factors for scattering of colourless particles. // Intern. Conference "DIFFRACTION 2010", September 10-15, 2010, Otranto (Lecce), Italy.
- [534] Fadin V.S. Möbius representation of small-x evolution kernels at NLO. // Intern. Conference "Hadron Structure and QCD: from LOW to HIGH energies", July 5 - 9, 2010, Gatchina, Russia.
- [535] Katkov V.M. Exact theory of the photoproduction of charged particles in external fields. // Intern. Conference "Channaling 2010", Ferrara, Italy. - Book of abstracts, P.15.
- [536] Sokolov V.V. Classical Versus Quantum Dynamical Chaos: Sensitivity to External Perturbations, Stability and Reversibility. // Intern. Conference Chaos 2010 "Chaotic Modeling and Simulation", June 1-4, 2010, Chania, Crete, Greece. - Electronic Proceedings, 2010, P.82.
- [537] Bogomyagkov A. Tuning of the interaction region for tau-charm factory in Novosibirsk. // XIII SuperB General Meeting, 30 May - 5 June, 2010, Isola d'Elba.
- [538] Bogomyagkov A., Levichev E. On other possible solutions for the crab-waist transformation. // XIV SuperB General Meeting, 27 September - 1 October, 2010, LNF.
- [539] Koop A., Bogomyagkov A.V., Otboev A.V. Longitudinally polarized electrons in Novosibirsk C-tau Factory. // 19th Intern. Spin Physics Symposium (SPIN-2010), September 27 - October 2, 2010, Juelich, Germany.
- [540] Milardi C., Levichev E.B., Nikitin S.A., Piminov P.A., Shatilov D.N., et al. DAFNE developments for the KLOE-2 experimental run [Electronic resource]. // 1st Intern. Particle Accelerator Conf. (IPAC'10), 23 - 28 May, 2010, Kyoto, Japan. - Kyoto: Kyoto Intern. Conf. Center, 2010. - P.1527-1529; [E-print: arXiv:1006.1487. TUPEB006, IPAC'10].
- [541] Barkov L.M., Fix A.I., Gauzshteyn V.V., Loginov A.Yu., Nikolenko D.M., Mishnev S.I., Osipov A.V., Rachek I.A., Sidorov A.A., Stibunov V.N., Toporkov D.K., Shestakov Yu.V., Zevakov S.A. Study of the spin-dependent observables in p-meson photoproduction on the tensor deuteron. Nucleus 2010: Methods of Nuclear Physics for Femto- and Nanotechnologies. // LX Intern. Conference on Nuclear Physics, St.Petersburg, July 6-9, 2010. - Book of Abstracts: St. Petersburg State University, 2010, P.193 (51638776).
- [542] Rachek I.A., Barkov L.M., Dmitriev V.F., Karnakov I.V., Lazarenko B.A., Mishnev S.I., Nikolenko D.M., Osipov A.V., Sadukov R.Sh., Stibunov V.N., Shestakov Yu.V., Toporkov D.K., Zevakov S.A. Photoreactions with tensor-polarized deuterium target at VEPP-3. // 19th Intern. Spin Physics Symposium (SPIN-2010), Julich, Germany, September 27 - October 2, 2010. - Julich: Forschungszentrum Julich Institute for Nuclear Physics, 2010, P.152 (54592329).
- [543] Stibunov V.N., Barkov L.M., Gauzshteyn V.V., Dmitriev V.F., Loginov A.Yu., Mishnev S.I., Nikolenko D.M., Osipov A.V., Rachek I.A., Sidorov A.A., Shestakov Yu.V., Toporkov D.K., Fix A.I., Zevakov S.A. Study of tensor analysing component T21 for the pi-meson photoproduction on

- the deuteron. // 19th Intern. Spin Physics Symposium (SPIN-2010), Julich, Germany, September 27 - October 2, 2010. - Julich: Forschungszentrum Julich Institute for Nuclear Physics, 2010, P.222 (41247514).
- [544] Abakumova E., Achasov M., Hai Yi Dong, Hua Min Qu, Krasnov A., Kosarev A., Muchnoi N., Pyata E., Qiong Xiao, Xiao Hu Mo, Yi Fang Wang, Zhukov A. Vacuum chamber for the measurement system of the beam energy. // 18th Intern. Vacuum Congress, August 23-27, 2010, Beijing, China.
- [545] Anashin V.V., Krasnov A.A. Method for investigation of low energy electron interaction with metal surface in presence of magnetic field. // 18th Intern. Vacuum Congress, August 23-27, 2010, Beijing, China.
- [546] Ukrainev Yu.G., Suslin V.P.. Technology of scanning visualization - method of the radiation dose decrease in radiology. // Proc. of the IV All-Russian National Congress of Radiation Diagnosticians and Therapists «Radiology - 2010», 25-27 May, 2010, Moscow. - P.460-462 (in Russian)
- [547] Rudneva T.V., Rudnev S.V., Ukrainev Yu.G. Method X-ray pelvimetri in obstetrics. // Materials of the I Congress of Doctors of Beam Diagnostics RFD «Achievements, prospects and the basic directions of development of beam diagnostics in Siberia», 7-8 October, 2010, Novosibirsk. - P.178-181.
- [548] Suslin V.P., Otrowenko V.A., Chikov V.A., Ukrainev Ju.G. Effective doses of an irradiation of patients at carrying out of radiological researches on digital and film devices. // Materials of the I Congress of Doctors of Beam Diagnostics RFD «Achievements, prospects and the basic directions of development of beam diagnostics in Siberia», 7-8 October, 2010, Novosibirsk. - P.216-220.
- [549] Babichev E.A., Baru S.E., Grigoriev D.N., Groshev V.R., Leonov V.V., Papushev P.A., Porosev V.V., Savinov G.A., Shayakhmetov V.R., Shekhtman L.I., Tikhonov Yu.A., Ukraintsev Yu.G., Yurchenko Yu.B. High-resolution detectors for medical applications and synchrotron radiation research. // Proc. of 12th Vienna Conference on Instrumentation. Vienna, Austria. 15-20 February, 2010.
- [550] Baru S.E. Radiographic systems with extremely low doses of an irradiation// Materials of the I Congress of Doctors of Beam Diagnostics RFD «Achievements, Prospects and the Basic Directions of Development of Beam Diagnostics in Siberia», 7-8 October, 2010, Novosibirsk. - P.27-30.
- [551] Druzhinin V.P. Recent BABAR results on two-photon physics. // 35th Intern. Conference of High Energy Physics (ICHEP 2010), July 22-28, 2010, Paris, France. - [arXiv:1011.6159 [hep-ex]].
- [552] Buzulutskov A. Advances in GEM-based cryogenic avalanche detectors. // Plenary talk at 12th Vienna Conference on Instrumentation (VCI 2010), 15-20 February 2010, Austria.
- [553] Buzulutskov A. Cryogenic avalanche detectors development in Budker INP. // Invited talk at BINP-KEK Workshop on Noble Liquid TPC, Nov. 24-25, 2010, KEK, Japan.
- [554] Buzulutskov A.F. The development of cryogenic avalanche detectors at BINP SB RAS. // Presentation at the Workshop RED Collaboration, 23 December, 2010, MIPI, Moscow.
- [555] Bondar A.E. Hot topics of Belle - Recent results on X(3872). // 4th Intern. Workshop on Charm Physics, October, 2010, Beijing, China.
- [556] Eidelman S. Precise measurement of the tau lepton lifetime at Belle. // XI Intern. Workshop on Tau Lepton Physics, September, 2010, Manchester, UK.
- [557] Kuzmin A.S. Heavy quarkonium and -like states. // Deep-Inelastic Scattering Workshop, April, 2010, Florence, Italy.
- [558] Bondar A.E. Electroweak related rare decays. // Moriond Electroweak 2010, March, 2010, La Thuile, Italy.
- [559] Telnov V.I. A high luminosity Photon collider without damping rings. // Talk at the Intern. Linear Collider Workshop (LCWS10), March 26-30, 2010, Beijing, China. - <http://ilcagenda.linearcollider.org/conferenceOtherViews.py?view=standard&confId=4175>.
- [560] Telnov V.I. A low emittance e- source without damping ring. // Talk at the Intern. Linear Collider Workshop (LCWS10), March 26-30, 2010, Beijing, China. - <http://ilcagenda.linearcollider.org/conferenceOtherViews.py?view=standard&confId=4175>.

- [561] Telnov V.I. Consideration of a photon collider without damping rings. // Talk at Intern. Workshop on Linear Colliders (IWLC2010), ECFA-CLIC-ILC Joint Meeting: October 18-22, 2010, CERN, Switzerland. - <http://ilcagenda.linearcollider.org/getFile.py/access?contribId=357&sessionId=42&resId=1&materialId=slides&confId=4507>.
- [562] Telnov V.I. FEL pumped solid state laser system for the photon collider at CLIC. // The talk Intern. Workshop on Linear Colliders (IWLC2010), ECFA-CLIC-ILC Joint Meeting: October 18-22, 2010, CERN, Switzerland. - <http://ilcagenda.linearcollider.org/getFile.py/access?contribId=358&sessionId=42&resId=0&materialId=slides&confId=4507>.
- [563] Moortgat-Pick G., Rinolfi Louis, Riemann S., Telnov V.I. Summary of the working groups polarization gamma-gamma technical aspects. // The talk Intern. Workshop on Linear Colliders (IWLC2010), ECFA-CLIC-ILC Joint Meeting: October 18-22, 2010, CERN, Switzerland. - <http://ilcagenda.linearcollider.org/getFile.py/access?contribId=590&sessionId=102&resId=1&materialId=slides&confId=4507>.
- [564] S.I. Eidelman, V.V. Anashin, V.M. Aulchenko, E.M. Baldin, A.K. Barladyan, A.Yu. Barnyakov, M.Yu. Barnyakov, S.E. Baru, I.V. Bedny, O.L. Beloborodova, A.E. Blinov, V.E. Blinov, A.V. Bobrov, V.S. Bobrovnikov, A.V. Bogomyagkov, A.E. Bondar, A.R. Buzykaev, Yu.M. Glukhovchenko, V.V. Gulevich, D.V. Gusev, S.E. Karnaev, S.V. Karpov, T.A. Kharlamova, V.A. Kiselev, S.A. Kononov, K.Yu. Kotov, E.A. Kravchenko, V.F. Kulikov, G.Ya. Kurkin, E.A. Kuper, E.B. Levichev, D.A. Maksimov, V.M. Malyshev, A.L. Maslennikov, A.S. Medvedko, O.I. Meshkov, S.I. Mishnev, I.I. Morozov, N.Yu. Muchnoi, V.V. Neufeld, S.A. Nikitin, I.B. Nikolaev, I.N. Okunev, A.P. Onuchin, S.B. Oreshkin, I.O. Orlov, A.A. Osipov, S.V. Peleganchuk, S.G. Pivovarov, P.A. Piminov, V.V. Petrov, A.O. Poluektov, I.N. Popkov, V.G. Prisekin, A.A. Ruban, V.K. Sandyrev, G.A. Savinov, A.G. Shamov, D.N. Shatilov, B.A. Shwartz, E.A. Simonov, S.V. Sinyatkin, Yu.I. Skovpen, A.N. Skrinsky, V.V. Smaluk, A.V. Sokolov, A.M. Sukharev, E.V. Starostina, A.A. Talyshev, V.A. Tayursky, V.I. Telnov, Yu.A. Tikhonov, K.Yu. Todyshev, G.M. Tumaikin, Yu.V. Usov, A.I. Vorobiov, A.N. Yushkov, V.N. Zhilich, V.V. Zhulanov, A.N. Zhuravlev, (KEDR Collab.). High-precision tau lepton mass measurement at KEDR. // XI Intern. Workshop on Tau Lepton Physics, September 2010, Manchester, UK.
- [565] E.M. Baldin, V.V. Anashin, V.M. Aulchenko, A.K. Barladyan, A.Yu. Barnyakov, M.Yu. Barnyakov, S.E. Baru, I.V. Bedny, O.L. Beloborodova, A.E. Blinov, V.E. Blinov, A.V. Bobrov, V.S. Bobrovnikov, A.V. Bogomyagkov, A.E. Bondar, A.R. Buzykaev, S.I. Eidelman, Yu.M. Glukhovchenko, V.V. Gulevich, D.V. Gusev, S.E. Karnaev, S.V. Karpov, T.A. Kharlamova, V.A. Kiselev, S.A. Kononov, K.Yu. Kotov, E.A. Kravchenko, V.F. Kulikov, G.Ya. Kurkin, E.A. Kuper, E.B. Levichev, D.A. Maksimov, V.M. Malyshev, A.L. Maslennikov, A.S. Medvedko, O.I. Meshkov, S.I. Mishnev, I.I. Morozov, N.Yu. Muchnoi, V.V. Neufeld, S.A. Nikitin, I.B. Nikolaev, I.N. Okunev, A.P. Onuchin, S.B. Oreshkin, I.O. Orlov, A.A. Osipov, S.V. Peleganchuk, S.G. Pivovarov, P.A. Piminov, V.V. Petrov, A.O. Poluektov, I.N. Popkov, V.G. Prisekin, A.A. Ruban, V.K. Sandyrev, G.A. Savinov, A.G. Shamov, D.N. Shatilov, B.A. Shwartz, E.A. Simonov, S.V. Sinyatkin, Yu.I. Skovpen, A.N. Skrinsky, V.V. Smaluk, A.V. Sokolov, A.M. Sukharev, E.V. Starostina, A.A. Talyshev, V.A. Tayursky, V.I. Telnov, Yu.A. Tikhonov, K.Yu. Todyshev, G.M. Tumaikin, Yu.V. Usov, A.I. Vorobiov, A.N. Yushkov, V.N. Zhilich, V.V. Zhulanov, A.N. Zhuravlev, et al. (KEDR Collab.). Measurement of  $\Gamma(J/\psi) \cdot B(J/\psi \rightarrow e^+e^-)$  and  $\Gamma(J/\psi) \cdot B(J/\psi \rightarrow \mu^+\mu^-)$ . // 35th Intern. Conference on High Energy Physics (ICHEP 2010), July 22-28, 2010, Paris, France. - Proceedings of Science (ICHEP 2010), P.222.
- [566] A.G. Shamov, V.V. Anashin, V.M. Aulchenko, E.M. Baldin, A.K. Barladyan, A.Yu. Barnyakov, M.Yu. Barnyakov, S.E. Baru, I.V. Bedny, O.L. Beloborodova, A.E. Blinov, V.E. Blinov, A.V. Bobrov, V.S. Bobrovnikov, A.V. Bogomyagkov, A.E. Bondar, A.R. Buzykaev, S.I. Eidelman, Yu.M. Glukhovchenko, V.V. Gulevich, D.V. Gusev, S.E. Karnaev, S.V. Karpov, T.A. Kharlamova, V.A. Kiselev, S.A. Kononov, K.Yu. Kotov, E.A. Kravchenko, V.F. Kulikov, G.Ya. Kurkin, E.A. Kuper, E.B. Levichev, D.A. Maksimov, V.M. Malyshev, A.L. Maslennikov, A.S. Medvedko, O.I. Meshkov, S.I. Mishnev, I.I. Morozov, N.Yu. Muchnoi, V.V. Neufeld, S.A. Nikitin, I.B. Nikolaev, I.N. Okunev, A.P. Onuchin, S.B. Oreshkin, I.O. Orlov, A.A. Osipov, S.V. Peleganchuk, S.G. Pivovarov, P.A. Piminov, V.V. Petrov, A.O. Poluektov, I.N. Popkov, V.G. Prisekin, A.A. Ruban, V.K. Sandyrev, G.A. Savinov, A.G. Shamov, D.N. Shatilov, B.A. Shwartz, E.A. Simonov, S.V. Sinyatkin, Yu.I. Skovpen,

- A.N. Skrinsky, V.V. Smaluk, A.V. Sokolov, A.M. Sukharev, E.V. Starostina, A.A. Talyshev, V.A. Tayursky, V.I. Telnov, Yu.A. Tikhonov, K.Yu. Todyshev, G.M. Tumaikin, Yu.V. Usov, A.I. Vorobiov, A.N. Yushkov, V.N. Zhilich, V.V. Zhulanov, A.N. Zhuravlev, et al. (KEDR Collab.). Measurement of  $J/\psi$ ,  $\psi(2S)$ ,  $\tau$  masses with KEDR detector at VEPP-M collider. // 35th Intern. Conference on High Energy Physics (ICHEP 2010), July 22-28 2010, Paris, France.
- [567] K.Yu. Todyshev, V.V. Anashin, V.M. Aulchenko, E.M. Baldin, A.K. Barladyan, A.Yu. Barnyakov, M.Yu. Barnyakov, S.E. Baru, I.V. Bedny, O.L. Beloborodova, A.E. Blinov, V.E. Blinov, A.V. Bobrov, V.S. Bobrovnikov, A.V. Bogomyagkov, A.E. Bondar, A.R. Buzykaev, S.I. Eidelman, Yu.M. Glukhovchenko, V.V. Gulevich, D.V. Gusev, S.E. Karnaev, S.V. Karpov, T.A. Kharlamova, V.A. Kiselev, S.A. Kononov, K.Yu. Kotov, E.A. Kravchenko, V.F. Kulikov, G.Ya. Kurkin, E.A. Kuper, E.B. Levichev, D.A. Maksimov, V.M. Malyshev, A.L. Maslennikov, A.S. Medvedko, O.I. Meshkov, S.I. Mishnev, I.I. Morozov, N.Yu. Muchnoi, V.V. Neufeld, S.A. Nikitin, I.B. Nikolaev, I.N. Okunev, A.P. Onuchin, S.B. Oreshkin, I.O. Orlov, A.A. Osipov, S.V. Peleganchuk, S.G. Pivovarov, P.A. Piminov, V.V. Petrov, A.O. Poluektov, I.N. Popkov, V.G. Prisekin, A.A. Ruban, V.K. Sandryev, G.A. Savinov, A.G. Shamov, D.N. Shatilov, B.A. Schwartz, E.A. Simonov, S.V. Sinyatkin, Yu.I. Skovpen, A.N. Skrinsky, V.V. Smaluk, A.V. Sokolov, A.M. Sukharev, E.V. Starostina, A.A. Talyshev, V.A. Tayursky, V.I. Telnov, Yu.A. Tikhonov, K.Yu. Todyshev, G.M. Tumaikin, Yu.V. Usov, A.I. Vorobiov, A.N. Yushkov, V.N. Zhilich, V.V. Zhulanov, A.N. Zhuravlev, et al. (KEDR Collab.). Measurement of  $\psi(3770)$  resonance parameters with KEDR detector at VEPP-4M. // 35th Intern. Conference on High Energy Physics (ICHEP2010), July 22-28 2010, Paris, France.
- [568] K.Yu. Todyshev, V.V. Anashin, V.M. Aulchenko, E.M. Baldin, A.K. Barladyan, A.Yu. Barnyakov, M.Yu. Barnyakov, S.E. Baru, I.V. Bedny, O.L. Beloborodova, A.E. Blinov, V.E. Blinov, A.V. Bobrov, V.S. Bobrovnikov, A.V. Bogomyagkov, A.E. Bondar, A.R. Buzykaev, S.I. Eidelman, Yu.M. Glukhovchenko, V.V. Gulevich, D.V. Gusev, S.E. Karnaev, S.V. Karpov, T.A. Kharlamova, V.A. Kiselev, S.A. Kononov, K.Yu. Kotov, E.A. Kravchenko, V.F. Kulikov, G.Ya. Kurkin, E.A. Kuper, E.B. Levichev, D.A. Maksimov, V.M. Malyshev, A.L. Maslennikov, A.S. Medvedko, O.I. Meshkov, S.I. Mishnev, I.I. Morozov, N.Yu. Muchnoi, V.V. Neufeld, S.A. Nikitin, I.B. Nikolaev, I.N. Okunev, A.P. Onuchin, S.B. Oreshkin, I.O. Orlov, A.A. Osipov, S.V. Peleganchuk, S.G. Pivovarov, P.A. Piminov, V.V. Petrov, A.O. Poluektov, I.N. Popkov, V.G. Prisekin, A.A. Ruban, V.K. Sandryev, G.A. Savinov, A.G. Shamov, D.N. Shatilov, B.A. Schwartz, E.A. Simonov, S.V. Sinyatkin, Yu.I. Skovpen, A.N. Skrinsky, V.V. Smaluk, A.V. Sokolov, A.M. Sukharev, E.V. Starostina, A.A. Talyshev, V.A. Tayursky, V.I. Telnov, Yu.A. Tikhonov, K.Yu. Todyshev, G.M. Tumaikin, Yu.V. Usov, A.I. Vorobiov, A.N. Yushkov, V.N. Zhilich, V.V. Zhulanov, A.N. Zhuravlev, et al., (KEDR Collab.). Recent results from the KEDR detector. // 4th Intern. Workshop on Charm Physics (Charm2010), Oct. 21-24, 2010, IHEP, Beijing, China.
- [569] K.Yu. Todyshev, V.V. Anashin, V.M. Aulchenko, E.M. Baldin, A.K. Barladyan, A.Yu. Barnyakov, M.Yu. Barnyakov, S.E. Baru, I.V. Bedny, O.L. Beloborodova, A.E. Blinov, V.E. Blinov, A.V. Bobrov, V.S. Bobrovnikov, A.V. Bogomyagkov, A.E. Bondar, A.R. Buzykaev, S.I. Eidelman, Yu.M. Glukhovchenko, V.V. Gulevich, D.V. Gusev, S.E. Karnaev, S.V. Karpov, T.A. Kharlamova, V.A. Kiselev, S.A. Kononov, K.Yu. Kotov, E.A. Kravchenko, V.F. Kulikov, G.Ya. Kurkin, E.A. Kuper, E.B. Levichev, D.A. Maksimov, V.M. Malyshev, A.L. Maslennikov, A.S. Medvedko, O.I. Meshkov, S.I. Mishnev, I.I. Morozov, N.Yu. Muchnoi, V.V. Neufeld, S.A. Nikitin, I.B. Nikolaev, I.N. Okunev, A.P. Onuchin, S.B. Oreshkin, I.O. Orlov, A.A. Osipov, S.V. Peleganchuk, S.G. Pivovarov, P.A. Piminov, V.V. Petrov, A.O. Poluektov, I.N. Popkov, V.G. Prisekin, A.A. Ruban, V.K. Sandryev, G.A. Savinov, A.G. Shamov, D.N. Shatilov, B.A. Schwartz, E.A. Simonov, S.V. Sinyatkin, Yu.I. Skovpen, A.N. Skrinsky, V.V. Smaluk, A.V. Sokolov, A.M. Sukharev, E.V. Starostina, A.A. Talyshev, V.A. Tayursky, V.I. Telnov, Yu.A. Tikhonov, K.Yu. Todyshev, G.M. Tumaikin, Yu.V. Usov, A.I. Vorobiov, A.N. Yushkov, V.N. Zhilich, V.V. Zhulanov, A.N. Zhuravlev, (KEDR Collab.). Measurement of  $\psi(3770)$  resonance parameters with KEDR. // 4th Intern. Workshop on Charm Physics (Charm2010), Oct. 21-24, 2010, IHEP, Beijing, China.
- [570] V.M. Malyshev, V.V. Anashin, V.M. Aulchenko, E.M. Baldin, A.K. Barladyan, A.Yu. Barnyakov, M.Yu. Barnyakov, S.E. Baru, I.V. Bedny, O.L. Beloborodova, A.E. Blinov, V.E. Blinov, A.V. Bobrov, V.S. Bobrovnikov, A.V. Bogomyagkov, A.E. Bondar, A.R. Buzykaev, S.I. Eidelman, Yu.M. Glukhovchenko, V.V. Gulevich, D.V. Gusev, S.E. Karnaev, S.V. Karpov, T.A. Kharlamova, V.A.

- Kiselev, S.A. Kononov, K.Yu. Kotov, E.A. Kravchenko, V.F. Kulikov, G.Ya. Kurkin, E.A. Kuper, E.B. Levichev, D.A. Maksimov, V.M. Malyshev, A.L. Maslennikov, A.S. Medvedko, O.I. Meshkov, S.I. Mishnev, I.I. Morozov, N.Yu. Muchnoi, V.V. Neufeld, S.A. Nikitin, I.B. Nikolaev, I.N. Okunev, A.P. Onuchin, S.B. Oreshkin, I.O. Orlov, A.A. Osipov, S.V. Peleganchuk, S.G. Pivovarov, P.A. Piminov, V.V. Petrov, A.O. Poluektov, I.N. Popkov, V.G. Prisekin, A.A. Ruban, V.K. Sandyrev, G.A. Savinov, A.G. Shamov, D.N. Shatilov, B.A. Shwartz, E.A. Simonov, S.V. Sinyatkin, Yu.I. Skovpen, A.N. Skrinsky, V.V. Smaluk, A.V. Sokolov, A.M. Sukharev, E.V. Starostina, A.A. Talyshev, V.A. Tayursky, V.I. Telnov, Yu.A. Tikhonov, K.Yu. Todyshev, G.M. Tumaikin, Yu.V. Usov, A.I. Vorobiov, A.N. Yushkov, V.N. Zhilich, V.V. Zhulanov, A.N. Zhuravlev, et al. (KEDR Collab.). Measurement of  $\text{Br}(J/\psi \rightarrow \eta_c \gamma)$  at KEDR. // 4th Int. Workshop on Charm Physics (Charm2010), Oct. 21-24, 2010, IHEP, Beijing, China.
- [571] Reva V.B., Parkhomchuk V.V., Yang X.D. Using electron cooling for obtaining ion beam with high intensity and brightness. // Intern. Conference (HB2010), September 27 - October 1, 2010, Morschach, Switzerland. - Proceedings, MOPD25.
- [572] Vostrikov V. Electron cooling application for cancer therapy accelerator facility. // Workshop "Physics for Health in Europe", 2-4 February 2010, CERN, Switzerland.
- [573] Levichev E., Parkhomchuk V., Skrinsky A., Vostrikov V. A project of the hadron cancer therapy synchrotron with electron cooling. // 2nd Joint Asian Accelerator Workshop (2JAAWS), 29-30 November, POSTECH, Pohang, Korea.
- [574] Chupyra A.G., Gusev G.A., Kondaurov M.N., Medvedko A.S., Singatulin Sh.R. BINP capacitive and ultrasoniltrasonic hydrostatic level sensors. // Proc. of the 11th Intern. Workshop on Accelerator Alignment (IWAA10), DESY, 13-17 September 2010, DESY, Hamburg.
- [575] Volk J., Shiltsev V. (Fermilab), Chupyra A., Kondurov M., Singatulin S. (BINP), Stetler L. (South Dakota School of Mines and Technology). Hydrostatic level systems at Fermilab and DUSEL. // Proc. of the 11th Intern. Workshop on Accelerator Alignment (IWAA10), 13-17 September 2010, DESY, Hamburg.
- [576] Batrakov A., Fatkin G., Ilyin I., Logatchev P., Pavlenko A., Sazanskiy V. The structure and hardware of control system for power linear accelerator. // IASTED Intern. Conference on Automation, Control and Instrumentation Technology (ACIT-CDA-2010), June 2010, Novosibirsk, Russia. - Proceedings. - P.164-167.
- [577] Arbuzov V.S., Biryuchevsky Yu.A., Gorniker E.I., Zavyalov N.V., Kozyrev Ye.V., Kondakov A.A., Krutikhin S.A., Kurkin G.Ya., Motyguin S.V., Osipov V.N., Petrov V.M., Serdobintzev G.V., Smetanin M.L., Telnov A.V., Tchernov K.N., Shorikov I.V. HF generator for electron resonance accelerator based on coaxial resonator // «XII Kharitonov Reading" of the Intern. Scientific Conference on High Energy Density Physics, 19 - 23 April, 2010, VNIIEF, Sarov, Nizhny Novgorod region. - P.28-32 (in Russian).
- [578] Davydenko V., Ivanov A., Kolmogorov A., Zelenski A. Production of high brightness H- beam by charge exchange of hydrogen atom beam in sodium jet. // 2nd Intern. Symposium on Negative Ions and Sources, November 16-19, 2010, Takayama, Gifu, Japan. - Book of Abstracts, P.50.
- [579] Kuznetsov A.S., Belchenko Yu.I., Burdakov A.V., Davydenko V.I., Ivanov A.A., Konstantinov S.G., Mekler K.I., Sanin A.L., Sorokin I.N., Sulyaev Yu.S., Taskaev S.Yu. Status and prospects of vacuum insulated tandem accelerator (VITA). // 21st Intern. Conference on the Application of Accelerators in Research and Industry, 2010, USA. - Book of Abstracts, 2010, P.175.
- [580] Sarff J.S., Abdrashitov G.F., Alfer A., Amarli A.F., Anderson J.K., et al. Overview of results in the MST reversed field pinch experiment. // 23rd IAEA Fusion Energy Conference, 11-16 October 2010, Daejeon, Republic of Korea. - Abstracts, P.21-22.
- [581] Bayanov B., Burdakov A., Ivanov A., Kuznetsov A., Taskaev S. Accelerator based epithermal neutron source for boron neutron capture therapy. // Physics for Health in Europe Workshop, 2-4 February 2010, CERN - Switzerland. - Book of Abstracts, P.11.
- [582] Aleynik V.I., Burdakov A.V., Grigorjeva E.V., Davydenko V.I., Ivanov A.A., Kanygin V.V., Kuznetsov a.S., Makarov A.N., Pakhomova Yu.V., Sorokin I.N., Taskaev S.Yu. Features and

- feasibilities of accelerator based epithermal neutron source at BINP. Proc. of the IV All-Russian National Congress of Radiation Diagnosticians and Therapeutists "Radiology-2010", Moscow, 25-27 May, 2010. - P.18-19. (In Russian).
- [583] Aleynik V.I., Bayanov B.F., Burdakov A.V., Kuznetsov A.S., Makarov A.N., Sinitskii S.L., Taskaev S.Yu. The time-of-flight technique for the neutron spectrum measurement on VITA-facility. // 3rd Intern. Conference "Current Problems in Nuclear Physics and Atomic Energy", June 7-11, 2010, Kyiv, Ukraine. - Book of Abstracts, P.138-139.
- [584] Sauerwein W., Kulakov V., Lipengolts A., Taskaev S., Doll C. The ISTC BNCT task force. // 14th Intern. Congress on Neutron Capture Therapy, October 25-29, 2010, Buenos Aires, Argentina. - Program and Abstracts, P.35.
- [585] Aleinik V., Burdakov V., Davydenko V., Ivanov A., Kanygin V., Kuznetsov A., Makarov A., Sorokin I. and Taskaev S. BINP accelerator based epithermal neutron source. // Proc. of 14th Intern. Congress on Neutron Capture Therapy. October 25-29, 2010, Buenos Aires, Argentina. - P.441-444.
- [586] Taskaev S., Bayanov B., Chudaev V., Kandiev Ya., Kashaeva E., Malyshkin G. A protective subsurface container for activated target holding and temporary storage. // Proc. of 14th Intern. Congress on Neutron Capture Therapy. October 25-29, 2010, Buenos Aires, Argentina. - P.503-506.
- [587] Kandiev Ya., Kashaeva E., Malyshkin G., Taskaev S., Bayanov B. Optimization of the target of an accelerator-driven neutron source through Monte Carlo numerical simulation of neutron and gamma transport by the PRIZMA code. // Proc. of 14th Intern. Congress on Neutron Capture Therapy. October 25-29, 2010, Buenos Aires, Argentina. - P.507-510.
- [588] Aleinik V., Bayanov B., Burdakov V., Makarov A., Sinitskiy S., Taskaev S. New technical solution for use the time-of-flight technique to measure neutron spectra. // Proc. of 14th Intern. Congress on Neutron Capture Therapy. October 25-29, 2010, Buenos Aires, Argentina. - P.511-514.
- [589] Sauerwein W., Kulakov V., Lipengolts A., Taskaev S., Doll C. The ISTC BNCT task force. // Proc. of 14th Intern. Congress on Neutron Capture Therapy. October 25-29, 2010, Buenos Aires, Argentina. - P.535.
- [590] Caldwell A., Xia G.X., Assmann R.W., Zimmermann F., Lotov K.V., Pukhov A.M. A proposed experiment on proton driven plasma wakefield acceleration. // 1st Intern. Particle Accelerator Conference, 2010, Kyoto, Japan. - Abstracts, P.402.
- [591] Lotov K.V., Maslov V.I., Onishchenko I.N. Long sequence of relativistic electron bunches as a driver in wakefield method of charged particles acceleration in plasma. // Intern. Conference-School on Plasma Physics and Controlled Fusion, Alushta, 2010. - Abstracts, P.18.
- [592] Maslov V.I., Lotov K.V., Onishchenko I.N. Vesnovskaya., M.S., Svistun E.N. Mechanism of plasma wakefield excitation by a nonresonant sequence of relativistic electron bunches with repetition frequency less than plasma frequency. // Intern. Conference-School on Plasma Physics and Controlled Fusion, Alushta, 2010, Abstracts, P.122.
- [593] Lotov K.V., Maslov V.I., Onishchenko I.N., Vesnovskaya M.S. New mechanism of instability development of relativistic electron beam in plasma, determined by its electron focusing/defocusing. // Intern. Conference-School on Plasma Physics and Controlled Fusion, Alushta, 2010. - Abstracts, P.128.
- [594] Pushkareva A.N. Plasma temperature measurements with Thompson scattering method on GDT facility. // Proc of the XLVII Intern. Student Scientific Conference "Student and Scientific-Technical Progress", 2010, Novosibirsk. - P.172.
- [595] Zaitsev K.V. Plasma vortex confinement theory supporting experiments. // Proc of the XLVII Intern. Student Scientific Conference "Student and Scientific-Technical Progress", 2010, Novosibirsk.
- [596] Yurov D.V. Energy spectrum investigation of the negative hydrogen ions beam. // XLVII Intern. Student Scientific Conference "Student and Scientific-Technical Progress", Novosibirsk, 2010. - Abstracts.

- [597] Simonen T.C., Anikeev A., Bagrynsky P., Beklemishev A., Ivanov A., Lizunov A., Maximov V., Prikhodko V., and Tsidulko Yu. In: Innovative Confinement Concepts Workshop, 2010, Princeton University, Princeton, NJ.
- [598] Arzhannikov A.V., Astrelin V.T., Ivanenko V.G. Makarov, M.A., Sinitsky S.L. Influence of diode geometry and voltage pulse profile on REB parameters of U-2 accelerator. // 8th Intern. Conf. on Open Magnetic Systems for Plasma Confinement, Novosibirsk, Russia, 2010. - Abstracts, Novosibirsk: BINP SB RAS, 2010, P.102.
- [599] Postupaev V.V., Arzhannikov A.V., Batkin V.I., Burdakov A.V., Burmasov V.S., Ivanov I.A., Ivantsivsky M.V., Kuklin K.N., Kuznetsov S.A., Makarov M.A., Mekler K.I., Polosatkin S.V., Popov S.S., Rovenskikh A.F., Sinitsky S.L., Sklyarov V.F., Sorokina N.V., Sudnikov A.V., Sulyaev Yu.S., and Vyacheslavov L.N. Experiments with gradual-energy-growth electron beam at GOL-3. // 8th Intern. Conf. on Open Magnetic Systems for Plasma Confinement, Novosibirsk, Russia. - Abstracts, Novosibirsk: BINP SB RAS, 2010, P.104.
- [600] Snytnikov A.V., Astrelin V.T., Burdakov A.V. Vshivkov, V.A., Dudnikova G.I. 3D Particle-in-cell simulation of the beam-plasma system. // 8th Intern. Conf. on Open Magnetic Systems for Plasma Confinement, Novosibirsk, Russia, 2010. - Abstracts, P.109.
- [601] Astrelin V.T., Burdakov A.V., Grigoriev S.V., Kandaurov I.V., Koval N.N., Teresov A.D. An influence of grid fields on beam characteristics in a diode with grid stabilization of plasma emitting surface // 16th Intern. Symposium on High Current Electronics: Publishing house of the IAO SB RAS, 2010. - Abstracts, P.15-18.
- [602] Grigoryev S.V., Astrelin V.T., Devjatkov V.N., Kandaurov I.V., Koval N.N., Kozyrev A.V., Moskvina P.V., Teresov A.D. Generation of submillisecond electron beam in the diode with the grid plasma cathode and the plasma anode generated by the asymmetrical reflective discharge // 16th Intern. Symposium on High Current Electronics, Tomsk: Publishing house of the IAO SB RAS, 2010. - Abstracts, P.19-22.
- [603] Teresov A.D., Astrelin V.T., Devjatkov V.N., Gavrilov N.V., Grigoriev S.V., Kandaurov I.V., Koval N.N. Investigation of characteristics of sub-millisecond electron source with the plasma cathode and the opened boundary of anode plasma // 16th Intern. Symposium on High Current Electronics, Tomsk: Publishing house of the IAO SB RAS, 2010. - Abstracts, P.92-95.
- [604] Trunov Yu.A., Avrorov A.P., Astrelin V.T., Burdakov A.V., Bykov P.V., Derevyankin G.E., Kandaurov I.V., Yarovoy V.A. A prototype long-pulse electron beam injector for GOL-3 multimirror plasma trap // 16th Intern. Symposium on High Current Electronics, Tomsk: Publishing house of the IAO SB RAS, 2010. - Abstracts, P.156-158.
- [605] Ivanov A.A., Burdakov A.V., Kruglyakov E.P. Modern magnetic mirrors and their fusion prospects // 37th EPS Conference on Plasma Physics, Ireland, 2010. - I2.105.
- [606] Postupaev V.V., Arzhannikov A.V., Astrelin V.T., Batkin V.I., Burdakov A.V., Burmasov V.S., Ivanov I.A., Ivantsivsky M.V., Kuklin K.N., Kuznetsov S.A., Makarov M.A., Mekler K.I., Polosatkin S.V., Popov S.S., Rovenskikh A.F., Shoshin A.A., Sinitsky S.L., Sklyarov V.F., Sorokina N.V., Sudnikov A.V., Sulyaev Yu.S. Vyacheslavov L.N. Experiments with “thin” electron beam at GOL-3 // 37th EPS Conference on Plasma Physics, Ireland, 2010. - P1.1080.
- [607] Sadykov Vladislav, Mezentseva Natalia, Usoltsev Vladimir, Sadovskaya Ekaterina, Ishchenko Arkady, Pavlova Svetlana, Bepalko Yulia, Kharlamova Tamara, Zevak Ekaterina, Salanov Aleksei, Krieger Tamara, Bobrenok Oleg, Uvarov Nikolai, Okhlupin Yury, Smorygo Oleg, Smirnova Alevtina, Singh Prabhakar, Vlasov Aleksandr, Korobeynikov Mikhail, Bryazgin Aleksandr, Kalinin Peter, Arzhannikov Andrei. SOFC composite cathodes based on perovskite and fluorite structures. // Proc. of 9th European Solid Oxide Fuel Cell Forum, 29 June - 2 July 2010, Lucerne, Switzerland. - Chapter 10. - P.4-16.
- [608] Sadykov V.A., Usoltsev V.V., Fedorova Yu.E., Mezentseva N.V., Smorygo O.L., Bobrenok O.F., Kalinin P.V., Arzhannikov A.V., Vlasov A., Korobeynikov M. V., Bryazgin A.A., Ulikhin A. IT SOFC with functionally graded cathode designed on metallic NiAl foam. // E-MRS Fall Meeting,

- 13-17 September 2010, Warsaw, Poland.
- [609] Kuznetsov S.A., Paulish A.G., Gelfand A.V., Fedorinin V.N. Implementation of novel type of IR-THz receivers based on matrix structures of optoacoustic cells. // 40th European Microwave Conference, September 28-30, 2010, Paris, France. - P.61-64.
- [610] Kuznetsov S.A., Navarro-Cía M., Gelfand A.V., Fedorinina N.I., Arzhannikov A.V., Paulish A.G., Beruete M., Falcone F., and Sorolla M. Ultra-thin subterahertz absorbers based on high-impedance metasurfaces. // 4th Intern. Congress on Advanced Electromagnetic Materials in Microwaves and Optics "Metamaterials-2010", September 13-18, 2010, Karlsruhe, Germany. - Abstracts, P.119-121.
- [611] Sorolla M., Beruete M., Navarro-Cía M., Falcone F., Campillo I., Kuznetsov S.A. Extraordinary transmission metamaterials: from millimeter-waves to terahertz. // 4th Intern. Congress on Advanced Electromagnetic Materials in Microwaves and Optics "Metamaterials-2010", September 13-18, 2010, Karlsruhe, Germany. - Abstracts, P.660-662.
- [612] Sorolla M., Beruete M., Navarro-Cía M., Falcone F., Campillo I., Kuznetsov S.A. Extraordinary-transmission-based devices. // Proc. of the 2nd Intern. Conference on Metamaterials, Photonic Crystals and Plasmonics META'10, February 22-25, 2010, Cairo, Egypt.
- [613] Kruglyakov E.P., Burdakov A.V., Ivanov A.A. Evolution of mirrors in Novosibirsk: past, present and future. // Intern. Conference-School on Plasma Physics and Controlled Fusion and 4th Intern. Workshop on the Role of Electric Fields in Plasma Confinement in Stellarators and Tokamaks, Ukraine, 2010, - Book of Abstracts of Alushta-2010, P.6.
- [614] Popov S.S., Vyacheslavov L.N., Ivantsivsky M.V., Burdakov A.V., Kasatov A.A., Polosatkin S.V., Postupaev V.V. Two-pulse Thomson scattering system for measurements of spatial dynamics of electron distribution function in multi-mirror trap GOL-3. // Intern. Conference-School on Plasma Physics and Controlled Fusion and 4th Intern. Workshop on the Role of Electric Fields in Plasma Confinement in Stellarators and Tokamaks, Ukraine, 2010. - Book of Abstracts of Alushta-2010, P.209.
- [615] Burdakov A.V., Avrorov A.P., Arzhannikov A.V., Astrelin V.T., Batkin V.I., Burmasov V.S., Bykov P.V., Vyacheslavov L.N., Derevyankin G.E., Ivanenko V.G., Ivanov I.A., Ivantsivsky M.V., Kandaurov I.V., S.A. Kuznetsov, Kuklin K.N., Makarov M.A., Mekler K.I., Polosatkin S.V., Popov S.S., Postupaev V.V., Rovenskikh A.F., Sinitsky S.L., Stepanov V.D., Sudnikov A.V., Sulyaev Yu.S., Timofeev I.V., Sklyarov V.F., Sorokina N.V., Shoshin A.A., Trunev Yu.A. New experiments on the GOL-3 multiple mirror trap. // Proc. of 23rd IAEA Fusion Energy Conference, 11-16 October 2010, Daejeon, Korea. - EXC/P4-03.
- [616] Kruglyakov E.P., Burdakov A.V., and Ivanov A.A. Progress in studies of magnetic mirror and their prospects. // Proc. of 23rd IAEA Fusion Energy Conference, 11-16 October 2010, Daejeon, Korea. - OV/P-6.
- [617] Berkaev D.E., Shatunov P.Yu. The automation system of the electron-positron collider VEPP-2000. // 13th ISTS SAC Seminar "New Perspectives of High Energy Physics", 1 - 5 Sept., 2010, Budker INP, Novosibirsk, Russia.
- [618] Berkaev D.E., Shatunov P.Yu. VEPP-2000 - new electron-positron collider at BINP. // 13th ISTS SAC Seminar "New Perspectives of High Energy Physics", 1 - 5 Sept., 2010, Budker INP, Novosibirsk, Russia.
- [619] Belikov O., Cheblakov P., Kasaev A., Kozak V., Podgorny F., Stankevich A. Control system for injection channels of VEPP-2000 collider. // 13th ISTC SAC Seminar "New Perspectives of High Energy Physics", 1 - 5 Sept., 2010, Budker INP, Novosibirsk, Russia.
- [620] Koop I., Levichev E., Nikitin S., Piminov P., Sinyatkin S., Shatilov D., et al. The Super-B project accelerator status [Electronic resource]. // 1st Intern. Particle Accelerator Conference (IPAC'10), Kyoto, Japan, 23 - 28 May, 2010. - Kyoto: Kyoto Intern. Conf. Centre, Japan, 2010. - P.1518-1520 IPAC-2010-TUPEB003, Jun 2010.

- [621] Golkovskiy M.G., Bataev I.A., Zhuravina T.V. Surface alloying of titanium by tantalum and niobium. // Proc. of All-Russian Scientific Conference of Young Scientists: Science. Technologies. Innovations, 3 - 5 December, 2010, Novosibirsk: NSTU. - Proceedings, P.188-189.
- [622] Golkovski. M.G., Zhuravina T.V., Bataev I.A., and Bataev V.A. Formation of alloyed layer of Ta-Nb-Ti system on the titanium substrate with using of focused electron beam injected in atmosphere. // 10th International Conference on Modification of Materials with Particle beams and Plasma Flows, Tomsk: Publishing house of the IAO SB RAS, 2010. - Proceedins, P.616-619.
- [623] Golkovski M.G., Poletika I.M., Krilova T.A., Tetiutskaya M.V., and Makarov S.A. Vacuum free electron beam fused deposition of multifunctional coatings on steel substrates. // 10th International Conference on Modification of Materials with Particle beams and Plasma Flows, Tomsk: Publishing house of the IAO SB RAS, 2010. - Proceedings, P.508-510.
- [624] Krilova T.A., Poletika I.M., Golkovski M.G., Ivanov Yu.F., and Teresov A.D. The combination of electron beam treatment technologies for forming the strengthening coatings on steel substrate. // 10th Intern. Conference on Modification of Materials with Particle beams and Plasma Flows, Tomsk: Publishing house of the IAO SB RAS, 2010. - Proceedings, P.121-123.
- [625] Golkovskiy M.G., Zhuravina T.V., Bataeva Z.B. Structural changes in alloys of Ti-Ta-Nb system on titanium substrate obtained using focused electron beam extracted into atmosphere. // V Intern. Scientific Conference, 2010, Kemerovo. - Proceedings, P.514-515.
- [626] Zhunusbaeva A.K., Gnjusov S.F., Golkovskiy M.G. Influence of extra-vacuum alloying by electron beam onto composition coatings structure and micro-solidity. // V Intern. Scientific Conference «Modern Problems of Machine Construction», November 23-26, 2010, National Research Tomsk Polytechnic University, Tomsk: TPU Publishing House. - Proceedings, 2010, P.345-350.1
- [627] Salimbaeva M.K., Gnjusov S.F., Golkovski M.G. Influence of a number of relativistic electron beam runs onto structurally-phase state and micro-solidity of coatings on the basis of high-speed steel. // V Intern. Scientific Conference "Modern Problems of Machine Construction", November 23-26, 2010, National Research Tomsk Polytechnic University, Tomsk: TPU Publishing House. - Proceedings, 2010, P.387-391.
- [628] Kuksanov N.K., Golubenko Yu.I., Nemytov P.I., Salimov R.A., Fadeev S.N., Lavruhkin A.V., Korchagin A.I., Kogut D.S., Semenov A.M. High energy electron accelerators in cross-linking of cables and pipes. // 1st Intern. Symposium on Polymer Modification with High Energy Electrons, 24-26 November, 2010, Dresden, Germany.
- [629] Goncharov V.B., Bardahanov S.P., Korchagin A.I., Cyril'nikov P.G., Nizovskiy A.I. Radiation-thermal synthesis of nano-powders of metals, oxides and coated catalysts. // VII Intern. Conference "Radiation-Thermal Effects and Processes in Inorganic Matters", 2010, Tomsk. - Proceedings 2010, P.68-73.
- [630] Ancharov A.I., Aulchenko V.M., Baryshev V.B., Churkin I.N., Gavrilov N.G., Goldenberg B.G., Knyazev B.A., Kochubei D.I., Kubarev V.V., Kulipanov G.N., Kuper K.E., Kuper E.A., Kuzin M.V., Kuzminikh V.S., Levichev E.B., Medvedko A.S., Mezentsev N.A., Mironenko L.A., Mishnev S.I., Nikolenko A.D., Panchenko V.E., Peltek S.E., Petrov A.K., Philipchenko A.V., Pindyurin V.F., Popik V.M., Shaporenko A.D., Sharafutdinov M.R., Sheglov M.A., Sheromov M.A., Shiyankov S.V., Shmakov A.N., Skrinsky A.N., Smalyuk V.V., Ten K.A., Tolochko B.P., Ushakov V.A., Utkin A. V., Zolotarev K.V. "Siberian Synchrotron and Terahertz Radiation Center" as a center of collective using in the field of fundamental and applied research: Strategy of development of large-scale research infrastructures of the Russian Federation and cooperation with the European Union. // III Intern. Workshop, October 29, 2010, Nancy, France. - Moscow: MISaA publ. house press, 2010. - P.32-33.
- [631] Korolkov V.P., Kudryashov S.I., Ionin A.A., Makarov S.V., Seleznev L.V., Sinityn D.V., Masliy A.I., Medvedev A.Zh., Semenov R., Goldenberg B.G. Femtosecond surface nanostructuring of electroformed nickel stamps in air or in various liquids. // Intern. Conference "Fundamentals of laser assisted micro- and nanotechnologies" (FLAMN-10), July 5-8, 2010, St. Petersburg - Pushkin,

- Russia. - Abstracts, St. Petersburg, 2010. - P. 92.
- [632] Korolkov V.P., Poleshchuk A.G., Veiko V.P., Yarchuk M.V., Malyshev A.I., Sametov A.R., Suhii S.A., Goldenberg B.G. Study of microstructure topography and hardness evolution at direct laser writing on chrome films. // Intern. Conference "Fundamentals of Laser Assisted Micro- and Nanotechnologies" (FLAMN-10), July 5-8, 2010, St. Petersburg - Pushkin, Russia. – Abstracts, St. Petersburg, 2010. - P.90-91.
- [633] Nikitin A.K., Khitrov O.V., Kyrianov A.P., Knyazev B.A., Zhizhin G.N. Surface plasmon dispersive spectroscopy of thin films at terahertz frequencies. // XII Intern. Conference on Laser Applications in Life Sciences (LALS-2010), June 9 - 11, 2010, Oulu, Finland. - Laser Applications in Life Sciences, edited by Matti Kinnunen, Risto Myllylä. - Proc. of SPIE, 2010, Vol.7376, P.73760U-1-11.
- [634] Knyazev B.A. Imaging, spectroscopy and metrology using coherent monochromatic radiation of terahertz free electron laser. // Digest Reports of Intern. Symposium "Terahertz Radiation: Generation and Application", 26-29 July, 2010, Novosibirsk: BINP, Russia. - P.30.
- [635] Gerasimov V.V., Knyazev B.A., Nikitin A.K., Nikitin V.V., Zhizhin G.N. Terahertz surface-plasmon microscopy using free-electron laser and microbolometer matrix. // Digest Reports of Intern. Symposium "Terahertz Radiation: Generation and Application", 26-29 July, 2010, Novosibirsk: BINP, Russia. - P.30.
- [636] Gerasimov Vasily V., Cherkassky Valery S., Choporova Yulia Yu., Knyazev Boris A., Nikitin Alexander A., Vlasenko Maxim G. Real-time imaging systems for optical experiments with the THz free-electron lasers. // XIX Intern. Conference on Coherent and Nonlinear Optics, Lasers, their Applications and Technology (ICONO / LAT 2010), 23 - 27 August 2010, Kazan (Tatarstan), Russia.
- [637] Knyazev B.A. Novosibirsk free electron laser: possibilities for the study of materials and objects. // School for Young Professionals on the Synchrotron Radiation": The program and lecture bank / Ed. M. Kuzin. 11-15 November 2010, Novosibirsk. - Novosibirsk: BINP SB RAS, 2010.
- [638] Valeev R.G., Romanov E.A., Deev A.N., Mezentsev N.A., Sharafutdinov M.R., Kriventsov V.V., Eliseev A.A. Study of the local structure of thin nanocomposite films and nanostructures based on ZnSe and ZnS by the EXAFS method. // 13th Intern. Symposium "Order, Disorder and Properties of Oxides" (ODPO-2010), Loo, September 16-21, 2010. - Proceedings of the Symposium, Rostov-on-Don. - 2010. - P.48
- [639] Kulipanov G.N. Prospects for the development of synchrotron radiation centers in Russia (44 slides). // Report at the XVIII Intern. Conference on Synchrotron Radiation (SR-2010), 19 - 22 July 2010, Novosibirsk: BINP SB RAS.
- [640] Kulipanov G.N. Introduction plenary lecture: History and perspective of terahertz science (40 transparency). // Intern. Symp. "Terahertz radiation: generation and application, 26-28 July, 2010, Budker INP, Novosibirsk.
- [641] Kulipanov G.N. High power THz FEL (39 слайдов). // Invited Talk: 2nd JAAWS at PAL, 28-29 November 2010, Pohang, Korea.
- [642] Bryazgin A.A., Korobeynikov M.V. Industrial electron accelerators produced in BINP and their applications. // NAARI Intern. Conference - 2010 (NIC-2010), Isotope Technologies and Applications - New Horizons, December 13-15, 2010, Powai, Mumbai, India. - Proceedings, P.52-55.
- [643] Bryazgin A. Industrial irradiation facilities based on electron accelerators developed by BINP. // International Conference on Radiation Processing, December 17-18, 2010, New Delhi, India. - Abstracts, P.29.
- [644] Kalinina T.S., Dygalo N.N., Chernolovskaya E.L., Korobeinikov M.V. Assessment of the efficacy and toxicity of oligonucleotide preparations using neonatal rats test system. // Annual Scientific Conference "Basic Sciences for the Medicine, Novosibirsk: Institute of Chemistry and Medicine and IHB & FM SB RAS, 7-10 September 2010. - P.61.
- [645] Kasaev A.S., Podgorny F.V. Application of high-voltage nanosecond pulses to the disintegration

- of biological objects. // Scientific Conference of Students Physicists, 22-29 April, 2010, Volgograd. - Theses, Vol.47-23 (42).
- [646] Zhmurikov E.I., Savchenko I.V., Stankus S.V., Tecchio L. Thermophysical properties measurements of graphite composites for the neutron target convertor. // 10th International Conference on Modification of Materials with Particle beams and Plasma Flows, 19-24 September, 2010, Tomsk. - (Plenary report).
- [647] Baru S.E. An optimal system for personal inspection checkpoint strategically important objects. // VI Intern. Conference «Technical Means to Counter Terrorism and Criminal Explosions», St.Petersburg, 2010. - Theses, P.91-101.
- [648] Moog E.R., Abliz M., Boerste K., Buffington T., Capatina D., Dejus R.J., Doose C., Hasse Q., Ivanyushenkov Y., Jaski M., Kasa M., Kim S.H., Kustom R., Trakhtenberg E., Vasserman I., Xu J.Z., Mezentsev N.A., Syrovatin V.M. Development status of a superconducting undulator for the advanced photon source (APS) [Electronic resource]. // The 1st Intern. Particle Accelerator Conf. (IPAC'10), Kyoto, 23 - 28 May, 2010. - Kyoto: Kyoto Intern. Conf. Center, 2010. - P.3198-3200.
- [649] Dadoun O., Chaikovska I., Lepereq P., Poirier F., Variola A., Rinolfi L., Vivoli A., Chehab R., Strakhovenko V., Xu C. The baseline positron production and capture scheme for CLIC [Electronic resource]. // The 1st Intern. Particle Accelerator Conf. (IPAC'10), Kyoto, 23 - 28 May, 2010. - Kyoto: Kyoto Intern. Conf. Center, 2010. - P.2389-2391.
- [650] Dobson M., ..., Bogdanchikov A., Korol A., Zaytsev A., et al. IT infrastructure design and implementation considerations for the Atlas TDAQ system. // Poster at 5th Intern. Conference on Software and Data Technologies, 22-24 July, 2010, Athenes, Greece.
- [651] Valsan M.L., ..., Bogdanchikov A., Korol A., Zaytsev A., et al. Role based access control system in the ATLAS experiment. // Poster at 18th Intern. Conference on Computing in High Energy and Nuclear Physics, 18-22 October, 2010, Taipei, Taiwan.
- [652] Kuznetsov A.S. Source of neutrons for neutron capture therapy and other applications on the based of accelerator // XXI Meeting on the Use of Neutron Scattering Studies of Condensed Matter, 16 -19 November, 2010, Russian Research Center «Kurchatov Institute», Moscow.
- [653] Epifanov D.A., Akhmetshin R.R., Anisyonkov A.V., Aulchenko V.M., Banzarov V.Sh., Barkov L.M., Bashtovoy N.S., Bondar A.E., Bragin A.V., Dneprovsky L.V., Eidelman S.I., Epshteyn L.B., Fedotovitch G.V., Grebenuk A.A., Grigoriev D.N., Ignatov F.V., Karpov S.V., Kazanin V.F., Khazin B.I., Kozyrev A.N., Kuzmin A.S., Logashenko I.B., Lukin P.A., Mikhailov K.Yu., Okhaphkin V.S., Pestov Yu.N., Pirogov S.A., Pivovarov S.G., Popov A.S., Popov Yu.S., Redin S.I., Ruban A.A., Ryskulov N.M., Ryzhenenkov A.E., Shebalin V.E., Shemyakin D.N., Shwartz B.A., Smolina E.V., Solodov E.P., Talyshv A.A., Titov V.M., Vorobiov A.I., Yudin Yu.V., Zaytsev A.S. Electromagnetic calorimeters of the CMD-3 detector. // XIV Intern. Conference on Calorimetry in High Energy Physics (Calor 2010), 10-14 May, 2010. Beijing, China.
- [654] Dudnikov A.V. Babailov S.P. Relaxation properties of perspective NMR contrasts - ultrafine hydrogels of the magnito-soft ferrite (in Russian). // Proc of the All-Russian Conference "Physical Chemistry 2010", June, 2010, Tuapse. - C.36.
- [655] Dudnikov A.V. Issledovanie vremyazreshennoi mikrovolnovoi lyuminescencii i biogradacii FMR - kontrastiruyushego nanofosfora K16 (in Russian). // Proc. of the Intern. Conference on Nanostructures for Biology and Medicine, Novosibirsk, Institute of Chemistry and Biology. - P.30.
- [656] Khriplovich I.B. Capture of dark matter by the Solar System. Simple estimates. // Intern. Conference in memory of V.N Gribov, June, Trieste, Italy; [E-print: ArXiv:1004.3171 [hep-ex]].
- [657] Kuper K.E., Kvasov A.A., Pruel E.R., Ten K.A., Zarko V.E. High resolution X-ray computed tomography of low-contrast samples with the use of synchrotron radiation. // 6th World Congress on Industrial Process Tomography, 6-9 September, 2010, Beijing, China.

## Preprints

- 1 V.V. Petrov, Yu.A. Pupkov. BINP testing of radiation resistance of the materials used for production of accelerator magnetic systems. // Новосибирск, 2010, 32с, Препринт: ИЯФ 2010-1.
- 2 V.L. Auslender, A.A. Bryazgin, K.N. Chernov, V.G. Cheskidov, B.L. Faktorovitch, V.A. Gorbunov, I.V. Gornakov, E.N. Kokin, G.I. Kuznetsov, A.N. Lukin, I.G. Makarov, S.A. Maximov, N.V. Matyash, G.N. Ostreiko, A.D. Panfilov, G.V. Serdobintsev, A.V. Sidorov, V.M. Radchenko, N.D. Romashko, V.V. Tarnetsky, M.A. Tiunov, V.O. Tkachenko. Development of ILU-14 accelerator and TEST of its prototype. // Novosibirsk, 2010, 31p, Preprint: INP 2010-2 (in Russian).
- 3 B. F. Bayanov, Ya. Z. Kandiev, E. A. Kashaeva, G. N. Malyshkin, S. Yu. Taskaev, and V. Ya. Chudaev. A protective subsurface container for holding and temporary storage of activated targets. // Novosibirsk, 2010, 14p, Preprint: INP 2010-4 (in Russian).
- 4 S. Eidelman, S. Ivashyn, A. Korchin, G. Pancheri and O. Shekhovtsova.  $e^+e^-$  annihilation to  $\pi^0\pi^0\gamma$  and  $\pi^0\eta\gamma$  as a source of information on scalar and vector mesons. // Novosibirsk, 2010, 35p, Preprint: Budker INP 2010-5.
- 5 V.M. Petrov, N.V. Mityanina. Defining RF system parameters for the Siberia-2 Electron Storage Ring, ensuring stability of electron longitudinal motion for synchrotron dipole oscillations. // Novosibirsk, 2010, 43p, Preprint: INP 2010-6 (in Russian).
- 6 E.Yu. Kolesnikov, Yu.A. Tsidulko. Stochastic transport of sloshing ions. // Novosibirsk, 2010, 28p, Preprint: INP 2010-15 (in Russian).
- 7 I.I. Averbukh, V.P. Belov, V.I. Davydenko, P.P. Deichuli, A.A. Ivanov, V.A. Kapitonov, A.A. Podymnugin A.V. Sorokin, I.V. Shikhovtsev. Single aperture 70 mA, 50 keV radio-frequency proton source. // Novosibirsk, 2010, 12p, Preprint: Budker INP 2010-24.
- 8 M.G. Kozlov, A.V. Reznichenko, V.S. Fadin. Check of the gluon Reggeization condition. in the next-to-leading order. Quark part. // Novosibirsk, 2010, 27p, Preprint: INP 2010-26 (in Russian).
- 9 E.I. Zhmurikov, I.V. Savchenko, S.V. Stankus, Tecchio L Thermophysical properties measurements of graphite composites for the neutron target convertor. // Novosibirsk, 2010, 23p, Preprint: INP 2010-27 (in Russian).
- 10 V.P. Druzhinin, L.V. Kardopoltsev, V.A. Tayursky. The event generator for the two-photon process  $e^+e^- \rightarrow e^+e^- R(J^{PC}=0^{++})$  with account of radiative corrections in the single-tag mode. // Novosibirsk, 2010, 23p, Preprint: INP 2010-30 (in Russian).
- 11 V.V. Repkov. High-voltage linear transistor amplifiers. // Novosibirsk, 2010, 18p, Preprint: INP 2010-32 (in Russian).
- 12 E.A. Biberdorf, N.I. Popova. Nonsymmetric spectral problem. // Novosibirsk, 2010, 48p, Preprint: INP 2010-39 (in Russian).
- 13 Anashin V.V., Aulchenko V.M., Baldin E.M., Barladyan A.K., Barnyakov A.Yu., Barnyakov M.Yu., Basok I.Yu., Baru S.E., Bedny I.V., Beloborodova O.L., Blinov A.E., Blinov V.E., Bobrov A.V., Bobrovnikov V.S., A.V., Bondar A.E., Buzykaev A.R., Vorobiev A.I., Gulevich V.V., Dneprovsky L.V., Zhilich V.N., Zhulanov V.V., Karnaev S.E., Karpov G.V., Karpov S.V., Kononov S.A., Kotov K.Yu., Kravchenko E.A., Kudryavtsev V.N., Kuzmin A.S., Kulikov V.F., Kuper E.A., Levichev E.B., Malyshchev V.M., Maksimov D.A., Maslennikov A.L., Medvedko A.S., Muchnoi N.Yu., Nikitin S.A., Nikolaev I.B., Onuchin A.P., Oreshkin S.B., Orlov I.O., Osipov A.A., Peleganchuk S.V., Pivovarov S.G., Poluektov A.O., Pospelov G.E., Prisekin V.G., Ruban A.A., Rodyakin v.A., Savinov G.A., Skovpen Yu.I., Skrinsky A.N., Smaluk V.V., Snopkov R.G., Sokolov A.V., Sukharev A.M., Talyshev A.A., Tayursky V.A., Telnov V.I., Tikhonov Yu.A., Todyshev K.Yu., Usov Yu.V., Kharlamova T.A., Shamov A.G., Shwartz B.A., Shekhtman L.I., Shusharo A.I., S.I., Yuskov A.N. Detector KEDR. // Novosibirsk 2010, Preprint INP 2010-40 (in Russian).
- 14 S.A. Nikitin, I.B. Nikolaev. Calculation of Touschek electrons intensity in the VEPP-4M storage ring. // Novosibirsk, 2010, 24p, Preprint: INP 2010-42 (in Russian).

- 15 Rudenko A.S., Khriplovich I.B.  $K_{13}^+\gamma$  decay revisited: branching ratio and T-odd momenta correlation. E-print: ArXiv:1012.0147 [hep-ex].
- 16 Khriplovich I.B. Capture of dark matter by the Solar System. Simple estimates. // E-print: ArXiv:1004.3171 [hep-ex].
- 17 Bondar A., Buzulutskov A., Grebenuk A., Sokolov A., Akimov D., Alexandrov I., Breskin A. Geiger mode APD performance in a cryogenic two-phase Ar avalanche detector based on THGEMs. // E-print: arXiv:1003.1597.
- 18 Bondar A., Buzulutskov A., Grebenuk A., Sokolov A., Akimov D., Alexandrov I., Breskin A. Direct observation of avalanche scintillations in a THGEM-based two-phase Ar avalanche detector using Geiger-mode APD. // E-print: arXiv:1005.5216.
- 19 Bondar A.E., Dmitriev V.F., Milstein A.I., Strakhovenko V.M. // Nucleon polarization in the process  $e^+e^- \rightarrow N\bar{N}$  near threshold. // arXiv:1012.4638 [hep-ph].
- 20 Abe T., Bondar A.E., Buzulutskov A., Shekhtman L., Telnov V., et al. (ILD Concept Group - Linear Collider Collab.). The International Large Detector: Letter of Intent. // arXiv:1006.3396 [hep-ex].
- 21 Aushev T., Bondar A., et al. Physics at Super B Factory. // arXiv:1002.5012 [hep-ex].
- 22 Guler H., ..., Arinstein K., Aulchenko V., Eidelman S., Kuzmin A., Poluektov A., Zhilich V., Zhulanov V., et al. (Belle Collab.). Study of the  $K^+\pi^+\pi^-$  final state in  $B^+ \rightarrow J/\psi K^+\pi^+\pi^-$  and  $B^+ \rightarrow \psi' K^+\pi^+\pi^-$ . // arXiv, 1009.5256 [hep-ex].
- 23 Abe T., Arinstein K., Aulchenko V., Bondar A., Eidelman S., Epifanov D., Gabyshev N., Garmash A., Kuzmin A., Poluektov A., Shebalin V., Shwartz B., Usov Y., Vinokurova A., Zhilich V., Zhilich V., Zyukova O., et al. (Belle Collab.). Belle II technical design report. // E-print: arXiv:1011.0352 [physics.ins-det].
- 24 Pakhlova G., ..., Arinstein K., Bondar A., Eidelman S., Epifanov D., Gabyshev N., Garmash A., Kuzmin A., Poluektov A., Shebalin V., Shwartz B., Vinokurova A., Zhilich V., Zyukova O., et al. (Belle Collab.). // arXiv:1011.4397 [hep-ex].
- 25 Bashkanov M., Shwartz B., et al. Exclusive Measurement of the  $pp \rightarrow nn p^+p^-$  Reaction at 1.1 GeV. // arXiv:1012.1463 [nucl-ex].
- 26 Asner D., Shwartz B., et al. (By Heavy Flavor Averaging Group), et al. Averages of b-hadron, c-hadron, and  $\tau$ -lepton Properties. // arXiv:1010.1589 [hep-ex].
- 27 Sciascia B., ..., Sibidanov A.L., et al. (KLOE Collaboration). Kaon physics with KLOE. // E-print: arXiv:1005.2873 [hep-ex].
- 28 Babusci D., ..., Lukin P.A., et al. (KLOE2 Collaboration). Proposal for taking data with the KLOE-2 detector at the DAFNE collider upgraded in energy. // E-print: arXiv:1007.5219 [hep-ex].
- 29 Webber D.M., ..., Logashenko I.B., et al. (MuLan Collab.). Measurement of the Positive Muon Lifetime and Determination of the Fermi Constant to Part-per-Million Precision. // E-print: arXiv:1010.0991 [hep-ex].
- 30 Sanchez P. del Amo, ..., Blinov V.E., Bukin A.D., Druzhinin V.P., Golubev V.B., Onuchin A.P., Serednyakov, S.I., Skovpen Yu.I., Solodov E.P., Todyshev K.Yu., et al. (BABAR Collab.). Observation of the Rare Decay  $B^+ \rightarrow K^+\pi^0\pi^0$ . // E-print: arXiv:1005.3717 [hep-ex].
- 31 Sanchez P. del Amo, ..., Blinov V.E., Bukin A.D., Druzhinin V.P., Golubev V.B., Onuchin A.P., Serednyakov, S.I., Skovpen Yu.I., Solodov E.P., Todyshev K.Yu., et al. (BABAR Collab.). Study of  $B \rightarrow \pi l \nu$  and  $B \rightarrow r l \nu$  decays and determination of  $|V_{ub}|$ . // E-print: arXiv:1005.3288 [hep-ex].
- 32 Lees J.P., ..., Blinov V.E., Bukin A.D., Druzhinin V.P., Golubev V.B., Onuchin A.P., Serednyakov, S.I., Skovpen Yu.I., Solodov E.P., Todyshev K.Yu., et al. (BABAR Collab.). Measurement of the Branching fraction for  $D_s^+ \rightarrow \tau^+ \nu_\tau$  and extraction of the decay constant  $f_{D_s}$ . // E-print: arXiv:1003.3063 [hep-ex].
- 33 Akhmetshin R.R., Aulchenko V.M., Banzarov V.Sh., Barkov L.M., Baru S.E., Bashtovoy N.S., Bondar A.E., Bragin A.V., Eidelman S.I., Epifanov D.A., Fedotov G.V., Gabyshev N.I., Grebenuk A.A., Grigoriev D.N., Ignatov F.V., Karpov S.V., Kazanin V.F., Khazin B.I., Koop I.A., Krokovny P.P., Kuzmin A.S., Logashenko I.B., Lukin P.A., Lysenko A.P., Mikhailov K.Yu., Okhapkin V.S., Perevedentsev E.A., Popov A.S., Redin S.I., Ruban A.A., Ryskulov N.M., Shatunov Yu.M., Shwartz B.A., Sibidanov A.L., Snopkov I.G., Solodov E.P., Yudin Yu.V., Zaytsev A.S., et al. (CMD-2 and CMD-2 Collab.). Measurement of  $\phi(1020)$  meson leptonic width with CMD-2 detector at VEPP-2M

- Collider. // E-print: arXiv:1010.4878 [hep-ex].
- 34 Cherepanov V., Eidelman S. CVC and  $\tau \rightarrow \eta \eta' \pi \pi^0 \nu_\tau$ . // E-print: arXiv:1012.2564 [hep-ex].
- 35 Brambilla N., Eidelman S., Levichev E. Heavy quarkonium: progress, puzzles, and opportunities. // E-print: arXiv:1010.5827 [hep-ph].
- 36 Eidelman S. Two-photon interactions at Belle and BaBar. // 13th Intern. Conference on Elastic and Diffractive Scattering (Blois Workshop) "Moving Forward into the LHC Era". / M. Deile, S. Eidelman, et al. - Feb 2010. - 514p. // E-print: arXiv:1002.3527 [hep-ph], P.330.
- 37 Lee R.N., Terekhov I.S. Application of the DRA method to the calculation of the four-loop QED-type tadpoles. // arXiv:1010.6117 [hep-ph].
- 38 Lee R.N., Smirnov A.V. Analytic epsilon expansions of master integrals corresponding to massless three-loop form factors and three-loop g-2 up to four-loop transcendentality weight. // arXiv:1010.1334 [hep-ph].
- 39 Blinov A.E., Rudenko A.S. Upper limits on electric and weak dipole moments of W-boson. // arXiv:1010.2018 [hep-ph].
- 40 Biagini M., Koop I., Levichev E.B., Nikitin S.A., Piminov P.A., Shatilov D.N., Sinyatkin S.V., et al. SuperB Progress Reports - Accelerator. // E-print: arXiv:1009.6178, 2010 [hep-ph].
- 41 Nikolenko D.M., et al., Mishnev S.I., Muchnoi N.Yu., Neifeld V.V. Two-photon exchange and elastic scattering of positrons/electrons on the proton. // PoS ICHEP2010:164, 2010 [hep-ph].
- 42 V.P. Druzhinin, L.A. Kardapolzev, V.A. Tayursky. The event generator for the two-photon process  $e^+e^- \rightarrow e^+e^- R(J^{PC}=0^{++})$  in the single-tag mode. // E-print: 5969v1 2010, 28 Oct 2010 [hep-ph].
- 43 Eidelman S.I., Fedotov G.V., Kuraev E.A., Sibidanov A.L. Monte-Carlo Generator Photon Jets for the process  $e^+e^- \rightarrow \gamma\gamma$ . // E-print: arXiv: 1009.3390 [hep-ex].
- 44 O.V. Zhironov, A.S. Pikovsky and D.L. Shepelyansky. Quantum compacton vacuum. // E-print: arXiv: 1005.0778v1 [cond-mat.stst-mech] (2010).
- 45 Wolski A., Korostelev M., Panagiotidis K., Thorley A., Malyshev O., Collomb N., Lucas J., Postlethwaite S., Zolotarev K. ILC damping ring design studies at the Cockcroft Institute. // Daresbury, 2010. - 91 p. - [ILC-NOTE-2010-057; Cockcroft-10-57].
- 46 G. Aad, ..., V.A. Kazanin, G.M. Kolachev, A. Korol, K.Yu. Kotov, V. Malyshev, A.L. Maslennikov, I. Orlov, V.S. Panin, S.V. Peleganchuk, K. Skovpen, A.G. Schamov, A. Soukharev, A. Talyshev, Yu. A. Tikhonov, A. Zaytsev, et al. (ATLAS Collab.). Measurement of inclusive jet and dijet cross sections in proton-proton collisions at 7 TeV centre-of-mass energy with the ATLAS detector. // E-print: arXiv:1009.5908, 2010.
- 47 G. Aad, ..., V.A. Kazanin, V. Malyshev, A.L. Maslennikov, I. Orlov, S.V. Peleganchuk, A.G. Schamov, K. Skovpen, A. Soukharev, A. Talyshev, Yu. A. Tikhonov, A. Zaytsev, et al. (ATLAS Collab.). Studies of the performance of the ATLAS detector using cosmic-ray muons. // E-print: arXiv:1011.6665, 2010.
- 48 G. Aad, ..., V.B. Bobrovnikov, A. Bogdanchikov, V.A. Kazanin, G.M. Kolachev, A. Korol, V. Malyshev, A.L. Maslennikov, I. Orlov, S.V. Peleganchuk, K. Skovpen, A.G. Schamov, A. Soukharev, A. Talyshev, Yu. A. Tikhonov, A. Zaytsev, et al. (ATLAS Collab.). Measurement of underlying event characteristics using charged particles in pp collisions at  $\sqrt{s} = 900$  GeV and 7 TeV with the ATLAS detector. // E-print: arXiv:1012.0791, 2010.
- 49 G. Aad, ..., V.B. Bobrovnikov, A. Bogdanchikov, V.A. Kazanin, G.M. Kolachev, A. Korol, V. Malyshev, A.L. Maslennikov, I. Orlov, S.V. Peleganchuk, K. Skovpen, A.G. Schamov, A. Soukharev, A. Talyshev, Yu. A. Tikhonov, A. Zaytsev, et al. (ATLAS Collab.). Measurement of the top quark-pair production cross section with ATLAS in pp collisions at  $\sqrt{s} = 7$  TeV. // E-print: arXiv:1012.1792, 2010.
- 50 G. Aad, ..., V.B. Bobrovnikov, A. Bogdanchikov, V.A. Kazanin, G.M. Kolachev, A. Korol, V. Malyshev, A.L. Maslennikov, I. Orlov, S.V. Peleganchuk, K. Skovpen, A.G. Schamov, A. Soukharev, A. Talyshev, Yu. A. Tikhonov, A. Zaytsev, et al. (ATLAS Collab.). Search for diphoton events with large missing transverse energy in 7 TeV proton-proton collisions with the ATLAS detector. // E-print: arXiv:1012.4272, 2010.
- 51 G. Aad, ..., V.B. Bobrovnikov, A. Bogdanchikov, V.A. Kazanin, G.M. Kolachev, A. Korol, V. Malyshev, A.L. Maslennikov, I. Orlov, S.V. Peleganchuk, K. Skovpen, A.G. Schamov, A. Soukharev, A. Talyshev, Yu. A. Tikhonov, A. Zaytsev, et al. (ATLAS Collab.). Measurement of the inclusive isolated

- prompt photon cross section in pp collisions at  $\sqrt{s} = 7$  TeV with the ATLAS detector. // E-print: arXiv:1012.4389, 2010.
- 52 G. Aad, ..., V.B. Bobrovnikov, A. Bogdanchikov, V.A. Kazanin, G.M. Kolachev, A. Korol, V. Malyshev, A.L. Maslennikov, I. Orlov, S.V. Peleganchuk, K. Skovpen, A.G. Schamov, A. Soukharev, A. Talyshev, Yu. A. Tikhonov, A. Zaytsev, et al. (ATLAS Collab.). Charged particle multiplicities in pp interactions measured with the ATLAS detector at the LHC. // E-print: arXiv:1012.5104, 2010.
- 53 G. Aad, ..., V.B. Bobrovnikov, A. Bogdanchikov, V.A. Kazanin, G.M. Kolachev, A. Korol, V. Malyshev, A.L. Maslennikov, I. Orlov, S.V. Peleganchuk, K. Skovpen, A.G. Schamov, A. Soukharev, A. Talyshev, Yu. A. Tikhonov, A. Zaytsev, et al. (ATLAS Collab.). Measurement of the production cross section for W bosons in association with jets in pp collisions at  $\sqrt{s} = 7$  TeV with the ATLAS detector. // E-print: arXiv:1012.5382, 2010.
- 54 G. Aad, ..., V.B. Bobrovnikov, A. Bogdanchikov, V.A. Kazanin, G.M. Kolachev, A. Korol, V. Malyshev, A.L. Maslennikov, I. Orlov, S.V. Peleganchuk, K. Skovpen, A.G. Schamov, A. Soukharev, A. Talyshev, Yu. A. Tikhonov, A. Zaytsev, et al. (ATLAS Collab.). Measurement of the centrality dependence of  $J/\psi$  yields and observation of Z production in lead-lead collisions with the ATLAS detector at the LHC. // E-print: arXiv:1012.5419, 2010.
- 55 Aamodt K., ALICE Collab., Pestov Yu., et al. Centrality dependence of the charged-particle multiplicity density at midrapidity in Pb-Pb collisions at radical  $\sqrt{s_{NN}}=2.76$  TeV. // E-print: arXiv:1012.1657, 2010.
- 56 Shepelyansky D.L., Zhiron O.V. Towards Google matrix of brain. // E-print: arXiv:1002.4583v2 [cond-mat.dis-nn] (2010).
- 57 Zhiron A.O., Zhiron O.V., Shepelyansky D.L. Two-dimensional ranking of Wikipedia articles. // E-print: arXiv:1006.4270v1 [cs.IR] (2010).
- 58 Rudenko A.S., Khriplovich I.B. Can CP-violation be observed in heavy-ion collisions? // E-print: ArXiv:1003.3339 [hep-ex].
- 59 V.M. Aulchenko, O.L. Beloborodova, A.V. Bobrov, A.E. Bondar, V.N. Zhilich, V.V. Zhulanov, V.N. Kudryavtsev, A.G. Shamov, L.I. Shekman. Triple-GEM detectors in the tagging system. // Novosibirsk 2010, Preprint INP 2010-41 (in Russian).

### Authorial papers-2010

1. Khilchenko A.D. Hardware infrastructure measurement and control systems of plasma traps INP SB RAS. // 01.04.01 – instruments and methods of experimental physics. Author. papers of thesis for the degree of doctor of technical science: Novosibirsk, 2010, BINP, SB RAS.
2. Meshkov O.I. Methods of optical diagnostics of the electron-positron beams and plasma interaction with a high-current electron beam. // 01.04.08 - physics of plasma; 01.04.20 - physics of charged particle beams and accelerator techniques, Author. papers of thesis for the degree of doctor of phys.-math. science: Novosibirsk, 2010, BINP, SB RAS.
3. Smalyuk V.V. The suppression of the collective beam instability in electron-positron storage // 01.04.20 - physics of charged particle beams and accelerator techniques, Author. papers of thesis for the degree of doctor of phys.-math. science: Novosibirsk, 2010, BINP, SB RAS.
4. Nemytov P.I. Systems of power and control a series of high-voltage industrial electron accelerators with the capacity of the extracted beam hundreds of kilowatts. // 01.04.20 - physics of charged particle beams and accelerator techniques, Author. papers of thesis for the degree of doctor of technical science: Novosibirsk, 2010, BINP, SB RAS.
5. Tolochko B.P. In situ investigation of the fast chemical reactions by X-ray methods at synchrotron radiation beams. // 02.00.21 - solid state chemistry. Author. papers of thesis for the degree of doctor of chemical science: Novosibirsk, 2010, BINP, SB RAS.
6. Grabovsky A.V. Möbius form of the BFKL kernel. // 01.04.02 - theoretical physics. Author. papers of thesis for the degree of doctor of phys.-math. science: Novosibirsk, 2010, BINP, SB RAS.

7. Belikov O.V. Current sources for the correction magnets in accelerators and storage rings. // 01.04.08 - physics of plasma, Author. papers of thesis for the degree of candidate of technical science: Novosibirsk, 2010, BINP, SB RAS.
8. Timofeev I.V. Nonlinear dynamics of powerful electron beam during evolution of plasma turbulence. // 01.04.08 - physics of plasma, Author. papers of thesis for the degree of candidate of phys.-math. science: Novosibirsk, 2009, BINP, SB RAS
9. Sulyaev Yu.S. Experimental investigation of plasma heating and confinement in multimirror trap GOL-3 by means of neutron emission. // 01.04.08 - physics of plasma, Author. papers of thesis for the degree of candidate of phys.-math. science: Novosibirsk, 2010, BINP, SB RAS
10. Berkaev D.E. Injection of electrons and positrons in the collider VEPP-2000. // 01.04.20 - physics of charged particle beams and accelerator techniques, Author. papers of thesis for the degree of candidate of phys.-math. science: Novosibirsk, 2010, BINP, SB RAS.
11. Baldin E.M. Measurement of the products of the electron width of the  $J/\psi$  meson and the branching fraction of its decays to the lepton pairs. // 01.04.16 - elementary particle physics, and atomic nuclear physics. Author. papers of thesis for the degree of candidate of phys.-math. science: Novosibirsk, 2009, BINP, SB RAS.
12. Kharlamov A.G. Study of the process  $e^+e^- \rightarrow \pi^+\pi^-\pi^0$  at energies  $2E < 1$  GeV with the SND detector. // 01.04.16 - elementary particle physics, and atomic nuclear physics. Author. papers of thesis for the degree of candidate of phys.-math. science: Novosibirsk, 2010, BINP, SB RAS.
13. Korobeinikov M.V. Complex electron-beam treatment on the basis of the upgraded accelerator ILU-6 and treatment technology medical products. // 01.04.20 - physics of charged particle beams and accelerator techniques, Author. papers of thesis for the degree of candidate of technical science: Novosibirsk, 2010, BINP, SB RAS.
14. Bondarenko A.V. A beam extraction scheme from a synchrotron using a magnetic shield. // 01.04.20 - physics of charged particle beams and accelerator techniques, Author. papers of thesis for the degree of candidate of phys.-math. science: Novosibirsk, 2010, BINP, SB RAS.
15. Erokhin A.I. Energy recuperation and extraction from the inductive and capacitive energy storage circuits. // 01.04.20 - physics of charged particle beams and accelerator techniques, Author. papers of thesis for the degree of candidate of technical science: Novosibirsk, 2010, BINP, SB RAS.
16. Piminov P.A. Numerical simulation and optimization of nonlinear motion parameters of particles in the circular accelerator. Numerical simulation and optimization of the nonlinear motion of particles in cyclic accelerators. // 01.04.20 - physics of charged particle beams and accelerator techniques, Author. papers of thesis for the degree of candidate of phys.-math. science: Novosibirsk, 2010, BINP, SB RAS.

### **Participation in conferences**

1. 3rd International Workshop "High Energy Physics in the LHC Era", January 4 - 8, 2010, Valparaiso, Chile.
2. Workshop "Physics for Health in Europe", Workshop Physics for Health in Europe Workshop, 2 - 4 February 2010, CERN - Switzerland.
3. XXXVII International Zvenigorod Conference on Plasma Physics and Controlled Fusion, 8 - 12 February, 2010, Zvenigorod, Russia.
4. 12th Vienna Conference on Instrumentation, 15-20 February, 2010, Vienna, Austria.
5. 2nd International Conference on Metamaterials, Photonic Crystals and Plasmonics (META'10), February 22 - 25, 2010, Cairo, Egypt.
6. THz-Bio Workshop, March 9 - 10, SNU, Korea.
7. XLIV PNPI Winter School, 9 - 14 March, 2010, Roschino, Russia.
8. Zababakhin readings: X International Conference, 15 - 19 March, 2010, Snezhinsk, Russia.
9. International Linear Collider Workshop (LCWS10), March 26 - 30, 2010, Beijing, China.
10. Deep-Inelastic Scattering Workshop, April, 2010, Florence, Italy.

11. «XII Kharitonov Reading" of the International Scientific Conference on High Energy Density Physics, 19 - 23 April, 2010, Sarov, Nizhny Novgorod region, Russia.
12. Scientific Conference of Students Physicists, 22-29 April, 2010, Volgograd, Russia.
13. XIV International Conference on Calorimetry in High Energy Physics (Calor 2010), 10 - 14 May, 2010, Beijing, China.
14. 1st International Particle Accelerator Conference (IPAC'10), 23 - 28 May, 2010, Kyoto, Japan.
15. IV All-Russian National Congress of Radiation Diagnosticians and Theraputists «Radiology - 2010», 25 - 27 May, 2010, Moscow, Russia.
16. XIII SuperB General Meeting, 30 May - 5 June, 2010, Isola d'Elba.
17. International Conference "Chaotic Modeling and Simulation" (Chaos 2010), June 1 - 4, 2010, Chania, Crete, Greece.
18. 3rd International Conference "Current Problems in Nuclear Physics and Atomic Energy", June 7 - 11, 2010, Kyiv, Ukraine.
19. XII International Conference on Laser Applications in Life Sciences (LALS-2010), June 9 - 11, 2010, Oulu, Finland.
20. 9th European Solid Oxide Fuel Cell Forum, 29 June - 2 July 2010, Lucerne, Switzerland.
21. IASTED International Conference on Automation, Control and Instrumentation Technology (ACIT-CDA-2010), June 2010, Novosibirsk, Russia.
22. All-Russian Conference "Physical Chemistry 2010", June, 2010, Tuapse.
23. International Conference of V.N Gribov memory, June, Trieste, Italy.
24. 8th International Conference on Open Magnetic Systems for Plasma Confinement, Novosibirsk: BINP, Russia.
25. International Conference "Hadron Structure and QCD: from Low to High Energies", July 5 - 9, 2010, Gatchina, Russia.
26. LX International Conference on Nuclear Physics, July 6 - 9, 2010, St.Petersburg.
27. XVIII International Conference on Synchrotron Radiation (SR-2010), 19 - 22 July 2010, Novosibirsk: BINP, Russia.
28. 5th International Conference on Software and Data Technologies, 22 - 24 July, 2010, Athenes, Greece.
29. 35th International Conference of High Energy Physics (ICHEP 2010), July 22 - 28, 2010, Paris, France.
30. International Symposium "Terahertz radiation: generation and application", 26 - 28 July 2010, Novosibirsk: BINP SB RAS, Russia.
31. International Conference on Nanostructures for Biology and Medicine, Novosibirsk: Institute of Chemistry and Biology. Russia.
32. 18th International Vacuum Congress, August 23 - 27, 2010, Beijing, China.
33. XIX International Conference on Coherent and Nonlinear Optics, Lasers, their Applications and Technology (ICONO/LAT 2010), 23 - 27 August, 2010, Kazan (Tatarstan), Russia.
34. 13th ISTC SAC Seminar "New Perspectives of High Energy Physics", 1 - 5 September, 2010, Novosibirsk: BINP SB RAS, Russia.
35. 35th International Conference on Infrared, Millimeter, and Terahertz Waves (IRMMW-THz 2010), 5 - 10 September, 2010, Rome, Italy.
36. 6th World Congress on Industrial Process Tomography, 6-9 September, 2010, Beijing, China.
37. Annual Scientific Conference "Basic Sciences - Medicine, Novosibirsk, Russia.
38. International Conference "Diffraction 2010", September 10 - 15, 2010, Otranto (Lecce), Italy.
39. E-MRS Fall Meeting, 13-17 September 2010, Warsaw, Poland.
40. 11th International Workshop on Accelerator Alignment (IWAA10), 13 - 17 September 2010, DESY, Hamburg.
41. 4th International Congress on Advanced Electromagnetic Materials in Microwaves and Optics "Metamaterials-2010", September 13 - 18, 2010, Karlsruhe, Germany.
42. 10th International Conference on Modification of Materials with Particle beams and Plasma Flows, 2010, 19 - 24 September, Tomsk, Russia.
43. X International Conf. on Actual Problems of Electronic Instrument Engineering (APEIE-2010), 22-24 September, 2010, Novosibirsk, Russia.
44. 40th European Microwave Conference, September 28-30, 2010, Paris, France.

45. RuPAC XXII: Russian Particle Accelerator Conference, September 27 - October 1, 2010, IHEP Protvino, Russia.
46. International Conference (HB2010), September 27 - October 1, 2010, Morschach, Switzerland.
47. XIV SuperB General Meeting, 27 September - 1 October, 2010, LNF.
48. 11th International Workshop on Tau Lepton Physics, September, 2010, Manchester, UK.
49. 19th Intern. Spin Physics Symposium (SPIN-2010), September 27 - October 2, 2010, Juelich, Germany.
50. I Congress of Doctors of Beam Diagnostics RFD «Achievements, prospects and the basic directions of development of beam diagnostics in Siberia», 7 - 8 October, 2010, Novosibirsk, Russia.
51. 3rd School for Young Professional, "Synchrotron Radiation in the Earth Sciences", 11 - 15 October, Novosibirsk: BINP SB RAS, Russia.
52. 23rd IAEA Fusion Energy Conference, 11 - 16 October 2010, Daejeon, Republic of Korea.
53. International Workshop on Linear Colliders (IWLC2010), ECFA-CLIC-ILC Joint Meeting, October 18-22, 2010, CERN, Switzerland.
54. 18th International Conference on Computing in High Energy and Nuclear Physics, 18-22 October, 2010, Taipei, Taiwan.
55. 4th International Workshop on Charm Physics (Charm2010), October 21-24, 2010, IHEP, Beijing, China.
56. 14th International Congress on Neutron Capture Therapy, October 25 - 29, 2010, Buenos Aires, Argentina.
57. 17th International Symposium on Laser Spectroscopy (SOLS 2010), November 4 - 5, 2010, Daejeon, Korea.
58. 2nd International Symposium on Negative Ions and Sources, November 16 - 19, 2010, Takayama, Gifu, Japan.
59. XXI Meeting on the use of Neutron Scattering Studies of Condensed Matter, 16 -19 November, 2010, Russian Research Center «Kurchatov Institute», Moscow, Russia.
60. V International Scientific Conference «Modern Problems of Machine Construction», 23 - 26 November, 2010, Tomsk, Russia
61. BINP-KEK Workshop on Noble Liquid TPC, 24 - 25 November, 2010, KEK, Japan.
62. 1st International Symposium on Polymer Modification with High Energy Electrons, 24-26 November, 2010, Dresden, Germany.
63. 2nd Joint Asian Accelerator Workshop (2JAAWS), 29-30 November, POSTECH, Pohang, Korea.
64. All-Russian Scientific Conference of Young Scientists: Science. Technologies. Innovations, 3 - 5 December, 2010, Novosibirsk: NSTU, Russia.
65. III All-Russia Meeting «Precision Physics and Fundamental Physical Constants», 7 - 10 December, 2010, St-Petersburg, Russia.
66. International Symposium «50 Years on the Road to Quantum Unit of SR», 6 December. 2010, St-Petersburg, Russia.
67. NAARI International Conference (NIC-2010): Isotope Technologies and Applications - New Horizons, December 13-15, 2010, Powai, Mumbai, India.
68. Plenary RED Collaboration Workshop, 23 December, Moscow, Russia.
69. International Conference "Channaling 2010", Ferrara, Italy.
70. 21st International Conference on the Application of Accelerators in Research and Industry, 2010, USA.
71. International Conference-School on Plasma Physics and Controlled Fusion and the 4th International Workshop on the Role of Electric Fields in Plasma Confinement in Stellarators and Tokamaks, 2010, Alushta, Ukraine.
72. Innovative Confinement Concepts Workshop, 2010, Princeton University, Princeton, NJ.
73. VII International Conference "Radiation-Thermal Effects and Processes in Inorganic Matters", 2010, Tomsk, Russia.
74. 16th International Symposium on High Current Electronics, 2010, Tomsk, Russia.
75. 37th EPS Conference on Plasma Physics, 2010, Ireland.
76. XLVII International Student Scientific Conference "Student and Scientific-Technical Progress", 2010, Novosibirsk, Russia.
77. VI International Conference «Technical Means to Counter Terrorism and Criminal Explosions», 2010, St.Petersburg, Russia.

## List of Collaboration Agreements between the Budker INP and Foreign Laboratories

Name of Laboratory		Title or Field of Collaboration	Dates	Principal Investigators
<i>N<sup>o</sup></i>	<i>1</i>	<i>2</i>	<i>3</i>	<i>4</i>
1	<i>Daresbury (England)</i>	Generation and utilization of SR.	1977	<i>G. Kulipanov (INP); I. Munro (Daresbury)</i>
2	<i>BESSY (Germany)</i>	Development of the wigglers for BESSY-2.	1993	<i>A. Skrinsky, N. Mezentsev (INP); E. Jaeschke (BESSY)</i>
3	<i>Research Centre Rossendorf (Germany)</i>	Physical foundations of a plasma neutron source.	1994	<i>E. Kruglyakov, A. Ivanov (INP); K. Noack (Germany)</i>
4	<i>Nuclear Centre "Karlsruhe" (Germany)</i>	1. Development of conceptual project and data base for neutron source on the basis of GDT device. 2. Simulation of processes in diverter of ITER device.	1994	<i>E. Kruglyakov, A. Ivanov, A. Burdakov (INP); G. Kessler (Germany)</i>
5	<i>GSI (Germany)</i>	Collaboration in the field of accelerator physics: electron cooling; electron-ion colliders.	1995	<i>Yu. Shatunov, V. Parkhomchuk (INP); H. Eickhoff (GSI)</i>
6	<i>DESY (Germany)</i>	Elementary-particle physics, synchrotron radiation, accelerator physics and technology, electronics and experimental equipment.	1995	<i>A. Skrynsky, G. Kulipanov (INP); A. Vagner, K. Scherff (DESY)</i>
7	<i>CELLS (Spain)</i>	Collaboration in the field of application of new equipment for SR sources.	2008	<i>E. Levichev (INP); Joan Bordas and Orpinell (CELLS)</i>
8	<i>CIEMAT (Spain)</i>	Accelerator technology and plasma physics.	2007	<i>E. Levichev (INP), J. Rubio (CIEMAT)</i>
9	<i>INFN (Italy)</i>	Development of intense source for radioactive ion beams for experiments in nuclear physics	1984	<i>P. Logachev (INP); L. Techio (INFN)</i>
10	<i>University of Milan (Italy)</i>	Theoretical and numerical studies of dynamic chaos in classic and quantum mechanics.	1991	<i>A. Skrynsky, V. Sokolov (INP); T. Montegazza, J. Kasati (Italy)</i>
11	<i>INFN-LNF (Italy)</i>	Development of collider project DAFNE-II	2004	<i>E. Levichev (INP); S. Biscari (INFN-LNF)</i>
12	<i>University of Padua (Italy)</i>	Development of cryogenic detectors for experiments in neutrino physicist.	2008	<i>Yu. Tikhonov, A. Bondar (INP); A. Gudlielmi (Italy)</i>
13	<i>National Nuclear Center. Park of Nuclear Technology (Kazakhstan)</i>	Development and application of industrial accelerators, generation and utilization of neutron beams, development of SR sources, RF-generators.	2007	<i>G. Kulipanov (INP); K. Kadyrzhanov, A. Kusainov (Kazakhstan)</i>

<i>№</i>	<i>1</i>	<i>2</i>	<i>3</i>	<i>4</i>
14	<i>National Nuclear Center. Al-Farabi National University (Kazakhstan)</i>	Creation and development of a multi-purpose research complex of radiation technology and terahertz radiation.	2009	<i>G. Kulipanov (INP); K. Kadyrzhanov, B. Zhumagulov (Kazakhstan)</i>
15	<i>Institute of Morden Physics and Techniques, Lanchzou (China)</i>	Collaboration in the field of accelerator physics: electron cooling	2000	<i>V. Parkhomchuk (INP); S. Yang (KHP)</i>
16	<i>WOER Company, Shenzhen, (China)</i>	Using of electron accelerator ILU-10, exchanging of personal, information and experimental equipment.	2005	<i>A. Bryazgin (INP); Leo Li (WOER)</i>
17	<i>SINAP Shanghai, (China)</i>	Researching in field of industrial electron accelerators.	2006	<i>A. Bryazgin (INP); Hu Hounku (SINAP)</i>
18	<i>IHEP (China)</i>	Work of Chinese scientists on BINP installations, work of BINP scientists on IHEP installations.	2007	<i>A. Skrinsky (INP); H. Chen (IHEP)</i>
19	<i>Industrial and Technological Center of Cooperation with Russia and Belorussia of Heilongjiang Province (P.R.C) (China)</i>	Exchange of information about BINP-developed devices and the technology and product demand of the Chinese factories	2009	<i>D. Grigoriev (INP); Zhan Hun-Vei (P.R.C)</i>
20	<i>POSTECH (Korea)</i>	Creation of beam accelerators, add-on devices, SR experiments.	1992	<i>A. Skrinsky, N. Mezentsev (INP); H. Kim (POSTECH)</i>
21	<i>KAERI (Korea)</i>	Development of FEL and accelerator-recuperator.	1999	<i>N. Vinokurov (INP); B.Ch. Lee (KAERI)</i>
22	<i>BNL, Brookhaven (USA)</i>	1. Measurement of the magnetic muon anomaly. 2. Joint research of RHIC spin.	1991 1993	<i>L. Barkov (INP); J. Bunse (BNL) Yu. Shatunov (INP); S. Ozaki (BNL)</i>
23	<i>ANL, Argonn (USA)</i>	1. Experiments with polarized gas jet target at VEPP-3. 2. SR instrumentation.	1988 1993	<i>L. Barkov (INP); R. Holt (ANL) G. Kulipanov, A. Skrinsky (INP); G. Shenoy (USA)</i>
24	<i>University of Pittsburgh (USA)</i>	Experiments on VEPP-2M and $\phi$ -factory.	1989	<i>S. Eidelman, E. Solodov (INP); V. Savinov (USA)</i>
25	<i>University of Duke (CIIA)</i>	Free electron lasers.	1992	<i>N. Vinokurov (INP); J. Wu (Duke)</i>

<i>№</i>	<i>1</i>	<i>2</i>	<i>3</i>	<i>4</i>
26	<i>BNL, Brookhaven (USA)</i>	Collaboration on electron-ion colliders.	1993	<i>V. Parkhomchuk (INP); I. Benzvi (USA)</i>
27	<i>FERMILAB (USA)</i>	Collaboration in the field of accelerator physics: electron cooling; conversion system.	1995	<i>V. Parkhomchuk (INP); O. Finli (FERMILAB)</i>
28	<i>FERMILAB (USA)</i>	Exchange of scientists and engineers for scientific research.	2005	<i>A. Skrinsky (INP); P. Oddone (FERMILAB)</i>
29	<i>SLAC, Stanford (USA)</i>	Obtainment of submicron beams and intensive positron beams, development of B-factory elements, detectors, RF-generators based on magnicons.	1994	<i>A. Skrinsky (INP); Persis Drel (SLAC)</i>
30	<i>Institute of Plasma Physics ASCR (Czech Republic)</i>	Collaboration in the field of plasma physics and plasma diagnostics research.	2008	<i>A. Ivanov (INP); P. Hruška (Czech Republic)</i>
31	<i>CERN (Switzerland)</i>	<b>1.</b> Research and development of the detectors for LHC.  <b>2.</b> Development of the LHC elements.	1992  1996	<i>A. Bondar, Yu. Tikhonov (INP); T. Nakada, P. Yenni (CERN)</i> <i>V. Anashin (INP); L. Evans (CERN)</i>
32	<i>Paul Scherrer Institute (Switzerland)</i>	Collaboration in the field of particle physics.	2009	<i>D. Grigoriev (INP); D. Mecom (Paul Scherrer Institute)</i>
33	<i>CERN (Switzerland)</i>	Research and development of micro-pattern detector technology..	2009	<i>Yu. Tikhonov (INP); S. Bertolucci (CERN)</i>
34	<i>CERN (Switzerland)</i>	Collaboration in the development of the electron-positron colliders with super-high luminosity.	2009	<i>E. Levichev (INP); S. Myers (CERN)</i>
35	<i>RIKEN Spring-8 (Japan)</i>	Collaboration in the field of accelerator physics and synchrotron radiation	1996	<i>G. Kulipanov (INP); H. Kamitsubo (Japan)</i>
36	<i>KEK (Japan)</i>	Research in accelerator physics and allied fields, development of elementary particle detectors.	1995	<i>A. Skrinsky (INP); A. Suzuki (KEK)</i>
37	<i>Center of Plasma Research, Tsukuba (Japan)</i>	Collaboration on Open traps.	2007	<i>A. Ivanov (INP); T. Imai (Japan)</i>

## Research Personnel

### Members of Russian Academy of Science

#### Academicians:

*Barkov Lev Mitrofanovich*

*Kruglyakov Edward Pavlovich*

*Kulipanov Gennady Nikolaevich*

*Skrinsky Alexandr Nikolaevich*

#### Corresponding members RAS:

*Bondar Alexandr Evgenievich*

*Dikansky Nikolai Sergeevich*

*Dimov Gennady Ivanovich*

*Parkhomchuk Vasily Vasilievich*

*Khriplovich Iosif Bentsionovich*

*Shatunov Yury Michailovich*

### Director Board

#### Director:

*Skrinsky Alexandr Nikolaevich*

#### Adviser RAS:

*Kruglyakov Edward Pavlovich*

#### Deputy Director (scientific):

*Ivanov Alexandr Alexandrovich*

*Kulipanov Gennady Nikolaevich*

*Levichev Evgeny Borisovich*

*Tikhonov Yury Anatolievich*

#### Scientific Secretary:

*Vasiliev Aleksei Vladimirovich*

### Scientific Council

- |   |                  |
|---|------------------|
| 1. Academician, Chairman                                  | Skrinsky A.N.    |
| 2. Doctor of phys.-math. science, Co-Chairman             | Ivanov A.A.      |
| 3. Academician, Co-Chairman                               | Kulipanov G.N.   |
| 4. Doctor of phys.-math. science, Co-Chairman             | Levichev E.B.    |
| 5. Doctor of phys.-math. science, Co-Chairman             | Tikhonov Yu.A.   |
| 6. Candidate of phys.-math. science, Scientific Secretary | Vasiliev A.V.    |
| 7. Candidate of techn. science                            | Anashin V.V.     |
| 8. Doctor of phys.-math. science, Professor               | Arzhannikov A.V. |
| 9. Academician  | Barkov L.M.      |
| 10. Candidate of phys.-math. science                      | Blinov V.E.      |
| 11. Corr. Member RAS                                      | Bondar A.E.      |
| 12. Doctor of phys.-math. science, Professor              | Burdakov A.V.    |

13. Doctor of phys.-math. science, Professor	Vinokurov N.A.
14. Corr. Member RAS	Dikansky N.S.
15. Corr. Member RAS	Dimov G.I.
16. Doctor of phys.-math. science	Druzhinin V.P.
17. Doctor of phys.-math. science	Koop I.A.
18. Academician	Kruglyakov E.P.
19. Doctor of techn. science	Kuper E.A.
20. Doctor of phys.-math. science	Logachev P.V.
21. Candidate of techn. science	Medvedko A.S.
22. Doctor of phys.-math. science	Mezentsev N.A.
23. Corr. Member RAS	Parkhomchuk V.V.
24. Doctor of techn. science, Professor	Salimov R.A.
25. Doctor of phys.-math. science, Professor	Serednyakov S.I.
26. Doctor of phys.-math. science, Professor	Fadin V.S.
27. Doctor of phys.-math. science	Khazin B.I.
28. Corr. Member RAS	Khriplovich I.B.
29. Corr. Member RAS	Shatunov Yu.M.
30. Candidate of techn. science	Shiaynkov S.V.
31. Candidate of phys.-math. science	Taskaev S.Yu. -- Representative of Trade Union
32. Candidate of phys.-math. science	Starostenko A.A. -- Representative of Council of Young scientists

## **Specialized Sections of Scientific Council**

### **Accelerators for Applied Purposes**

Kulipanov G.N. (Chrmn)	Korchagin A.I.	Rakshun Ya.V.
Gorbunov V.A. (Secr.)	Kuksanov N.K.	Salimov R.A.
Miginsky S.V.(Secr.)	Kuper E.A.	Shatunov Yu.M.
Anashin V.V.	Kuper K.E.	Sheromov M.A.
Antokhin E.I.	Kurkin G.Ya.	Shevchenko O.A.
Bryazgin A.A.	Kuznetsov G.I.	Shkaruba V.A.
Chernyakin A.D.	Levichev E.B.	Skrinsky A.N.
Cheskidov V.G.	Medvedko A.S.	Sukhina B.N.
Churkin I.N.	Mezentsev N.A.	Tkachenko V.O.
Dikansky N.S.	Nemytov P.I.	Tribendis A.G.
Fadeev S.N.	Nikolenko A.D.	Tumaikin G.M.
Goldenberg B.G.	Parkhomchuk V.V.	Tuvik A.F.
Ivanov A.A.	Petrichenkov M.V.	Vinokurov N.A.
Knyazev B.A.	Petrov V.M.	Vostrikov V.A.
Kolmogorov V.V.	Pindyurin V.F.	Zolotarev K.V.

## Plasma Physics and Controlled Fusion Problems

Ivanov A.A. (Chrmn)  
Kandaurov I.V. (Secr.)  
Akhmetov T.D.  
Anikeev A.V.  
Arzhannikov A.V.  
Astrelin V.T.  
Bagryansky P.A.  
Beklemishev A.D.  
Belchenko Yu.I.  
Burdakov A.V.  
Burmasov V.S.  
Davydenko V.I.  
Dimov G.I.  
Ivanov I.A.  
Kapitonov V.A.

Khilchenko A.D.  
Kulipanov G.N.  
Kuznetsov A.S.  
Konstantinov S.G.  
Kotelnikov I.A.  
Kruglyakov E.P.  
Lizunov A.A.  
Lotov K.V.  
Mekler K.I.  
Murakhtin S.V.  
Polosatkin S.V.  
Popov S.S.  
Postupaev V.V.  
Prihodko V.V.

Sanin A.L.  
Shiyankov S.V.  
Sinitsky S.L.  
Skrinsky A.N.  
Soldatkina E.I.  
Solomakhin A.L.  
Sorokin A.V.  
Sulyaev Yu.S.  
Taskaev S.Yu.  
Timofeev I.V.  
Vasiliev A.V.  
Volosov V.I.  
Voskoboinikov R.V.  
Vyacheslavov L.N.

## Colliding Beams

Parkhomchuk V.V. (Chrmn)  
Petrov V.V. (Secr.)  
Anashin V.V.  
Barkov L.M.  
Berkaev D.E.  
Bondar A.E.  
Dikansky N.S.  
Erokhin A.I.  
Gorniker E.I.  
Gurov S.M.  
Karpov G.V.  
Khazin B.I.  
Kiselev V.A.  
Kolmogorov V.V.  
Koop I.A.  
Krasnov A.A.  
Kulipanov G.N.

Kuper E.A.  
Kurkin G.Ya.  
Levichev E.B.  
Logachev P.V.  
Medvedko A.S.  
Meshkov O.I.  
Mezentsev N.A.  
Mishnev S.I.  
Nesterenko I.N.  
Nikitin S.A.  
Onuchin A.P.  
Ostreiko G.N.  
Perevedentsev E.A.  
Pestrikov D.V.  
Petrov V.M.  
Reva V.B.

Salimov R.A.  
Shatilov D.N.  
Shatunov P.Yu.  
Shatunov Yu.M.  
Shwartz D.B.  
Shiyankov S.V.  
Simonov E.A.  
Skrinsky A.N.  
Smalyuk V.V.  
Solodov E.P.  
Starostenko A.A.  
Tikhonov Yu.A.  
Tumaikin G.M.  
Vinokurov N.A.  
Vobly P.D.  
Zolotarev K.V.

## Physics of Elementary Particles

Bondar A.E.(Chrmn)	Khazin B.I.	Rachek I.A.
Strakhovenko V.M. (Secr.)	Khriplovich I.B.	Redin S.I.
Achasov M.N.	Kirilin G.G.	Ryskulov N.M.
Aulchenko V.M.	Koop I.A.	Serednyakov S.I.
Barkov L.M.	Kravchenko E.A.	Shamov A.G.
Baru S.E.	Kuzmin A.S.	Shatunov Yu.M.
Berkaev D.E.	Lee R.N.	Shekhtman L.I.
Blinov A.E.	Levichev E.B.	Shwartz B.A.
Blinov V.E.	Logachev P.V.	Sibidanov A.L.
Buzulutskov A.F.	Logashenko I.B.	Silagadze Z.K.
Chernyak V.L.	Lukin P.A.	Skovpen Yu.I.
Eidelman S.I.	Malyshev V.M.	Skrinsky A.N.
Epifanov D.A.	Maslennikov A.L.	Smalyuk V.V.
Dimova T.V.	Milshtein A.I.	Sokolov A.V.
Dmitriev V.F.	Muchnoi N.Yu.	Solodov E.P.
Druzhinin V.P.	Nikolenko D.M.	Sokolov V.V.
Fadin V.S.	Obrazovsky A.E.	Tayursky V.A.
Fedotov G.V.	Onuchin A.P.	Telnov V.I.
Golubev V.B.	Pakhtusova E.V.	Terekhov I.S.
Grebenyuk A.A.	Parkhomchuk V.V.	Todyshev K.Yu.
Grigoriev D.N.	Peleganchuk S.V.	Tikhonov Yu.A.
Groshev V.P.	Pestov Yu.N.	Toporkov D.K.
Grozin A.G.	Pivovarov S.G.	Vasiliev A.V.
Ignatov F.V.	Pomeransky A.A.	Vorob'ev A.I.
Katkov V.M.	Popov A.S.	Zhilich V.N.
Kharlamov A.G.		

## Automation

Tikhonov Yu.A. (Chrmn)	Faktorovich B.P.	Levichev E.B.
Kuper E.A. (Co-Chrmn)	Frolovskaya N.N.	Logashenko I.B.
Baldin E.M.(Secr.)	Grozin A.G.	Maximova S.V.
Dubrov S.V. (Secr.)	Kaplin V.I.	Medvedko A.S.
Aleshaev A.N.	Karnaev S.E.	Mezentsev N.A.
Amosov S.A.	Khilchenko A.D.	Nekhanevich E.L.
Aulchenko V.M.	Klimenko A.S.	Shatunov Yu.M.
Banzarov V.Sh.	Koop I.A.	Shukaev A.N.
Baru S.E.	Korol A.A.	Shuvalov B.N.
Belov S.D.	Kozak V.R.	Solodov E.P.
Berkaev D.E.	Kovalenko Yu.V.	Sukharev A.M.
Bogdanchikov A.G.	Kuzin M.V.	Tararyshkin S.V.
Bolkhovityanov D.Yu.	Kupchik V.I.	Tsukanov V.M.
Buzykaev A.R.	Kurilin O.Yu.	Vasiliev A.V.
Egorychev M.N.	Kvashnin A.N.	Zaitsev A.S.

Skrinsky A.N.	2, 11, 30, 54, 78, 200, 238, 239, 240, 241, 242, 246, 358, 403, 457, 495, 496, 503, 511, 564, 565, 566, 567, 568, 569, 570, 573, 630, 13π	Arapov L.N.	
Anashin V.V.	238, 239, 240, 241, 242, 329, 380, 545, 564, 565, 566, 567, 568, 569, 570, 13π	Arbuzov V.S.	
Ivanov A.A.	89, 91, 131, 248, 252, 253, 255, 277, 367, 373, 387, 388, 389, 391, 417, 427, 440, 442, 443, 447, 455, 578, 579, 581, 582, 585, 597, 605, 613, 616, 7π	Arzhannikov A.V.	35, 103, 279, 280, 321, 322, 393, 417, 420, 428, 444, 452, 465, 598, 599, 606, 607, 608, 610, 615
Kruglyakov E.P.	89, 255, 373, 387, 389, 417, 605, 613, 616	Arinstein K.E.	67, 72, 74, 75, 84, 105, 111, 115, 117, 118, 124, 125, 214, 215, 216, 219, 222, 223, 224, 225, 226, 22π, 23π, 24π
Kulipanov G.N.	17, 43, 82, 284, 292, 320, 329, 350, 457, 458, 464, 475, 630, 639, 640, 641	Astigeevich P.M.	503
Levichev E.B.	2, 56, 92, 238, 239, 240, 241, 242, 246, 285, 380, 517, 523, 538, 540, 564, 565, 566, 567, 568, 569, 570, 573	Astrelin V.T.	277, 361, 378, 417, 418, 428, 454, 456, 598, 600, 601, 602, 603, 604, 606, 615
Tikhonov Yu.A.	2, 167, 170, 200, 201, 212, 238, 239, 240, 241, 242, 308, 309, 314, 315, 316, 317, 318, 319, 324, 325, 326, 358, 403, 412, 503, 549, 564, 565, 566, 567, 568, 569, 570, 13π, 46π, 47π, 48π, 49π, 50π, 51π, 52π, 53π, 54π	Astrelina K.V.	
***	***	Aulchenko V.M.	16, 72, 74, 83, 84, 105, 111, 113, 115, 117, 118, 177, 181, 203, 214, 215, 216, 217, 226, 238, 239, 240, 241, 242, 331, 340, 358, 414, 503, 564, 565, 566, 567, 568, 569, 570, 630, 653, 13p, 22p, 23π, 33π, 59π
Abakumova E.V.	380, 544	Akhmetov T.D.	391
Abdrashitov A.G.	446	Akhmetshin R.R.	181, 358, 653, 33π
Abdrashitov G.F.	15, 446, 580	Achasov M.N.	30, 54, 78, 85, 88, 175, 180, 200, 304, 311, 403, 503, 544
Abdulmanov V.G.	323	***	***
Avdeeva E.G.	49	Babichev E.A.	549
Averbukh I.I.	447, 7π	Bagryansky P.A.	13, 89, 90, 252, 261, 276, 362, 363, 364, 365, 373, 389, 390, 422, 423, 424, 425, 438, 439, 597, 70, 157
Avilov M.S.	94	<b>Baier V.N.</b>	513
Avrorov A.P.	418, 604, 615	Bak P.A.	513
Akberdin R.R.		Baldin E.M.	238, 239, 240, 241, 242, 564, 565, 566, 567, 568, 569, 570
Akimov A.V.	167, 244	Banzarov V.I.	181, 358, 653, 33π
Aleinik	582, 583, 585, 588	Barkov L.M.	18, 29, 181, 194, 195, 358, 541, 542, 543, 653, 33π
Alinovsky N.I.		Barladyan A.K.	238, 239, 240, 241, 242, 564, 565, 566, 567, 568, 569, 570
Anikeev A.V.	13, 252, 362, 363, 364, 366, 373, 389, 390, 423, 429, 438, 597	Barnyakov A.Yu.	14, 238, 239, 240, 241, 242, 503, 564, 565, 566, 567, 568, 569, 570, 13π
Anisenkov A.V.	119, 183, 394, 653	Barnyakov A.M.	199
Antokhin E.I.		Barnyakov M.Yu.	199, 238, 239, 240, 241, 242
Arakcheev A.S.	441		

Baru S.E.	181, 203, 206, 208, 209, 238, 239, 240, 241, 242, 549, 550, 564, 565, 566, 567, 568, 569, 570, 647, 13π, 33π	Bobylev V.B.	442, 451
Baryshev V.B.	630	Bogdanchikov A.G.	30, 49, 54, 78, 309, 326, 413, 503, 650, 651, 48π, 49π, 50π, 51π, 52π, 53π, 54π
Basok I.Yu.	13π	Bogomyagkov A.V.	2, 238, 239, 240, 241, 242, 397, 537, 538, 539, 564, 565, 566, 567, 568, 569, 570
Batazova M.A.	522	Bolkhovitjanov D.Yu.	12
Batkin V.I.	48, 361, 428, 442, 599, 606, 615,	Bondarenko A.V.	10, 515, 14A
Batrakov A.M.	38, 297, 298, 330, 383, 576		
Bashtovoy N.S.	181, 194, 358, 653, 33π		
Bayanov B.F.	51, 268, 581, 583, 586, 587, 588, 3π		
Bezuglov V.V.	303, 499		
Beklemishev A.D.	13, 89, 90, 252, 253, 261, 360, 374, 375, 389, 417, 421, 422, 424, 431, 434, 597	Bondar A.E.	72, 73, 74, 84, 105, 113, 115, 118, 125, 181, 211, 212, 213, 214, 217, 218, 219, 220, 222, 223, 224, 225, 226, 228, 229, 230, 238, 239, 240, 241, 242, 358, 414, 492, 555, 558, 564, 565, 566, 567, 568, 569, 570, 653, 13π, 17π, 18π, 19π, 20π, 21π, 23π, 24π, 33π, 59π
Belikov O.V.	58, 102, 251, 490, 619, 7A	Borisov A.A.	
Beloborodov K.I.	30, 54, 78, 199, 200, 403, 503	Botov A.A.	49, 200, 403, 503
Beloborodova O.L.	201, 238, 239, 240, 241, 242, 564, 565, 566, 567, 568, 569, 570, 13π, 59π	Bocharov V.N.	498
Belov V.P.	132, 248, 427, 447, 7π	Bragin A.V.	181, 194, 358, 653, 33π
Belov S.D.		Bryzgunov M.I.	36, 98, 398, 488, 494, 497, 498, 516
Belykh V.V.	440	Bryazgin A.A.	247, 279, 280, 303, 499, 607, 608, 642, 643, 2π
Belchenko Yu.I.	579	Bubley A.V.	36, 99, 398, 488, 498
Berdyugin A.V.	30, 54, 78, 200, 403, 503	Buzulutskov A.F.	211, 212, 522, 553, 554, 17π, 18π, 20π
Berkaev D.E.	396, 491, 495, 514, 617, 618, 10A	Buzykaev A.R.	65, 69, 71, 76, 77, 79, 80, 86, 87, 106, 107, 108, 109, 110, 112, 114, 116, 126, 127, 128, 129, 188, 189, 190, 199, 210, 238, 239, 240, 241, 242, 564, 565, 566, 567, 568, 569, 570
Bekhtenev E.A.	298, 301, 479, 480, 483	Bukin D.A.	30, 49, 54, 78, 503
Biryuchevsky Yu.A.	577	Burdakov A.V.	9, 164, 254, 255, 268, 277, 278, 282, 322, 361, 368, 372, 376, 377, 378, 387, 393, 417, 418, 420, 428, 432, 433, 442, 444, 448, 449, 454, 456, 462, 505, 579, 581, 582, 583, 585, 588, 599, 600, 601, 604, 605, 606, 613, 614, 615, 616
Blinov A.E.	238, 239, 240, 241, 242, 564, 565, 566, 567, 568, 569, 570, 13π, 39π	Burmasov V.S.	361, 428, 451, 599, 606, 615
Blinov V.E.	2, 65, 69, 71, 76, 77, 79, 80, 86, 87, 106, 107, 108, 109, 110, 112, 114, 116, 126, 127, 128, 129, 175, 185, 186, 187, 188, 189, 190, 191, 192, 193, 210, 238, 239, 240, 241, 242, 395, 503, 564, 565, 566, 567, 568, 569, 570, 13π, 30π, 31π	Bykov E.V.	396
Blinov M.F.	12		
Bobrov A.V.	229, 230, 238, 239, 240, 241, 242, 305, 492, 564, 565, 566, 567, 568, 569, 570, 13π, 59π		
Bobrovnikov V.S.	199, 201, 238, 239, 240, 241, 242, 564, 565, 566, 567, 568, 569, 570, 13π, 48π, 49π, 50π, 51π, 52π, 53π, 54π		

Bykov P.V.	277, 418, 604, 615	Golubev V.B.	30, 49, 54, 65, 69, 71, 76, 77, 78, 79, 80, 86, 87, 106, 107, 108, 109, 110, 112, 114, 116, 126, 127, 128, 129, 185, 186, 187, 188, 189, 190, 191, 192, 193, 199, 200, 210, 403, 503, 30π, 31π, 32π
***	***	Golubev P.A.	
Vasiljev A.V.	30, 49, 54, 78, 102, 200, 203, 403, 503	Golubenko Yu.I.	1, 39, 481, 493, 628
Vasichev S.S.		Goldenberg B.G.	17, 294, 335, 336, 339, 359, 384, 465, 630, 631, 632
Veremeenko V.F.	58	Goncharov A.D.	485, 497, 498, 516
Vesenev V.M.	49, 199	Gorbovsky A.I.	427
Vinokurov N.A.	10, 82, 118, 214, 285, 286, 292, 400, 457, 458, 464, 475, 496, 510, 511, 515	Gorbunov V.A.	247, 303, 499, 2π
Vinokurova A.N.	72, 75, 111, 115, 118, 214, 23π, 24π	Gornakov I.V.	247, 499, 2π
Vlasenko M.G.	287, 355, 457, 460, 461, 472, 477, 478, 496, 529, 636	Gorniker E.I.	577
Vlasov A. Yu.	303, 607, 608	Gorchakov K.M.	
Vobly P.D.	330, 383, 436, 457, 496, 511, 523, 527	Grabovsky A.V.	61, 135, 533, 6A
Volkov A.A.	2	Gramolin A.V.	29, 401
Volkov V.N.	250	Grebenyuk A.A.	181, 194, 211, 212, 358, 653, 17π, 18π, 33π
Volosov V.I.	437	Grigoriev V.N.	102, 133, 166
Vorob'ev A.I.	238, 239, 240, 241, 242, 564, 565, 566, 567, 568, 569, 570, 653, 13π	Grigoriev D.N.	181, 204, 205, 358, 549, 653, 3π
Voronin L.A.	303	Grishnyaev E.S.	6
Voskoboinikov R.V.		Grozin A.G.	141, 142, 143
Vostretsov A.G.	9	Groshev V.R.	549
Vostrikov V.A.	36, 59, 398, 486, 512, 572, 573	Gubin K.V.	245
Vyacheslavov L.N.	262, 263, 264, 322, 361, 420, 428, 449, 462, 599, 606, 614, 615	Gudkov B.A.	
***	***	Gulevich V.V.	238, 239, 240, 241, 242, 564, 565, 566, 567, 568, 569, 570, 13π
Gabyshv N.I.	66, 67, 68, 73, 74, 75, 84, 104, 105, 111, 113, 115, 118, 181, 214, 215, 216, 217, 218, 220, 224, 358, 23π, 24π, 33π	Gurov D.S.	330
Galt A.A.	251, 496	Gurov S.M.	
Garmash A. Yu.	115, 118, 214, 23π, 24π	Gusev G.A.	574
Gentshev A.N.	342, 343, 345, 346, 347, 349, 359, 384	Gusev D.V.	238, 239, 240, 241, 242, 564, 565, 566, 567, 568, 569, 570
Gerasimov V.V.	19, 52, 53, 289, 290, 291, 292, 293, 355, 457, 458, 460, 467, 468, 470, 472, 473, 477, 478, 529, 635, 636	Gusev E.A.	
Gerasimov R.E.	21	Gusev I.A.	484
Getmanov Ya.V.	400, 457, 496, 510, 511	***	***
Glukhov S.A.		Davidovsky V.G.	
Glukhovchenko Yu.M.	238, 239, 240, 241, 242, 564, 565, 566, 567, 568, 569, 570	Davydenko V.I.	6, 131, 132, 248, 427, 440, 442, 443, 447, 578, 579, 582, 583, 7π
Golkovsky M.G.	621, 622, 623, 624, 625, 626, 627	Devyataikina T.A.	
		Deichuli P.P.	131, 132, 248, 388, 427, 446, 447, 7π
		Dementjev E.N.	249, 457, 496, 511
		Derevyankin G.E.	418, 604, 615
		Dikansky N.S.	57, 323
		Dimov G.I.	7, 387, 435, 436
		Dimova T.V.	30, 49, 54, 78, 200, 403, 503

Dmitriev V.F.	18, 29, 138, 150, 195, 542, 543, 19π	Zaitsev A.S.	181, 183, 308, 309, 314, 315, 316, 317, 318, 319, 324, 325, 326, 358, 413, 650, 651, 653, 33π, 46π, 47π, 48π, 49π, 50π, 51π, 52π, 53π, 54π
Dneprovsky L.V.	653, 13π	Zapryagaev I.A.	47
Dovzhenko B.A.	457, 496, 5π	Zverev S.I.	
Donin A.S.	369, 373, 389, 446	Zevakov S.A.	18, 29, 195, 196, 541, 542, 543
Dorokhov D.V.		Zemlyansky I.M.	495
Druzhinin V.P.	30, 49, 54, 65, 69, 71, 76, 77, 78, 79, 80, 86, 87, 106, 107, 108, 109, 110, 112, 114, 116, 126, 127, 128, 129, 174, 185, 186, 187, 188, 189, 190, 191, 192, 193, 200, 210, 403, 503, 551, 10π 30π, 31π, 32π, 42π	Zinin E.I.	34, 178, 386
Dubrovin A.N.		Zolotarev K.V.	42, 338, 351, 380, 523, 524, 525, 630, 45π
Dudnikov A.V.	130, 654, 655	Zubarev P.V.	369, 446
***	***	***	***
Eliseev A.A.	33, 295, 296, 638	Ivanenko V.G.	361, 377, 433, 598, 615
Emanov F.A.		Ivanenko S.V.	425, 451
Emelev I.S.	7, 436	Ivanov A.V.	23, 133, 166, 270, 488, 499
Epifanov D.A.	66, 68, 111, 115, 118, 181, 214, 215, 220, 358, 653, 23π, 24π, 33π	Ivanov I.A.	6, 254, 277, 282, 361, 372, 376, 377, 393, 428, 432, 433, 444, 599, 606, 615
Erokhin A.I.	5, 15A	Ivantsivsky M.V.	361, 417, 428, 449, 599, 606, 614, 615
Ershov V.V.	167	Ignatov F.V.	95, 181, 182, 183, 198, 204, 358, 402, 653, 33π
***	***	Iljin I.V.	330, 383, 576
Zhilich V.N.	67, 74, 83, 105, 111, 115, 118, 214, 216, 217, 218, 219, 222, 224, 226, 238, 239, 240, 241, 242, 564, 565, 566, 567, 568, 569, 570, 13π, 22π, 23π, 24π, 59π	***	***
Zhirov O.V.	148, 151, 152, 163, 44π, 56π, 57π	Kazanin V.F.	181, 205, 358, 653, 33π
Zhmurikov E.I.	12, 94, 245, 646, 9π	Kairan D.A.	
Zhukov A.A.	175, 180, 380, 544	Kalinin P.V.	103, 278, 279, 280, 322, 462, 607, 608
Zhulanov V.V.	16, 67, 73, 75, 104, 105, 111, 113, 115, 117, 118, 203, 214, 218, 220, 221, 225, 238, 239, 240, 241, 242, 340, 414, 564, 565, 566, 567, 568, 569, 570, 13π, 22π, 59π	Kandaurov I.V.	378, 417, 418, 454, 601, 602, 603, 604, 615
Zhuravlev A.N.	2, 179, 238, 239, 240, 241, 242, 564, 565, 566, 567, 568, 569, 570	Kapitonov V.A.	418, 440, 442, 447, 7π
***	***	Kaplin V.I.	133, 166, 269
Zabrodin V.D.		Karavdina A.V.	182
Zaigraeva N.S.	457, 496, 511	Kardapoltsev L.V.	200, 10π
		Karmakulov K.V.	
		Karnaev S.E.	2, 238, 239, 240, 241, 242, 249, 564, 565, 566, 567, 568, 569, 570
		Karnakov I.V.	29, 542
		Karpov G.V.	479, 480, 13π
		Karpov S.V.	181, 194, 238, 239, 240, 241, 242, 358, 564, 565, 566, 567, 568, 569, 570, 653, 33π
		Kasaev A.S.	619, 645
		Katkov V.M.	157, 535
		Kvashnin A.N.	425
		Kenzhebulatov E.K.	
		Kirilin G.G.	162
		Kirillov K.Yu.	363, 373
		Kirpotin A.N.	491, 495, 514

Kiselev V.A.	2, 31, 238, 239, 240, 241, 242, 564, 565, 566, 567, 568, 569, 570	Kravchenko E.A.	199, 238, 239, 240, 241, 242, 503, 564, 565, 566, 567, 568, 569, 570, 13п
Klyuev V.F.	485, 486, 512	Krasnov A.A.	175, 180, 380, 544, 545
Knyazev B.A.	19, 25, 26, 52, 53, 82, 287, 288, 289, 290, 291, 292, 293, 355, 457, 458, 460, 461, 468, 471, 472, 473, 474, 477, 478, 496, 511, 529, 630, 633, 634, 635, 636, 637	Krivashin D.S.	119
Kobets V.V.	251, 436, 500	Krivenko A.S.	445
Kovalenko N.V.	3	Krutikhin S.A.	249, 577
Kovalenko Yu.V.	373, 389, 425	Kryuchkov A.M.	498
Kovrizhin D.P.	200, 403, 503	Kryuchkov Ya.G	
Kogut D.A.	493, 628	Kubarev V.V.	103, 321, 457, 459, 465, 466, 475, 476, 630
Kozak V.R.	396, 490, 619	Kudryavtsev V.N.	13п, 59п
Kozlov M.G.	8п	Kuzin M.V.	630
Kozyrev A.N.	8, 415, 544, 653	Kuznetsov A.S.	9, 268, 579, 581, 582, 583, 585, 652
Kozyrev E.V.	577	Kuznetsov G.I.	247, 508, 522, 2п
Kokin E.N.	303, 499, 2п	Kuznetsov S.A.	35, 103, 281, 321, 322, 345, 359, 361, 368, 384, 420, 428, 462, 465, 504, 505, 506, 507, 599, 606, 609, 610, 611, 612, 615
Kolesnikov E.Yu.	6п	Kuzmin A.S.	66, 67, 74, 75, 104, 111, 113, 115, 118, 125, 181, 214, 215, 216, 217, 221, 225, 231, 358, 414, 557, 653, 13п, 22п, 23п, 24п, 33п
Kolmogorov A.V.	578	Kuzminykh V.S.	380, 630
Kolmogorov V.V.	15	Kuklin K.N.	254, 277, 282, 361, 393, 428, 444, 451, 599, 606, 615
Kolobanov E.I.	457, 496, 511	Kuksanov N.K.	1, 39, 283, 493, 628
Kolokolnikov Yu.M.	3	Kulikov V.F.	238, 239, 240, 241, 242, 564, 565, 566, 567, 568, 569, 570, 13п
Kondakov A.A.	577	Kuper K.E.	44, 335, 336, 352, 353, 384, 630, 657
Kondaurov M.N.	574, 575	Kuper E.A.	238, 239, 240, 241, 242, 486, 512, 564, 565, 566, 567, 568, 569, 570, 630, 13п
Kondratjev V.I.	32, 294, 332, 336, 342, 343, 345, 346, 347, 384	Kurkin G.Ya.	47, 238, 239, 240, 241, 242, 249, 564, 565, 566, 567, 568, 569, 570, 577
Kononov S.A.	199, 238, 239, 240, 241, 242, 416, 564, 565, 566, 567, 568, 569, 570, 13п	Kuskov R.E.	***
Konstantinov E.S.	485, 486, 512	Lavrukhin A.V.	493, 628
Konstantinov S.G.	277, 485, 579	Lazarenko B.A.	18, 29, 196, 542
Koop I.A.	30, 54, 78, 181, 200, 403, 495, 514, 521, 539, 620, 33п, 40п	Lapic R.M.	
Korepanov A.A.	513	Lebedev N.N.	
Korzhevina M.S.	362, 363, 373, 389, 423	Lev V.H.	382
Korobeinikov M.V.	279, 280, 303, 499, 607, 608, 642, 644, 13A	Levichev A.E.	24
Korol A.A.	30, 49, 54, 78, 200, 308, 309, 326, 403, 413, 503, 650, 651, 46п, 48п, 49п, 50п, 51п, 52п, 53п, 54п	Legkodymov A.A.	3, 50, 60, 344, 354, 385
Korchagin A.I.	493, 628, 629	Leonov V.V.	203, 549
Kot N.H.	12	Lee R.N.	153, 154, 155, 156, 37п, 38п
Kotelnikov I.A.	256, 265, 266, 267, 363, 392, 417, 422, 463	Lizunov A.A.	13, 89, 252, 363, 373, 389, 425, 446, 587
Kotov K.Yu.	238, 239, 240, 241, 242, 308, 314, 315, 317, 318, 319, 324, 325, 326, 564, 565, 566, 567, 568, 569, 570, 13п, 46п		
Koshuba S.V.	30, 49, 54, 78, 200,, 403, 503		

Listopad A.A.	131, 443	Mekler K.I.	277, 322, 361, 368, 372, 377, 393, 420, 428, 432, 433, 442, 444, 448, 462, 505, 579, 599, 606, 615
Logachev P.V.	38, 164, 244, 245, 251, 500, 576,	Meshkov O.I.	2, 179, 238, 239, 240, 241, 242, 564, 565, 566, 567, 568, 569, 570, 2A
Logashenko I.B.	173, 181, 358, 653, 29п, 33п	Miginskaya E.G.	382
Lotov K.V.	27, 40, 123, 164, 165, 271, 272, 273, 274, 306, 307, 441, 453, 526, 590, 591, 592, 593	Miginsky S.V.	10, 379, 457, 469, 496, 511, 515, 530
Lukin A.N.	3036 499	Milstein A.I.	121, 122, 138, 139, 140, 240, 19п
Lukin P.A.	95, 134, 181, 358, 653, 28п, 33п	Mironenko L.A.	496, 511, 630
Lysenko A.P.	78, 181, 495, 33п	Mityanina N.V.	5п
Lyakh V.V.	3, 60, 332, 344	Mikhailov K.Yu.	181, 358, 653, 33п
***	***	Mishagin V.V.	131, 427, 440
Makarov A.N.	582, 583, 585, 588	Misnev S.I.	2, 18, 29, 195, 196, 238, 239, 240, 241, 242, 541, 542, 543, 564, 565, 566, 567, 568, 569, 570, 630, 41п
Makarov I.G.	247, 499, 2п	Moiseev D.V.	369, 446
Makarov M.A.	322, 361, 372, 377, 393, 420, 428, 432, 433, 448, 451, 462, 505, 598, 599, 606, 615	Morozov I.I.	2, 238, 239, 240, 241, 242, 564, 565, 566, 567, 568, 569, 570
Maximov V.V.	13, 89, 252, 362, 363, 367, 370, 373, 389, 422, 439, 597	Motygin S.V.	249, 577
Maximov D.A.	201, 238, 239, 240, 241, 242, 564, 565, 566, 567, 568, 569, 570, 13п	Murakhtin S.V.	13, 89, 362, 363, 369, 373, 389, 445, 446
Maximov S.A.	499, 2п	Muchnoi N.Yu.	2, 29, 85, 88, 175, 180, 238, 239, 240, 241, 242, 304, 544, 564, 565, 566, 567, 568, 569, 570, 13п, 41п
Maximovskaya V.V.	351, 385	Mjakin S.V.	283
Malyshev V.M.	238, 239, 240, 241, 242, 308, 309, 314, 315, 316, 317, 318, 319, 324, 325, 326, 564, 565, 566, 567, 568, 569, 570, 13п, 46п, 47п, 48п, 49п, 50п, 51п, 52п, 53п, 54п	***	
Malyutin D.A.		Neyfeld V.V.	238, 239, 240, 241, 242, 564, 565, 566, 567, 568, 569, 570
Mamkin V.R.	486, 512	Nemytov P.I.	1, 39, 481, 486, 493, 512, 628, 4A
Martin K.A.	199, 503	Nesterenko I.N.	482, 491, 495
Martyshkin P.V.		Nekhaev V.E.	303
Maslennikov A.L.	167, 201, 238, 239, 240, 241, 242, 308, 309, 314, 315, 316, 317, 318, 319, 324, 325, 326, 564, 565, 566, 567, 568, 569, 570, 13п, 46п, 47п, 48п, 49п, 50п, 51п, 52п, 53п, 54п	Nikitin S.A.	2, 238, 239, 240, 241, 242, 489, 521, 540, 564, 565, 566, 567, 568, 569, 570, 620, 13п, 14п, 40п
Matveenko A.N.		Nikolaev I.B.	2, 175, 238, 239, 240, 241, 242, 564, 565, 566, 567, 568, 569, 570, 13п, 14п,
Matyash N.V.	247, 499, 2п	Nikolenko A.D.	3, 46, 50, 60, 332, 334, 339, 344, 354, 630
Medvedev L.E.	457, 496, 511	Nikolenko D.M.	18, 20, 29, 195, 196, 197, 541, 542, 543, 41п
Medvedko A.S.	5, 238, 239, 240, 241, 242, 249, 251, 481, 484, 486, 490, 512, 564, 565, 566, 567, 568, 569, 570, 574, 630, 13п	***	***
Mezsetsev N.A.	33, 45, 295, 296, 382, 630, 638, 648	Obrazovsky A.E.	49, 200, 403, 404, 503
		Ovchar V.K.	457, 496, 511
		Ogurtsov A.B.	330

Окунев И.Н. Okunev I.N.	238, 239, 240, 241, 242, 405, 564, 565, 566, 567, 568, 569, 570	Pestov Yu.N.	96, 102, 133, 166, 257, 310, 312, 313, 653, 55п
Onuchin A.P.	55, 65, 69, 71, 76, 77, 79, 80, 86, 87, 106, 107, 108, 109, 110, 112, 114, 116, 126, 127, 128, 129, 185, 186, 187, 188, 189, 190, 191, 192, 193, 199, 210, 238, 239, 240, 241, 242, 503, 564, 565, 566, 567, 568, 569, 570, 13п, 30п, 31п, 32п	Pestrikov D.V.	57, 243
Oreshkin S.B.	238, 239, 240, 241, 242, 564, 565, 566, 567, 568, 569, 570, 13п	Petrenko A.V.	164
Oreshonok V.V.	249, 487	Petrichenkov M.V.	246, 485
Orlov I.O.	167, 238, 239, 240, 241, 242, 308, 309, 314, 315, 316, 317, 318, 319, 324, 325, 326, 564, 565, 566, 567, 568, 569, 570, 13п, 46п, 47п, 48п, 49п, 50п, 51п, 52п, 53п, 54п	Petrov V.V.	2, 238, 239, 240, 241, 242, 564, 565, 566, 567, 568, 569, 570, 1п
Osipov A.A.	238, 239, 240, 241, 242, 305, 564, 565, 566, 567, 568, 569, 570, 13п	Petrov V.M.	167, 249, 577, 5п
Osipov V.N.	249, 577	Petrova E.V.	339, 384
<b>Ostreiko G.N.</b>	10, 247, 499, 2п	Petrozhitsky A.V.	406, 485
Otboev A.V.	539	Pivovarov I.L.	
Ottmar A.V.	300	Pivovarov S.G.	167, 182, 194, 238, 239, 240, 241, 242, 564, 565, 566, 567, 568, 569, 570, 653, 13п
Okhapkin O.S.	181, 182, 194, 358, 653, 33п	Pilipenko R.V.	
***	***	Piminov P.A.	2, 92, 238, 239, 240, 241, 242, 407, 509, 540, 564, 565, 566, 567, 568, 569, 570, 620, 40п, 16A
Pavlenko A.V.	38	Pindyurin V.F.	3, 17, 60, 332, 339, 342, 343, 344, 345, 346, 347, 384, 630
Pavlov V.M.	24, 251, 500, 518	Pinzhenin E.I.	363, 367, 370, 373, 389, 439
Palagin K.S.		Pirogov S.A.	183, 653
Panasyuk V.M.	36, 98, 99, 398, 498	Podgorny F.V.	619, 645
Panov A.N.	302	Podobaev V.S.	499
Panfilov A.D.	247, 303, 499, 2п	Podyminogin A.A.	6, 132, 248, 447, 7п
Panchenko V.E.	630	Polosatkin S.V.	6, 254, 277, 282, 322, 361, 368, 372, 376, 377, 393, 417, 420, 428, 432, 433, 440, 442, 444, 448, 462, 599, 606, 614, 615
Papushev P.A.	203, 549	Poluektov A.O.	74, 111, 113, 115, 118, 124, 214, 215, 216, 223, 227, 228, 229, 230, 238, 239, 240, 241, 242, 564, 565, 566, 567, 568, 569, 570, 13п, 22п, 23п, 24п
Parkhomchuk V.V.	36, 59, 99, 100, 101, 171, 246, 337, 398, 485, 488, 497, 498, 501, 516, 571, 573	Pomeransky A.A.	
Pakhtusova E.V.	30, 49, 54, 78, 200, 403, 503	Popik V.M.	17, 457, 464, 496, 511, 630
Pachkov A.A.		Popkov I.N.	238, 239, 240, 241, 242, 564, 565, 566, 567, 568, 569, 570
Peleganchuk S.V.	167, 201, 238, 239, 240, 241, 242, 308, 309, 314, 315, 316, 317, 318, 319, 324, 325, 326, 564, 565, 566, 567, 568, 569, 570, 13п, 46п, 47п, 48п, 49п, 50п, 51п, 52п, 53п, 54п	Popov A.S.	181, 182, 204, 358, 653, 33п
Perevedentsev E.A.	181, 495, 514, 33п	Popov S.S.	254, 282, 361, 428, 448, 451, 599, 606, 614, 615
Persov B.Z.	457, 496, 511	Popov Yu.S.	194, 653
		Popova N.I.	12п
		Porosev V.V.	203, 206, 549

Postupaev V.V.	254, 277, 282, 322, 361, 368, 372, 376, 377, 393, 417, 420, 428, 432, 433, 442, 444, 448, 454, 462, 505, 599, 606, 614, 615	Salikova T.V.	381, 457, 496, 511
Prisekin V.G.	238, 239, 240, 241, 242, 564, 565, 566, 567, 568, 569, 570, 13π	Salimov R.A.	1, 486, 493, 512, 628
Prikhodko V.V.	13, 89, 252, 261, 276, 362, 363, 373, 389, 391, 422, 423, 424, 439, 597	Salnikov S.G.	138
Protopopov A. Yu.	484	Sandyrev V.K.	238, 239, 240, 241, 242, 564, 565, 566, 567, 568, 569, 570
Pupkov Yu.A.	1π	Sanin A.L.	263, 264, 579
Pureskin D.N.	481, 484	Sedlyarov I.K.	
Putmakov A.A.	498	Selivanov A.N.	341
Pyata E.E.	175, 180	Selivanov P.A.	5
***	***	Semenov A.V.	486, 512
Radchenko V.M.	9, 303, 499, 2π	Semenov E.P.	329, 380, 493, 628
Razorenov V.V.		Semenov Yu.I.	
Rakshun Ya.V.	41, 64, 333, 351, 385	Sen'kov R.A.	481, 484, 486, 512
Rastigeev S.A.	337, 485	Serdobintsev G.V..	247, 499, 577, 2π
Rachek I.A.	18, 29, 195, 196, 197, 541, 542, 543	Serednyakov S.I.	30, 49, 54, 65, 69, 71, 76, 77, 78, 79, 80, 86, 87, 106, 107, 108, 109, 110, 112, 114, 116, 126, 127, 128, 129, 185, 186, 187, 188, 189, 190, 191, 192, 193, 199, 200, 210, 403, 503, 30π, 31π, 32π
Raschenko V.V.	299	Serednyakov S.S.	301, 457, 496, 511
Reva V.B.	23, 36, 59, 98, 99, 100, 101, 171, 270, 398, 486, 488, 494, 497, 498, 501, 512, 516, 571	Sibidanov A.L.	95, 169, 181, 182, 183, 184, 213, 358, 27π, 33π, 43π
Redin S.I.	181, 358, 653, 33π	Sidorov A.V.	303, 424, 499, 2π
Reznichenko A.V.	8π	Sidorov I.V.	
Repkov V.V.	396, 486, 512, 11π	Silagadze Z.K.	28, 30, 54, 78, 172, 176, 200, 202, 327, 328, 403, 503
Rovenskiikh A.F.	254, 277, 282, 322, 361, 368, 372, 376, 377, 393, 418, 420, 428, 432, 433, 442, 444, 448, 451, 462, 505, 599, 606, 615	Simonov E.A.	2, 238, 239, 240, 241, 242, 517, 564, 565, 566, 567, 568, 569, 570
Rogovsky Yu.A.	482, 483, 491, 495, 514	Singatulin Sh.R.	574, 575
Rodyakin V.A.	13π	Sinitsky S.L.	268, 277, 322, 361, 368, 372, 377, 393, 417, 418, 420, 428, 432, 433, 444, 448, 452, 454, 462, 505, 583, 588, 598, 599, 606, 615
Romanov A.L.	97, 491, 495, 508, 514, 519	Sirotkin A.A.	49
Romashko N.D.	499, 2π	Sinyatkin S.V.	2, 238, 239, 240, 241, 242, 411, 509, 521, 523, 564, 565, 566, 567, 568, 569, 570, 620, 40π
Rotov E.A.	249	Skarbo B.A.	522
Ruban A.A.	181, 182, 194, 238, 239, 240, 241, 242, 358, 564, 565, 566, 567, 568, 569, 570, 653, 13π, 33π	Skovorodin D.I.	375, 434
Rudenko A.S.	149, 356, 408, 15π, 39π, 58π	Skovpen K. Yu.	308, 309, 325, 326, 410, 46π, 47π, 48π, 49π, 50π, 51π, 52π, 53π, 54π
Rybitskaya T.V.			
Ryskulov N.M.	181, 358, 653, 33π		
***	***		
Savinov G.A.	203, 238, 239, 240, 241, 242, 549, 564, 565, 566, 567, 568, 569, 570, 13π		
Savkin V.Ya.	131, 373, 389, 425, 445		
Sadykov R.Sh.	195, 196, 542		
Sazansky V.Ya.	38, 576		

Skovpen Yu.I.	65, 69, 71, 76, 77, 79, 80, 86, 87, 106, 107, 108, 109, 110, 112, 114, 116, 126, 127, 128, 129, 185, 186, 187, 188, 189, 190, 191, 192, 193, 210, 238, 239, 240, 241, 242, 503, 564, 565, 566, 567, 568, 569, 570, 13п, 30п, 31п, 32п	Sukharev A.M.	238, 239, 240, 241, 242, 308, 309, 314, 315, 316, 317, 318, 319, 324, 325, 326, 564, 565, 566, 567, 568, 569, 570, 13п, 46п, 47п, 48п, 49п, 50п, 51п, 52п, 53п, 54п
Skorobogatov D.N.	5, 100, 101, 171, 497, 498, 516	Sukhina B.N.	
Smalyuk V.V.	2, 31, 92, 179, 238, 239, 240, 241, 242, 249, 380, 487, 564, 565, 566, 567, 568, 569, 570, 630, 13п, 3A	Syrovatina V.M.	382, 648
Smolina E.V.	653	***	***
Snopkov I.G.	181, 182	Talyshev A.A.	120, 167, 201, 238, 239, 240, 241, 242, 308, 309, 314, 315, 316, 317, 318, 319, 324, 325, 326, 564, 565, 566, 567, 568, 569, 570, 653, 13п, 46п, 47п, 48п, 49п, 50п, 51п, 52п, 53п, 54п
Snopkov R.G.	13п, 33п	Tararyshkin S.V.	
Sokolov A.V.	72, 83, 84, 211, 214, 238, 239, 240, 241, 242, 564, 565, 566, 567, 568, 569, 570, 17п, 18п	Tarnetsky V.V.	47, 247, 499, 2п
Sokolov V.V.	146, 147, 148, 211, 214, 238, 239, 240, 241, 242	Taskaev S.Yu.	51, 268, 579, 581, 582, 583, 584, 585, 586, 587, 588, 589, 3п
Soltatkina E.I.	90	Tayursky V.A.	238, 239, 240, 241, 242, 564, 565, 566, 567, 568, 569, 570, 10п, 13п, 42п
Solodov E.P.	126, 127, 128, 129, 181, 185, 186, 187, 188, 189, 190, 191, 192, 193, 210, 358, 653, 30п, 31п, 32п, 33п	Telnov V.I.	237, 238, 239, 240, 241, 242, 559, 560, 561, 562, 563, 564, 565, 566, 567, 568, 569, 570, 13п, 20п
Solomakhin A.L.	13, 363, 365, 371, 373, 389, 425, 450	Terekhov A.V.	27, 168, 275, 419
Sorokin A.V.	132, 248, 427, 446, 7п	Terekhov I.S.	121, 37п
Sorokin I.N.	579, 582, 585	Timofeev I.V.	27, 275, 417, 419, 453, 454, 615, 8A
Sorokina N.V.	254, 282, 361, 376, 428, 442, 448, 599, 606, 615	Titov V.M.	203, 653
Sorokoletov D.S.	336, 384	Tiunov M.A.	132, 247, 248, 436, 499, 2п
Starostenko A.A.		Tkachenko V.O.	303, 499, 2п
Starostenko D.A.		Todyshev K.Yu.	65, 69, 71, 76, 77, 79, 80, 86, 87, 106, 107, 108, 109, 110, 112, 114, 116, 127, 128, 129, 185, 186, 187, 188, 189, 190, 191, 192, 193, 210, 238, 239, 240, 241, 242, 564, 565, 566, 567, 568, 569, 570, 13п, 30п, 31п, 32п
Starostina E.V.	238, 239, 240, 241, 242, 564, 565, 566, 567, 568, 569, 570	Tokarev Yu.F.	457, 511
Startseva E.P.		Tolochko B.P.	16, 177, 203, 331, 340, 348, 630, 5A
Stepanov V.D.	322, 361, 448, 452, 462, 615	Toporkov D.K.	18, 29, 195, 196, 541, 542, 543
Strakhovenko V.M.	161, 649, 19п	Tribendis A.G.	
Stupishin N.V.	131, 132, 248, 388, 427	Trunev Yu.A.	418, 442, 604, 615
Sudnikov A.V.	361, 372, 377, 428, 432, 433, 599, 606, 615	Tumaikin G.M.	2, 238, 239, 240, 241, 242, 564, 565, 566, 567, 568, 569, 570
Sulyaev Yu.S.	9, 268, 322, 361, 420, 428, 442, 462, 579, 599, 606, 615, 9A	***	***
Surin I.K.	49		
Sukhanov A.V.			
Sukhanov D.P.	249, 487		

Ukrantsev Yu.G.	206, 207, 546, 547, 548, 549	Churkin I.N.	630
Usov Yu.V.	49, 72, 73, 74, 84, 105, 111, 113, 115, 118, 167, 201, 214, 216, 226, 238, 239, 240, 241, 242, 414, 503, 564, 565, 566, 567, 568, 569, 570, 13п, 23п	***	***
Utkin A.V.	330, 383, 630	Shamov A.G.	2, 175, 238, 239, 240, 241, 242, 308, 309, 314, 315, 316, 317, 318, 319, 324, 325, 326, 564, 565, 566, 567, 568, 569, 570, 13п, 46п, 47п, 48п, 49п, 50п, 51п, 52п, 53п, 54п, 59п
Ushakov V.A.	329, 630	Sharafutdinov M.R.	203
***	***	Shatilov D.N.	2, 92, 238, 239, 240, 241, 242, 517, 520, 540, 564, 565, 566, 567, 568, 569, 570, 620, 40п
Fadeev S.N.	493, 628	Shatunov P.Yu.	495, 514, 617, 618, 33п
Fadin V.S.	21, 61, 135, 136, 137, 531, 532, 533, 534, 8п	Shatunov Yu.M.	30, 54, 78, 181, 200, 403, 495, 503
Faktorovich B.L.	247, 303, 499, 2п	Shayakhmetov V.R.	549
Fatkin G.A.	38, 300, 302	Shwartz B.A.	66, 67, 68, 73, 74, 75, 104, 105, 111, 113, 115, 117, 118, 125, 181, 214, 215, 216, 217, 218, 219, 220, 222, 224, 231, 232, 233, 238, 239, 240, 241, 242, 305, 358, 414, 564, 565, 566, 567, 568, 569, 570, 653, 13п, 23п, 24п, 25п, 26п, 33п
Fedotov M.G.	341	Shwartz D.B.	495, 514
Fedotov G.V.	95, 134, 169, 181, 358, 653, 33п, 43п	Shvedov D.A.	2
Filatov P.V.	49	Shebalin V.E.	72, 75, 111, 115, 118, 124, 214, 223, 409, 414, 653, 23п, 24п
Filipchenko A.V.	329, 630	Shevchenko O.A.	400, 457, 475, 478, 496, 510, 511
Frolov A.R.	96, 102, 133, 166, 260, 269, 485	Sheromov M.A.	348, 630
***	***	Shestakov Yu.V.	18, 29, 195, 196, 197, 541, 542, 543
Khavin N.G.	330	Shekhtman L.I.	16, 29, 203, 229, 230, 340, 549, 13п, 20п, 59п
Khazin B.I.	181, 182, 194, 358, 653, 33п	Shikhovtsev I.V.	6, 132, 248, 427, 447, 7п
Kharlamov A.G.	49, 200, 403, 503, 12A	Shichkov D.S.	330, 383
Kharlamova T.A.	238, 239, 240, 241, 242, 564, 565, 566, 567, 568, 569, 570, 13п	Shiyankov S.V.	630
Khatsymovsky V.M.	158, 159, 160	Shkaruba V.A.	382
Khilchenko A.D.	425, 440, 446, 1A	Shoshin A.A.	254, 282, 361, 376, 377, 393, 428, 433, 444, 606, 615
Khilchenko V.A.	440	Shtarklev E.A.	303
Kholopov M.A.	330, 333, 385	Shtol D.A.	30, 200, 503
Khriplovich I.B.	22, 81, 93, 149, 356, 408, 656, 15п, 16п, 58п	Shubin E.I.	479
Khrushev S.V.	382	Shukaev A.N.	503
***	***	Shulzhenko G.I.	131, 132, 427
Tsydulko Yu.A.	37, 252, 258, 259, 423, 426, 430, 438, 597, 6п	Shusharo A.I.	13п
Tsukanov V.M.	2, 382	***	***
Tsyganov A.S.		Scheglov M.A.	17, 457, 464, 496, 511, 630
***		Schegolev L.M.	329
Cheblakov P.B.	619	***	***
Cherepanov V.P.	95, 249, 396, 487, 34п		
Cherepkov V.G.	486, 512		
Chernov V.A.	333, 338		
Chernov K.N.	47, 247, 499, 577, 2п		
Chernoshtanov I.S.	37, 423, 426		
Chernyak V.L.	62, 63, 144, 145		
Chernyakin A.D.			
Cheskidov V.G.	247, 457, 496, 498, 499, 511, 2п		
Chudaev V.Ya.	51, 586, 3п		
Chupyra A.G.	58, 574, 575		

Eidelman S.I.	4, 66, 67, 68, 73, 74, 75, 83, 84, 95, 104, 105, 111, 113, 115, 117, 118, 124, 125, 134, 181, 214, 215, 216, 217, 218, 219, 220, 221, 222, 223, 224, 225, 226, 229, 230, 234, 235, 236, 238, 239, 240, 241, 242, 357, 358, 502, 556, 564, 565, 566, 567, 568, 569, 570, 653, 4п, 22п, 23п, 24п, 33п, 34п, 35п, 36п, 43п
Eidelman Yu.I.	
Epstein L.B.	399, 653
***	***
Yudin Yu.V.	181, 204, 358, 653, 33п
Yurchenko Yu.B.	549
Yushkov A.N.	71, 79, 106, 107, 108, 109, 110, 112, 115, 116, 127, 128, 129, 187, 188, 190, 238, 239, 240, 241, 242, 564, 565, 566, 567, 568, 569, 570, 13п
***	
Yarovoi V.A.	418, 604

SIBERIAN BRANCH OF RUSSIAN ACADEMY OF SCIENCE

---

BUDKER INSTITUTE OF NUCLEAR PHYSICS

ANNUAL REPORT

2010

Cover E.D. Bender

Ответственный за выпуск А.В. Васильев

Работа поступила 16.04. 2011 г.

---

Сдано в набор 15.05. 2011 г.

Подписано в печать 3.08. 2011 г.

Формат 60x90 1/16 Объем 20,2 печ.л., 16,2 уч.-изд.л.

Тираж 200 экз. Бесплатно. Заказ № 22

---

Обработано на РС и отпечатано  
на ротапинтере «ИЯФ им. Г.И. Будкера» СО РАН,  
Новосибирск, 630090, пр. Академика Лаврентьева, 11